frontiers | Research Topics

Challenges and their implications for the clinical practice of head and neck cancer

Edited by
Steffi Ulrike Pigorsch and Markus Wirth

Published in
Frontiers in Oncology

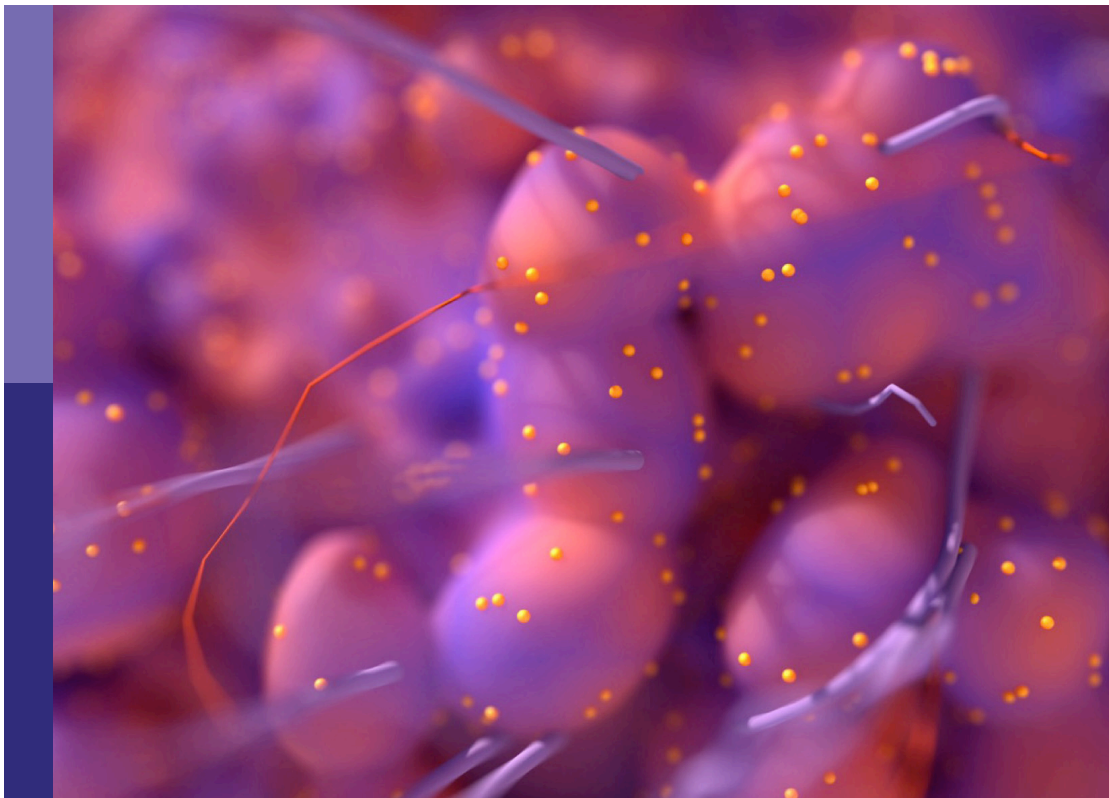

ISSN 1664-8714
ISBN 978-2-83251-532-7
DOI 10.3389/978-2-83251-532-7

About Frontiers

Frontiers is more than just an open access publisher of scholarly articles: it is a pioneering approach to the world of academia, radically improving the way scholarly research is managed. The grand vision of Frontiers is a world where all people have an equal opportunity to seek, share and generate knowledge. Frontiers provides immediate and permanent online open access to all its publications, but this alone is not enough to realize our grand goals.

Frontiers journal series

The Frontiers journal series is a multi-tier and interdisciplinary set of open-access, online journals, promising a paradigm shift from the current review, selection and dissemination processes in academic publishing. All Frontiers journals are driven by researchers for researchers; therefore, they constitute a service to the scholarly community. At the same time, the *Frontiers journal series* operates on a revolutionary invention, the tiered publishing system, initially addressing specific communities of scholars, and gradually climbing up to broader public understanding, thus serving the interests of the lay society, too.

Dedication to quality

Each Frontiers article is a landmark of the highest quality, thanks to genuinely collaborative interactions between authors and review editors, who include some of the world's best academicians. Research must be certified by peers before entering a stream of knowledge that may eventually reach the public - and shape society; therefore, Frontiers only applies the most rigorous and unbiased reviews. Frontiers revolutionizes research publishing by freely delivering the most outstanding research, evaluated with no bias from both the academic and social point of view. By applying the most advanced information technologies, Frontiers is catapulting scholarly publishing into a new generation.

What are Frontiers Research Topics?

Frontiers Research Topics are very popular trademarks of the *Frontiers journals series*: they are collections of at least ten articles, all centered on a particular subject. With their unique mix of varied contributions from Original Research to Review Articles, Frontiers Research Topics unify the most influential researchers, the latest key findings and historical advances in a hot research area.

Find out more on how to host your own Frontiers Research Topic or contribute to one as an author by contacting the Frontiers editorial office: frontiersin.org/about/contact

Challenges and their implications for the clinical practice of head and neck cancer

Topic editors

Steffi Ulrike Pigorsch — Technical University of Munich, Germany

Markus Wirth — Klinikum rechts der Isar, department of otorhinolaryngology, Germany

Citation

Pigorsch, S. U., Wirth, M., eds. (2023). *Challenges and their implications for the clinical practice of head and neck cancer*. Lausanne: Frontiers Media SA. doi: 10.3389/978-2-83251-532-7

Table of contents

frontiers | Frontiers in Oncology

TYPE Editorial
PUBLISHED 18 January 2023
DOI 10.3389/fonc.2023.1131639

OPEN ACCESS

EDITED AND REVIEWED BY
Jan Baptist Vermorken,
University of Antwerp, Belgium

*CORRESPONDENCE
Markus Wirth
markus.wirth@tum.de

SPECIALTY SECTION
This article was submitted to Head and Neck Cancer, a section of the journal Frontiers in Oncology

RECEIVED 25 December 2022
ACCEPTED 04 January 2023
PUBLISHED 18 January 2023

CITATION
Wirth M, Schmidl B, Wollenberg B and Pigorsch S (2023) Editorial: Challenges and their implications for the clinical practice of head and neck cancer.
Front. Oncol. 13:1131639.
doi: 10.3389/fonc.2023.1131639

Editorial: Challenges and their implications for the clinical practice of head and neck cancer

Markus Wirth[1]*, Benedikt Schmidl[1], Barbara Wollenberg[1] and Steffi Pigorsch[2]

[1]Department of Otolaryngology Head and Neck Surgery, Klinikum rechts der Isar, Technical University Munich, Munich, Germany, [2]Department of RadioOncology and Radiotherapy, Klinikum rechts der Isar, Technical University Munich, Munich, Germany

KEYWORDS

HNSCC, treatment related side effects, quality of life, surgery, radiotherapy - adverse effects

Editorial on the Research Topic
Challenges and their implications for the clinical practice of head and neck cancer

Head and neck squamous cell carcinoma (HNSCC) with its heterogeneous character, in part limited survival rates, and therapeutic options with significant side effects pose a serious challenge in clinical practice. A multidisciplinary and if needed multimodal approach including surgery, radio(chemo)therapy, and immuno- or chemotherapy is therefore the treatment of choice, with strategies changing and evolving constantly. In this special edition, latest advances in therapy, the quality of life and treatment-related side effects are highlighted.

In the clinical practice, the presentation with advanced clinical stages at the time of diagnosis is a defining feature for many head and neck cancers. Early diagnosis proved to be one of the most important prognostic factors, with late diagnosis leading to significantly impaired survival rates. The first section of this special edition therefore involves the advances in head and neck cancer diagnostics, including strategies for earlier diagnosis, but also prevention and prediction of patients most at risk. The articles range from nomograms predicting outcomes and important prognostic factors in laryngeal squamous cell carcinoma to saliva-based liquid biopsies, detecting tumor-derived components in a non-invasive way. In another attempt to improve the diagnostic options for head and neck cancer, diffusion-weighted MRI imaging is introduced to differentiate benign and malignant tumors of the parotid gland.

The second subject of this issue are advances in the treatment of head and neck cancer, with a special focus on the balance between the safe elimination of cancer, while also preserving functionality and the quality of life of patients. A selection of articles highlights the latest strategies in surgery. Based on the sonographic depth of tumor invasion, the stratified surgical dissection of the neck lymph nodes in tongue squamous cell carcinoma without apparent clinical lymph node metastasis is investigated. Another study sheds light on risk factors for postoperative complications in head and neck cancer patients after reconstruction with a free flap. Patients with certain preoperative conditions need to be screened adequately, to either monitor potential adverse effects more closely or stratify patients into different risk groups to design a more personalized treatment.

The third and last subject of this special edition are advances in chemo- and radiotherapy in HNSCC. There is a special focus on nasopharyngeal carcinoma, one of the most challenging entities of cancer of the head and neck, at the crossroads of surgery, radio- and chemotherapy. Intensity-modulated radiotherapy, prophylactic neck irradiation, and induction chemotherapy followed by concurrent chemotherapy are discussed. Furthermore, transcatheter arterial chemoembolization for oral cancer with the comorbidity of oral hemorrhage is introduced. Many therapies result in acceptable outcome, but patients are paying with side effects. One of the treatment modalities discussed in this special edition is cisplatin in advanced nasopharyngeal carcinoma, a highly effective chemotherapeutic agent, but at the cost of severe drug-induced adverse effects. The use of a lower dose of cisplatin, as demonstrated in a phase 2 trial in nasopharyngeal carcinoma, leads to similar outcomes, with a significantly lower number of side effects. In addition, the safety of intensity-modulated radiotherapy is demonstrated, while cerebrovascular disease after radiotherapy is another example of a potential side effect. Therefore, the patients need to be informed during the process of shared decision making on the indicated therapy. All these interacting factors in treating patients for cancer should be considered when selecting a treatment modality in clinical practice.

In summary, the articles in this special edition provide a comprehensive overview on the challenges in the daily treatment of patients with head and neck cancer. Surgery, radiotherapy, immunotherapy, and chemotherapy go hand in hand in the current oncological therapy. While radical therapeutic options were the treatment of choice in the past decades, the treatment strategies highlighted in this special edition display ways to preserve the patient's quality of life and ensure a sufficient elimination of head and neck cancer.

Author contributions

All authors listed have made a substantial, direct, and intellectual contribution to the work and approved it for publication.

Conflict of interest

MW has received honoraria from Merck Sharp Dome.

The remaining authors declare that the research was conducted in the absence of any commercial or financial relationships that could be construed as a potential conflict of interest.

Publisher's note

frontiers in Oncology

ORIGINAL RESEARCH
published: 20 September 2021
doi: 10.3389/fonc.2021.727991

Different Primary Sites of Hypopharyngeal Cancer Have Different Lymph Node Metastasis Patterns: A Retrospective Analysis From Multi-Center Data

Xiwei Zhang[1†], Ye Zhang[2†], Xiaoduo Yu[3†], Ying Sun[4], Susheng Miao[5], Shaoyan Liu[1], Zhengjiang Li[1], Junlin Yi[2] and Changming An[1*]*

[1] Department of Head and Neck Surgery, National Cancer Center/National Clinical Research Center for Cancer/Cancer Hospital, Chinese Academy of Medical Sciences and Peking Union Medical College, Beijing, China, [2] Departments of Radiation Oncology, National Cancer Center/National Clinical Research Center for Cancer/Cancer Hospital, Chinese Academy of Medical Sciences and Peking Union Medical College, Beijing, China, [3] Departments of Radiation, National Cancer Center/National Clinical Research Center for Cancer/Cancer Hospital, Chinese Academy of Medical Sciences and Peking Union Medical College, Beijing, China, [4] State Key Laboratory of Oncology in South China, Collaborative Innovation Center of Cancer Medicine, Guangdong Key Laboratory of Nasopharyngeal Carcinoma Diagnosis and Therapy, Sun Yat-sen University Cancer Center, Guangzhou, China, [5] Department of Radiation Oncology, Harbin Medical University Cancer Hospital, Harbin, China

OPEN ACCESS

Edited by:
Markus Wirth,
Klinikum rechts der Isar, Germany

Reviewed by:
Franz Rödel,
University Hospital Frankfurt, Germany
Hui Gan,
Olivia Newton-John Cancer Research Institute, Australia

***Correspondence:**
Junlin Yi
yijunlin1969@163.com
Changming An
anchangming@cicams.ac.cn

[†]These authors have contributed equally to this work

Specialty section:
This article was submitted to Head and Neck Cancer, a section of the journal Frontiers in Oncology

Received: *20 June 2021*
Accepted: *01 September 2021*
Published: *20 September 2021*

Citation:
Zhang X, Zhang Y, Yu X, Sun Y, Miao S, Liu S, Li Z, Yi J and An C (2021) Different Primary Sites of Hypopharyngeal Cancer Have Different Lymph Node Metastasis Patterns: A Retrospective Analysis From Multi-Center Data. Front. Oncol. 11:727991. doi: 10.3389/fonc.2021.727991

Background: Most hypopharyngeal cancers (HPCs) develop lymph node metastasis (LNM) at initial diagnosis. Understanding the pattern of LNM in HPC could help both surgeons and radiologists make decisions in the management of cervical lymph nodes.

Methods: A total of 244 newly diagnosed HPC patients between January 2010 and December 2018 were recruited from three specialized cancer hospitals in mainland China. All patients received pre-treatment magnetic resonance imaging (MRI), and definitive radiotherapy with or without concurrent chemotherapy. We reassessed the features of the primary tumor (tumor size, primary location, and extent of invasion) and the involvement of lymph nodes at each level. According to the incidence of LNM, these levels were sequenced and sorted into drainage stations. Univariate and multivariate analyses were used to determine the risk factors for bilateral and regional lymph node metastasis.

Results: The cohort consisted of 195 piriform sinus cancers (PSC), 47 posterior wall cancers (PWC), and 2 post-cricoid cancers (PCC). A total of 176 patients (72.1%) presented with MRI-detectable LNMs. The overall LNM rates for level II-VI and retropharyngeal lymph nodes (RPLNs) were 59.0%, 52.9%, 14.3%, 1.6%, 2.9%, and 16.4%, respectively. Based on the prevalence of LNM at each level, we hypothesize that the lymphatic drainage of PSC was carried out in sequence along three stations: Level II and III (61.0% and 55.4%), Level IV and RPLN (15.9% and 11.3%), and Level V and VI (1.5% and 3.1%). For PWCs, lymphatic drainage is carried out at two stations: Level II, III, and RPLN (48.9%, 40.4%, and 34.0%) and Level IV-VI (6.4%, 0%, and 2.1%). According to univariate and multivariate analyses, posterior wall invasion was significantly correlated

with bilateral LNM (P = 0.030, HR = 2.853 95%CI, 1.110-7.338) and RPLN metastasis (P = 0.017, HR = 2.880 95%CI, 1.209-6.862). However, pyriform sinus invasion was less likely to present with bilateral LNM (P = 0.027, HR = 0.311, 95%CI, 0.111-0.875) and RPLN metastasis (P = 0.028, HR = 0.346, 95%CI, 0.134-0.891).

Conclusions and Relevance: The primary tumor site and extent of invasion are related to the pattern of lymph node metastasis. That is, the metastasis would drainage station by station along different directions.

Keywords: hypopharyngeal cancer (HPC), lymph node metastasis (LNM), magnetic resonance imaging (MRI), retropharyngeal lymph nodes (RPLN), pattern, bilateral

INTRODUCTION

The hypopharynx, which connects the oropharynx, larynx, and cervical esophagus, is the junction of the upper respiratory and digestive tracks. Hypopharyngeal cancer (HPC) is dominated by squamous cell cancer and accounts for only 6% of all head and neck cancers (1). The prognosis of HPC is relatively poor compared with that of other head and neck cancers, with a 5-year overall survival of only 30%–35% (2, 3).

Due to the lack of obvious symptoms, most HPC patients have developed a progressive disease at their initial diagnosis, with lymph node metastasis (LNM) incidence as high as 60% (4). Therefore, management of lymph nodes must be considered in the treatment planning of most patients with HPC. Since lymphatic drainage of the hypopharynx is abundant, the primary tumors may spread along different paths to the lateral neck or posteriorly to the posterior wall. Understanding the pattern of lymph node metastasis in HPC and the relationship between the primary tumor and LNM could help both surgeons and radiologists make decisions in cervical lymph node management.

Magnetic resonance imaging (MRI), with a higher ability for detailed presentation of soft tissue, is superior to computed tomography (CT) in the evaluation of cervical lymph node involvement. Here, we collected pre-treatment MRIs of HPC from three cancer centers in mainland China for review and aimed to determine the pattern of nodal spread and the correlation between the features of the primary tumor and LNM.

MATERIALS AND METHODS

Patients with pathologically proven hypopharyngeal squamous cell cancer from three specialized cancer hospitals in mainland China (Cancer Hospital, Chinese Academy of Medical Sciences; Sun Yat-sen University Cancer Center; Harbin Medical University Cancer Hospital) between January 2010 and December 2018 were recruited. All patients received definitive radiotherapy (GTV ≥ 66Gy) with or without concurrent chemotherapy, and cervical MRI was performed before treatment. Unavailable pre-treatment MRI, distant metastasis before initial treatment, and second primary cancer were the exclusion criteria. This study was approved by the institutional ethics committee of Cancer Hospital, Chinese Academy of Medical Sciences (NCC2018J-004). Informed consent was obtained before surgery.

All pre-treatment MRIs were reviewed by two dedicated head and neck radiologists. The features of the primary tumor and the presence of lymph nodes at each level of the neck were reassessed. Tumor information included tumor size, tumor location, and extent of invasion. Lymph nodes were assigned according to the RGOT guidelines. Seven groups of lymph nodes, levels I-VI and retropharyngeal lymph nodes (RPLN), were assessed. The following criteria were considered as a radiographically positive LN: in the axial plane, the largest short diameter of the retropharyngeal node ≥ 5 mm, ≥ 11 mm at level II, ≥ 10 mm at other level, and any visible median RPLN; three lymph node grouping (each of which should have a minimal axial dimension of 8–10 mm); lymph node with circular enhancement or central necrosis; and lymph node with extracapsular spread (5). If MRI cannot determine the metastasis, we will evaluate it in combination with pre-treatment CT scans and ultrasound.

The prevalence of each cervical level was calculated using descriptive statistics with SPSS 25.0 (IBM Corp. Released 2017. IBM SPSS Statistics for Windows, Version 25.0. Armonk, NY: IBM Corp.). Predictors (tumor size, lesion location, and the extent of invasion) of the presence of bilateral LNM were examined using univariate and multivariate logistic regression. A two-sided p-value of less than 0.05 was considered statistically significant.

RESULTS

Baseline Characteristics of Patients

Of the 244 patients, 262 (96.0%) were male, only 11 (4.0%) were female. The median age of the cohort was 56 years (range: 36–85 years). The primary anatomical site of the tumor was located at pyriform sinus for 195 patients (79.9%), posterior pharyngeal wall for 47 patients (19.3%), and postcricoid area for only 2 patients (0.8%). According to the AJCC 8th staging-system, 122 patients (50.0%) were restaged as T1-2, 122 patients (50.0%) were T3-4. N0-1 were observed in 116 patients (47.5%). N2-3 were observed in 128 patients (52.5%). Among them, 37 patients (15.2%) were of stage I-II and 207 patients (84.8%) were of stage III-IV. In our group, all patients received definitive radiotherapy (GTV ≥ 66Gy). Among them, 92 (37.7%) and 161 patients (66.0%) received induced or concurrent chemotherapy

respectably. (**Table 1**) The 3-year and 5-year overall survival (OS) of our group were 49.9% and 36.4%.

LNM Incidence

In our cohort, a total of 176 patients (72.1%) presented with MRI-detectable LNM. No LNM was found in level I in any of the patients. The most common LNM regions are Levels II and III, with incidences of 59.0% and 52.9%, respectively. Level IV and RPLN followed with incidences of 14.3% and 16.4%, respectively. LNMs in Levels V and VI were rare, with an incidence of only 1.6% and 2.9%, respectively. In our cohort, 40 patients (16.4%) presented with bilateral LNMs, all of which were restricted to levels II, III, and RPLNs (**Table 2**).

Patterns of LNM

Of the 195 PSC patients, 143 (73.3%) were diagnosed with cervical LNMs. More than half of the patients had LNMs in levels II and III, with metastasis rates of 61.0% and 55.4%, respectively. For Level IV and RPLNs, the LNM rates were 15.9% and 11.3%, respectively. However, LNMs were rare in Levels V and VI, with incidences of only 1.5% and 3.1%, respectively (**Figure 1A** shows a specific distribution). Based on the incidence of LNM at each level, we concluded that lymphatic drainage of PSC was carried out sequentially along three stations (See **Figure 2A**). These are Levels II and III for the 1st station, Level IV and RPLN for the 2nd station, and Levels V and VI for the 3rd station. Based on our hypothesis, lymph node skip metastasis was rare in the cohort, as it was found in only four patients (2.8%).

Of the 47 PWCs, LNMs were detected in 31 patients (66.0%). Besides Levels II (48.9%) and III (40.4%), RPLNs (38.3%) also presented a high incidence of LNM. However, LNMs in level IV were less common than those in PSC. The LNM rates in Levels IV-VI were only 6.4%, 0%, and 2.1%, respectively. (**Figure 1B** shows specific distributions). Therefore, we hypothesize that the lymphatic drainage of PWC is carried out along two stations: Levels II, III, and RPLN as the 1st station, and Levels IV-VI as the 2nd station (**Figure 2B**). No lymph node skip metastasizes were found based on this hypothesis. **Figure 3** shows the T1 with contrast images of a patient with PWC (**Figure 3A**). The patient has LNMs in left RPLN (**Figure 3B**) and right Level II (**Figure 3C**).

Only two PCCs were included in our cohort. A patient was diagnosed with LNMs in ipsilateral II-IV. The other patient had LNMs in bilateral levels II and III.

TABLE 1 | The baseline characteristics of the patients.

Characteristic	Patients (%)
Gender	
Male	237 (97.1)
Female	7 (2.9)
Age (y.)	
<50	63 (25.8)
≥50	181 (74.2)
Tumor location	
Pyriform sinus	195 (79.9)
Posterior pharyngeal wall	47 (19.3)
Postcricoid	2 (0.8)
T-stage	
T1-2	122 (50.0)
T3-4	122 (50.0)
N-stage	
N0-1	116 (47.5)
N2-3	128 (52.5)
TNM stage	
I-II	37 (15.2)
III-IV	207 (84.8)
Induced chemotherapy	
Yes	92 (37.7)
No	152 (62.3)
Concurrent chemoradiotherapy	
Yes	161 (66.0)
No	83 (34.0)

TABLE 2 | The incidence of lymph nodes metastasis at each level among 244 patients.

Level	Unilateral (%)	Bilateral (%)	Total (%)
I	0	0	0
II	120 (49.2)	24 (9.8)	144 (59.0)
III	121 (49.6)	8 (3.3)	129 (52.9)
IV	35 (14.3)	0	35 (14.3)
V	4 (1.6)	0	4 (1.6)
VI	7 (2.9)	0	7 (2.9)
RPLN*	25 (10.2)	15 (6.1)	40 (16.4)
Total (%)	136 (55.7)	40 (16.4)	176 (72.1)

*Retropharyngeal Lymph node.

Univariate and Multivariate Analyses

To determine the risk factors for bilateral and regional LNM, univariate and multivariate analyses were used, the results of which are displayed in **Table 3**. According to univariate analysis, invasion of the posterior wall was a risk factor for bilateral LNM. Patients with pyriform sinus invasion were less likely to develop bilateral LN. Further multivariate analysis showed that posterior wall and pyriform sinus invasion were still statistically significant, with P = 0.002 (HR = 3.524 95%CI, 1.559-7.964) and P = 0.027 (HR = 0.311, 95%CI, 0.111-0.875), respectively.

Univariate analysis revealed that the presence of retropharyngeal lymph nodes was associated with larger tumor size (> 4 cm) and posterior wall invasion. However, HPCs with pyriform sinus invasion were less likely to have PRLN metastasis. However, only posterior wall invasion (P = 0.017, HR = 2.880, 95%CI, 1.209-6.862) and pyriform sinus invasion (P = 0.028, HR = 0.346, 95%CI, 0.134-0.891) were associated with PRLN metastasis in multivariate analysis.

DISCUSSION

Hypopharyngeal cancer is a relatively rare malignancy with poor prognosis. Due to the lack of obvious symptoms, most patients with HPC have lymph node metastasis at the initial diagnosis. Therefore, the management of lymph nodes must be considered in the treatment plan of most patients with HPC. Understanding the lymph node metastasis pattern of HPC and the relationship between primary tumor and LNM can help clinicians make decisions in the treatment of cervical lymph nodes.

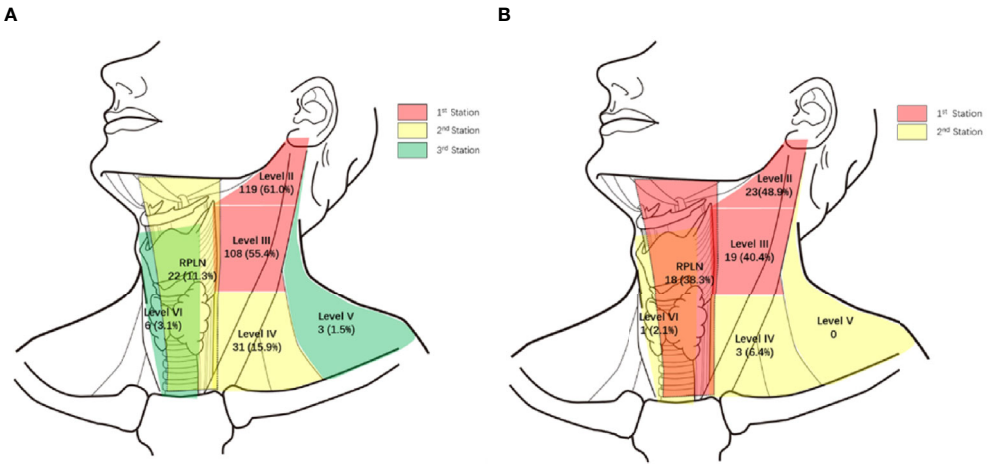

FIGURE 1 | Specific distribution of LNMs. **(A)** Specific distribution of LNM in 195 piriform sinus cancers. **(B)** Specific distribution of LNMs in 47 posterior wall cancers. (%) Percent of LNMs in all 195 piriform sinus cancers or 47 posterior wall cancers.

Various imaging technologies, such as CT, MRI, and ^{18}F-FDG, have been widely used in the evaluation of head neck cancer (6, 7). MRI has a higher ability in the presentation of soft tissue than CT or PET, especially in the evaluation of primary tumors, since the tumor may extend to the mucous membrane alone. Moreover, MRI has been shown to be superior to CT imaging for the detection of metastatic RPLNs (8). Therefore, we chose pre-treatment MRI as mandatory in identifying both the primary tumor and LNM in HPC patients in our cohort. Hypopharyngeal cancer is a relatively rare disease among head and neck tumors. Therefore, it is difficult to obtain large-sample-size image data, especially MRIs, in a single center. Here, we combined three specialized cancer hospitals and collected the pre-treatment MRIs of 244 patients.

Because of the abundant lymphatic drainage in the hypopharynx, most patients will have developed lymph node metastasis at the initial treatment. The reported LNM rate at diagnosis is 65% (5, 9, 10). Among them, the most common metastasis was located at levels II and III, followed by level IV. The LNM rate of our group is similar to that of previous reports. However, in our cohort, the incidence of RPLN metastasis was as high as 16.4%, which is equivalent to that of level IV (14.3%). This may be because MRI is superior in detecting RPLNs than other imaging methods such as CT scans and ultrasound imaging (8). Since the anatomic cross-lymphatic drainage of the hypopharyngeal region links both sides, contralateral LNM should not be neglected (11). In our group, the rate of bilateral

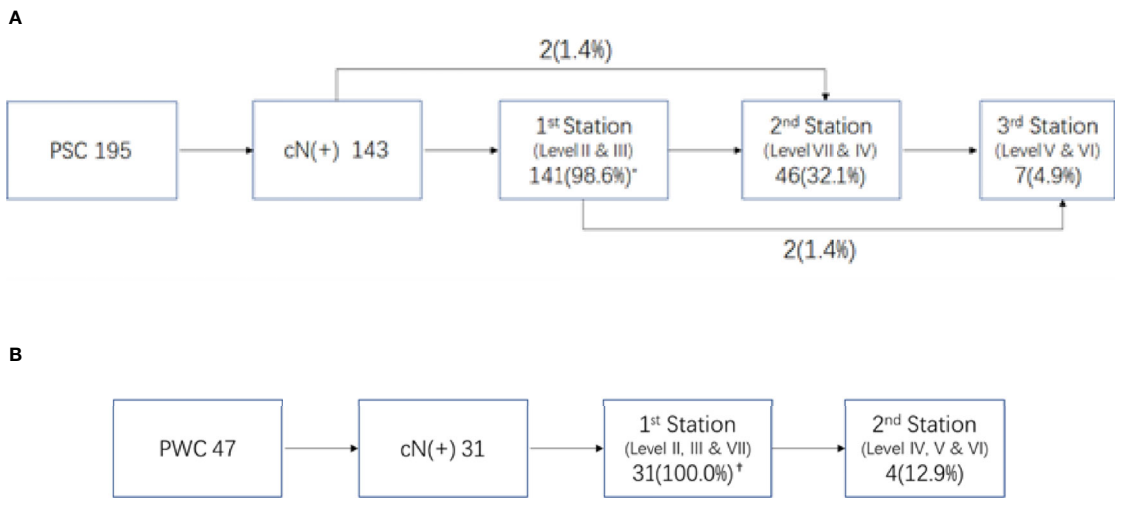

FIGURE 2 | Lymphnode metastasis pattern in different primary site of hypopharyngeal cancer. **(A)** Pattern of LNM in piriform sinus cancer (PSC) * Percent of LNMs in 143 N(+) patients. **(B)** Pattern of LNM in posterior wall (PPC). †Percent of LNMs in 31 N(+) patients.

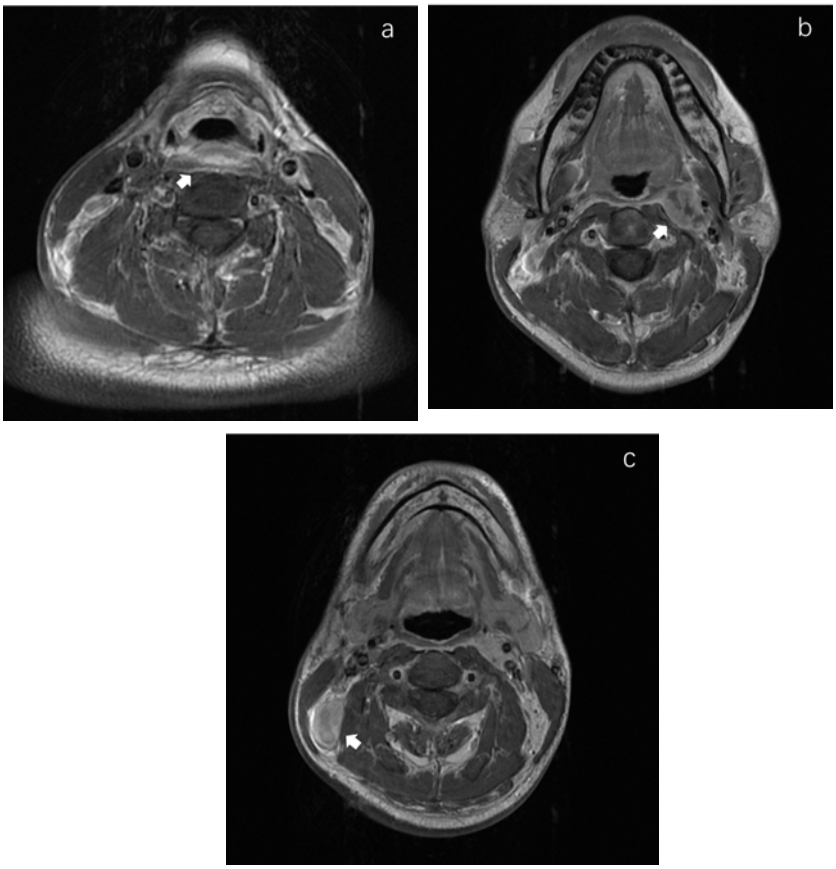

FIGURE 3 | MRI images in T1 with contrast of a posterior wall cancer patient. **(A)** The primary focus of posterior wall cancer. **(B)** The left retropharyngeal lymphnode metastasis. **(C)** The metastatic lymphnode in right Level II.

LNM was 16.8%, and all contralateral LNMs were limited to levels II, III, and RPLNs.

Because of the prevalence of LNM in levels II and III, they are generally considered to be the first station for all hypopharyngeal cancers (6, 12), including the preliminary report from our center (13). However, through further we study found that the drainage route varied with different primary sites. In pyriform sinus cancer, almost all N+ patients presented with level II and/or III LNMs. Therefore, we assumed that they were the first drainage stations for PSC. Level IV and RPLNs, with LNM rates following closely behind, were considered as the second station. The third station consisted of Level V and VI because of their rarity. The lymph node drainage diagram (**Figure 2A**) supports our hypothesis. Only 4/143 patients exhibited skipping metastases.

In contrast with PSC, the metastasis rate of RPLN in posterior wall cancer was as high as 38.3%, which was similar to that in levels II and III. Therefore, we assumed that the RPLN along with levels II and III was the first station of LNM for PWCs. In the PSC group, only three

TABLE 3 | The risk factors for bilateral LNM and PRLN metastasis.

Factors		Univariate analysis		Multivariate analysis	
		HR (95%CI)	*p*	HR (95%CI)	*p*
Bilateral LNM	Pyriform sinus invasion	0.165 (0.064-0.430)	0.000	0.311 (0.111-0.875)	0.027
	Posterior wall invasion	4.812 (2.259-10.252)	0.000	3.524 (1.559-7.964)	0.002
PRLN metastasis	Tumor Size				
	≤2cm		0.023		
	2-4cm	6.206 (0.809-47.618)	0.079		
	>4cm	12.364 (1.561-97.907)	0.017		
	Pyriform sinus invasion	0.213 (0.095-0.481)	0.000	0.346 (0.134-0.891)	0.028
	Posterior wall invasion	4.543 (2.201-9.378)	0.000	2.471 (1.047-5.832)	0.039

patients presented with LNM in Level IV. Therefore, together with Level V and VI, Level IV was also considered to belong to station 2. This hypothesis could also be proved by the simulation diagram (**Figure 2B**), as no skipping metastasis was found.

Another reason why RPLNs were not recognized as the first drainage station before was based on the reports that RPLN metastasis does not appear in N0 patients (6, 14). In other words, pure RPLN metastasis is rare. However, there have been other reports where RPLN metastasis may be present among cN0 HPC patients (15, 16). In our cohort, RPLN metastasis was detected in four patients with negative lateral cervical findings. These results indicate that it is reasonable that the RPLNs are presumed to belong to the 1st station LNMs for PWCs.

According to our finding we suggest that, for cN0 patients with PSC, the elective neck dissection should include level II and III, while for PWC level II, III and RPLNs. When metastasis is considered in the first station LNs, the second station lymph node should be further treated.

The other purpose of this paper is to explore the direction of metastasis of HPC. So we focus on the bilateral and retropharyngeal metastasis, which indicate transfer contralaterally and backward respectively. As a midline organ, the hypopharynx is also drained along the anatomic cross route to the contralateral lymph nodes. Olzowy (17) et al. reported that the incidence of contralateral metastasis was above 20% for HPCs affecting the midline and those involving the medial wall of the PSCs. The overall bilateral LNM rate in our cohort was 16.4%, which is similar to that found in previous reports. Through logistic analysis, we found that HPC with pyriform sinus invasion is more likely to metastasize to the ipsilateral lymph nodes, since pyriform sinus invasion is a protective factor for bilateral LNM. Posterior wall invasion in both univariate and multivariate analyses was proven to be correlated with bilateral LNM, indicating that posterior wall invasion was prone to drainage to the bilateral neck. This phenomenon is easy to explain—posterior wall cancer is located at the midline areas and is prone to drain bilaterally to the neck. However, the pyriform sinus is a lateral structure, and so lymphatic drainage mainly flows in the ipsilateral direction.

The retropharyngeal lymph node has been widely studied in nasopharyngeal cancer and was regarded as the first station for nasopharyngeal lymphatic drainage (14, 18). In recent years, its significance in HPC has received increasing attention (6). Our preliminary study (13, 19) reported RPLN metastasis was related to PWC, posterior wall invasion and cervical LN status. And we found that RPLN metastasis is a poor prognosticator for survival. And in this further study, on multivariate analysis, we found not only posterior wall invasion as a risk factor, but also pyriform sinus invasion was a protective factor for LNM in RPLNs. We could conclude this trend: posterior wall invasion tends to drain back directly to the posterior pharyngeal region, while HPCs with piriform sinus invasion are less likely to drain backward.

Therefore, for radiologists, if pure piriform sinus is invaded, it can be considered that the retropharyngeal area and contralateral neck could not be included in clinical treatment volume (CTV). While, for patients with tumor invading the posterior wall, not only the retropharyngeal area but also both necks should be included in CTV.

Our study was based only on pre-treatment MRI images; thus, occult metastasis could not be evaluated. In fact, due to the wide use of laryngeal conservative strategies, hypopharyngeal cancer mainly adopts radiotherapy-based multidisciplinary treatment. Therefore, it is difficult to admit a large sample of HPCs from the head and neck department. In this study, we obtained a large sample of MRI data from three major cancer hospitals. We believe that this was sufficient for evaluating lymph node metastasis patterns. However, only two cases of PCC were included in the cohort; therefore, more data are needed to understand the metastasis pattern of PCC.

In conclusion, we analyzed 244 pre-treatment MRIs of HPC in three specialized cancer hospitals in mainland China and found that the primary tumor subsite and the extent of invasion were related to the pattern of LNM. PSC tends to metastasize along three stations, while PWC tends to metastasize along two stations. HPCs with piriform invasion were less likely to metastasize to contralateral and retropharyngeal LNs, while posterior wall invasion was a risk factor for bilateral and retropharyngeal LNM.

DATA AVAILABILITY STATEMENT

The raw data supporting the conclusions of this article will be made available by the authors, without undue reservation.

ETHICS STATEMENT

Written informed consent was obtained from the individual(s) for the publication of any potentially identifiable images or data included in this article.

AUTHOR CONTRIBUTIONS

XZ, YZ, and XY contributed equally to this work. XZ statistical analysis and wrote paper. YZ and XY reevaluated the MRIs. CA, YS, and SM collected the patient data. SL, ZL, and JY: supervision. All authors contributed to the article and approved the submitted version.

FUNDING

Supported by the Non-profit Central Research Institute Fund of Chinese Academy of Medical Science (2019-RC-HL-004) and Beijing Hope Run Special Fund of Cancer Foundation of China (No. LC2018L06).

ACKNOWLEDGMENTS

The authors would like to acknowledge the colleagues of three cancer centers for their support with the data.

REFERENCES

1. Carvalho AL, Nishimoto IN, Califano JA, Kowalski LP. Trends in Incidence and Prognosis for Head and Neck Cancer in the United States: A Site-Specific Analysis of the SEER Database. *Int J Cancer* (2005) 114(5):806–16. doi: 10.1002/ijc.20740
2. Newman JR, Connolly TM, Illing EA, Kilgore ML, Locher JL, Carroll WR. Survival Trends in Hypopharyngeal Cancer: A Population-Based Review. *Laryngoscope* (2015) 125(3):624–9. doi: 10.1002/lary.24915
3. Hall SF, Groome PA, Irish J, O'Sullivan B. The Natural History of Patients With Squamous Cell Carcinoma of the Hypopharynx. *Laryngoscope* (2008) 118(8):1362–71. doi: 10.1097/MLG.0b013e318173dc4a
4. Kotwall C, Sako K, Razack MS, Rao U, Bakamjian V, Shedd DP. Metastatic Patterns in Squamous Cell Cancer of the Head and Neck. *Am J Surg* (1987) 154(4):439–42. doi: 10.1016/0002-9610(89)90020-2
5. Biau J, Lapeyre M, Troussier I, Budach W, Giralt J, Grau C, et al. Selection of Lymph Node Target Volumes for Definitive Head and Neck Radiation Therapy: A 2019 Update. *Radiother Oncol* (2019) 134:1–9. doi: 10.1016/j.radonc.2019.01.018
6. Wu Z, Deng XY, Zeng RF, Su Y, Gu MF, Zhang Y, et al. Analysis of Risk Factors for Retropharyngeal Lymph Node Metastasis in Carcinoma of the Hypopharynx. *Head Neck* (2013) 35(9):1274–7. doi: 10.1002/hed.23112
7. Wu IS, Hung GU, Chang BL, Liu CK, Chang TH, Lee HS, et al. Is Unenhanced 18F-FDG-PET/CT Better Than Enhanced CT in the Detection of Retropharyngeal Lymph Node Metastasis in Nasopharyngeal Carcinoma? *Ear Nose Throat J* (2016) 95(4-5):178–84. doi: 10.1177/0145561316095004-506
8. Kato H, Kanematsu M, Watanabe H, Mizuta K, Aoki M. Metastatic Retropharyngeal Lymph Nodes: Comparison of CT and MR Imaging for Diagnostic Accuracy. *Eur J Radiol* (2014) 83(7):1157–62. doi: 10.1016/j.ejrad.2014.02.027
9. Garneau JC, Bakst RL, Miles BA. Hypopharyngeal Cancer: A State of the Art Review. *Oral Oncol* (2018) 86:244–50. doi: 10.1016/j.oraloncology.2018.09.025
10. Riviere D, Mancini J, Santini L, Giovanni A, Dessi P, Fakhry N. Lymph-Node Metastasis Following Total Laryngectomy and Total Pharyngolaryngectomy for Laryngeal and Hypopharyngeal Squamous Cell Carcinoma: Frequency, Distribution and Risk Factors. *Eur Ann Otorhinolaryngol Head Neck Dis* (2018) 135(3):163–6. doi: 10.1016/j.anorl.2017.11.008
11. Mukherji SK, Armao D, Joshi VM. Cervical Nodal Metastases in Squamous Cell Carcinoma of the Head and Neck: What to Expect. *Head Neck* (2001) 23(11):995–1005. doi: 10.1002/hed.1144
12. Shah JP. Patterns of Cervical Lymph Node Metastasis From Squamous Carcinomas of the Upper Aerodigestive Tract. *Am J Surg* (1990) 160(4): 405–9. doi: 10.1016/S0002-9610(05)80554-9
13. Wang H, Wu R, Huang X, Qu Y, Wang K, Liu Q, et al. The Pattern of Cervical Lymph Node Metastasis and Risk Factors of Retropharyngeal Lymph Node Metastasis Based on Magnetic Resonance Imaging in Different Sites of Hypopharyngeal Carcinoma. *Cancer Manag Res* (2020) 12:8581–7. doi: 10.2147/CMAR.S245988
14. McLaughlin MP, Mendenhall WM, Mancuso AA, Parsons JT, McCarty PJ, Cassisi NJ, et al. Retropharyngeal Adenopathy as a Predictor of Outcome in Squamous Cell Carcinoma of the Head and Neck. *Head Neck* (1995) 17 (3):190–8. doi: 10.1002/hed.2880170304
15. Amatsu M, Mohri M, Kinishi M. Significance of Retropharyngeal Node Dissection at Radical Surgery for Carcinoma of the Hypopharynx and Cervical Esophagus. *Laryngoscope* (2001) 111(6):1099–103. doi: 10.1097/00005537-200106000-00031
16. Kamiyama R, Saikawa M, Kishimoto S. Significance of Retropharyngeal Lymph Node Dissection in Hypopharyngeal Cancer. *Jpn J Clin Oncol* (2009) 39(10):632–7. doi: 10.1093/jjco/hyp080
17. Olzowy B, Hillebrand M, Harreus U. Frequency of Bilateral Cervical Metastases in Hypopharyngeal Squamous Cell Carcinoma: A Retrospective Analysis of 203 Cases After Bilateral Neck Dissection. *Eur Arch Otorhinolaryngol* (2017) 274(11):3965–70. doi: 10.1007/s00405-017-4724-3
18. Huang L, Zhang Y, Liu Y, Li H, Wang S, Liang S, et al. Prognostic Value of Retropharyngeal Lymph Node Metastasis Laterality in Nasopharyngeal Carcinoma and a Proposed Modification to the UICC/AJCC N Staging System. *Radiother Oncol* (2019) 140:90–7. doi: 10.1016/j.radonc.2019.04.024
19. An C, Sun Y, Miao S, Yu X, Zhang Y, Zhang X, et al. Retropharyngeal Lymph Node Metastasis Diagnosed by Magnetic Resonance Imaging in Hypopharyngeal Carcinoma: A Retrospective Analysis From Chinese Multi-Center Data. *Front Oncol* (2021) 11:649540. doi: 10.3389/fonc.2021.649540

Conflict of Interest: The authors declare that the research was conducted in the absence of any commercial or financial relationships that could be construed as a potential conflict of interest.

frontiers in Oncology

ORIGINAL RESEARCH
published: 10 November 2021
doi: 10.3389/fonc.2021.737080

Standardized Diagnostic Workup and Patient-Centered Decision Making for Surgery and Neck Dissection Followed by Risk-Factor Adapted Adjuvant Therapy Improve Loco-Regional Control in Local Advanced Oral Squamous Cell Carcinoma

Gunnar Wichmann[1†], Mykola Pavlychenko[1†], Maria Willner[1], Dirk Halama[2], Thomas Kuhnt[3], Regine Kluge[4], Tanja Gradistanac[5], Sandra Fest[1], Theresa Wald[1], Bernd Lethaus[2], Andreas Dietz[1], Susanne Wiegand[1‡] and Veit Zebralla[1‡]*

[1] Department of Otorhinolaryngology, Head and Neck Surgery, University Hospital Leipzig, Leipzig, Germany, [2] Department of Maxillofacial Surgery, University Hospital Leipzig, Leipzig, Germany, [3] Department of Radiation Oncology, University Hospital Leipzig, Leipzig, Germany, [4] Department of Nuclear Medicine, University Hospital Leipzig, Leipzig, Germany, [5] Department of Pathology, University Hospital Leipzig, Leipzig, Germany

Background: Standardized staging procedures and presentation of oral squamous cell carcinoma (OSCC) patients in multidisciplinary tumor boards (MDTB) before treatment and utilization of elective neck dissection (ND) are expected to improve the outcome, especially in local advanced LAOSCC (UICC stages III–IVB). As standardized diagnostics but also increased heterogeneity in treatment applied so far have not been demonstrated to improve outcome in LAOSCC, a retrospective study was initiated.

Methods: As MDTB was introduced into clinical routine in 2007, 316 LAOSCC patients treated during 1991-2017 in our hospital were stratified into cohort 1 treated before (n=104) and cohort 2 since 2007 (n=212). Clinical characteristics, diagnostic procedures and treatment modality of patients were compared using Chi-square tests and outcome analyzed applying Kaplan-Meier plots and log-rank tests as well as Cox proportional hazard regression. Propensity scores (PS) were used to elucidate predictors for impaired distant metastasis-free survival (DMFS) in PS-matched patients.

Results: Most patient characteristics and treatment modalities applied showed insignificant alteration. Surgical treatment included significantly more often resection of the primary tumor plus neck dissection, tracheostomy and percutaneous endoscopic gastrostomy tube use. Cisplatin-based chemo-radiotherapy was the most frequent. Only insignificant improved disease- (DFS), progression- (PFS) and event-free (EFS) as well as tumor-specific (TSS) and overall survival (OS) were found after 2006 as local (LC) and loco-regional control (LRC) were significantly improved but DMFS significantly impaired.

OPEN ACCESS

Edited by:
Markus Wirth,
Klinikum Rechts der Isar, Germany

Reviewed by:
Johannes Döscher,
Ulm University Medical Center, Germany
Shankargouda Patil,
Jazan University, Saudi Arabia

***Correspondence:**
Gunnar Wichmann
Gunnar.Wichmann@medizin.uni-leipzig.de

[†]These authors have contributed equally to this work and share first authorship

[‡]These authors share senior authorship

Specialty section:
This article was submitted to Head and Neck Cancer, a section of the journal Frontiers in Oncology

Received: 06 July 2021
Accepted: 19 October 2021
Published: 10 November 2021

Citation:
Wichmann G, Pavlychenko M, Willner M, Halama D, Kuhnt T, Kluge R, Gradistanac T, Fest S, Wald T, Lethaus B, Dietz A, Wiegand S and Zebralla V (2021) Standardized Diagnostic Workup and Patient-Centered Decision Making for Surgery and Neck Dissection Followed by Risk-Factor Adapted Adjuvant Therapy Improve Loco-Regional Control in Local Advanced Oral Squamous Cell Carcinoma. Front. Oncol. 11:737080. doi: 10.3389/fonc.2021.737080

Cox regression applied to PS-matched patients elucidated N3, belonging to cohort 2 and cisplatin-based chemo-radiotherapy as independent predictors for shortened DMFS. The along chemo-radiotherapy increased dexamethasone use in cohort 2 correlates with increased DM.

Conclusions: Despite standardized diagnostic procedures, decision-making considering clear indications and improved therapy algorithms leading to improved LC and LRC, shortened DMFS hypothetically linked to increased dexamethasone use had a detrimental effect on TSS and OS.

Keywords: oral squamous cell carcinoma (OSCC), head and neck cancer, outcome research, elective neck dissection (ND), local control (LC), distant metastasis free survival (DMFS), overall survival (OS), multidisciplinary tumor board (MDTB)

INTRODUCTION

Surgery followed by postoperative radio- (Op+PORT) or platinum-based concomitant radio-chemotherapy (Op +PORCT) represent the recommended standard of care in local and/or loco-regional advanced oral squamous cell carcinoma (LAOSCC) in Germany. Definitive radiotherapy (RT) and concomitant radio-chemotherapy (CRT) are only recommended to LAOSCC patients diagnosed with very advanced disease without a chance to achieve by resection both aims, disease-free resection margins (R0) and good functional outcome. The general use of computed tomography (CT) imaging, in selected cases combined with positron-emission tomography (PET-CT) (1) together with standardized staging procedures (2) and presentation of LAOSCC patients in multidisciplinary tumor boards (MDTB) before treatment (3, 4) as well as utilization of elective neck dissection (ND) even in absence of suspect neck nodes (radiologic N0 category) are shown to improve outcome (5). The implementation of evidence-based decision-making for particular diagnostic and therapy according to institutional guidelines by adhering to NCCN (6) and ASCO guidelines (7) and the discussion of the individual case in the light of results obtained with the modern diagnostic and therapeutic procedures should improve survival rates especially in LAOSCC, as we recently demonstrated improved outcome since 2007 for neck squamous cell carcinoma of unknown primary (8). However, the now more patient-centered decision-making processes that consider individual preferences of the patient as well as more intense counselling of the patient that includes offering to get second opinion from another health care provider, sometimes associated with a delay in starting the treatment, and other factors may lead to increased heterogeneity in treatment applied and the individual clinical course of the patient and hence also influence the outcome. Our aim was to assess outcome differences before and after introduction of standardized diagnostic workup and patient-centered decision making for surgery and neck dissection followed by risk-factor adapted adjuvant therapy that was simultaneously implemented by establishing our MDTB.

MATERIALS AND METHODS

Patients and Pathologic Tumor Data

The tumor database of the ENT department of University Leipzig comprises data of 5,586 patients diagnosed with malignant disease. **Figure 1** (CONSORT diagram) summarizes eligibility criteria and the selection process. Eligibility criteria included: i) oral cancer as primary tumor site (ICD-10-C02, C03, C04, C06, C41); ii) patho-histological confirmed squamous cell carcinoma of advanced stage (UICC III-IVB according to TNM 2010; T1-T4N+ and T3-T4N0 (2)) excluding patients with distant metastasis (M1; UICC IVC); iii) absence of any prior or synchronous malignancy of other histology than SCC; iv) date of first diagnosis between 1991 and 2017; v) patho-histological report with information about the number of positive neck nodes (N+) and the N category. Patho-histological characteristics including ECE (+/-) and epidemiological risk factors (alcohol and tobacco smoking history) were recorded. The study was approved by the ethics committee of the University Leipzig the (votes 201-10-12072010 and 202-10-12072010), and conducted according to the guidelines of the Declaration of Helsinki. All patients provided written informed consent.

Clinical Work-Up for LAOSCC

Clinical work-up for LAOSCC-P until 2006 (cohort 1) varied and included *e.g.* clinical examination, ultrasound sonography and other variable procedures (**Table 1**) before treatment. Since 2007 (cohort 2) clinical work-up was standardized and included, as recommended (6), clinical examination, ultrasound sonography, contrast-enhanced CT or even PET-CT/PET-MRI followed by panendoscopy including excision biopsies from suspect tissue.

Decision-Making Process in the MDTB

Our weekly MDTB established in 2007 comprises all professions involved in the diagnostics and therapy of head and neck cancer patients. These are head and neck surgeons from the departments of ENT and maxillofacial surgery, radiologists and a board-certified nuclear radiologist, pathologist, medical oncologist, hematologic oncologist, radiation oncologist,

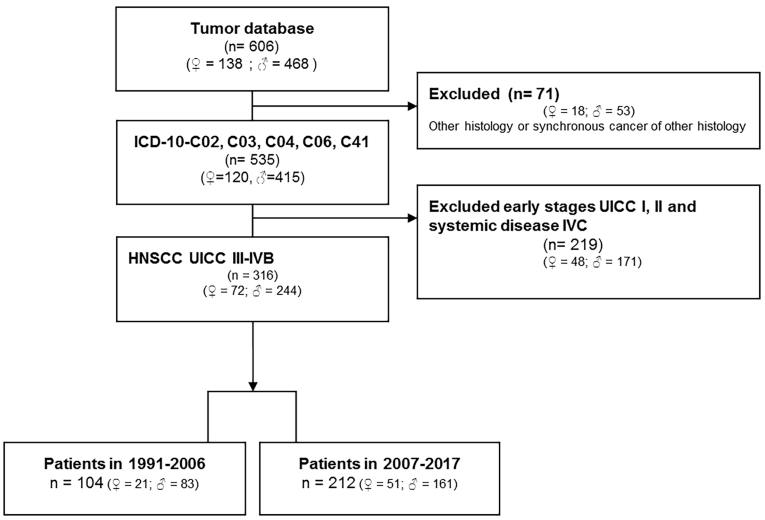

FIGURE 1 | CONSORT diagram showing the selection of patients under study.

prosthodontic dentist, and specialists from other departments, whenever required. The decision-making process in the MDTB for treatment of pathologic confirmed LAOSCC followed NCCN and ASCO guidelines (6, 7) or participation in open clinical trials including randomized controlled trials (RCT). Briefly, radiologist and nuclear medicine specialist presented all radiological imaging. Since 2007 (cohort 2), the pre-therapeutic MDTB discussed results of diagnostic procedures. Whenever patients where eligible for a RCT, offering participation was consented. According to guidelines (6), the MDTB mostly recommended ND as part of the surgical treatment.

After ND, the pathologist defined ECE being present whenever a capsule was missing (soft tissue deposit) or a disrupted lymph node capsule was visible macroscopically or microscopically (9). Every initially according to TNM 7th ed. 2010 staged patient was reclassified according to TNM 8th ed. 2017 (**Table 1**).

Considering the pathologic report as well as general health and comorbidity of the patient, the post-surgical MDTB consented a recommendation for treatment according to NCCN-Guidelines (6, 10). Smaller LAOSCC without local metastases (N0) and clear margins (R0 >5 mm) were treated by surgery alone (Op). However, most LAOSCC due to local metastases (N+) and/or extension of the primary required adjuvant treatment and received post-operative (adjuvant) radiotherapy (Op+PORT) or radio-chemotherapy (Op+PORCT). However, definitive primary radiotherapy (pRT) or concomitant chemo-radiotherapy (CRT) were recommended, whenever R0 resection and good functional outcome seemed to be impossible to achieve or were performed according to the patient's preference, whenever he denied extensive surgery and reconstruction.

Best supportive care +/- palliative treatment was offered to patients without curative treatment options or if refused by the patient.

Treatment Modalities

The treatment modalities applied to LAOSCC patients of cohort 1 and 2 are shown in **Table 2**. Also since 2004 intensity-modulated radiotherapy (IMRT) was available and used for PORT and PORCT, pRT and CRT. Irradiation plans for pRT and CRT without upfront surgery were scheduled to achieve 70 to 72 Gy totally in the gross tumor volume given in 35 fractions within 7 weeks. Cisplatin-based CRT used 3 cycles of single cisplatin infusions (100 mg/m^2 at days 1, 22, and 43). In cohort 2, the LAOSCC-P with ND and detection of only unilateral N+ (N2b) without risk factors present (up to 2 N+ <6 cm, no ECE, R0/no incision biopsy) received PORT of 60 Gy ipsilateral and 50 Gy contralateral, independent from ND also of the unaffected site or not. Irradiation after resection of a single node without risk factors (<6 cm, no ECE, R0/no incision biopsy) was unilateral 60 Gy (8, 9). Whenever risk factors for local recurrence (bilateral N+, *i.e.* N2c, or one node ≥6 cm, *i.e.* N3, or ECE+, R1) were detected, bilateral irradiation with 64 Gy was accompanied by concomitant cisplatin (8, 9). Cisplatin was given either in up to 3 cycles of single infusions (100 mg/m^2 at days 1, 22, and 43) or fractionated in five daily doses of 20 mg/m^2 (days 1-5, 22-26, and 43-47) (8, 9). To reduce acute toxicity and combat cisplatin-related side effects, the latter regimen was predominantly used since 2007 (**Table 2**). To prevent vomiting and unwanted side effects of CRT and PORCT, dexamethasone was given adjuvant before and during infusion.

Statistical Analysis and Propensity-Score Matching

Statistical analyses using SPSS version 24 (11) included *Pearson's Chi*-square (χ^2) tests to assess differences between categorical variables. Time-dependent covariates were measured from date of diagnosis to date of event. They included overall

TABLE 1 | Baseline characteristics of the study population.

Characteristics		Total		Cohort 1		Cohort 2		*p* value†
		(*N*=316)		(*N*=104)		(*N*=212)		(*N*=316)
		n (%)		*n* (%)		*n* (%)		*n* (%)
Age (years)	<=50	78	(24.7)	28	(26.9)	50	(23.6)	0.5919
	<=60	112	(35.4)	38	(36.5)	74	(34.9)	
	<=70	72	(22.8)	23	(22.1)	49	(23.1)	
	<=80	44	(13.9)	14	(13.5)	30	(14.2)	
	>80	10	(3.2)	1	(1.0)	9	(4.2)	
Sex	Female	72	(22.8)	21	(20.2)	51	(24.1)	0.4415
	Male	244	(77.2)	83	(79.8)	161	(75.9)	
Tumor localization, stage, T & N category								
	Tongue (C02)	152	(48.1)	59	(56.7)	93	(43.9)	0.0145
	Mandible (C03)	27	(8.5)	2	(1.9)	25	(11.8)	
	Floor of mouth (C04)	116	(36.7)	36	(34.6)	80	(37.7)	
	Other (C06, C41)	21	(6.6)	7	(6.7)	14	(6.6)	
ICD-10 C02 *vs*	C02	152	(48.1)	59	(56.7)	93	(43.9)	0.0315
other	Other	164	(51.9)	45	(43.3)	119	(56.1)	
TNM 7th ed. 2010‡,	Stage III	73	(23.1)	35	(33.7)	38	(17.9)	0.0009
UICC	Stage IVA	225	(71.2)	60	(57.7)	165	(77.8)	
	Stage IVB	18	(5.7)	9	(8.7)	9	(4.2)	
TNM 8th ed. 2017‡‡,	Stage III	69	(21.8)	35	(33.7)	34	(16.0)	0.0001
UICC	Stage IVA	186	(58.9)	59	(56.7)	127	(59.9)	
	Stage IVB	61	(19.3)	10	(9.6)	51	(24.1)	
T categories‡;								
TNM 7th ed. 2010	T1	35	(11.1)	10	(9.6)	25	(11.8)	1.9×10^{-5}
	T2	60	(19.0)	24	(23.1)	36	(17.0)	
	T3	65	(20.6)	33	(31.7)	32	(15.1)	
	T4a	148	(46.8)	31	(29.8)	117	(55.2)	
	T4b	8	(2.5)	6	(5.8)	2	(0.9)	
N categories TNM 7th ed. 2010‡	N0	57	(18.0)	19	(18.3)	38	(17.9)	0.3642
	N1	70	(22.2)	28	(26.9)	42	(19.8)	
	N2	175	(55.3)	51	(49.0)	124	(58.5)	
	N2a	*9*	*(2.8)*	*2*	*(1.9)*	*7*	*(3.3)*	
	N2b	*91*	*(28.8)*	*31*	*(29.8)*	*60*	*(28.3)*	
	N2c	*75*	*(23.7)*	*18*	*(17.3)*	*57*	*(26.9)*	
	N3	14	(4.4)	6	(5.8)	8	(3.8)	
N categories TNM 8th ed. 2017‡‡	N0	57	(18.0)	19	(18.3)	38	(17.9)	2.4×10^{-5}
	N1	64	(20.3)	28	(26.9)	36	(17.0)	
	N2	138	(43.7)	50	(48.0)	88	(41.5)	
	N2a	12	(3.8)	2	(1.9)	10	(4.7)	
	N2b	74	(23.4)	31	(29.8)	43	(20.3)	
	N2c	52	(16.5)	17	(16.3)	35	(16.5)	
	N3a	10	(3.2)	6	(5.8)	4	(1.9)	
	N3b	47	(14.9)	1	(1.0)	46	(21.7)	
Grading	G1 and G2	233	(73.7)	76	(73.1)	157	(74.1)	0.3865
	G3 and G4	70	(22.2)	19	(18.3)	51	(24.1)	
	Missing	*13*	*(4.1)*	*9*	*(8.7)*	*4*	*(1.9)*	
R status	R0	184	(58.2)	36	(34.6)	148	(69.8)	0.0011
	R1	8	(2.5)	5	(4.8)	3	(1.4)	
	R2	1	(0.3)	1	(1.0)	-	(0)	
	no Op	92	(29.1)	32	(30.8)	60	(28.3)	
	Missing	*31*	*(9.8)*	*30*	*(28.8)*	*1*	*(0.5)*	
Pn status	Pn0	144	(45.6)	42	(40.4)	102	(48.1)	1.7×10^{-4}
	Pn1	52	(16.5)	2	(1.9)	50	(23.6)	
	Missing	*120*	*(38.0)*	*60*	*(57.7)*	*60*	*(28.3)*	
L status	L0	72	(22.8)	34	(32.7)	38	(17.9)	3.8×10^{-9}
	L1	132	(41.8)	14	(13.5)	118	(55.7)	
	Missing	*112*	*(35.4)*	*56*	*(53.8)*	*56*	*(26.4)*	
V status	V0	159	(50.3)	43	(41.3)	116	(54.7)	0.0232
	V1	40	(12.7)	4	(3.8)	36	(17.0)	
	Missing	*117*	*(37.0)*	*57*	*(54.8)*	*60*	*(28.3)*	
Any soft risk factor	None	59	(18.7)	33	(31.7)	26	(12.3)	3.4×10^{-12}
	Any (Pn1, V1, L1)	145	(45.9)	15	(14.4)	130	(61.3)	
	Missing	*112*	*(35.4)*	*56*	*(53.8)*	*56*	*26.4)*	

(Continued)

TABLE 1 | Continued

Characteristics		Total		Cohort 1		Cohort 2		*p* value†
		(*N*=316)		(*N*=104)		(*N*=212)		(*N*=316)
		n (%)		*n* (%)		*n* (%)		*n* (%)
ECE§ with N0	ECE-	66	(20.9)	5	(4.8)	61	(28.8)	2.1×10^{-6}
	ECE+	53	(16.8)	1	(1.0)	52	(24.5)	
	No ECE (N0)	57	(18.0)	19	(18.3)	38	(17.9)	
	Missing	*140*	*(44.3)*	*79*	*(76.0)*	*61*	*(28.8)*	
p16 Status	p16-	105	(33.2)	2	(1.9)	103	(48.6)	0.2691
	p16+	15	(4.7)	1	(1.0)	14	(6.6)	
	Missing	*196*	*(62.0)*	*101*	*(97.1)*	*95*	*(44.8)*	
Smoking	Never	37	(11.7)	7	(6.7)	30	(14.2)	0.2776
	Former	32	(10.1)	6	(5.8)	26	(12.3)	
	Current	217	(68.7)	62	(59.6)	155	(73.1)	
	Missing	*30*	*(9.5)*	*29*	*(27.9)*	*1*	*(0.5)*	
Smoking categories	<5PY	42	(13.3)	8	(7.7)	34	(16.0)	0.5729
	<15PY	18	(5.7)	6	(5.8)	12	(5.7)	
	<35PY	112	(35.4)	29	(27.9)	83	(39.2)	
	<45PY	62	(19.6)	18	(17.3)	44	(20.8)	
	<55PY	32	(10.1)	10	(9.6)	22	(10.4)	
	>=55PY	16	(5.1)	2	(1.9)	14	(6.6)	
	Missing	*34*	*(10.8)*	*31*	*(29.8)*	*3*	*(1.4)*	
Smoking quintiles	<=10PY	53	(16.8)	11	(10.6)	42	(19.8)	0.7786
	<=25PY	63	(19.9)	15	(14.4)	48	(22.6)	
	<=32PY	51	(16.1)	13	(12.5)	38	(17.9)	
	<=40PY	62	(19.6)	19	(18.3)	43	(20.3)	
	>40PY	53	(16.8)	15	(14.4)	38	(17.9)	
	Missing	*34*	*(10.8)*	*31*	*(29.8)*	*3*	*(1.4)*	
Alcohol drinking	Never	27	(8.5)	8	(7.7)	19	(9.0)	0.8919
	Former	37	(11.7)	9	(8.7)	28	(13.2)	
	Current	222	(70.3)	60	(57.7)	162	(76.4)	
	Missing	*30*	*(9.5)*	*27*	*(26.0)*	*3*	*(1.4)*	
Alcohol categories	0 g/day	27	(8.5)	8	(7.7)	19	(9.0)	0.0001
	1-30 g/day	65	(20.6)	5	(4.8)	60	(28.3)	
	31-60 g/day	47	(14.9)	9	(8.7)	38	(17.9)	
	>60 g/day	146	(46.2)	54	(51.9)	92	(43.4)	
	Missing	*31*	*(9.8)*	*28*	*(26.9)*	*3*	*(1.4)*	
Age at diagnosis	Mean (95% CI)	57.6	(55.5 - 59.7)	58.8	(57.1 - 60.4)			0.3751
Pack years	Mean (95% CI)	29.3	(25.7 - 32.8)	28.0	(25.6 - 30.4)			0.5694
N assessed	Mean (95% CI)	10.1	(6.9 - 13.4)	26.9	(23.9 - 29.9)			4.4×10^{-12}
N+	Mean (95% CI)	1.1	(0.8 - 1.4)	2.0	(1.6 - 2.4)			0.0003

† Pearson's Chi-square (χ^2) test for contingency tables; ‡ TNM staging according to 7th ed. 2010 (2); ‡‡ TNM staging according to 8th ed. 2017; ‡; T categories according to TNM 8th edition now are considering depth of invasion not completely recorded in both cohorts; § ECE, extracapsular extension; heteroscedastic t-test for cardinal metric data.
Distributions are shown with number of cases and percentage in brackets.
Missing values in table are not included in analyses and therefore presented italic.

survival (OS; the time span from diagnosis until death of any cause by censoring patients alive at end of follow-up), tumor-specific survival (TSS; the time span from diagnosis until cancer-related death censoring patients alive at end of follow-up or death from other cause) and event-free survival (EFS; the interval from date of diagnosis until relapse or death from any cause, censoring patients at time of last follow-up alive without signs of any cancer). Disease-free survival (DFS) was measured from date of R0 resection or receipt of the last irradiation dose applied in PORT or PORCT in R1 resected cases or definitive pRT and CRT until the date of either relapse or cancer-related death censoring patients alive at last follow up without signs of disease.

Progression free survival (PFS) was defined as the time span from diagnosis until relapse or cancer-related death censoring patients alive at end of follow-up or death from other cause. Local control (LC) was measured as the time span from diagnosis until local recurrence or second primary squamous cell carcinoma in the head and neck region; nodal control (NC) as time to relapse in the draining neck nodes (N+ only). We measured loco-regional control (LRC) as the time from diagnosis until loco-regional relapse (sum of local and nodal relapse), and distant control (DC) as distant metastasis-free survival (DMFS), the time to diagnosis of distant metastasis (M1), censoring all other PFS events at time of last follow-up. Outcome differences between groups were analyzed using KM cumulative survival plots and log-rank tests. Univariate and multivariate Cox regression models were utilized to estimate a covariate's hazard ratio (*HR*) and to identify independent predictors (*Pi*) of PFS, LC,

TABLE 2 | Treatment and outcome in advanced squamous cell carcinoma in cohort 1 (1993-2006) and 2 (2007-2017).

Characteristics		Total		Cohort 1		Cohort 2		*p* value†
		(*N*=316)		(*N*=104)		(*N*=212)		(*N*=316)
		n (%)		*n* (%)		*n* (%)		*n* (%)
Therapy concept (2 groups)	Curative	272	(86.1)	89	(85.6)	183	(86.3)	0.8575
	Palliative or incomplete	44	(13.9)	15	(14.4)	29	(13.7)	
Therapy concept (3 groups)	Curative	272	(86.1)	89	(85.6)	183	(86.3)	0.7940
	Palliative	32	(10.1)	10	(9.6)	22	(10.4)	
	Incomplete	12	(3.8)	5	(4.8)	7	(3.3)	
Tracheostomy	No	170	(53.8)	81	(77.9)	89	(42.0)	1.7×10^{-9}
	Yes	146	(46.2)	23	(22.1)	123	(58.0)	
PEG	No	128	(40.5)	63	(60.6)	65	(30.7)	3.5×10^{-7}
	Yes	188	(59.5)	41	(39.4)	147	(69.3)	
Neck dissection (yes or no)	No ND	104	(32.9)	44	(42.3)	60	(28.3)	0.0127
	SND, mRND, RND	212	(67.1)	60	(57.7)	152	(71.7)	
Neck dissection	No ND	104	(32.9)	44	(42.3)	60	(28.3)	0.0003
	SND	194	(61.4)	49	(47.1)	145	(68.4)	
	RND, mRND	18	(5.7)	11	(10.6)	7	(3.3)	
Neck dissection and Op	No Op and no ND	91	(28.8)	32	(30.8)	59	(27.8)	1.0×10^{-5}
	Op or ND	13	(4.1)	12	(11.5)	1	(0.5)	
	Op and ND	212	(67.1)	60	(57.7)	152	(71.7)	
Op (yes or no) ‡	No Op	91	(28.8)	32	(30.8)	59	(27.8)	0.5877
	Op	225	(71.2)	72	(69.2)	153	(72.2)	
RT and RChT *vs* none	None	64	(20.3)	22	(21.2)	42	(19.8)	0.7802
	RT, RChT	252	(79.7)	82	(78.8)	170	(80.2)	
RT *vs*. RChT *vs*. none	None	64	(20.3)	22	(21.2)	42	(19.8)	0.7322
	RT	136	(43.0)	47	(45.2)	89	(42.0)	
	RChT	116	(36.7)	35	(33.7)	81	(38.2)	
Therapy modality (detail)	no RT	64	(20.3)	22	(21.2)	42	(19.8)	0.5320
	PORT	93	(29.4)	31	(29.8)	62	(29.2)	
	PORCT	75	(23.7)	23	(22.1)	52	(24.5)	
	RT	43	(13.6)	16	(15.4)	27	(12.7)	
	CRT	34	(10.8)	12	(11.5)	22	(10.4)	
	IC+Op+POR(C)T‡	7	(2.2)	0	(0)	7	(3.3)	
Chemotherapy	CRT Carboplatin	1	(0.9)	1	(2.9)	0	(0)	2.9×10^{-5}
	CRT Cisplatin	28	(24.1)	8	(22.9)	20	(24.7)	
	RT Cetuximab	2	(1.7)	0	(0)	2	(2.5)	
	CRT other chemo	3	(2.6)	3	(8.6)	0	(0)	
	PORT Carboplatin	7	(6.0)	7	(20.0)	0	(0)	
	PORT Cisplatin	60	(51.7)	14	(40.0)	46	(56.8)	
	PORT Cetuximab	5	(4.3)	0	(0.0)	5	(6.2)	
	PORT other chemo	3	(2.6)	2	(5.7)	1	(1.2)	
	IC+Op+POR(C)T‡	7	(6.0)	0	(0)	7	(8.6)	
	No chemotherapy	*200*		*69*		*131*		
Overall survival	Alive	147	(46.5)	42	(40.4)	105	(49.5)	0.1257
	Dead	169	(53.5)	62	(59.6)	107	(50.5)	
Overall survival	Alive	147	(46.5)	42	(40.4)	105	(49.5)	0.2971
	NCRD	55	(17.4)	21	(20.2)	34	(16.0)	
	CRD	114	(36.1)	41	(39.4)	73	(34.4)	
Tumor-specific survival (TSS) §	Alive or NCRD	223	(70.6)	67	(64.4)	156	(73.6)	0.0931
	CRD	93	(29.4)	37	(35.6)	56	(26.4)	
Event-free survival (EFS)	No event	99	(31.3)	25	(24.0)	74	(34.9)	0.0503
	event	217	(68.7)	79	(76.0)	138	(65.1)	
Disease-free survival (DFS)	Disease-free	164	(51.9)	51	(49.0)	113	(53.3)	0.4759
	Relapse or CRD	152	(48.1)	53	(51.0)	99	(46.7)	
Progression-free survival (PFS)	None	162	(51.3)	51	(49.0)	111	(52.4)	0.5790
	Relapse or PD	154	(48.7)	53	(51.0)	101	(47.6)	
LC	None	201	(63.6)	57	(54.8)	144	(67.9)	0.0227
	Relapse, PD	115	(36.4)	47	(45.2)	68	(32.1)	
NC	None	247	(78.2)	80	(76.9)	167	(78.8)	0.7082
	Relapse, PD	69	(21.8)	24	(23.1)	45	(21.2)	
LRC	None	191	(60.4)	55	(52.9)	136	(64.2)	0.0542
	Relapse, PD	125	(39.6)	49	(47.1)	76	(35.8)	
DC	None	272	(86.1)	98	(94.2)	174	(82.1)	0.0033
	Relapse, PD	44	(13.9)	6	(5.8)	38	(17.9)	

(Continued)

TABLE 2 | Continued

Characteristics		Total (*N*=316)		Cohort 1 (*N*=104)		Cohort 2 (*N*=212)		*p* value† (*N*=316)
		n (%)		*n* (%)		*n* (%)		*n* (%)
Other cancer entity	None	306	(96.8)	102	(98.1)	204	(96.2)	0.3772
	Other cancer	10	(3.2)	2	(1.9)	8	(3.8)	
Time to intervention (d)	Mean (95% CI)	23.2	(19.5 - 26.9)			32.8 (29.3 - 36.4)		0.0002
Therapy interval (d)	Mean (95% CI)	56.4	(46.5 - 66.2)			59.9 (53.9 - 65.9)		0.5459

† Pearson's Chi-square (χ^2) test for contingency tables; ‡ IC+Op+POR(C)T TPF-induction-chemotherapy followed by surgery and postoperative radiotherapy or radio-chemotherapy; Op, only surgery; Op+PORT, Op followed by postoperative radiotherapy; Op+PORCT, Op followed by postoperative radio-chemotherapy; RT, definitive radiotherapy alone or PORT; RChT, concurrent radio-chemotherapy or PORCT; CRT, concurrent radio-chemotherapy; other, 3 cycles 40 mg/m² taxol or mitomycin ± 5-fluorouracil (not further specified); § OS, overall survival; TSS, tumor-specific survival; EFS, event-free survival; DFS, disease-free survival; PFS, progression-free survival; LC, local control; ¶ heteroscedastic t-test for cardinal metric data. Missing values in table are not included in analyses and therefore presented italic.

LRC, DC, EFS, DFS, TSS, and OS. *P* values below 0.05 in 2-sided tests were considered being significant.

Logistic regression and propensity-score matching (PS-matching) was used to identify patients with identical or most similar characteristics, and 1:1 PS-matching was performed using SPSS version 24 (11) with a caliper width of 0.1 standard deviations of the linear predictor (12).

RESULTS

Table 1 shows the characteristics of patients in cohort 1 (104 patients) and 2 (212 patients). Whereas most epidemiologic risk factors remained mostly unchanged, significant differences are found in the localization of the primary advanced OSCC with reduced frequency of tongue cancer and increased in the mandible, associated with increased frequency in T4 cancer (+25.4%), N2 categories (especially N2c, +9.6%), and UICC stage IVA (+20.1%). According to increased frequency of ECE+ in cohort 2 ($p=2.1\cdot10^{-6}$) and by applying TNM 2017 (13), frequencies in N categories changed significantly (all $p<0.0001$): N1 and N2b were reduced (-9.9% and -9.5%), whereas the (new) category N3b increased by 20.7% having the highest impact on the also increased frequency in stage IVB (+14.5%). Overall, the information provided in pathology reports since 2007 was more comprehensive and in all cases treated by surgical resection included data about the number of analyzed neck nodes, resection margins as well as information about perineural (Pn1), lymphatic (L1) or vascular infiltration (V1) of the primary lesion or absence of those (Pn0, L0, and V0, respectively). In line with increased use of (according to institutional guidelines standardized) neck dissection, the number of neck nodes examined (mean and 95% confidence interval) increased from 10.1 (6.9-13.4) to 26.9 (23.9-29.9; $p=4.4\cdot10^{-12}$) and led to increased numbers of N+ identified in cohort 2 (2.0, 95% CI 1.6-2.4) compared to cohort 1 (1.1, 95% CI 0.8-1.4; $p=0.0003$).

We achieved the goal of pre-therapeutic presentation of all head and neck cancer patients. Since 2007 more than 95% of all new diagnosed head and neck cancer patients were pre-therapeutic discussed in the MDTB and additionally post-therapy after availability of the pathology report for decision-making towards adjuvant (post-operative) treatment. Cisplatin-based PORCT was used more frequently. In addition, use of cetuximab added to pRT or PORT emerged as new treatment option for LAOSCC-P with rather poor organ function. Aiming on reducing chemo-related side effects, dexamethasone and histamine-receptor ± neurokinin inhibitors were used in general and treatment protocols modified to reduce acute toxicity. The higher fractionated schema applying the total cisplatin dose in 2 to 3 cycles of five daily doses each of 20 mg/m² (days 1-5, 22-26, and 43-47) was more frequently used since 2007 (cohort 2).

The therapy concepts applied to cohorts 1 and 2 as well as treatment modalities, Op, Op+PORT or Op+PORCT, or treatment without surgery by pRT or CRT, almost differed not significantly in frequency but with some exceptions (**Table 2**). Related to standardized work-up and the adherence to standard operating procedures (SOP) and internal guidelines, the surgical treatment included significantly more often the use of neck dissections (ND) and in particular selective ND (SND) as well as surgical placement of tracheostomas and percutaneous endoscopic gastrostomy (PEG) feeding tubes (**Table 2**). Besides 7 patients treated in an induction-chemotherapy RCT with 3 cycles TPF (docetaxel, cisplatin, 5-fluorouracil) before surgical resection, the only significant changes observed in treatment modality frequencies were the reduced use of carboplatin and significant increase in cisplatin-based PORCT and also use of cetuximab added to PORT (**Table 2**). To reduce acute toxicity and combat cisplatin-related side effects, the latter regimen was predominantly used since 2007 (**Table 2**). In parallel, adjuvant treatment with dexamethasone was given during CRT and PORCT over a mean total time of 8.5 (95% CI 7.6 - 9.4) days in cohort 1 and 10.1 (95% CI 9.3 - 10.8) days in cohort 2 ($p=0.0102$). The mean total dexamethasone doses of patients receiving CRT and PORCT were 100.1 (95% CI 87.2 - 113.0) mg dexamethasone in cohort 1 and 119.6 (95% CI 110.5 - 128.7) mg dexamethasone in cohort 2 ($p=0.0203$).

Comparisons revealed increased numbers in T4 and higher N categories accompanied by impaired distant control (DC; $p=0.0033$) after 2006. The outcome, however, differed significantly regarding improved local (LC; $p=0.0227$) and loco-regional control (LRC; $p=0.0542$). Only insignificant

improved DFS, PFS and EFS as well as slightly improved TSS and OS were detectable (**Figure 2**).

The diagnosis of distant metastasis (M1) in cohort 2 increased in parallel to standardized follow-up and higher frequency of post-therapeutic CT-imaging including chest and abdomen or even PET-CT imaging. Whereas in cohort 1 only 1 of 6 DC events (16.7%) was detected before loss in LRC, this was the case in 18 of 38 DC events (47.4%) in cohort 2 (p=0.158). In line with earlier detection and independent diagnosis of distant failure, the frequency of M1 not accompanied by loss in LC, NC or LRC was increased and the survival of patients after M1 diagnosis prolonged (mean 3.5, 95% CI 0.9 – 6.1, *vs*. 5.5, 95% CI 3.3 – 7.8 months in cohort 1 and 2; p=0.288).

Kaplan-Meier plots of cumulative survival (**Figure 2**) with the only exception of DC show improved outcome of cohort 2. LC was significantly improved (p=0.034), but DC reduced (p=0.005). The net effect, however, was slightly (insignificant) improved DFS, PFS, EFS, TSS and OS. To clarify reasons for opposing trends respective to LC and DC, multivariate analyses applying Cox proportional hazard models were used (**Figure 3**). DFS besides being dependent on LC, NC and DC and per-protocol completed curative treatment was found being improved in patients who had ND and tracheostomy but impaired in those with N3. LC itself has a predictor in use of Op, belonging to cohort 2, and NC (nodal control); reciprocally, NC was dependent on LC and improved by applying Op and RT or CRT (independent from being used in postoperative or definitive setting). LC, despite the opposing trends in cohort 1 and 2, predicted DC. To solve the problem of improved LC in cohort 2 and despite improved LC reduced DC, analyses in propensity-score (PS) matched patients were done.

In the prior univariate analyses applying log-rank tests to Kaplan-Meier analyses or Cox proportional hazard models, we identified various predictive factors for DC/DMFS: high level of smoking (pack years), alcohol consumption, T1/T2 *vs.* T3/T4, N0 *vs.* N+, N3 *vs.* other, higher age at diagnosis, localization of the primary OSCC, male sex, alcohol consumption, and tobacco smoking. Therefore, a significantly higher prevalence of these factors in LAOSCC-P in cohort 2 had to be expected. A 1:1 PS-matching with a caliper width of 0.1 standard deviations of the linear predictor (12) was used to identify 70 LAOSCC-P in each cohort with according to z-scores nearly identical profile in the before mentioned characteristics. We applied multivariate Cox proportional hazard regression models for analysis of DC in these 140 cases (70 PS-matched patients from each of the two cohorts). We used the conditional stepwise-forward method in Cox proportional hazard regression to identify those covariates exerting strongest impact on DC in the PS-matched cases, the three covariates N3, cisplatin, and cohort 1 or 2. By including them, all other covariates (sex, age at diagnosis, level of daily alcohol consumption, history of tobacco smoking and pack years smoked, localization of the primary as well as individual treatment components [surgical operation, neck dissection, RT or CRT] applied or not as well as T and N categories, and also LC and NC) no longer had any impact on DC in these PS-matched patients. The exclusion of the formerly predictive covariates demonstrates absence of relevant residual confounding. The final model automatically built using the conditional stepwise-forward method extracted only 3 independent predictors for losing DC: belonging to cohort 2 (*HR* 4.25, 95% CI 1.41-12.85; p=0.0103); N3 (*HR* 6.23, 95% CI 1.66-23.44; p=0.0068); and cisplatin-based chemo-radiation (*HR* 1.96, 95% CI 0.78-4.94; p=0.1531). Bootstrapping utilizing 1,000 iterations revealed significance of the model ($p=4.99\cdot10^{-5}$) and of these 3 independent predictors (all $p<0.001$) within the PS-matched LAOSCC-P. Therefore, being treated with cisplatin-based chemo-radiation is an independent predictor of DC loss but, however, not itself a significant contributor in our sample of LAOSCC-P.

DISCUSSION

Decision-making after standardized diagnostics in the MDTB can improve the efficiency of multidisciplinary patient management. Our MDTB allowed for implementation of clinical practice guidelines and quality control for diagnostic workflow, decision-making and therapy. Moreover, it helped to capture cases for clinical trials and allowed for quicker translation of their findings into our daily practice. These additional efforts should improve survival. Indeed, we found an improved outcome of LAOSCC patients diagnosed and treated in our university hospital after establishing the MDTB, and significantly improved LRC in particular. This confirms findings in our university hospital (8) and of other centers (14). After introduction of a MDTB at the University of Philadelphia the disease-specific survival of patients with head and neck cancer increased significantly from 52% to 75% (p=0.003) and the post-tumor board cohort had a better OS and a lower mortality risk (HR: 0.48) (14). In Germany, the guidelines of the oncologic societies and the National Cancer Plan as well force the implementation of MDTB as prerequisite standard of oncologic treatment to become a certified center. In our certified center's weekly head & neck MDTB, the presence of at least two head neck surgeons, two maxillofacial surgeons, one radiologist, one pathologist, one radio-oncologist, and one oncologist is obligatory; further disciplines participate if necessary.

Pre-therapeutic presentation of LAOSCC cases in the MDTB and the standardized diagnostic workup and patient-centered decision making for surgery and neck dissection followed by risk-factor adapted adjuvant therapy improves LC and LRC in LAOSCC as demonstrated here in our retrospective analysis of 316 cases. Related to improved LC and LRC in cohort 2, there was a trend to improved outcome. Despite significantly improved LC and LRC, the DC appeared to be reduced (p=0.0033). A reduced DC/DMFS was also reported for neck squamous cell carcinoma of unknown primary tumors (8). Impaired DC in our sample was found to be significantly associated with N3 category ($p=2.97\cdot10^{-4}$), localization in the tongue (C02; p=0.049), ECE+ ($p=3.16\cdot10^{-5}$), and history of tobacco smoking (≤40 vs. >40 pack years, p=0.044). According to NCCN guidelines, unresectable disease demands CRT, and

resectable N3 and/or ECE+ demand PORCT. Such LAOSCC patients received either 100 mg/m^2 cisplatin in 3 cycles (days 1, 22, and 43) as recommended or fractionated in five doses of 20 mg/m^2 days 1-5, 22-26, and 43-47 (7, 10). A tendency for loss of DC was found for cisplatin-based CRT or PORCT (p=0.059). The associations of reduced DC with high level smoking, localization of the OSCC in the tongue, presence of ECE+, T4 and N3 categories, and the consequent cisplatin-use are even more relevant as the loss of DC exerts the strongest impact on TSS and OS (**Figure 3**).

The particular reasons for the increased number of distant metastasis diagnosed in cohort 2 are currently unclear. One possible explanation is the increased use of more sensitive diagnostic tools (15). Our standardized workup and the staging procedure before the presentation of the case in the MDTB consists of at least a CT-scan of head and neck and the chest, either ultrasound or CT-scan of the abdomen, and a bone scan in all advanced stages (≥T3 or N+). Since 2006, a PET-CT system is available at our center, and [^{18}F]-FDG-PET-CT scans are used for pre-therapeutic imaging of all cases presenting with bulky disease (≥T4a or N3), suspected residual disease after completed therapy or relapse. This functional imaging may have led to an earlier detection of otherwise occult

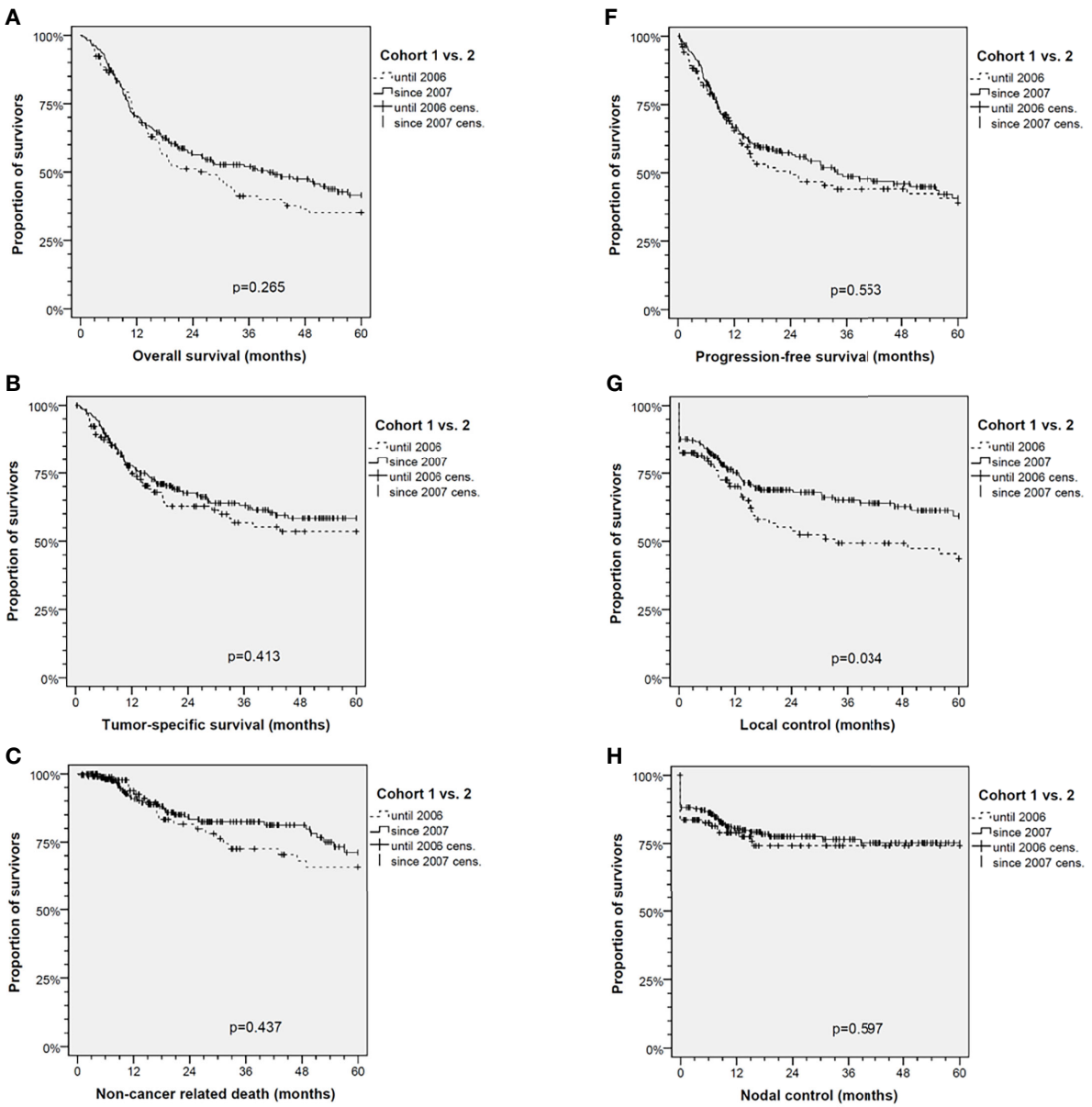

FIGURE 2 | Continued

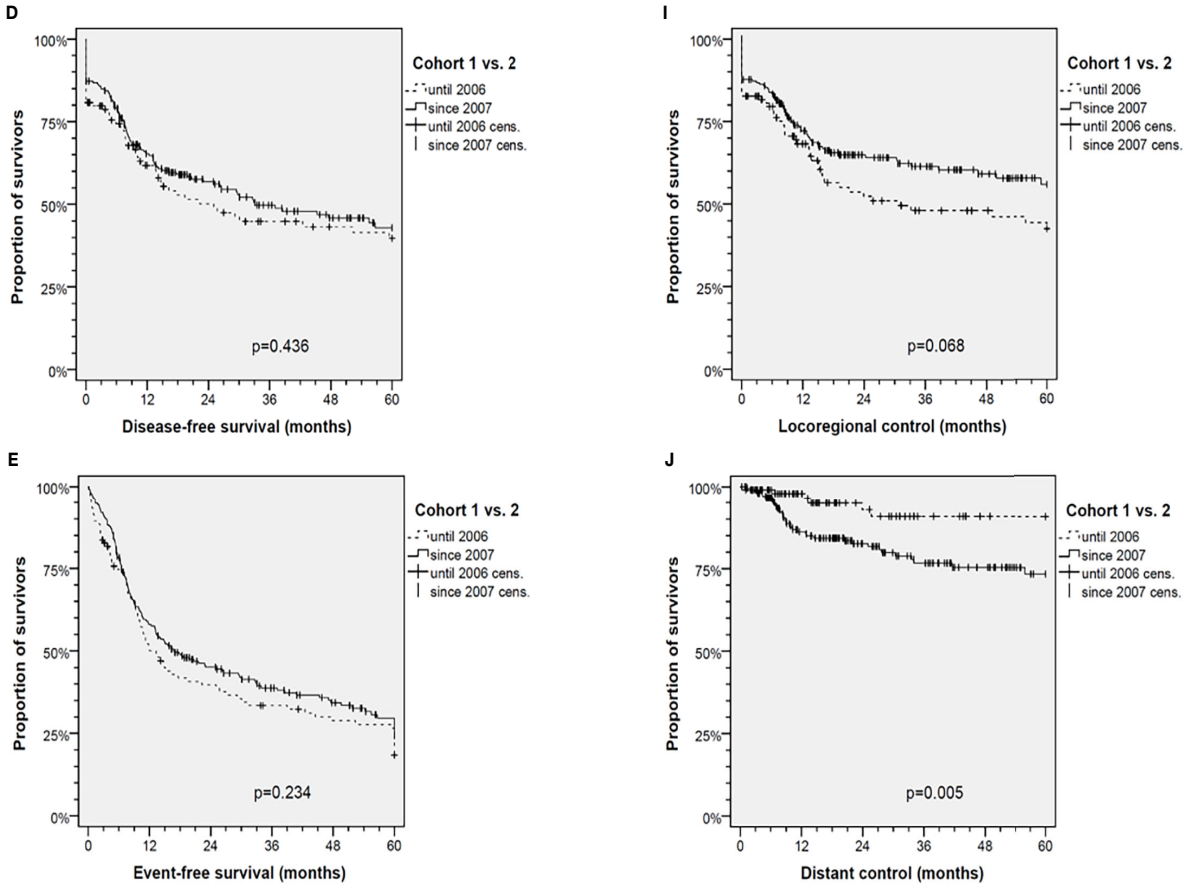

FIGURE 2 | Kaplan-Meier cumulative survival analyses of advanced oral squamous cell carcinoma (OSCC) patients before (Cohort 1, 1993-2006) and after standardization of diagnostic workup and therapy (Cohort 2, 2007-2017) for **(A)** overall survival; **(B)** tumor-specific survival; **(C)** survival according to non-cancer death/death from other cause; **(D)** disease-free survival; **(E)** event-free survival; **(F)** progression-free survival; **(G)** local control; **(H)** nodal control; **(I)** loco-regional control; and **(J)** distant control. *P* values shown are from 2-sided log-rank tests.

asymptomatic distant metastasis and therefore linked to earlier detection of (at this time) rather treatable M1 but caused formally an impaired DC. Indeed, 16.7% vs. 47.4% distant failures (DF) were detected *before* loss in LRC in cohort 1 vs. 2. This may suggest that the DC could be impaired but OS and TSS have, nevertheless, improved to some extent. Due to the missing negative impact on survival, diagnostic improvements and use of PET/CT imaging in particular may have led to detection of otherwise occult distant metastases and caused the observed loss in DC. Early detection of single or oligo metastases and their surgical removal or irradiation may have contributed to prolonged OS in cohort 2 despite higher frequent loss of DC in cohort 2.

There was a difference between the two cohorts regarding participation in randomized controlled trials (RCT). In cohort 1, only 2 patients were included in an RCT but 35 patients of cohort 2 (and these patients underwent additional imaging including PET-CT). The increased use of CT and PET-CT imaging in patients within RCT may also have contributed to M1 detection: 26 of 35 LAOSCC patients in RCT of cohort 2 had M1 and 20 of them had their M1 diagnosis simultaneous to the LRC event leading to recommendation for systemic treatment and enrollment in one of the first-line RCT.

Since 2006, more LAOSCC (UICC Stage III-IVB, TNM 2010 and 2017) diagnosed underwent a complex risk factor-adapted multimodal treatment with curative intent. Specifically, more radical procedures were performed in a curative intent in cohort 2 in patients who before 2006 were declared being in a palliative state. However, patients with a more advanced tumor category and nodal metastasis (N+) have a higher risk for distant metastasis (15, 16). The proportion of tracheostomy, percutaneous gastrostomy and applied neck dissection increased, and consequently both the detection of N+ neck and ECE+ increased significantly, too.

During the study period, the rate of neck dissections increased. This is probably a main contributor to improved LRC. Before 2006, 42.3% of all patients did not undergo neck dissection whilst after 2006 only 28.3% did not. The increase in the number of neck dissections and the increased number of resected nodes examined by the pathologist per case led to a higher frequency of removed disease-positive nodes in particular. This change is attributable to the adherence and better implementation of the guidelines linked

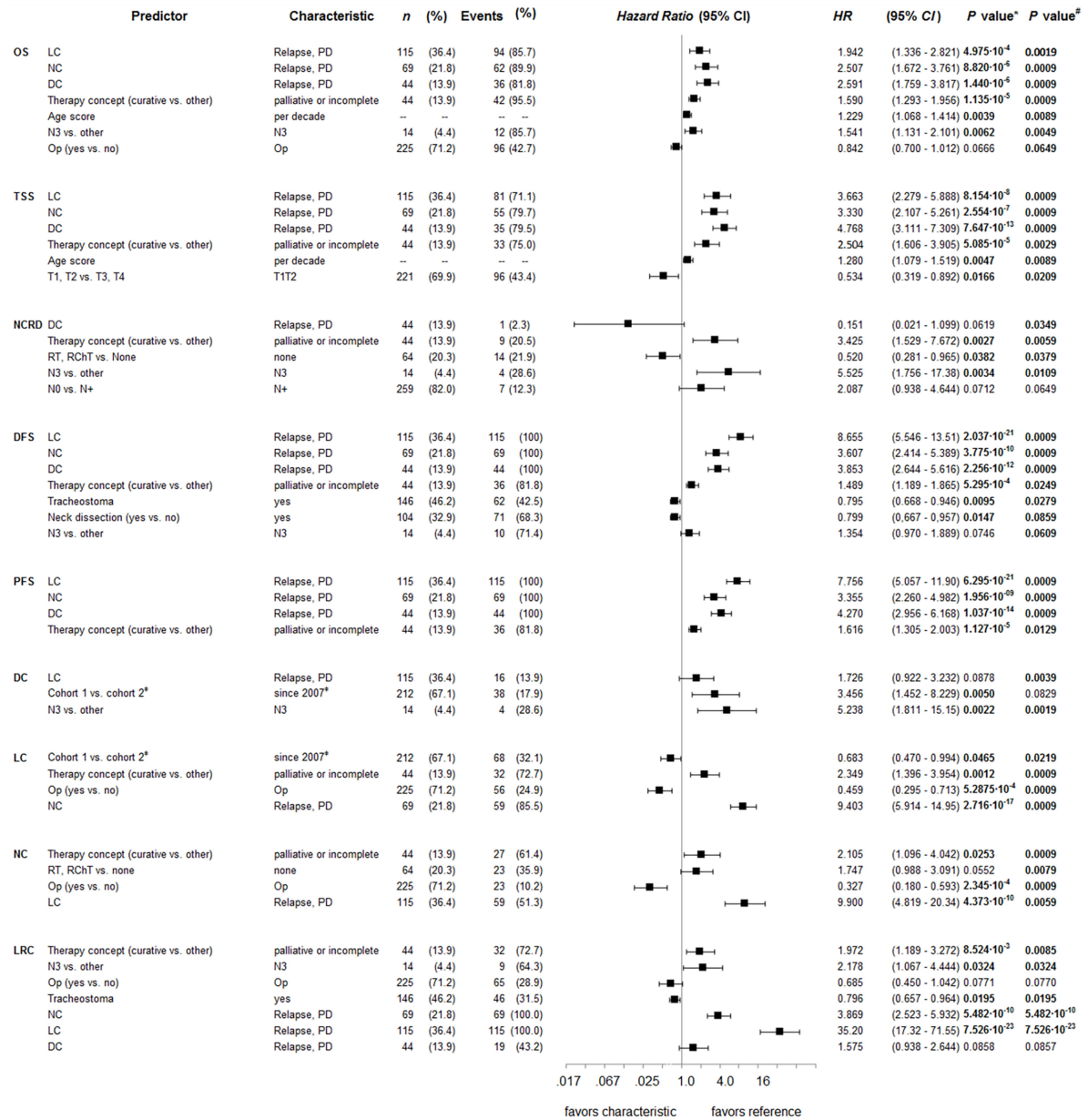

FIGURE 3 | Forest plots for outcome predictors in advanced oral squamous cell carcinoma according to multivariate Cox proportional hazard regression analyses. Shown are hazard ratios (HR) and 95% confidence intervals for OS, overall survival; TSS, tumor-specific survival; NCRD, survival according to non-cancer death/death from other cause; DFS, disease-free survival; PFS, progression-free survival; DC, distant control; LC, local control; NC, nodal control; LRC, loco-regional control. *, *P* values for independent predictors in the Cox proportional hazard model of highest significance; #, *P* values from bootstrap validation of the same Cox proportional hazard model applying 1,000 iterations. ;#‡Cohort 2 comprises patients diagnosed since 2007 (standardized workup and prediagnostic presentation in the multidisciplinary tumor board).

to decision-making and quality control of results in the MDTB. The benefit of an elective neck dissection for survival was demonstrated in cN0 oral cancer in several studies (5, 8, 10, 17). The mean number of assessed lymph nodes (nodal yield) increased from 10.1 before 2006 to 26.9 after 2006, respectively, suggesting the quality of neck dissection improved during the study period. The literature strongly suggests that a higher nodal yield is associated with a better survival and loco-regional control in head and neck cancer even when all dissected lymph nodes are negative. The optimal threshold for nodal yield in cN0 OSCC seems to be between 16 and 18 (18–20). Furthermore, the number of assessed nodes correlates with a higher N classification due to detection of occult lymph node metastases and detection of ECE+ as recorded in this study.

Cisplatin-based chemo-radiotherapy showed a tendency to predict impaired DC/DMFS and was found to predict distant

metastasis in the PS-matched subgroup. Patients with larger tumor stages at diagnosis will more often receive platinum-based chemotherapy than those with smaller ones (21). Indeed, due to higher frequency in higher T and N categories, and in particular more T4 tongue cancer compared to cohort 1 and aiming on preventing glossectomy, patients in cohort 2 more often were treated by cisplatin-based CRT or PORCT (**Table 2**). Cisplatin seems to be unable to delete peripheral (circulating or already tissue-infiltrating) tumor cells completely for preventing distant metastasis in a patient cohort with more advanced disease (cohort 2).

As high level of smoking history (pack years), alcohol consumption, T1/T2 vs. T3/T4, N0 vs. N+, N3 vs. other N categories, of the primary LAOSCC sub-localization as well as age and sex were identified as independent predictive factors (*Pi*) for loss of DC (reduced DMFS) and, therefore, were expected to be significantly higher in LAOSCC-P of cohort 2 in general and hence potential confounders, logistic regression and propensity-score matching (PS-matching) was used to identify patients with identical or most similar characteristics in cohort 1 and 2). Cox hazard regression indeed identified N3, cisplatin-based PORCT/CRT and belonging to cohort 2 as independent predictors for losing DC in these 70 PS-matched LAOSCC-P pairs. However, the role of possible confounders and additional risk factors (*e.g.* smoking) and unwanted side effects of adjuvant treatment probably also linked to loss of DC have to be further clarified. However, it is conceivable that cisplatin not only could be unable to completely delete peripheral (circulating or already tissue-infiltrating) tumor cells and prevent distant metastasis in a patient cohort with more advanced disease (as in our cohort 2). However, belonging to cohort 2 emerged as independent predictor for distant metastasis in the 70 PS-matched LAOSCC-P, and therefore a closer look at differences into treatment regimens appear to be warranted.

Cisplatin-based CRT or PORCT may have the potential to trigger resistance to cisplatin and distant metastasis. Besides earlier observations that incomplete per-protocol treatment or use of inadequately low cisplatin doses are accompanied by loss of sensitivity to cisplatin treatment, recent papers highlight at least two additional mechanisms potentially involved in resistance to cisplatin and increased frequency of distant metastasis after cisplatin treatment due to unwanted side effects occurring whenever cisplatin is given combined with dexamethasone. Pan and collaborators demonstrated cisplatin-mediated activation of the glucocorticoid receptor (GR). The cisplatin-GR complex translocates into the nucleus. This complex induces platinum resistance *via* activating expression of MAST1, a critical platinum resistance factor component (22). A recent study by Zhang et al. demonstrated in various mice models pro-metastatic effects of dexamethasone *via* a PI3K-SGK1-CTGF pathway (23). Ligation of the GR by dexamethasone activated the PI3K signaling pathway and upregulated serum glucocorticoid-inducible kinase 1 (SGK1) expression, and then increased the expression of connective tissue growth factor (CTGF) through Nedd4l-Smad2 (23). Moreover, dexamethasone-induced SGK1 upregulated CTGF induced the expression of integrins Itgα6 and Itgβ1, and either SGK1 inhibition or CTGF knockdown downregulated these integrin genes. Interestingly, dexamethasone did not impair the response of the primary tumor towards paclitaxel in their *in vivo* models (23). This is different to Pan et al. (22) who demonstrated a prometastatic effect of dexamethasone combined with cisplatin and rather reduced efficacy of cisplatin after dexamethasone treatment. However, dexamethasone in concentrations and dosing schemata used in clinical routine induced increased migration of tumor cells and enhanced metastasis into the lung (23). This prometastatic effect was independent of immunosuppressive ability of dexamethasone (23).

Aiming on reducing chemo-related side effects, dexamethasone and histamine-receptor blockade ± neurokinin inhibitors were increasingly used since their approval and are part of guideline-conform treatment of LAOSCC (10). We noticed a 10% increase in use of cisplatin-based CRT and PORCT in cohort 2 (**Table 2**). Moreover, also treatment protocols were modified and cisplatin-based PORCT used more often the more fractionated schema applying the total cisplatin dose in 3 cycles of five daily doses each of 20 mg/m^2 (days 1-5, 22-26, and 43-47) since 2007 (cohort 2) accompanied by prolonged adjuvant dexamethasone administration. Looking at dexamethasone dosing only in LAOSCC-P during CRT or PORCT, cohort 2 patients received dexamethasone on more days (10.1 *versus* 8.5 days; p=0.01018) summing up to a higher mean total dose (119.6 *versus* 100.1 mg dexamethasone; p=0.02032). Just for comparison: The mean total dexamethasone doses per patients calculated for all patients independent of receiving chemo-radiotherapy or not would result in 27.7 (95% CI 18.4 - 36.9) mg dexamethasone in cohort 1 and 40.5 (95% CI 32.4 - 48.6) mg dexamethasone in cohort 2 (p=0.04503). The association of higher proportion of patients receiving dexamethasone (also in higher mean dexamethasone doses) and higher frequency of distant metastasis in cohort 2 requires an explanation.

In the light of the studies by Pan et al. (22) and Zhang et al. (23) and other recent papers dealing with unwanted side effects of dexamethasone pointing towards elevated distant metastasis, either a reduction of dexamethasone use or targeting the GR signaling pathway components appear to be desirable. After demonstrating dexamethasone-induced cisplatin-resistant tumor growth *in vivo* in patient-derived xenograft (PDX) mouse models of head and neck cancer, Pan et al. demonstrated that treatment with lestaurtinib, an inhibitor of MAST1, fully revived cisplatin sensitivity in the dexamethasone-treated (prior cisplatin-resistant group) and even further attenuated tumor growth compared to the group treated with cisplatin alone (22). On the other hand, targeting SGK1 with a small molecule (GSK650394) could inhibit dexamethasone-induced lung metastasis without affecting antitumor capacity, as demonstrated in a murine breast cancer model (23). Besides aiming on a reduction of dexamethasone use in solid cancers including HNSCC, research is needed respective to hormone receptor signaling and its impact on distant metastasis and blocking these pathways, *e.g.* by using inhibitors for MAST1 (22) or SGK1 (23).

Since the implementation of a standardized MDTB in 2007, the mean time to intervention (TTI) in our cohort extends from 23.2 days to 32.8 days, respectively. Even after exclusion of TTI as a significant factor for DC, OS, TSS and other outcome measures (p>0.5 in all Cox models), the impact of this delay on OS and DC in our dataset remains unclear. A negative correlation of extended

TTI on OS has been published by several authors (24–26). However, the delay in treatment initiation in our trial was not that huge as in the cited studies (45-68 days). Despite being without significant impact on outcome in our study, we are now aiming on shortening the interval between diagnosis and treatment to not potentially compromise the gains form MDTBs ensuring standardized cancer care and improve decision-making.

In our analysis, the patient volume increased from 6.5 cases per year to 21.2 cases per year. The impact of hospital and surgeon volume on the outcome of head and neck cancer patients was demonstrated in several trials (27–29). We assume that the increase in patient number is due to the improved structural and process quality (selective referral theory (27–29)) which is among other things certainly also a result of the implementation of the MDTB.

The limitations of our study are the small sample size in particular in subgroups analyzed and its retrospective nature. Inherent to the design we have to deal with missing data that could have impact on our results. Attributable to treatment of the most LAOSCC cases in routine ("real-world setting"), comorbidity led in a minority of cases to deviations between treatment recommended by the MDTB and applied. The distribution in localization of the primary lesions within the oral cavity and the shift towards higher age and presentation with more advanced tumors (T4) and higher N+ numbers and increased frequency in ECE+ reported represents a bias with not completely clarified impact on outcome including reduced DC in elderly patients and those with more advanced disease. Moreover, we could only report about a correlation between increased frequency of distant metastasis and increased use of cisplatin-based CRT and PORCT and simultaneously increased utilization of dexamethasone along altered fractionation protocols. This, however, remains an unproven hypothesis as long as evidence is missing that prolonged use of dexamethasone before and during chemotherapy to reduce acute toxicity and unwanted cisplatin-related side effects indeed comes at the price of an increase in distant metastasis and reduced DC in LAOSCC. However, one of the strength of our study is its intent-to-treat character and the validation of findings in sensitivity analyses based on propensity-score matched cases, which revealed stability of effects observed in comparison of both total cohorts and subgroups.

CONCLUSION

Despite standardized diagnostic procedures, decision-making in the MDTB considering clear indications and improved therapy algorithms leading to improved LC and LRC only a slightly improved TSS and OS was achieved. The increased frequency of distant failure in cohort 2 accompanies changes in patient characteristics. Altered characteristics include age at diagnosis and increased proportions of T4 and N2-3 categories. Consequently, the use of cisplatin, BSC or palliative treatment according to patient's preference increased. The identification of distant metastases, however, predominantly relates to diagnostic procedures during follow-up including use of advanced imaging methods including CT, MRI or PET-CT utilized in cohort 2. As simultaneous to cisplatin-based CRT and PORCT increased use of dexamethasone may have partly contributed to impaired DC based on its ability to induce expression of MAST1 (22) and of CTGF *via* SGK1 (23) the targeting of these critical proteins with inhibitors like lestaurtinib and GSK650394, respectively, may help to eliminate the unwanted side effects of steroids and re-sensitize LAOSCC and distant metastases to cisplatin treatment.

DATA AVAILABILITY STATEMENT

The raw data supporting the conclusions of this article will be made available by the authors, without undue reservation.

ETHICS STATEMENT

The studies involving human participants were reviewed and approved by Ethics Committee of the University Leipzig. The patients/participants provided their written informed consent to participate in this study.

AUTHOR CONTRIBUTIONS

Conceptualization, GW. Methodology, GW. Validation, GW and MP. Formal analysis, GW and MP. Investigation, GW and MP. Resources, GW, DH, TK, RK, TG, BL, AD, SW, and VZ. Data curation, GW and MP. Writing—original draft preparation, GW and MP. Writing— review and editing, all authors. Visualization, GW and MP. Supervision, GW, SW, AD, and VZ. Project administration, GW. Funding acquisition, GW and AD. All authors contributed to the article and approved the submitted version.

FUNDING

The study was partly supported by the grants LIFE-006 B7 and LIFE-007 D9 of the Leipzig Research Center for Civilization Diseases (LIFE), University Leipzig. LIFE is funded by the European Union, the European Fund for Regional Development (EFRE), and the Free State of Saxony. The funding sources did not influence the design of the study, collection, interpretation and analysis of the data, the preparation of this report, or the decision to publish.

ACKNOWLEDGMENTS

We thank all patients participating in the investigation and their families. We especially thank all contributing physicians providing clinical data, and the entire technical staff, all nurses and physicians in the involved departments. We acknowledge support from Leipzig University for Open Access Publishing.

REFERENCES

1. Lonneaux M, Hamoir M, Reychler H, Maingon P, Duvillard C, Calais G, et al. Positron Emission Tomography With [^{18}f]Fluorodeoxyglucose Improves Staging and Patient Management in Patients With HNSCC - A Multicenter Prospective Study. *J Clin Oncol* (2010) 28:1190–5. doi: 10.1200/JCO.2009.24.6298
2. Sobin LH, Gospodarowicz MK, Wittekind C. *Hrsg. TNM Classification of Malignant Tumours. 7. Aufl.* New York, NY: John Wiley & Sons (2011).
3. Oeser A, Gaebel J, Dietz A, Wiegand S, Oeltze-Jafra S. Update on the Management of Advanced Head and Neck Cancer. *Otorinolaringologia* (2010) 60(2):65–80. doi: 10.1007/s11548-018-1741-7
4. Oeser A, Gaebel J, Dietz A, Wiegand A, Oeltze-Jafra S. Information Architecture for a Patient-Specific Dashboard in Head and Neck Tumor Boards. *Int J CARS* (2018) 3:1283–90. doi: 10.1007/s11548-018-1741-7
5. D'Cruz AK, Vaish R, Kapre N, Dandekar M, Gupta S, Hawaldar R, et al. Elective *Versus* Therapeutic Neck Dissection in Node-Negative Oral Cancer. *N Engl J Med* (2015) 373:521 – 529. doi: 10.1056/NEJMoa1506007
6. National Comprehensive Cancer Network (NCCN). *NCCN Clinical Practice Guidelines in Oncology: Head and Neck Cancers* Plymouth Meeting, PA: nccn.org 2. (2012). p. 2011.
7. Geiger JL, Ismaila N, Beadle B, Caudell JJ, Chau N, Deschler D, et al. Management of Salivary Gland Malignancy: ASCO Guideline. *J Clin Oncol* (2021) 39:1909–41. doi: 10.1200/JCO.21.00449
8. Wichmann G, Willner M, Kuhnt T, Kluge R, Gradistanac T, Wald T, et al. Standardized Diagnostics Including PET-CT Imaging, Bilateral Tonsillectomy and Neck Dissection Followed by Risk-Adapted Post-Operative Treatment Favoring Radio-Chemotherapy Improve Survival of Neck Squamous Cell Carcinoma of Unknown Primary Patients. *Front Oncol* (2021) 11:682088. doi: 10.3389/fonc.2021.682088
9. Freitag J, Wald T, Kuhnt T, Gradistanac T, Kolb M, Dietz A, et al. Extracapsular Extension of Neck Nodes and Absence of Human Papillomavirus 16-DNA Are Predictors of Impaired Survival in P16-Positive Oropharyngeal Squamous Cell Carcinoma. *Cancer* (2020) 126:1856–72. doi: 10.1002/cncr.32667
10. *[Clinical Guideline for Diagnostic and Treatment of the Oral Carcinoma]; Leitlinienprogramm Onkologie (Deutsche Krebsgesellschaft, Deutsche Krebshilfe, AWMF): S3-Leitlinie Diagnostik Und Therapie Des Mundhöhlenkarzinoms, Langversion 3.0, 2021, AWMF Registernummer: 007/100ol.* Available at: https://www.leitlinienprogramm-onkologie.de/leitlinien/mundhoehlenkarzinom/ (Accessed last accessed 22.09.2021).
11. IBM Corp. *IBM SPSS Statistics for Windows, Version 24.0*. Armonk, NY: IBM Corp (2016).
12. Kuss O, Blettner M, Börgermann J. Propensity Score: An Alternative Method of Analyzing Treatment Effects. *Dtsch Arztebl Int* (2016) 113:597–603. doi: 10.3238/arztebl.2016.0597
13. Amin MB, Greene FL, Edge SB, Compton CC, Gershenwald JE, Brookland RK, et al. The Eighth Edition AJCC Cancer Staging Manual: Continuing to Build a Bridge From a Population-Based to a More "Personalized" Approach to Cancer Staging. *CA Cancer J Clin* (2017) 67:93–9. doi: 10.3322/caac.21388
14. Liu JC, Kaplon A, Blackman E, Miyamoto C, Savior D, Ragin C. The Impact of the Multidisciplinary Tumor Board on Head and Neck Cancer Outcomes. *Laryngoscope* (2019) 130:946–50. doi: 10.1002/lary.28066
15. Kim Y, Roh J-L, Kim JS, Lee JH, Choi S-H, Nam SY, et al. Chest Radiography or Chest CT Plus Head and Neck CT *Versus* ^{18}F-FDG PET/CT for Detection of Distant Metastasis and Synchronous Cancer in Patients With Head and Neck Cancer. *Oral Oncol* (2019) 88:109–14. doi: 10.1016/j.oraloncology.2018.11.026
16. Carvalho AL, Nishimoto IN, Califano JA, Kowalski LP. Trends in Incidence and Prognosis for Head and Neck Cancer in the United States: A Site-Specific Analysis of the SEER Database. *Int J Cancer* (2005) 114:806–16. doi: 10.1002/ijc.20740
17. Fasunla AJ, Greene BH, Timmesfeld N, Wiegand S, Werner JA, Sesterhenn AM. A Meta-Analysis of the Randomized Controlled Trials on Elective Neck Dissection *Versus* Therapeutic Neck Dissection in Oral Cavity Cancers With Clinically Node-Negative Neck. *Oral Oncol* (2011) 47:320–4. doi: 10.1016/j.oraloncology.2011.03.009
18. de Kort WWB, Maas SLN, van Es RJJ, Willems SM. Prognostic Value of the Nodal Yield in Head and Neck Squamous Cell Carcinoma: A Systematic Review. *Head Neck* (2019) 41:2801–10. doi: 10.1002/hed.25764
19. Ebrahimi A, Clark JR, Amit M, Yen TC, Liao C-T, Kowalski LP, et al. Minimum Nodal Yield in Oral Squamous Cell Carcinoma: Defining the Standard of Care in a Multicenter International Pooled Validation Study. *Ann Surg Oncol* (2014) 21(9):3049–55. doi: 10.1245/s10434-014-3702-x
20. Kuo P, Mehra S, Sosa JA, Roman SA, Husain ZA, Burtness BA, et al. Proposing Prognostic Thresholds for Lymph Node Yield in Clinically Lymph Node-Negative and Lymph Node-Positive Cancers of the Oral Cavity. *Cancer* (2016) 122(23):3624–31. doi: 10.1002/cncr.30227
21. Shetty A, W D. Systemic Treatment for Squamous Cell Carcinoma of the Head and Neck. *Otolaryngol Clin North Am* (2017) 50(4):775–82. doi: 10.1016/j.otc.2017.03.013
22. Pan C, Kang J, Hwang JS, Li J, Boese AC, Wang X, et al. Cisplatin-Mediated Activation of Glucocorticoid Receptor Induces Platinum Resistance *via* MAST1. *Nat Commun* (2021) 12:4960. doi: 10.1038/s41467-021-24845-8
23. Zhang Y, Shi G, Zhang H, Xiong Q, Cheng F, Wang H, et al. Dexamethasone Enhances the Lung Metastasis of Breast Cancer *via* a PI3K-SGK1-CTGF Pathway. *Oncogene* (2021) 40:5367–78. doi: 10.1038/s41388-021-01944-w
24. Murphy CT, Galloway TJ, Handorf EA, Egleston BL, Wang LS, Mehra R, et al. Survival Impact of Increasing Time to Treatment Initiation for Patients With Head and Neck Cancer in the United States. *J Clin Oncol* (2016) 34:169–78. doi: 10.1200/JCO.2015.61.5906
25. Suzuki H, Terada H, Hanai N, Nishikawa D, Koide Y, Beppu S, et al. Treatment Package Time Predicts Cancer-Specific Survival and Distant Metastasis in Laryngeal Cancer. *Oncol Lett* (2019) 17:1384–90. doi: 10.1016/j.oraloncology.2017.02.009
26. Polesel J, Furlan C, Birri S, Giacomarra V, Vaccher E, Grando G, et al. The Impact of Time to Treatment Initiation on Survival From Head and Neck Cancer in North-Eastern Italy. *Oral Oncol* (2017) 67:175–82. doi: 10.1016/j.oraloncology.2017.02.009
27. Cheung MC, Koniaris LG, Perez EA, Molina MA, Goodwin WJ, Salloum RM. Impact of Hospital Volume on Surgical Outcome for Head and Neck Cancer. *Ann Surg Oncol* (2009) 16:1001–9. doi: 10.1245/s10434-008-0191-9
28. Eskander A, Irish J, Groome PA, Freeman J, Gullane P, Gilbert R, et al. Volume-Outcome Relationships for Head and Neck Cancer Surgery in a Universal Health Care System. *Laryngoscope* (2014) 124:2081–8. doi: 10.1002/lary.24704
29. Eskander A, Merdad M, Irish JC, Hall SF, Groome PA, Freeman JL, et al. Volume-Outcome Associations in Head and Neck Cancer Treatment: A Systematic Review and Meta-Analysis. *Head Neck* (2014) 36:1820–34. doi: 10.1002/hed.23498

Conflict of Interest: The authors declare that the research was conducted in the absence of any commercial or financial relationships that could be construed as a potential conflict of interest.

frontiers in Oncology

ORIGINAL RESEARCH
published: 26 November 2021
doi: 10.3389/fonc.2021.728230

Rare Metastasis to the Submandibular Gland in Oral Squamous Cell Carcinoma

Ping Zhou[1†], *Jing-Xin Chen*[2†], *Yuan Zhou*[1†], *Chen-Lu Lian*[1], *Bing Yan*[3*] *and San-Gang Wu*[1*]

[1] Department of Radiation Oncology, The First Affiliated Hospital of Xiamen University, Xiamen, China, [2] Department of Stomatology, Hainan General Hospital (Hainan Affiliated Hospital of Hainan Medical University), Haikou, China, [3] Department of Otolaryngology Head and Neck Surgery, The First Affiliated Hospital of Xiamen University, Xiamen, China

OPEN ACCESS

Edited by:
Markus Wirth,
Klinikum rechts der Isar, Germany

Reviewed by:
Daniel Jira,
Technical University of Munich, Germany
Alfredo Mauricio Batista De Paula,
Unimontes, Brazil
Maria Buchberger,
Technical University of Munich, Germany

***Correspondence:**
Bing Yan
yanbing_west@163.com
San-Gang Wu
wusg@xmu.edu.cn

[†]These authors have contributed equally to this work

Specialty section:
This article was submitted to Head and Neck Cancer, a section of the journal Frontiers in Oncology

Received: 21 June 2021
Accepted: 01 November 2021
Published: 26 November 2021

Citation:
Zhou P, Chen J-X, Zhou Y, Lian C-L, Yan B and Wu S-G (2021) Rare Metastasis to the Submandibular Gland in Oral Squamous Cell Carcinoma. Front. Oncol. 11:728230. doi: 10.3389/fonc.2021.728230

Purpose: In the current recommendation of neck dissection in oral squamous cell carcinoma (OSCC), the submandibular gland (SMG) should also be removed. This study aimed to investigate the incidence and the patterns of SMG involvement in OSCC patients.

Methods: Patients initially diagnosed with OSCC between January 2018 and October 2020 were included. The distribution of lymph nodes metastasis in level IB was analyzed.

Results: We included 145 patients who underwent primary surgery and neck dissection in this study. All patients had level IB lymph node dissection and simultaneous removal of the SMG. Of these patients, only one patient (0.7%) had involvement in SMG by directly infiltrating from the primary tumor. A total of 18 positive lymph nodes were found in level IB in 16 patients, and no positive lymph nodes were located in the SMG. There were 6 lymph nodes located in the lateral part of the SMG and 12 lymph nodes located in the anterior of the SMG. Patients with tumors located in the buccal mucosa and N3 stage were the independent predictive factors associated with level IB nodal metastasis.

Conclusion: Involvement of SMG in OSCC is quite rare. Preservation of the SMG during neck dissection in selected patients with OSCC seems to be feasible and oncologically safe.

Keywords: oral squamous cell carcinoma, submandibular gland, organ preservation, level IB metastasis, head and neck cancer

INTRODUCTION

According to the GLOBOCAN 2020, cancers developed in the lip and oral cavity accounted for approximately 2% of all cancers in the world, with over 370,000 cases newly diagnosed with lip and oral cavity cancers and 170,000 disease-related deaths occurring annually (1). The majority of oral cavity cancers are squamous cell carcinoma (SCC) (2). Approximately 29%–36% of oral squamous cell carcinoma (OSCC) patients had cervical lymph node involvement (3, 4). In patients with early-stage (T1) and clinically lymph node-negative disease, 23% of them had occult lymph node

metastasis during neck dissection (5). Therefore, primary surgery and neck dissection remain the most important management for OSCC (6).

The submandibular gland (SMG), which is located in the submandibular triangle, has the predominant function of saliva secretion. According to the 2013 edition of the neck nodal classification in the neck, SMG is one of the contents of level IB (7). A large case series from a literature review included 2,750 patients with OSCC, and only 2 patients (0.07%) had intraglandular lymph node metastases (8). In addition, the probability of direct involvement to SMG by primary tumor or periglandular nodal extension through the capsule was only 0%–4.5% (8). Moreover, the prior study also showed comparable survival outcomes between the SMG preservation group and the removal group (9). However, in the current clinical practice, SMG excision is a regular part of level IB dissection in OSCC. In this study, we aimed to investigate the incidence and risk factors of SMG involvement in OSCC patients, which could add to the knowledge regarding the preservation of SMG in this patient subset.

MATERIALS AND METHODS

Data Collection and Patient's Selection Criteria

We retrospectively included patients diagnosed with OSCC between January 2018 and October 2020. Patients who met the following criteria were included in this study: (1) histopathologically confirmed SCC, (2) primary tumor located in the oral cavity, (3) received primary tumor resection and ipsilateral with or without contralateral neck dissection, and (4) removal of ipsilateral level IB and simultaneous removal of the SMG. All cases of OSCC were confirmed by histopathology. Patients who received preoperative chemotherapy, preoperative radiotherapy, or preoperative chemoradiotherapy were excluded. The study was approved by the Institutional Review Board of the First Affiliated Hospital of Xiamen University (approval number: XMYY-2021KY052). Written informed consent for participation was not required for this study in accordance with the national legislation and the institutional requirements.

Measures

OSCC in our institution was generally treated with primary surgical resection with concomitant neck dissection. All patients received standard neck dissection due to the higher incidence of occult nodal metastasis in OSCC (10, 11). The extent of neck dissection included a minimum of levels I–III with SMG resection in all cases. Bilateral neck dissection was conducted in those with tumors involving or approaching the midline. The following clinicopathologic characteristics were identified, including gender, age, primary tumor sites, smoking use, alcohol use, tumor grade, tumor (T) stage, nodal (N) stage, American Joint Committee on Cancer (AJCC) stage, surgery margin status, and the details of neck dissection. Slides stained with hematoxylin and eosin were assessed to confirm the diagnosis and to perform histopathological grading of the tumors based on the adaptation from Bryne et al. (12). The distribution of lymph node involvement in level IB and around the SMG was analyzed. The eighth edition of the AJCC staging was used in this study, which integrated the depth of invasion and extranodal extension into the tumor–node–metastasis (TNM) classification systems, respectively (13).

Statistical Analysis

The logistic regression analysis was performed to identify predictive factors associated with level IB lymph node metastasis. SPSS statistical software (version 25.0, IBM Corporation, Armonk, NY, USA) was used for data analysis. $p < 0.05$ was considered to be statistically significant.

RESULTS

Patients' Clinicopathological Characteristics

A total of 145 patients were identified in this study, namely, 96 males (66.2%) and 49 females (33.8%). The median age was 60 years (range, 27–83 years). **Table 1** lists the baseline characteristics of patients. Of these patients, 106 (73.1%), 20 (13.8%), 9 (6.2%), and 7 (4.8%) had tumors developed in the tongue, buccal mucosa, the floor of the mouth, and gingiva, respectively. In patients with available tumor grade (n = 143), moderately differentiated disease predominated with 76.2% (n = 109), and 11.9% (n = 17) and 11.9% (n = 17) of them were poorly differentiated and well-differentiated, respectively. There were 49 (33.8%), 64 (44.1%), 54 (14.5%), and 11 (7.6%) patients who had stage T1, T2, T3, and T4 diseases, respectively. A total of 117 (80.7%) patients underwent ipsilateral neck dissection and 28 (19.3%) underwent bilateral neck dissection. Sixty-one patients (42.1%) were pathologically diagnosed with lymph node metastases, including 11 (18.0%), 36 (59.0%), and 14 (23.0%) patients who had stage N1, N2, and N3 diseases, respectively. According to the 8th TNM staging, there were 38 (26.2%), 34 (23.4%), 20 (13.8%), and 53 (36.6%) patients who were pathologically diagnosed with stage I, II, III, and IVA diseases, respectively. Most of the patients (95.9%) had negative surgical margins.

Among all patients, 76 (52.4%) had a history of alcohol use, including 31 (40.8%, 31/76) patients with a history of alcohol abuse. In patients with alcohol abuse, the median daily Chinese Baijiu consumption was 150 ml (range, 50–700 ml), and the median alcohol intake time was 30 years (range, 2–40 years). In addition, there were 64 (44.1%) patients who had a history of smoking, the median smoking intensity was 20 (range, 2–60) cigarettes per day, the median smoking time was 30 years (range, 5–50 years), and the median smoking index was 30 pack-years (range, 2–120 pack-years).

SMG Invasion

Only one patient (0.7%) with stage IVA disease and primary tumor located in the tongue had involvement of the SMG.

TABLE 1 | Patient characteristics.

Variables	Number (%)
Gender	
Male	96 (66.2)
Female	49 (33.8)
Age	
<50 years	33 (22.8)
≥50 years	112 (77.2)
Primary site	
Lip	1 (0.7)
Upper jaw	1 (0.7)
Buccal mucosa	20 (13.8)
Mouth floor	9 (6.2)
Retromolar trigone	1 (0.7)
Tongue	106 (73.1)
Gingiva	7 (4.8)
Smoking pack-year index	
0	81 (55.9)
<20	17 (11.7)
≥20	47 (32.4)
Alcohol use	
Never	69 (47.6)
Normal	45 (31.0)
Abuse	31 (21.4)
Tumor grade	
Well differentiation	17 (11.7)
Moderate differentiation	109 (75.2)
Poor differentiation	17 (11.7)
Unknown	2 (1.4)
Tumor stage	
T1	49 (33.8)
T2	64 (44.1)
T3	21 (14.5)
T4	11 (7.6)
Nodal stage	
N0	84 (57.9)
N1	11 (7.6)
N2	36 (24.8)
N3	14 (9.7)
AJCC stage	
I	38 (26.2)
II	34 (23.4)
III	20 (13.8)
IVA	53 (36.6)
Margin status	
Negative	139 (95.9)
Positive	6 (4.1)
Neck dissection	
Ipsilateral	117 (80.7)
Bilateral	28 (19.3)
Submandibular gland involved	
No	144 (99.3)
Yes	1 (0.7)

AJCC, American Joint Committee on Cancer; T, tumor; N, nodal.

The SMG was involved by direct infiltration from the ventral tongue (**Figure 1**). This patient was a 57-year-old man who was clinically diagnosed with T4N2bM0 oral tongue cancer. The maximum diameter of the primary tumor was 6.8 cm. Ipsilateral neck dissection was performed. There were 36 lymph nodes that were dissected and 2 were metastasized. A preoperative computed tomography scan showed that the SMG was directly infiltrated by the primary tumor.

Peri-Submandibular Node Involvement

In the 61 patients with pathologically nodal positive diseases, level II was the most common site of regional lymph node metastasis (n = 57), followed by level III (n = 21), level IB (n = 16), level IA (n = 2), and level IV (n = 1). A total of 18 positive lymph nodes were found in level IB in 16 patients. The median maximum diameter of the positive lymph nodes around level IB was 1.49 cm (range, 1.17–2.61 cm). The patterns of peri-submandibular lymph node metastases are displayed in **Figures 2–4**. There were 6 lymph nodes in the lateral part of the SMG, and 12 were shown in the anterior of the SMG. However, no positive lymph node was observed in the medial or internal side of the SMG.

Risk Factors Associated With Level IB Lymph Node Metastasis

The logistic regression test was performed to determine the predictive factors associated with level IB lymph node metastasis (**Table 2**). The results showed that patients with tumors located in the buccal mucosa (the odds ratio [OR] for buccal mucosal cancer compared to tongue cancer was 6.852, 95% confidence interval [CI] 1.375–34.144, p = 0.019) and N3 stage (the OR for stage N3 disease compared to stage N1 disease was 13.333, 95%CI 1.321–134.615, p = 0.028) were the independent predictive factors associated with level IB lymph node metastasis.

DISCUSSION

In our study, we aimed to investigate the rationality of SMG-sparing neck dissection among patients with OSCC. Our study showed that only one patient (0.7%) had SMG involvement, and direct involvement was the most common way of SMG involvement in OSCC patients.

Although the neck dissection procedure has undergone several improvements, the SMG dissection was always recommended in OSCC (14, 15). In recent years, a growing number of evidence showed that the preservation of non-invaded SMG may be feasible in OSCC (8, 9, 16). There are three potential patterns of SMG involvement: anatomic proximity, hematogenous metastasis, and lymphatic spread (17). SMG is thought to lack a blood vessel network, which is different from other glands (17). Although a prior literature review showed a low risk of SMG metastasis in breast, lung, and renal cancers (18), no hematogenous metastasis in SMG was found in OSCC patients (17, 19, 20). In addition, SMG was thought to lack a lymphatic vessel network (17). Zeng et al. made a literature review that included 2,750 patients, and they found that only 0.07% of patients had intraglandular lymph node metastases (8). Furthermore, direct involvement was the main pattern of SMG involvement in OSCC (1%–2.9%) (16, 17, 19, 21). In our study, there was only one (0.7%) OSCC patient who had SMG involvement by direct infiltration from the primary tumor, which was similar to the above studies. Therefore, direct

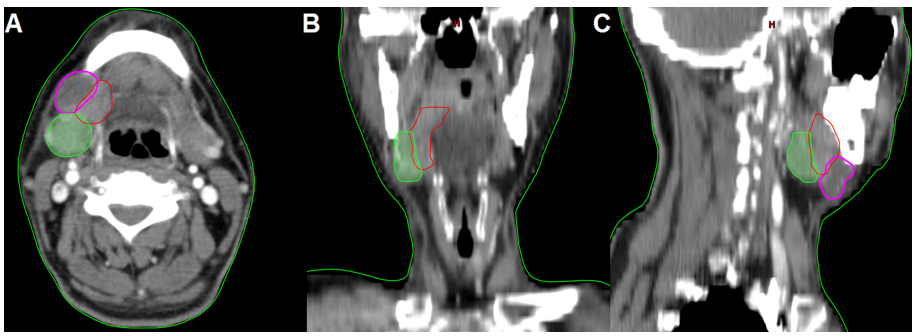

FIGURE 1 | The preoperative computed tomography image of submandibular gland involvement in axial **(A)**, coronal **(B)**, and sagittal views **(C)** (red, primary tumor; purple, lymphadenopathy in level IB; green, submandibular gland).

involvement is the most common pattern of SMG involvement in OSCC patients.

SMG is located in level IB according to the current recommendation of neck nodes delineation guideline (7). Fives et al. reported that approximately 44.4% of OSCC patients had pathologically confirmed positive lymph nodes in level I (4). In our study, 61 patients had pathologically nodal positive diseases and 26.2% of them ($n = 18$) had positive lymph nodes in level IB. Although the rate of level IB lymph node metastasis was relatively high in OSCC, the literature review showed that only 2.05% of patients had SMG involvement (8). In our study, no SMG involvement was observed through periglandular nodal extension. Peri-SMG lymph nodes are divided into six subgroups, and the deep groups have fewer lymph nodes, which have little clinical significance (22). In our study, there were 6 lymph nodes in the lateral part of SMG, 12 in the anterior of SMG, and no lymph node was observed in the medial or internal side of SMG. A large cohort of patients with nasopharyngeal carcinoma also showed no patients had SMG metastasis or metastasis to the medial edge of SMG (23). In the

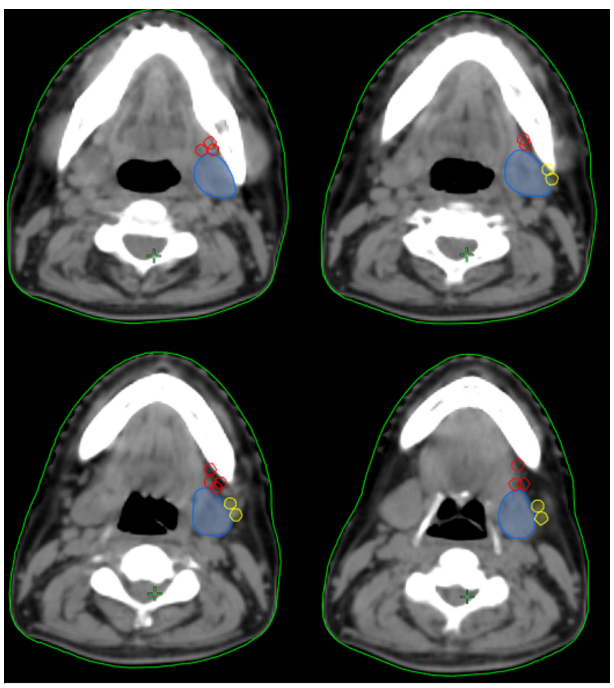

FIGURE 2 | The patterns of peri-submandibular lymph node metastases in oral squamous cell carcinoma (blue, submandibular gland; red, lymph node metastases in the anterior part of the submandibular gland; yellow, lymph node metastases in the lateral part of the submandibular gland).

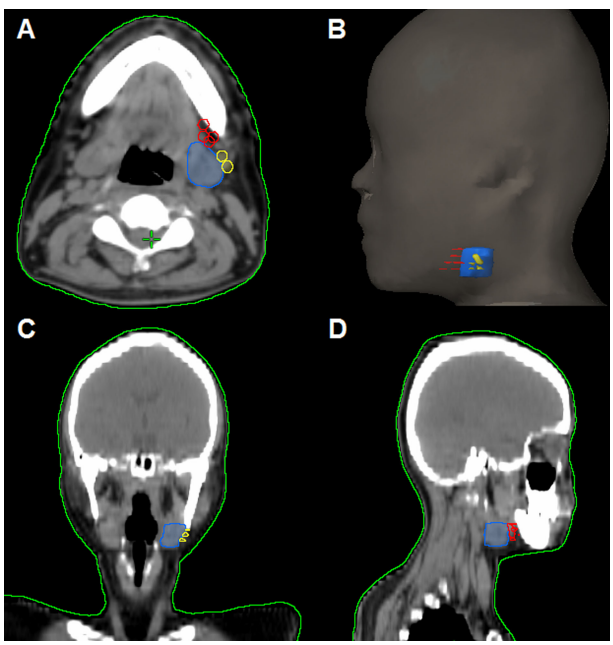

FIGURE 3 | The patterns of peri-submandibular lymph node metastases in axial **(A)**, three-dimensional **(B)**, coronal **(C)**, and sagittal views **(D)** (blue, submandibular gland; red, lymph node metastases in the anterior part of the submandibular gland; yellow, lymph node metastases in the lateral part of the submandibular gland).

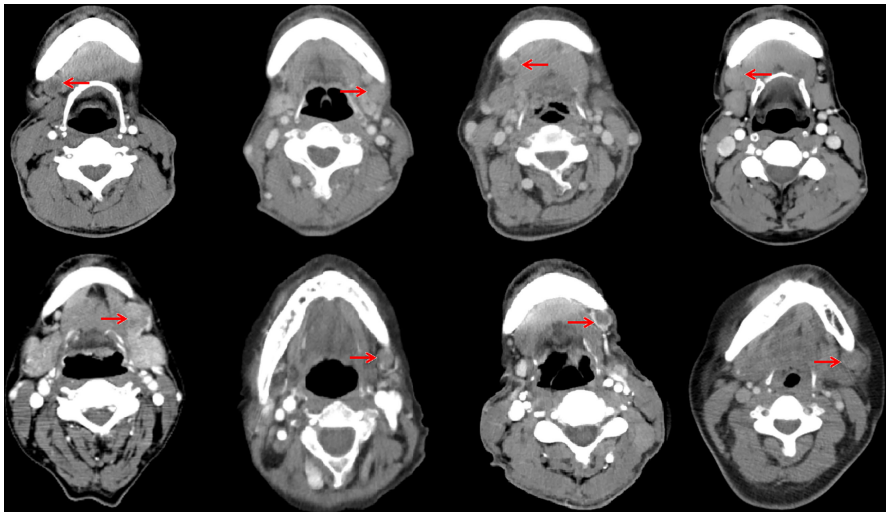

FIGURE 4 | Computed tomography axial images from patients with lymphadenopathy in level IB (red arrow, lymphadenopathy in level IB).

TABLE 2 | Independent predictive factors associated with level IB lymph node metastasis in patients with node-positive disease (n = 61).

Variables	OR	95% CI	p
Gender			
Male	1		
Female	0.418	0.104–1.689	0.221
Age			
<50 years	1		
≥50 years	0.553	0.138–2.217	0.403
Primary sites			
Tongue	1		
Buccal mucosa	6.852	1.375–34.144	0.019
Others	1.644	0.273–9.892	0.587
Alcohol use			
No	1		
Normal	1.971	0.527–7.374	0.313
Abuse	0.821	0.179–3.374	0.800
Smoking pack-year index			
0	1		
<20	1.667	0.329–8.434	0.537
≥20	0.741	0.194–2.830	0.661
Tumor differentiation			
Well differentiation	1		
Moderate differentiation	0.455	0.066–3.113	0.422
Poor differentiation	0.667	0.078–5.678	0.711
Tumor stage			
T1	1		
T2	0.913	0.193–4.330	0.909
T3	0.667	0.089–4.994	0.693
T4	3.000	0.447–20.153	0.258
Nodal stage			
N1	1		
N2	2.414	0.263–22.117	0.436
N3	13.333	1.321–134.615	0.028
Margin status			
Negative	1		
Positive	0.933	0.090–9.677	0.954

OR, odds ratio; CI, confidence interval; T, tumor; N, nodal.

current clinical practice, resection of all lymph nodes in level IB and preservation of the SMG are technically feasible for OSCC patients (24). Therefore, with careful preoperative imaging evaluation and intraoperative evaluation of the relationship between primary tumor and metastatic lymph nodes or SMG, SMG-sparing neck dissection may be feasible and safe if the SMG is not involved.

The SMG secretes approximately 70%–90% of the amount of unstimulated salivary, especially at night (25). Saliva plays an important role in oral cavity lubrication, oral antimicrobial activity maintenance, tooth remineralization, and oral mucosal immunity (17). Removal of SMG would increase the incidence of xerostomia and influence the quality of life (17). In addition, in OSCC patients receiving adjuvant radiotherapy, the irradiation of the contralateral SMG could further increase xerostomia because SMG is a part of level IB treatment in the consensus guidelines (7). Moreover, resection of the SMG may also result in external contour defects in the neck (26). Several studies have found that the SMG may be involved by direct invasion of the primary lesion or by spread from adjacent metastatic cervical lymph nodes (21, 27). Advanced T stage and mouth floor tumors were also the risk factors for a direct invasion of SMG (17, 22, 26, 28). In our study, we did not analyze the relationship between clinicopathological factors associated with SMG involvement because limited patients had SMG involvement. We only found one patient with T4N2bM0 oral tongue cancer who had a tumor infiltrated to SMG.

In the recent two decades, there has been controversy over whether SMG needs to be removed in OSCC. With the in-depth understanding of the patterns of lymph node metastases in the neck, selective neck dissection has become widely accepted in the treatment of OSCC. The distribution of lymph node metastases in the neck in our study was similar to the previous studies (29,

30). Since the SMG does not contain intraglandular lymph nodes, removal of an uninvolved SMG may not always be necessary, which has the potential benefit to reduce postoperative xerostomia (26). We also only found one patient with SMG involvement by direct invasion of the primary tumor. The study from Chen et al. showed that stage T4 disease and N2b–N3 tumors were the risk factor for SMG invasion, especially for those with buccal mucosal cancer and cancer located in the alveolar ridge (28). Therefore, the anatomical proximity of primary cancer must be taken into consideration while evaluating the patient for SMG preservation.

According to previous studies, the true infiltration of the SMG by OSCC is quite rare, suggesting that the SMG might not be contaminated and thus be considered to be preserved during level IB lymph node dissection (17, 26, 28). However, we should emphasize the limited insight into the operating field when preserving the SMG during neck dissection, including the risk of nerve injuries and the risk of missing affected lymph nodes (9, 31). In the clinical practice, the protection of SMG may also be safe. Zeng et al. confirmed the oncological safety of SMG flaps in repairing postoperative OSCC defects (8). Moreover, SMG transplantation to the anterior submental region has been found to protect the gland from the dry mouth during radiotherapy (32). Regarding the contemporary radiotherapy techniques, William et al. demonstrated the feasibility of SMG preservation by maintaining a mean dose to the gland of ≤39 Gy (33).

In our study, patients with buccal mucosal cancer and N3 stage have a higher risk of level IB metastasis. However, there was no significant association between T stage and level IB metastasis. Several studies also have shown that the T stage was not a risk factor for level IB metastasis (16, 26, 34).

Several limitations should be acknowledged in the current study. First, it was a retrospective study with relatively small sample size. Second, our study does not include information on actual complaints by patients concerning the removal of SMG. Third, as the follow-up time in our study was relatively short, a long-term observation is required to determine the risk of tumor recurrence in level IB. Finally, the long-term safety of SMG preservation in OSCC should be performed by the prospective studies. Despite these limitations, we believe that our findings add the knowledge regarding the preservation of SMG for OSCC patients.

CONCLUSION

In conclusion, our study suggests that the involvement of SMG is extremely rare in OSCC. Preservation of the SMG during neck dissection in selected patients with OSCC seems to be feasible and oncologically safe. More studies are needed to investigate the candidates who may be feasible and safe to preserve SMG.

DATA AVAILABILITY STATEMENT

The raw data supporting the conclusions of this article is available from the corresponding author on reasonable request.

ETHICS STATEMENT

The study was approved by the Institutional Review Board of the First Affiliated Hospital of Xiamen University. Written informed consent for participation was not required for this study in accordance with the national legislation and the institutional requirements.

AUTHOR CONTRIBUTIONS

PZ, J-XC, YZ, BY, and S-GW are lead authors who participated in data collection, manuscript drafting, tables/figures creation, and manuscript revision. PZ and C-LL aided in data collection. PZ, J-XC, and YZ are senior authors who aided in drafting the manuscript and manuscript revision. BY and S-GW are the corresponding authors who initially developed the concept and drafted and revised the manuscript. All authors contributed to the article and approved the submitted version.

FUNDING

This work was partly supported by the Key R&D Plan of Hainan Province (No. ZDYF2021SHFZ115).

REFERENCES

1. Sung H, Ferlay J, Siegel RL, Laversanne M, Soerjomataram I, Jemal A, et al. Global Cancer Statistics 2020: GLOBOCAN Estimates of Incidence and Mortality Worldwide for 36 Cancers in 185 Countries. *CA Cancer J Clin* (2021) 71(3):209–49. doi: 10.3322/caac.21660
2. Pulte D, Brenner H. Changes in Survival in Head and Neck Cancers in the Late 20th and Early 21st Century: A Period Analysis. *Oncologist* (2010) 15 (9):994–1001. doi: 10.1634/theoncologist.2009-0289
3. Zanoni DK, Montero PH, Migliacci JC, Shah JP, Wong RJ, Ganly I, et al. Survival Outcomes After Treatment of Cancer of the Oral Cavity (1985-2015). *Oral Oncol* (2019) 90:115–21. doi: 10.1016/j.oraloncology.2019.02.001
4. Fives C, Feeley L, Sadadcharam M, O'Leary G, Sheahan P. Incidence of Intraglandular Lymph Nodes Within Submandibular Gland, and Involvement by Floor of Mouth Cancer. *Eur Arch Otorhinolaryngol* (2017) 274(1):461–6. doi: 10.1007/s00405-016-4205-0
5. Peng KA, Chu AC, Lai C, Grogan T, Elashoff D, Abemayor E, et al. Is There a Role for Neck Dissection in T1 Oral Tongue Squamous Cell Carcinoma? The UCLA Experience. *Am J Otolaryngol* (2014) 35(6):741–6. doi: 10.1016/j.amjoto.2014.06.019
6. Omura K. Current Status of Oral Cancer Treatment Strategies: Surgical Treatments for Oral Squamous Cell Carcinoma. *Int J Clin Oncol* (2014) 19 (3):423–30. doi: 10.1007/s10147-014-0689-z
7. Grégoire V, Ang K, Budach W, Grau C, Hamoir M, Langendijk JA, et al. Delineation of the Neck Node Levels for Head and Neck Tumors: A 2013 Update. DAHANCA, EORTC, HKNPCSG, NCIC CTG, NCRI, RTOG, TROG Consensus Guidelines. *Radiother Oncol* (2014) 110(1):172–81. doi: 10.1016/j.radonc.2013.10.010
8. Zeng W, Qiu CY, Liu JF, Pan Y, Li R, Luo K, et al. The Preservation and Application of the Submandibular Gland in Oral Squamous Cell Carcinoma

(STROBE). *Med (Baltimore)* (2019) 98(52):e18520. doi: 10.1097/MD.0000000000018520
9. Gu B, Fang Q, Wu Y, Du W, Zhang X, Chen D. Impact of Submandibular Gland Preservation in Neck Management of Early-Stage Buccal Squamous Cell Carcinoma on Locoregional Control and Disease-Specific Survival. *BMC Cancer* (2020) 20(1):1034. doi: 10.1186/s12885-020-07534-5
10. Arain AA, Rajput MSA, Ansari SA, Mahmood Z, Ahmad AN, Dogar MR, et al. Occult Nodal Metastasis in Oral Cavity Cancers. *Cureus* (2020) 12(11): e11640. doi: 10.7759/cureus.11640
11. d'Alessandro AF, Pinto FR, Lin CS, Kulcsar MA, Cernea CR, Brandão LG, et al. Oral Cavity Squamous Cell Carcinoma: Factors Related to Occult Lymph Node Metastasis. *Braz J Otorhinolaryngol* (2015) 81(3):248–54. doi: 10.1016/j.bjorl.2015.03.004
12. Bryne M, Koppang HS, Lilleng R, Kjaerheim A. Malignancy Grading of the Deep Invasive Margins of Oral Squamous Cell Carcinomas has High Prognostic Value. *J Pathol* (1992) 166(4):375–81. doi: 10.1002/path.1711660409
13. Lydiatt WM, Patel SG, O'Sullivan B, Brandwein MS, Ridge JA, Migliacci JC, et al. Head and Neck Cancers-Major Changes in the American Joint Committee on Cancer Eighth Edition Cancer Staging Manual. *CA Cancer J Clin* (2017) 67(2):122–37. doi: 10.3322/caac.21389
14. Crile GIII. On the Technique of Operations Upon the Head and Neck. *Ann Surg* (1906) 44(6):842–50. doi: 10.1097/00000658-190612000-00003
15. Bocca E, Pignataro O. A Conservation Technique in Radical Neck Dissection. *Ann Otol Rhinol Laryngol* (1967) 76(5):975–87. doi: 10.1177/000348946707600508
16. Cakir Cetin A, Dogan E, Ozay H, Kumus O, Erdag TK, Karabay N, et al. Submandibular Gland Invasion and Feasibility of Gland-Sparing Neck Dissection in Oral Cavity Carcinoma. *J Laryngol Otol* (2018) 132(5):446–51. doi: 10.1017/S0022215118000592
17. Byeon HK, Lim YC, Koo BS, Choi EC. Metastasis to the Submandibular Gland in Oral Cavity Squamous Cell Carcinomas: Pathologic Analysis. *Acta Otolaryngol* (2009) 129(1):96–100. doi: 10.1080/00016480802032801
18. Vessecchia G, Di Palma S, Giardini R. Submandibular Gland Metastasis of Breast Carcinoma: A Case Report and Review of the Literature. *Virchows Arch* (1995) 427(3):349–51. doi: 10.1007/BF00203404
19. Naidu TK, Naidoo SK, Ramdial PK. Oral Cavity Squamous Cell Carcinoma Metastasis to the Submandibular Gland. *J Laryngol Otol* (2012) 126(3):279–84. doi: 10.1017/S0022215111002660
20. Ebrahim AK, Loock JW, Afrogheh A, Hille J. Is it Oncologically Safe to Leave the Ipsilateral Submandibular Gland During Neck Dissection for Head and Neck Squamous Cell Carcinoma? *J Laryngol Otol* (2011) 125(8):837–40. doi: 10.1017/S0022215111001095
21. Yang S, Su JZ, Gao Y, Yu GY. Clinicopathological Study of Involvement of the Submandibular Gland in Oral Squamous Cell Carcinoma. *Br J Oral Maxillofac Surg* (2020) 58(2):203–7. doi: 10.1016/j.bjoms.2019.11.016
22. DiNardo LJ. Lymphatics of the Submandibular Space: An Anatomic, Clinical, and Pathologic Study With Applications to Floor-of-Mouth Carcinoma. *Laryngoscope* (1998) 108(2):206–14. doi: 10.1097/00005537-199802000-00009
23. Lin L, Lu Y, Wang XJ, Chen H, Yu S, Tian J, et al. Delineation of Neck Clinical Target Volume Specific to Nasopharyngeal Carcinoma Based on Lymph Node Distribution and the International Consensus Guidelines. *Int J Radiat Oncol Biol Phys* (2018) 100(4):891–902. doi: 10.1016/j.ijrobp.2017.11.004
24. Dhiwakar M, Ronen O, Malone J, Rao K, Bell S, Phillips R, et al. Feasibility of Submandibular Gland Preservation in Neck Dissection: A Prospective Anatomic-Pathologic Study. *Head Neck* (2011) 33(5):603–9. doi: 10.1002/hed.21499
25. Jacob RF, Weber RS, King GE. Whole Salivary Flow Rates Following Submandibular Gland Resection. *Head Neck* (1996) 18(3):242–7. doi: 10.1002/(SICI)1097-0347(199605/06)18:3<242::AID-HED6>3.0.CO;2-#
26. Razfar A, Walvekar RR, Melkane A, Johnson JT, Myers EN. Incidence and Patterns of Regional Metastasis in Early Oral Squamous Cell Cancers: Feasibility of Submandibular Gland Preservation. *Head Neck* (2009) 31 (12):1619–23. doi: 10.1002/hed.21129
27. Malgonde MS, Kumar M. Practicability of Submandibular Gland in Squamous Cell Carcinomas of Oral Cavity. *Indian J Otolaryngol Head Neck Surg* (2015) 67(Suppl 1):138–40. doi: 10.1007/s12070-014-0803-6
28. Chen TC, Lo WC, Ko JY, Lou PJ, Yang TL, Wang CP. Rare Involvement of Submandibular Gland by Oral Squamous Cell Carcinoma. *Head Neck* (2009) 31(7):877–81. doi: 10.1002/hed.21039
29. Lim YC, Koo BS, Lee JS, Lim JY, Choi EC. Distributions of Cervical Lymph Node Metastases in Oropharyngeal Carcinoma: Therapeutic Implications for the N0 Neck. *Laryngoscope* (2006) 116(7):1148–52. doi: 10.1097/01.mlg.0000217543.40027.1d
30. Dogan E, Cetinayak HO, Sarioglu S, Erdag TK, Ikiz AO. Patterns of Cervical Lymph Node Metastases in Oral Tongue Squamous Cell Carcinoma: Implications for Elective and Therapeutic Neck Dissection. *J Laryngol Otol* (2014) 128(3):268–73. doi: 10.1017/S0022215114000267
31. Markey JD, Morrel WG, Wang SJ, Ryan WR. The Effect of Submandibular Gland Preservation During Level 1B Neck Dissection on Postoperative Xerostomia. *Auris Nasus Larynx* (2018) 45(1):123–7. doi: 10.1016/j.anl.2017.03.005
32. Jha N, Seikaly H, McGaw T, Coulter L. Submandibular Salivary Gland Transfer Prevents Radiation-Induced Xerostomia. *Int J Radiat Oncol Biol Phys* (2000) 46(1):7–11. doi: 10.1016/s0360-3016(99)00460-5
33. Jackson WC, Hawkins PG, Arnould GS, Yao J, Mayo C, Mierzwa M. Submandibular Gland Sparing When Irradiating Neck Level IB in the Treatment of Oral Squamous Cell Carcinoma. *Med Dosim* (2019) 44 (2):144–9. doi: 10.1016/j.meddos.2018.04.003
34. Subramaniam N, Balasubramanian D, Reddy R, Rathod P, Murthy S, Vidhyadharan S, et al. Determinants of Level Ib Involvement in Oral Squamous Cell Carcinoma and Implications for Submandibular Gland-Sparing Neck Dissection. *Int J Oral Maxillofac Surg* (2018) 47(12):1507–10. doi: 10.1016/j.ijom.2017.11.019

Conflict of Interest: The authors declare that the research was conducted in the absence of any commercial or financial relationships that could be construed as a potential conflict of interest.

frontiers in Oncology

ORIGINAL RESEARCH
published: 05 January 2022
doi: 10.3389/fonc.2021.789248

Salivary Metabolomics for Prognosis of Oral Squamous Cell Carcinoma

Shigeo Ishikawa[1], Masahiro Sugimoto[2], Tsuneo Konta[3], Kenichiro Kitabatake[1], Shohei Ueda[1], Kaoru Edamatsu[1], Naoki Okuyama[1], Kazuyuki Yusa[1] and Mitsuyoshi Iino[1]*

[1] Department of Dentistry, Oral and Maxillofacial Plastic and Reconstructive Surgery, Faculty of Medicine, Yamagata University, Iida-nishi, Japan, [2] Health Promotion and Pre-emptive Medicine, Research and Development Center for Minimally Invasive Therapies, Tokyo Medical University, Shinjuku, Japan, [3] Department of Public Health and Hygiene, Yamagata University Graduate School of Medicine, Iida-nishi, Japan

This study aimed to identify salivary metabolomic biomarkers for predicting the prognosis of oral squamous cell carcinoma (OSCC) based on comprehensive metabolomic analyses. Quantified metabolomics data of unstimulated saliva samples collected from patients with OSCC (n = 72) were randomly divided into the training (n = 35) and validation groups (n = 37). The training data were used to develop a Cox proportional hazards regression model for identifying significant metabolites as prognostic factors for overall survival (OS) and disease-free survival. Moreover, the validation group was used to develop another Cox proportional hazards regression model using the previously identified metabolites. There were no significant between-group differences in the participants' characteristics, including age, sex, and the median follow-up periods (55 months [range: 3–100] *vs.* 43 months [range: 0–97]). The concentrations of 5-hydroxylysine (p = 0.009) and 3-methylhistidine (p = 0.012) were identified as significant prognostic factors for OS in the training group. Among them, the concentration of 3-methylhistidine was a significant prognostic factor for OS in the validation group (p = 0.048). Our findings revealed that salivary 3-methylhistidine is a prognostic factor for OS in patients with OSCC.

Keywords: metabolomics, oral squamous cell carcinoma (OSCC), prognosis, saliva, overall survival, disease-free survival

OPEN ACCESS

Edited by:
Steffi Ulrike Pigorsch, Technical University of Munich, Germany

Reviewed by:
Vito Carlo Alberto Caponio, University of Foggia, Italy
Lucas Delmonico, Federal University of Rio de Janeiro, Brazil

****Correspondence:***
Masahiro Sugimoto
mshrsgmt@gmail.com

Specialty section:
This article was submitted to Head and Neck Cancer, a section of the journal Frontiers in Oncology

Received: *04 October 2021*
Accepted: *14 December 2021*
Published: *05 January 2022*

Citation:
Ishikawa S, Sugimoto M, Konta T, Kitabatake K, Ueda S, Edamatsu K, Okuyama N, Yusa K and Iino M (2022) Salivary Metabolomics for Prognosis of Oral Squamous Cell Carcinoma. Front. Oncol. 11:789248. doi: 10.3389/fonc.2021.789248

INTRODUCTION

Oral cancer occurs in the oral cavity, with oral squamous cell carcinoma (OSCC) accounting for 90% of all cases of oral cancer (https://gco.iarc.fr/). The oral cavity can be visualized without using special devices; therefore, OSCC is assumed to be easily detected. However, most OSCCs are frequently detected in advanced stages (1, 2), with these OSCCs showing a poor prognosis. Furthermore, there has been no substantial improvement in the long-term survival rate of OSCC in advanced stages over the past few decades (3–6). Therefore, there is a critical need to improve the prognosis of OSCC.

Moreover, it is critical to accurately predict the prognosis of OSCC before oncological treatment. Various clinicopathological parameters can accurately predict the prognosis of OSCC, with cancer

staging being the most common predictor (7). An advanced tumor-node-metastasis stage, including cervical lymph node metastasis or distant metastasis, is widely considered to be indicative of a poor prognosis of OSCC (3, 4, 8). Further, the invasion mode and tumor grade are established pathological parameters for predicting prognosis (4). Additionally, the clinical type of tumor growth, including extraversion or inward, is a clinical parameter for predicting the prognosis of oral cancer (4). However, these clinicopathological prognostic parameters should be far from optimal evidence because these predictors have relatively low efficiency and specificity.

Accordingly, molecular biomarkers provide a more objective criterion for prognostic prediction. There is a need for novel strategies to facilitate biomarker-guided treatment selection based on individual tumor differences (2, 9). Recent studies have demonstrated that molecular biomarkers can predict OSCC given the development of analytical methods. Specifically, there has been remarkable development in the application of sequencing technology; moreover, there are numerous ribonucleic acid biomarkers for predicting the prognosis of OSCC (9–11). Additionally, the metabolomic approach to cancer-specific biomarkers is promising. Cancer-specific abnormal metabolism, including the Warburg effect, which utilizes adenosine triphosphate synthesis to sustain rapidly growing cancerous cells rather than readily available oxygen from the surrounding environment, is well described (12, 13). Moreover, salivary metabolomics is an emerging approach for the diagnosis or screening of oral cancers, including OSCC, leukoplakia, and lichen planus (13). Saliva is an ideal biofluid with vast information reflecting the systemic health status that could be used to detect various diseases (12, 13). Applying salivary metabolites is plausible since these molecules may be transferred into saliva by various cells, including OSCC, present in the oral cavity and salivary glands; moreover, saliva allows non-invasive analysis (12). However, to our knowledge, the identification of the prognostic biomarkers of OSCC using salivary metabolomics has not been reported. We aimed to identify salivary metabolomic biomarkers for predicting the prognosis of OSCC.

MATERIALS AND METHODS

This study was performed as part of ongoing research on salivary biomarkers for cancer screening at Yamagata University. The study protocol was approved by the Ethics Committee of Yamagata University Faculty of Medicine (#2021-176). All study procedures involving human participants were conducted following the ethical standards of the institutional and/or national research committee, as well as the 1964 Declaration of Helsinki and its later amendments or comparable ethical standards.

Consent was obtained through an online opt-out method, with none of the eligible patients declining participation. Patients with OSCC were recruited from the Department of Dentistry, Oral and Maxillofacial Surgery, Yamagata University Hospital between April 2012 and March 2017. Patients who received curative treatment, such as radical surgery or chemoradiotherapy, were included in this study, whereas patients who received non-curative treatment, such as palliative treatment or symptomatic treatment, were excluded. The total number of patients was 72. One patient rejected surgery and received super-selective intra-arterial chemotherapy and daily concurrent radiotherapy, with the remaining patients undergoing resection surgery. All the patients underwent pathological diagnosis through incisional open biopsy and excised specimens.

Saliva Collection and Sample Preparation

The protocol for saliva collection has been described previously (13–16). Briefly, before saliva collection, a skilled dentist and dental hygienist checked the oral hygiene of all participants. Remarkable dental plaque and calculus deposits were removed using a toothbrush without dentifrice and ultrasonic scaling at ≥ 3 h before saliva collection. All participants were asked to refrain from eating and drinking for ≥ 1.5 h before saliva collection. The participants rinsed their mouths with water before sample collection and split their saliva into 50 cc Falcon tubes (Corning, Inc., Corning, NY, USA) in a paper cup filled with crushed ice. Subsequently, approximately 3 mL of unstimulated whole saliva was collected for approximately 5 min. Finally, the samples were aliquoted into smaller volumes and stored at -80°C.

Metabolomic Analysis of Saliva

We performed a metabolomic analysis of saliva samples as previously described (13–17). Briefly, frozen saliva was thawed and dissolved at room temperature. To remove macromolecules, the samples were centrifuged through a 5-kDa cut-off filter (Pall, Tokyo, Japan) at 9100 × g. The filtrate (45 μL) was removed and added to a 1.5-mL Eppendorf tube, followed by the addition and mixing of 5 μL of water containing 2 mM methionine sulphone, 2-(N-morpholino) ethane sulfonic acid, d-camphor-10-sulphonic acid, sodium salt, 3-aminopyrrolidine, and trimesate. Capillary electrophoresis time-of-flight mass spectrometry was performed to quantify the charged metabolites in the positive and negative modes. Raw data were processed using MasterHands software (Keio University, Yamagata, Japan). Metabolites were identified by matching the corresponding m/z values and migration times; further, absolute concentrations were calculated by comparing the peak area (normalized by those of internal standards) with those of standard mixtures (13–17). Our metabolomics data were comprised of two batches of data obtained from 23 (batch 1) and 49 (batch 2) participants, respectively. The data of 20 of the 23 participants in batch 1 were retrieved from a previous study (13), and the data of 3 of the 23 participants in batch 1 were unpublished data. The data of 20 of the 49 participants in batch 2 were retrieved from another previous study (15), and the data of 29 of the 49 participants in batch 2 were unpublished data. Both studies assessed screening of oral cancer using different concepts.

Statistical Analyses

As aforementioned, we evaluated the unexpected bias caused by two batches. We performed a principal component analysis (PCA) to confirm the between-batch similarity. The distribution of quantitative and qualitative variables was analyzed using the

Mann–Whitney U test and chi-square test, respectively. For salivary metabolites, frequently detected metabolites (> 30% of all participants) were used for subsequent analyses. All data (n = 72) were randomly divided into the training (n = 35) and validation (n = 37) groups. Using data from the training group, we calculated the hazard ratios (HRs) and 95% confidence intervals (CIs) using the Cox proportional hazards regression model to assess prognostic factors for overall survival (OS) and disease-free survival (DFS). The multivariate-adjusted model was performed using backward elimination. Significant variables in the multivariate-adjusted model using the training group were included in the Cox proportional hazards regression model using the validation group. Specifically, using significant variables identified from the training group, we calculated HR and 95% CI for assessing the prognostic factors for OS and DFS in the validation group. Regarding the significant variables in the validation group, the survival curves were drawn using the Kaplan-Meier method and compared using the log-rank test. Spearman's rank correlation coefficient was used to evaluate the relationship between salivary metabolites and continuous variables (age, stage, early phase standard uptake value, and late phase standard uptake value). Furthermore, Mann-Whitney U test was used to evaluate the relationship between salivary metabolites and discrete variable (sex). Statistical analyses were performed using SPSS software, version 20 (SPSS, Inc., Chicago, IL, USA) and MetaboAnalyst (18) (http://www.metaboanalyst.ca/).

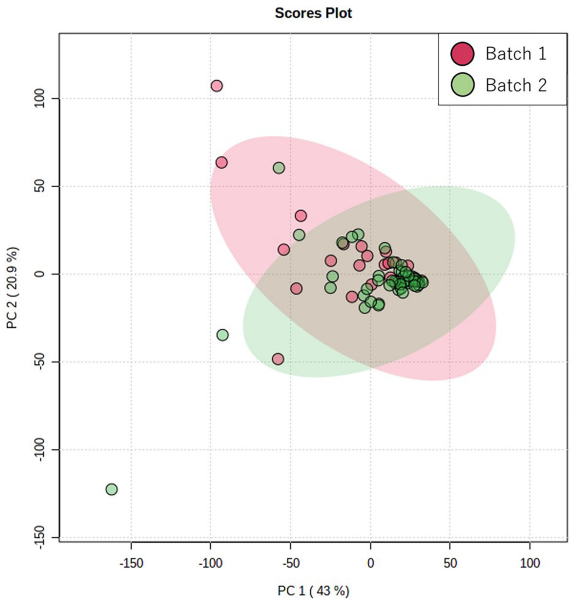

FIGURE 1 | Score plots of principal component analysis using Pareto scaling PC1 and PC2 indicate the first and second principal components, respectively. The red and green plots indicate the samples collected in batches 1 and 2, respectively. The contribution rates of PC1 and PC2 were 43.1% and 20.95%, respectively.

RESULTS

Figure 1 shows the score plots of the PCA of two batches. The distance of the plots is inversely related to the similarities in the metabolite concentration patterns of the two batches. Most of the batch 1 (red) and batch 2 plots (green) converged at similar parts of the score plots. These distributions were indicative of the similarity between samples from batch 1 and batch 2. **Table 1** shows the participants' characteristics, including age, sex, and smoking habit, as well as clinical parameters, including staging, OSCC antigen levels, standard uptake values of positron emission tomography/computed tomography (CT) in the early/late phases, and follow-up durations. None of the clinical parameters showed significant between-group differences. The median follow-up periods were 57 (range: 3–100) months and 43 (range: 0–97) months in the training and validation groups, respectively.

TABLE 1 | Characteristics of all participants (n = 72).

Variable		Training Group (n = 35)	Validation Group (n = 37)	p-value[†]
Sex	Male (%)	20 (57.1)	18 (48.6)	0.314
	Female (%)	15 (42.9)	19 (51.4)	
Smoking	Yes (%)	2 (5.7)	6 (16.2)	0.149
Stage	0 (CIS) (%)	2 (5.7)	1 (2.7)	0.059
	I (%)	16 (45.7)	8 (21.6)	
	II (%)	6 (17.1)	8 (21.6)	
	III (%)	3 (8.6)	10 (27.0)	
	IV (%)	8 (22.9)	10 (27.0)	
SCC antigen[§]	1.5< (%)	9 (25.7)	8 (21.6)	0.423
	1.5≥ (%)	16 (45.7)	19 (51.3)	
				p-value[‡]
Age	median (min-max)	65.0 (26-89)	69 (23-94)	0.313
Early phase Standard Uptake Value	median (min-max)	10.7 (2.2-23.2)	11.1 (3.0-22.0)	0.245
Late phase Standard Uptake Value	median (min-max)	11.6 (1.8-26.9)	13.44 (4.0-30.0)	0.172
Follow-up period(month)	median (min-max)	55 (3-100)	43 (0-97)	0.101

[†]*p-value by chi-square test.*
[‡]*p-value by Mann-Whitney U-test.*
[§]*Missing data were 28.6% and 27.0% of each group.*
SCC, squamous cell carcinoma.

Supplementary Table 1 shows the unadjusted and adjusted HRs for variables associated with OS in the training group. Univariate analysis of the training data identified proline (HR = 1.001, p = 0.020), carnitine (HR = 1.047, p = 0.042), 5-hydroxylysine (HR = 1.110, p = 0.019), 3-methylhistidine (HR = 3.261, p = 0.035), adenosine (HR = 8.301, p = 0.003), inosine (HR = 1.369, p = 0.040), and *N*-acetylglucosamine (HR = 1.027, p = 0.004) as significant prognostic factors for predicting OS in patients with OSCC. Subsequent multivariate analysis using training data revealed that 3-methylhistidine and 5-hydroxylysine were significant prognostic factors for OS in patients with OSCC (HR = 4.865 and 1.142, p = 0.012 and 0.009, respectively). **Table 2** shows the adjusted HRs for variables associated with OS in the validation group. Two metabolites, 3-methylhistidine and 5-hydroxylysine, were adopted in the multivariate analysis of the validation group, with only 3-methylhistidine being identified as a significant prognostic factor (HR = 1.711, p = 0.048). **Supplementary Table 2** shows the unadjusted and adjusted HRs for variables associated with DFS in the training group. Univariate analysis using training data revealed that creatinine (HR = 1.157, p = 0.048), proline (HR = 1.002, p = 0.029), and *N*-acetylglucosamine (HR = 1.026, p = 0.016) were significant prognostic factors for DFS in OSCC. Subsequent multivariate analysis showed that salivary *N*-acetylglucosamine was a significant prognostic factor for DFS in patients with OSCC (HR = 1.026, p = 0.016). Accordingly, salivary *N*-acetylglucosamine was adopted in the model in the validation group; however, it was not identified as a significant prognostic factor for DFS (HR = 0.988, p = 0.099) (**Table 3**). **Figures 2**, **3** show Kaplan-Meier survival curves for OS and DFS, respectively, based on the definitive variable adopted in the Cox hazard model for the validation group. Participants with higher levels of salivary 3-methylhistidine (> median) had significantly lower OS rates than those with lower levels of salivary 3-methylhistidine (< median) in the validation group (p = 0.020). Participants with lower levels of salivary N-acetylglucosamine (< median) had significantly lower DFS rates than those with higher levels of salivary *N*-acetylglucosamine (> median) in the validation group (p = 0.048). **Supplementary Tables 3, 4** show the correlation coefficient between salivary metabolites and continuous clinical variables in the training and validation groups, respectively. Despite the correlations among age and a few metabolites, most metabolites showed no correlations with stage, early phase standard uptake value, and late phase standard uptake value. **Supplementary Tables 5, 6** show the sex-dependency of salivary metabolites. Only two metabolites (creatinine and indole-3-acetate) showed a significant difference between male and female participants.

DISCUSSION

This study analyzed the relationships between salivary metabolites and the prognosis of OSCC. We found that salivary 3-methylhistidine was a significant prognostic biomarker for predicting OS in patients with OSCC in both the training and validation groups. OSCC staging, including the TN-stage, and surgical margin status are the most established clinical prognostic factors (19). Imaging-based biomarkers, including CT, magnetic resonance imaging, and F-fluorodeoxyglucose positron emission tomography/CT parameters, are established prognostic factors for OSCC (20, 21). Recently, molecular biomarkers quantified through liquid and tissue biopsy have been reported (2, 22, 23). However, the liquid biopsy applied to blood, rather than saliva, as the biofluid (2, 22, 23). Most surveys were performed using genomics, transcriptomics, or proteomics approaches, rather than a metabolomics approach (2, 24, 25). To our knowledge, this is the first study to identify salivary metabolites for predicting the prognosis of OSCC, which makes our findings significant.

Two studies have used blood metabolomics approaches to identify prognostic biomarkers of OSCC (26, 27). Cadoni et al. reported that 12 serum metabolites, including 3-methylhistidine, were biomarkers for predicting OS in head and neck cancer, including OSCC (27). We found that salivary 3-methylhistidine was a significant prognostic biomarker for OS. Generally, 3-methylhistidine is considered a marker of muscle proteolysis; moreover, increased 3-methylhistidine levels could be biomarkers of frailty and sarcopenia (27, 28). General statuses, including Karnofsky performance status, sarcopenia status, and frailty status, are well-known prognostic factors for OS in head and neck

TABLE 2 | Adjusted hazard ratios and 95% confidence intervals for variables associated with overall survival in the validation group.

Variable		Adjusted HR	(95% CI)	p-value	
3-Methylhistidine	(per 1 increase)	1.711	1.004-2.916	0.048	*

**statistically significant (p <0.05).*
HR, hazard ratio; CI, confidence interval.
Adjusted for variables with p <0.05 in the multivariate analysis in the training group: 3-Methylhistidine and 5-Hydroxylysine.

TABLE 3 | Unadjusted hazard ratios and 95% confidence intervals for variables associated with disease-free survival in the validation group.

Variable		Unadjusted HR	(95% CI)	p-value
N-Acetylglucosamine	(per 1 increase)	0.988	0.973-1.002	0.099

HR, hazard ratio; CI, confidence interval.
N-Acetylglucosamine was adopted for the final model in this validation set because only N-acetylglucosamine had a p-value <0.05 in the multivariate analysis in the training group.

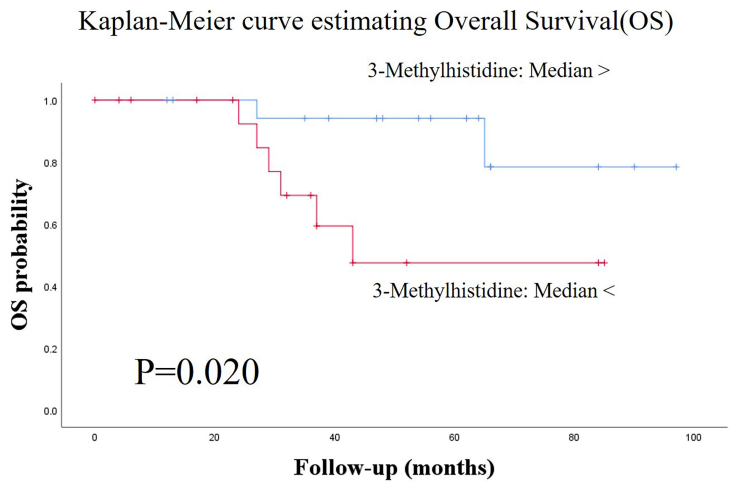

FIGURE 2 | Kaplan-Meier survival curves for estimating overall survival (OS) based on the definitive variable, which is adopted in the Cox hazard model in the validation group. Patients with higher salivary 3-methylhistidine levels (> median) had significantly lower OS rates than those with lower salivary 3-methylhistidine levels (< median) in the test group (p = 0.020). OS, overall survival.

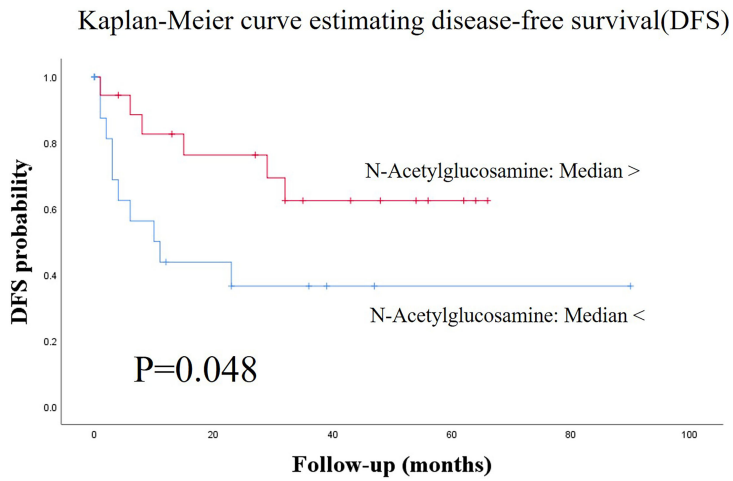

FIGURE 3 | Kaplan-Meier survival curves for estimating disease-free survival (DFS) based on the definitive variable, which is adopted in the Cox hazard model in the validation group. Patients with lower salivary N-acetylglucosamine levels (< median) had significantly lower DFS than those with higher salivary N-acetylglucosamine levels (> median) in the validation group (p = 0.048). DFS, disease-free survival.

cancer (29–32). Therefore, 3-methylhistidine levels may indicate host factors, such as general status, rather than cancer aggressiveness. Prognostic biomarkers for OSCC, especially tissue-based biomarkers, are based on tumor aggressiveness in general (2, 9, 33, 34). As we mentioned above, our candidate salivary biomarkers, such as 3-methylhistidine, could be derived from the non-cancerous tissue. However, further studies are required to confirm from which tissue our candidate biomarkers are derived. Compared with healthy controls, patients with head and neck cancer have significantly higher serum, but not salivary levels of 3-methylhistidine (35). These reports are consistent with our findings that higher salivary levels of 3-methylhistidine were indicative of poor prognosis of OS in patients with OSCC.

We selected salivary *N*-acetylglucosamine, proline, and creatinine as candidate biomarkers for predicting the prognosis of DFS of OSCC in the training group; however, they were not significant in the validation group. The addition of *N*-acetylglucosamine at the hydroxyl groups of serine and/or threonine residues in cytosolic and nuclear proteins involved in various intracellular processes is involved in cancer cell biology (36–38). However, there have been no reports regarding the prognostic biomarkers of OSCC from this

perspective. Proline is considered an indicator of amino acid utilization in tumor tissues (39). Several studies have reported differences in the serum and salivary proline levels between healthy controls and patients with head and neck cancer, including oral cancer (39, 40). These differences in proline levels have been confirmed in renal cell carcinoma and esophageal cancer (39, 41, 42). Although we did not find these salivary metabolites to be significant prognostic biomarkers for predicting DFS in OSCC, future studies are warranted to assess these salivary biomarkers as candidate biomarkers.

A notable strength of this study is its design. After randomly dividing the participants into the training and validation groups, we performed univariate and multivariate analyses to identify prognostic biomarkers in both the groups. In both the groups, the candidate salivary metabolite showed statistical significance. To our knowledge, no studies have performed multivariate analyses to identify prognostic biomarkers of OSCC in the training and validation groups. Despite our small sample size, the aforementioned points can be considered as strengths of this study.

This study has several limitations. First, this study included a small sample size, which could have led to oversight of potentially significant factors or over/underestimation of the results. Second, we combined our data with data derived from two different batches. The use of only one batch to analyze analytes is desirable due to batch effects (43). However, we performed the PCA, which revealed similarities between both batches. Therefore, there were no unexpected batch effects. There is a need for further studies, including multi-center studies, to collect numerous cases all at once. However, it is difficult to collect numerous cases of OSCC simultaneously in Japan given its low prevalence. Third, we did not survey the status of human papillomavirus (HPV). Several types of HPV, including type 16, are related to OSCC, especially its prognosis (44, 45). Patients with OSCC infected with HPV have a better prognosis (44, 45). Jung et al. have revealed that HPV-positive head and neck squamous cell carcinoma cells rely on mitochondrial respiration with decreased glucose metabolism. Contrastingly, smoking-associated/chemically induced HPV-positive head and neck squamous cell carcinoma cells rely heavily on glycolytic pathways (17, 46). Therefore, there could be differences in the profiles of salivary metabolites between HPV-positive and HPV-negative patients with OSCC (17, 46). Further studies are required to collect data regarding HPV infection to determine the prognosis of OSCC.

In conclusion, our assessment of the associations between salivary metabolites and prognosis of OSCC revealed that salivary 3-methylhistidine is a significant biomarker for predicting the prognosis of OS in OSCC.

DATA AVAILABILITY STATEMENT

The original contributions presented in the study are included in the article/**Supplementary Material**. Further inquiries can be directed to the corresponding author.

ETHICS STATEMENT

The studies involving human participants were reviewed and approved by the Ethics Committee of Yamagata University Faculty of Medicine (#2021-176). Written informed consent for participation was not required for this study in accordance with the national legislation and the institutional requirements.

AUTHOR CONTRIBUTIONS

NO, KK, SU, KE, KY, and MI collected the saliva samples. MS conducted metabolomic analysis. SI designed the study. SI, TK, and MS conducted the statistical analysis. SI wrote the main manuscript and prepared all tables and figures. MS, TK, and MI reviewed and edited the manuscript. All authors reviewed the manuscript. All authors contributed to manuscript revision, read, and approved the submitted version.

FUNDING

This work was supported by grants from YU-COE(C) from Yamagata University and the Ministry of Education, Culture, Sports, Science and Technology (MEXT) KAKENHI (16K11742, 17K11897, 19K10304, and 20H05743), and research funds from Yamagata Prefectural Government and Tsuruoka City, Japan.

ACKNOWLEDGMENTS

The authors thank all the patients who provided the samples and Editage for editing our manuscript.

SUPPLEMENTARY MATERIAL

The Supplementary Material for this article can be found online at: https://www.frontiersin.org/articles/10.3389/fonc.2021.789248/full#supplementary-material

REFERENCES

1. Shahabinejad M, Zare R, Asadi Z, Mohajertehran F. LAMP3 (CD208) Expression in Squamous Cell Carcinoma and Epithelial Dysplasia of the Oral Cavity and Clinicopathological Characteristics of Unfavorable Prognosis. *Rep Biochem Mol Biol* (2021) 9:373–8. doi: 10.52547/rbmb.9.4.373
2. Gatta G, Botta L, Sanchez MJ, Anderson LA, Pierannunzio D, Licitra L, et al. Prognoses and Improvement for Head and Neck Cancers Diagnosed in Europe in Early 2000s: The EUROCARE-5 Population-Based Study. *Eur J Cancer* (2015) 51:2130–43. doi: 10.1016/j.ejca.2015.07.043
3. Budach V, Tinhofer I. Novel Prognostic Clinical Factors and Biomarkers for Outcome Prediction in Head and Neck Cancer: A Systematic Review. *Lancet Oncol* (2019) 20:e313–26. doi: 10.1016/S1470-2045(19)30177-9
4. Mello FW, Kammer PV, Silva CAB, Parkinson EK, Monteiro L, Warnakulasuriya S, et al. Prognostic and Clinicopathological Significance of Podoplanin Immunoexpression in Oral and Oropharyngeal Squamous Cell

Carcinoma: A Systematic Review. *J Oral Pathol Med* (2021) 50:1–9. doi: 10.1111/jop.13041
5. Nemeth Z, Velich N, Bogdan S, Ujpal M, Szabo G, Suba ZS. The Prognostic Role of Clinical, Morphological and Molecular Markers in Oral Squamous Cell Tumors. *Neoplasma* (2005) 52:95–102.
6. Rivera C. Essentials of Oral Cancer. *Int J Clin Exp Pathol* (2015) 8:11884–94.
7. Graillon N, Iocca O, Carey RM, Benjamin K, Cannady SB, Hartner L, et al. What has the National Cancer Database Taught Us About Oral Cavity Squamous Cell Carcinoma? *Int J Oral Maxillofac Surg* (2021) S0901-5027:00125–9. doi: 10.1016/j.ijom.2021.03.015
8. Lenze NR, Farquhar DR, Sheth S, Zevallos JP, Lumley C, Blumberg J, et al. Prognostic Impact of Socioeconomic Status Compared to Overall Stage for HPV-Negative Head and Neck Squamous Cell Carcinoma. *Oral Oncol* (2021) 119:105377. doi: 10.1016/j.oraloncology.2021.105377
9. Xu Y, Xu F, Lv Y, Wang S, Li J, Zhou C, et al. A ceRNA-Associated Risk Model Predicts the Poor Prognosis for Head and Neck Squamous Cell Carcinoma Patients. *Sci Rep* (2021) 11:6374. doi: 10.1038/s41598-021-86048-x
10. Fang XN, Yin M, Li H, Liang C, Xu C, Yang GW, et al. Comprehensive Analysis of Competitive Endogenous RNAs Network Associated With Head and Neck Squamous Cell Carcinoma. *Sci Rep* (2018) 8:10544. doi: 10.1038/s41598-018-28957-y
11. Pan Y, Liu G, Wang D, Li Y. Analysis of lncRNA-Mediated ceRNA Crosstalk and Identification of Prognostic Signature in Head and Neck Squamous Cell Carcinoma. *Front Pharmacol* (2019) 10:150. doi: 10.3389/fphar.2019.00150
12. Sugimoto M. Salivary Metabolomics for Cancer Detection. *Expert Rev Proteomics* (2020) 17:639–48. doi: 10.1080/14789450.2020.1846524
13. Ishikawa S, Sugimoto M, Kitabatake K, Sugano A, Nakamura M, Kaneko M, et al. Identification of Salivary Metabolomic Biomarkers for Oral Cancer Screening. *Sci Rep* (2016) 6:31520. doi: 10.1038/srep31520
14. Ishikawa S, Hiraka T, Kirii K, Sugimoto M, Shimamoto H, Sugano A, et al. Relationship Between Standard Uptake Values of Positron Emission Tomography/Computed Tomography and Salivary Metabolites in Oral Cancer: A Pilot Study. *J Clin Med* (2020) 9:3958. doi: 10.3390/jcm9123958
15. Ishikawa S, Sugimoto M, Edamatsu K, Sugano A, Kitabatake K, Iino M. Discrimination of Oral Squamous Cell Carcinoma From Oral Lichen Planus by Salivary Metabolomics. *Oral Dis* (2020) 26:35–42. doi: 10.1111/odi.13209
16. Ishikawa S, Sugimoto M, Kitabatake K, Tu M, Sugano A, Yamamori I, et al. Effect of Timing of Collection of Salivary Metabolomic Biomarkers on Oral Cancer Detection. *Amino Acids* (2017) 49:761–70. doi: 10.1007/s00726-017-2378-5
17. Ishikawa S, Wong DTW, Sugimoto M, Gleber-Netto FO, Li F, Tu M, et al. Identification of Salivary Metabolites for Oral Squamous Cell Carcinoma and Oral Epithelial Dysplasia Screening From Persistent Suspicious Oral Mucosal Lesions. *Clin Oral Investig* (2019) 23:3557–63. doi: 10.1007/s00784-018-2777-3
18. Pang Z, Chong J, Zhou G, de Lima Morais DA, Chang L, Barrette M, et al. MetaboAnalyst 5.0: Narrowing the Gap Between Raw Spectra and Functional Insights. *Nucleic Acids Res* (2021) 49:W388–96. doi: 10.1093/nar/gkab382
19. Lin MC, Leu YS, Chiang CJ, Ko JY, Wang CP, Yang TL, et al. Adequate Surgical Margins for Oral Cancer: A Taiwan Cancer Registry National Database Analysis. *Oral Oncol* (2021) 119:105358. doi: 10.1016/j.oraloncology.2021.105358
20. Spanier G, Weidt D, Hellwig D, Meier JKH, Reichert TE, Grosse J. Total Lesion Glycolysis in Oral Squamous Cell Carcinoma as a Biomarker Derived From Pre-Operative FDG PET/CT Outperforms Established Prognostic Factors in a Newly Developed Multivariate Prediction Model. *Oncotarget* (2021) 12:37–48. doi: 10.18632/oncotarget.27857
21. Ou D, Blanchard P, Rosellini S, Levy A, Nguyen F, Leijenaar RTH, et al. Predictive and Prognostic Value of CT Based Radiomics Signature in Locally Advanced Head and Neck Cancers Patients Treated With Concurrent Chemoradiotherapy or Bioradiotherapy and its Added Value to Human Papillomavirus Status. *Oral Oncol* (2017) 71:150–5. doi: 10.1016/j.oraloncology.2017.06.015
22. Park MJ, Roh JL, Kim SB, Choi SH, Nam SY, Kim SY. Prognostic Value of Circulating Biomarker Score in Advanced-Stage Head and Neck Squamous Cell Carcinoma. *Eur J Cancer* (2018) 92:69–76. doi: 10.1016/j.ejca.2018.01.069
23. Zhou S, Wang L, Zhang W, Liu F, Zhang Y, Jiang B, et al. Circulating Tumor Cells Correlate With Prognosis in Head and Neck Squamous Cell Carcinoma. *Technol Cancer Res Treat* (2021) 20:1533033821990037. doi: 10.1177/1533033821990037
24. Liu M, Tong L, Liang B, Song X, Xie L, Peng H, et al. A 15-Gene Signature and Prognostic Nomogram for Predicting Overall Survival in non-Distant Metastatic Oral Tongue Squamous Cell Carcinoma. *Front Oncol* (2021) 11:587548. doi: 10.3389/fonc.2021.587548
25. Lim E, Kuo CC, Tu HF, Yang CC. The Prognosis Outcome of Oral Squamous Cell Carcinoma Using HIF-2α. *J Chin Med Assoc* (2017) 80:651–6. doi: 10.1016/j.jcma.2017.06.005
26. Vsiansky V, Svobodova M, Gumulec J, Cernei N, Sterbova D, Zitka O, et al. Prognostic Significance of Serum Free Amino Acids in Head and Neck Cancers. *Cells* (2019) 8:428. doi: 10.3390/cells8050428
27. Cadoni G, Giraldi L, Chiarla C, Gervasoni J, Persichilli S, Primiano A, et al. Prognostic Role of Serum Amino Acids in Head and Neck Cancer. *Dis Markers* (2020) 2020:2291759. doi: 10.1155/2020/2291759
28. Kochlik B, Stuetz W, Peres K, Feart C, Tegner J, Rodriguez-Manas L, et al. Associations of Plasma 3-Methylhistidine With Frailty Status in French Cohorts of the FRAILOMIC Initiative. *J Clin Med* (2019) 8:1010. doi: 10.3390/jcm8071010
29. Janecka-Widla A, Mucha-Malecka A, Majchrzyk K, Halaszka K, Przewoznik M, Slonina D, et al. Active HPV Infection and its Influence on Survival in Head and Neck Squamous-Cell Cancer. *J Cancer Res Clin Oncol* (2020) 146:1677–92. doi: 10.1007/s00432-020-03218-6
30. Goel AN, Frangos MI, Raghavan G, Lazaro SL, Tang B, Chhetri DK, et al. The Impact of Treatment Package Time on Survival in Surgically Managed Head and Neck Cancer in the United States. *Oral Oncol* (2019) 88:39–48. doi: 10.1016/j.oraloncology.2018.11.021
31. Urba S, Gatz J, Shen W, Hossain A, Winfree K, Koustenis A, et al. Quality of Life Scores as Prognostic Factors of Overall Survival in Advanced Head and Neck Cancer: Analysis of a Phase III Randomized Trial of Pemetrexed Plus Cisplatin Versus Cisplatin Monotherapy. *Oral Oncol* (2012) 48:723–9. doi: 10.1016/j.oraloncology.2012.02.016
32. Galli A, Colombo M, Carrara G, Lira Luce F, Paesano PL, Giordano L, et al. Low Skeletal Muscle Mass as Predictor of Postoperative Complications and Decreased Overall Survival in Locally Advanced Head and Neck Squamous Cell Carcinoma: The Role of Ultrasound of Rectus Femoris Muscle. *Eur Arch Otorhinolaryngol* (2020) 277:3489–502. doi: 10.1007/s00405-020-06123-3
33. Liang L, Huang Q, Gan M, Jiang L, Yan H, Lin Z, et al. High SEC61G Expression Predicts Poor Prognosis in Patients With Head and Neck Squamous Cell Carcinomas. *J Cancer* (2021) 12:3887–99. doi: 10.7150/jca.51467
34. Hu X, Xia K, Xiong HF, Su T. G3BP1 may Serve as a Potential Biomarker of Proliferation, Apoptosis, and Prognosis in Oral Squamous Cell Carcinoma. *J Oral Pathol Med* (2021) 50:995–1004. doi: 10.1111/jop.13199
35. Scioscia KA, Snyderman CH, Wagner R. Altered Serum Amino Acid Profiles in Head and Neck Cancer. *Nutr Cancer* (1998) 30:144–7. doi: 10.1080/01635589809514654
36. Kongkaew T, Aung WPP, Supanchart C, Makeudom A, Langsa-Ard S, Sastraruji T, et al. O-GlcNAcylation in Oral Squamous Cell Carcinoma. *J Oral Pathol Med* (2018) 47:260–7. doi: 10.1111/jop.12680
37. Ma Z, Vosseller K. O-GlcNAc in Cancer Biology. *Amino Acids* (2013) 45:719–33. doi: 10.1007/s00726-013-1543-8
38. Ferrer CM, Sodi VL, Reginato MJ. O-GlcNAcylation in Cancer Biology: Linking Metabolism and Signaling. *J Mol Biol* (2016) 428:3282–94. doi: 10.1016/j.jmb.2016.05.028
39. Mikkonen JJW, Singh SP, Akhi R, Salo T, Lappalainen R, Gonzalez-Arriagada WA, et al. Potential Role of Nuclear Magnetic Resonance Spectroscopy to Identify Salivary Metabolite Alterations in Patients With Head and Neck Cancer. *Oncol Lett* (2018) 16:6795–800. doi: 10.3892/ol.2018.9419
40. Tiziani S, Lopes V, Gunther UL. Early Stage Diagnosis of Oral Cancer Using 1H NMR-Based Metabolomics. *Neoplasia* (2009) 11:269–76. doi: 10.1593/neo.81396
41. Mustafa A, Gupta S, Hudes GR, Egleston BL, Uzzo RG, Kruger WD. Serum Amino Acid Levels as a Biomarker for Renal Cell Carcinoma. *J Urol* (2011) 186:1206–12. doi: 10.1016/j.juro.2011.05.085
42. Liang S, Sanchez-Espiridion B, Xie H, Ma J, Wu X, Liang D. Determination of Proline in Human Serum by a Robust LC-MS/MS Method: Application to Identification of Human Metabolites as Candidate Biomarkers for Esophageal Cancer Early Detection and Risk Stratification. *BioMed Chromatogr* (2015) 29:570–7. doi: 10.1002/bmc.3315
43. Han W, Li L. Evaluating and Minimizing Batch Effects in Metabolomics. *Mass Spectrom Rev* (2020) 10.1002/mas.21672:1–22. doi: 10.1002/mas.21672
44. Sugiyama M, Bhawal UK, Kawamura M, Ishioka Y, Shigeishi H, Higashikawa K, et al. Human Papillomavirus-16 in Oral Squamous Cell Carcinoma:

Clinical Correlates and 5-Year Survival. *Br J Oral Maxillofac Surg* (2007) 45:116–22. doi: 10.1016/j.bjoms.2006.04.012
45. Ghantous Y, Akrish S, Leiser Y, Abu El-Naaj I. The Possible Role of Human Papillomavirus Infection in the Prognosis of Oral Squamous Cell Carcinoma in a Northern Israel Population. *Isr Med Assoc J* (2018) 20:155–60.
46. Jung YS, Najy AJ, Huang W, Sethi S, Snyder M, Sakr W, et al. HPV-Associated Differential Regulation of Tumor Metabolism in Oropharyngeal Head and Neck Cancer. *Oncotarget* (2017) 8:51530–41. doi: 10.18632/oncotarget.17887

Conflict of Interest: The authors declare that the research was conducted in the absence of any commercial or financial relationships that could be construed as a potential conflict of interest.

frontiers in Oncology

ORIGINAL RESEARCH
published: 24 January 2022
doi: 10.3389/fonc.2021.786258

Neck Management in cT1N0 Tongue Squamous Cell Carcinoma as Determined by Sonographic Depth of Invasion

*Yao Wu, Xu Zhang, Liyuan Dai, Qigen Fang and Wei Du**

Department of Head Neck and Thyroid, Affiliated Cancer Hospital of Zhengzhou University, Henan Cancer Hospital, Zhengzhou, China

OPEN ACCESS

Edited by:
Steffi Ulrike Pigorsch, Technical University of Munich, Germany

Reviewed by:
Aviram Mizrachi, Rabin Medical Center, Israel
Phillipp Brockmeyer, University Medical Center Göttingen, Germany
Marco Mascitti, Marche Polytechnic University, Italy

***Correspondence:**
Wei Du
duweitj@126.com

Specialty section:
This article was submitted to Head and Neck Cancer, a section of the journal Frontiers in Oncology

Received: *30 September 2021*
Accepted: *28 December 2021*
Published: *24 January 2022*

Citation:
Wu Y, Zhang X, Dai L, Fang Q and Du W (2022) Neck Management in cT1N0 Tongue Squamous Cell Carcinoma as Determined by Sonographic Depth of Invasion. Front. Oncol. 11:786258. doi: 10.3389/fonc.2021.786258

Objectives: To compare the oncologic outcomes in patients with cT1N0 tongue squamous cell carcinoma (SCC) who underwent different neck management strategies stratified by sonographic depth of invasion (DOI).

Methods: The included patients were retrospectively enrolled, and divided into two groups: observation (OBS) and elective neck dissection (END). The regional control (RC) and disease-specific survival (DSS) rates were compared and stratified by sonographic DOI.

Results: The mean sonographic and pathologic DOIs were 3.8 and 3.7 mm, respectively; the two DOIs were significantly correlated (Spearman correlation coefficient 0.974. p <0.001). In patients with sonographic DOI <4.0 mm, the 5-year RC rates were 73 and 89% in the OBS and END groups, respectively, and were not significantly different. However, in patients with sonographic DOI ≥4.0 mm, the 5-year RC rate was significantly different between the OBS (57%) and END (80%) groups (p = 0.031). In patients with sonographic DOI <4.0 mm, the 5-year DSS rates were 79 and 89% in OBS and END groups, respectively, and were not significantly different. However, in patients with sonographic DOI ≥4.0 mm, the 5-year DSS rate was significantly different between the OBS (67%) and END (86%) groups (p = 0.033).

Conclusions: Sonographic DOI was notably correlated with pathologic DOI. Moreover, there was a significant survival difference between the OBS and END groups in cT1N0 tongue SCC patients with sonographic DOI ≥4.0 mm but not in those with sonographic DOI <4.0 mm. Our study provides a useful method to aid decision-making in the clinical setting for this patient group.

Keywords: depth of invasion, tongue squamous cell carcinoma, head and neck squamous cell carcinoma, observation, elective neck dissection

INTRODUCTION

Surgical excision is the preferred method for managing squamous cell carcinoma (SCC) of the tongue, which is the most common oral malignancy (1). Neck dissection is usually included in the initial treatment of cT3–T4 disease; however, the optimal neck management in cases of cT1N0 tongue SCC is still controversial owing to the wide range of the occult metastasis rate (2). Observation (OBS) and elective neck dissection (END) are two potential approaches for management. Vandenbrouck et al. (3), Fakih et al. (4), and Yuen et al. (5) reported that a comparison of oncologic outcomes between patients undergoing OBS and those indicated for END revealed a similar disease-specific survival (DSS) in both groups. However, some high-quality studies also showed that END could reduce the frequency of regional nodal recurrence and improve DSS in patients with cT1-2N0 oral SCC (6–8). To achieve successful outcomes in such cases, reliable predictors indicating cervical lymph node metastasis, which can be assessed preoperatively, must be identified.

Factors contributing to lymph node metastasis include tumor size, tumor differentiation grade, perineural invasion (PNI), and lymphovascular invasion (LVI) (9–11). Caponio et al. (12) reported that PNI occurred in 40.5% of 200 patients with tongue SCC, and PNI was associated with a higher tendency of lymph node metastasis and a worse disease prognosis. However, the depth of invasion (DOI) is considered the best predictor of occult lymph node metastasis (13). Studies have suggested that neck dissection should be performed if the DOI exceeds 4 mm (14–16). However, in such studies, the DOI was measured postoperatively based on hematoxylin and eosin staining results; this is known as pathologic DOI, which provides little benefit in preoperative decision-making.

Intraoral ultrasound, CT, and MRI are used to evaluate clinical DOI (17, 18). Takamura et al. (17) reported that compared to pathologic DOI, clinical DOI derived by ultrasound was overestimated by an average of 0.2 mm, while CT and MRI-based radiological DOIs were overestimated by an average of 2–3 mm. These findings, combined with the reports of Klein et al. (19) and Marchi et al. (20), highlight the accuracy of ultrasound in determining the clinical DOI. However, to our knowledge, no study has analyzed whether sonographic DOI can be used to guide neck management in cT1N0 tongue SCC. Therefore, this study aimed to compare the oncologic outcomes in patients that underwent different neck management strategies stratified by sonographic DOI.

PATIENTS AND METHODS

Ethical Considerations

This study was approved by the Institutional Research Committee of our hospital, and all the participants provided informed consent. All procedures involving human participants were conducted according to the ethical standards of the Institutional and National Research Committees and the 1964 Helsinki Declaration and its later amendments or comparable ethical standards.

Patient Selection

We retrospectively reviewed the medical records of patients that underwent surgical treatment for primary tongue SCC between January 2015 and January 2021. The following were the criteria for study enrollment: a disease stage of cT1N0 according to the 8th AJCC classification system and the availability of follow-up data. Patients with a history of any other malignancy were excluded. Information on demography, treatment, pathology, and follow-up was extracted and analyzed.

Important Definitions of Variables

A cT1 tumor was defined as a tumor with a maximum diameter of 2 cm and a maximum clinical DOI of 5 mm based on imaging examination. A cN0 neck referred to a neck with no clinically enlarged lymph nodes on palpation and imaging. PNI was considered present if tumor cells were identified within the perineural space and/or nerve bundle. LVI was considered present if tumor cells were noted within the lymphovascular channels (21, 22).

Evaluation of Clinical DOI

Sonographic DOI was defined as the vertical distance between the deepest part of the tumor and the virtual line connecting the normal mucosal basal portion adjacent to the tumor (17). Before evaluation, all patients were required to rinse the mouth. Stationary B-mode ultrasound was performed with a 10–12 MHz intracavitary probe (SonoScape, Shenzhen, China) using degassed water as the coupling agent. The tongues of the patients were lightly held with gauze, and the intraoral probes were positioned according to the longitudinal axis of the maximum diameter of the tumor. Scanning was performed with the probe in contact with the lesion, but without compression, to avoid distortion and alteration of the DOI (**Figure 1**).

Treatment Principle

Sonographic DOI was frequently assessed for tongue SCC patients from January 2015 in our department. Resection of the primary tumor was performed with a margin of at least 1 cm. The neck management consisted of two strategies: OBS and END. END consisted of suprahyoid neck dissection (SOND) and modified radical neck dissection (MRND). SOND is referred to as a dissection of level I to III, whereas MRND is referred to as a dissection of level I to IV/V. The final neck treatment was based on the preference of the surgeon and the condition of the patient. Postoperative radiotherapy was suggested in cases with cervical nodal disease, positive margin, PNI, LVI, and extracapsular extension. Patients were followed up every three months for the first two years, every six months for the third to fourth year, and once yearly thereafter.

Statistical Analysis

The ROC curve was used to analyze the optimal cutoff value of sonographic DOI in predicting occult metastasis. Bland–Altman and Spearman rank correlation analyses were used to compare

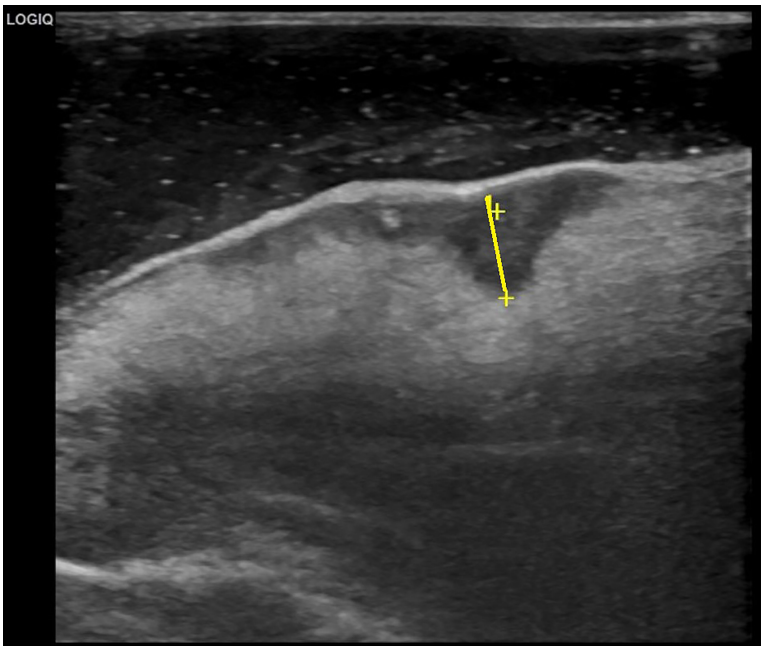

FIGURE 1 | Measurement of sonographic depth of invasion (yellow line).

sonographic and pathologic DOIs. The chi-square test was used to compare the clinicopathologic variables between the two DOI groups. The main study endpoints were regional control (RC) and DSS. RC time was calculated from the date of surgery to the date of the first neck cancer recurrence or the last follow-up. DSS was calculated from the date of surgery to the date of cancer-related death or the last follow-up. The Kaplan–Meier method (univariate analysis) was used to analyze the RC and DSS rates. Factors which were significant in univariate analyses were then analyzed in Cox model to find out the independent predictor for the survival. All statistical analyses were performed using SPSS 20.0, and $p < 0.05$ was considered significant.

RESULTS

Baseline Data

A total of 178 patients (135 men, 42 women) were included in the analysis; the median age was 53 (range: 28–78) years. Smokers and drinkers comprised 100 (56.2%) and 50 (28.1%) patients, respectively. Sixty-five (36.5%) patients underwent OBS for neck treatment, and 113 (63.5%) patients underwent END, with 70 (39.3%) undergoing SOND and 43 (24.2%) undergoing MRND. The mean sonographic DOI was 3.8 (range: 0.4–5.0) mm.

Postoperatively, all patients were pathologic stage T1, and clear margins were noted on histopathologic examination. Pathologic neck lymph node metastasis occurred in 12 patients (10.6%, 12/113), of whom six received SOND and six received MRND. Level I, II, III, and IV metastases were noted in 10 (5.6%), three (2.7%), three (2.7%), and one (0.9%) patient, respectively. PNI and LVI were present in 17 (9.6%) and 13 (7.3%) patients, respectively. The tumors showed good differentiation in 72 (40.4%), intermediate differentiation in 84 (47.2%), and poor differentiation in 22 (12.4%) patients. The two groups had similar distributions regarding clinical and pathologic variables (all $p > 0.05$, **Table 1**).

Adjuvant Treatment

Radiotherapy was performed for 30 patients, of whom six underwent radiation for the primary site, 12 underwent radiation for the primary site and ipsilateral upper neck area, and 12 underwent radiation for the primary site and ipsilateral neck area.

ROC Curve of Sonographic DOI

In the END group, the mean sonographic DOI was 3.8 (range: 0.5–5.0) mm. ROC analysis indicated that the best cutoff value for sonographic DOI in predicting occult metastasis was 4.0 mm, with an AUC of 0.759 (**Figure 2**), sensitivity of 75%, and specificity of 59.4%. Eighteen percent of the 50 tumors with sonographic DOI ≥4.0 mm had occult metastases, which was significantly higher than the 4.8% of the 63 tumors with sonographic DOI <4.0 mm ($p = 0.031$).

Association Between Sonographic DOI and Pathologic DOI

The mean pathologic DOI was 3.7 (range: 0.3–4.8) mm. Spearman analysis of the relationship between sonographic and pathologic DOI yielded a correlation coefficient of 0.974 ($p < 0.001$). Bland–

TABLE 1 | Comparison of clinical and pathologic variables between the observation and elective neck dissection groups.

Variables	Observation (n = 65)	Elective neck dissection (n = 113)	p
Age			
<40	8	14	
≥40	57	99	0.987
Sex			
Male	50	86	
Female	15	27	0.902
Smoking	40	60	0.274
Drinking	20	30	0.546
Sonographic DOI*			
<4.0 mm	37	63	
≥4.0 mm	28	50	0.880
PNI[&]	7	10	0.675
LVI[^]	5	8	1.000
Differentiation			
Well	24	47	
Intermediate	33	52	
Poor	8	14	0.810

**DOI, depth of invasion.*
[&]PNI, perineural invasion.
^LVI, lymphovascular invasion.

Altman analysis indicated that the sonographic DOI corresponded to the pathologic DOI (**Figure 3**).

Neck Recurrence Pattern

In tumors with sonographic DOI <4.0 mm, neck recurrence occurred in six and five patients in the OBS and END groups, respectively. In the OBS group, the most common recurrent site was level I; contralateral level II and III recurrence occurred in one patient each. In the END group, the most common recurrent site was level I, while contralateral level II recurrence occurred in one patient. The two groups had a similar recurrence pattern (**Table 2**).

In tumors with sonographic DOI ≥4.0 mm, neck recurrence occurred in 12 and nine patients in the OBS and END groups, respectively. In the OBS group, level V recurrence occurred in two patients, while level I, II, and III recurrence occurred in one patient each. In the END group, the most common recurrent site was level I, while contralateral level II and III recurrence occurred in one and two patients, respectively. The recurrence pattern in the OBS group was more complex (**Table 2**).

RC and DSS

After a median follow-up of 2.8 (range: 0.3–6.3) years, in patients with sonographic DOI <4.0 mm, the 5-year RC rates were 73 and

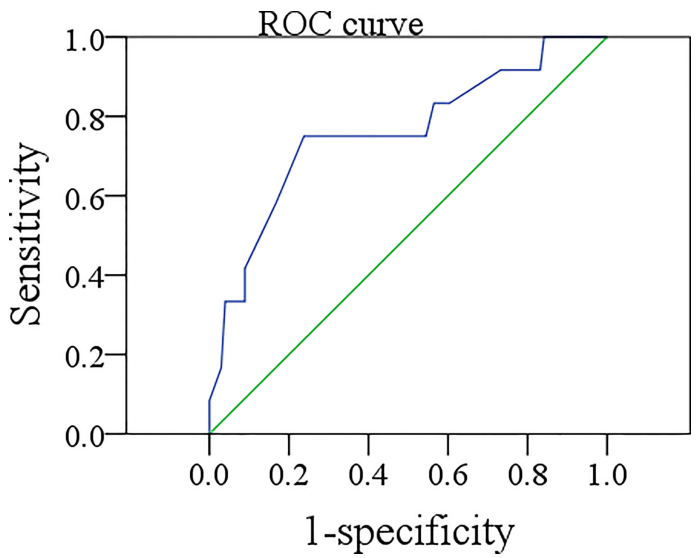

FIGURE 2 | ROC curve of the sonographic depth of invasion in predicting occult metastasis.

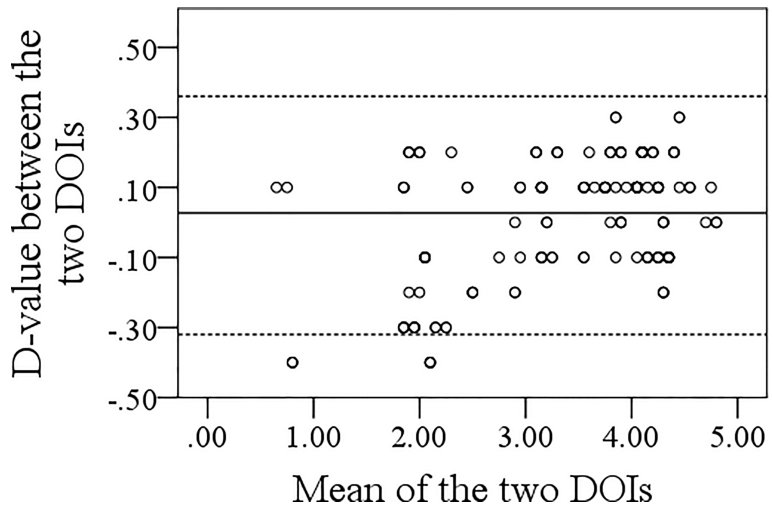

FIGURE 3 | Bland–Altman analysis of the association between sonographic and pathologic depth of invasion.

89% in the OBS and END groups, respectively; the difference was not significant (**Figure 4A**, p = 0.139). In patients with sonographic DOI ≥4.0 mm, the 5-year RC rates were 57 and 80% in the OBS and END groups, respectively, and the difference was significant (**Figure 4B**, p = 0.031). Further, Cox model analysis confirmed that neck dissection was an independent factor for improving RC (**Table 3**).

In patients with sonographic DOI <4.0 mm, the 5-year DSS rates were 79 and 89% in the OBS and END groups, respectively, and the difference was not significant (**Figure 5A**, p = 0.381). In patients with sonographic DOI ≥4.0 mm, the 5-year DSS rates were 67 and 86% in the OBS and END groups, respectively, and the difference was significant (**Figure 5B**, p = 0.033). Further, Cox model analysis confirmed that neck dissection was an independent factor for improving DSS (**Table 4**).

DISCUSSION

The most important finding in this study was that the sonographic DOI corresponded with pathologic DOI. There was a significant survival difference between the OBS and END groups in patients with cT1N0 tongue SCC with sonographic DOI ≥4.0 mm but not in patients with sonographic DOI <4.0 mm. This finding provides a clear indicator for neck management; hence, END was suggested if there was a presence of sonographic DOI ≥4.0 mm.

Neck lymph node metastasis is an important feature of tongue SCC, and its prevalence differs with tumor stage; END is usually recommended when the estimated risk of lymph node metastasis exceeds 20% (23). However, current evidence suggests that the incidence of occult metastasis in cT1N0 tongue SCC varies from 5 to 10% (6), contributing to debates regarding neck management in patients. A recent high-quality study by D'Cruz et al. (8) showed that, in the results of the first 500 patients with early-stage oral SCC, END resulted in higher overall survival and DSS rates than OBS. However, de Bree et al. (24) discussed the importance of a clear definition of cN0. Questioning the reliability of investigations for this diagnosis, they argued that cN0 was not clearly defined in the Tata Memorial Centre prospective randomized trial; further, to examine the role of ultrasound, some patients with suspicious findings were included, and more importantly, the ultrasound scoring criteria were not described. It was clear that the incidence of delayed metastases and neck recurrence would have been higher if the neck status was staged only by palpation compared with staging

TABLE 2 | Neck recurrence pattern in the observation and elective neck dissection groups stratified by different ultrasound derived depth of invasion (DOI).

Level	Observation (n = 18)				Elective neck dissection (n = 14)			
	Ultrasound derived DOI <4.0 mm		Ultrasound derived DOI≥ 4.0 mm		Ultrasound derived DOI <4.0 mm		Ultrasound derived DOI ≥4.0 mm	
	Ipsilateral	Contralateral	Ipsilateral	Contralateral	Ipsilateral	Contralateral	Ipsilateral	Contralateral
I	4		4		3		5	
II	2	2	4	2	2	1	3	1
III	2	1	4	2	1		2	2
IV	1		2	2	1		1	
V			2					

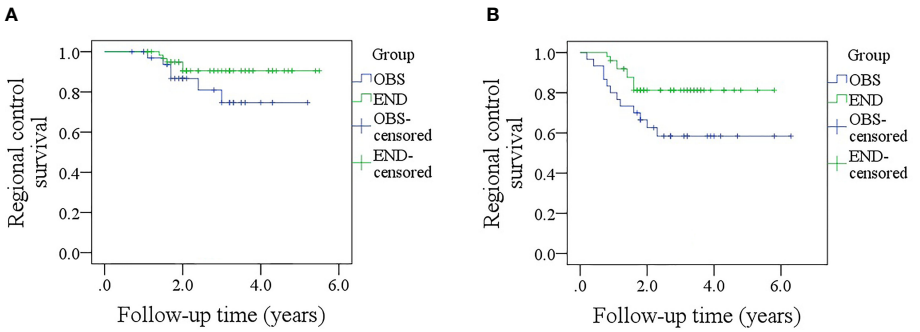

FIGURE 4 | **(A)** Comparison of regional control rates between the elective neck dissection and observation groups in patients with a sonographic depth of invasion <4.0 mm (p = 0.139); **(B)** Comparison of regional control survival between the elective neck dissection and observation groups in patients with a sonographic depth of invasion ≥4.0 mm (p = 0.031).

using advanced diagnostic techniques. Similar studies reported conflicting results on the benefits of OBS vs END (3–7); thus, there is a need for a reliable preoperative predictor of lymph node metastasis.

DOI was considered for tumor staging in the newest version of the AJCC classification, and it was confirmed as the strongest predictor of lymph node metastasis (11–16), according to the NCCN guidelines (13), END was suggested if pathologic DOI >4.0 mm existed. Pathologic DOI was calculated from the basement membrane to the deepest of invasion, although it was impossible to take the same measurement method, it was important to draft an alternative preoperative indicator of pathologic DOI to create a balance between overtreatment and necessity of lymphadenectomy.

Intraoral ultrasound has gained interest since its introduction by Iro et al. for assessing the tongue and the floor of the mouth (25), and a number of researchers have analyzed the accuracy of intraoral ultrasound in evaluating the DOI of oral SCC patients. Iida et al. (26) found in 56 cases of tongue tumor that the median ultrasound DOI was 3.6 (range: 0.7–9.2) mm, and the median histologic DOI was 3.5 (range: 0–12.0 mm). Compared to histologic DOI, there was an overestimation by only 0.1 mm for ultrasound DOI, with a coefficient of 0.867. If only superficial tumors were analyzed, the compatibility between the two DOIs improved. In another study by Yoon et al. (27) consisting of 22 patients, the mean sonographic DOI and histologic DOI were 6.6 ± 3.4 and 6.4 ± 4.4 mm, respectively, and there was excellent correlation between sonographic and histologic measurement for DOI, with a Pearson correlation coefficient of 0.95 (95%CI: 0.87–0.98). Filauro et al. (28) also noted that the mean difference between sonographic DOI and histologic DOI was only 0.3 mm after analyzing the outcome of 49 patients with cT1-3 tongue SCC, and the two DOIs were significantly related. Together with our results, these findings indicate the high reliability and accuracy of DOI evaluation by ultrasound even in cT1 tumors.

The association between the necessity of END and DOI has been frequently analyzed. Nguyen et al. (29) included 70 patients with cT1N0 oral SCC, of whom 27 underwent END and 43 were observed. Regional relapse occurred in 16.3% of patients who were observed and in 3.7% patients who underwent surgery. Risk factor analysis reported that DOI ≥3.0 mm was related to a poor prognosis, and it was concluded that END should be recommended if DOI ≥3.0 mm. However, the sample size of this study was notably small, and more importantly, it analyzed

TABLE 3 | Univariate and cox model analyses of regional control survival in patients with ultrasound derived DOI ≥4.0 mm.

Variable	Univariate analysis	Cox model	
	Log-rank	p	HR [95% CI]
Age (<40 vs ≥40)	0.356		
Sex	0.667		
Smoking	0.214		
Drinking	0.772		
DOI of ultrasound			
<4.0 mm			
≥4.0 mm	0.031	0.011	2.565 [1.223–4.787]
Positive lymph node	<0.001	<0.001	3.227 [1.835–7.218]
PNI	0.034	0.103	2.643 [0.785–9.116]
LVI	0.117	0.345	
Differentiation			
Well			
Intermediate		0.056	2.082 [0.946–4.897]
Poor	<0.001	<0.001	3.776 [2.001–6.438]

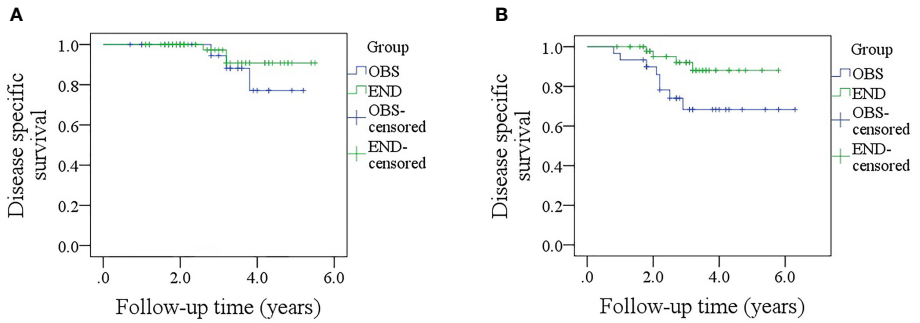

FIGURE 5 | **(A)** Comparison of disease-specific survival between the elective neck dissection and observation groups in patients with a sonographic depth of invasion <4.0 mm (p = 0.381); **(B)** Comparison of disease-specific between the elective neck dissection and observation groups in patients with a sonographic depth of invasion ≥4.0 mm (p = 0.033).

all regions of the oral cavity together. It is well known that tongue SCC has a significantly different biologic behavior compared to SCC of other oral regions. Kuan et al. (30) recently conduct a review to determine the optimal cutoff DOI value for predicting regional disease for early-stage tongue SCC, and noted that patients with cT1-2N0 oral/tongue SCC with known DOI >3.0 mm should be counseled on the possible survival benefits of END with primary tumor resection. However, the review only focused on the association between regional metastasis and DOI without considering the oncologic outcome. However, compared to T2 disease, a T1 tumor has a lower possibility of occult metastasis, which necessitates a search for a corresponding DOI for each disease stage. To the best of our knowledge, this is the first study to analyze how clinical sonography affects oncologic outcomes in patients undergoing different neck management strategies. Our study indicated that END improved patient prognosis for sonographic DOI ≥4.0 mm, but there was no apparent survival benefit associated with END for sonographic DOI <4.0 mm. This finding provides a useful method to aid decision-making in clinics.

Other studies have compared END and OBS in early-stage oral SCC. In a previous study, we enrolled 175 patients with cT1N0 buccal SCC, and the 5-year locoregional control rates in the END and OBS groups were 92 and 90%, respectively, and the difference was not significant. Moreover, the two groups had comparable 5-year DSS rates. Therefore, we concluded that END did not provide any survival benefit compared to a wait-and-watch policy and could not be suggested for patients with cT1N0 buccal SCC (31). A similar viewpoint was offered by Vandenbrouck et al. (3), Fakih et al. (4), and Yuen et al. (5). However, Huang et al. (32) analyzed the outcome of 380 patients with cT1-2N0 tongue SCC and reported the 5-year overall survival and neck control rates were significantly better in the END group than in the OBS group. Their conclusion was also supported by Abu-Ghanem et al. (6), Ren et al. (7), D'Cruz et al. (8), and de Bree et al. (24). However, these studies did not present the results stratified by the clinical DOI. As DOI is the strongest predictor of occult metastasis, the significance of our study is well highlighted.

The limitations in current study must be acknowledged. First, the study was retrospective with the attendant bias. Second, our sample size was not sufficiently large, we could not analyze the effect of the END extend on the outcome; hence, future studies with a larger sample size need to be conducted.

TABLE 4 | Univariate and cox model analyses of disease specific survival in patients with ultrasound derived DOI ≥4.0 mm.

Variable	Univariate analysis	Cox model	
	Log-rank	p	HR [95% CI]
Age (<40 vs ≥40)	0.221		
Sex	0.436		
Smoking	0.178		
Drinking	0.383		
DOI of ultrasound			
<4.0 mm			
≥4.0 mm	0.033	0.009	2.667 [1.567–4.328]
Positive lymph node	<0.001	<0.001	3.415 [1.675–9.287]
PNI	0.026	0.176	2.007 [0.811–8.142]
LVI	0.228	0.226	
Differentiation			
Well			
Intermediate		0.026	2.432 [1.761–5.205]
Poor	<0.001	<0.001	4.036 [1.935–8.328]

In conclusion, sonographic DOI corresponded well with pathologic DOI, and there was a significant survival difference between the OBS and END groups in patients with cT1N0 tongue SCC with sonographic DOI ≥4.0 mm but not in patients with sonographic DOI <4.0 mm. Our findings provide a useful method to aid decision-making in the clinic setting for this patient group.

DATA AVAILABILITY STATEMENT

The original contributions presented in the study are included in the article/supplementary material. Further inquiries can be directed to the corresponding author.

ETHICS STATEMENT

This study was approved by the Institutional Research Committee of our hospital, and all the participants signed an informed consent. The patients/participants provided their written informed consent to participate in this study.

AUTHOR CONTRIBUTIONS

All authors listed have made a substantial, direct, and intellectual contribution to the work and approved it for publication.

REFERENCES

1. Fang Q, Li P, Qi J, Luo R, Chen D, Zhang X. Value of Lingual Lymph Node Metastasis in Patients With Squamous Cell Carcinoma of the Tongue. *Laryngoscope* (2019) 129:2527–30. doi: 10.1002/lary.27927
2. Bruschini R, Maffini F, Chiesa F, Lepanto D, De Berardinis R, Chu F, et al. Oral Cancer: Changing the Aim of the Biopsy in the Age of Precision Medicine. A Review. *Acta Otorhinolaryngol Ital* (2021) 41:108–19. doi: 10.14639/0392-100X-N1056
3. Vandenbrouck C, Sancho-Garnier H, Chassagne D, Saravane D, Cachin Y, Micheau C. Elective Versus Therapeutic Radical Neck Dissection in Epidermoid Carcinoma of the Oral Cavity: Results of a Randomized Clinical Trial. *Cancer* (1980) 46:386–90. doi: 10.1002/1097-0142(19800715)46:2<386::AID-CNCR2820460229>3.0.CO;2-9
4. Fakih AR, Rao RS, Borges AM, Patel AR. Elective Versus Therapeutic Neck Dissection in Early Carcinoma of the Oral Tongue. *Am J Surg* (1989) 158:309–13. doi: 10.1016/0002-9610(89)90122-0
5. Yuen AP, Ho CM, Chow TL, Tang LC, Cheung WY, Ng RW, et al. Prospective Randomized Study of Selective Neck Dissection Versus Observation for N0 Neck of Early Tongue Carcinoma. *Head Neck* (2009) 31:765–72. doi: 10.1002/hed.21033
6. Abu-Ghanem S, Yehuda M, Carmel NN, Leshno M, Abergel A, Gutfeld O, et al. Elective Neck Dissection vs Observation in Early-Stage Squamous Cell Carcinoma of the Oral Tongue With No Clinically Apparent Lymph Node Metastasis in the Neck: A Systematic Review and Meta-Analysis. *JAMA Otolaryngol Head Neck Surg* (2016) 142:857–65. doi: 10.1001/jamaoto.2016.1281
7. Ren ZH, Xu JL, Li B, Fan TF, Ji T, Zhang CP. Elective Versus Therapeutic Neck Dissection in Node-Negative Oral Cancer: Evidence From Five Randomized Controlled Trials. *Oral Oncol* (2015) 51:976–81. doi: 10.1016/j.oraloncology.2015.08.009
8. D'Cruz AK, Vaish R, Kapre N, Dandekar M, Gupta S, Hawaldar R, et al. Elective Versus Therapeutic Neck Dissection in Node-Negative Oral Cancer. *N Engl J Med* (2015) 373:521–9. doi: 10.1056/NEJMoa1506007
9. Jin W, Zhu M, Zheng Y, Wu Y, Ding X, Wu H, et al. Perineural Invasion, Lactate Dehydrogenase, Globulin, and Serum Sodium Predicting Occult Metastasis in Oral Cancer. *Oral Dis* (2020) 28(1):132–41. doi: 10.1111/odi.13750
10. Vassiliou LV, Acero J, Gulati A, Hölzle F, Hutchison IL, Prabhu S, et al. Management of the Clinically N0 Neck in Early-Stage Oral Squamous Cell Carcinoma (OSCC). An EACMFS Position Paper. *J Craniomaxillofac Surg* (2020) 48:711–8. doi: 10.1016/j.jcms.2020.06.004
11. Jiang Q, Tang A, Long S, Qi Q, Song C, Xin Y, et al. Development and Validation of a Nomogram to Predict the Risk of Occult Cervical Lymph Node Metastases in Cn0 Squamous Cell Carcinoma of the Tongue. *Br J Oral Maxillofac Surg* (2019) 57:1092–7. doi: 10.1016/j.bjoms.2019.09.024
12. Caponio VCA, Troiano G, Togni L, Zhurakivska K, Santarelli A, Laino L, et al. Pattern and Localization of Perineural Invasion Predict Poor Survival in Oral Tongue Carcinoma. *Oral Dis* (2021). doi: 10.1111/odi.13900
13. National Comprehensive Cancer Network. *NCCN Clinical Practice Guidelines in Oncology (NCCN Guidelines®) Head and Neck. Version 1.* (2016). p. 2016.
14. van Lanschot CGF, Klazen YP, de Ridder MAJ, Mast H, Ten Hove I, Hardillo JA, et al. Depth of Invasion in Early Stage Oral Cavity Squamous Cell Carcinoma: The Optimal Cut-Off Value for Elective Neck Dissection. *Oral Oncol* (2020) 111:104940. doi: 10.1016/j.oraloncology.2020.104940
15. Tam S, Amit M, Zafereo M, Bell D, Weber RS. Depth of Invasion as a Predictor of Nodal Disease and Survival in Patients With Oral Tongue Squamous Cell Carcinoma. *Head Neck* (2019) 41:177–84. doi: 10.1002/hed.25506
16. Faisal M, Abu Bakar M, Sarwar A, Adeel M, Batool F, Malik KI, et al. Depth of Invasion (DOI) as a Predictor of Cervical Nodal Metastasis and Local Recurrence in Early Stage Squamous Cell Carcinoma of Oral Tongue (ESSCOT). *PloS One* (2018) 13:e0202632. doi: 10.1371/journal.pone.0202632
17. Takamura M, Kobayashi T, Nikkuni Y, Katsura K, Yamazaki M, Maruyama S, et al. A Comparative Study Between CT, MRI, and Intraoral US for the Evaluation of the Depth of Invasion in Early Stage (T1/T2) Tongue Squamous Cell Carcinoma. *Oral Radiol* (2021) 38(1):114–25. doi: 10.1007/s11282-021-00533-7
18. Xu C, Yuan J, Kang L, Zhang X, Wang L, Chen X, et al. Significance of Depth of Invasion Determined by MRI in Ct1n0 Tongue Squamous Cell Carcinoma. *Sci Rep.:4695 Sci Rep* (2020) 10:4695. doi: 10.1038/s41598-020-61474-5
19. Klein Nulent TJW, Noorlag R, Van Cann EM, Pameijer FA, Willems SM, Yesuratnam A, et al. Intraoral Ultrasonography to Measure Tumor Thickness of Oral Cancer: A Systematic Review and Meta-Analysis. *Oral Oncol* (2018) 77:29–36. doi: 10.1016/j.oraloncology.2017.12.007
20. Marchi F, Filauro M, Iandelli A, Carobbio ALC, Mazzola F, Santori G, et al. Magnetic Resonance vs. Intraoral Ultrasonography in the Preoperative Assessment of Oral Squamous Cell Carcinoma: A Systematic Review and Meta-Analysis. *Front Oncol* (2019) 9:1571. doi: 10.3389/fonc.2019.01571
21. Du W, Fang Q, Liu S, Chen D, Luo R, Zhang X. Feasibility of Submandibular Gland Preservation in Ct1-2N0 Squamous Cell Carcinoma in the Floor of the Mouth. *Front Oncol* (2020) 10:579. doi: 10.3389/fonc.2020.00579
22. Gu B, Fang Q, Wu Y, Du W, Zhang X, Chen D. Impact of Submandibular Gland Preservation in Neck Management of Early-Stage Buccal Squamous Cell Carcinoma on Locoregional Control and Disease-Specific Survival. *BMC Cancer* (2020) 20:1034. doi: 10.1186/s12885-020-07534-5
23. Weiss MH, Harrison LB, Isaacs RS. Use of Decision Analysis in Planning a Management Strategy for the Stage N0 Neck. *Arch Otolaryngol Head Neck Surg* (1994) 120:699–702. doi: 10.1001/archotol.1994.01880310005001
24. de Bree R, van den Brekel MWM. Elective Neck Dissection Versus Observation in the Clinically Node Negative Neck in Early Oral Cancer: Do We Have the Answer Yet? *Oral Oncol* (2015) 51:963–5. doi: 10.1016/j.oraloncology.2015.08.013
25. Iro H, Nitsche N. Intra-Oral Sonography in Neoplasms of the Mouth and Base of the Tongue. *HNO* (1989) 37:329–32.
26. Iida Y, Kamijo T, Kusafuka K, Omae K, Nishiya Y, Hamaguchi N, et al. Depth of Invasion in Superficial Oral Tongue Carcinoma Quantified Using Intraoral Ultrasonography. *Laryngoscope* (2018) 128:2778–82. doi: 10.1002/lary.27305
27. Yoon BC, Bulbul MD, Sadow PM, Faquin WC, Curtin HD, Varvares MA, et al. Comparison of Intraoperative Sonography and Histopathologic Evaluation of Tumor Thickness and Depth of Invasion in Oral Tongue

Cancer: A Pilot Study. *AJNR Am J Neuroradiol* (2020) 41:1245–50. doi: 10.3174/ajnr.A6625
28. Filauro M, Missale F, Marchi F, Iandelli A, Carobbio ALC, Mazzola F, et al. Intraoral Ultrasonography in the Assessment of DOI in Oral Cavity Squamous Cell Carcinoma: A Comparison With Magnetic Resonance and Histopathology. *Eur Arch Otorhinolaryngol* (2021) 278:2943–52. doi: 10.1007/s00405-020-06421-w
29. Nguyen E, McKenzie J, Clarke R, Lou S, Singh T. The Indications for Elective Neck Dissection in T1N0M0 Oral Cavity Squamous Cell Carcinoma. *J Oral Maxillofac Surg* (2021) 79:1779–93. doi: 10.1016/j.joms.2021.01.042
30. Kuan EC, Mallen-St Clair J, Badran KW, St John MA. How Does Depth of Invasion Influence the Decision to do a Neck Dissection in Clinically N0 Oral Cavity Cancer? *Laryngoscope* (2016) 126:547–8. doi: 10.1002/lary.25707
31. Fang Q, Gao H, Gao Q, Sun J, Li P, Cui M, et al. Elective Neck Dissection Versus Wait-and-See Policy in Ct1n0 Buccal Squamous Cell Carcinoma. *BMC Cancer* (2020) 20:537. doi: 10.1186/s12885-020-07006-w
32. Huang SF, Kang CJ, Lin CY, Fan KH, Yen TC, Wang HM, et al. Neck Treatment of Patients With Early Stage Oral Tongue Cancer: Comparison Between Observation,Supraomohyoid Dissection, and Extended Dissection. *Cancer* (2008) 112:1066–75. doi: 10.1002/cncr.23278

Conflict of Interest: The authors declare that the research was conducted in the absence of any commercial or financial relationships that could be construed as a potential conflict of interest.

Publisher's Note: All claims expressed in this article are solely those of the authors and do not necessarily represent those of their affiliated organizations, or those of the publisher, the editors and the reviewers. Any product that may be evaluated in this article, or claim that may be made by its manufacturer, is not guaranteed or endorsed by the publisher.

frontiers in Oncology

ORIGINAL RESEARCH
published: 15 February 2022
doi: 10.3389/fonc.2022.814082

Carbon Ion Beam Boost Irradiation in Malignant Tumors of the Nasal Vestibule and the Anterior Nasal Cavity as an Organ-Preserving Therapy

Fabian Eberle[1,2], Rita Engenhart-Cabillic[1,2], Markus M. Schymalla[1,2], Christoph Dumke[1,2], Ulrike Schötz[1,2], Florentine S.B. Subtil[1,2], Kilian-Simon Baumann[1,2], Boris A. Stuck[3], Christine Langer[4], Alexandra D. Jensen[1,5], Henrik Hauswald[2,6] and Stefan Lautenschläger[1,2]*

[1] Department of Radiation Oncology, Marburg University Hospital, Marburg, Germany, [2] Marburg Ion-Beam Therapy Center (MIT), Department of Radiation Oncology, Marburg University Hospital, Marburg, Germany, [3] Department of Otolaryngology/Head & Neck Surgery, Marburg University Hospital, Marburg, Germany, [4] Department of Otolaryngology/Head & Neck Surgery, Gießen University Hospital, Gießen, Germany, [5] Department of Radiation Oncology, Gießen University Hospital, Gießen, Germany, [6] Department of Radiation Oncology, Heidelberg University Hospital, Heidelberg, Germany

OPEN ACCESS

Edited by:
Jordi Giralt,
Vall d'Hebron University Hospital, Spain

Reviewed by:
Franz Rödel,
University Hospital Frankfurt, Germany
Christiane Matuschek,
University Hospital of Düsseldorf, Germany

***Correspondence:**
Fabian Eberle
Fabian.eberle@uk-gm.de
orcid.org/0000-0002-1473-6065

Specialty section:
This article was submitted to Head and Neck Cancer, a section of the journal Frontiers in Oncology

Received: 12 November 2021
Accepted: 19 January 2022
Published: 15 February 2022

Citation:
Eberle F, Engenhart-Cabillic R, Schymalla MM, Dumke C, Schötz U, Subtil FSB, Baumann K-S, Stuck BA, Langer C, Jensen AD, Hauswald H and Lautenschläger S (2022) Carbon Ion Beam Boost Irradiation in Malignant Tumors of the Nasal Vestibule and the Anterior Nasal Cavity as an Organ-Preserving Therapy. Front. Oncol. 12:814082. doi: 10.3389/fonc.2022.814082

Background: Surgery and radiotherapy are current therapeutic options for malignant tumors involving the nasal vestibule. Depending on the location, organ-preserving resection is not always possible, even for small tumors. Definitive radiotherapy is an alternative as an organ-preserving procedure. Carbon ion beam radiotherapy offers highly conformal dose distributions and more complex biological radiation effects eventually resulting in optimized normal tissue sparing and improved outcome. The aim of the current study was to analyze toxicity, local control (LC), and organ preserving survival (OPS) after irradiation of carcinoma of the nasal vestibule with raster-scanned carbon ion radiotherapy boost (CIRT-B) combined with volumetric intensity modulated arc therapy (VMAT) with photons.

Methods: Between 12/2015 and 05/2021, 21 patients with malignant tumors involving the nasal vestibule were irradiated with CIRT-B combined with VMAT and retrospectively analyzed. Diagnosis was based on histologic findings. A total of 17 patients had squamous cell carcinoma (SCC) and 4 had other histologies. In this series, 10%, 67%, and 24% of patients had Wang stages 1, 2, and 3 tumors, respectively. Three patients had pathologic cervical nodes on MRI. The median CIRT-B dose was 24 Gy(RBE), while the median VMAT dose was 50 Gy. All patients with pathologic cervical nodes received simultaneously integrated boost with photons (SIB) up to a median dose of 62.5 Gy to the pathological lymph nodes. Eight patients received cisplatin chemotherapy. All patients received regular follow-up imaging after irradiation. Kaplan–Meier estimation was used for statistical assessment.

Results: The median follow-up after irradiation was 18.9 months. There were no common toxicity criteria grade 5 or 4 adverse events. A total of 20 patients showed grade 3 adverse events mainly on skin and mucosa. All patients were alive at the end of follow-up. The median OPS after treatment was 56.5 months. The 6- and 24-month OPS were 100% and 83.3%, respectively. All local recurrences occurred within 12 months after radiotherapy. The median progression free survival (PFS) after treatment was 52.4 months. The 6-, 12-, and 24-month PFS rates were 95%, 83.6%, and 74.3%, respectively.

Conclusion: CIRT-B combined with VMAT in malignant tumors of the nasal vestibule is safe and feasible, results in high local control rates, and thus is a good option as organ-preserving therapy. No radiation-associated grade 4 or 5 acute or late AE was documented.

Keywords: malignancy of the nasal vestibule, malignancy of the nasal cavity, organ-preserving therapy, irradiation, carbon ion beam therapy, particle beam therapy, radiotherapy, nasal cancer

INTRODUCTION

Malignant tumors of the nasal vestibule and the anterior nasal cavity are rare and account for less than 1% of all head and neck tumors (1, 2). Primary tumors of the nasal vestibule had an estimated standardized incidence of 0.4 per 100,000 inhabitants (3). There are three main staging systems: the American Joint Committee on Cancer (AJCC) (4), the Union for International Cancer Control (UICC) (5), and the Wang system (6) (**Table 1**). The Wang classification is a staging system based primarily on clinical tumor characteristics. It is considered the most appropriate classification system for malignancy of the nasal vestibule (7–9). Standard of care includes surgery, with or without adjuvant radiotherapy in certain postoperative risk constellations or definitive radiotherapy. Although surgery can yield high control rates, organ preservation may not always be possible, even for small tumors (10–12). Definitive radiotherapy for malignant tumors of the nasal vestibule and the anterior nasal cavity involving the nasal vestibule may be preferable as an organ-preserving procedure (13). Different irradiation techniques such as brachytherapy (9, 14, 15) or external beam radiotherapy (EBRT) (8, 16) or a combination of both (17) are available. Especially in early stages, any of these treatment options leads to high local control rates and can yield good cosmetic and functional results. For larger lesions, control rates decrease after definitive EBRT with photons (8). Carbon ions have different radiobiological effects eventually being able to overcome radioresistance (18, 19). For example, carbon ions could eradicate hypoxic and stem cell-like tumor cells and create an antiangiogenic and less immunosuppressive state (20, 21). Furthermore, due to the specific energy deposition resulting in the Bragg-Peak, carbon ions offer improved normal tissue sparing. Therefore, carbon ion beam radiotherapy might be more effective in eliminating tumor cells while showing less adverse events compared to photon beam radiotherapy. Currently, there are no clinical data on radiotherapy with carbon ion boost (CIRT-B) combined with volumetric intensity modulated arc therapy (VMAT) for tumors of the nasal vestibule and the anterior nasal cavity. For other tumors in the head and neck region, excellent results have been achieved with the use of carbon ions (22–26). The aim of the current study was to analyze toxicity, local control, and organ-preserving survival after irradiation of malignant tumors of the nasal vestibule and the anterior nasal cavity with raster-scanned CIRT-B combined with VMAT with photons as organ-preserving therapy at the Marburg Ion-Beam Therapy Center/ Marburg University Hospital.

Abbreviations: AE, Adverse events; CIRT, carbon ion radiotherapy; CIRT-B, carbon ion radiotherapy boost; CT, computed tomography; CTC, common toxicity criteria; CTV, clinical target volume; CTV-B, clinical target volume—boost; CTV-SIB, clinical target volume—simultaneously integrated boost; DSS, disease-specific survival; EBRT, external beam radiotherapy; ENI, elective nodal irradiation; EQD2, equivalent dose in 2 Gy; Gy, Gray; Gy(RBE), Gray (Relative biological effectiveness); GTV, gross tumor volume; GTV-B, gross tumor volume—boost; GTV-SIB, gross tumor volume—simultaneously integrated boost; IMRT, intensity modulated radiotherapy; IR, interventional/interstitial radiotherapy; LC, local control; LEM, local effect model; LRC, locoregional control; MRI, magnetic resonance imaging; OPS, organ-preserving survival; OS, overall survival; PFS, progression-free survival; PTV, planning target volume; RBE, relative biological effectiveness; RT, radiotherapy; SCC, squamous cell carcinoma; SD, single dose; TD, total dose; VMAT, volumetric intensity modulated arc therapy.

MATERIALS AND METHODS

Patients' Characteristics

Between November 2015 and May 2021, 21 patients from Marburg and Gießen University Hospital mainly with SCC of the nasal vestibule and the anterior nasal cavity were irradiated at the Marburg Ion-Beam Therapy Center with CIRT-B combined with VMAT carried out at the Department of Radiation Oncology of the Marburg University Hospital. Diagnosis was primarily based on histologic findings and on magnetic resonance imaging (MRI). Further patients' and treatment characteristics are found in **Tables 2**, **3**.

Initial Treatment

Two patients underwent organ-preserving surgery at initial diagnosis. Due to the early stages and missing evidence of tumor after surgery, no adjuvant treatment was performed.

TABLE 1 | Classification systems for malignancies of the nasal cavity/paranasal sinuses and the nasal vestibule.

	American Joint Committee on Cancer (AJCC)	Union International Centre le Cancer (UICC 2002)	Wang-classification for malignancy of the nasal vestibule
T1	Tumor restricted to any 1 subsite, with or without bony invasion	Limited to 1 subsite	Limited to the nasal vestibule, relative superficial, involving 1 or more sites within
T2	Tumor invading 2 subsites in a single region or extending to involve an adjacent region within the nasoethmoidal complex, with or without bony invasion	Involves 2 subsites or adjacent nasoethmoidal site	Extended from the nasal vestibule to adjacent structures, such as the upper nasal septum, upper lip, philtrum, skin of the nose, and/or nasolabial fold, but not fixed to the underlying bone
T3	Tumor extends to invade the medial wall or floor of the orbit, maxillary sinus, palate, or cribriform plate	Invasion of medial wall/floor orbit, maxillary sinus, palate,cribriform plate	Massive with extension to the hard palate, buccogingival sulcus, large portion of the upper lip, upper nasal septum, turbinate, and/or paranasal sinuses, fixed with deep muscle or bone involvement
T4a	Tumor invades any of the following: anterior orbital contents, skin of the nose or cheek, minimal extension to the anterior cranial fossa, pterygoid plates, sphenoid or frontal sinuses	Involvement of anterior orbit, skin of nose/cheek, anterior cranial fossa, pterygoid plates,sphenoid/frontal sinuses	undefined
T4b	Tumor invades any of the following: orbital apex, dura, brain, middle cranial fossa, cranial nerves other than maxillary division of trigeminal nerve (V2), nasopharynx, or clivus	Involvement of orbital apex, dura, brain, middle cranial fossa, cranial nerves other than V2, nasopharynx, clivus	undefined

Macroscopic recurrence occurred during regular oncologic follow-up, and definitive salvage RT was performed. For these two patients, the time interval between resection and diagnosis of recurrent disease was 19 and 30 months, respectively. No patient received prior chemotherapy or radiotherapy.

Immobilization and Target Volume Definition

For patient immobilization, a thermoplastic head-shoulder-mask was used. Computed tomography (CT, 3-mm slices) was used for treatment planning. For precise contouring, a T1-weighted contrast-enhanced MRI was three-dimensionally registered to the planning CT. The gross tumor volume (GTV-B) was defined as the contrast-enhancing primary tumor on a T1 contrast-enhanced MRI. If there was nodal involvement, a second GTV (GTV-SIB) was delineated. Separate clinical target volumes (CTVs) were delineated. The clinical target volume for the CIRT boost (CTV-B) was defined as a 5-mm expansion to the GTV-B respecting anatomical borders. CTV-photons were the extended target volume and included CTV-B, typical pathways of spread, and in advanced stages and in patients with nodal involvement elective lymph node levels (facial, Ib, II, III). The clinical target volume for SIB (CTV-SIB) was defined as a 5- to 7-mm expansion of the GTV-SIB. The planning target volume (PTV) was defined as the CTV plus a 3-mm margin.

Treatment Planning

Treatment planning for raster-scanned CIRT-B was performed with the Siemens Syngo.via PT planning software. Biological dose optimization was performed based on the local effect model (LEM) 1. VMAT plans were calculated with the Varian ECLIPSE V 15.6 planning software.

Treatment

CIRT-B was performed at the Marburg Ion-Beam Therapy Center with carbon ion (^{12}C) beams *via* the active raster scanning method with 2 to 4 noncoplanar treatment beams under daily image guidance with orthogonal X-rays and weekly CT-based recalculations. Photon treatment was carried out in Rapid Arc IMRT technique at the Department of Radiation Oncology of the Marburg University Hospital. A Varian True Beam linear accelerator with a motoric multileaf collimator of 0.5-cm leaf width under daily image guidance with CBCT in the treatment position was used. The prescribed dose was normalized to the median dose of the target volume. Furthermore, the PTV was encompassed within the 95–107% isodose level of the prescribed dose. Patients received a CIRT-B with 18–24 Gy(RBE) to PTV-B in 6–8 fractions followed by 50–56 Gy photon VMAT to PTV-photons in 2 Gy per fraction. Patients with nodal involvement received simultaneously integrated photon boost (SIB) up to 62.1–64.4 Gy with 2.3 Gy per fraction to PTV-SIB. Five fractions per week were administered.

In advanced stages and in patients with nodal involvement on MRI elective nodal irradiation (ENI) with simultaneously integrated boost (SIB) was performed with photons and cisplatin chemotherapy was administered simultaneously to photon treatment (40 mg/m^2 weekly). Further treatment characteristics are found in **Table 3**.

Evaluation

Prospectively collected datasets and medical reports of all patients who received irradiation treatment with CIRT-B followed by VMAT between 2015 and 2021 for malignancies of the anterior nasal cavity with involvement of the nasal vestibule were evaluated. Treatment and follow-up was performed according to a fixed scheme at our center. The first clinical follow-up examination was 6 weeks after finishing radiotherapy; the first follow-up examination including MRI of the head and neck was 3 months after finishing radiotherapy and every 3 months thereafter. Adverse events (AEs) were classified

TABLE 2 | Patients' characteristics.

Parameter	N	%
Gender		
Male	12	57
Female	9	43
Age, years		
Median	57	
Range	44-89	
ECOG Score at RT		
0	17	81
1	4	19
Smoking history		
Smoker	7	34
Non-Smoker	14	66
Histology		
SCC	17	81
Others (AC, AS, MYC, MEC)	4	9
Grading		
G1	3	14
G2	11	52
G3	7	33
HPV status (p16)		
negative	6	29
positive	2	10
n.a.	13	61
Tumor site		
vestibule	2	10
vestibule and anterior nasal cavity	19	90
Largest diameter, mm		
Median	22.5	
Range	14-43	
PT Stage		
Wang		
1	2	9
2	14	67
3	5	24
AJCC		
1	2	10
2	15	71
3	-	-
4a	4	19
4b	-	-
UICC		
1	2	10
2	15	71
3	-	-
4a	4	19
4b	-	-
Nodal stage		
N0	18	86
N1	-	-
N2a	-	-
N2b	1	5
N2c	2	9
Skin invasion		
Yes	4	19
No	17	81
Bone invasion		
Yes	3	14
No	18	86

SCC, squamous cell carcinoma; AC, adenocarcinoma; AS, angiosarcoma; MYC, myoepithelial carcinoma; MEC, mucoepidermoid carcinoma; n.a., not available; RT, radiotherapy; PT, primary tumor.

according to the common toxicity criteria for adverse events version 5 (CTCAE V.5).

Statistical Design and Classifications

Toxicity, organ-preserving survival (OPS), local control (LC), and progression-free survival (PFS) were evaluated. Time estimates refer to the date of treatment planning CT. LC was defined as the absence of local tumor progression including all cases of stable disease (less than 50% tumor mass reduction), partial remission (tumor mass reduction of at least 50%), and complete remission (requiring no detectable disease). Survival analyses were carried out with I.B.M. SPSS 21 using Kaplan–Meier estimation and log rank test.

Ethics

The local ethics committee approved the study (Marburg, Germany, study number EK_MR_31_03_21). All patients gave informed consent. This study was conducted in accordance with the Declaration of Helsinki.

Data Sharing Statement

Due to the legal aspects of the patients' informed consent, sharing of data is not possible.

RESULTS

Adverse Events

According to CTCAE V 5.0, none of the patients developed CTC grade 5 or 4 AE. At the end of treatment, 61.9% of the patients developed grade 3 and 38.1% of the patients developed grade 2 acute AE mostly on skin, mucosa, and on swallowing. Rapid recovery from skin and mucosal toxicity was seen in the majority of the patients. Six weeks after completion of treatment, 14.3% of the patients showed grade 3 acute AE. CTC grades 1 and 2 acute AE at the end of treatment and 6 weeks after treatment were seen in 38.1% and 81.0% of the patients, respectively (**Figure 1** and **Table 4**).

The most frequent acute AE CTC grade 3 at the end of treatment were dermatitis, dry mouth with inability to adequately aliment orally, mucositis with severe pain affecting oral intake, and dysphagia with severely altered eating/swallowing in 52.4%, 28.6%, 52.4%, and 33.3% of the patients, respectively. Inpatient treatment of patients with mucosal AE and impaired swallowing during radiotherapy was required in 8 patients (38.1%). Tube feeding was indicated in 7 patients (33.3%). In the CTCAE classification (V 5.0), there is no separate category for therapy-related complaints in the area of the nasal vestibule. Complaints in this region are thus best represented within the CTCAE term "sinus disorders." Sinus disorders CTCAE grade 2 with impairment of airflow or CTCAE grade 3 with significant nasal obstruction occurred in 52.4% and

TABLE 3 | Treatment characteristics.

Parameter	N	%
RT setting		
primary	19	90
salvage	2	10
Resection performed (before RT)		
Yes	2	10
No	19	90
Intervall between resection and RT, months		
Median	24.5	
Range	19-30	
Dose C_{12} Boost, Gy(RBE)		
Total dose (median)	24	
Range	18-24	
Single dose	3	
GTV Boost, ccm		
Median	4.1	
Range	1.2-26.4	
CTV Boost, ccm		
Median	171.3	
Range	7.3-	
PTV Boost, ccm		
Median	28.8	
Range	1	
Dose Photons, Gy		
Total dose (median)	50	
Range	50-56	
Single dose	2	
CTV Photons, ccm		
Median	171.3	
Range	7.3-436.6	
ENI performed		
Yes	14	67
No	7	33
Platinbased chemotherapy administered		
Yes	8	38
No	13	62
Duration of RT, days		
Median	48.5	
Range	38-52	

SCC, squamous cell carcinoma; AC, adenocarcinoma; AS, angiosarcoma; MYC, myoepithelial carcinoma; MEC, mucoepidermoid carcinoma; n.a., not available; RT, radiotherapy; PT, primary tumor; Gy(RBE), Gray (relative biological effectiveness); Gy, Gray; GTV, gross tumor volume; CTV, clinical target volume; PTV, planning target volume; Ccm, cubic centimeter; ENI, elective node irradiation; C_{12}, carbon ions.

23.8% of the patients, respectively. One case of cisplatin-related hearing loss without indication for intervention or hearing aid fitting occurred. At the end of treatment, CTCAE grade 1 dry eyes with mild symptoms relieved by lubricants were common in 52.4% of the patients. Grade 1 epistaxis without indication for intervention was seen in 42.9% of the patients.

Rapid and extensive recovery from skin and mucosal toxicity, xerostomia, dysphagia, and sinus disorders were observed in a majority of patients. Six weeks after completion of treatment, residual dry mouth or dysphagia and residual sinus disorders CTCAE grade 3 were present in 9.5% and 4.8% of the patients, respectively.

Late AE CTC grade 3 occurred in 14.2% (after 3 months), 21.1% (after 6 months), 21.4% (after 12 months), and 25.0% (after 24 months) of patients mostly consisting of nasal obstruction or cisplatin related hearing impairment that required medical intervention. In our series, 80.9%, 73.7%, 78.6%, and 75% of the patients had grade 1 or 2 sinus disorders with mucosal crusting or symptomatic stenosis at the level of the nasal vestibule interfering with airflow 3, 6, 12 and 24 months after radiotherapy, respectively. Additional three patients developed CTCAE grade 3 stenosis with significant nasal obstruction and limited airflow at the level of the nasal vestibule within the first 3–6 months after completion of radiotherapy, which required intervention. These limitations were most likely due to the formation of synechiae at the level of the nasal vestibule caused by therapy-related mucosal ulceration. Surgical intervention with removal of adhesions restored good airflow and respiratory function. One patient receiving radiochemotherapy developed cisplatin-related CTCAE grade 3 hearing loss 6 months after treatment, and a bilateral hearing aid was needed. CTC grades 1 and 2 AE 3, 6, 12, and 24 months after treatment were seen in 80.9%, 57.9%, 50.0%, and 50.0% of the patients, respectively (**Figure 1** and **Table 4**). Fibrotic changes CTCAE grade 2 of the soft tissue occurred at the earliest 3 months after the end of therapy. After 3, 6, 12, and 24 months, 23.8%, 47.4%, 50.0%, and 50.0% of the patients showed therapy-related fibrotic processes CTCAE grade 2 of the nasal soft tissue, respectively. No patient developed cartilage necrosis during follow-up. One patient with nose piercing developed a small soft tissue necrosis of the ala nasi, which required local wound care. No surgical intervention was required in this case. Six months after the end of treatment, there was no CTCAE grade 3 dysphagia or dry mouth. However, moderate dry mouth CTCAE grade 2 persisted after 6, 12, and 24 months in 47.4%, 21.4%, and 12.5% of the patients, respectively. Altered taste/unpleasant taste was present after 6 and 12 months in 2 patients. Further parameters regarding acute and late AE are found in **Table 4**.

Local Control and Survival

The median follow-up after treatment was 18.9 months (range, 3–64 months). All patients were alive at the end of follow-up. The estimated median LC after diagnosis was 56 months (range, 46–66 months). The actuarial 24-month LC rates after diagnosis for all patients (**Figure 2A**) and patients with Wang stage 3 tumors (**Figure 2B**) were 84% and 75%, respectively. Eighty percent of the patients showed complete clinical response without evidence of tumor on MRI 3 months after radiotherapy. There were three patients with local tumor progression after treatment. In all patients, this occurred within the first 12 months after therapy. Out-of-field (CIRT-B) progression of a single submandibular node was seen in one patient. In field (CIRT-B) progression was seen in two patients. Median time to progression at the initial tumor site was 6 months (range, 4–8 months). Two patients with local tumor progression underwent non organ-preserving salvage surgery; in one patient, organ-preserving salvage resection was feasible. Median time to salvage surgery after finishing initial treatment was 6 months (range, 5–10 months). None of the patients who had undergone salvage surgery developed tumor recurrence during further follow-up.

For malignant tumors of the nasal vestibule and the anterior nasal cavity, the median organ-preserving survival (OPS) after

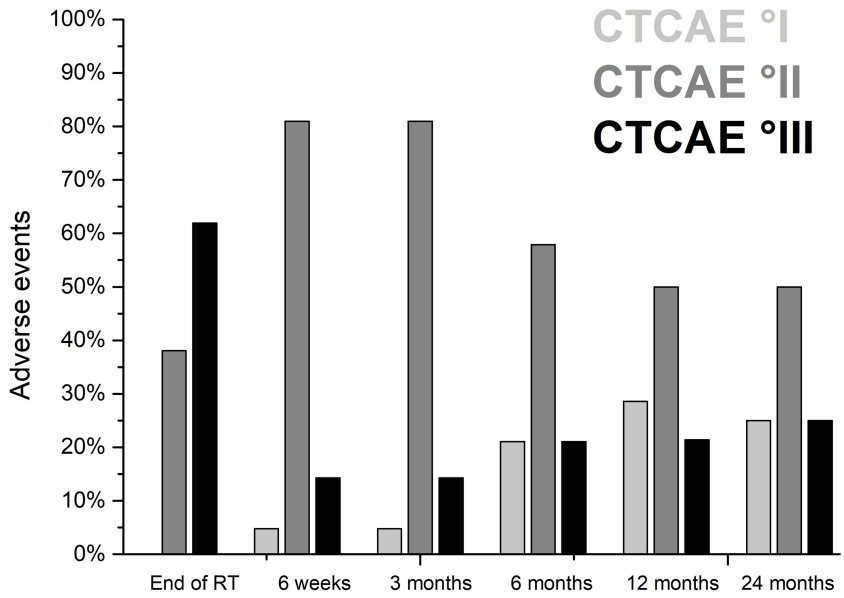

FIGURE 1 | Acute and late adverse events after definitive radiotherapy of 21 patients with malignant tumors involving the nasal vestibule irradiated with CIRT-B combined with VMAT according to common toxicity criteria for adverse events (CTCAE V 5.0).

diagnosis was 60 months (range, 52–68 months). The corresponding 6- and 12-month OPS rates after diagnosis for all patients were 100% and 90%, respectively (**Figure 3A**). For patients with Wang stage 3 tumors, the 12-month OPS rate was 75% (**Figure 3B**).

The median PFS after diagnosis was 52 months (range, 40–64 months). The corresponding 12- and 24-month PFS rates after diagnosis were 84% and 74%, respectively (**Figure 4**). There was one patient with locoregional relapse of a single submandibular node without evidence of tumor at the primary site. Initial treatment was performed as a local radiotherapy without ENI and without chemotherapy due to tumor stage. Nodal relapse occurred 19 months after end of radiotherapy. Salvage surgery followed by adjuvant elective irradiation of the lymphatic drain was performed. This patient remained free of tumor until the end of follow-up.

Prognostic Factors for LC

In univariate analysis on factors impacting on LC histology (SCC versus others, p=0.44), Wang stage (all stages, p=0.77), AJCC

TABLE 4 | Treatment-related acute and late adverse events according to common toxicity criteria for adverse events (CTCAE V 5.0).

	End of RT			6 weeks			3 months			6 months			12 months			24 months		
CTCAE grade	**I**	**II**	**III**	**I**	**II**	**III**	**I**	**II**	**III**	**I**	**II**	**III**	**I**	**II**	**III**	**I**	**II**	**III**
Number of patients at FU	**n=21**			**n=21**			**n=21**			**n=19**			**n=14**			**n=8**		
Dermatitis [%]	0.0	47.6	52.4	85.7	14.3	0.0	28.6	4.8	0.0	26.3	0.0	0.0	7.1	0.0	0.0	0.0	0.0	0.0
Mucositis [%]	19.0	23.8	52.4	38.1	28.6	0.0	19.0	4.8	0.0	10.5	0.0	0.0	0.0	0.0	0.0	0.0	0.0	0.0
Dysphagia [%]	19.0	33.3	33.3	28.6	33.3	9.5	42.9	14.3	4.8	15.8	5.3	0.0	14.3	0.0	0.0	0.0	0.0	0.0
Dysgeusia [%]	19.0	66.7	undefined	33.3	52.4	undefined	47.6	23.8	undefined	52.6	10.5	undefined	50.0	14.3	undefined	37.5	0.0	undefined
Dry mouth [%]	9.5	52.4	28.6	14.3	66.7	9.5	19.0	66.7	4.8	36.8	47.4	0.0	64.3	21.4	0.0	50.0	12.5	0.0
Dry eye [%]	52.4	0.0	0.0	38.1	0.0	0.0	19.0	0.0	0.0	10.5	0.0	0.0	14.3	0.0	0.0	12.5	0.0	0.0
Optic nerve disorder [%]	0.0	0.0	0.0	0.0	0.0	0.0	0.0	0.0	0.0	0.0	0.0	0.0	0.0	0.0	0.0	0.0	0.0	0.0
Hearing impaired [%]	4.8	4.8	0.0	4.8	4.8	0.0	4.8	9.5	0.0	5.3	5.3	5.3	7.1	7.1	7.1	0.0	0.0	12.5
Epistaxis [%]	42.9	0.0	0.0	28.6	0.0	0.0	19.0	0.0	0.0	15.8	0.0	0.0	14.3	0.0	0.0	12.5	0.0	0.0
Sinus disorders [%]	23.8	52.4	23.8	23.8	71.4	4.8	47.6	33.3	9.5	57.9	15.8	15.8	64.3	14.3	14.3	75.0	0.0	12.5
Soft tissue fibrosis [%]	9.5	0.0	0.0	19.0	0.0	0.0	28.6	23.8	0.0	21.1	47.4	0.0	14.3	50.0	0.0	12.5	50.0	0.0

stage (all stages, p=0.71), UICC stage (all stages, p=0.72), size of GTV (>3.9 ccm versus <3.9 ccm, p=0.46), size of CTV (>8.2 ccm versus <8.2 ccm, p=0.83), size of PTV (>31.8 ccm versus <31.8 ccm, p=0.24), maximal tumor diameter (>20 mm versus <20 mm, p=0.28), presence of bone infiltration (yes versus no, p=0.31), presence of skin infiltration (yes versus no, p=0.51), upper lip involvement (yes versus no, p=0.66), upper septum involvement (yes versus no, p=0.86), delivery of chemotherapy (delivery versus no delivery, p=0.53), and previously tumor resection (yes versus no, p=0.15) did not demonstrate statistically significant effects. Further parameters are demonstrated in **Table 5**. Multivariable analysis on LC was not performed due to missing prognostic factors in univariate analysis and the limited number of patients.

Prognostic Factors for Survival

Histology (SCC versus others, p=0.50), tumor stage (Wang stage, p=0.50; AJCC stage, p=0.48); UICC stage, p=0.49), and presence of bone invasion (yes versus no, p=0.12) did not demonstrate statistically significant effects on OPS. Furthermore, target volume and tumor size had no statistically significant effect on OPS (GTV>3.9 ccm, p=0.54; CTV>8.2 ccm, p=0.83; PTV>31.8 ccm, p=0.62; maximal tumor diameter>20 mm, p=0.76). Additional parameters are found in **Table 6**. Multivariable analysis on survival was not performed due to missing prognostic factors in univariate analysis.

DISCUSSION

We have analyzed all patients with malignant tumors of the vestibule or the anterior nasal cavity with involvement of the nasal vestibule consecutively treated with CIRT-B combined with VMAT at Marburg Ion-Beam Therapy Center and Department of Radiation Oncology of the Marburg University Hospital between December 2015 and May 2021.

It was our aim to retrospectively assess the treatment results in our patients and help finding ways to improve the outcome in this rare and challenging disease. To our knowledge, this is the first report on clinical outcomes after irradiation with CIRT-B followed by photon EBRT in malignant tumors of the vestibule or the anterior nasal cavity with involvement of the nasal vestibule.

Langendijk et al. evaluated the results of primary RT for SCC of the nasal vestibule. A total of 56 patients with Stage T1 and T2 tumors (Wang classification) were treated. The 2-year LC-rate was 88% after EBRT. The 2-year locoregional control (LRC) was 87% (16). As with our patients, none of the patients developed distant metastases. Out of 10 patients with local recurrence at the primary tumor site, 8 were successfully salvaged by surgery. The ultimate local control rate after 5 years was 95%. In our collective ultimate LC and LRC following surgical salvage treatment (local (n = 3), locoregional (n = 1)) was 100% after a median follow-up for these patients of 18.2 months. In a retrospective analysis of 174 patients receiving surgery, radiotherapy, or both treatment modalities conducted by Agger et al., LC and disease-specific survival for all patients after 5 years were 80% and 74%, respectively (8). In a stratified analysis of T1 tumors (Wang), the authors found a higher 5-year LRC for surgery compared to the hypofractionated high-dose radiotherapy group (EQD2 67.5) (94% versus 87%). The subgroup of patients who were treated with RT doses below 66 Gy performed worse with LRC rates of 60% after 5 years. This suggests that for RT alone, a sufficiently high dose is crucial for the outcome of therapy. Vanneste et al. reported on 81 patients who were treated with EBRT (TD 59.4 Gy, SD 2.7) or interstitial brachytherapy (60 Gy) for primary, localized, SCC of the nasal vestibule. LC at 5 years over all stages was 85%; T1 tumors performed better with LC of 97% (17). Interventional radiotherapeutic (IR) procedures are mainly used for small tumors (Wang stages 1 and 2). Good clinical results with LC rates of 80–90% after 5 years can be achieved when IR for Wang stages 1 and 2 tumors is used. For all patients with local recurrence, salvage resection was possible and performed (9, 14, 27). Primary CIRT-B and EBRT treatment resulted in LC and PFS rates of 84% and 74% after 24 months, respectively, in our cohort. These results are in the range of those reported by others on primary RT in malignancy of the nasal vestibule. However, direct comparability with other published data is difficult due to the use of different treatment concepts, radiation techniques, staging systems, small and inhomogeneous patient collectives, and various endpoints.

There are no data on the treatment of malignant tumors of the nasal vestibule with carbon ions, but clinical data exist on the treatment of head and neck and paranasal sinus tumors with this irradiation technique. Studies showed that carbon ion radiotherapy can yield favorable outcomes for patients with certain head and neck tumors, e.g., adenoid cystic carcinoma, recurrent head and neck cancer, or mucosal melanoma (22–26). In a retrospective analysis of 95 patients with locally advanced adenoid cystic carcinoma of the head and neck, definitive raster-scanned C12 therapy was compared with modern photon techniques. LC, PFS, and OS at 5 years were significantly higher in the C12 group (59.6%, 48.4%, and 76.5%, respectively) compared with the photon group (39.9%, 27%, and 58.7%, respectively) (25). In a retrospective study, 229 patients with recurrent head and neck cancer were treated with carbon ion radiotherapy (CIRT). CIRT seems to be an effective treatment with acceptable toxicity resulting in good LC rates. Median local PFS and OS after radiotherapy with carbon ions were 24.2 and 26.1 months, respectively (28). In a retrospective analysis performed by Mohr et al., CIRT was used for the treatment of mucosal melanoma of the paranasal sinuses. LC at 3 years was 58.3% at mild toxicity. OS was poor due to the occurrence of distant metastases (29).

Surgical resection is often performed for malignancies of the nasal vestibule and is considered a reliable local treatment option especially for advanced stages or as salvage treatment (30). Resection, even if cosmetically compromising, can achieve high local control rates between 82% and 94% after 3 years similar to RT in appropriately selected patients (3, 8, 10, 31, 32). Depending on tumor location and extension, organ-preserving resection is not always possible, and in advanced stages, resection should be combined with postoperative RT (10, 15, 31–33).

In the report by Kummer et al., all 47 patients experienced acute RT AE, mainly dermatitis (28% °III), mucositis (30% °III),

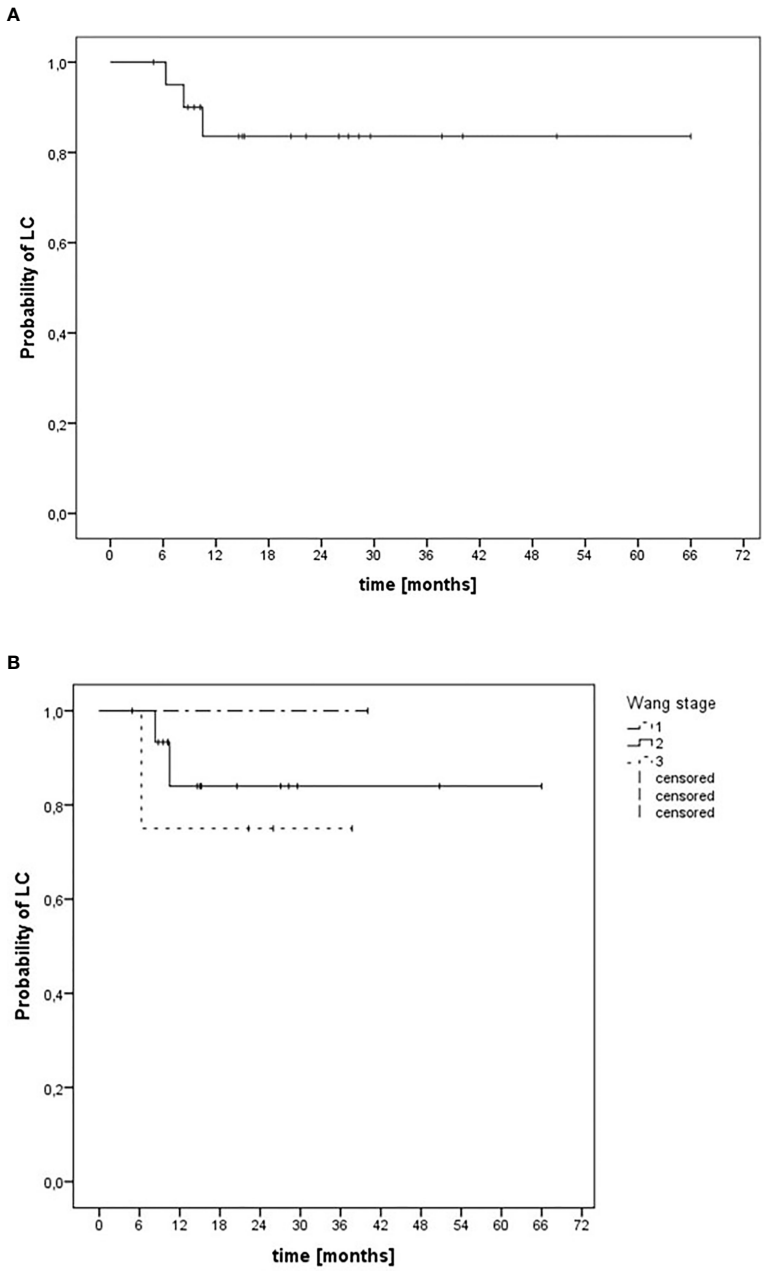

FIGURE 2 | Kaplan–Meier estimation of local control after definitive radiotherapy of 21 patients with malignant tumors involving the nasal vestibule irradiated with CIRT-B combined with VMAT. **(A)** LC independent of tumor stage. **(B)** LC depending on Wang stage.

and crust. Acute mucosal and skin AE grade 3 occurred in 30% and 28% of the patients, respectively. Late radiation AE was reported only in a few patients. A perforated nasal septum due to cartilage necrosis occurred in three patients (6%); severe stenosis of the nasal airway was reported for two cases (4%) (34). In the cohort by Vanneste et al., all patients experienced acute dermatitis of the nasal skin and mucositis of the nasal cavity. Grade III mucositis of the oral cavity was seen in 10% of the patients. About 72% of the patients survived long-term without AE. Three patients (3%) experienced a perforated septum; in 2 cases, the nasal septum showed tumor infiltration. Two patients (2.5%) experienced severe stenosis of the nasal airway (17). The patients in the study of Wallace et al. mainly reported moderate soft tissue AE (21%) that resolved without intervention. Severe complications occurred in 4.2% of the patients treated with RT (35). In addition, Langendijk et al. reported that the most common late AE were rhinorrhea (45%), nasal dryness (39%), and adhesions (4%) (16). There was no

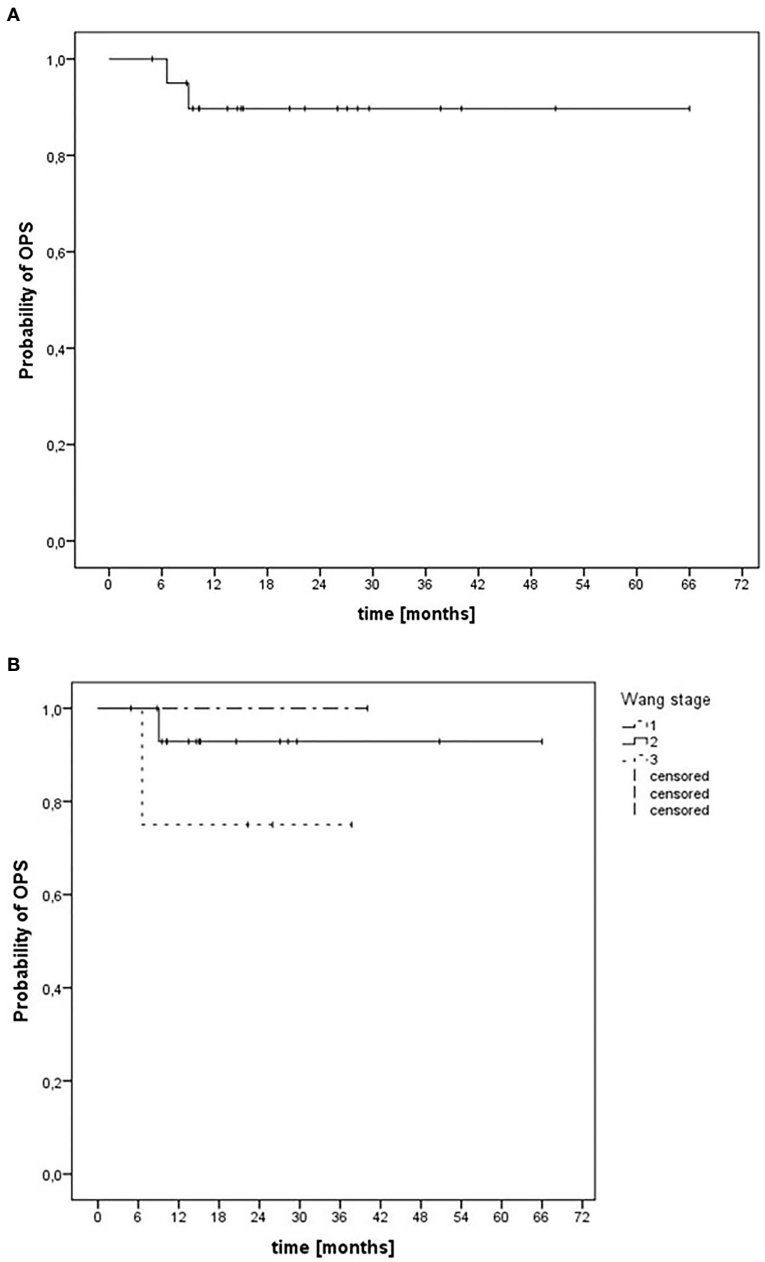

FIGURE 3 | Kaplan–Meier estimation of organ-preserving survival (OPS) after CIRT-B combined with VMAT. **(A)** OPS independent of tumor stage. **(B)** OPS depending on Wang stage.

CTC grade 5 or 4 AE, but 20 patients showed grade 3 adverse events mainly on the skin and mucosa. However, even though there was no grade 4 or 5 AE in our cohort, 20 patients developed CTC grade 3 acute AE, requiring medical intervention. The high rate of AE, especially at the skin and mucosa, is consistent with the data for RT of malignancies of the nasal vestibule mentioned above. In our cohort, relevant stenoses CTCAE grade 3 at the level of the nasal vestibule occurred as a long-term AE in 15% of the patients. However, long-term low-grade stenoses at the level of the nasal vestibule are frequent. They do also affect the patient and complicate the oncological clinical follow-up due to changes of the nasal passage and are therefore clinically highly relevant. Despite the high dose applied, no patient developed cartilage necrosis during follow-up, and the cosmetic results after combined RT with CIRT-B were excellent.

There is disagreement in the literature regarding prognostic factors for LC and survival after RT for malignancies of the nasal vestibule. Vanneste et al. found that increasing T classification

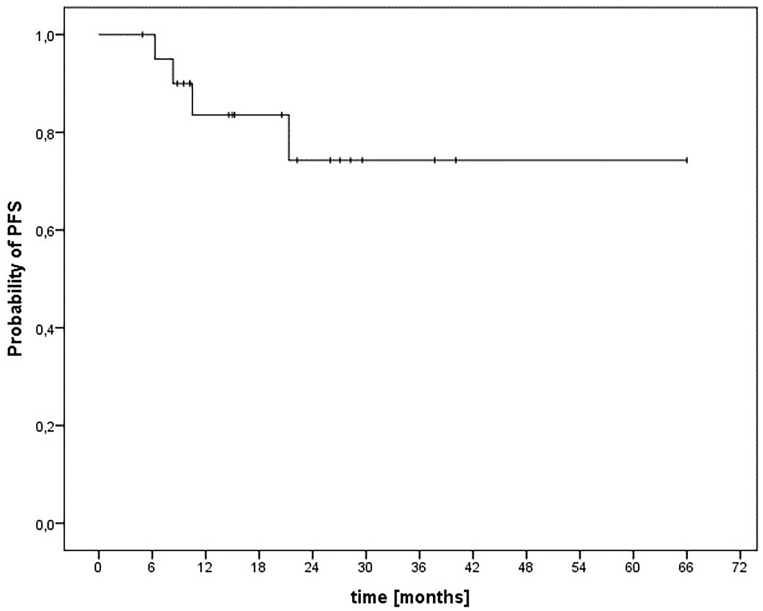

FIGURE 4 | Kaplan–Meier estimation of progression-free survival after CIRT-B combined with VMAT.

TABLE 5 | Univariate analyses on local control (Log Rank Test).

Parameter	p-value
Smoker	0.82
Gender	0.83
Age (>56.4 years)	0.59
Histology	
Histology (SCC versus others)	0.44
Grading	0.33
HPV status	0.51
Stage	
Wang (all stages)	0.77
Wang (3 versus 1)	0.62
Wang (3 versus other stages)	0.53
AJCC (all stages)	0.71
AJCC (4 versus 1)	0.48
AJCC (4 versus other stages)	0.52
UICC (all stages)	0.72
UICC (4 versus 1)	0.48
UICC (4 versus other stages)	0.53
Tumor size	
GTV size (>3.9ccm)	0.46
CTV size (>8.2ccm)	0.83
PTV size (>31.8ccm)	0.24
Tumor diameter (>20mm)	0.28
Clinical parameters	
Presence of skin infiltration	0.51
Presence of bone infiltration	0.31
Upper lip involvement	0.66
Upper septum involvement	0.86
Delivery of chemotherapy	0.53
Previously tumor resection	0.15

*$p < 0.05$.
GTV, gross tumor volume; CTV, clinical target volume; PTV, planning target volume; SCC, squamous cell carcinoma.

was linked with poorer LC and LRC, and the risk of a local recurrence increased with tumor size (17). In a retrospective series of cancer of the nasal vestibule, Agger et al. found no statistically significant effects in 5-year LRC with regard to sex, age, or smoking status. However, Wang classification was prognostic for LRC and DSS in this series of patients (8). Kummer et al. could show that the effect of RT (DSS) is significantly correlated with tumor stage, and hence RT is less successful in T3 lesions. Limited success for T3 lesions should be interpreted with caution because only three patients were included, and no chemotherapy was applied in advanced stages (34). In a series published by Wallace et al., cause-specific survival was lower in patients with unfavorable T4 tumors (>4 cm with bone invasion) after definitive RT (35). A total of 56 patients with SCC of the nasal vestibule were treated and retrospectively evaluated by Langendijk et al. No significant association between Wang stage, tumor diameter, or tumor localization and LC was found by the authors (16). Our analysis did not identify prognostic factors related to LC and survival. This may possibly be explained by the small number of patients and the short follow-up.

Finally, the limitations of our analysis were the retrospective character and the limited patient number. Furthermore, patients had different tumor types, and 9.5% had resection alone during their treatment at initial diagnosis and RT was performed as salvage treatment. However, this is the first analysis reporting on CIRT-B combined with VMAT as an organ-preserving, primary procedure in malignant tumors of the vestibule or the anterior nasal cavity with involvement of the nasal vestibule and has a

TABLE 6 | Univariate analyses on organ-preserving survival (OPS) (Log Rank Test).

Parameter	p-value
Smoker	0.56
Gender	0.25
Age (>56.4 years)	0.16
Histology	
Histology (SCC versus others)	0.50
Grading	0.12
HPV status	0.56
Stage	
Wang (all stages)	*0.50*
Wang (3 versus 1)	0.61
Wang (3 versus other stages)	0.25
AJCC (all stages)	*0.48*
AJCC (4 versus 1)	0.48
AJCC (4 versus other stages)	0.24
UICC (all stages)	*0.49*
UICC (4 versus 1)	0.48
UICC (4 versus other stages)	0.25
Tumor size	
GTV size (>3.9ccm)	0.54
CTV size (>8.2ccm)	0.83
PTV size (>31.8ccm)	0.62
Tumor diameter (>20mm)	0.76
Clinical parameters	
Presence of skin infiltration	0.24
Presence of bone infiltration	0.12
Upper lip involvement	0.74
Upper septum involvement	0.58
Delivery of chemotherapy	1.00
Previously tumor resection	0.07

*$p < 0.05$.
GTV, gross tumor volume; CTV, clinical target volume; PTV, planning target volume; SCC, squamous cell carcinoma.

reasonable number of patients treated with a homogenous treatment approach.

CONCLUSIONS

CIRT-B combined with VMAT with photons in the primary treatment of malignant tumors of the nasal vestibule and the anterior nasal cavity is safe and feasible, resulting in high local control and survival rates and thus is a good option as an organ-preserving therapy. In local or locoregional recurrences after definitive RT, there are good surgical salvage options for the patients.

No radiation-associated grade 4 or higher AE were documented, and the treatment was tolerated well. However, a relevant number of patients developed grade 3 acute AE mostly regarding the skin, mucosa, and swallowing at the end of treatment. A more limited proportion of patients developed late AE mostly at the paranasal sinuses or cisplatin-related hearing impairment that required medical interventions. Further investigations including the issue of potential target volume reduction within prospective trials on carbon ion beam irradiation in malignancy of the nasal vestibule and the anterior nasal cavity are warranted.

DATA AVAILABILITY STATEMENT

The raw data supporting the conclusions of this article will be made available by the authors, without undue reservation.

ETHICS STATEMENT

The studies involving human participants were reviewed and approved by Ethikkommission des Fachbereichs Humanmedizin der Philipps-Universität Marburg. The patients/participants provided their written informed consent to participate in this study.

AUTHOR CONTRIBUTIONS

FE, SL, HH, and RE-C developed and planned the study. FE and SL performed data management. FE and SL performed data analysis. FE, SL, and RE-C performed data interpretation. FE and SL drafted the manuscript. RE-C, CD, US, FS, K-SB, BS, CL, AJ, and HH critically revised the manuscript for important intellectual content. All authors read and approved the final manuscript and agreed to be accountable for all aspects of the work.

ACKNOWLEDGMENTS

We thank Inga Stanger for data management.

REFERENCES

1. Pantelakos ST, McGuirt WF, Nussear DW. Squamous Cell Carcinoma of the Nasal Vestibule and Anterior Nasal Passages. *Am J Otolaryngol* (1994) 15 (1):33–6. doi: 10.1016/0196-0709(94)90037-x
2. Patel P, Tiwari R, Karim AB, Nauta JJ, Snow GB. Squamous Cell Carcinoma of the Nasal Vestibule. *J Laryngol Otol* (1992) 106(4):332–6. doi: 10.1017/s0022215100119425
3. Vital D, Morand G, Huber GF, Studer G, Holzmann D. Outcome in Squamous Cell Carcinoma of the Nasal Vestibule: A Single Center Experience. *Head Neck* (2015) 37(1):46–51. doi: 10.1002/hed.23549
4. Amin B, Edge SB, Green F, Byrd DR, Brooklan RK, Washington MK, et al. eds. *AJCC Cancer Staging Manual. 8 ed*. Basel: Springer International Publishing (2017).
5. MKG James, D Brierley, C Wittekind eds. *TNM Classification of Malignant Tumours. 8th Edition*. Hoboken: Wiley-Blackwell (2016).
6. Wang CC. Treatment of Carcinoma of the Nasal Vestibule by Irradiation. *Cancer* (1976) 38(1):100–6. doi: 10.1002/1097-0142(197607)38:1<100::aid-cncr2820380118>3.0.co;2-9
7. Jeannon JP, Riddle PJ, Irish J, O'sullivan B, Brown DH, Gullane P. Prognostic Indicators in Carcinoma of the Nasal Vestibule. *Clin Otolaryngol* (2007) 32 (1):19–23. doi: 10.1111/j.1365-2273.2007.01353.x
8. Agger A, von Buchwald C, Madsen AR, Yde J, Lesnikova I, Christensen CB, Foghsgaard S, et al. Squamous Cell Carcinoma of the Nasal Vestibule 1993-2002: A Nationwide Retrospective Study From DAHANCA. *Head Neck* (2009) 31(12):1593–9. doi: 10.1002/hed.21132
9. Levendag PC, Nijdam WM, Van Moolenburgh SE, Tan L, Noever I, Van Rooy P, et al. Interstitial Radiation Therapy for Early-Stage Nasal Vestibule Cancer:

A Continuing Quest for Optimal Tumor Control and Cosmesis. *Int J Radiat Oncol Biol Phys* (2006) 66(1):160–9. doi: 10.1016/j.ijrobp.2006.03.041
10. Lambertoni A, Cherubino M, Battaglia P, De Col A, Giovannardi M, Antognoni P, et al. Squamous Cell Carcinoma of Nasal Vestibule and Pyramid: Outcomes and Reconstructive Strategies. *Laryngoscope* (2020) 131 (4):E1198–E1208, 04 2021. doi: 10.1002/lary.29107
11. Becker C, Kayser G, Pfeiffer J. Squamous Cell Cancer of the Nasal Cavity: New Insights and Implications for Diagnosis and Treatment. *Head Neck* (2016) 38 Suppl 1:E2112–7, 04. doi: 10.1002/hed.24391
12. Girardi FM, Hauth LA, Abentroth AL. Total Rhinectomy for Nasal Carcinomas. *Braz J Otorhinolaryngol* (2019) 763–6. doi: 10.1016/j.bjorl.2019.06.002
13. Bussu F, Tagliaferri L, Mattiucci G, Parrilla C, Dinapoli N, Micciche F, et al. Comparison of Interstitial Brachytherapy and Surgery as Primary Treatments for Nasal Vestibule Carcinomas. *Laryngoscope* (2016) 126(2):367–71. doi: 10.1002/lary.25498
14. Lipman D, Verhoef LC, Takes RP, Kaanders JH, Janssens GO. Outcome and Toxicity Profile After Brachytherapy for Squamous Cell Carcinoma of the Nasal Vestibule. *Head Neck* (2015) 37(9):1297–303. doi: 10.1002/hed.23758
15. Bussu F, Tagliaferri L, De Corso E, Passali GS, Lancellotta V, Mattiucci GC, et al. Functional Results of Exclusive Interventional Radiotherapy (Brachytherapy) in the Treatment of Nasal Vestibule Carcinomas. *Brachytherapy* (2021) 20(1):178–84. doi: 10.1016/j.brachy.2020.08.008
16. Langendijk JA, Poorter R, Leemans CR, de Bree R, Doornaert P, Slotman BJ. Radiotherapy of Squamous Cell Carcinoma of the Nasal Vestibule. *Int J Radiat Oncol Biol Phys* (2004) 59(5):1319–25. doi: 10.1016/j.ijrobp.2004.01.007
17. Vanneste BG, Lopez-Yurda M, Tan IB, Balm AJ, Borst GR, Rasch CR. Irradiation of Localized Squamous Cell Carcinoma of the Nasal Vestibule. *Head Neck* (2016) 38 Suppl 1:E1870–5. doi: 10.1002/hed.24337
18. Schlaff CD, Krauze A, Belard A, O'Connell JJ, Camphausen KA. Bringing the Heavy: Carbon Ion Therapy in the Radiobiological and Clinical Context. *Radiat Oncol* (2014) 9(1):88. doi: 10.1186/1748-717X-9-88
19. Fokas E, Kraft G, An H, Engenhart-Cabillic R. Ion Beam Radiobiology and Cancer: Time to Update Ourselves. *Biochim Biophys Acta* (2009) 1796(2):216–29. doi: 10.1016/j.bbcan.2009.07.005
20. Karger CP, Peschke P. RBE and Related Modeling in Carbon-Ion Therapy. *Phys Med Biol* (2017) 63(1):01TR02. doi: 10.1088/1361-6560/aa9102
21. Subtil FS, Wilhelm J, Bill V, Westholt N, Rudolph S, Fischer J, et al. Carbon Ion Radiotherapy of Human Lung Cancer Attenuates HIF-1 Signaling and Acts With Considerably Enhanced Therapeutic Efficiency. *FASEB J* (2014) 28 (3):1412–21. doi: 10.1096/fj.13-242230
22. Mizoe JE, Hasegawa A, Jingu K, Takagi R, Bessyo H, Morikawa T, et al. Results of Carbon Ion Radiotherapy for Head and Neck Cancer. *Radiother Oncol* (2012) 103(1):32–7. doi: 10.1016/j.radonc.2011.12.013
23. Kamada T, Tsujii H, Blakely EA, Debus J, De Neve W, Durante M, et al. Carbon Ion Radiotherapy in Japan: An Assessment of 20 Years of Clinical Experience. *Lancet Oncol* (2015) 16(2):e93–e100. doi: 10.1016/S1470-2045 (14)70412-7
24. Jensen AD. Particle Therapy: Protons and Heavy Ions. *Adv Otorhinolaryngol* (2020) 84:87–105. doi: 10.1159/000457929
25. Jensen AD, Nikoghosyan AV, Poulakis M, Hoess A, Haberer T, Jaekel O, et al. Combined Intensity-Modulated Radiotherapy Plus Raster-Scanned Carbon Ion Boost for Advanced Adenoid Cystic Carcinoma of the Head and Neck Results in Superior Locoregional Control and Overall Survival. *Cancer* (2015) 121(17):3001–9. doi: 10.1002/cncr.29443
26. Koto M, Demizu Y, Saitoh JI, Suefuji H, Tsuji H, Okimoto T, et al. Definitive Carbon-Ion Radiation Therapy for Locally Advanced Sinonasal Malignant Tumors: Subgroup Analysis of a Multicenter Study by the Japan Carbon-Ion Radiation Oncology Study Group (J-CROS). *Int J Radiat Oncol Biol Phys* (2018) 102(2):353–61. doi: 10.1016/j.ijrobp.2018.05.074
27. Tagliaferri L, Carra N, Lancellotta V, Rizzo D, Casà C, Mattiucci G, et al. Interventional Radiotherapy as Exclusive Treatment for Primary Nasal Vestibule Cancer: Single-Institution Experience. *J Contemp Brachytherapy* (2020) 12(5):413–9. doi: 10.5114/jcb.2020.100373
28. Held T, Windisch P, Akbaba S, Lang K, El Shafie R, Bernhardt D, et al. Carbon Ion Reirradiation for Recurrent Head and Neck Cancer: A Single-Institutional Experience. *Int J Radiat Oncol Biol Phys* (2019) 105(4):803–11. doi: 10.1016/j.ijrobp.2019.07.021
29. Mohr A, Chaudhri N, Hassel JC, Federspil PA, Vanoni V, Debus J, et al. Raster-Scanned Intensity-Controlled Carbon Ion Therapy for Mucosal Melanoma of the Paranasal Sinus. *Head Neck* (2016) 38 Suppl 1:E1445–51. doi: 10.1002/hed.24256
30. Ledderose GJ, Reu S, Englhard AS, Krause E. Endonasal Resection of Early Stage Squamous Cell Carcinoma of the Nasal Vestibule. *Eur Arch Otorhinolaryngol* (2014) 271(5):1051–5. doi: 10.1007/s00405-013-2660-4
31. Zaoui K, Plinkert PK, Federspil PA. Primary Surgical Treatment of Nasal Vestibule Cancer - Therapeutic Outcome and Reconstructive Strategies. *Rhinology* (2018) 56(4):393–9. doi: 10.4193/Rhin17.157
32. Koopmann M, Weiss D, Savvas E, Rudack C, Stenner M. Clinicopathological and Immunohistochemical Characteristics of Surgically Treated Primary Carcinoma of the Nasal Vestibule - An Evaluation of 30 Cases. *Clin Otolaryngol* (2015) 40(3):240–7. doi: 10.1111/coa.12359
33. Dowley A, Hoskison E, Allibone R, Jones NS. Squamous Cell Carcinoma of the Nasal Vestibule: A 20-Year Case Series and Literature Review. *J Laryngol Otol* (2008) 122(10):1019–23. doi: 10.1017/S0022215108002259
34. Kummer E, Rasch CR, Keus RB, Tan IB, Balm AJ. T Stage as Prognostic Factor in Irradiated Localized Squamous Cell Carcinoma of the Nasal Vestibule. *Head Neck* (2002) 24(3):268–73. doi: 10.1002/hed.10023
35. Wallace A, Morris CG, Kirwan J, Amdur RJ, Werning JW, Mendenhall WM. Radiotherapy for Squamous Cell Carcinoma of the Nasal Vestibule. *Am J Clin Oncol* (2007) 30(6):612–6. doi: 10.1097/COC.0b013e31815aff1f

Conflict of Interest: The authors declare that the research was conducted in the absence of any commercial or financial relationships that could be construed as a potential conflict of interest.

Publisher's Note: All claims expressed in this article are solely those of the authors and do not necessarily represent those of their affiliated organizations, or those of the publisher, the editors and the reviewers. Any product that may be evaluated in this article, or claim that may be made by its manufacturer, is not guaranteed or endorsed by the publisher.

frontiers in Oncology

ORIGINAL RESEARCH
published: 24 February 2022
doi: 10.3389/fonc.2022.801090

Second Primary Lung Adenocarcinoma After Intensity-Modulated Radiotherapy for Nasopharyngeal Carcinoma

Fen Xue[1,2,3†], *Xiaoshuang Niu*[1,2,3†], *Chaosu Hu*[1,2,3] *and Xiayun He*[1,2,3*]

[1] Department of Radiation Oncology, Fudan University Shanghai Cancer Center, Shanghai, China, [2] Department of Oncology, Shanghai Medical College, Fudan University, Shanghai, China, [3] Shanghai Key Laboratory of Radiation Oncology, Fudan University Shanghai Cancer Center, Shanghai, China

Objective: The improvement of the efficacy of intensity-modulated radiotherapy (IMRT) for nasopharyngeal cancer (NPC) has prolonged the survival of patients, and the incidence of the second tumor has gradually increased. Among them, second primary lung adenocarcinoma (SPLAC) attributes the highest incidence. This study aimed to determine the long-term risk of SPLAC in NPC patients after IMRT.

Methods: From May 2005 to May 2018, a total of 1,102 non-metastatic NPC patients who received IMRT in our hospital were enrolled, and the incidence and efficacy of SPLAC were followed up in the long term.

Results: Over a median follow-up period of 66 months, a total of 22 cases of SPLAC were observed, with an incidence of 2.0%. The 1-, 2-, 3-, 4-, and 5-year cumulative risks of SPLAC were 0.4%, 0.7%, 0.8%, 1.1%, and 1.7%, respectively. During follow-up, 90.9% (20/22) of the SPLAC detected was in early stage, and the recurrence rate of surgery alone was 5.3% (1/19).

Conclusion: In NPC patients, the proportion of SPLAC after IMRT was similar to that of the normal population, and most of them were found in early stage during follow-up, with good surgical efficacy.

Keywords: nasopharyngeal carcinoma, intensity-modulated radiotherapy, second primary lung adenocarcinoma, cumulative incidence risk, survival

OPEN ACCESS

Edited by:
Steffi Ulrike Pigorsch, Technical University of Munich, Germany

Reviewed by:
Jianxin Shi, Shanghai Jiaotong University, China
Yingbin Liu, Shanghai Jiaotong University, China

***Correspondence:**
Xiayun He
hexiayun1962@163.com

*These authors have contributed equally to this work

Specialty section:
This article was submitted to Head and Neck Cancer, a section of the journal Frontiers in Oncology

Received: *24 October 2021*
Accepted: *25 January 2022*
Published: *24 February 2022*

Citation:
Xue F, Niu X, Hu C and He X (2022) Second Primary Lung Adenocarcinoma After Intensity-Modulated Radiotherapy for Nasopharyngeal Carcinoma. Front. Oncol. 12:801090. doi: 10.3389/fonc.2022.801090

INTRODUCTION

Compared to the era of 2-dimensional radiotherapy (2DRT), the efficacy of treatment for nasopharyngeal carcinoma (NPC) has been significantly improved by intensity-modulated radiotherapy (IMRT), and IMRT has now become the main treatment for NPC. It has been reported that the 10-year overall survival (OS) rate of NPC patients after IMRT is about 72.6%–75.0% (1, 2). The main reasons impairing long-term survival were distant metastasis and locoregional recurrence, with 10-year local failure-free survival (LFFS), regional failure-free survival (RFFS), and distant metastasis-free survival (DMFS) around 89.0%–90.0%, 95.0%–95.9%, and 79.8%–83.3%

according to the literature. While the second tumor is also an important reason (1–5). The incidence of the second primary tumor after IMRT in NPC patients was 3.0%–9.2%, with second primary lung adenocarcinoma (SPLAC) contributing the highest incidence (6, 7). With the prolongation of survival, the incidence of the second primary tumor gradually increased. Zhang et al. (6) conducted a long-term follow-up study of 6,377 NPC patients who received IMRT and found that 189 (3.0%) patients developed the second primary tumor. The 1-, 2-, 3-, 4-, and 5-year cumulative risks of second primary tumor were 0.4%, 0.9%, 1.6%, 2.2% and 2.6%, respectively. Among them, lung cancer had the highest incidence (50/6,377, 0.78%), followed by oral cancer, liver cancer, colorectal cancer, and thyroid cancer. According to the results of a chest low-dose computed tomography (LDCT) screening study in China (8), the proportion of lung squamous cell carcinoma was relatively low and lung adenocarcinoma and disease with early stage (0/I) are relatively high, which suggested that more attention were needed for distinguishing SPLAC from lung metastasis of NPC. At present, there are rare reports about the incidence and outcome of SPLAC after IMRT for NPC. Therefore, we conducted this retrospective study to compare the difference of SPLAC incidence and outcome between NPC survivors after treatment and the general population.

PATIENTS AND METHODS

Patient Selection and Evaluation

From May 2005 to May 2018, 1,102 patients with newly diagnosed, pathologically proven, non-metastatic, previously untreated NPC treated with IMRT ± chemotherapy at Fudan University Shanghai Cancer Center were retrospectively enrolled. The exclusion criteria were as follows: 1) pathologically proven non-squamous cell carcinoma; 2) history of previous malignancy before NPC diagnosis or other concomitant malignancy; 3) incomplete clinicopathologic and treatment data available; 4) incomplete radiotherapy. All patients were restaged according to the eighth edition of the International Union against Cancer/American Joint Committee on Cancer (UICC/AJCC) system. The diagnostic criteria of SPLAC were as follows: 1) histopathology- or cytology-proven SPLAC; 2) elimination of the possibility of metastasis from the primary tumor or other second primary tumor; 3) SPLAC occurrence at least after 6 months from IMRT completion.

Initial evaluation included a complete history and physical examination, blood routine and biochemistry tests, fiberoptic nasopharyngoscopy, pathological diagnosis of nasopharynx, enhanced magnetic resonance imaging (MRI) of the nasopharynx, enhanced MRI/CT of the neck. Other assessments included positron emission tomography-CT (PET-CT) or replaced by chest CT, abdominal ultrasound/CT, and bone emission CT. All patients underwent a multidisciplinary discussion before treatment.

Treatment

All the patients received definitive IMRT. The primary gross tumor volume (GTV) included lesion of nasopharynx and positive lymph nodes. The prescribed doses were 66.0–70.4 Gy/30–32 fractions for the PTVp [the planning target volume (PTV) covering the GTV with an additional 5-mm margin]. Clinical target volume (CTV) included the PTVp, the nasopharynx, parapharyngeal space, posterior one-third of the nasal cavity and maxillary sinus, anterior part of clivus, pterygoid plate, pterygoid fossa, skull base, inferior sphenoid sinus, retropharyngeal lymph nodes, drainage region of the neck (levels II, III, and VA for N0 patients and levels II, III, IV, and VA-B for N1 patients). PTVc was created by expanding a 5-mm margin around the CTV to compensate for geometric uncertainties and patient movement. The prescribed doses were 60.0 and 54.0 Gy for high-risk PTVc and low-risk PTVc, respectively. All patients received five daily fractions per week.

Patients with stage I disease were not administered chemotherapy. Part of the patients with stage II disease and all patients with stage III–IVA disease received platinum-based chemotherapy, including concurrent chemoradiotherapy (CCRT) with or without neoadjuvant chemotherapy (IC)/adjuvant chemotherapy (AC). CCRT regimen included cisplatin 30–40 mg/m^2/day on day 1 every week or cisplatin 80 mg/m^2/day on day 1 every 3 weeks. IC and AC regimens included TPF regimen (docetaxel 60 mg/m^2/day, day 1, cisplatin 25 mg/m^2/day, days 1–3, and 5-fluorouracil 0.5 g/m^2/day with a 120-h infusion, repeated every 3 weeks), PF regimen (cisplatin 25 mg/m^2/day, days 1–3, and 5-fluorouracil 0.5 g/m^2/day with a 120-h infusion, repeated every 3 weeks), and GP regimen (gemcitabine 1,000 mg/m^2/day, days 1 and 8, and cisplatin 25 mg/m^2/day, days 1–3, repeated every 3 weeks). Generally, IMRT was implemented 3 weeks after IC. AC was administered 4 weeks after the completion of radiotherapy for tolerable patients.

Follow-Up and Evaluation

During the follow-up, patients were evaluated at 3-month intervals for the first 2 years, at 6-month intervals for the following 3 years, and then annually. Each follow-up visit included a complete history, physical examination, nasopharyngoscopy, an MRI scan of the nasopharynx, and MRI/CT scan of the neck. Chest CT and abdominal sonography/CT were conducted annually. Additional tests like bone scintigraphy were ordered whenever clinically indicated.

Statistical Analysis

SPSS 26.0 (SPSS Inc, Chicago, IL, USA) was used for statistical analysis in this study. Statistical data were tested by χ^2 test or by Fisher's exact test if theoretical frequency $T < 1$ or $n < 40$. The actuarial LFFS, RFFS, DMFS, and OS were measured from the date of diagnosis to a documented event or the last follow-up visit. Cumulative incidence of SPLAC in the corresponding observed years and survival rates of patients were calculated using the Kaplan–Meier method and compared with log-rank test between different groups. A two-sided p-value <0.05 was statistically significant.

RESULTS

Patient Demographics

Of the 1,102 patients in this study, there are 809 men and 293 women. The median age at diagnosis of NPC was 50 years old (range, 18–78 years). According to AJCC eighth staging edition, there are 44, 222, 413, and 423 patients with stage I, II, III, and IVA disease, respectively. Most patients (928/1,102, 84.2%) received IMRT with chemotherapy and 174/1,102 (15.8%) received IMRT alone. The median follow-up duration for the whole group was 66 months (range, 4–154 months). The 5- and 10-year LFFS, RFFS, DMFS, and OS rates were 93.3% and 84.4%, 95.3% and 86.3%, 89.6% and 81.3%, and 86.6% and 73.4%, respectively. During follow-up, 22 SPLAC cases were observed with a crude incidence of 2.0% (22/1102). The baseline data were similar in age, sex, stage, and with or without chemotherapy for NPC patients with or without SPLAC (**Table 1**). The 10-year OS rates for NPC patients with or without SPLAC were 71.2% and 73.6% (P = 0.699), respectively (**Figure 1**).

Second Primary Lung Adenocarcinoma Incidence and Related Details

The median latency from the diagnosis of NPC to the diagnosis of SPLAC was 48 months (range, 7–99 months). The 1-, 2-, 3-, 4-, and 5-year cumulative risks of SPLAC were 0.4%, 0.7%, 0.8%, 1.1%, and 1.7%, respectively (**Figure 2**). Of the 22 patients, 16 (72.7%) developed SPLAC within 5 years and 6 (27.3%) developed SPLAC after 5 years. Male incidence and female incidence were similar, with 2.0% (16/809) and 2.0% (6/293). The age range of patients at diagnosis of SPLAC was 29–72 years old. Among them, 50.0% (3/6) female SPLAC patients and 12.5% (2/16) male SPLAC patients were ≤50 years old. During the follow-up, 200 patients died, of whom 4 (2.0%) died of SPLAC. The details of 22 SPLAC cases were shown in **Table 2**. Routine chest CT during follow-up detected pulmonary lesions of 5–9 mm in diameter in 10 patients, 10–14 mm in 6 patients, and 15–20 mm in 4 patients. Adenocarcinoma cells were found in 1 patient's pleural effusion. Another patient was found with a burr lump of 42 * 37 mm in diameter at the apex of the left lung, lymph node metastasis to the left supraclavicular, mediastinum, and hilar, as well as brain metastasis (with puncture of pulmonary lump defined as adenocarcinoma). These two patients were unqualified for surgery. The lesions of 3 cases were in the apex of the lung, and 19 cases were in different pulmonary lobes. Among the 22 patients, 20 cases (90.9%) were stage 0/I and 19 patients underwent surgery with postoperative pathology-proven adenocarcinoma. Four cases received lobectomy, seven cases received segmentectomy, and eight cases received wedge resection. One patient refused surgery and received medication after biopsy of pulmonary nodule was confirmed as adenocarcinoma. One of the 19 patients died of SPLAC recurrence 84 months after operation, and the recurrence rate of surgery was 5.3% (1/19).

DISCUSSION

The second primary cancer was found in many patients with posttreatment primary malignancies during their follow-up, and the proportion of which is higher than that in the general population (9–13). Results of a retrospective study indicated that the overall risk of developing a second primary cancer is

TABLE 1 | Baseline characteristics of NPC patients with or without SPLAC.

Characteristic	No. of patients	Without SPLAC	With SPLAC	P
Total patients	1,102	1,080	22	/
Age				0.103
≤50 years old	590	582	8	
>50 years old	512	498	14	
Gender				0.941
Male	809	793	16	
Female	293	287	6	
T category				0.227
T1	184	177	7	
T2	355	348	7	
T3	345	341	4	
T4	218	214	4	
N stage				0.062
N0	155	147	8	
N1	381	375	6	
N2	332	327	5	
N3	234	231	3	
Clinical stage				0.051
I	44	41	3	
II	222	215	7	
III	413	408	5	
IVA	423	416	7	
chemotherapy				0.74
No	174	167	7	
Yes	928	913	15	

NPC, nasopharyngeal carcinoma; SPLAC, second primary lung adenocarcinoma.

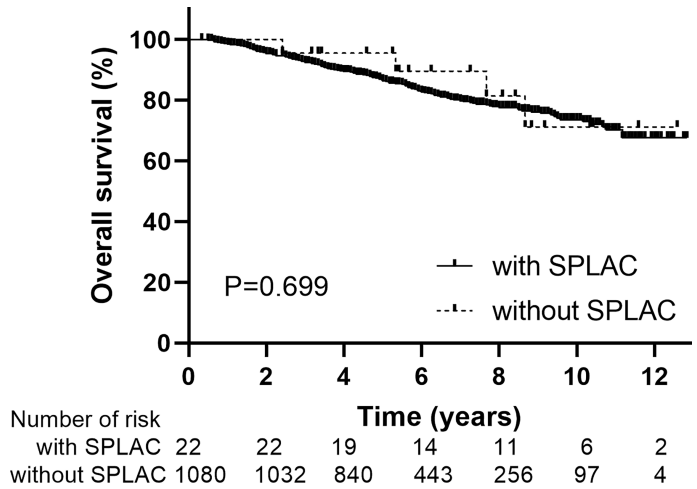

FIGURE 1 | Overall survival for patients with or without second primary lung adenocarcinoma.

statistically significantly higher for 18 of 30 primary malignancies in men and 21 of 31 primary malignancies in women when compared with the general population (14). Song et al. (9) reported that among 2,285 patients with second primary lung cancer, the most common first primary malignancies were prostate cancer, breast cancer, bladder cancer, colorectal cancer, esophageal cancer, thyroid cancer, and cervical cancer. In general, the longer a life span is for primary malignancies after treatment, the more likely it is to develop a second primary cancer. The second primary cancer for NPC patients after radiotherapy was also reported by some previous studies (4, 6, 7, 15). Survivors of NPC patients had a higher risk of cancer than the general population. With a median follow-up of 10.8 years, a total of 290 cases of second primary cancer were observed in NPC patients treated at six centers in Hong Kong, with an incidence of 9.2% (290/3,166) (7). The most common second primary cancer was lung cancer (1.6%, 51/3,166), oral cancer, colorectal cancer, and bone and soft tissue tumors. During the follow-up, 1,188 patients died, of whom 114 (9.6%) died of the second primary malignancy. Zhang et al. (6) reported an incidence of 3.0% of second primary cancer for NPC patients, with 1-, 2-, 3-, 4-, and 5-year cumulative risks of 0.4%, 0.9%, 1.6%, 2.2%, and 2.6%, respectively. The median time from IMRT to the diagnosis of the second primary cancer was 37 months (6–102 months), with 14.3% patients within 1 year, 38.1% within 1–3 years, 33.9% within 3–5 years, and 13.7% after 5 years, respectively. Among them, lung cancer also had the highest incidence (50/6,377, 0.78%). The 5-year OS rates were 70.0% and 95.0% for NPC patients with or without the second primary cancer ($P < 0.001$), respectively. Similar to previous studies, the median latency from the diagnosis of NPC to the diagnosis of SPLAC

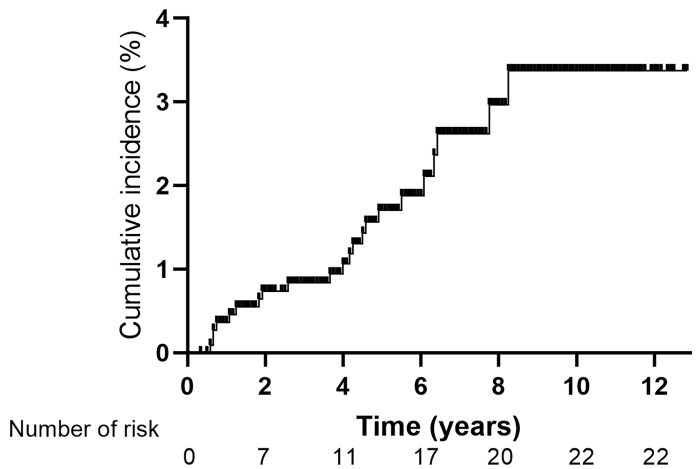

FIGURE 2 | Cumulative incidence of second primary lung adenocarcinoma for 1,102 patients with non-metastatic nasopharyngeal carcinoma.

TABLE 2 | Status of pulmonary lesions in SPLAC.

Patient No.	Location	Type	Size mm	Diagnosis months	Therapy	Response	Status	Survival months
1	Right middle lobe	GGO	<10	73	Surgery	Complete response	Alive	151
2	Right lobe	GGO	<10	13	Surgery	Complete response	Alive	139
3	Left superior lobe	solid nodule	<10	55	Surgery	Complete response	Alive	125
4	Right superior lobe	solid nodule	<10	99	Surgery	Complete response	Alive	106
5	Right superior lobe	GGO	<10	8	Surgery	Recurrence	Died	92
6	Right superior lobe	GGO	<10	66	Surgery	Complete response	Alive	97
7	Apex of left lung	GGO	<10	77	Surgery	Complete response	Alive	87
8	Left superior lobe	GGO	<10	54	Surgery	Complete response	Alive	75
9	Right superior lobe	GGO	<10	22	Surgery	Complete response	Alive	40
10	Right superior lobe	GGO	<10	15	Surgery	Complete response	Alive	41
11	Left superior lobe	solid nodule	10	31	Surgery	Complete response	Alive	128
12	Right superior lobe	GGO	10	59	Surgery	Complete response	Alive	101
13	Right superior lobe	GGO	10	48	Surgery	Complete response	Alive	65
14	Right middle lobe	GGO	10	23	Surgery	Complete response	Alive	68
15	Right superior lobe	GGO	12	76	Surgery	Complete response	Alive	110
16	Apex of left lung	GGO	14	7	Surgery	Complete response	Alive	38
17	Right superior lobe	GGO	15	51	Surgery	Complete response	Alive	124
18	Right inferior lobe	GGO	15	44	Surgery	Complete response	Alive	63
19	Right inferior lobe	GGO	15	8	Surgery	Complete response	Alive	55
20	Left superior lobe	solid nodule	20	50	Medication	Progression	Died	64
21	pleural effusion	/	/	9	Medication	Progression	Died	29
22	Apex, mediastinal lymph nodes	lump	42	93	Medication	Progression	Died	104

SPLAC, second primary lung adenocarcinoma; GGO, ground-glass opacity.

was 48 months (range, 7–99 months) in our study, with 72.7% (16/22) patients within 5 years and 27.3% (6/22) patients after 5 years. The 1-, 2-, 3-, 4-, and 5-year cumulative risks of SPLAC were 0.4%, 0.7%, 0.8%, 1.1%, and 1.7%, respectively. Of 200 patients who died in this whole group, 2.0% (4/200) died of SPLAC. There was no difference in OS between NPC patients with or without SPLAC because of the good postoperative effect of early lung cancer (10-year OS: 71.2% vs. 73.6%, P = 0.699) in our study.

With the prevalence of chest LDCT screening, the likelihood of early detection of lung cancer increased. Two important studies were conducted in China on the results of LDCT screening. The first study was LDCT for high-risk individuals (16). From August 2013 to August 2014, 11,332 people (7,144 males and 4,188 females) were selected from Minhang Community of Shanghai. Screening results suggested 27 cases of primary lung cancer (0.24%), including 24 cases (0.21%) of adenocarcinoma, and 22 cases (81.48%) of stage 0/I lung cancer. The detection rate of primary lung cancer was 238.26 cases per 100,000 people/year. The second study was LDCT for regular health examination (17). From 2012 to 2018, lung cancer (pathologically confirmed) was detected in 179 (2.1%) of 8,392 hospital staff in six hospitals in China. The incidence rate was significantly higher in women than in men (2.5% vs. 1.3%, P = 0.001). The detection rates of lung cancer in age ≤40-year-old group, 40–55-year-old group, and >55-year-old group were 1.0%, 2.6%, and 2.9%, respectively. In the previous two screening studies in China, there was a high proportion of adenocarcinoma (92.6%–98.8%), a low proportion of squamous cell carcinoma (0.6%–7.4%), and a high proportion of early (stage 0/I) disease (81.5%–97.2%). These data were similar to those released by the Shanghai Municipal Center for Disease Control and Prevention and those released in the United States (18, 19). In this study, the incidence of SPLAC was 2.0% (22/1102) with a median follow-up interval of 66 months. There was no significant increase compared with the general population. The incidence rate in female was not lower than that in male (both 2.0%). Among 22 cases of SPLAC found in this group, 90.9% were in early stage, and the proportion of young female was higher than that of male (50.0% vs. 12.5%).

Commonly, 95.5% of lung cancer detected by CT was represented as ground-glass opacity (GGO). GGO may be benign lesions such as inflammation or bleeding, atypical adenomatoid hyperplasia, or lung cancer (17). In surveillance of NPC, follow-up of 4–6 months was suggested for newly discovered ≤5-mm GGO (20). Generally, benign GGO will decrease or disappear, while malignant GGO will persist or develop. Aggressive surgical treatment is necessary for lesions that are highly suspected to be invasive lung adenocarcinoma radiographically and for GGO with increased diameter or solid components during follow-up. As reported by our hospital (8), the proportion of benign lesions in all surgically removed lung GGO is less than 10%, and the surgical efficacy of the early SPLAC is similar to that of the first primary lung adenocarcinoma. Good postoperative prognosis for the SPLAC was found in those with controlled first primary tumor. Ko et al. (21) also reported similar 5-year OS for first primary lung adenocarcinoma and SPLAC (81.8% vs. 72.9%, P = 0.069). Different surgical approaches may affect the outcomes of early-stage lung adenocarcinoma. According to Shi et al. (22), the OS of patients with early-stage non-small cell lung cancer who underwent lobectomy/segmentectomy was higher than those who underwent wedge resection. However, regarding disease-free survival and relapse-free survival, the three surgical approaches showed no significant difference. Among 19

patients who received surgery in this study, only 1 patient died of lung cancer recurrence 84 months after wedge resection. The rest were alive with complete response.

The causative agent of the second primary tumors is unclear at present and may be related to family history, genetic defects, infection, chemotherapy, radiotherapy, hormones, alcohol, tobacco, environment, and so on (23). Epstein–Barr virus was identified to be the dominant contributor to NPC but was only identified in a very small proportion of the second primary tumors. Literature suggested that low-dose radiation may be associated with the second primary tumor (7). Compared with 2DRT and 3-dimensional conformal radiotherapy (3DCRT), it was reported that IMRT could improve local control and survival rates for NPC patients as well as reduce dose exposure to parotid glands, temporal lobes, and other organs at risk. As a result, the incidence of late toxicities such as dry mouth, trismus, and temporal lobe injury was significantly decreased in the IMRT group (24). Therefore, volumes of peripheral normal tissues (like oral cavity, neck, and so on) receiving low-dose radiation increased in the IMRT group and may contribute to the incidence of second primary tumors (25). Chow et al. (7) reported that 51 of the 290 second primary tumors were found in the head and neck in NPC patients treated with IMRT, with the highest incidence. Only 5%–15% of primary sarcomas occurred in the head and neck region (26). However, 21 (84%) of the 25 second primary sarcomas occurred in the head and neck region after IMRT in NPC patients. And 6 of the 51 second primary lung cancers occurred in the apex of the lung (7). From 1996 to 2002, Goggins et al. (27) analyzed the standardized incidence of the second primary tumor in all parts of NPC patients after 2DRT, which was consistent with that after IMRT (1.93 vs. 1.90). Also, the second oral cancer and lung cancer contributed to the highest incidence in both 2DRT and IMRT groups. The potentially negative effect of the wider low-dose zone in IMRT may be counteracted by the potentially negative effect of the larger high-dose zone of 2DRT or 3DCRT (28). Ardenfors et al. (29) made IMRT and CRT (conformal radiotherapy) plans for 10 head and neck patients, and the treatment plan data were obtained to calculate the risk of radiation-induced malignancy in four different tissues using different risk models. The results showed that the total lifetime risks of developing radiation-induced secondary tumor from CRT and IMRT were comparable and in the interval 0.9%–2.5%. The incidence of SPLAC after radiotherapy for NPC patients in this group was 2.0% (22/1102), which was similar to that reported by other authors and that reported in the general population (7, 16, 17). The proportion of SPLAC occurring in lung apex (3/22) in this group was also similar to that reported by literature (6/51) (7).

Limitations for this study include a single-center retrospective experience with a limited number of cases without a control cohort. Prospective multicenter studies are needed to confirm the result. Besides, literature showed that some biomarkers are important for lung cancer screening or detecting recurrence, such as circulating microRNAs (miRNAs), circulating tumor DNA (ctDNA), or methylation markers (30, 31). It may be also meaningful to investigate these biomarkers in SPLAC in the future when we have enough cases.

CONCLUSION

In conclusion, the proportion of SPLAC after IMRT for NPC patients in our single-institution study was similar to that of the normal population. Most SPLACs were found in early stage with good surgical efficacy. Attributing to early detection of chest CT during routine follow-up, long-term survival of NPC patients with SPLAC is not inferior to those without SPLAC. Therefore, close surveillance of NPC survivors for SPLAC is warranted.

DATA AVAILABILITY STATEMENT

The raw data supporting the conclusions of this article will be made available by the authors without undue reservation.

ETHICS STATEMENT

The studies involving human participants were reviewed and approved by the institutional review board of Fudan University Shanghai Cancer Center. The patients/participants provided their written informed consent to participate in this study.

AUTHOR CONTRIBUTIONS

FX and XN collected the data and finished the quality control of data. XH and CH provided the study concepts. FX, XN, and XH designed the study and performed the statistical analysis. FX and XH wrote the article. All authors contributed to the article and approved the submitted version.

FUNDING

This work was supported by the Shanghai Sailing Program (grant no. 21YF1408400), Scientific and Innovative Action Plan of Shanghai (grant no. 21Y11911900), and institutional grant of Fudan University Shanghai Cancer Center (grant no. YJQN202023).

ACKNOWLEDGMENTS

We acknowledge the support of the Department of Radiation Oncology, Fudan University Shanghai Cancer Center. The views expressed in this publication are those of the authors. We thank the patients and their families for their support and participation in this trial.

REFERENCES

1. Chen L, Zhang Y, Lai SZ, Li WF, Hu WH, Sun R, et al. 10-Year Results of Therapeutic Ratio by Intensity-Modulated Radiotherapy Versus Two-Dimensional Radiotherapy in Patients With Nasopharyngeal Carcinoma. *Oncologist* (2019) 24:e38–45. doi: 10.1634/theoncologist.2017-0577
2. Wu LR, Liu YT, Jiang N, Fan YX, Wen J, Huang SF, et al. Ten-Year Survival Outcomes for Patients With Nasopharyngeal Carcinoma Receiving Intensity-Modulated Radiotherapy: An Analysis of 614 Patients From a Single Center. *Oral Oncol* (2017) 69:26–32. doi: 10.1016/j.oraloncology.2017.03.015
3. Zhao W, Lei H, Zhu X, Li L, Qu S, Liang X, et al. The Clinical Characteristics of Secondary Primary Tumors in Patients With Nasopharyngeal Carcinoma After Intensity-Modulated Radiotherapy: A Retrospective Analysis. *Med (Baltimore)* (2016) 95:e5364. doi: 10.1097/MD.0000000000005364
4. Chow JCH, Au KH, Mang OWK, Cheung KM, Ngan RKC. Risk, Pattern and Survival Impact of Second Primary Tumors in Patients With Nasopharyngeal Carcinoma Following Definitive Intensity-Modulated Radiotherapy. *Asia Pac J Clin Oncol* (2019) 15:48–55. doi: 10.1111/ajco.12994
5. Zhao C, Miao JJ, Hua YJ, Wang L, Han F, Lu LX, et al. Locoregional Control and Mild Late Toxicity After Reducing Target Volumes and Radiation Doses in Patients With Locoregionally Advanced Nasopharyngeal Carcinoma Treated With Induction Chemotherapy (IC) Followed by Concurrent Chemoradiotherapy: 10-Year Results of a Phase 2 Study. *Int J Radiat Oncol Biol Phys* (2019) 104:836–44. doi: 10.1016/j.ijrobp.2019.03.043
6. Zhang LL, Li GH, Li YY, Qi ZY, Lin AH, Sun Y. Risk Assessment of Secondary Primary Malignancies in Nasopharyngeal Carcinoma: A Big-Data Intelligence Platform-Based Analysis of 6,377 Long-Term Survivors From an Endemic Area Treated With Intensity-Modulated Radiation Therapy During 2003-2013. *Cancer Res Treat* (2019) 51:982–91. doi: 10.4143/crt.2018.298
7. Chow JCH, Tam AHP, Cheung KM, Lee VHF, Chiang CL, Tong M, et al. Second Primary Cancer After Intensity-Modulated Radiotherapy for Nasopharyngeal Carcinoma: A Territory-Wide Study by HKNPCSG. *Oral Oncol* (2020) 111:105012. doi: 10.1016/j.oraloncology.2020.105012
8. Zhang Y, Chen H. Lung Cancer Screening: Who Pays? Who Receives?-the Chinese Perspective. *Transl Lung Cancer Res* (2021) 10:2389–94. doi: 10.21037/tlcr.2020.03.16
9. Song C, Yu D, Wang Y, Wang Q, Guo Z, Huang J, et al. Dual Primary Cancer Patients With Lung Cancer as a Second Primary Malignancy: A Population-Based Study. *Front Oncol* (2020) 10:515606:515606. doi: 10.3389/fonc.2020.515606
10. Zheng X, Li X, Wang M, Shen J, Sisti G, He Z, et al. Second Primary Malignancies Among Cancer Patients. *Ann Transl Med* (2020) 8:638. doi: 10.21037/atm-20-2059
11. Liu YY, Chen YM, Yen SH, Tsai CM, Perng RP. Multiple Primary Malignancies Involving Lung Cancer-Clinical Characteristics and Prognosis. *Lung Cancer* (2002) 35:189–94. doi: 10.1016/s0169-5002(01)00408-1
12. Li F, Zhong WZ, Niu FY, Zhao N, Yang JJ, Yan HH, et al. Multiple Primary Malignancies Involving Lung Cancer. *BMC Cancer* (2015) 15:696. doi: 10.1186/s12885-015-1733-8
13. Ben Arie G, Shafat T, Belochitski O, El-Saied S, Joshua BZ. Treatment Modality and Second Primary Tumors of the Head and Neck. *ORL J Otorhinolaryngol Relat Spec* (2021) 83:1–8. doi: 10.1159/000513617
14. Sung H, Hyun N, Leach CR, Yabroff KR, Jemal A. Association of First Primary Cancer With Risk of Subsequent Primary Cancer Among Survivors of Adult-Onset Cancers in the United States. *JAMA* (2020) 324:2521–35. doi: 10.1001/jama.2020.23130
15. Niu X, Xue F, Liu P, Hu C, He X. Long-Term Outcomes of Induction Chemotherapy Followed by Intensity-Modulated Radiotherapy and Adjuvant Chemotherapy in Nasopharyngeal Carcinoma Patients With N3 Disease. *Transl Oncol* (2021) 14:101216. doi: 10.1016/j.tranon.2021.101216
16. Luo X, Zheng S, Liu Q, Wang S, Li Y, Shen L, et al. Should Nonsmokers Be Excluded From Early Lung Cancer Screening With Low-Dose Spiral Computed Tomography? Community-Based Practice in Shanghai. *Transl Oncol* (2017) 10:485–90. doi: 10.1016/j.tranon.2017.02.002
17. Zhang Y, Jheon S, Li H, Zhang H, Xie Y, Qian B, et al. Results of Low-Dose Computed Tomography as a Regular Health Examination Among Chinese Hospital Employees. *J Thorac Cardiovasc Surg* (2020) 160:824–31 e4. doi: 10.1016/j.jtcvs.2019.10.145
18. Liang F, Wu C, Gu H, Zhu M, Xuan Z, Jiang Y, et al. Lung Cancer Incidence in Female Rises Significantly in Urban Sprawl of Shanghai After Introduction of LDCT Screening. *Lung Cancer* (2019) 132:114–8. doi: 10.1016/j.lungcan.2019.04.020
19. Handy JR Jr, Skokan M, Rauch E, Zinck S, Sanborn RE, Kotova S, et al. Results of Lung Cancer Screening in the Community. *Ann Fam Med* (2020) 18:243–9. doi: 10.1370/afm.2519
20. Ma Z, Zhang Y, Huang Q, Fu F, Deng C, Wang S, et al. Decreasing Prevalence of Benign Etiology in Resected Lung Nodules Suspicious for Lung Cancer Over the Last Decade. *Semin Thorac Cardiovasc Surg* (2021) 21:1043–9. doi: 10.1053/j.semtcvs.2021.06.024
21. Ko KH, Huang HK, Chen YI, Chang YH, Tsai WC, Huang TW. Surgical Outcomes of Second Primary Lung Cancer After the Extrapulmonary Malignancy. *J Cancer Res Clin Oncol* (2020) 146:3323–32. doi: 10.1007/s00432-020-03310-x
22. Shi Y, Wu S, Ma S, Lyu Y, Xu H, Deng L, et al. Comparison Between Wedge Resection and Lobectomy/Segmentectomy for Early-Stage Non-Small Cell Lung Cancer: A Bayesian Meta-Analysis and Systematic Review. *Ann Surg Oncol* (2021) 29:1868–79. doi: 10.1245/s10434-021-10857-7
23. Copur MS, Manapuram S. Multiple Primary Tumors Over a Lifetime. *Oncol (Williston Park)* (2019) 33:629384.
24. Zhang B, Mo Z, Du W, Wang Y, Liu L, Wei Y. Intensity-Modulated Radiation Therapy Versus 2D-RT or 3D-CRT for the Treatment of Nasopharyngeal Carcinoma: A Systematic Review and Meta-Analysis. *Oral Oncol* (2015) 51:1041–6. doi: 10.1016/j.oraloncology.2015.08.005
25. Chargari C, Goodman KA, Diallo I, Guy JB, Rancoule C, Cosset JM, et al. Risk of Second Cancers in the Era of Modern Radiation Therapy: Does the Risk/Benefit Analysis Overcome Theoretical Models? *Cancer Metastasis Rev* (2016) 35:277–88. doi: 10.1007/s10555-016-9616-2
26. Sturgis EM, Potter BO. Sarcomas of the Head and Neck Region. *Curr Opin Oncol* (2003) 15:239–52. doi: 10.1097/00001622-200305000-00011
27. Goggins WB, Yu IT, Tse LA, Leung SF, Tung SY, Yu KS. Risk of Second Primary Malignancies Following Nasopharyngeal Carcinoma in Hong Kong. *Cancer Causes Control* (2010) 21:1461–6. doi: 10.1007/s10552-010-9574-x
28. Filippi AR, Vanoni V, Meduri B, Cozzi L, Scorsetti M, Ricardi U, et al. Intensity Modulated Radiation Therapy and Second Cancer Risk in Adults. *Int J Radiat Oncol Biol Phys* (2018) 100:17–20. doi: 10.1016/j.ijrobp.2017.09.039
29. Ardenfors O, Josefsson D, Dasu A. Are IMRT Treatments in the Head and Neck Region Increasing the Risk of Secondary Cancers? *Acta Oncol* (2014) 53:1041–7. doi: 10.3109/0284186X.2014.925581
30. Seijo LM, Peled N, Ajona D, Boeri M, Field JK, Sozzi G, et al. Biomarkers in Lung Cancer Screening: Achievements, Promises, and Challenges. *J Thorac Oncol* (2019) 14:343–57. doi: 10.1016/j.jtho.2018.11.023
31. Gu C, Chen C. Methylation in Lung Cancer: A Brief Review. *Methods Mol Biol* (2020) 2204:91–7. doi: 10.1007/978-1-0716-0904-0_8

Conflict of Interest: The authors declare that the research was conducted in the absence of any commercial or financial relationships that could be construed as a potential conflict of interest.

frontiers in Oncology

ORIGINAL RESEARCH
published: 02 March 2022
doi: 10.3389/fonc.2022.786207

A Predictive Nomogram for Lymph Node Metastasis in Supraglottic Laryngeal Squamous Cell Carcinoma

*Lulu Song, Yu Heng, Chi-Yao Hsueh, Huiying Huang, Lei Tao, Liang Zhou and Ming Zhang**

Department of Otolaryngology, Shanghai Key Clinical Disciplines of Otorhinolaryngology, Eye & ENT Hospital, Fudan University, Shanghai, China

Purpose: Lymph node metastasis (LNM) has a negative impact on the survival of patients with laryngeal squamous cell carcinoma (LSCC). Supraglottic LSCC is the most common cause of cervical lymph node metastases due to the extensive submucosal lymphatic plexus. The accurate evaluation of LNM before surgery can inform improved decisions in the clinic. In this study, we aimed to construct a nomogram to predict LNM in primary supraglottic LSCC patients.

Methods: The data from 314 patients with clinico-pathological confirmed supraglottic LSCC who underwent partial or total laryngectomy in our department from 2016 to 2020 were retrospectively analyzed (243 cases in the training set and 71 cases in the validation set). A multivariate logistic regression model was used to screen out independent risk factors and a nomogram was established. The accuracy and discrimination ability of the nomogram was evaluated using a consistency index and calibration curves.

Results: Tumor size, tumor differentiation degree and LMR (lymphocyte-monocyte ratio) were selected to construct the nomogram. The C-index was 0.731 in the training set and 0.707 in the validation set. The calibration curves of the training and validation group both exhibited close agreement between the predicted and the actual presence of LNM.

Conclusions: A nomogram was established based on routinely measured pretreatment variables and the predicted results improved the management of patients with LNM.

Keywords: supraglottic squamous cell laryngeal cancer, lymph node metastasis, nomogram, diagnosis, C-index

OPEN ACCESS

Edited by:
Panagiotis Balermpas, University Hospital Zürich, Switzerland

Reviewed by:
Richa Vaish, Tata Memorial Hospital, India
Annett Linge, University Hospital Carl Gustav Carus, Germany

***Correspondence:**
Ming Zhang
zmzlm@163.com

Specialty section:
This article was submitted to Head and Neck Cancer, a section of the journal Frontiers in Oncology

Received: *29 September 2021*
Accepted: *31 January 2022*
Published: *02 March 2022*

Citation:
Song L, Heng Y, Hsueh C-Y, Huang H, Tao L, Zhou L and Zhang M (2022) A Predictive Nomogram for Lymph Node Metastasis in Supraglottic Laryngeal Squamous Cell Carcinoma. Front. Oncol. 12:786207. doi: 10.3389/fonc.2022.786207

INTRODUCTION

Laryngeal cancer (LC) is one of the most common tumors of the respiratory tract (1). LC can be anatomically subdivided into glottic, supraglottic, and subglottic cancer based on its primary site. 60-70% of cases originate from the glottis and approximately 35% of cases originate from the supraglottic site (2). The supraglottic area is characterized by a rich lymphatic network resulting in a high potential for the development of regional metastases (3). The involvement of metastatic cervical lymph nodes has been shown to negatively impact survival (4). In clinical practice, positive lymph nodes may be palpable or can be detected by ultrasonography, computed tomography (CT), or magnetic resonance imaging (MRI). However, false positive results are frequently caused by

inflammatory conditions whilst false negatives can be due to the small size of metastatic lymph nodes or cystic changes (5).

Several studies have identified indicators that may be independent factors for LNM such as the tumor depth, the degree of tumor differentiation, T-stage, thyroid cartilage invasion, and extra laryngeal extension. Traditional methods for determining the factors related to LNM are largely qualitative and there remains a need to develop quantitative measures to assess the factors associated with the risk of LNM (6, 7). The accurate preoperative evaluation of LNM risk may guide the use of optimized treatment strategies in patients with supraglottic LSCC and provide important prognostic information. In this study, we retrospectively analyzed data from 314 patients with supraglottic LSCC admitted to hospital between 2016 and 2020. These data were used to develop a nomogram prediction model for LNM in supraglottic LSCC patients.

METHODS

Patient Cohort

This study retrospectively collected 314 clinical cases of newly diagnosed primary supraglottic LSCC confirmed by postoperative pathology in the Eye, Ear, Nose, and Throat Hospital of Fudan University. We defined the training and the validation groups by time in this study. The training group consisted of 243 patients who were admitted between January 2016 and December 2018 and the validation group consisted of 71 patients who were hospitalized between January 2019 and December 2020. The training group was used to establish the model, and the validation group was used to verify the performance of the model. The inclusion criteria for the study were as follows: (1) supraglottic laryngeal squamous cancer confirmed by postoperative pathology; (2) no preoperative chemotherapy or radiotherapy; (3) complete clinical and pathological data; (3) no history of other cancers; (4) no distant metastasis.

This study was approved by the Institutional Ethics Committee of the Eye and ENT Hospital of Fudan University.

Surgical Treatments and Data Collection

Clinical and pathological data including the demographic data, blood test report, tumor size, clinical tumor stages, and differentiation grades were collected. The following pretreatment hematological parameters were collected within 4 weeks before initial treatment: neutrophil, lymphocyte, monocyte and platelet counts. The platelet-lymphocyte (PLR), neutrophil-lymphocyte (NLR) and lymphocyte-monocyte (LMR) ratios were calculated by dividing the absolute values of the corresponding hematological parameters. The degree of tumor differentiation was obtained by pre-operative biopsy. The postoperative pathology reports were screened to confirm whether the patients met the criteria for inclusion. Tumor size was defined as the maximum diameter of the primary tumor based on computed tomography measurements. Staging was performed according to AJCC 8th edition guidelines.

The primary tumor resection was conducted for all patients in our study, while neck dissection was performed therapeutically or prophylactically in 180 patients. In patients receiving neck dissection, lymph node status (no metastasis, N0, or lymph node metastasis, N+) was verified based on the final pathological assessments. In 63 patients who didn't receive neck dissection, if positive LNM was found by postoperative follow-up six months after initial operation, they were regarded as having occult lymph node involvement at the time of initial surgery, and thus be classified as LNM group (**Figure 1**).

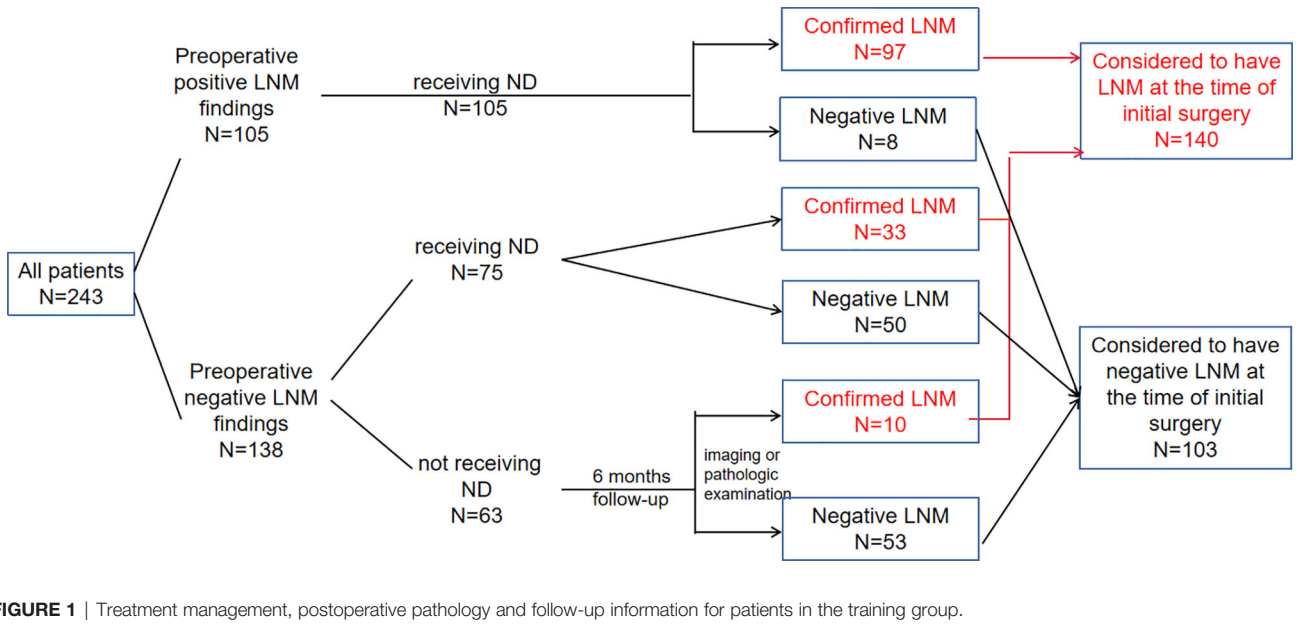

FIGURE 1 | Treatment management, postoperative pathology and follow-up information for patients in the training group.

Variable Analysis

The variables analyzed in this study included the following clinicopathologic data: sex, age, drinking history, smoking history, tumor size, differentiation, PLR, NLR and LMR. The optimal cut-off values were calculated according to the receiver operating characteristic (ROC) curve. Based on the cut-off values, the continuous variables were transformed into categorical variables.

Statistical Analysis

A Chi-square test was used to compare the categorical variables. Multivariable logistic regression analysis was performed with the following clinical and pathological candidate predictors: age, gender, tumor size, tumor differentiation degree, LMR, NLR and PLR, which were applied to develop a diagnostic model for LNM using the primary cohort. A bi-direction stepwise selection process with the Akaike information criterion as the stopping rule was performed. The nomogram was formulated based on the results. To evaluate the discrimination of our predictive model, the concordance index (C-index) and receiver operating characteristic (ROC) curve were constructed, and a calibration curve was used to assess the consensus degree of our models. In this study, SPSS 26.0 and R software (version 3.6.1, www.rproject.org) were used in statistical analyses.

RESULTS

Patients Characteristics

The characteristics of the training and validation groups are shown in **Table 1**. Between 2016 and 2018, 243 patients served as the training group to create the predictive model. The other 71 patients admitted between 2019 and 2020 served as external validation group for verifying the model. The mean age of all patients enrolled was 64 years, 63 years for training and 66 years for validation group. In all patients, the cervical metastasis rates are 45.9% with early-stage (pT1/2) and 64.2% in patients with pT3/4 tumors. There were no significant differences between the two cohorts in LNM prevalence (P = 0.493). LNM positivity was 57.6% in the primary cohort and 52.1% in the validation cohort. The cut-off values (PLR = 129.41, NLR = 2.76, LMR= 3.12, tumor size = 2.7) were calculated according to the receiver operating characteristic (ROC) curve. Based on the cut-off values, the continuous variables were transformed into categorical variables. In the training group, LNM was associated with the following clinicopathological parameters: tumor differentiation degree (P<0.001), LMR (P = 0.023), clinical T stage (P = 0.031), NLR (P=0.05) and tumor size (P<0.001) (**Table 2**).

Surgical Treatments and Follow-up Information

All patients received partial or total laryngectomy and neck dissection was performed in patients with positive or highly suspicious LNM. In the training group, neck dissection was performed on 180 (74.1%) patients, 105 of which had clinically detectable LNM. 33 of the 75 patients who were preoperatively negative but highly suspicious LNM were found to have LNM on postoperative pathology. In patients that did not receive neck dissection, 10 out of 63 were diagnosed with LNM by imaging tests or pathologic examination during the postoperative 6 months follow-up. In total, 140 (57.6%) patients were regarded as having LNM at the time of initial treatment (**Figure 1**).

TABLE 1 | Clinicopathological characteristics of all patients.

Variables	Total (314)	Training (243)	Validation (71)	p
HBP				< 0.01
NO	221	186	35	
Yes	93	57	36	
DM				0.07
NO	285	225	60	
Yes	29	18	11	
Smoking				0.53
NO	59	48	11	
Yes	255	195	60	
Drinking				1.00
NO	131	101	30	
Yes	183	142	41	
Sex				0.05
Female	14	14	0	
Male	300	229	71	
cT stage				0.05
1	11	8	3	
2	124	98	26	
3	154	113	41	
4	25	24	1	
Age				0.10
<65	171	139	32	
≥65	143	104	39	
Grading				0.16
moderate to high	50	43	7	
moderate	264	200	64	
TS				0.46
<2.7	123	92	31	
≥2.7	191	151	40	
NLR				1.00
<2.76	193	149	44	
≥2.76	121	94	27	
LMR				0.29
<3.12	118	87	31	
≥3.12	196	156	40	
PLR				1.00
<129.41	158	122	36	
≥129.41	156	121	35	

HBP, High blood pressure; DM, Diabetes mellitus; TS, tumor size; PLR, Platelet/lymphocyte; NLR, Neutrophil/lymphocyte; LMR, Lymphocyte.

Risk Factors for LNM and Construction of the Nomogram

Multivariable logistic regression analysis was performed with the following clinical and pathological candidate predictors: age, gender, tumor size, tumor differentiation degree, LMR, NLR and PLR. The results indicated that tumor differentiation degree (OR=3.752, P=0.001), tumor size (OR=3.103, P<0.001) were associated with LNM. Patients older than 65 years were more likely to have LNM with an odds ratio of 1.692. Patients with a LMR greater than 3.12 were less likely to develop LNM with an odds ratio of 0.562 (**Table 3**). The multivariate logistic model was used to develop a diagnostic model for LNM using the training

TABLE 2 | Relationship between lymph node metastasis and clinicopathologic variables in training set.

Variables	Total n = 243	LNM(-) n = 103	LNM(+) n = 140	P-value
HBP				0.102
NO	186	73	113	
Yes	57	30	27	
DM				1
NO	225	95	130	
Yes	18	8	10	
Smoking				0.482
NO	48	23	25	
Yes	195	80	115	
Drinking				0.479
NO	101	46	55	
Yes	142	57	85	
Sex				0.153
Female	14	9	5	
Male	229	94	135	
CT stage				0.031
1	8	7	1	
2	98	45	53	
3	113	41	72	
4	24	10	14	
Age				0.143
<65	139	65	74	
≥65	104	38	66	
Grading				<0.001
moderate to high	43	30	13	
moderate	200	73	127	
TS				< 0.001
<2.7	92	54	38	
≥2.7	151	49	102	
NLR				0.05
<2.76	149	71	78	
≥2.76	94	32	62	
LMR				0.023
<3.12	87	28	59	
≥3.12	156	75	81	
PLR				0.956
<129.41	122	51	71	
≥129.41	121	52	69	

HBP, High bloodpressure; DM, Diabetes mellitus; TS, tumor size; PLR, Platelet/ lymphocyte; NLR, Neutrophil/lymphocyte; LMR, Lymphocyte/ monocyte; CT stage, clinical Tumor Stage.

TABLE 3 | Multivatiate logistic regression analysis for predicting lymph node metastasis.

Variables		95%C1	P
Sex	Female	–	
	Male	1.360 (0.426-4.811)	0.612
Age	<65	–	
	≥65	1.692 (0.958-3.028)	0.072
Grading	moderate to high	–	
	moderate	3.752 (1.790-8.246)	0.001
Tumor size	<2.7	–	
	≥2.7	3.103 (1.750-5.594)	< 0.001
PLR	<140.84	–	
	≥140.84	0.668 (0.347-1.267)	0.22
NLR	<2.76	–	
	≥2.76	1.572 (0.786-3.180)	0.203
LMR	<3.12	–	
	≥3.12	0.562 (0.285-1.093)	0.092

PLR, Platelet/lymphocyte; NLR, NeutrophiVlymphocyte; LMR, Lymphocyte/ monocyte.

cohort, and a bi-direction stepwise selection process was performed to select variables with the Akaike information criterion as the stopping rule. Finally, tumor differentiation degree, age, LMR and tumor size were selected to establish the nomogram to predict the risk of LNM in patients with newly diagnosed primary supraglottic LSCC cancer (**Figure 2**).

Evaluation and Validation of the Nomogram

A logistic regression model was used to develop a multivariate model to predict the LNM of the patients. Each variable corresponded to a specific point by drawing a straight line upwards to the point axis. All of the points were added to obtain the total. Finally, the risk value corresponding to the total score was determined. For example, the total score of moderate differentiation with TS≥2.7 cm and age≥65 plus LMR≥3.12 in patients with supraglottic LSCC was 37 + 84+100+0 = 221. Then, the corresponding risk for LNM was 73% (**Figure 2**). The bootstrap method was used to evaluate the precision of the nomogram internally and externally. The C-index was 0.731 in the training set and 0.707 in the validation set. The calibration curves of the training and validation group are displayed in **Figures 3**, **4**. Both exhibited satisfying accordance between the predicted and the actual presence of LNM.

DISCUSSION

Supraglottic LSCC is commonly associated with cervical LNM due to the extensive submucosal lymphatic plexus (8). According to a previous study, high cervical metastasis rates are common across all stages of supraglottic laryngeal cancer ranging from 55% in patients with early-stage (pT1/2) to 67% in patients with pT3/4 tumors (9). In our study, the rate of LNM rates were 45.9%

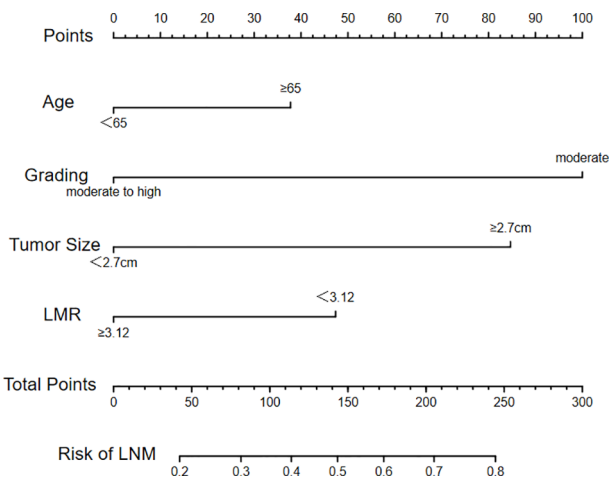

FIGURE 2 | Nomogram constructed according to selected variables.

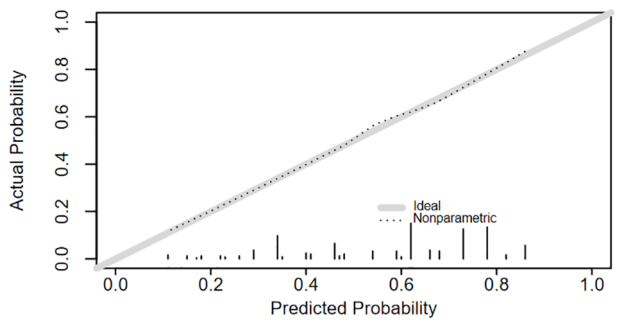

FIGURE 3 | The calibration curve of the nomogram for predicting LNM in training group.

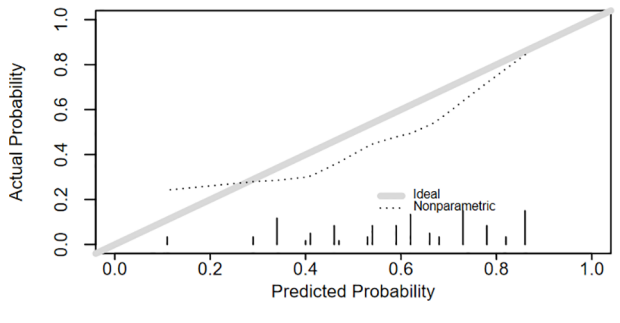

FIGURE 4 | The calibration curve of the nomogram for predicting LNM in test group.

and 64.2%, respectively for these stages of the disease. LNM has been shown to correlate with a high risk of distant metastases and the number of metastatic nodes is a predominant independent factor of mortality (10). Allen et al. found that the risk of mortality escalated continuously with an increasing number of metastatic nodes. Also, the hazard per node (hazard ratio [HR], 1.19; 95% CI, 1.16-1.23; P < 0.001) was most pronounced when up to 5 positive lymph nodes were detected (11). These data suggest that cervical lymph node management is vital and identifying the objective determinants for LNM could lead to the development of improved individualized therapy decisions.

The current clinically established methods for detecting LNM have several limitations. As for the physical examination, the sensitivity and specificity of findings are unsatisfactorily low with false-negative rates as high as 15-25% and similar false-positive rates (12). In contrast, the detection of LNM by radiological imaging is more accurate compared to clinical examination. Commonly, CT is used for the staging of lymph nodes in the neck. The criteria for assessing nodal metastases include nodal size, shape, presence of central necrosis, and grouping of nodes in an expected draining nodal station (5, 13). However, imaging assessment of LNM in the head and neck can be challenging for the radiologist as there are multiple cervical levels to review and various criteria have been proposed (14). False-positive results can be caused by inflammatory conditions and false-negative results due to small size and cystic change of metastatic lymph nodes (5). As for the comparison of CT and MR imaging, it showed no significant difference between the two imaging tests for either sensitivity (P = 0.1317) or specificity (P = 0.3173) (15). PET/CT can be used to achieve a 21% increase in the diagnosis of nodal metastasis compared with conventional images yet it has limited cost-effectiveness (16). Accordingly, a practical and comprehensive prediction model that integrates multiple indicators could facilitate the accurate assessment of LNM in patients with supraglottic LSCC.

In this study, the four variables obtained before surgery (age, tumor size, tumor differentiation degree and LMR) were selected to construct the nomogram. The continuous variables were transformed into categorical variables with the optimal cut-off values (PLR = 129.41, NLR = 2.76, LMR= 3.12, tumor size = 2.7) calculated according to the receiver operating characteristic (ROC) curve. Several previous studies have shown that patients with poorly differentiated and larger primary tumors have a higher incidence of lymph node involvement (17, 18). Consistent with previous studies, two primary related factors including a maximum tumor diameter ≥ 2.7 cm and poorly differentiated tumors were shown to be independent risk factors for LNM in supraglottic LSCC patients. Of the hematological parameters assessed in this study, our data showed that patients with a LMR lower than 3.12 were more likely to develop LNM. This may be due to the ability of monocytes to secrete various proinflammatory cytokines that promote tumorigenesis, angiogenesis and distant metastasis and low lymphocyte levels are associated with poor tumor control (19, 20).

The National Comprehensive Cancer Network (NCCN) Clinical Practice Guidelines specify that patients with supraglottic lesions should have neck treatment even in N0 cases. However, Sessions et al. conducted a retrospective study of 653 patients with supraglottic laryngeal squamous cell cancer and found that patients with N0 disease may be safely observed with no loss of survival advantage (21). Also, Ömer et al. found a very low incidence of LNM in T1-T2 stage and well-differentiated tumors. These data suggested that a watchful waiting strategy can be used in T1-T2 and selected T3 cases with well-differentiated tumors (6).

Elective neck dissection is widely accepted as the standard surgical treatment for clinically node-negative patients (22). However, neck dissection may result in complications such as recurrent laryngeal nerve palsy (while clearing central compartment nodes in partial laryngectomy), hematoma, chyle leakage, and spinal accessory nerve dysfunction (23). This approach is a form of overtreatment in patients that have no lymph node involvement. Based on our nomogram, the individual risk of LNM can be determined and doctors can identify patients with a high risk of LNM. The model can be used to avoid overtreatment and reduce the risk of dissection–related complications. Also, our nomogram can directly inform the

lymph node dissection strategy for those with a high risk of occult LNM.

To the best of our knowledge, this is the first study to develop a nomogram to predict LNM in supraglottic LSCC, which can be used to predict the individual risk of LNM and to identify patients with a high LNM risk. It can be useful in evaluating the optimized treatment strategies and provide important prognostic information. However, our study had several limitations. Our study was performed as a retrospective study and may have had inherent section bias. Also, all of the enrolled patients were from a single institution which may be a source or bias. Multicentre studies are required to validate our model.

CONCLUSION

Based on tumor differentiation degree, age, LMR and tumor size, a nomogram model was established to predict the incidence of LNM in patients with supraglottic LSCC. This model has potential value in predicting the LNM risk. However, further multicentre studies with larger samples are needed to validate these findings.

DATA AVAILABILITY STATEMENT

The raw data supporting the conclusions of this article will be made available by the authors, without undue reservation.

ETHICS STATEMENT

The studies involving human participants were reviewed and approved by the Institutional Ethics Committee of the Eye and ENT Hospital of Fudan University. Written informed consent to participate in this study was provided by the participants' legal guardian/next of kin.

AUTHOR CONTRIBUTIONS

The data was collected and analyzed by LS. YH, C-YH, and HH helped design the project. The manuscript was written by LS, and revised by MZ, LT, and LZ. All authors contributed to the article and approved the submission.

REFERENCES

1. Steuer CE, El-Deiry M, Parks JR, Higgins KA, Saba NF. An Update on Larynx Cancer. *CA: Cancer J Clin* (2017) 67(1):31–50. doi: 10.3322/caac.21386
2. Patel TD, Echanique KA, Yip C, Hsueh WD, Baredes S, Park RCW, et al. Supraglottic Squamous Cell Carcinoma: A Population-Based Study of 22,675 Cases. *Laryngoscope* (2019) 129(8):1822–7. doi: 10.1002/lary.27592
3. Zhang Y, Xu S, Liu W, Wang X, Wang K, Liu S, et al. Rational Choice of Neck Dissection in Clinically N0 Patients With Supraglottic Cancer. *Head Neck* (2020) 42(3):365–73. doi: 10.1002/hed.26014
4. Barroso Ribeiro R, Ribeiro Breda E, Fernandes Monteiro E. Prognostic Significance of Nodal Metastasis in Advanced Tumors of the Larynx and Hypopharynx. *Acta Otorrinolaringologica Espanola* (2012) 63(4):292–8. doi: 10.1016/j.otorri.2012.02.012
5. Saindane AM. Pitfalls in the Staging of Cervical Lymph Node Metastasis. *Neuroimaging Clinics North Am* (2013) 23(1):147–66. doi: 10.1016/j.nic.2012.08.011
6. Bayır Ö, Toptaş G, Saylam G, İzgi TC, Han Ü, Keseroğlu K, et al. Occult Lymph Node Metastasis in Patients With Laryngeal Cancer and Relevant Predicting Factors: A Single-Center Experience. *Tumori* (2021) 3008916211026977. doi: 10.1177/03008916211026977
7. Ye LL, Rao J, Fan XW, Kong FF, Hu CS, Ying HM. The Prognostic Value of Tumor Depth for Cervical Lymph Node Metastasis in Hypopharyngeal and Supraglottic Carcinomas. *Head Neck* (2019) 41(7):2116–22. doi: 10.1002/hed.25667
8. Yılmaz T, Süslü N, Atay G, Günaydın R, Bajin MD, Özer S. The Effect of Midline Crossing of Lateral Supraglottic Cancer on Contralateral Cervical Lymph Node Metastasis. *Acta Oto-Laryngol* (2015) 135(5):484–8. doi: 10.3109/00016489.2014.986759
9. Kürten CHL, Zioga E, Gauler T, Stuschke M, Guberina M, Ludwig JM, et al. Patterns of Cervical Lymph Node Metastasis in Supraglottic Laryngeal Cancer and Therapeutic Implications of Surgical Staging of the Neck. *Eur Arch Oto-Rhino-Laryngol: Off J Eur Fed Oto-Rhino-Laryngol Societies (EUFOS): Aff German Soc Oto-Rhino-Laryngol - Head Neck Surg* (2021) 278(12):5021–7. doi: 10.1007/s00405-021-06753-1
10. Oosterkamp S, de Jong JM, Van den Ende PL, Manni JJ, Dehing-Oberije C, Kremer B. Predictive Value of Lymph Node Metastases and Extracapsular Extension for the Risk of Distant Metastases in Laryngeal Carcinoma. *Laryngoscope* (2006) 116(11):2067–70. doi: 10.1097/01.mlg.0000240263.05198.a0
11. Ho AS, Kim S, Tighiouart M, Gudino C, Mita A, Scher KS, et al. Association of Quantitative Metastatic Lymph Node Burden With Survival in Hypopharyngeal and Laryngeal Cancer. *JAMA Oncol* (2018) 4(7):985–9. doi: 10.1001/jamaoncol.2017.3852
12. Johnson JT. A Surgeon Looks at Cervical Lymph Nodes. *Radiology* (1990) 175 (3):607–10. doi: 10.1148/radiology.175.3.2188292
13. van den Brekel MW, Stel HV, Castelijns JA, Nauta JJ, van der Waal I, Valk J, et al. Cervical Lymph Node Metastasis: Assessment of Radiologic Criteria. *Radiology* (1990) 177(2):379–84. doi: 10.1148/radiology.177.2.2217772
14. Chung MS, Choi YJ, Kim SO, Lee YS, Hong JY, Lee JH, et al. A Scoring System for Prediction of Cervical Lymph Node Metastasis in Patients With Head and Neck Squamous Cell Carcinoma. *AJNR Am J Neuroradiol* (2019) 40(6):1049–54. doi: 10.3174/ajnr.A6066
15. King AD, Tse GM, Yuen EH, To EW, Vlantis AC, Zee B, et al. Comparison of CT and MR Imaging for the Detection of Extranodal Neoplastic Spread in Metastatic Neck Nodes. *Eur J Radiol* (2004) 52(3):264–70. doi: 10.1016/j.ejrad.2004.03.004
16. Sun R, Tang X, Yang Y, Zhang C. (18)FDG-PET/CT for the Detection of Regional Nodal Metastasis in Patients With Head and Neck Cancer: A Meta-Analysis. *Oral Oncol* (2015) 51(4):314–20. doi: 10.1016/j.oraloncology.2015.01.004
17. Al-Kaabi A, van der Post RS, Huising J, Rosman C, Nagtegaal ID, Siersema PD. Predicting Lymph Node Metastases With Endoscopic Resection in Ct2n0m0 Oesophageal Cancer: A Systematic Review and Meta-Analysis. *U Eur Gastroenterol J* (2020) 8(1):35–43. doi: 10.1177/2050640619879007
18. Redaelli de Zinis LO, Nicolai P, Tomenzoli D, Ghizzardi D, Trimarchi M, Cappiello J, et al. The Distribution of Lymph Node Metastases in Supraglottic Squamous Cell Carcinoma: Therapeutic Implications. *Head Neck* (2002) 24 (10):913–20. doi: 10.1002/hed.10152
19. Pollard JW. Tumour-Educated Macrophages Promote Tumour Progression and Metastasis. *Nat Rev Cancer* (2004) 4(1):71–8. doi: 10.1038/nrc1256
20. Kastelan Z, Lukac J, Derezić D, Pasini J, Kusić Z, Sosić H, et al. Lymphocyte Subsets, Lymphocyte Reactivity to Mitogens, NK Cell Activity and Neutrophil and Monocyte Phagocytic Functions in Patients With Bladder Carcinoma. *Anticancer Res* (2003) 23(6d):5185–9.
21. Sessions DG, Lenox J, Spector GJ. Supraglottic Laryngeal Cancer: Analysis of Treatment Results. *Laryngoscope* (2005) 115(8):1402–10. doi: 10.1097/01.Mlg.0000166896.67924.B7
22. Coskun HH, Medina JE, Robbins KT, Silver CE, Strojan P, Teymoortash A, et al. Current Philosophy in the Surgical Management of Neck Metastases for

Head and Neck Squamous Cell Carcinoma. *Head Neck* (2015) 37(6):915–26. doi: 10.1002/hed.23689
23. Shaha AR. Complications of Neck Dissection for Thyroid Cancer. *Ann Surg Oncol* (2008) 15(2):397–9. doi: 10.1245/s10434-007-9724-x

Conflict of Interest: The authors declare that the research was conducted in the absence of any commercial or financial relationships that could be construed as a potential conflict of interest.

Publisher's Note: All claims expressed in this article are solely those of the authors and do not necessarily represent those of their affiliated organizations, or those of the publisher, the editors and the reviewers. Any product that may be evaluated in this article, or claim that may be made by its manufacturer, is not guaranteed or endorsed by the publisher.

frontiers in Oncology

REVIEW
published: 21 March 2022
doi: 10.3389/fonc.2022.828434

Saliva Based Liquid Biopsies in Head and Neck Cancer: How Far Are We From the Clinic?

Aditi Patel[1], *Shanaya Patel*[1], *Parina Patel*[1] *and Vivek Tanavde*[1,2]*

[1] *Biological and Life Sciences, School of Arts and Sciences, Ahmedabad University, Ahmedabad, India,* [2] *Bioinformatics Institute, Agency for Science Technology and Research (ASTAR), Singapore, Singapore*

Head and neck cancer (HNC) remains to be a major cause of mortality worldwide because of confounding factors such as late-stage tumor diagnosis, loco-regional aggressiveness and distant metastasis. The current standardized diagnostic regime for HNC is tissue biopsy which fails to determine the thorough tumor dynamics. Therefore, due to the ease of collection, recent studies have focused on the utility of saliva based liquid biopsy approach for serial sampling, early diagnosis, prognosis, longitudinal monitoring of disease progression and treatment response in HNC patients. Saliva collection is convenient, non-invasive, and pain-free and offers repetitive sampling along with real time monitoring of the disease. Moreover, the detection, isolation and analysis of tumor-derived components such as Circulating Tumor Nucleic Acids (CTNAs), Extracellular Vesicles (EVs), Circulating Tumor Cells (CTCs) and metabolites from saliva can be used for genomic and proteomic examination of HNC patients. Although, these circulatory biomarkers have a wide range of applications in clinical settings, no validated data has yet been established for their usage in clinical practice for HNC. Improvements in isolation and detection technologies and next-generation sequencing analysis have resolved many technological hurdles, allowing a wide range of saliva based liquid biopsy application in clinical backgrounds. Thus, in this review, we discussed the rationality of saliva as plausible biofluid and clinical sample for diagnosis, prognosis and therapeutics of HNC. We have described the molecular components of saliva that could mirror the disease status, recent outcomes of salivaomics associated with HNC and current technologies which have the potential to improve the clinical value of saliva in HNC.

Keywords: head and neck cancer, liquid biopsy, saliva, biomarker, circulating tumor nucleic acids, extracellular vesicles, metabolomics

OPEN ACCESS

Edited by:
Markus Wirth,
Klinikum rechts der Isar, Germany

Reviewed by:
Vito Carlo Alberto Caponio,
University of Foggia, Italy
Gilda Alves Brown,
Rio de Janeiro State University, Brazil

***Correspondence:**
Vivek Tanavde
vivek.tanavde@ahduni.edu.in

Specialty section:
This article was submitted to Head and Neck Cancer, a section of the journal Frontiers in Oncology

Received: *03 December 2021*
Accepted: *25 February 2022*
Published: *21 March 2022*

Citation:
Patel A, Patel S, Patel P and Tanavde V (2022) Saliva Based Liquid Biopsies in Head and Neck Cancer: How Far Are We From the Clinic?. Front. Oncol. 12:828434. doi: 10.3389/fonc.2022.828434

INTRODUCTION

Head and Neck Cancer (HNC) is the sixth most prevalent cancer worldwide attributed to etiological factors like tobacco and alcohol consumption, HPV infections and to a certain extent genetic predisposition (1–3). Despite advancements in diagnostic and therapeutic regime, the overall survival of HNC patients has remained dismal for over four decades. Conventional diagnostic strategies comprise of physical examination, imaging techniques such as computed tomography (CT) scan, Ultrasound (US), magnetic resonance imaging (MRI) and tissue biopsies followed by

histopathological analysis. Till date, tissue biopsy is the most commonly used method for diagnosis; however, this technique is invasive, quite challenging, painful, time-consuming, and potentially risky for the patient. Moreover, the intra-tumoral and metastatic heterogeneity remains undetected, affecting the specificity, sensitivity and accuracy of assessment (4). Therefore the 'liquid biopsy approach' that focuses on detecting tumor-derived components in circulatory fluids for the diagnosis, screening and prognosis of cancer (5) is becoming increasingly important. Liquid biopsies are anticipated to demonstrate high accuracy in terms of representation of tumor genome landscape and mutations. They also provide reproducibility and feasibility of real-time therapeutic monitoring while being minimally invasive and cost effective (6). For HNC cancers, serum, plasma and saliva have been identified as the most frequently used sources for liquid biopsies (7).

Saliva as a potential source for liquid biopsy of HNC patients has several advantages compared to other body fluids as it (i) reflects any genomic, epigenomic, proteomic and physiological/pathological alterations in the oral cavity, larynx and pharynx; (ii) serves as a non-invasive, inexpensive, easier and more accessible screening tool (8); and (iii) provides the opportunity for real-time monitoring of HNC patients by having the flexibility of repetitive sampling and larger volumes for examination without the requirement of trained medical staff for collections (8–10). Despite the potential value in utilizing saliva derived biomarkers as diagnostic tool, its clinical utility is limited due to some challenges. Primarily, the complex composition of saliva comprises of various non-tumorigenic components hampering the ability to detect biomolecules of tumor origin. Moreover, relative contribution of different subsites into the salivary milieu makes the identification of HNC specific markers difficult (11). However, the potential utility of saliva as a liquid biopsy tool for diagnosis, prognosis and therapeutic monitoring of HNC is being extensively explored. Presently, the most common components for liquid biopsy of HNCs comprise cell-free tumor nucleic acids (DNA, mRNA and miRNAs), extracellular vesicles, circulating tumor cells (CTCs) and salivary metabolites (**Figure 1**). This review encompasses the recent developments, technologies, clinical applications and limitations of saliva derived biomarkers in HNC diagnosis, prognosis, and therapeutics.

CIRCULATORY TUMOR NUCLEIC ACIDS

Circulatory tumor nucleic acids (ctNAs) are fragments of cell-free genomic/viral DNA and/or RNA that are shed by tumor cells

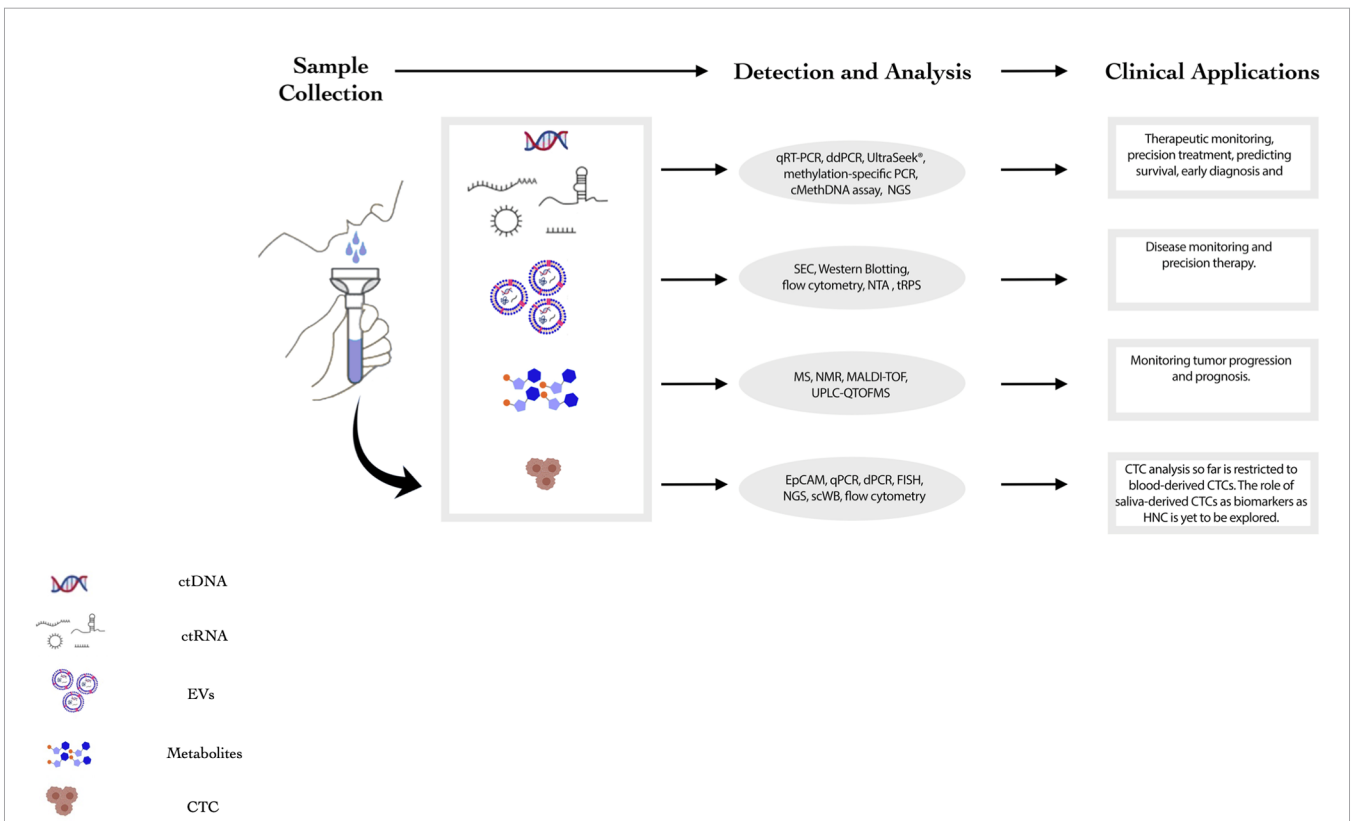

FIGURE 1 | Summary of salivary components that can potentially act as biomarkers for HNC. This figure summarizes the current landscape of salivary components that may act as biomarkers for HNC. The detection and analysis techniques and clinical applications for each component are mentioned in the figure. (NMR: Nuclear Magnetic Resonance, MS: Mass Spectrometry, HNC: Head and Neck Cancer, ddPCR: Droplet Digital Polymerase Chain Reaction, qPCR: quantitative Polymerase Chain Reaction, NGS: Next Generation Sequencing, SEC: Size-Exclusion Chromatography, NTA: Nanoparticle Tracking Analysis).

through passive processes like necrosis and apoptosis or *via* active mechanisms like spontaneous release of nucleic acids in systemic circulation (12, 13). These fragments of circulating tumor DNA (ctDNA) and RNA (ctRNA), are found in various body fluids including saliva. They reflect the genetic information of the bulk tumor and reflect clonal heterogeneity and tumor evolution. The rate at which these circulatory nucleic acids release into circulation depends on the tumor's location, vascularity, scale, resulting in variability across patients (14). Analysis of ctDNA relies more on identifying and targeting certain tumor specific mutations and understanding the epigenetic landscape, whereas ctRNA emphasizes on identifying novel or differential expression patterns of messenger RNA (mRNAs), microRNA (miRNAs), and long ncRNAs (lncRNAs) as a potential salivary biomarker. ctRNA based biomarkers probably gives better dynamic insights about cell-state and regulation as compared to ctDNA biomarkers.

Detection and analysis of ctNAs is quite challenging. Currently, real-time PCR (qRT-PCR), digital droplet PCR (ddPCR) and UltraSeek® (Agena Bioscience) mass-spectrometry-based PCR method are the most widely used techniques, as it helps in optimizing samples with low ctNA concentration in HNCs. ddPCR is still the most preferred method demonstrating higher sensitivity, specificity and multiplexing capacity (15, 16). Further, techniques such as methylation-specific PCR (17, 18), methylation on beads (19), and cMethDNA assay (20, 21) are used to detect the difference in methylation patterns on promoter of ctDNA in HNC patient samples. PCR based techniques are preferred when there are low number of target regions (≤ 20 targets), limited sample input and when there is limited assessment of tumor heterogeneity or identification of known variants. Next Generation Sequencing (NGS) methods such as CAPP-Seq (cancer personalized profiling by deep sequencing), TAm-Seq (tagged amplicon deep sequencing), Safe-Seq (safe sequencing system), and AmpliSeq are being used to isolate and capture ctNAs; each with relatively higher strengths in sensitivity, specificity and scalability (22–24). These NGS techniques can detect both known and unknown tumor-specific mutations and analyze differential expression patterns of single markers or a panel of markers. Targeted NGS methods are less time-consuming, result in fewer wastage of resources and offer a higher discovery rate, thus aiding in identification of novel variants. Despite the current limitations, these techniques have demonstrated potential to detect and isolate smaller concentrations of ctDNA from saliva, thus opening new avenues for clinical applications (25). With technological advancements, higher specificity and sensitivity of ctDNA detection could effectively increase their clinical applications. Nonetheless development of cost-effective NGS assays is crucial for their widespread clinical utility (26, 27).

CIRCULATORY TUMOR DNA (ctDNA)

ctDNA represents a trivial fraction (<1%) of whole cfDNA shed from tumor cells into the circulation. However, this small subpopulation is believed to reflect the somatic mutations and genomic landscape from primary tumors that can be useful in early diagnosis and risk prediction of HNC. Recently, few studies have emphasized utilizing ctDNA derived from saliva in early detection of cancer. Wang et al., conducted a comprehensive analysis of somatic mutations (*TP53, CDKN2A, NRAS*, *NOTCH1, PIK3CA, FBXW7*, and *HRAS*) and HPV (HPV16 and 18) genes in saliva and plasma of 93 HNC patient samples comprising of oral cavity, oropharynx, larynx, and hypopharynx subsites. The study demonstrated detection of ctDNA at 96% rate irrespective of the tumor size, stage and location. Moreover, recurrence post-surgery was observed in majority of patients having these somatic mutations. In OSCC patients, the detection rate of ctDNA was higher in saliva as compared to plasma, indicating that salivary ctDNA can be used for OSCC detection (28).. Similarly, p53 mutation in exon 4 codon 63 was detected in saliva of early stage OSCC patients (93.33% of cases, $p<0.05$) with a similar detection rate as patient tumor samples (29). However, Perdomo et al. reported that, targeted mutation detection approach failed to demonstrate significant concordance in detecting *TP53* mutations from tumor and saliva derived ctDNA. El Naggar *et al.* and Spafford et al., detected microsatellite instability and loss of heterozygosity at certain chromosomes in oral mucosal cells from HNC patients and saliva ($p < 0.001$) with different sensitivity and specificity based on sample size and sampling subsites (30, 31). Moreover, genetic alterations in *PMAIP1* and *PTPN1* genes had the potential to discern HNC patients from healthy individuals (32). Collectively, these studies suggest that assessment of somatic mutations from salivary ctDNA can be an effective non-invasive substitute to tissue biopsy for early diagnosis, disease surveillance and prognosis of HNC patients. However, multiple mutation detection-based studies with standardized protocols and larger cohort of patients will be required for clinical translation (33) of this approach. Low yields of ctDNA after purification from saliva is also a key limiting factor. To increase the efficacy and sensitivity of salivary ctDNA as a biomarker, specific ctDNA panels need to be designed that can help detect and monitor HNC cases in real-time and a cost-effective manner.

Several studies have highlighted the importance and feasibility of detecting epigenetic alterations in ctDNA from body fluids and its immense diagnostic potential. Promoter hyper-methylation of genes such as *EDNRB* ($\kappa = 0.60$), *KIF1A* ($\kappa = 0.64$), *NID2*($\kappa = 0.60$), and *HOXA9* ($\kappa = 0.60$) in salivary DNA have shown potential utility for early detection of oral cancer patients (34–36). Few studies have demonstrated a significant clinical correlation between hypermethylation in promoter region of salivary ctDNA with prognosis and risk prediction in HNC patients. Specifically, methylated gene loci were identified in both tissue and preoperative saliva samples and could serve as a classifier to differentiate between preoperative and postoperative samples for HNC patients (37). Analogous to this, Carvalho et al. indicated that detection of promoter hypermethylation of either or all genes (*TIMP-3, CCNA1, DCC, MGMT, MINT-31, DAPK p16*) in pre-treated salivary DNA could effectively predict poor survival (HR=2.8;

95% CI=1.2–6.5; p=0.016) and recurrence (HR=12.2; 95% CI=1.8–80.6; p= 0.010) of HNC patients (38).These findings suggest that elevated ctDNA hypermethylation patterns have the potential to predict disease aggressiveness, overall survival rate and therapeutic monitoring and surveillance of HNC patients (**Table 1**). As we thrive towards the development of epigenetic-based diagnostic tests, we need to consider the challenges that come along with it. One of the major challenges: Given the epigenetic plasticity in non-cancerous cells, we need to develop tools that can filter the false positive signals and enhance the specificity and sensitivity of these assays making them more translatable.

Collectively, somatic mutations and methylation patterns of salivary DNA could be utilized as potential biomarkers and prognosticators in HNC. This approach can accelerate the diagnosis and risk prediction of HNC and pave the path for improved patient outcomes by monitoring their therapeutic response.

CIRCULATORY TUMOR RNA (ctRNA)

Analysis of transcriptomic profiles of circulating body fluids is a widely explored method for early cancer detection and several studies have shown significant association of the transcriptome with disease progression. Several studies have demonstrated the association of salivary mRNAs with development and detection of HNC. Li et al. demonstrated a significant 3.5-fold elevation in OSCC saliva with significant sensitivity (91%) and specificity (91%) ($P < 0.01$) of transcripts of salivary *SAT, IL8, S100P, IL1B, OAZ1, DUSP1* and *HA3*, in oral cancer patients as compared to their healthy counterparts (41). David Elashoff and colleagues (42) substantiated the effectiveness of these biomarkers in a larger patient cohort (382 patients), suggesting the potential role of salivary mRNA markers in oral cancer detection. With respect to individual marker performance across the five cohorts, the increase in *IL8* and *SAT* was statistically significant($p<0.02$). The validation of these biomarkers in larger patient cohorts shows their feasibility in the discrimination of OSCCs from healthy controls (42). Transcript level expression of tumor suppressor gene transgelin was observed to be significantly elevated in saliva of OSCC patients as compared to the normal counterparts. The salivary gene expression levels were in concordance with the tumor tissue and associated with overall survival (p=0.011) of patients, demonstrating its immense potential as a promising biomarker and an independent prognosticator in OSCC (43). *HPV-16* has also been identified as a major etiological factor responsible for HNSCC tumorigenesis. *HPV-16* mRNA showed a significantly altered expression in salivary rinses of HNSCC patients with a simultaneous effect on p16(INK4a), a known tumor suppressor having a vital role in regulating the cell cycle($p<0.05$) (44). Thus, the expression pattern of different salivary mRNAs correlates with various important clinical parameters including tumor progression, differentiation, and overall survival. More importantly, the expression of salivary mRNA depicts an independent prognosis factor for HNC, suggesting that salivary mRNA might be a potential biomarker for early detection of HNC and predicting the prognosis for HNC patients.

Tumor derived circulating RNA profile is complex as it comprises of distinctive components such as noncoding RNAs (e.g., lncRNA and piwi-interacting RNAs) and microRNAs (miRNAs). Alterations in miRNA and lncRNAs expression can be exploited to investigate their potential in differentiating HNC patients from healthy volunteers (45, 46), given the fact that substantial research has been conducted in exploring the diagnostic and prognostic potential of ncRNAs derived from saliva of HNC patients (**Table 2**) (55). Various saliva-derived circulatory miRNAs such *as miR-139-5p* in TSCC (49) *miR-3612, miR-650, miR-4259, miR-937-5p* and *miR-4478* in NPC (51) and *miR-125a, miR-200a*, and *miR-21* have been identified as plausible biomarkers for different subsites of HNC (46, 48). In a preliminary study, expression of 314 salivary miRNAs was assessed in OSCC patients in comparison to their healthy counterparts. *miR-200a* and *miR-125* were observed to be significantly down regulated ($p<0.05$) in the patient cohort as compared to the healthy volunteers. This study emphasized that salivary miRNAs were stable in saliva and could be utilized in early detection of oral cancers (46). These findings were validated by Wiklund and colleagues demonstrating that differential expression of *miR-200a* and *miR-375* along with promoter methylation of miR-200c-141 in oral rinses and saliva of OSCC patients can be utilized for early detection of oral cancers (56). The potential role of circulatory miRNAs in

TABLE 1 | ctDNA biomarkers for HNSCC.

Marker	Type of Marker	Findings	Sample Size	Reference
E7 (HPV16 and HPV18), TP53, PIK3CA, CDKN2A, FBXW7, HRAS, and NRAS	Diagnostic	The sensitivity of detection of ctDNA increased when both saliva and plasma assays were combined (96% of the samples). Moreover, oral cavity tumor ctDNA was preferentially enriched in saliva as opposed to ctDNA from other sites.	93	(28)
CDKN1A and DDB2	Post-treatment monitoring	Salivary CDKN1A and DDB2 were significantly upregulated post-treatment in HNSCC patients and the rate of upregulation was correlated with the received treatment dose.	8	(39)
HPV DNA	Prognostic	Salivary HPV DNA levels in patients with LR HPV^+ OPSCC were correlated to total tumor burden. A rise of salivary HPV DNA was correlated with recurrence and a fall in HPV DNA levels was observed during treatment. Higher levels of plasma HPV cfDNA were associated with poor prognosis.	21	(40)

TABLE 2 | Circulating miRNA markers for HNSCC.

Marker	Type of Marker	Findings	Tumor Sample Size	Author
miR-31	Diagnostic	Upregulation of salivary miR-31 in OC patients.	35	(47)
miR-21 and miR-184	Diagnostic	Highly significant upregulation of miR-21 and miR-184 ($P < 0.001$) in OSCC and PMD samples as compared to healthy controls.	40	(48)
miR-139-5p	Diagnostic	Significant downregulation of salivary miR-139-5p in TSCC patients as compared to healthy controls. Levels returned to normal after treatment (surgery).	25	(49)
miR-93 and miR-200a	Treatment monitoring	Increase in expression of miR-93 and miR-200a in OSCC patients 12 months after radiotherapy thereby highlighting their potential as biomarkers for post-radiation treatment monitoring in HNSCC patients.	33	(50)
miR-937-5p, miR-650, miR-3612, miR-4478, miR-4259, miR-3714, miR-4730, miR-1203, miR-30b-3p, miR-1321, miR-1202 and miR-575	Diagnostic	Identified 12 miRNAs that were significantly downregulated in the saliva of NPSCC patients and could potentially serve as diagnostic biomarkers.	22	(51)
miR-let-7a-5p and miR- 3928	Diagnostic	Salivary miR- let-7a-5p and miR- 3928 were significantly downregulated in HNSCC patients as compared to healthy controls. Both of these miRNAs showed significant specificity and sensitivity in differentiating between healthy controls and HNSCC patients.	12	(52)
miR-24-3p	Diagnostic	Significantly high expression of exosomal miR-24-3p was observed in saliva of OSCC patients.	30	(53)
miR-21 and miR-31	Diagnostic	Upregulation of salivary miR-31 and miR-21 in patients with severe dysplasia relative to healthy controls. Leucoplakia had the most significant upregulation of the aforementioned markers out of all the lesions.	36	(54)

effectively monitoring tumor progression, therapeutic response and recurrence have been reported in several studies – (i) Salivary miR-21 is associated with T-stage classification (p=0.02) (54) (ii) and miR-136 expression showed significant correlation with complete remission cases (AUC=0.904 CI=0.75-1 P<0.05) (25) Moreover, a preliminary study conducted by Greither et al. demonstrated differential expression of salivary miR-200a (p=0.036) and miR-93 (p=0.047) in HNSCC patients post-radiotherapy (50). Similarly, another study identified significant correlation between increased expression of salivary miR-15a-5p and disease-free survival in post-intensity modulated radiotherapy patients (HR=0.25; 95% CI=0.05-0.78; p<0.016) (57). These studies highlighted the utility and efficacy of saliva-based miRNA biomarkers in predicting therapeutic response despite the significant alterations in salivary components post-radiation.

The other arm of ncRNAs are long non-coding RNAs (lncRNAs) which are approximately more than 200 nucleotides long and are not translated into protein. Considering their inevitable role in tumor progression and metastasis, signatures of saliva derived lncRNAs have been explored as probable biomarkers for monitoring disease progression of OSCC. A pilot study has reported measurable levels of HOTAIR and MALAT lncRNAs in the saliva of OSCC patients (58). Furthermore, these elevated levels were associated with nodal metastasis ascertaining its potential as a predictive marker.

Recently, circular RNAs (circRNAs) have attracted attention globally, because of their stability (owing to the circular structure) in comparison to lncRNAs and miRNAs (45). Various circRNAs secreted into the saliva of HNC patients regulate several biological and physical processes (59). A study found differential expression of 32 salivary circRNAs in OSCC patients as compared to matched controls. The upregulation of hsa-circ-0001874 clinically correlated with tumor grade and staging. Expression level of hsa-circ-0001971 was associated with TNM stage. Further, these circRNAs could also differentiate OSCC from oral leucoplakias (AUC of 0.895) (60). These findings prompt towards their potential role as diagnostic biomarkers for OSCC; however, additional investigation on circRNAs as probable non-invasive biomarkers for HNCs will be needed to assess their prognostic and diagnostic value.

The use of salivary ctRNAs as biomarkers for detection, disease surveillance, therapy response, and prognosis sound promising but a major limitation of salivary RNA quantification is the risk of RNA degradation due to the presence of enzymes including RNases in the saliva. This in turn affects the quality of RNA extracted thereby increasing the false-positive and false-negative detection rates. Moreover, the risk of sample contamination with blood from the oral mucosa and lesions due to inflammation are other limiting factors. Multicentric preclinical/clinical studies with standardized protocols are required to verify the existing findings before establishing the clinical utility of circulatory RNAs.

EXTRACELLULAR VESICLES

Extracellular vesicles (EVs) are 30-200 nm membrane encapsulated organelles that are secreted by cells into the extracellular space in response to various physiological conditions such as proteases, growth factors, apoptotic signals, biomechanical shear and stress conditions (61, 62). Developing evidence suggests that tumor-derived EVs enable the tumor bulk to manipulate its microenvironment as they have the potential to mediate intercellular communication by transporting their

molecular cargo (DNA, RNA and protein) to local or distant sites through circulatory fluids (63).

Conventional EV isolation techniques are dependent on their physical and biological properties such as size, density and surface marker expression (64). Conventionally utilized techniques for EV isolation and purification based on size include filtration and size-exclusion chromatography (SEC) whereas immune-affinity capture method identifies the EV population based on surface markers. Currently, the widely used methods for EV isolation are ultracentrifugation and/or differential centrifugation and polymer precipitation method which is commonly used in commercially available kits. Recently developed microfluidics-based technologies for EV isolation comprise of antibody-functionalized microfluidic channels (65), nanoscale size-based filtration (66) and spiral inertial microfluidic devices (67). After isolation, western blotting and flow cytometry using surface protein markers CD9, CD63, CD81, Alix, TSG101, are the most conventionally used analytical methodologies for characterisation of EVs (68–71). Nanoparticle Tracking Analysis (NTA) that works on the principle of determining Brownian motion of the particles is another extensively used technique and has higher resolution as compared to flow cytometry (72). Similar to NTA, Tunable Resistive Pulse Sensing (tRPS) is an emerging technology that estimates the EV concentration based on the particle movement and flow rates in fluid cells corresponding to the pulses/voltage applied (73, 74). However, the clinical applicability of tRPS remains to be challenging considering the heterogenous size of the EV population. Several techniques have been explored for isolation and characterisation of EVs using various patient samples; however, sensitivity and specificity of these techniques in terms of clinical utility for liquid biopsies requires comprehensive standardization of protocols and larger patient cohort studies.

Various findings have revealed that saliva harbors ample numbers of EVs, the components of which differ based on the physiological or pathological state of an individual (75). Some of the advantages of salivary EVs as compared to serum and plasma derived EVs are – (i) the collection process is non-invasive; (ii) they contain less protein content that makes their identification and quantification simpler (76, 77); and (iii) they do not undergo coagulation which stimulates a persistent secretion of EVs from platelets, thus altering the composition of circulating EVs (78). Recently, the possibility of potential biomarkers from circulatory EVs derived from saliva of HNC patients is gaining interest (**Table 3**). On comparing plasma and salivary EVs derived from oral cancer patients it was found that salivary EVs were concomitantly elevated as the plasma derived EVs and demonstrated a clinical association with tumor staging ($p<0.01$) and loco-regional aggressiveness ($p<0.01$) (81). These results are in corroboration with previous studies showing that salivary EVs from oral cancer patients have an irregular morphology, are greater in size and formed more aggregates as compared to EVs from normal controls (82–84).

Recent studies have found a significant role of salivary EV derived non-coding miRNAs as potential biomarkers for early diagnosis, prognosis and therapeutic targets in HNC patients given their stability within the EV and ability to regulate both oncogenes and tumor suppressor genes. Significantly, elevated levels of *miR-21, miR-494-3p, miR-412-3p, miR-184, miR-27a-3p*, and *miR-512-3p* ($p<0.05$) were observed in salivary exosomes derived from OSCC patients compared to the control cohort (9, 85). A recent study demonstrated that salivary miR-24-3p was enriched in OSCC and tongue cancer patients and could significantly increase the proliferation of these cells (53). Collectively these findings suggest that salivary exosomal miRNAs can be an asset for convenient and non-invasive sampling as well as pave way for early diagnosis, disease monitoring and therapeutic response evaluation in various HNC subsites (86–88).

Recent studies have reported that EVs contain long non coding RNAs (lncRNAs), however their expression has not been explored extensively in salivary EVs. High expression of a subset of lncRNAs, including HOTAIR, has been reported in the saliva of metastatic HNC patients. Thus, besides miRNAs, lncRNAs in salivary EVs could be a valued prognostic and diagnostic asset for HNC (89, 90).

TABLE 3 | Exosomal biomarkers for HNSCC.

Author	Type of Marker	Findings	Tumor Sample Size	Reference
RNA				
miR-21	Diagnostic	Hypoxic OSCC derived exosomes expressed higher levels of miR-21 and the expression was closely associated with lymph node metastasis and T-stage of the cancer.	108	(79)
miR-302b-3p, miR-517b-3p, miR-512-3p and miR-412-3p	Diagnostic	miR-302b-3p and miR-517b-3p were exclusively expressed in salivary EVs isolated from OSCC samples. miR-412-3p and miR-512-3p were significantly upregulated in salivary EVs of OSCC patients as compared to healthy controls ($p < 0.02$).	21	(9)
miR-24-3p	Diagnostic	Salivary exosomal miR-24-3p levels significantly increased in OSCC patients. miR-24-3p interacts with *PER1* thereby promoting the proliferation of OSCC.	49	(53)
Proteins				
MMP-9, myosin-9 (NMMHC II-a), complement C3, S100A9, complement factor B (CFB), Rab GDI and complement C4-B	Diagnostic	Differentially expressed proteins were reported in salivary OSCC samples as compared to control samples. Out of the group of 38 proteins that were identified only in OSCC samples, 5 were identified in patients without any lesions.	21	(80)

The discovery of tumor associated proteins in saliva is accredited to high-throughput mass spectrometry screening of patient samples. From these studies, a series of protein biomarkers has been detected in salivary EVs for OSCC, such as *LGALS3BP, PKM1/M2, A2M, MUC5B, IGHA1, HPa, and PIP* (80, 91). Moreover, these tumor-associated proteins have been reported to be involved in multiple signaling pathways, including metal transport, cell proliferation, and tumor immune responses (80). Additionally, exosomal *EGFR, ANXA1* and programmed cell death (PD)-1/PD-ligand 1 (*PD-L1*) pathway (tumor suppressor in HNSCC) have been identified as potential biomarkers for predicting prognosis and therapeutic monitoring in tumor derived exosomes of HNSCC patients (92).

There are several benefits of EVs as compared to ctDNA and CTCs. However, a wide range of isolation and analysis techniques for EVs and lack of universally accepted EV reference standards are some of the major hurdles for developing diagnostic assays to enumerate EVs from patient samples. Moreover, interference from hemolytic, lipaemic and platelet contaminated samples and issues with sample stability compromise the reproducibility of EV detection, modify EV's physical and biological properties and affect their purity and recovery rate (93). Hence, developing a consistent external quality assessment (EQA) scheme involving application of strict but attainable sample requirements for assays, establishing standardized collection and storage environments that can minimize EV degradation and applying standard methods of EV characterization and enumeration is needed.

Salivary EVs have enormous potential for future diagnostic and therapeutic modalities, but this potential needs to be underpinned with solid scientific groundwork. A comprehensive understanding about the mechanism of how cancer cells utilize EVs to promote carcinogenesis may direct the advancement of novel therapies for HNC.

SALIVARY METABOLOMICS

Metabolomics focusses on identification and quantification of small metabolites produced during the process of metabolism from biological samples including body fluids, cells, and tissues. Increasing evidence has highlighted the importance and potential clinical utility of metabolomics in differentiating between HNC patients and controls using bio-fluids such as saliva, plasma and serum of HNC patients.

Currently, mass spectrometry (MS) and nuclear magnetic resonance (NMR) are the most frequently used procedures for screening salivary metabolites for early diagnosis and therapeutic monitoring of HNC patients (94). For salivary metabolite-based analysis, solution state NMR is the most preferred technique and protons (1H) are the most commonly analyzed NMR-active nuclei (95). One of the major advantages of this technique is that simple steps such as centrifugation are sufficient and no other pre-processing is required for sample preparation (96). The utility of MS techniques such as matrix-assisted laser desorption ionization (MALDI) in combination with time-of-flight (TOF) is being explored in salivary metabolomics as it can provide a high-throughput profile from a small sample volume without the requirement of a separation step (97, 98). Apart from this, liquid chromatography MS (LC-MS) is a frequently used technique for screening saliva samples for metabolites. Capillary electrophoresis MS (CE-MS) is an emerging technique that utilizes high voltages to induce an electrophoretic flow of ions through a capillary (20–200 μm i.d.) using very small sample volumes (10-100 nanolitre). The unique advantage of CE-MS is its ability to boost the range of detectable polar metabolites; however complex assembly and the high possibility of capillary blockage are confounders (99, 100). Therefore, it is crucial to develop a standard protocol for processing saliva samples for metabolomic analysis for successful clinical translation.

Identification of salivary metabolites such as d-glycerate-2-phosphate, pseudouridine, norcocaine nitroxide, 1-methylhistidine, 2-oxoarginine, inositol 1,3,4-triphosphate, sphinganine-1-phosphate, and 4-nitroquinoline-1-oxide demonstrated the potential of this technique to differentiate between malignant and precancerous lesions (94). Wei et al. used ultra-performance liquid chromatography combined with quadrupole/time-of-flight spectrometry (UPLC-QTOFMS) analysis to identify a signature panel of salivary metabolites (valine, lactic acid, γ-aminobutyric acid, n-eicosanoic acid, and phenylalanine) in 37 OSCC patient samples that could distinguish between OSCC from their normal counterparts with 86.5% sensitivity and 82.4% specificity. Furthermore, lactic acid and valine were significantly elevated in OSCC with respect to oral leucoplakia (OLK) with a fold change of 2.97 ($p = 0.0032$) and 1.60 ($p = 0.0034$) respectively (101). Similarly, Sugimoto et al., and Ishikawa et al. analyzed the salivary metabolomic profiles in oral cancer patients in two independent studies. These studies identified several metabolites such as cadaverine, glutamic acid, pyrrolinehydrocarboxylic acid, choline, threonine, beta-alanine, piperidine, carnitine, tryptophan, glutamine, taurine, leucine plus isoleucine, pipecolic acid, alanine, valine, and histidine that were consistently elevated in the saliva and tumor tissues of the patient samples as compared to controls (102, 103). Sugimoto's group identified taurine and piperdine as the key oral cancer-specific markers ($p < 0.05$) in a pool of 69 OSCC saliva fluid samples, suggesting that metabolites in saliva can be used as biomarkers for HNC screening. Ishikawa et al. reported a high fold change value for kynurenine ($FC = 38.1$, $p < 0.0001$) (a metabolite associated with reactive oxygen species mediated stress) in tumor samples from oral cancer patients. Collectively these findings suggest that salivary metabolites reflect changes in metabolites found in tumor tissues and thus could be used for diagnosis and prognosis of oral cancers (101, 102).

Among these differentially expressed metabolites, several studies observed significantly higher levels of salivary polyamine in oral cancer patients which showed a clinical association with tumor invasion and metastasis (102). A study conducted by Hsu et al. confirmed the elevation of polyamine along with its intermediate metabolites and demonstrated a vital involvement of polyamine pathway in oral cancer progression (103, 104). These findings highlight the importance of polyamine homeostasis and its clinical utility in identifying and understanding tumor progression.

Although many studies have successfully utilized salivary metabolomics to detect HNC, inconsistency in saliva/serum derived metabolite profiles hampers the clinical utility of this approach (105). To resolve this, more evidence using larger patient cohorts is warranted. Additionally, establishing standardized protocols, analyzing intracellular metabolites and their role in HNC and understanding the underlying mechanisms behind metabolomic alterations are required in order to identify genes or proteins affected by metabolomic changes. The salivary metabolites profile tends to fluctuate as it is highly responsive to various conditions including stress. Such factors need to be accounted for as they directly impact the reproducibility of the results as well as the sample collection protocol. Salivary metabolomics is still at a nascent stage and may develop into a diagnostic tool for early detection of oral cancer.

SALIVARY MICROBIOME

Recent studies have highlighted the role of oral microbiome in the development, progression and treatment monitoring of HNC (106). Moreover, oral microbiota has also been reported to influence salivary metabolomic profiles of HNC patients (107). Studies based on identification of bacterial spectra on the surface of OSCC mucosa in comparison to normal oral mucosa of patients revealed that there was a predominance of anaerobic pathogens in OSCC patients, compared to normal oral mucosa (108, 109). However, very little is known about the relationship between the oral microbiota and disease progression in HNC patients.

The past approaches for identification of bacterial taxa were culture dependent. However the diversity of the oral microbiome cannot be completely identified by these approaches. PCR technology and DNA-DNA hybridization methods are commonly used to describe oral microflora. However this experimental design can only identify limited changes in the microflora of a tissue (110–112). With the emergence of NGS technology, rRNA sequencing is promoted to discover the associations between microbial flora and HNC.

Pushalkar et al. examined the saliva microbiome of OSCC patients and suggested its potential application as a diagnostic tool (113). A 16S rRNA gene sequencing study on Caucasian participants found that a panel of Capnocytophaga, Corynebacterium, Porphyromonas, Haemophilus, Oribacterium, Rothia, and Paludibacter could discriminate between patients with oropharyngeal cancers and oral cavity cancers from age-matched controls ($p<0.05$) (114). A recent study demonstrated that an elevated presence of Capnocytophaga (AUC= 0.81 $p<0.05$) in saliva could be used as a probable screening tool for prognosis and diagnosis of HNC patients (115). Similarly, abundance of Dialister ($p<0.05$) in HNC patients correlated with aggressive laryngeal and oral tumors (116). Collectively, these studies suggest that salivary microbiota maybe useful in diagnosis and early detection of HNC.

The comprehensive role of oral microbiome in HNC development and progression is still at a nascent stage, but has been explored considerably in the last decade. However, it is still difficult to understand the exact mechanisms by which the oral microbiome contributes to HNC pathogenesis. Recently, data that links specific microbiome species to HNC aetiopathogenesis has been reported (106); however, studies based on longitudinal time frames with larger patient cohorts are needed. Longitudinal studies are critical in evaluating the dynamic nature of salivary oral microbiome before, during and after HNC development. Further research along these lines for identifying microbial biomarkers involved in tumor progression may assist in better understanding of the process of tumorigenesis and development of personalized treatments for better patient management in HNC.

CIRCULATING TUMOR CELLS (CTCs)

The tumor mass tends to shed a large number of cells through the process of apoptosis/necrosis. These cells are known as Circulating Tumor Cells (CTCs) that have the potential to create metastatic niches (117) by migrating to adjacent or distant tissues through the blood or lymphatic system. Thus, these cells are considered as seeds of metastasis or risk predictors of disease aggressiveness. CTCs have a promising role in early risk prediction, disease progression and therapeutic monitoring, and as potential drug targets (118).

CTC detection is a two-step process that involves an initial enrichment step followed by a detection step. The enrichment process comprises of two alternative approaches namely –(i) negative depletion: which focuses on removal of undesired cells (RBCs and lymphocytes) either *via* lysis or by immuno-magnetic bead-based depletion of CD45+ leukocytes; and (ii) positive selection: that involves isolation of epithelial cells using surface markers like epithelial cell adhesion molecule (EpCAM) or cytokeratins in order to distinguish the CTCs from contaminating leukocytes. The subsequent detection step is carried out using techniques ranging from quantitative PCR (qPCR) and digital PCR (dPCR) for mutational profiling to whole-genome sequencing, fluorescence *in situ* hybridization (FISH) based cytogenetic analysis and targeted NGS (119, 120). Targeted NGS-based detection of CTCs is a relatively recent advancement and is being explored for various types of cancers, including HNC (121). Immunocytochemistry (122) and flow cytometry (123) are used for single-CTC analysis but a major drawback of these two techniques is their poor multiplexing capacity. To overcome this limitation new technologies are emerging such as single-cell Western Blotting (scWB), a microfluidics-based technique used to evaluate protein levels in metastatic cancers (124). In addition, CellSearch® is an EpCAM-based CTC detection system that is the only system clinically approved by the FDA for enumerating epithelial CTCs. Recent studies have highlighted the heterogeneity of CTC populations and CellSearch® fails to detect CTCs with low or no expression of EpCAM and is unable to detect non epithelial tumors like sarcomas or other mesenchymal tumors. This shortcoming is overcome by using antigen-independent systems that identify CTCs based on their biophysical characteristics like density, size, and electrical properties.

CTCs can predict the risk of metastasis in HNC patients even before clinical examination (125). Hence, they may be useful for risk prediction in HNC. The presence of CTCs has been detected in saliva, however, the current landscape of CTC-based studies in HNSCC have utilized blood/plasma/serum-derived samples. Moreover, CTC evaluation is a challenge in saliva due to their limited numbers which makes isolation and detection difficult (126). The feasibility of EpCAM markers in salivary detection of CTCs, remains uncertain because of the shedding of normal epithelial cells along with cancerous cells in saliva. Nonetheless, existing studies have shown promising potential of circulatory CTCs for diagnosis, prognosis, and therapeutic monitoring in HNSCC, which suggests that further research can lead to better prospects for salivary CTCs in HNC (127–130).

DISCUSSION

Several studies conducted in the last decade demonstrated the plausibility of identification of potential biomarkers from biofluids and their relevance in clinical settings. Liquid biopsy has paved the way for early diagnosis and prognosis, recurrence and therapy monitoring as well as screening of high-risk populations. Although blood-based liquid biopsies have been the utmost common avenue of research, the use of salivary or oral rinse-based liquid biopsies for HNC offer a unique opportunity, as these cancers are of upper aerodigestive mucosal origin and can shed tumor cells, tumor DNA, and EVs directly into saliva. Moreover, this biopsy approach is minimally invasive, entails analysis of various circulating biomarkers and enables real time monitoring of tumor progression using repetitive testing. Such real time monitoring is simply not possible with traditional biopsies. As cancer treatment moves toward an attention on targeted precision medicine, liquid biopsy has the potential to guide such treatments based on real time monitoring of patients. The current review highlights new technological advancements and potential clinical applications of saliva as a liquid biopsy tool in HNC. CTCs, ctNAs, EVs, and salivary metabolome can yield useful biomarkers using non-invasive techniques. These biomarkers could reflect actual tumor biomarkers. The copious work, involving an extensive variety of assays based on diverse principles, has been quite productive in terms of utility of these biomarkers in diagnosis and disease monitoring of head and neck cancers. However, a major obstacle for all biomolecules in liquid biopsy remains the relatively low and fluctuating concentration derived from a tumor against the background of normal counterparts; in most patient samples. Such hurdles are tackled using the approaches highlighted in the technologies addressed above. These methods are presently sensitive enough to detect and analyze very rare mutation events. Nevertheless, it is crucial that laboratories working with such techniques must be consistent in their methodologies to avoid inaccurate results. Though passé, the association of a needle in a haystack relates and is fitting for each of these practices.

The investigation of ctNAs and EVs has benefitted from advances in the field of enrichment former to the analytical procedures. While at a nascent stage, reports have revealed that isolation and enrichment techniques will be an important asset in refining nucleic acid-based assays and as an individual diagnostic in the future.

Evidently, EVs have various advantages for prognosis and diagnosis. They aid in extraction of high-quality RNA from fresh or frozen saliva, thus enhancing the scope of detectable mutations that comprise of splice variants, mutations, fusions along with expression-based assays for mRNA, microRNA, lncRNA and other non-coding RNAs. ctDNA contains all genes at an equal level, while RNA originating from a highly expressed gene could be present in thousands of copies/cells. Nevertheless, as mutations exist on both ctRNA (dying/apoptotic process) and exosome RNA (living process), developing a platform that can aid in both will have palpable advantages for detecting rare mutations. This can be of great help in the case of patients who do not have an ample quantity of mutated nucleic acid in circulatory fluid. Moreover, as DNA mutations will only notify limited information of the disease, investigating RNA expression in biofluids such as saliva can further help in understanding the processes within the HNC patient. Although saliva is a promising source of all these biomolecules it is currently unclear which one of these (ctNAs, EVs or metabolites) will eventually be useful in early diagnosis, tumor prognosis and real time therapeutic monitoring. It is entirely possible that each of these end points require monitoring different biomolecule levels. Advances in technologies for sensitive, robust and inexpensive detection of such biomolecules will enable the use of saliva based liquid biopsies in routine clinical use.

Cancer is a multifaceted and dynamic disease that can undergo quick changes. To copiously deliver on the assurance and surety of personalized medicine, development of reliable non-invasive avenues for the diagnosis, prognosis, patient stratification and treatment response monitoring are paramount. Further studies in clinical settings and in large patient cohorts with well-annotated data are needed to validate the salivary transcriptomic, genomic and proteomic data. The several liquid biopsy platforms explained in this review have the ability to add immense value to the care of cancer patients.

AUTHORS CONTRIBUTIONS

AP and **SP** participated in the literature analysis. **AP** and **PP** searched the literature, drafted the manuscript and created the figures and tables. **SP** and **VT** designed, conceptualized, finalized and contributed to the critical review of the manuscript. All authors contributed to the article and approved the submission.

ACKNOWLEDGMENTS

Financial support to SP from the DBT-RA Program in Biotechnology and Life Sciences from the Department of Biotechnology, Government of India is gratefully acknowledged.

REFERENCES

1. Ferlay J, Colombet M, Soerjomataram I, Mathers C, Parkin DM, Piñeros M, et al. Estimating the Global Cancer Incidence and Mortality in 2018: GLOBOCAN Sources and Methods. *Int J Cancer* (2019) 144(8):1941–53. doi: 10.1002/ijc.31937
2. Johnson DE, Burtness B, Leemans CR, Lui VWY, Bauman JE, Grandis JR. Head and Neck Squamous Cell Carcinoma. *Nat Rev Dis Primer* (2020) 6 (1):1–22. doi: 10.1038/s41572-020-00224-3
3. Bray F, Ferlay J, Soerjomataram I, Siegel RL, Torre LA, Jemal A. Global Cancer Statistics 2018: GLOBOCAN Estimates of Incidence and Mortality Worldwide for 36 Cancers in 185 Countries. *CA Cancer J Clin* (2018) 68 (6):394–424. doi: 10.3322/caac.21492
4. Yates LR, Gerstung M, Knappskog S, Desmedt C, Gundem G, Van Loo P, et al. Subclonal Diversification of Primary Breast Cancer Revealed by Multiregion Sequencing. *Nat Med* (2015) 21(7):751–9. doi: 10.1038/nm.3886
5. Siravegna G, Marsoni S, Siena S, Bardelli A. Integrating Liquid Biopsies Into the Management of Cancer. *Nat Rev Clin Oncol* (2017) 14(9):531–48. doi: 10.1038/nrclinonc.2017.14
6. Crowley E, Di Nicolantonio F, Loupakis F, Bardelli A. Liquid Biopsy: Monitoring Cancer-Genetics in the Blood. *Nat Rev Clin Oncol* (2013) 10 (8):472–84. doi: 10.1038/nrclinonc.2013.110
7. Spector ME, Farlow JL, Haring CT, Brenner JC, Birkeland AC. The Potential for Liquid Biopsies in Head and Neck Cancer. *Discovery Med* (2018) 125 (139):251.
8. Kaczor-Urbanowicz KE, Carreras-Presas CM, Aro K, Tu M, Garcia-Godoy F, Wong DT. Saliva Diagnostics - Current Views and Directions. *Exp Biol Med Maywood NJ* (2017) 242(5):459–72. doi: 10.1177/1535370216681550
9. Gai C, Camussi F, Broccoletti R, Gambino A, Cabras M, Molinaro L, et al. Salivary Extracellular Vesicle-Associated miRNAs as Potential Biomarkers in Oral Squamous Cell Carcinoma. *BMC Cancer* (2018) 1818(1):1–11. doi: 10.1186/s12885-018-4364-z
10. Khurshid Z, Zafar MS, Khan RS, Najeeb S, Slowey PD, Rehman IU. Role of Salivary Biomarkers in Oral Cancer Detection. *Adv Clin Chem* (2018) 86:23–70. doi: 10.1016/bs.acc.2018.05.002
11. Miller SM. Saliva Testing–a Nontraditional Diagnostic Tool. *Clin Lab Sci J Am Soc Med Technol* (1994) 7(1):39–44.
12. Schwarzenbach H, Hoon DSB, Pantel K. Cell-Free Nucleic Acids as Biomarkers in Cancer Patients. *Nat Rev Cancer* (2011) 11(6):426–37. doi: 10.1038/nrc3066
13. Stroun M, Lyautey J, Lederrey C, Olson-Sand A, Anker P. About the Possible Origin and Mechanism of Circulating DNA Apoptosis and Active DNA Release. *Clin Chim Acta Int J Clin Chem* (2001) 313(1–2):139–42. doi: 10.1016/S0009-8981(01)00665-9
14. Haber DA, Velculescu VE. Blood-Based Analyses of Cancer: Circulating Tumor Cells and Circulating Tumor DNA. *Cancer Discovery* (2014) 4 (6):650–61. doi: 10.1158/2159-8290.CD-13-1014
15. Dressman D, Yan H, Traverso G, Kinzler KW, Vogelstein B. Transforming Single DNA Molecules Into Fluorescent Magnetic Particles for Detection and Enumeration of Genetic Variations. *Proc Natl Acad Sci* (2003) 100 (15):8817–22. doi: 10.1073/pnas.1133470100
16. Sorber L, Zwaenepoel K, Deschoolmeester V, Van Schil PEY, Van Meerbeeck J, Lardon F, et al. Circulating Cell-Free Nucleic Acids and Platelets as a Liquid Biopsy in the Provision of Personalized Therapy for Lung Cancer Patients. *Lung Cancer Amst Neth* (2017) 107:100–7. doi: 10.1016/j.lungcan.2016.04.026
17. Herman JG, Graff JR, Myöhänen S, Nelkin BD, Baylin SB. Methylation-Specific PCR: A Novel PCR Assay for Methylation Status of CpG Islands. *Proc Natl Acad Sci* (1996) 93(18):9821–6. doi: 10.1073/pnas.93.18.9821
18. Licchesi JDF, Herman JG. Methylation-Specific PCR. *Methods Mol Biol Clifton NJ* (2009) 507:305–23. doi: 10.1007/978-1-59745-522-0_22
19. Bailey VJ, Zhang Y, Keeley BP, Yin C, Pelosky KL, Brock M, et al. Single-Tube Analysis of DNA Methylation With Silica Superparamagnetic Beads. *Clin Chem* (2010) 56(6):1022–5. doi: 10.1373/clinchem.2009.140244
20. Fackler MJ, Sukumar S. Quantitation of DNA Methylation by Quantitative Multiplex Methylation-Specific PCR (QM-MSP) Assay. *Methods Mol Biol* (2018) 1708:473–96. doi: 10.1007/978-1-4939-7481-8_24
21. Fackler MJ, Lopez Bujanda Z, Umbricht C, Teo WW, Cho S, Zhang Z, et al. Novel Methylated Biomarkers and a Robust Assay to Detect Circulating Tumor DNA in Metastatic Breast Cancer. *Cancer Res* (2014) 74(8):2160–70. doi: 10.1158/0008-5472.CAN-13-3392
22. Liu Q, Sommer SS. Pyrophosphorolysis-Activated Polymerization (PAP): Application to Allele-Specific Amplification. *BioTechniques* (2000) 29 (5):1072–83. doi: 10.2144/00295rr03
23. Diaz LA, Bardelli A. Liquid Biopsies: Genotyping Circulating Tumor DNA. *J Clin Oncol* (2014) 32(6):579–86. doi: 10.1200/JCO.2012.45.2011
24. Han X, Wang J, Sun Y. Circulating Tumor DNA as Biomarkers for Cancer Detection. *Genomics Proteomics Bioinf* (2017) 15(2):59–72. doi: 10.1016/j.gpb.2016.12.004
25. Momen-Heravi F, Trachtenberg AJ, Kuo WP, Cheng YS. Genomewide Study of Salivary MicroRNAs for Detection of Oral Cancer. *J Dent Res* (2014) 93(7_suppl):86S–93S. doi: 10.1177/0022034514531018
26. Zaporozhchenko IA, Ponomaryova AA, Rykova EY, Laktionov PP. The Potential of Circulating Cell-Free RNA as a Cancer Biomarker: Challenges and Opportunities. *Expert Rev Mol Diagn* (2018) 18(2):133–45. doi: 10.1080/14737159.2018.1425143
27. Zhang H, Liu R, Yan C, Liu L, Tong Z, Jiang W, et al. Advantage of Next-Generation Sequencing in Dynamic Monitoring of Circulating Tumor DNA Over Droplet Digital PCR in Cetuximab Treated Colorectal Cancer Patients. *Transl Oncol* (2019) 12(3):426–31. doi: 10.1016/j.tranon.2018.11.015
28. Wang Y, Springer S, Mulvey CL, Silliman N, Schaefer J, Sausen M, et al. Detection of Somatic Mutations and HPV in the Saliva and Plasma of Patients With Head and Neck Squamous Cell Carcinomas. *Sci Transl Med* (2015) 7(293):293ra104. doi: 10.1126/scitranslmed.aaa8507
29. Mewara A, Gadbail AR, Patil S, Chaudary M, Chavhan SD. C-Deletion Mutation of the P53 Gene at Exon 4 of Codon 63 in the Saliva of Oral Squamous Cell Carcinoma in Central India: A Preliminary Study. *J Investig Clin Dent* (2010) 1(2):108–13. doi: 10.1111/j.2041-1626.2010.00014.x
30. El-Naggar AK, Mao L, Staerkel G, Coombes MM, Tucker SL, Luna MA, et al. Genetic Heterogeneity in Saliva From Patients With Oral Squamous Carcinomas: Implications in Molecular Diagnosis and Screening. *J Mol Diagn* (2001) 3(4):164–70. doi: 10.1016/S1525-1578(10)60668-X
31. Spafford MF, Koch WM, Reed AL, Califano JA, Xu LH, Eisenberger CF, et al. Detection of Head and Neck Squamous Cell Carcinoma Among Exfoliated Oral Mucosal Cells by Microsatellite Analysis. *Clin Cancer Res* (2001) 7 (3):607–12.
32. Sethi S, Benninger MS, Lu M, Havard S, Worsham MJ. Noninvasive Molecular Detection of Head and Neck Squamous Cell Carcinoma: An Exploratory Analysis. *Diagn Mol Pathol* (2009) 18(2):81–7. doi: 10.1097/PDM.0b013e3181804b82
33. Liao P-H, Chang Y-C, Huang M-F, Tai K-W, Chou M-Y. Mutation of P53 Gene Codon 63 in Saliva as a Molecular Marker for Oral Squamous Cell Carcinomas. *Oral Oncol* (2000) 36(3):272–6. doi: 10.1016/S1368-8375(00)00005-1
34. Guerrero-Preston R, Soudry E, Acero J, Orera M, Moreno-López L, Macía-Colón G, et al. NID2 and HOXA9 Promoter Hypermethylation as Biomarkers for Prevention and Early Detection in Oral Cavity Squamous Cell Carcinoma Tissues and Saliva. *Cancer Prev Res (Phila Pa)* (2011) 4 (7):1061–72. doi: 10.1158/1940-6207.CAPR-11-0006
35. Demokan S, Chang X, Chuang A, Mydlarz WK, Kaur J, Huang P, et al. KIF1A and EDNRB are Differentially Methylated in Primary HNSCC and Salivary Rinses. *Int J Cancer* (2010) 127(10):2351–9. doi: 10.1002/ijc.25248
36. Ovchinnikov DA, Cooper MA, Pandit P, Coman WB, Cooper-White JJ, Keith P, et al. Tumor-Suppressor Gene Promoter Hypermethylation in Saliva of Head and Neck Cancer Patients. *Transl Oncol* (2012) 5(5):321–6. doi: 10.1593/tlo.12232
37. Viet CT, Schmidt BL. Methylation Array Analysis of Preoperative and Postoperative Saliva DNA in Oral Cancer Patients. *Cancer Epidemiol Biomarkers Prev* (2008) 17(12):3603–11. doi: 10.1158/1055-9965.EPI-08-0507
38. Carvalho AL, Henrique R, Jeronimo C, Nayak CS, Reddy AN, Hoque MO, et al. Detection of Promoter Hypermethylation in Salivary Rinses as a Biomarker for Head and Neck Squamous Cell Carcinoma Surveillance. *Clin Cancer Res Off J Am Assoc Cancer Res* (2011) 17(14):4782–9. doi: 10.1158/1078-0432.CCR-11-0324

39. Lacombe J, Brooks C, Hu C, Menashi E, Korn R, Yang F, et al. Analysis of Saliva Gene Expression During Head and Neck Cancer Radiotherapy: A Pilot Study. *Radiat Res* (2017) 188(1):75–81. doi: 10.1667/RR14707.1
40. Hanna GJ, Lau CJ, Mahmood U, Supplee JG, Mogili AR, Haddad RI, et al. Salivary HPV DNA Informs Locoregional Disease Status in Advanced HPV-Associated Oropharyngeal Cancer. *Oral Oncol* (2019) 95:120–6. doi: 10.1016/j.oraloncology.2019.06.019
41. Li Y, St. John MAR, Zhou X, Kim Y, Sinha U, Jordan RCK, et al. Salivary Transcriptome Diagnostics for Oral Cancer Detection. *Clin Cancer Res* (2004) 10(24):8442–50. doi: 10.1158/1078-0432.CCR-04-1167
42. Elashoff D, Zhou H, Reiss J, Wang J, Xiao H, Henson B, et al. Prevalidation of Salivary Biomarkers for Oral Cancer Detection. *Cancer Epidemiol Biomarkers Prev* (2012) 21(4):664–72. doi: 10.1158/1055-9965.EPI-11-1093
43. Bu J, Bu X, Liu B, Chen F, Chen P. Increased Expression of Tissue/Salivary Transgelin mRNA Predicts Poor Prognosis in Patients With Oral Squamous Cell Carcinoma (OSCC). *Med Sci Monit* (2015) 21:2275–81. doi: 10.12659/msm.893925
44. Chai RC, Lim Y, Frazer IH, Wan Y, Perry C, Jones L, et al. A Pilot Study to Compare the Detection of HPV-16 Biomarkers in Salivary Oral Rinses with Tumour p16(INK4a) Expression in Head and Neck Squamous Cell Carcinoma Patients. *BMC Cancer* (2016) 16(1):178. doi: 10.1186/s12885-016-2217-1
45. Han B, Chao J, Yao H. Circular RNA and its Mechanisms in Disease: From the Bench to the Clinic. *Pharmacol Ther* (2018) 187:31–44. doi: 10.1016/j.pharmthera.2018.01.010
46. Park NJ, Zhou H, Elashoff D, Henson BS, Kastratovic DA, Abemayor E, et al. Salivary microRNA: Discovery, Characterization, and Clinical Utility for Oral Cancer Detection. *Clin Cancer Res Off J Am Assoc Cancer Res* (2009) 15(17):5473–7. doi: 10.1158/1078-0432.CCR-09-0736
47. Al-Malkey MK, Abbas AA, Khalaf NF, Mubarak IA, Jasim IA. Expression Analysis of Salivary Microrna-31 in Oral Cancer Patients. *Int J Curr Microbiol App Sci* (2015) 4(12):375–82.
48. Zahran F, Ghalwash D, Shaker O, Al-Johani K, Scully C. Salivary microRNAs in Oral Cancer. *Oral Dis* (2015) 21(6):739–47. doi: 10.1111/odi.12340
49. Duz MB, Karatas OF, Guzel E, Turgut NF, Yilmaz M, Creighton CJ, et al. Identification of miR-139-5p as a Saliva Biomarker for Tongue Squamous Cell Carcinoma: A Pilot Study. *Cell Oncol Dordr* (2016) 39(2):187–93. doi: 10.1007/s13402-015-0259-z
50. Greither T, Vorwerk F, Kappler M, Bache M, Taubert H, Kuhnt T, et al. Salivary miR-93 and miR-200a as Post-Radiotherapy Biomarkers in Head and Neck Squamous Cell Carcinoma. *Oncol Rep* (2017) 38(2):1268–75. doi: 10.3892/or.2017.5764
51. Wu L, Zheng K, Yan C, Pan X, Liu Y, Liu J, et al. Genome-Wide Study of Salivary microRNAs as Potential Noninvasive Biomarkers for Detection of Nasopharyngeal Carcinoma. *BMC Cancer* (2019) 19(1):843. doi: 10.1186/s12885-019-6037-y.
52. Fadhil RS, Wei MQ, Nikolarakos D, Good D, Nair RG. Salivary microRNA miR-Let-7a-5p and miR-3928 Could be Used as Potential Diagnostic Bio-Markers for Head and Neck Squamous Cell Carcinoma. *PloS One* (2020) 15(3):e0221779. Ahmad A, editor. doi: 10.1371/journal.pone.0221779
53. He L, Ping F, Fan Z, Zhang C, Deng M, Cheng B, et al. Salivary Exosomal miR-24-3p Serves as a Potential Detective Biomarker for Oral Squamous Cell Carcinoma Screening. *BioMed Pharmacother* (2020) 121:109553. doi: 10.1016/j.biopha.2019.109553
54. Uma Maheswari TN, Nivedhitha MS, Ramani P. Expression Profile of Salivary Micro RNA-21 and 31 in Oral Potentially Malignant Disorders. *Braz Oral Res* (2020) 34:e002. doi: 10.1590/1807-3107bor-2020.vol34.0002
55. Guo Y, Yang J, Huang Q, Hsueh C, Zheng J, Wu C, et al. Circular RNAs and Their Roles in Head and Neck Cancers. *Mol Cancer* (2019) 18(1):1–18. doi: 10.1186/s12943-019-1003-5
56. Wiklund ED, Gao S, Hulf T, Sibbritt T, Nair S, Costea DE, et al. MicroRNA Alterations and Associated Aberrant DNA Methylation Patterns Across Multiple Sample Types in Oral Squamous Cell Carcinoma. *Zhang B editor PloS One* (2011) 6(11):e27840. doi: 10.1371/journal.pone.0027840
57. Ahmad P, Sana J, Slavik M, Gurin D, Radova L, Gablo N, et al. MicroRNA-15b-5p Predicts Locoregional Relapse in Head and Neck Carcinoma Patients Treated With Intensity-Modulated Radiotherapy. *Cancer Genomics Proteomics* (2019) 16(2):139–46. doi: 10.21873/cgp.20119
58. Tang H, Wu Z, Zhang J, Su B. Salivary lncRNA as a Potential Marker for Oral Squamous Cell Carcinoma Diagnosis. *Mol Med Rep* (2013) 7(3):761–6. doi: 10.3892/mmr.2012.1254
59. Bahn JH, Zhang Q, Li F, Chan TM, Lin X, Kim Y, et al. The Landscape of microRNA, Piwi-Interacting RNA, and Circular RNA in Human Saliva. *Clin Chem* (2015) 61(1):221–30. doi: 10.1373/clinchem.2014.230433
60. Zhao S-Y, Wang J, Ouyang S-B, Huang Z-K, Liao L. Salivary Circular RNAs Hsa_Circ_0001874 and Hsa_Circ_0001971 as Novel Biomarkers for the Diagnosis of Oral Squamous Cell Carcinoma. *Cell Physiol Biochem* (2018) 47(6):2511–21. doi: 10.1159/000491624
61. Liu J, Chen Y, Pei F, Zeng C, Yao Y, Liao W, et al. Extracellular Vesicles in Liquid Biopsies: Potential for Disease Diagnosis. *BioMed Res Int* (2021) 2021:6611244. doi: 10.1155/2021/6611244
62. Taylor J, Bebawy M. Proteins Regulating Microvesicle Biogenesis and Multidrug Resistance in Cancer. *Proteomics* (2019) 19(1–2):e1800165. doi: 10.1002/pmic.201800165
63. van Niel G, D'Angelo G, Raposo G. Shedding Light on the Cell Biology of Extracellular Vesicles. *Nat Rev Mol Cell Biol* (2018) 19(4):213–28. doi: 10.1038/nrm.2017.125
64. Armstrong D, Wildman DE. Extracellular Vesicles and the Promise of Continuous Liquid Biopsies. *J Pathol Transl Med* (2018) 52(1):1. doi: 10.4132/jptm.2017.05.21
65. Kanwar SS, Dunlay CJ, Simeone DM, Nagrath S. Microfluidic Device (ExoChip) for on-Chip Isolation, Quantification and Characterization of Circulating Exosomes. *Lab Chip* (2014) 14(11):1891–900. doi: 10.1039/C4LC00136B
66. Wang Z, Wu H, Fine D, Schmulen J, Hu Y, Godin B, et al. Ciliated Micropillars for the Microfluidic-Based Isolation of Nanoscale Lipid Vesicles. *Lab Chip* (2013) 13(15):2879. doi: 10.1039/c3lc41343h
67. Tay HM, Kharel S, Dalan R, Chen ZJ, Tan KK, Boehm BO, et al. Rapid Purification of Sub-Micrometer Particles for Enhanced Drug Release and Microvesicles Isolation. *NPG Asia Mater* (2017) 9(9):e434–e434. doi: 10.1038/am.2017.175
68. Liu C, Xu X, Li B, Situ B, Pan W, Hu Y, et al. Single-Exosome-Counting Immunoassays for Cancer Diagnostics. *Nano Lett* (2018) 18(7):4226–32. doi: 10.1021/acs.nanolett.8b01184
69. van Niel G, Charin S, Simoes S, Romao M, Rochin L, Saftig P, et al. The Tetraspanin CD63 Regulates ESCRT-Independent and -Dependent Endosomal Sorting During Melanogenesis. *Dev Cell* (2011) 21(4):708–21. doi: 10.1016/j.devcel.2011.08.019
70. Verweij FJ, van Eijndhoven MA, Hopmans ES, Vendrig T, Wurdinger T, Cahir-McFarland E, et al. LMP1 Association With CD63 in Endosomes and Secretion *via* Exosomes Limits Constitutive NF-κb Activation. *EMBO J* (2011) 30(11):2115–29. doi: 10.1038/emboj.2011.123
71. Ma C, Jiang F, Ma Y, Wang J, Li H, Zhang J. Isolation and Detection Technologies of Extracellular Vesicles and Application on Cancer Diagnostic. *Dose-Response* (2019) 17(4):1559325819891004. doi: 10.1177/1559325819891004
72. Carnell-Morris P, Tannetta D, Siupa A, Hole P, Dragovic R. Analysis of Extracellular Vesicles Using Fluorescence Nanoparticle Tracking Analysis. *Methods Mol Biol Clifton NJ* (2017) 1660:153–73. doi: 10.1007/978-1-4939-7253-1_13
73. Rupert DLM, Lässer C, Eldh M, Block S, Zhdanov VP, Lotvall JO, et al. Determination of Exosome Concentration in Solution Using Surface Plasmon Resonance Spectroscopy. *Anal Chem* (2014) 86(12):5929–36. doi: 10.1021/ac500931f
74. Grasso L, Wyss R, Weidenauer L, Thampi A, Demurtas D, Prudent M, et al. Molecular Screening of Cancer-Derived Exosomes by Surface Plasmon Resonance Spectroscopy. *Anal Bioanal Chem* (2015) 407(18):5425–32. doi: 10.1007/s00216-015-8711-5
75. Michael A, Bajracharya S, Yuen P, Zhou H, Star R, Illei G, et al. Exosomes From Human Saliva as a Source of microRNA Biomarkers: microRNA Biomarkers in Salivary Exosomes. *Oral Dis* (2010) 16(1):34–8. doi: 10.1111/j.1601-0825.2009.01604.x
76. Topkas E, Keith P, Dimeski G, Cooper-White J, Punyadeera C. Evaluation of Saliva Collection Devices for the Analysis of Proteins. *Clin Chim Acta* (2012) 413(13–14):1066–70. doi: 10.1016/j.cca.2012.02.020

77. Schulz BL, Cooper-White J, Punyadeera CK. Saliva Proteome Research: Current Status and Future Outlook. *Crit Rev Biotechnol* (2013) 33(3):246–59. doi: 10.3109/07388551.2012.687361
78. Gemmell CH, Sefton MV, Yeo EL. Platelet-Derived Microparticle Formation Involves Glycoprotein IIb-IIIa. Inhibition by RGDS and a Glanzmann's Thrombasthenia Defect. *J Biol Chem* (1993) 268(20):14586–9. doi: 10.1016/S0021-9258(18)82371-7
79. Li L, Li C, Wang S, Wang Z, Jiang J, Wang W, et al. Exosomes Derived From Hypoxic Oral Squamous Cell Carcinoma Cells Deliver miR-21 to Normoxic Cells to Elicit a Prometastatic Phenotype. *Cancer Res* (2016) 76(7):1770–80. doi: 10.1158/0008-5472.CAN-15-1625
80. Winck FV, Prado Ribeiro AC, Ramos Domingues R, Ling LY, Riaño-Pachón DM, Rivera C, et al. Insights Into Immune Responses in Oral Cancer Through Proteomic Analysis of Saliva and Salivary Extracellular Vesicles. *Sci Rep* (2015) 5(1):16305. doi: 10.1038/srep16305
81. Zhong W, Ren J, Xiong X, Man Q, Zhang W, Gao L, et al. Increased Salivary Microvesicles are Associated With the Prognosis of Patients With Oral Squamous Cell Carcinoma. *J Cell Mol Med* (2019) 23(6):4054. doi: 10.1111/jcmm.14291
82. Ogawa Y, Miura Y, Harazono A, Kanai-Azuma M, Akimoto Y, Kawakami H, et al. Proteomic Analysis of Two Types of Exosomes in Human Whole Saliva. *Biol Pharm Bull* (2011) 34(1):13–23. doi: 10.1248/bpb.34.13
83. Sharma S, Gillespie BM, Palanisamy V, Gimzewski JK. Quantitative Nanostructural and Single-Molecule Force Spectroscopy Biomolecular Analysis of Human-Saliva-Derived Exosomes. *Langmuir ACS J Surf Colloids* (2011) 27(23):14394–400. doi: 10.1021/la2038763
84. Zlotogorski-Hurvitz A, Dayan D, Chaushu G, Salo T, Vered M. Morphological and Molecular Features of Oral Fluid-Derived Exosomes: Oral Cancer Patients Versus Healthy Individuals. *J Cancer Res Clin Oncol* (2016) 142(1):101–10. doi: 10.1007/s00432-015-2005-3
85. Xiao C, Song F, Zheng YL, Lv J, Wang QF, Xu N. Exosomes in Head and Neck Squamous Cell Carcinoma. *Front Oncol* (2019) 9:894. doi: 10.3389/fonc.2019.00894
86. Hadavand M, Hasni S. Exosomal Biomarkers in Oral Diseases. *Oral Dis* (2019) 25(1):10–5. doi: 10.1111/odi.12878
87. Wang X, Kaczor-Urbanowicz KE, Wong DTW. Salivary Biomarkers in Cancer Detection. *Med Oncol Northwood Lond Engl* (2017) 34(1):7. doi: 10.1007/s12032-016-0863-4
88. Xie C, Ji N, Tang Z, Li J, Chen Q. The Role of Extracellular Vesicles From Different Origin in the Microenvironment of Head and Neck Cancers. *Mol Cancer* (2019) 18(1):1–15. doi: 10.1186/s12943-019-0985-3
89. Arantes L, De Carvalho AC, Melendez ME, Lopes Carvalho A. Serum, Plasma and Saliva Biomarkers for Head and Neck Cancer. *Expert Rev Mol Diagn* (2018) 18(1):85–112. doi: 10.1080/14737159.2017.1404906
90. Chiabotto, Gai, Deregibus, Camussi. Salivary Extracellular Vesicle-Associated exRNA as Cancer Biomarker. *Cancers* (2019) 11(7):891. doi: 10.3390/cancers11070891
91. Cheng J, Nonaka T, Wong D. Salivary Exosomes as Nanocarriers for Cancer Biomarker Delivery. *Mater* (2019) 12(4):654. doi: 10.3390/ma12040654
92. Hofmann L, Ludwig S, Vahl JM, Brunner C, Hoffmann TK, Theodoraki M-N. The Emerging Role of Exosomes in Diagnosis, Prognosis, and Therapy in Head and Neck Cancer. *Int J Mol Sci* (2020) 21(11):4072. doi: 10.3390/ijms21114072
93. Clayton A, Buschmann D, Byrd JB, Carter DRF, Cheng L, Compton C, et al. Summary of the ISEV Workshop on Extracellular Vesicles as Disease Biomarkers, Held in Birmingham, UK, During December 2017. *J Extracell Vesicles* (2018) 7(1):1473707. doi: 10.1080/20013078.2018.1473707
94. Yan SK, Wei BJ, Lin ZY, Yang Y, Zhou ZT, Zhang WD. A Metabonomic Approach to the Diagnosis of Oral Squamous Cell Carcinoma, Oral Lichen Planus and Oral Leukoplakia. *Oral Oncol* (2008) 44(5):477–83. doi: 10.1016/j.oraloncology.2007.06.007
95. Silwood CJL, Lynch E, Claxson AWD, Grootveld MC. ^{1}H and ^{13}C NMR Spectroscopic Analysis of Human Saliva. *J Dent Res* (2002) 81(6):422–7. doi: 10.1177/154405910208100613
96. Gardner A, Carpenter G, So P-W. Salivary Metabolomics: From Diagnostic Biomarker Discovery to Investigating Biological Function. *Metabolites* (2020) 10(2):47. doi: 10.3390/metabo10020047
97. Schipper R, Loof A, de Groot J, Harthoorn L, Dransfield E, van Heerde W. SELDI-TOF-MS of Saliva: Methodology and Pre-Treatment Effects. *J Chromatogr B* (2007) 847(1):45–53. doi: 10.1016/j.jchromb.2006.10.005
98. Ploypetch S, Roytrakul S, Jaresitthikunchai J, Phaonakrop N, Krobthong S, Suriyaphol G. Salivary Proteomics of Canine Oral Tumors Using MALDI-TOF Mass Spectrometry and LC-Tandem Mass Spectrometry. *PloS One* (2019) 14(7):e0219390. Bencharit S, editor. doi: 10.1371/journal.pone.0219390
99. Buko A. Capillary Electrophoresis Mass Spectrometry Based Metabolomics. *J Appl Bioanal* (2017) 3(1):5–20. doi: 10.17145/jab.17.002
100. Beale DJ, Jones OAH, Karpe AV, Dayalan S, Oh DY, Kouremenos KA, et al. A Review of Analytical Techniques and Their Application in Disease Diagnosis in Breathomics and Salivaomics Research. *Int J Mol Sci* (2016) 18(1):E24. doi: 10.3390/ijms18010024
101. Wei J, Xie G, Zhou Z, Shi P, Qiu Y, Zheng X, et al. Salivary Metabolite Signatures of Oral Cancer and Leukoplakia. *Int J Cancer* (2011) 129(9):2207–17. doi: 10.1002/ijc.25881
102. Sugimoto M, Wong DT, Hirayama A, Soga T, Tomita M. Capillary Electrophoresis Mass Spectrometry-Based Saliva Metabolomics Identified Oral, Breast and Pancreatic Cancer-Specific Profiles. *Metabolomics* (2010) 6(1):78–95. doi: 10.1007/s11306-009-0178-y
103. Ishikawa S, Sugimoto M, Kitabatake K, Sugano A, Nakamura M, Kaneko M, et al. Identification of Salivary Metabolomic Biomarkers for Oral Cancer Screening. *Sci Rep* (2016) 6(1):31520. doi: 10.1038/srep31520
104. Hsu C-W, Chen Y-T, Hsieh Y-J, Chang K-P, Hsueh P-C, Chen T-W, et al. Integrated Analyses Utilizing Metabolomics and Transcriptomics Reveal Perturbation of the Polyamine Pathway in Oral Cavity Squamous Cell Carcinoma. *Anal Chim Acta* (2019) 1050:113–22. doi: 10.1016/j.aca.2018.10.070
105. Sridharan G, Ramani P, Patankar S, Vijayaraghavan R. Evaluation of Salivary Metabolomics in Oral Leukoplakia and Oral Squamous Cell Carcinoma. *J Oral Pathol Med* (2019) 48(4):299–306. doi: 10.1111/jop.12835
106. Sami A, Elimairi I, Stanton C, Ross RP, Ryan CA. The Role of the Microbiome in Oral Squamous Cell Carcinoma With Insight Into the Microbiome–Treatment Axis. *IJMS* (2020) 21(21):8061. doi: 10.3390/ijms21218061
107. Chattopadhyay I, Verma M, Panda M. Role of Oral Microbiome Signatures in Diagnosis and Prognosis of Oral Cancer. *Technol Cancer Res Treat* (2019) 18:153303381986735. doi: 10.1177/1533033819867354
108. Nagy KN, Sonkodi I, Szöke I, Nagy E, Newman HN. The Microflora Associated With Human Oral Carcinomas. *Oral Oncol* (1998) 34(4):304–8. doi: 10.1016/S1368-8375(98)80012-2
109. Bolz J, Dosá E, Schubert J, Eckert AW. Bacterial Colonization of Microbial Biofilms in Oral Squamous Cell Carcinoma. *Clin Oral Invest* (2014) 18(2):409–14. doi: 10.1007/s00784-013-1007-2
110. Tateda M, Shiga K, Saijo S, Sone M, Hori T, Yokoyama J, et al. Streptococcus Anginosus in Head and Neck Squamous Cell Carcinoma: Implication in Carcinogenesis. *Int J Mol Med* (2000) 6(6):699–703. doi: 10.3892/ijmm.6.6.699
111. Morita E, Narikiyo M, Yano A, Nishimura E, Igaki H, Sasaki H, et al. Different Frequencies of Streptococcus Anginosus Infection in Oral Cancer and Esophageal Cancer. *Cancer Sci* (2003) 94(6):492–6. doi: 10.1111/j.1349-7006.2003.tb01471.x
112. Mager D, Haffajee A, Devlin P, Norris C, Posner M, Goodson J. The Salivary Microbiota as a Diagnostic Indicator of Oral Cancer: A Descriptive, non-Randomized Study of Cancer-Free and Oral Squamous Cell Carcinoma Subjects. *J Transl Med* (2005) 3(1):27. doi: 10.1186/1479-5876-3-27
113. Pushalkar S, Mane SP, Ji X, Li Y, Evans C, Crasta OR, et al. Microbial Diversity in Saliva of Oral Squamous Cell Carcinoma. *FEMS Immunol Med Microbiol* (2011) 61(3):269–77. doi: 10.1111/j.1574-695X.2010.00773.x
114. Lim Y, Fukuma N, Totsika M, Kenny L, Morrison M, Punyadeera C. The Performance of an Oral Microbiome Biomarker Panel in Predicting Oral Cavity and Oropharyngeal Cancers. *Front Cell Infect Microbiol* (2018) 8(AUG):267. doi: 10.3389/fcimb.2018.00267
115. Zuo H-J, Fu MR, Zhao H-L, Du X-W, Hu Z-Y, Zhao X-Y, et al. Study on the Salivary Microbial Alteration of Men With Head and Neck Cancer and Its Relationship With Symptoms in Southwest China. *Front Cell Infect Microbiol* (2020) 0:690. doi: 10.3389/fcimb.2020.514943
116. Guerrero-Preston R, Godoy-Vitorino F, Jedlicka A, Rodríguez-Hilario A, González H, Bondy J, et al. 16s rRNA Amplicon Sequencing Identifies Microbiota Associated With Oral Cancer, Human Papilloma Virus Infection

and Surgical Treatment. *Oncotarget* (2016) 7(32):51320–34. doi: 10.18632/oncotarget.9710
117. Chaffer CL, Weinberg RA. A Perspective on Cancer Cell Metastasis. *Sci* (2011) 331(6024):1559–64. doi: 10.1126/science.1203543
118. Sharma S, Zhuang R, Long M, Pavlovic M, Kang Y, Ilyas A, et al. Circulating Tumor Cell Isolation, Culture, and Downstream Molecular Analysis. *Biotechnol Adv* (2018) 36(4):1063–78. doi: 10.1016/j.biotechadv.2018.03.007
119. Catelain C, Pailler E, Oulhen M, Faugeroux V, Pommier A-L, Farace F. Detection of Gene Rearrangements in Circulating Tumor Cells: Examples of ALK-, ROS1-, RET-Rearrangements in Non-Small-Cell Lung Cancer and ERG-Rearrangements in Prostate Cancer. In: MJM Magbanua, JW Park, editors. *Isolation and Molecular Characterization of Circulating Tumor Cells [Internet]*, vol. 994 . Cham: Springer International Publishing (2017). p. 169–79. Available at: http://link.springer.com/10.1007/978-3-319-55947-6_9.
120. Liu K, Chen N, Wei J, Ma L, Yang S, Zhang X. Clinical Significance of Circulating Tumor Cells in Patients With Locally Advanced Head and Neck Squamous Cell Carcinoma. *Oncol Rep* (2020) 43(5):1525–35. doi: 10.3892/or.2020.7536
121. Onidani K, Shoji H, Kakizaki T, Yoshimoto S, Okaya S, Miura N, et al. Monitoring of Cancer Patients *via* Next-Generation Sequencing of Patient-Derived Circulating Tumor Cells and Tumor DNA. *Cancer Sci* (2019) 110(8):2590–9. doi: 10.1111/cas.14092
122. Jatana KR, Balasubramanian P, Lang JC, Yang L, Jatana CA, White E, et al. Significance of Circulating Tumor Cells in Patients With Squamous Cell Carcinoma of the Head and Neck: Initial Results. *Arch Otolaryngol Head Neck Surg* (2010) 136(12):1274–9. doi: 10.1001/archoto.2010.223
123. Hristozova T, Konschak R, Stromberger C, Fusi A, Liu Z, Weichert W, et al. The Presence of Circulating Tumor Cells (CTCs) Correlates With Lymph Node Metastasis in Nonresectable Squamous Cell Carcinoma of the Head and Neck Region (SCCHN). *Ann Oncol* (2011) 22(8):1878–85. doi: 10.1093/annonc/mdr130
124. Sinkala E, Sollier-Christen E, Renier C, Rosàs-Canyelles E, Che J, Heirich K, et al. Profiling Protein Expression in Circulating Tumour Cells Using Microfluidic Western Blotting. *Nat Commun* (2017) 8(1):14622. doi: 10.1038/ncomms14622
125. Schmidt H, Kulasinghe A, Perry C, Nelson C, Punyadeera C, liquid biopsy for head A. And Neck Cancers. *Expert Rev Mol Diagn* (2016) 16(2):165–72. doi: 10.1586/14737159.2016.1127758
126. Heitzer E, Auer M, Ulz P, Geigl JB, Speicher MR. Circulating Tumor Cells and DNA as Liquid Biopsies. *Genome Med* (2013) 5(8):73. doi: 10.1186/gm477
127. Grisanti S, Almici C, Consoli F, Buglione M, Verardi R, Bolzoni-Villaret A, et al. Circulating Tumor Cells in Patients With Recurrent or Metastatic Head and Neck Carcinoma: Prognostic and Predictive Significance. *PloS One* (2014) 9(8):e103918. doi: 10.1371/journal.pone.0103918
128. Inhestern J, Oertel K, Stemmann V, Schmalenberg H, Dietz A, Rotter N, et al. Prognostic Role of Circulating Tumor Cells During Induction Chemotherapy Followed by Curative Surgery Combined With Postoperative Radiotherapy in Patients With Locally Advanced Oral and Oropharyngeal Squamous Cell Cancer. *PloS One* (2015) 10(7):e0132901. doi: 10.1371/journal.pone.0132901
129. Economopoulou P, Kladi-Skandali A, Strati A, Koytsodontis G, Kirodimos E, Giotakis E, et al. Prognostic Impact of Indoleamine 2,3-Dioxygenase 1 (IDO1) mRNA Expression on Circulating Tumour Cells of Patients With Head and Neck Squamous Cell Carcinoma. *ESMO Open* (2020) 5(3):e000646. doi: 10.1136/esmoopen-2019-000646
130. Patel S, Shah K, Mirza S, Shah K, Rawal R. Circulating Tumor Stem Like Cells in Oral Squamous Cell Carcinoma: An Unresolved Paradox. *Oral Oncol* (2016) 62:139–46. doi: 10.1016/j.oraloncology.2016.10.019

Conflict of Interest: The authors declare that the research was conducted in the absence of any commercial or financial relationships that could be construed as a potential conflict of interest.

Publisher's Note: All claims expressed in this article are solely those of the authors and do not necessarily represent those of their affiliated organizations, or those of the publisher, the editors and the reviewers. Any product that may be evaluated in this article, or claim that may be made by its manufacturer, is not guaranteed or endorsed by the publisher.

frontiers | Frontiers in Oncology

ORIGINAL RESEARCH
published: 04 April 2022
doi: 10.3389/fonc.2022.792297

Genomic and Molecular Signatures of Successful Patient-Derived Xenografts for Oral Cavity Squamous Cell Carcinoma

Wei-Chen Yen[1,2†], Ian Yi-Feng Chang[2,3†], Kai-Ping Chang[1,2,4†], Chun-Nan Ouyang[2], Chiao-Rou Liu[2,5,6], Ting-Lin Tsai[5,7], Yi-Cheng Zhang[5,7], Chun-I Wang[8], Ya-Hui Wang[9], Alice L. Yu[9,10], Hsuan Liu[2,5,11,12], Chih-Ching Wu[1,2,5,6], Yu-Sun Chang[1,2,5], Jau-Song Yu[2,5,12,13] and Chia-Yu Yang[1,2,5,7]*

[1] Department of Otolaryngology Head and Neck Surgery, Chang Gung Memorial Hospital, Taoyuan, Taiwan, [2] Molecular Medicine Research Center, Chang Gung University, Taoyuan, Taiwan, [3] Department of Neurosurgery, Chang Gung Memorial Hospital, Taoyuan, Taiwan, [4] College of Medicine, Chang Gung University, Taoyuan, Taiwan, [5] Graduate Institute of Biomedical Sciences, College of Medicine, Chang Gung University, Taoyuan, Taiwan, [6] Department of Medical Biotechnology and Laboratory Sciences, College of Medicine, Chang Gung University, Taoyuan, Taiwan, [7] Department of Microbiology and Immunology, College of Medicine, Chang Gung University, Taoyuan, Taiwan, [8] Radiation Biology Research Center, Institute for Radiological Research, Chang Gung University/Chang Gung Memorial Hospital, Linkou, Taiwan, [9] Institute of Stem Cell and Translational Cancer Research, Chang Gung Memorial Hospital at Linkou, Taoyuan, Taiwan, [10] University of California San Diego, San Diego, CA, United States, [11] Division of Colon and Rectal Surgery, Chang Gung Memorial Hospital, Taoyuan, Taiwan, [12] Department of Biochemistry and Molecular Biology, College of Medicine, Chang Gung University, Taoyuan, Taiwan, [13] Liver Research Center, Chang Gung Memorial Hospital, Linkou, Taiwan

OPEN ACCESS

Edited by:
Moran Amit,
University of Texas MD Anderson Cancer Center, United States

Reviewed by:
Camila Oliveira Rodini,
University of São Paulo, Brazil
Eliska Svastova,
Slovak Academy of Sciences, Slovakia

***Correspondence:**
Chia-Yu Yang
chiayu-yang@mail.cgu.edu.tw

[†]These authors have contributed equally to this work

Specialty section:
This article was submitted to Head and Neck Cancer, a section of the journal Frontiers in Oncology

Received: 10 October 2021
Accepted: 02 March 2022
Published: 04 April 2022

Citation:
Yen W-C, Chang IY-F, Chang K-P, Ouyang C-N, Liu C-R, Tsai T-L, Zhang Y-C, Wang C-I, Wang Y-H, Yu AL, Liu H, Wu C-C, Chang Y-S, Yu J-S and Yang C-Y (2022) Genomic and Molecular Signatures of Successful Patient-Derived Xenografts for Oral Cavity Squamous Cell Carcinoma. Front. Oncol. 12:792297. doi: 10.3389/fonc.2022.792297

Background: Oral cavity squamous cell carcinoma (OSCC) is an aggressive malignant tumor with high recurrence and poor prognosis in the advanced stage. Patient-derived xenografts (PDXs) serve as powerful preclinical platforms for drug testing and precision medicine for cancer therapy. We assess which molecular signatures affect tumor engraftment ability and tumor growth rate in OSCC PDXs.

Methods: Treatment-naïve OSCC primary tumors were collected for PDX models establishment. Comprehensive genomic analysis, including whole-exome sequencing and RNA-seq, was performed on case-matched tumors and PDXs. Regulatory genes/pathways were analyzed to clarify which molecular signatures affect tumor engraftment ability and the tumor growth rate in OSCC PDXs.

Results: Perineural invasion was found as an important pathological feature related to engraftment ability. Tumor microenvironment with enriched hypoxia, PI3K-Akt, and epithelial–mesenchymal transition pathways and decreased inflammatory responses had high engraftment ability and tumor growth rates in OSCC PDXs. High matrix metalloproteinase-1 (MMP1) expression was found that have a great graft advantage in xenografts and is associated with pooled disease-free survival in cancer patients.

Conclusion: This study provides a panel with detailed genomic characteristics of OSCC PDXs, enabling preclinical studies on personalized therapy options for oral cancer. MMP1 could serve as a biomarker for predicting successful xenografts in OSCC patients.

Keywords: patient-derived xenografts, oral cavity squamous cell carcinoma, whole-exome sequencing, transcriptome sequencing, engraftment ability

INTRODUCTION

Oral cavity squamous cell carcinoma (OSCC) is an aggressive disease globally; the overall 5-year survival rate of patients with advanced stage disease has remained lower than 40% (1). OSCC often occurs in the oral cavity due to many etiological factors. Smoking, areca nut products, and alcohol consumption remain the most common risk factors for OSCC in the world (2). Environmental factors such as irradiation, air pollution, and viral infection may increase the risk of gene mutations (3, 4). The activation of oncogenes (such as EGFR, PIK3CA and AKT) and the inhibition of tumor suppressor genes (such as TP53) promote the tumorigenesis of OSCC (5). Most OSCC tumors in male patients occur at the buccal area and tongue (6). The high mortality of OSCC patients is attributed to a late diagnosis, suggesting that early detection is the most effective strategy to ameliorate the outcome and therapy (7).

Many human tumor models have been generated in immune-deficient mice by the subcutaneous or orthotropic injection of various cancer cell lines established from humans to predict the treatment responses of various cancer therapies, including chemotherapy, targeted therapy, and small molecule inhibitors (8). Cell line-derived xenografts serve as well-known models because they are quickly and easily created, and tumors can be quickly acquired (after approximately two to three weeks). However, cancer cell lines may develop different phenotypes during *in vitro* culture conditions. Cell line-derived xenografts may not entirely resemble their parental tumors. Patient-derived xenograft models (PDXs) have been established as useful tools to retain the genetic signatures of patients' primary tumors (9). Small pieces of tumors from cancer patients were surgically transplanted into immune-deficient mice, followed by tumor growth and transplantation into a second mouse model. PDXs often maintain the cellular and histopathological structures of the original tumors (10). All of these characteristics demonstrate that PDXs are more useful models that are authentic to the environment of the original patient than cell-line xenografts (11). These models can be used for clinical outcome prediction, preclinical drug evaluation, biomarker identification, biologic studies, and personalized medicine strategies (12).

In the present study, we established a panel of OSCC xenografts from a Taiwanese population and characterized the clinical characteristics, genomic landscapes, and transcriptomic signatures between the primary tumors and their matched PDXs. We performed whole-exome sequencing (WES) and RNA sequencing (RNA-seq) analyses on 12 case-matched tumors and PDXs. Our study demonstrated that the genomic and transcriptomic signatures were conserved in most OSCC PDXs. Furthermore, we identified the impact of some biological pathways that were highly associated with tumor engraftment ability in xenografts. Patients with increased activation of the HIF-1 signaling, PI3K-Akt signaling, or epithelial-mesenchymal transition (EMT) pathway and decreased interferon or IL6 immune responses might facilitate the tumor engraftment ability. Overall, we provide a panel of OSCC PDXs for preclinical drug testing and predictive biomarkers for successful engraftment.

Abbreviations: OSCC, oral cavity squamous cell carcinomas; PDX, patient-derived xenografts; MMP1, matrix metalloproteinase-1; HNSCC, head and neck squamous cell carcinoma; EMT, epithelial–mesenchymal transition; WES, whole-exome sequencing; RNA-seq, RNA sequencing; OS, overall survival; DFS, disease-free survival.

MATERIALS AND METHODS

Patient Characteristics

Treatment-naïve OSCC patients were enrolled at Chang Gung Memorial Hospital, Taiwan. This study was approved by the Institutional Review Board at Chang Gung Memorial Hospital, Taiwan (Protocol Nos.: 201800700B0, 102-5685A3). Prior to sample collection, written informed consent was obtained from all participants. Patients underwent clinical examinations, including a physical examination, computed tomography or magnetic resonance imaging of the head and neck, chest radiography, a bone scan and an abdominal ultrasound, according to standard procedures. Primary tumors were excised and transplanted into immune-deficient mice. The demographics, clinical characteristics, and histopathological features of the patients (N = 49) are shown in **Table 1** and **Supplementary Table 1**. All patients had regular follow-ups every 2 months for the first year, every 3 months for the second year, and every 6 months thereafter. Twelve OSCC PDXs were successfully established, and the clinicopathological characteristics were shown in **Table 2**. Primary tumors, adjacent normal tissues, and xenograft tumors were subjected to pathology, WES, transcriptome sequencing, and pathway analyses (**Figure 1**).

PDX Model Establishment

NOD.Cg-Prkdcscid Il2rgtm1Wjl/SzJ (NSG) mice (obtained from The Jackson Laboratory) were used in this study and housed in a specific-pathogen-free animal room. All animal experiments were conducted in accordance with the Institutional Animal Care and Use Committee of Chang Gung University (Protocol Nos.: CGU106-114 and CGU107-074). For PDX establishment, tumors from the surgical specimens of OSCC patients were

TABLE 1 | Clinical characteristics of total patients (n = 49) in this study.

Patient categories	Case number n = 49	Engrafter		*p* value
		Yesn = 12	Non = 37	
Age (years)[a]	52 ± 10	51 ± 8	53 ± 10	0.667
Sex				
Male	45	11	34	1.000
Female	4	1	3	
Tumor classification				
T1 - T2	19	4	15	0.743
T3 - T4	30	8	22	
Node classification				
N = 0	18	4	14	1.000
N > 0	31	8	23	
Overall TNM stage				
I - II	5	2	3	0.584
III - IV	44	10	34	
Extranodal extension				
No	27	5	22	0.331
Yes	22	7	15	
Perineural invasion				
No	18	1	17	0.035[b]
Yes	31	11	20	
Tumor depth (mm)[a]	21 ± 16	22 ± 14	21 ± 16	0.925

[a]*These data are presented as mean ± standard deviation.*
[b]*This is considered statistically significant.*

TABLE 2 | The clinicopathological characteristics of 12 OSCC PDX grafters.

Patient number	Age (years)	Gender	T stage	N stage	Pathology	Overall stage	Alcohol drinking	Betel quid chewing	Cigarette smoking	Site
6	54	M	2	0	Well	II	Y	N	N	Buccal mucosa
7	45	M	1	2B	Poorly	IV	Y	Y	Y	Mouth floor
11	48	F	4A	2C	Moderately	IV	N	N	N	Tongue
12	44	M	4A	2C	Poorly	IV	Y	Y	Y	Tongue
22	56	M	4A	0	Well	IV	Y	Y	Y	Buccal mucosa
24	60	M	2	2B	Moderately	IV	Y	Y	Y	Buccal mucosa
29	66	M	4A	0	Moderately	IV	Y	Y	Y	Others
32	60	M	2	0	Moderately	II	Y	Y	Y	Buccal mucosa
34	47	M	4A	2B	Moderately	IV	Y	Y	N	Tongue
41	41	M	4A	2B	Moderately	IV	Y	Y	Y	Others
44	40	M	2	0	Moderately	II	N	Y	Y	Buccal mucosa
48	49	M	3	1	Moderately	IV	N	Y	Y	Others

Y, Yes; N, No; M, male; F, female.

engrafted into NSG mice. In brief, fresh tumor tissues were first washed with PBS containing antibiotic-antimycotic solution (Gibco, USA) and then cut into small pieces of approximately 1 mm^3. To establish the first-generation (P1) PDX, tumor fragments weighing 50–100 mg were subcutaneously inoculated into the left flank of NSG mice. Tumors reaching approximately 1000 to 1500 mm^3 were harvested and passaged into another mouse to establish the next generation (P2).

Histological Characterization

Tumor tissues were formalin fixed and paraffin embedded (FFPE), and tissue sections were stained with hematoxylin and eosin (H&E). Tissue sections (5 μm thick) were subjected to antigen retrieval using Bond Epitope Retrieval Solution 2 in a Bond-Max automated immunostainer (Leica Biosystems) and stained with antibodies against cytokeratin 17 (Cell Signaling Technology) and Ki-67 (Cell Signaling Technology). The procedures were performed in accordance with standard protocols.

Whole Exome Sequencing (WES)

Genomic DNA was extracted from paired adjacent normal tissues, tumor tissues, and xenograft tissues using the QIAamp DNA Mini Kit (Qiagen), and high-quality genomic DNA was captured using a SureSelect Human All Exon V6 + COSMIC Kit (Agilent Technologies) for exome-captured libraries. The libraries were sequenced using a HiSeq 2000 with the TruSeq PE Cluster kit v3 and TruSeq SBS kit v3 (all from Illumina) according to the manufacturer's protocol.

PDX FASTQ Cleaning

To remove mouse genomic DNA from the PDX WES or RNA-seq paired-end reads, we first used Trimmomatic (version 0.38) (13)

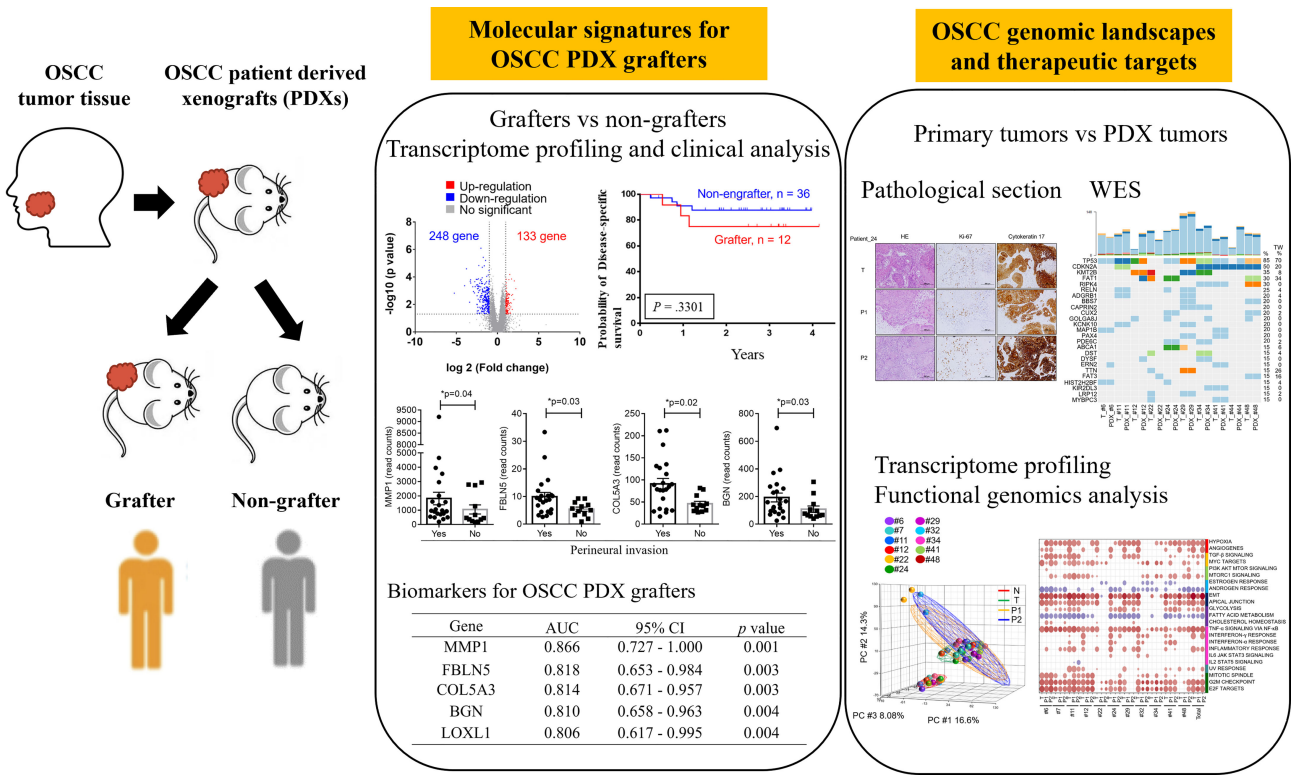

Gene	AUC	95% CI	*p* value
MMP1	0.866	0.727 - 1.000	0.001
FBLN5	0.818	0.653 - 0.984	0.003
COL5A3	0.814	0.671 - 0.957	0.003
BGN	0.810	0.658 - 0.963	0.004
LOXL1	0.806	0.617 - 0.995	0.004

FIGURE 1 | Workflow for the establishment and characterization of OSCC PDX models. Overall, 49 OSCC patients were enrolled in this study. Of the 49 tumors, 12 were successfully engrafted in NSG mice as PDX passage 1 (P1) and PDX passage 2 (P2). The specimens were subjected to pathology analysis, whole-exome sequencing, and RNA-seq. Finally, genomic landscape analysis and gene expression pathway annotation were performed to characterize the molecular signatures in patients and their matched xenografts.

to remove sequencing adapters and low-quality bases ("ILLUMINACLIP:/trimmomatic-0.38/adapters/TruSeq3-PE.fa:2:30:10" SLIDINGWINDOW:4:5 LEADING:5 TRAILING:5 MINLEN:25). Second, BWA-mem (0.7.15) (for WES data) (https://arxiv.org/abs/1303.3997) or STAR 2.7.3a (14) (for RNA-seq) was used to align the trimmed paired-end reads to the GENCODE V32 human hg38 genome (https://www.gencodegenes.org/human/release_32.html) and to the GENCODE M22 mouse genome (https://www.gencodegenes.org/mouse/release_M22.html). Third, we sorted the human and mouse BAM files by read names with the SAMtools (version 1.9) sort module. Finally, we used Disambiguate (15) and the GATK SamToFastq module to extract human-specific aligned reads from the sorted BAM files.

WES Data Analysis

We processed the human-specific WES reads into analysis-ready BAM files following the data preprocessing workflow with GATK version 4.1.4.1 (https://gatk.broadinstitute.org/hc/en-us/articles/360035535912-Data-pre-processing-for-variant-discovery). The sequenced reads were mapped to the hg38 reference genome by BWA-mem (0.7.15). The BWA genome index and known single-nucleotide polymorphisms (SNPs), germline resources, and associated files were downloaded from the Google Cloud bucket of the GATK resource bundle (Grch38/Hg38 Resources, https://gatk.broadinstitute.org/hc/en-us/articles/360035890811-Resource-bundle). Read group information was added to SAM files at the alignment stage. SAM files were converted to BAM files with the GATK MergeSamFiles module. The BAM files were further processed by marking duplicates, sorting by chromosome coordinates, and recalibrated by the base quality score with the GATK MarkDuplicates, SortSam, BaseRecalibrator, and ApplyBQSR modules. The CollectHSMetrics module of GATK was used to create the coverage report from the analysis-ready BAM files. The somatic variant calling pipeline was adopted from the GATK guidelines (https://gatk.broadinstitute.org/hc/en-us/articles/360035894731-Somatic-short-variant-discovery-SNVs-Indels-). The candidate somatic short variants were identified from the analysis-ready BAM files by the GATK Mutect2 module. Next, we used the GATK GetPileupSummaries and Calculate Contamination modules to construct an estimated fraction of reads due to cross-sample contamination. Finally, we used GATK FilterMutectCalls to identify somatic single-nucleotide variants (SNVs) and indel mutations. The identified SNVs/indels were annotated by Annovar (16) with GENCODE V32 annotation. The R package CopywriteR (version 2.18.0) (17) with default parameters was used to analyze the somatic copy number alterations (SCNAs) from the analysis-ready BAM files. Next,

we used GISTIC2 (version 2.0.23) (18) to identify significant SCNA regions from the paired WES BAM files (with parameters -ta=0.4, -td=0.4, and -conf=0.99). Because we used the hg38 reference genome for WES data processing, in GISTIC2, we downloaded the hg38 version of the reference file hg38.UCSC.add_miR.160920.refgene.mat from the Broad Institute FTP site (ftp://ftp.broadinstitute.org/pub/GISTIC2.0/refgenes/). GISTIC2 reported arm- and focal-level SCNAs for the cohort with the G-Score and false discovery rate (FDR) Q value. Only genes located in the focal region with a GISTIC2 Q value less than 0.25 were used for further analysis.

RNA-Seq, Gene Expression and Pathway Analyses

RNA-seq and data analyses were performed according to our previous reports (19). Briefly, total RNA from paired adjacent normal tissues, tumor tissues, and xenograft tissues was extracted using TRIzol Reagent (Gibco BRL). For RNA-seq, 2 μg purified total RNA was enriched by poly-A tail beads, fragmented and then reverse transcribed into cDNA, and libraries were prepared using the TruSeq Stranded mRNA Sample Preparation Guide (Part # 15031047 Rev. E; Illumina) according to the manufacturer's instructions. Sequencing was conducted on an Illumina NextSeq 500 instrument. The human-specific RNA reads were mapped to the hg38 reference by STAR (version 2.7.3a). Aligned reads were then normalized and quantified for quantitative representation. Cancer hallmark enrichment analysis was performed according to the gene set enrichment analysis (GSEA)/Molecular Signatures Database (MSigDB; 6.2), and the enrichment score was determined by calculating the probability of overlap between the test set and the hallmark sets using the DoGsea function of the Bioconductor package clusterProfiler (3.12.0). Differentially expressed genes (DEGs, 2-fold difference between groups, p value < 0.05, FDR < 0.05) were selected and subjected to the Database for Annotation, Visualization and Integrated Discovery (DAVID) v6.8 for pathway annotations.

Statistical Analysis

Patient characteristics were analyzed by the chi-square test, Fisher's exact test, or the Wilcoxon test. Multivariate models were applied to analyze overall survival and disease-free survival. Survival rates were estimated by Kaplan–Meier plotting and compared by the log-rank test. Statistical analyses were performed using SAS software (v.9.3) or SPSS software (version 20). The significance level was set at $p < 0.05$.

RESULTS

Establishment of OSCC PDX Models

Between 2015 and 2019, we performed a PDX study of OSCC across 49 specimens from treatment-naïve primary patients (**Table 1**). The surgically resected tumor specimens were immediately implanted subcutaneously into NOD/SCID/IL2Rγ null (NSG) mice as passage 1 (P1) generation PDXs; tumors from established P1 PDXs were then transplanted to other NSG mice as passage 2 (P2) generation PDXs and so on (**Figure 1**). Of these 49 specimens, 12 PDXs were successfully established (**Table 2**). There was no significant difference in tumor stage (T), nodal stage (N), overall clinical stage, pathology, or tumor sites between grafters (n = 12) and nongrafters (n = 37) (**Table 1** and **Supplementary Table 1**). However, compared with only 54% of nongrafters who were positive for perineural invasion, approximately 91.6% of grafters were positive (p = 0.035; **Table 1**). The overall survival (OS) and disease-specific survival (DSS) differences in grafters versus nongrafters were investigated. The 4-year OS rate was slightly lower for grafters than for nongrafters (p = 0.619) (**Supplementary Figure 1**). The 4-year disease-specific survival rate of grafters was also slightly lower (p = 0.33) (**Supplementary Figure 1**). Tumors from passage 1 (P1) generation PDXs were harvested to create second generation (P2) xenografts when the tumor size reached approximately 1000 mm^3 to 1500 mm^3, with a median time to passage of 84 days (range, 42-105 days). The patients' primary tumors and their matched P1 and P2 xenografts were further analyzed for pathology, genomic landscapes, and gene expression profiles (**Figure 1**). Histological comparison of PDXs and corresponding primary tumors revealed a high degree of similarity (**Supplementary Figure 2**). Cytokeratin 17 (CK17) is an epithelial marker for squamous cell carcinoma, and its expression is associated with the differentiation and malignancy of OSCC (20). The expression levels of CK17 and the proliferation marker protein Ki-67 were immunohistochemically examined in 12 patients with OSCC and their matched PDX tissues using human-specific anti-CK17 and anti-Ki-67 antibodies, respectively. As shown in **Supplementary Figure 2**, the immunohistochemical staining patterns of CK17 and Ki-67 were similar in most tumors from the two represented patients and their matched PDXs. Pathological examination of the primary tumors and xenografts also confirmed the histopathology of squamous cell carcinoma in our samples.

Molecular Signatures of Successful Grafters Versus Nongrafters

Although PDX models have emerged as powerful tools for reflecting the original features of patient tumors, the low success rate of PDX establishment is an obstacle that needs to be overcome. Among the 49 OSCC patients enrolled in this study, a total of 34, including grafters (n = 11) and nongrafters (n = 23), underwent RNA-seq analysis to determine the gene signatures that may serve as biomarkers for predicting the successful establishment of PDXs in OSCC patients. The log2 value of the expression fold change and the -log10 value of the p value between nongrafters and grafters were visualized in a volcano plot (**Figure 2A**). The volcano plot revealed 381 significantly altered transcripts (248 (65.1%) downregulated genes and 133 (34.9%) upregulated genes) in the engrafter group. Pathway analysis revealed that the screened genes were significantly associated with several common cancer-associated pathways (**Figure 2B**). The grafter group was significantly enriched in EMT (NES = 5.348, p = 0.004), hypoxia (NES = 1.791, p = 0.013) and apical junctions (NES = 1.771, p = 0.015), and the nonengrafter group was significantly enriched in the interferon gamma response (NES = -3.424, p = 0.001), interferon alpha response (NES = -3.180, p = 0.001), inflammatory response

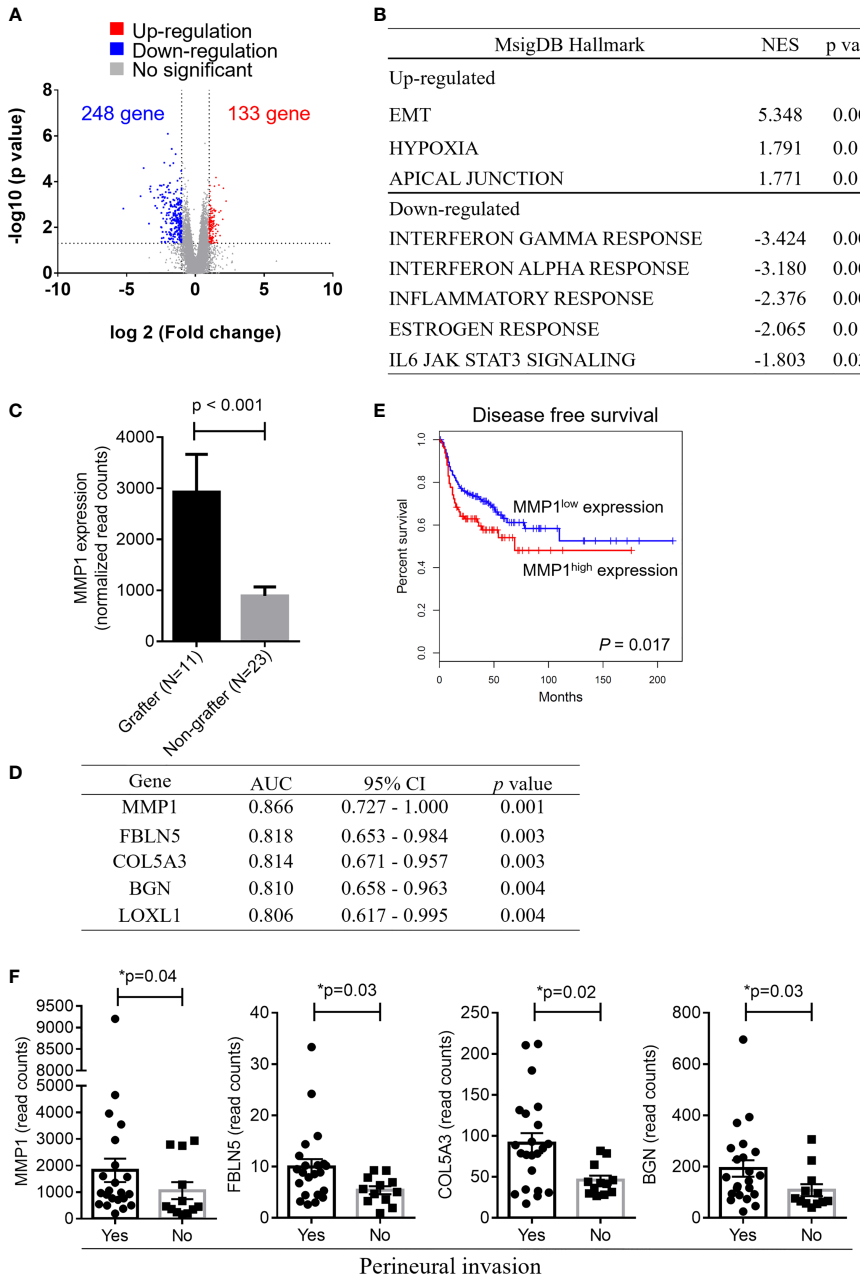

MsigDB Hallmark	NES	p value
Up-regulated		
EMT	5.348	0.004
HYPOXIA	1.791	0.013
APICAL JUNCTION	1.771	0.015
Down-regulated		
INTERFERON GAMMA RESPONSE	-3.424	0.001
INTERFERON ALPHA RESPONSE	-3.180	0.001
INFLAMMATORY RESPONSE	-2.376	0.003
ESTROGEN RESPONSE	-2.065	0.013
IL6 JAK STAT3 SIGNALING	-1.803	0.033

Gene	AUC	95% CI	*p* value
MMP1	0.866	0.727 - 1.000	0.001
FBLN5	0.818	0.653 - 0.984	0.003
COL5A3	0.814	0.671 - 0.957	0.003
BGN	0.810	0.658 - 0.963	0.004
LOXL1	0.806	0.617 - 0.995	0.004

FIGURE 2 | Gene expression signatures in OSCC grafters for PDXs. Among the 49 OSCC patients enrolled in this study, 34 OSCC, including grafters (n = 11) and nongrafters (n = 23), were subjected to RNA-seq analysis. **(A)** The volcano plot displays DEGs from RNA-seq data between the grafter and nonengrafter groups. The x-axis shows the log2-fold change values, and the y-axis shows the -log10 p values for the differentially expressed genes. **(B)** The differentially expressed pathways between nongrafters and grafters were determined by GSEA. **(C)** A bar chart of MMP1 expression between grafters (n=11) and nongrafters (n=23) by RNA-seq. **(D)** An AUC ranking table of the top five genes (MMP1, FBLN5, COL5A3, BGN, and LOXL1) with an AUC higher than 0.8 for distinguishing grafters from nongrafters. **(E)** Kaplan-Meier plot showing the disease-free survival for patient subgroups stratified by high versus low gene expression of MMP1 among the 514 patients in the HNSCC-TCGA dataset. The p values were calculated using log-rank tests. **(F)** The expression of MMP1, FBLN5, COL5A3, and BGN by RNA-seq analysis in oral cancer patients with or without perineural invasion. The p values were calculated using the Mann–Whitney U test. The P value < 0.05 indicated statistical significance (*: p < 0.05).

(NES= -2.376, p = 0.003), estrogen response (NES = -2.065, p = 0.013) and IL6 JAK STAT3 signaling (NES = -1.803, p = 0.033). We then selected genes involved in the regulation of EMT biological processes or immune responses and calculated the score based on the geometric mean of their expression levels. The EMT score was also significantly upregulated in grafters compared with nongrafters (**Supplementary Figure 3A**, left panel). However, we observed that the immune response score

was slightly increased in nongrafters compared with grafters (**Supplementary Figure 3A**, right panel). A heat map of the top 30 dysregulated genes in the EMT or immune response pathway is shown in **Supplementary Figure 3B**. These results revealed that an immunosuppressive microenvironment and activation of the EMT pathway could improve tumor growth in PDX models. Further, the top differentially expressed genes which involved in hypoxia and PI3K signaling pathways in grafters and nongrafters were shown in **Supplementary Figure 3C**.

As shown in **Figure 2C**, the expression of matrix metalloproteinase-1 (MMP-1), which was the most dominant expressed gene in our cohort of grafters, was significantly higher than that in nongrafters. The ability to distinguish between grafter and nonengrafter genes was evaluated by the area under the receiver operating characteristic (ROC) curve (AUC) and ranked in **Figure 2D**. The AUC values of the top five genes (MMP1, FBLN5, COL5A3, BGN and LOXL1) were above 0.800, and their *p* values were less than 0.01. We selected a marker panel with top three differentially expressed genes (MMP1, FBLN5 and COL5A3), which had an AUC value of 0.917 (95% CI = 0.792–1.042) in discriminating grafters from the non-grafters. MMP-1 is a part of the matrix metalloproteinase family that enzymatically degrades the extracellular matrix (ECM) or basement membrane (21). Numerous studies have suggested that MMP1 is associated with tumor invasion and metastasis (22, 23). MMP1 has also been reported as a potential diagnostic and prognostic biomarker in oral cancer (24). Disease-free survival was analyzed on head and neck cancer samples from The Cancer Genome Atlas (TCGA), and the results revealed that patients with higher MMP1 expression exhibited significantly poorer survival than those with lower MMP1 expression ($p = 0.017$) (**Figure 2E**). Furthermore, the expression of MMP1, FBLN5, COL5A3 and BGN was significantly increased in patients with perineural invasion (**Figure 2F).** Collectively, these results indicate that OSCC patients with high MMP1 expression and/or perineural invasion may benefit from the establishment of their matched PDX models.

RNA-Seq Analysis Reveals Enriched HIF and PI3K-AKT Pathways in Faster Growing Tumors Compared With Slower Growing Tumors

We also observed that the tumor growth rates were different in these 12 PDX lines. According to the tumor sizes in the first generation within 9 weeks of transplantation in NSG mice, the patients were divided into either faster (tumor > 200 mm^3) or slower (tumor < 200 mm^3) growing groups (**Figure 3A**). The transcriptional profiles of the faster (n=5) and slower (n=6) growing groups were compared by RNA-seq analysis of the primary tumors. Compared with the slower growing group, 854 transcripts were significantly altered (2-fold difference, p value < 0.05). Among these, 730 (85.5%) were downregulated and 124 (14.5%) were upregulated in the faster growing group (**Figure 3B**). Kyoto Encyclopedia of Genes and Genomes (KEGG) pathway analysis demonstrated that the upregulated genes were involved in the HIF-1 signaling pathway and PI3K-Akt signaling pathway (**Figure 3C**). The read counts of these genes (PDK1, EIF4EBP1, EGLN3, VEGFC, ITGAV, MTCP1 and CDK6), which are involved in the HIF-1 signaling pathway and PI3K-Akt signaling pathway, were significantly higher in the faster growing group than in the slower growing group (**Figure 3D**). These results may demonstrate that primary tumors under hypoxic conditions or with increased PI3K-Akt activation enhance tumor cell growth in xenografts.

Genomic Landscapes Are Conserved in Paired Primary Tumors and Xenografts

Next, we determined the DNA mutations and copy number variations (CNVs) in primary tumors and their matched PDXs using WES. Among the 12 PDXs, the quality of genomic DNA from the tumor tissues of 2 patients (patients #7 and #32) was deemed unsuitable for WES. A total of 30 samples, including 10 case-matched patient adjacent normal tissues and tumor tissues and their P1 PDXs, were subjected to WES and analyzed by bioinformatics. Clustering analysis of variant allele frequency (VAF) distributions showed that the matched samples were corrected for paired normal tissues, tumor tissues, and their matched P1 PDXs (**Figure 4A**). The correlation coefficient between primary tumors and their matched PDXs was high and ranged from 0.92 to 0.97 (**Figure 4B**). The top 25 most frequent mutations were also retained in 10 patients with OSCC, and their matched PDXs were listed in **Figure 4C**. Consistent with our previous report, the common mutations in this cohort of 49 OSCC patients were similar to those in most cohorts of Taiwanese OSCC patients (25). In this cohort, these mutations include those in TP53 (n = 8), CDKN2A (n = 5), KMT2B (n = 3), FAT (n = 3), and RIPK4 (n=3) (**Figure 4C**). The numbers of transition and transversion mutations were similar between patients and their matched PDXs (**Supplementary Table 2**).

In addition, WES analysis indicated that the CNVs in individual patients were comparable to those in their corresponding PDXs, including those in significantly amplified/deleted regions encompassing genes such as EGFR, FADD, CCND1, CDKN2A, and FAT1 (**Figure 4D**). Overall, consistent with our previous report, our PDX cohort retained the significantly mutated genes and CNVs from the OSCC Taiwan and head and neck squamous cell carcinoma (HNSCC) TCGA cohorts.

PDX Models Retain the Gene Expression Profiles of Their Paired Primary Tumors

We then analyzed the transcriptome profiles of these patients and their matched PDXs in the P1 and P2 generations. Of these 12 PDXs, the RNA quality from 1 sample was unsuitable for RNA-seq experiments. A total of 44 case-matched samples, including OSCC patient normal tissues (n = 11), tumor tissues (n = 11), P1 PDXs (n = 11), and P2 PDXs (n = 11), were subjected to RNA-seq and bioinformatics analyses. Our RNA-seq analyses revealed 32,200 genes, and the mean read count was 36.5 ± 0.76 million in the 44 case-matched samples. Principal component analysis (PCA) revealed similar gene expression patterns for case-matched tumors and PDXs (**Figure 5A**). The gene expression profiles of 2 patients (#22 and #32) were slightly different from those of the other 9 patients (**Figure 5A**). Comparative analysis of this transcriptome dataset allowed us

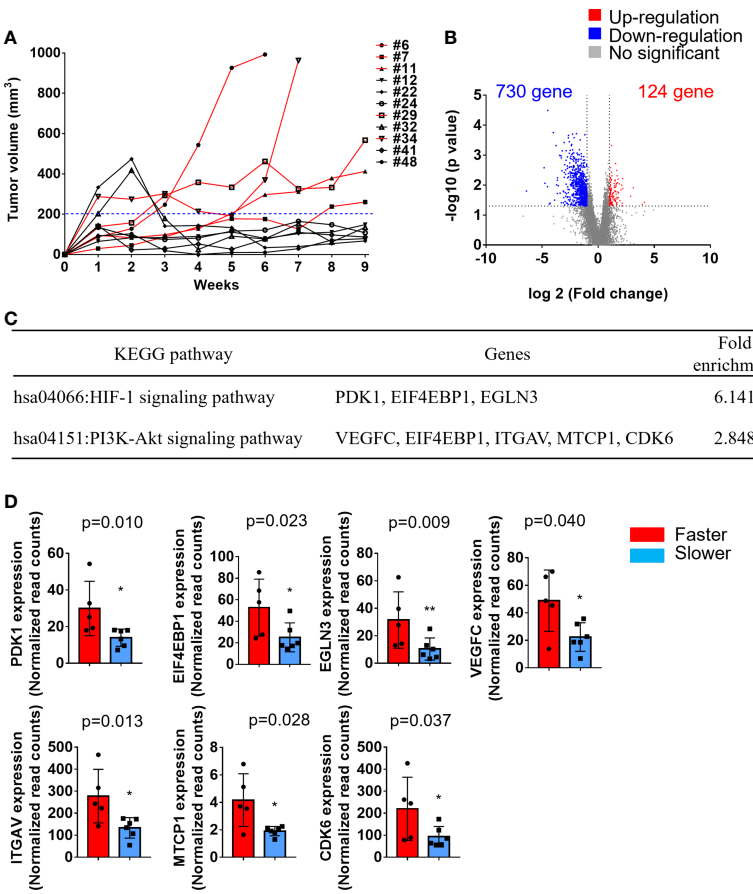

C

KEGG pathway	Genes	Fold enrichment
hsa04066:HIF-1 signaling pathway	PDK1, EIF4EBP1, EGLN3	6.141
hsa04151:PI3K-Akt signaling pathway	VEGFC, EIF4EBP1, ITGAV, MTCP1, CDK6	2.848

FIGURE 3 | Transcriptomic analysis of faster growing tumors compared with slower growing tumors. Primary tumors were excised and transplanted into immune-deficient mice. The tumor volumes in the flanks of mice were monitored twice a week. **(A)** Tumor growth curve of these 11 PDXs. The patients were divided into either a faster (red lines, tumor > 200 mm^3) or slower (black lines, tumor < 200 mm^3) growing group. **(B)** Volcano plot displays the DEGs between faster and slower growing tumors from RNA-seq analysis. The x-axis shows the log2-fold change values, and the y-axis shows the -log10 p values for the differentially expressed genes. **(C)** A total of 124 upregulated and 730 downregulated genes were subjected to KEGG pathway analysis. The significantly upregulated pathways are shown. **(D)** The expression of PDK1, EIF4EBP1, EGLN3, VEGFC, ITGAV, MTCP1, and CDK6 was significantly upregulated in the faster growing group. The p values were calculated using the Mann–Whitney U test. The P value < 0.05 indicated statistical significance. (*p<0.05, **p<0.01).

to identify 1,768 genes as DEGs (2-fold difference, p value < 0.05, FDR < 0.05); these included 1,066 upregulated and 702 downregulated genes in tumor tissue compared to normal tissue in 11 OSCC patients (**Figure 5B**). Then, the selected DEGs were subjected to clustering analysis to evaluate the dysregulated gene expression profiles of paired primary tumors and xenografts. The hierarchical clustering analysis of 11 case-matched normal tissues, tumor tissues, P1 PDXs, and P2 PDXs revealed clearly separated gene expression profiles between tumor and normal tissue and that PDXs retained the majority of the molecular signatures of their matched patient tissues (**Figure 5C**). The scatterplots displayed the correlation between the PDX RNA-seq and tumor RNA-seq results (**Figures 5D, E**). The Pearson correlation coefficient between matched tumors and PDXs in the P1 generation ranged from 0.24 to 0.87, with a median of 0.7 (**Figure 5D**). We found that the Pearson correlation coefficient between PDX P1 and P2 generation was positively associated, ranging from 0.85 to 0.97 (**Figure 5E**).

To explore the dysregulated pathways in patients and xenografts, the 2-fold-upregulated genes with a p value lower than 0.5 in patients or P1 PDXs compared with normal tissues were separately subjected to pathway annotation with DAVID software. KEGG pathway analysis revealed that dysregulated pathways in xenografts were similar to those in patients, such as the ECM-receptor interaction, cell cycle, focal adhesion, and PI3K-AKT signaling pathways (**Supplementary Figure 4**). In addition, compared with normal tissues, the genes with a 2-fold change in tumor tissues, P1 PDXs, or P2 PDXs were subjected to Venn diagram analysis. A total of 650 upregulated and 537 downregulated genes were conserved in primary tumor tissues, P1 PDXs, and P2 PDXs (**Supplementary Figure 5**). KEGG pathway analysis revealed that the 650 upregulated genes were enriched in cancer progression pathways, including the cell cycle, pathways in cancer, and ECM-receptor interactions (**Figure 6A**), whereas the downregulated genes were enriched in metabolic pathways (**Figure 6B**). Furthermore, pathways associated with

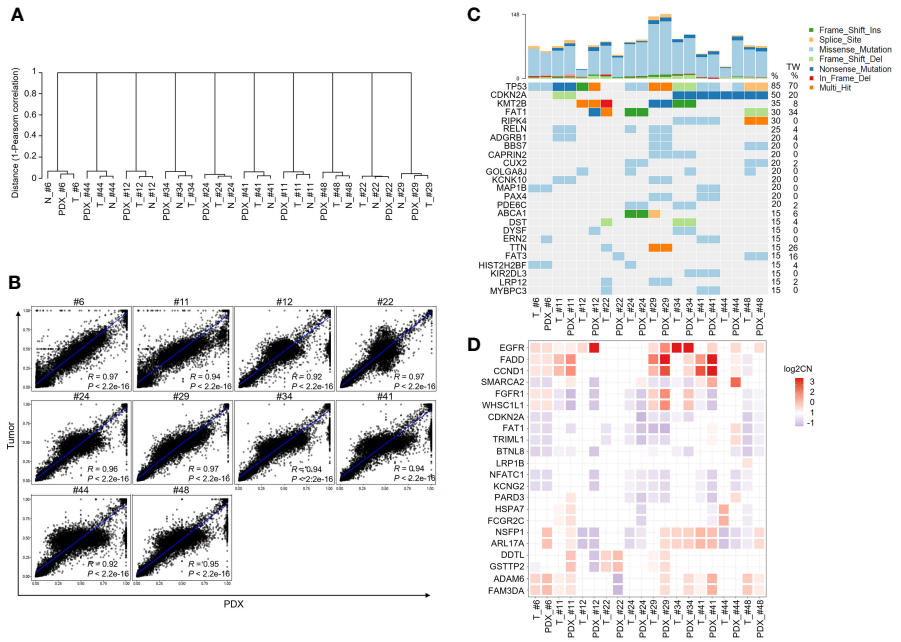

FIGURE 4 | Comparison of genomic landscape alterations in OSCC patients and PDXs. The genomic landscapes of paired normal tissues, tumor tissues, and xenografts were determined by whole-exome sequencing. **(A)** Unsupervised clustering analysis of variant allele frequency (VAF) distributions in paired normal tissues, tumor tissues, and their matched P1 PDXs. **(B)** The correlation coefficients of variants between primary tumors and matched PDXs were calculated. **(C)** The comparison of total genomic mutation counts in OSCC patients and their matched PDXs was shown in the upper panel. The y-axis shows the number of mutation events in the WES data. Heatmap representation of genes frequently mutated between OSCC patients and their matched PDXs. The numbers in the left lane represent the mutation frequencies of specific genes in these 10 paired specimens and in our previously published OSCC cohort (TW; n = 50). **(D)** Heatmap representation of the copy number variation (CNV) of targeted genes in OSCC patients and their matched PDXs.

cancer progression were investigated and plotted according to their normalized enrichment scores (NESs) for the hallmark pathway gene sets, as shown in **Figure 6C**. These results may indicate that our OSCC cohort used to investigate xenograft establishment represents the phenotypes of oral cancer patients and that the transcriptome profiles of these xenografts are similar to those of the primary tumors.

DISCUSSION

In this study, we established and comprehensively characterized WES and RNA-seq results in paired primary tumors and their matched OSCC PDXs in a Taiwanese population. Our cohort of 49 patients included those with primary tumors who were only newly diagnosed with treatment-naïve OSCC. Among the 49 OSCC samples, 12 successfully generated PDXs, most of which were derived from the buccal mucosa and tongue. The xenograft rate was approximately 25% in treatment-naïve primary tumors in our study. The 12 OSCC xenografts closely represented their parental tumors both in cancer-associated mutations (such as TP53 mutation, CDKN2A mutation, EGFR amplification, and CCND1 amplification) and transcriptome profiles (enriched in the cell cycle, pathways in cancer, ECM-receptor interaction, and PI3K-Akt pathways). Our study also demonstrated that some cellular pathways (hypoxia, PI3K-Akt, and EMT) were associated with high engraftment ability in OSCC. These pathways also contribute to the aggressiveness of various tumor types including oral cancer. In the present study, we first reported that three cancer-associated biological pathways were essential for successful xenograft transplantation.

Paired normal and tumor tissues from patients and their matched PDX models clustered together, demonstrating the relative similarity and stability of the whole-exome analysis between patients and their matched xenografts. Our study validated the use of these preclinical PDX models for OSCC patients and provided a useful biological and preclinical platform for studying tumor biology and testing anticancer therapies, including small molecule inhibitors, monoclonal antibodies, recombinant proteins, or Chinese herbal medicines.

The current study first unveiled that OSCC patients whose cells successfully generated PDXs had a high frequency of perineural invasion, which is a poor prognostic factor for the OSCC treatment outcome (26). Additionally, there was a trend of slightly lower 4-year OS and DFS rates in grafters than in nongrafters. Oral cancer is a highly heterogeneous cancer and genetic variation of individual tumor cells affect patients' clinical outcomes. Many clinical parameters or molecules have been reported as prognostic biomarkers for oral cancer. The genomics analysis showed that primary tumor with multiple dysregulated

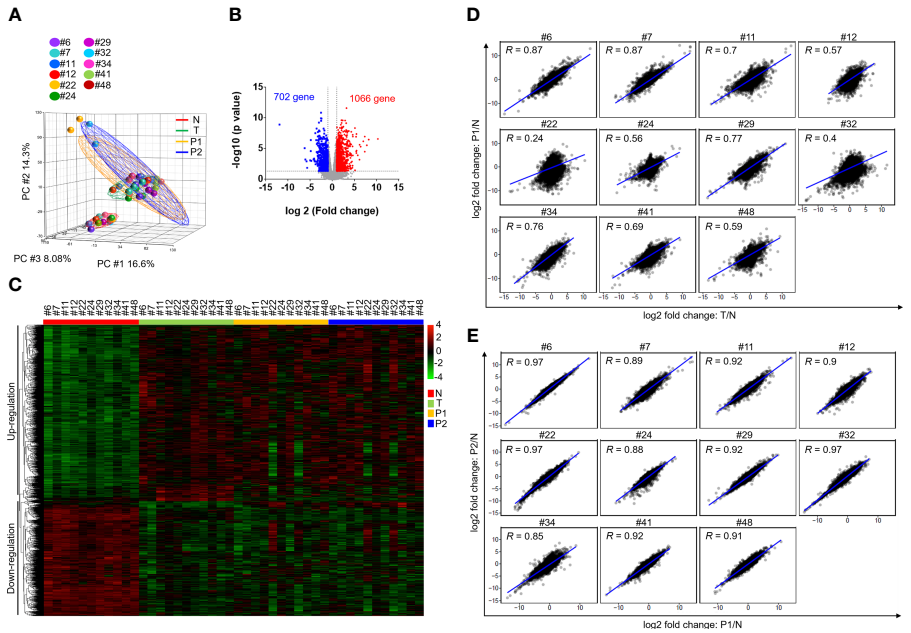

FIGURE 5 | Comparison of transcriptome profiles in OSCC patients and PDXs. The transcriptome profiles of paired normal tissues, tumor tissues, and xenografts were determined by RNA-seq. **(A)** Principal component analysis of the adjacent normal tissues (N), tumor tissues (T) and their matched PDXs at passage 1 (P1) and passage 2 (P2) of OSCC patients. **(B)** Volcano plot of differentially expressed genes between normal tissues and tumor tissues. The x-axis shows the log2-fold change values, and the y-axis shows the -log10 p values for the differentially expressed genes. **(C)** Expression heatmap analysis of transcriptome datasets from the adjacent normal tissues (N), tumor tissues (T) and their matched PDXs at passage 1 (P1) and passage 2 (P2) of OSCC patients. **(D)** Gene expression in patient tumor tissues or PDXs was normalized to that in patient adjacent normal tissues. Correlation of gene expression between patient primary tumor tissues and P1 PDXs. **(E)** Correlation of gene expression between P1 and P2 PDXs.

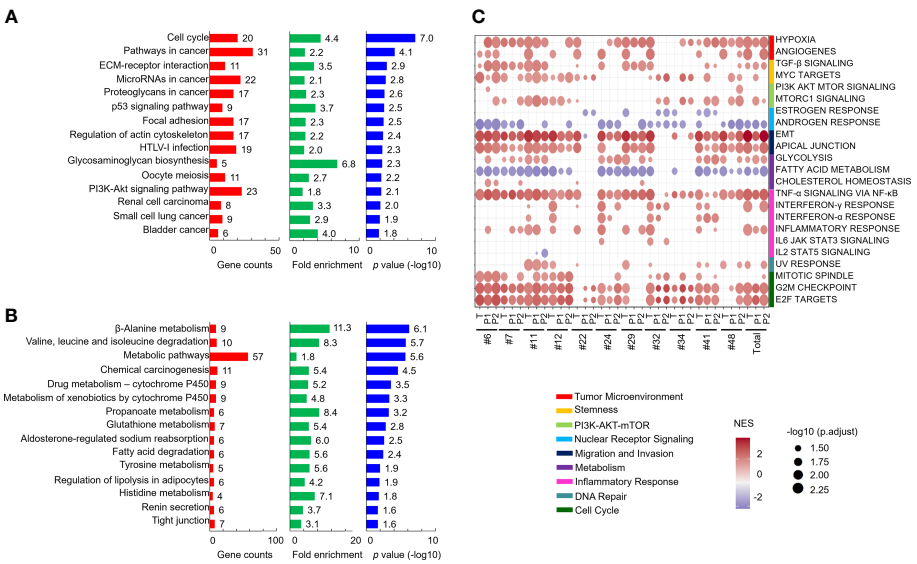

FIGURE 6 | Comparison of the similar pathways in patients and their PDXs. Genes with a 2-fold change and $p < 0.05$ in both patient tumor tissues and PDXs compared with patient adjacent normal tissues were subjected to KEGG pathway analysis. The results of the pathway analysis are summarized by bar charts and show the gene counts, fold enrichment, and -log p value. The pathways are labeled along the y-axis. The upregulated **(A)** and downregulated **(B)** genes were subjected to pathway annotation. Enriched cancer hallmarks in paired OSCC patients and xenografts were shown in **(C)**.

pathways have better engraftment rates in our study. However, the 4-year OS and DFS rates were slightly decreased, but no statistical difference, for grafters than for nongrafters. One possibility is the limited sample size in the small cohort; the other possibility is that a marker panel of specific molecules may be better for predicating cancer patients' survival in oral cancer.

Hypoxia is observed selectively around large tumor masses because of an inefficient blood supply and oxygen delivery (27, 28). Our study revealed that tumor hypoxia, which was not only the top enriched pathway in faster growing xenografts but was also enriched in successful grafters compared with nongrafters, was enriched according to RNA-seq analysis. Hypoxia promotes cancer progression *via* the hypoxia-inducible factor (HIF)-associated signaling pathway, resulting in the increased expression of many oncogenic proteins (29). Hypoxia also promotes drug resistance, including chemotherapy and some targeted therapies, in cancer cells (27). Some reports indicate that hypoxia is a marker of a poor prognosis and chemoradiotherapy failure in HNSCC (30). One of the hypoxia-inducible genes, MMP1, was the best biomarker (AUC = 0.866) for predicting the ability of a patient to successfully generate matched PDXs in our study. It has been reported by us and others that MMP1 in the saliva is a good biomarker for the screening and diagnosis of OSCC (31–33). Furthermore, salivary MMP-1 may be a useful biomarker that is better than CD44 for OSCC diagnosis in the Taiwanese population (31). In the present study, our results indicated that MMP1 expression was significantly increased in patients with perineural invasion and that hypoxic conditions may increase the expression of MMP-1 in human primary tumors, which might help transplanted tumor cells spread and evade in mice.

One limitation of our study is no external validation cohort. There is currently no public database of primary tumor's genomics analysis between successful grafters and non-grafters in PDXs platform. Our study generated the first public database of comprehensive genomics information for predicting tumor engraftment ability. The patient-derived-xenograft experiment takes an average of three months for establishing one generation of a mouse strain in oral cancer. We will further establish the validation cohort in the future. Some unexpected findings were noted in the current study. Some primary tumor-specific mutations were missed in their matched PDX. The intratumor heterogeneity and different pieces of resected tissues either for genomic sequencing or for transplantation in mice could have caused this inconsistency. Furthermore, some somatic mutations were undetected in xenografts. This may also be explained by the low sequencing coverage or low mutation frequency. Notably, although some variations in gene expression profiles were observed between primary tumors and their matched P1 PDXs, the correlation coefficient of the transcriptome profile between matched P1 and P2 PDXs was at least 85%. The correlation coefficient of some samples was even higher than 97%. These results may be due to specific cell types of these heterogeneous primary tumors surviving and establishing communities in mice. These cell populations have adapted to the new environment and could passage to the next generation, but indeed, some cell populations may be lost in the first xenograft generation.

CONCLUSIONS

Overall, our study demonstrates, for the first time in the literature, that 12 OSCC PDX models were successfully established and the genomic landscapes of paired primary tumor tissues and xenografts were comprehensively profiled by exome-seq and RNA-seq. Our PDX strains maintained common genetic mutation profiles in OSCC, suggesting that this platform might be quite useful for many anticancer drugs that are now widely used in clinical practice. A panel of five genes (MMP1, FBLN5, COL5A3, BGN and LOXL1) was useful for predication the successful grafters among oral cancer patients.

DATA AVAILABILITY STATEMENT

The sequencing data was deposited to NCBI SRA and the BioProject accession was PRJNA780253.

ETHICS STATEMENT

This study was approved by the Institutional Review Board at Chang Gung Memorial Hospital, Taiwan (Protocol Nos.: 201800700B0, 102-5685A3). Prior to sample collection, written informed consent was obtained from all participants. The patients/participants provided their written informed consent to participate in this study. All animal experiments were conducted in accordance with the Institutional Animal Care and Use Committee of Chang Gung University (Protocol Nos.: CGU106-114 and CGU107-074).

AUTHOR CONTRIBUTIONS

W-CY contributed to the experiments, data analysis, and writing and revising the manuscript. IY-FC performed the bioinformatics analysis and writing the manuscript. K-PC contributed to the study design, clinical sample collection, clinical data analysis, and writing and revising the manuscript. C-NO, C-RL, T-LT, Y-CZ, C-IW, Y-HW, AY, HL, C-CW, Y-SC and J-SY contributed to the experiments and provided technical support. C-YY contributed to the study design, experiments, data analysis, and writing and revising the manuscript. All authors have approved the final version of the work.

FUNDING

This work was supported by grants from the Ministry of Science and Technology (MOST) (K-PC, MOST 108-2314-B-182A-108-

MY3; and C-YY, MOST 110-2314-B-182-046 and MOST 107-2314-B-182-075-MY3) and Chang Gung Memorial Hospital (K-PC, CMRPG3H0853 and CMRPG3J1252; and C-YY, CORPD1J0103, CMRPD1K0402). The authors thank the "Molecular Medicine Research Center, Chang Gung University" from The Featured Areas Research Center Program within the framework of the Higher Education Sprout Project by the Ministry of Education (MOE) in Taiwan (EMRPD1M0281). NGS experiments and bioinformatics analyses were performed at the Genomics NGS Laboratory Molecular Medicine Research Center, Chang Gung University, Taiwan (EMRPD1M0231).

ACKNOWLEDGMENTS

We also acknowledge the Next-Generation Sequencing Core, Bioinformatics Core, Pathology Core, and Core Instrument Center at Chang Gung University, Taoyuan, Taiwan, for technical support (CLRPD1J0013).

SUPPLEMENTARY MATERIAL

The Supplementary Material for this article can be found online at: https://www.frontiersin.org/articles/10.3389/fonc.2022.792297/full#supplementary-material

REFERENCES

1. Bugshan A, Farooq I. Oral Squamous Cell Carcinoma: Metastasis, Potentially Associated Malignant Disorders, Etiology and Recent Advancements in Diagnosis. *F1000Res* (2020) 9:229. doi: 10.12688/f1000research.22941.1
2. Kumar M, Nanavati R, Modi TG, Dobariya C. Oral Cancer: Etiology and Risk Factors: A Review. *J Cancer Res Ther* (2016) 12:458–63. doi: 10.4103/0973-1482.186696
3. Parsa N. Environmental Factors Inducing Human Cancers. *Iran J Public Health* (2012) 41:1–9.
4. Vigneswaran N, Williams MD. Epidemiologic Trends in Head and Neck Cancer and Aids in Diagnosis. *Oral Maxillofac Surg Clin North Am* (2014) 26:123–41. doi: 10.1016/j.coms.2014.01.001
5. Manvikar V, Kulkarni R, Koneru A, Vanishree M. Role of Human Papillomavirus and Tumor Suppressor Genes in Oral Cancer. *J Oral Maxillofac Pathol* (2016) 20:106–10. doi: 10.4103/0973-029X.180958
6. Chi AC, Day TA, Neville BW. Oral Cavity and Oropharyngeal Squamous Cell Carcinoma–An Update. *CA Cancer J Clin* (2015) 65:401–21.doi: 10.3322/caac.21293
7. Buch SA, Chatra L. Saliva as a Non-Invasive Diagnostic Medium in Proteomics for Oral Squamous Cell Carcinoma Detection. *Int J Med Rev* (2019) 6:73–6. doi: 10.3390/proteomes4040041
8. Yoshida GJ. Applications of Patient-Derived Tumor Xenograft Models and Tumor Organoids. *J Hematol Oncol* (2020) 13:4. doi: 10.1186/s13045-019-0829-z
9. Bhimani J, Ball K, Stebbing J. Patient-Derived Xenograft Models-The Future of Personalised Cancer Treatment. *Br J Cancer* (2020) 122:601–2. doi: 10.1038/s41416-019-0678-0
10. Hidalgo M, Amant F, Biankin AV, Budinska E, Byrne AT, Caldas C, et al. Patient-Derived Xenograft Models: An Emerging Platform for Translational Cancer Research. *Cancer Discov* (2014) 4:998–1013. doi: 10.1158/2159-8290.CD-14-0001
11. Tentler JJ, Tan AC, Weekes CD, Jimeno A, Leong S, Pitts TM, et al. Patient-Derived Tumour Xenografts as Models for Oncology Drug Development. *Nat Rev Clin Oncol* (2012) 9:338–50. doi: 10.1038/nrclinonc.2012.61
12. Okada S, Vaeteewoottacharn K, Kariya R. Establishment of a Patient-Derived Tumor Xenograft Model and Application for Precision Cancer Medicine. *Chem Pharm Bull (Tokyo)* (2018) 66:225–30. doi: 10.1248/cpb.c17-00789
13. Bolger AM, Lohse M, Usadel B. Trimmomatic: A Flexible Trimmer for Illumina Sequence Data. *Bioinformatics* (2014) 30:2114–20. doi: 10.1093/bioinformatics/btu170
14. Dobin A, Davis CA, Schlesinger F, Drenkow J, Zaleski C, Jha S, et al. STAR: Ultrafast Universal RNA-Seq Aligner. *Bioinformatics* (2013) 29:15–21. doi: 10.1093/bioinformatics/bts635
15. Ahdesmaki MJ, Gray SR, Johnson JH, Lai Z. Disambiguate: An Open-Source Application for Disambiguating Two Species in Next Generation Sequencing Data From Grafted Samples. *F1000Res* (2016) 5:2741. doi: 10.12688/f1000research.10082.1
16. Wang K, Li M, Hakonarson H. ANNOVAR: Functional Annotation of Genetic Variants From High-Throughput Sequencing Data. *Nucleic Acids Res* (2010) 38:e164. doi: 10.1093/nar/gkq603
17. Kuilman T, Velds A, Kemper K, Ranzani M, Bombardelli L, Hoogstraat M, et al. CopywriteR: DNA Copy Number Detection From Off-Target Sequence Data. *Genome Biol* (2015) 16:49. doi: 10.1186/s13059-015-0617-1
18. Mermel CH, Schumacher SE, Hill B, Meyerson ML, Beroukhim R, Getz G. GISTIC2.0 Facilitates Sensitive and Confident Localization of the Targets of Focal Somatic Copy-Number Alteration in Human Cancers. *Genome Biol* (2011) 12:R41. doi: 10.1186/gb-2011-12-4-r41
19. Yang CY, Liu CR, Chang IY, OuYang CN, Hsieh CH, Huang YL, et al. Cotargeting CHK1 and PI3K Synergistically Suppresses Tumor Growth of Oral Cavity Squamous Cell Carcinoma in Patient-Derived Xenografts. *Cancers (Basel)* (2020) 12:1726. doi: 10.3390/cancers12071726
20. Kitamura R, Toyoshima T, Tanaka H, Kawano S, Kiyosue T, Matsubara R, et al. Association of Cytokeratin 17 Expression With Differentiation in Oral Squamous Cell Carcinoma. *J Cancer Res Clin Oncol* (2012) 138:1299–310. doi: 10.1007/s00432-012-1202-6
21. Ren ZH, Wu K, Yang R, Liu ZQ, Cao W. Differential Expression of Matrix Metalloproteinases and miRNAs in the Metastasis of Oral Squamous Cell Carcinoma. *BMC Oral Health* (2020) 20:24. doi: 10.1186/s12903-020-1013-0
22. Stott-Miller M, Houck JR, Lohavanichbutr P, Mendez E, Upton MP, Futran ND, et al. Tumor and Salivary Matrix Metalloproteinase Levels Are Strong Diagnostic Markers of Oral Squamous Cell Carcinoma. *Cancer Epidemiol Biomark Prev* (2011) 20:2628–36. doi: 10.1158/1055-9965.EPI-11-0503
23. Sauter W, Rosenberger A, Beckmann L, Kropp S, Mittelstrass K, Timofeeva M, et al. Matrix Metalloproteinase 1 (MMP1) Is Associated With Early-Onset Lung Cancer. *Cancer Epidemiol Biomark Prev* (2008) 17:1127–35. doi: 10.1158/1055-9965.EPI-07-2840
24. Yen CY, Chen CH, Chang CH, Tseng HF, Liu SY, Chuang LY, et al. Matrix Metalloproteinases (MMP) 1 and MMP10 But Not MMP12 Are Potential Oral Cancer Markers. *Biomarkers* (2009) 14:244–9. doi: 10.1080/13547500902829375
25. Chen TW, Lee CC, Liu H, Wu CS, Pickering CR, Huang PJ, et al. APOBEC3A Is an Oral Cancer Prognostic Biomarker in Taiwanese Carriers of an APOBEC Deletion Polymorphism. *Nat Commun* (2017) 8:465. doi: 10.1038/s41467-017-00493-9
26. Varsha BK, Radhika MB, Makarla S, Kuriakose MA, Kiran GS, Padmalatha GV. Perineural Invasion in Oral Squamous Cell Carcinoma: Case Series and Review of Literature. *J Oral Maxillofac Pathol* (2015) 19:335–41. doi: 10.4103/0973-029X.174630
27. Jing X, Yang F, Shao C, Wei K, Xie M, Shen H, et al. Role of Hypoxia in Cancer Therapy by Regulating the Tumor Microenvironment. *Mol Cancer* (2019) 18:157. doi: 10.1186/s12943-019-1089-9
28. Joseph JP, Harishankar MK, Pillai AA, Devi A, Hypoxia induced EMT. A Review on the Mechanism of Tumor Progression and Metastasis in OSCC. *Oral Oncol* (2018) 80:23–32. doi: 10.1016/j.oraloncology.2018.03.004
29. Petrova V, Annicchiarico-Petruzzelli M, Melino G, Amelio I. The Hypoxic Tumour Microenvironment. *Oncogenesis* (2018) 7:10. doi: 10.1038/s41389-017-0011-9
30. Harms JK, Lee TW, Wang T, Lai A, Kee D, Chaplin JM, et al. Impact of Tumour Hypoxia on Evofosfamide Sensitivity in Head and Neck Squamous Cell Carcinoma Patient-Derived Xenograft Models. *Cells* (2019) 8:717. doi: 10.3390/cells8070717

31. Chang YT, Chu LJ, Liu YC, Chen CJ, Wu SF, Chen CH, et al. Verification of Saliva Matrix Metalloproteinase-1 as a Strong Diagnostic Marker of Oral Cavity Cancer. *Cancers (Basel)* (2020) 12:2273. doi: 10.3390/cancers12082273
32. Yu JS, Chen YT, Chiang WF, Hsiao YC, Chu LJ, See LC, et al. Saliva Protein Biomarkers to Detect Oral Squamous Cell Carcinoma in a High-Risk Population in Taiwan. *Proc Natl Acad Sci USA* (2016) 113:11549–54. doi: 10.1073/pnas.1616695113
33. Feng Y, Li Q, Chen J, Yi P, Xu X, Fan Y, et al. Salivary Protease Spectrum Biomarkers of Oral Cancer. *Int J Oral Sci* (2019) 11:7. doi: 10.1038/s41368-018-0032-z

Conflict of Interest: The authors declare that the research was conducted in the absence of any commercial or financial relationships that could be construed as a potential conflict of interest.

Publisher's Note: All claims expressed in this article are solely those of the authors and do not necessarily represent those of their affiliated organizations, or those of the publisher, the editors and the reviewers. Any product that may be evaluated in this article, or claim that may be made by its manufacturer, is not guaranteed or endorsed by the publisher.

frontiers | Frontiers in Oncology

ORIGINAL RESEARCH
published: 07 April 2022
doi: 10.3389/fonc.2022.812358

Predicting Bone Metastasis Risk Based on Skull Base Invasion in Locally Advanced Nasopharyngeal Carcinoma

Bo Wu[1,2], *Yu Guo*[2], *Hai-hua Yang*[3], *Qian-gang Gao*[2] *and Ye Tian*[1]*

[1] Department of Radiotherapy and Oncology, The Second Affiliated Hospital of Soochow University, Suzhou, China, [2] Department of Radiotherapy, Taizhou Central Hospital (Taizhou University Hospital), Taizhou, China, [3] Department of Radiotherapy, Taizhou Hospital, Linhai, China

Objective: To develop and validate a bone metastasis prediction model based on skull base invasion (SBI) in patients with locally advanced nasopharyngeal carcinoma (LA-NPC).

Methods: This retrospective cohort study enrolled 290 patients with LA-NPC who received intensity-modulated radiation therapy in two hospitals from 2010 to 2020. Patient characteristics were grouped by SBI and hospital. Both unadjusted and multivariate-adjusted models were used to determine bone metastasis risk based on SBI status. Subgroup analysis was performed to investigate heterogeneity using a forest graph. Cox proportional hazard regression analysis was used to screen for risk factors of bone metastasis-free survival (BMFS). A nomogram of BMFS based on SBI was developed and validated using C-index, receiver operating characteristic curve, calibration curves, and decision curve analysis after Cox proportional hazard regression analysis.

Results: The incidence of bone metastasis was 14.83% (43/290), 20.69% (24/116), and 10.92% (19/174) in the overall population, SBI-positive group, and SBI-negative group, respectively. In the unadjusted model, SBI was associated with reduced BMFS [HR 2.43 (1.32–4.47), P = 0.004], and the results remained stable after three continuous adjustments (P <0.05). No significant interaction was found in the subgroup analyses (P for interaction >0.05). According to Cox proportional hazard regression analysis and clinical value results, potential risk factors included SBI, Karnofsky performance status, TNM stage, induction chemotherapy, concurrent chemoradiotherapy, and adjuvant chemotherapy. Using a training C-index of 0.80 and a validation C-index of 0.79, the nomogram predicted BMFS and demonstrated satisfactory prognostic capability in 2, 3, and 5 years (area under curve: 83.7% vs. 79.6%, 81.7% vs. 88.2%, and 79.0% vs. 93.8%, respectively).

Conclusion: Skull base invasion is a risk factor for bone metastasis in patients with LA-NPC. The SBI-based nomogram model can be used to predict bone metastasis and may assist in identifying LA-NPC patients at the highest risk of bone metastasis.

Keywords: nasopharyngeal carcinoma, skull base invasion, bone metastasis, bone metastasis-free survival, prediction model, nomogram, intensity modulated radiation therapy

OPEN ACCESS

Edited by:
Steffi Ulrike Pigorsch, Technical University of Munich, Germany

Reviewed by:
Victor Lewitzki, University Hospital Würzburg, Germany
Jinyi Lang, Sichuan Cancer Hospital, China
Lucas Etzel, Technical University of Munich, Germany

***Correspondence:**
Ye Tian
dryetian@126.com

Specialty section:
This article was submitted to Head and Neck Cancer, a section of the journal Frontiers in Oncology

Received: *10 November 2021*
Accepted: *16 March 2022*
Published: *07 April 2022*

Citation:
Wu B, Guo Y, Yang H-h, Gao Q-g and Tian Y (2022) Predicting Bone Metastasis Risk Based on Skull Base Invasion in Locally Advanced Nasopharyngeal Carcinoma. Front. Oncol. 12:812358. doi: 10.3389/fonc.2022.812358

INTRODUCTION

Nasopharyngeal carcinoma (NPC), a squamous cell carcinoma that develops on the nasopharyngeal epithelium, is one of the most common malignant tumors in South China, with more than 70% of patients diagnosed with locally advanced NPC (LA-NPC) (1–3). Although treatments like intensity-modulated radiation therapy (IMRT) can improve local control rate, the incidence of distant metastasis ranges from 11.00 to 27.08% and remains a significant concern (4–7). Multiple studies have correlated distant metastasis with poor prognosis (8, 9). NPC is associated with pulmonary, liver, and bone metastasis, with bone being the most common, occurring concurrent with or before other distant metastases (10, 11). Thus, it is critical to identify risk factors that may influence bone metastasis in LA-NPC patients.

The skull base is a common site of tumor invasion in LA-NPC patients (12). Zou et al. (13) studied 518 LA-NPC patients and found that those with skull base invasion (SBI) had a higher risk of bone metastasis than those without (16.4% vs. 6.6%, respectively; $P < 0.05$). Other studies have shown that SBI detected by computed tomography (CT) was predictive of bone metastasis in patients with early N-stage NPC [2.478 (1.146–5.358), $P = 0.021$] (14). However, more research is needed to determine the independent prognostic value of SBI to the risk of bone metastasis. Furthermore, there is no international consensus on the best model to predict bone metastasis in LA-NPC patients based on SBI (15).

A nomogram is a visual depiction of a complicated mathematical formula that offers the overall likelihood of a specific outcome (16). Nomograms generated by regression analysis are widely used in regimen selection, tumor recurrence/metastasis prediction, and prognostic evaluation (17, 18). In addition, the prediction model can be integrated into TNM staging (19). This retrospective study was designed to assess the relationship between SBI and bone metastasis and to develop a bone metastasis risk model based on SBI.

MATERIALS AND METHODS

Study Design and Data Source

A retrospective study was conducted by consecutively enrolling LA-NPC patients seen at Taizhou Central Hospital (Taizhou University Hospital) and Taizhou Hospital from 2010 to 2020 (**Figure 1**). The local Institutional Review Boards approved the study (No. 2019-SC-019, Date: 2019/06/09). Because the study was retrospective, the requirement for informed consent was waived.

Inclusion criteria included (1) a pathological diagnosis of NPC, (2) complete imaging results confirming LA-NPC (stage III or IVa, AJCC 8th edition), (3) CT or magnetic resonance imaging (MRI) diagnosis of SBI, and (4) receipt of IMRT alone or in combination with induction chemotherapy (IC), concurrent chemoradiotherapy (CCRT), or adjuvant chemotherapy (AC). Exclusion criteria included (1) stage I, II, and IVb (n = 67), (2) presence of other primary malignant tumors (n = 10), (3) incomplete clinical data (n = 26), and (4) loss to follow-up (n = 27). Based on these criteria, 290 LA-NPC patients were included in the study.

The times from inclusion in the study to bone metastasis, distant metastasis, or death were defined as bone metastasis-free survival (BMFS), distant metastasis-free survival (DMFS), or overall survival (OS), respectively. Follow-up was conducted during outpatient visits or by phone every 3 months for the first 2 years and every 6 months for the next 3–5 years. The end of follow-up was defined as the date of death or June 2021.

Predictor Variables

Potential predictor variables were collected before and during treatment. Patient information, including demographics, clinical features, imaging findings, and treatment, was obtained from the hospital information systems. SBI was separately assessed for each patient by two radiologists using contrast-enhanced CT and/or MRI (14, 20). Any disagreements were reviewed until a consensus was reached.

All enrolled LA-NPC patients were treated with IMRT as described previously (21, 22). In brief, the prescription doses of 70-76Gy, 66-70Gy, 60-66Gy, or 56-60Gy were administered to the primary tumor volume of the gross tumor (GTVnx) and the involved lymph nodes (GTVnd), with the clinical target volume including high- and low-risk regions (CTV1/2). IC, CCRT, or AC was usually recommended for these patients in the form of single-agent cisplatin or platinum-based regimen. The combination chemotherapy regimens included platinum/fluorouracil, gemcitabine/platinum, docetaxel/platinum, and docetaxel/platinum/fluorouracil (**Supplementary S1**).

Association Analyses of Skull Base Invasion With Covariables and Outcomes

Unadjusted and multivariable-adjusted models were used to determine the relationship between SBI and LA-NPC outcomes. Covariables were added to a Cox regression model and dropped one by one. The coefficients of the corresponding regression were compared. Effect modification based on TNM stage, IC, CCRT, and AC treatment was investigated by including an interaction term with SBI in the Cox regression model for bone metastasis. The findings were presented as a hazard ratio (HR) with 95% confidence intervals (CI).

Feature Extraction and Model Building

Univariate and multivariate Cox regression analyses were performed to identify clinically important variables related to bone metastasis risk ($P < 0.1$). A nomogram predicting bone metastasis was then established to visualize model efficiency using a training dataset from Taizhou Central Hospital (Taizhou University Hospital). The results were validated with a validation dataset from Taizhou Hospital. The area under the curve (AUC) of the receiver operating characteristic curve (ROC) was used to evaluate the accuracy of the nomogram model. The concordance index (C-index) was calculated to assess the model's discrimination ability and a calibration curve was plotted to calibrate the model (23). The clinical usefulness of the nomogram was estimated using decision curve analysis (24).

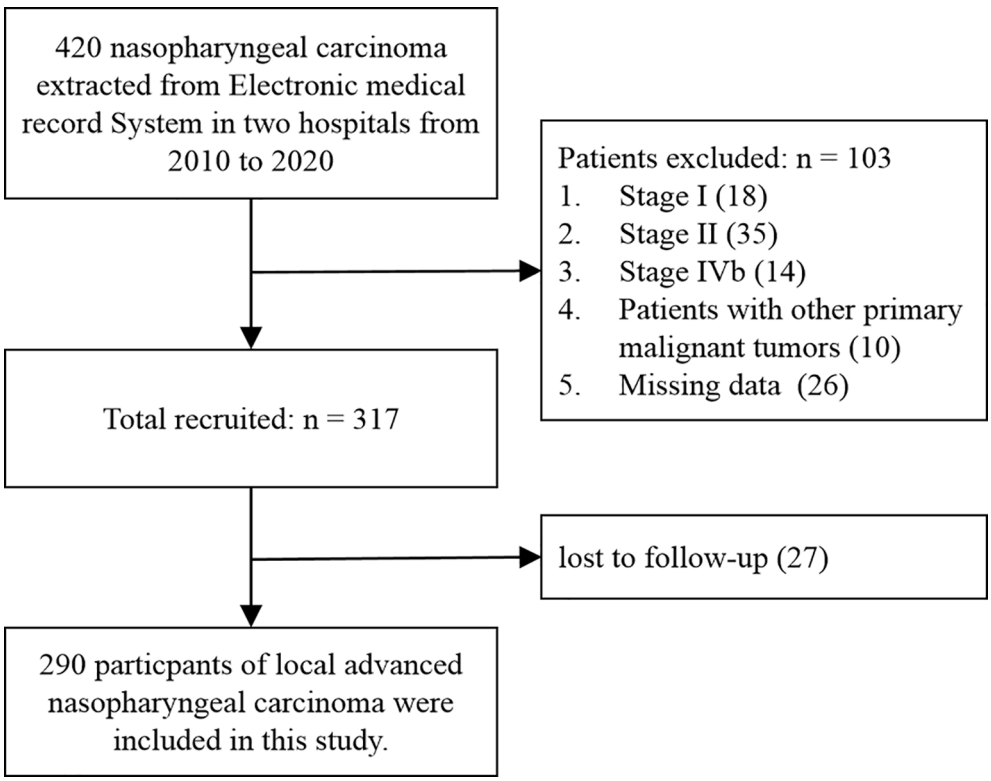

FIGURE 1 | Flow diagram of the study selection process.

Statistical Analyses

Descriptive analysis was used to characterize the study participants. Categorical variables were expressed as proportions (%), and continuous variables were expressed as the mean plus standard deviation. The correlation between clinical covariables and SBI or hospital was analyzed using χ^2 and *t* tests. $P < 0.05$ denoted a statistically significant difference (two-tailed test). Pearson's coefficients of association were calculated to assess the collinearity between SBI and the covariables. The threshold was set at r <0.6 with $P < 0.05$. All data were processed using Free Statistics software version 1.3 and SPSS software version 25.0.

RESULTS

Study Population

In total, 290 cases were included in the study with a median 49.5-month follow-up (range: 6–60 months). Of these, 198 cases were from Taizhou central hospital (Taizhou university hospital) and 92 cases were from Taizhou Hospital. Baseline characteristics of the patients, grouped by the presence or absence of SBI, are shown in **Table 1**. The patients were an average of 54.9 ± 11.6 years of age and 74.5% (216/290) were male. Most participants (71.3%, 207/290) had TNM stage III, while the remaining 83 had TNM stage IVa. Forty percent (116/290) of the patients had SBI. There were significant differences in T category, N category, TNM stage, and IC between the SBI-positive and SBI-negative groups ($P < 0.05$). However, no statistically significant differences in hospital, age, sex, Karnofsky performance status (KPS), smoking index, histological type, CCRT, and AC were observed between the groups ($P > 0.05$). **Table S1** summarizes the baseline characteristics by hospital. While there was a significant difference in CCRT (77.3% vs. 65.2%, $P = 0.043$), no statistically significant differences were reported in SBI, bone metastasis, age, sex, KPS, smoking index, histological type, T category, N category, TNM stage, IC, and AC ($P > 0.05$).

Association of Skull Base Invasion With Covariables and Outcomes

The incidence of bone metastasis was 14.83% (43/290), 20.69% (24/116), and 10.92% (19/174) in the study population, SBI-positive group, and SBI-negative group, respectively. Collinearity analysis revealed strong collinearity between SBI and T category (r = 0.657) (**Table S2**), while SBI and TNM stage (r = 0.293) did not show collinearity. Thus, TNM stage was chosen for subsequent analyses.

The HRs and 95% CIs for tumor progression and survival analyses determined by SBI are shown in **Table 2**. SBI-positive patients had a shorter BMFS in the unadjusted model [HR: 2.43, 95%CI (1.32–4.47)] (**Table 2** and **Figure 2A**). After adjusting for hospital, age, sex, KPS, smoking index, histological type, TNM

TABLE 1 | Baseline characteristics of 290 locally advanced nasopharyngeal carcinoma patients grouped by presence of skull base invasion.

Variable	Total (n = 290)	SBI: No (n = 174)	SBI: Yes (n = 116)	*p* value
Hospital				0.938
TZCH	198 (68.3)	118 (67.8)	80 (69)	
TZH	92 (31.7)	56 (32.2)	36 (31)	
Age(years), Mean ± SD	54.9 ± 11.6	54.7 ± 11.6	55.2 ± 11.5	0.694
Age(years)				0.981
≤55	144 (49.7)	87 (50)	57 (49.1)	
>55	146 (50.3)	87 (50)	59 (50.9)	
Sex				0.978
Female	74 (25.5)	45 (25.9)	29 (25)	
Male	216 (74.5)	129 (74.1)	87 (75)	
KPS scores				0.145
≤70	66 (22.8)	34 (19.5)	32 (27.6)	
>70	224 (77.2)	140 (80.5)	84 (72.4)	
Smoking index				1.000
≤400	207 (71.4)	124 (71.3)	83 (71.6)	
>400	83 (28.6)	50 (28.7)	33 (28.4)	
Histological type				0.751
Keratinizing	22 (7.6)	12 (6.9)	10 (8.6)	
Non-keratinizing	268 (92.4)	162 (93.1)	106 (91.4)	
T category				< 0.001
T1-2	114 (39.3)	114 (65.5)	0 (0)	
T3-4	176 (60.7)	60 (34.5)	116 (100)	
N category				0.003
N0-1	57 (19.7)	24 (13.8)	33 (28.4)	
N2-3	233 (80.3)	150 (86.2)	83 (71.6)	
TNM stage				< 0.001
III	207 (71.4)	143 (82.2)	64 (55.2)	
IVa	83 (28.6)	31 (17.8)	52 (44.8)	
IC				< 0.001
No	125 (43.1)	90 (51.7)	35 (30.2)	
Yes	165 (56.9)	84 (48.3)	81 (69.8)	
CCRT				0.849
No	77 (26.6)	45 (25.9)	32 (27.6)	
Yes	213 (73.4)	129 (74.1)	84 (72.4)	
AC				0.747
No	183 (63.1)	108 (62.1)	75 (64.7)	
Yes	107 (36.9)	66 (37.9)	41 (35.3)	

SBI, skull base invasion; TZCH, Taizhou Central Hospital (Taizhou University Hospital); TZH, Taizhou Hospital; KPS, karnofsky performance status; IC, induction chemotherapy; CCRT, concurrent chemoradiotherapy; AC, adjuvant chemotherapy.

stage, IC, CCRT, and AC, the HRs were 2.52 (1.36–4.66), 2.28 (1.23–4.22), and 2.31 (1.17–4.54), respectively (P <0.05). A correlation was observed between SBI and bone metastasis in unadjusted and multivariable-adjusted models. While the Kaplan–Meier survival curve showed that SBI-positive patients had a lower DMFS and OS than SBI-negative ones, the HRs was 1.56 (0.92–2.65) and 1.56 (0.85–2.89) for DMFS and OS after adjusting for all covariables (**Table 2** and **Figures 2B, C**).

Stratified and interactive analyses were used to determine if the relationships between SBI and bone metastasis were stable in the TNM stage, IC, CCRT, and AC subgroups (**Figure 3**). However, no significant interaction effects were found in the four subgroups (P for interaction > 0.05).

Feature Selection and Model Building

Cox proportional hazard regression revealed that SBI, KPS, TNM stage, IC, and CCRT were independent risk factors for BMFS (**Table 3**). AC was also selected due to its clinical value for tumor prognosis. A nomogram with the six factors is shown in **Figure 4**. The C-index for BMFS prediction in the training and validation datasets was 0.80 (95% CI 0.694–0.905) and 0.79 (95% CI 0.621–0.963), respectively. According to ROC analyses on both the training and validation datasets, the AUCs were 83.7% vs. 79.6%, 81.7% vs. 88.2%, and 79.0% vs. 93.8% for predicting 2-, 3-, and 5-year BMFS, respectively (**Figures 5A, B**). In addition, the calibration plot of the nomogram for the probability of BMFS at 2, 3, and 5 years showed strong agreement (**Figures 6A**–**F**), and the decision curve results indicated that the nomogram was clinically applicable (**Figures 7A**–**F**).

DISCUSSION

Novel treatments like IMRT have steadily reduced the rate of local/regional recurrence during LA-NPC, but distant metastasis still results in treatment failures (2). According to the "seed and soil" theory, bone metastasis most often results from nutrient-rich bone tissue, chemokine and cytokine mediation, and the unique ecological niche of the bone metastasis (5, 25). The present study developed a risk prediction model by

TABLE 2 | Tumor progression and survival analyses by the presence of skull base invasion.

Variable	SBI	Unadjusted model		Adjusted 1[a]		Adjusted 2[b]		Adjusted 3[c]	
		HR (95%CI)	*P* value	HR (95%CI)	*P* value	HR (95%CI)	*P* value	HR (95%CI)	*P* value
BMFS	–	1		1		1		1	
	+	2.43 (1.32-4.47)	0.004	2.52 (1.36-4.66)	0.003	2.28 (1.23-4.22)	0.009	2.31 (1.17-4.54)	0.015
DMFS	–	1		1		1		1	
	+	1.75 (1.05-2.93)	0.032	1.75 (1.04-2.93)	0.034	1.69 (1.01-2.83)	0.047	1.56 (0.92-2.65)	0.098
OS	–	1		1		1		1	
	+	1.69 (0.98-2.9)	0.057	1.84 (1.06-3.21)	0.031	1.64 (0.93-2.87)	0.086	1.56 (0.85-2.89)	0.153

SBI, skull base invasion; BMFS, bone metastasis free survival; DMFS, distant metastasis free survival; OS, overall survival.
[a]*Adjusted for hospital, age and sex.*
[b]*Adjusted for hospital, age, sex, karnofsky performance status, smoking index and histological type.*
[c]*Adjusted for all the variables.*

investigating the relationship between SBI and bone metastasis. SBI was significantly correlated with a higher incidence of bone metastasis and shorter BMFS. Even in multivariable-adjusted models, the results remained robust and stable. A nomogram of BMFS was developed and validated based on SBI and found to perform well in terms of calibration and discrimination.

Prior studies have assessed the risk factors for bone metastasis in NPC patients. Zhao et al. (26) suggested that bone metastasis is related to N but not T classification. Another study yielded comparable results (27). These studies did not specifically investigate the risk of bone metastasis caused by SBI, however. In the current study, 14.83% (43/290) patients had bone metastasis and SBI was significantly associated with increased risk of bone metastasis (20.69% vs. 10.92% for SBI-positive vs. SBI-negative patients, respectively) and shorter BMFS [HR 2.43 (1.32–4.47), $P < 0.05$]. A Cox proportional hazard model with major covariable adjustment was used to examine the effect of SBI on bone metastasis. The results remained robust and stable even after three adjustments ($P < 0.05$). Yi et al. (14) demonstrated the predictive value of SBI for bone metastasis, particularly in patients with early N-staging NPC. While SBI was associated with poor DMFS and OS in this study, however, the covariable adjusted model showed that SBI may not be an independent factor. Feng et al. has demonstrated that extensive SBI is not an independent prognostic factor for DMFS and OS (28). In a separate study of 181 N0 NPC patients, the high-risk advanced T category, which included SBI, was an independent prognostic factor for PFS, OS, and locoregional relapse-free survival (29). Subgroup analysis assessed the relationship between SBI and bone metastasis based on TNM stage, IC, CCRT, and AC. Of note, no significant interaction effects were found in the four subgroups (P for interaction >0.05). There is a strong link between SBI and bone metastasis in different subgroups, which is consistent with prior studies (30–32). Collectively, these data confirm a correlation between SBI and a greater risk of bone metastasis.

This study suggests that the development of a prediction model of bone metastasis based on SBI is both feasible and meaningful. Collinearity, which exists in variables that are similar or have a strong association, should be checked before modeling, and variables with significant collinearity should not be included (33–35). Given that SBI and T category had strong collinearity (r = 0.657) in this study, while TNM stage did not (r = 0.293), TNM stage was selected for subsequent analyses. Chen et al. (36) developed a prognostic score for NPC patients with bone

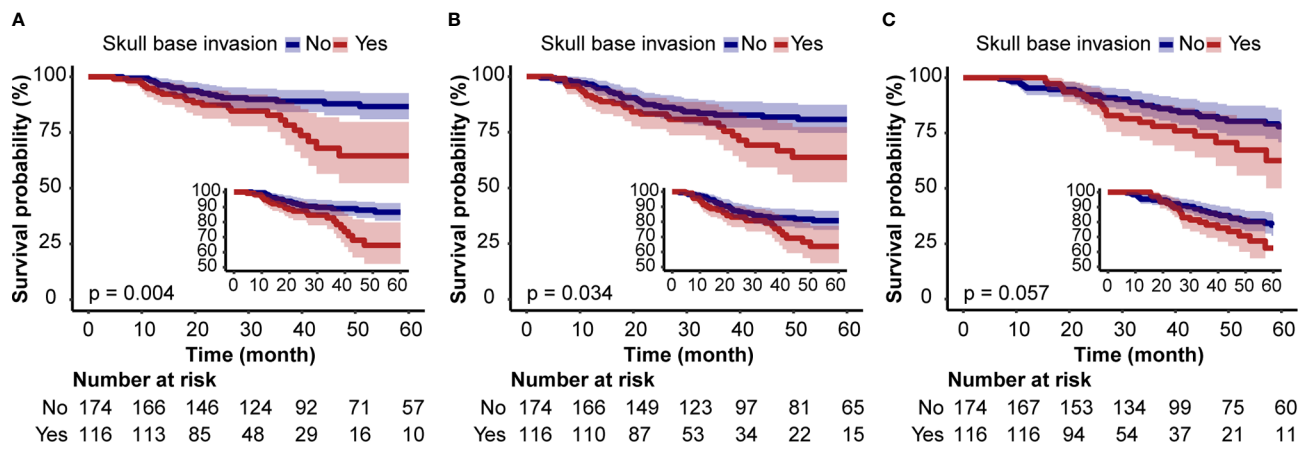

FIGURE 2 | Kaplan–Meier Survival Curves for bone metastasis-free survival **(A)**, distant metastasis-free survival, **(B)** and overall survival **(C)** of locally advanced nasopharyngeal carcinoma patients based on skull base invasion.

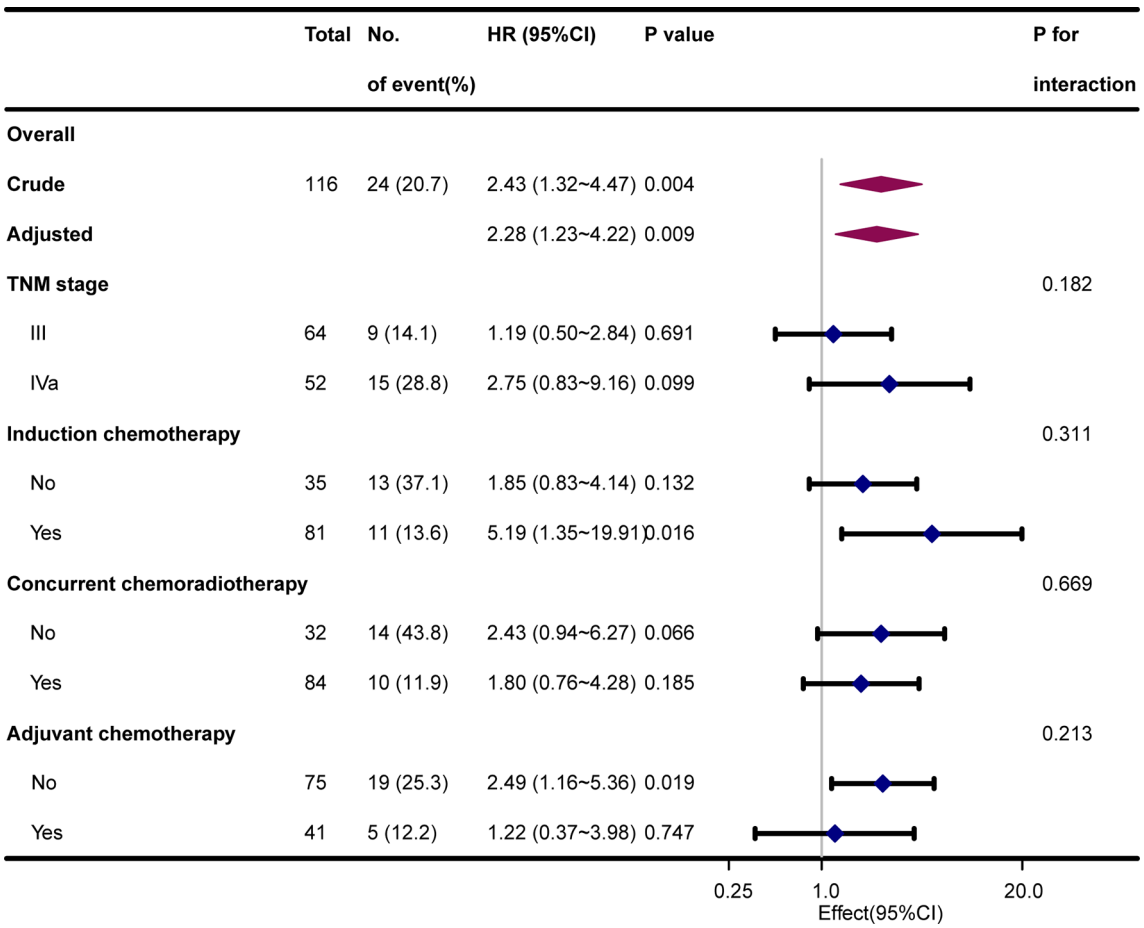

FIGURE 3 | Hazard risk of bone metastasis in subgroup analyses after adjustment for hospital, age, sex, Karnofsky performance status, smoking index, and histological type.

metastasis based on clinical routine factors. Another study (15) developed a nomogram using data from the Surveillance, Epidemiology, and End Results database to predict the prognosis of distant metastases. Yao et al. (37) used a nomogram to assess the benefits of adding IC to CCRT for N2-3 NPC patients and found that those in the high-risk group benefited more from combination therapy (DMFS: 69.5% vs. 56.7%, $P = 0.004$). There is no prediction model for bone metastasis risk in the Chinese population, however.

TABLE 3 | Risk factors selected by Cox proportional hazard regression analysis.

Variable	Univariable		Multivariable	
	HR (95%CI)	*P* value	HR (95%CI)	*P* value
SBI: +	2.43 (1.32-4.47)	0.003	2.17 (1.13-4.15)	0.020
Age: >55	2.66 (1.39-5.11)	0.002	1.01 (0.98-1.04)	0.416
Sex: male	1.25 (0.60-2.61)	0.540		
KPS: >70	2.30 (1.24-4.27)	0.012	1.78 (0.94-3.38)	0.078
Smoking index: >400	1.53 (0.82-2.84)	0.187		
Histological type: Non-keratinizing	1.75 (0.42-7.24)	0.399		
T category: T3-4	0.83 (0.45-1.53)	0.555		
N category: N2-3	3.66 (1.13-11.83)	0.009		
TNM stage: IVa stage	2.17 (1.18-3.96)	0.014	1.84 (0.98-3.46)	0.059
IC: Yes	0.36 (0.19-0.68)	< 0.001	0.26 (0.13-0.50)	0.000
CCRT: Yes	0.26 (0.14-0.47)	< 0.001	0.31 (0.16-0.60)	0.001
AC: Yes	0.58 (0.30-1.13)	0.100	0.61 (0.30-1.27)	0.187

SBI, skull base invasion; KPS, karnofsky performance status; IC, induction chemotherapy; CCRT, concurrent chemoradiotherapy; AC, adjuvant chemotherapy.

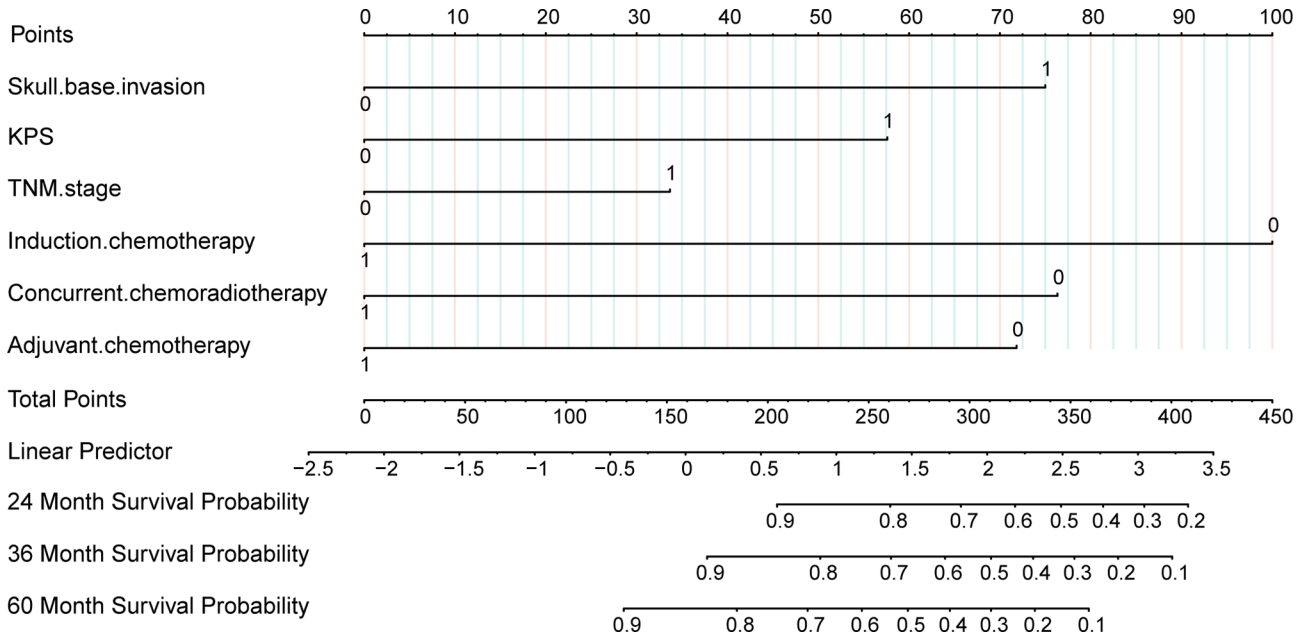

FIGURE 4 | Nomogram predicting 24, 36, and 60 months of bone metastasis-free survival.

Thus, a BMFS predictive model was developed based on SBI and visualized using a nomogram. The model included the following six components: SBI, KPS, TNM stage, IC, CCRT, and AC, and the nomogram performed well in both the training and validation datasets (C-index 0.80 vs. 0.79), which was consistent with the AUC at 2, 3, and 5 years. Calibration curves and DCA demonstrated the effectiveness of the nomogram. As a result, a nomogram based on SBI may provide an individual assessment of bone metastasis risk in LA-NPC patients.

The present study has several limitations. First, because it is a retrospective study, there is the possibility of both selection bias and confounding bias. Second, although the established nomogram model was trained and validated using data from two different hospitals, the sample size was small and external validation was not performed. Third, several variables including Epstein Barr Virus were not included in the analysis. Fourth, this study was conducted in an endemic area. So, extrapolation of the current results should be done with caution. Future studies should

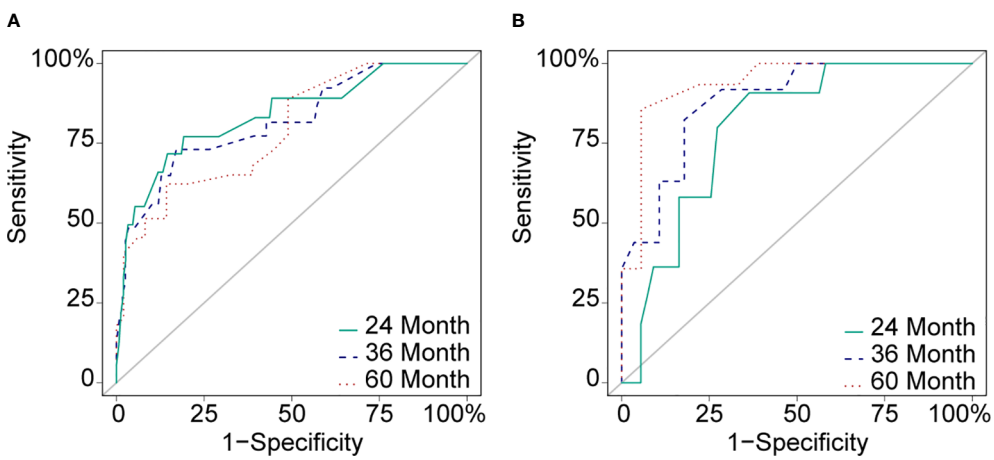

FIGURE 5 | ROC curves of the training dataset **(A)** and the validation dataset **(B)** in 24 months (AUC: 83.7% vs. 79.6%), 36 months (AUC: 81.7% vs. 88.2%) and 60 months (AUC: 79.0% vs. 93.8%).

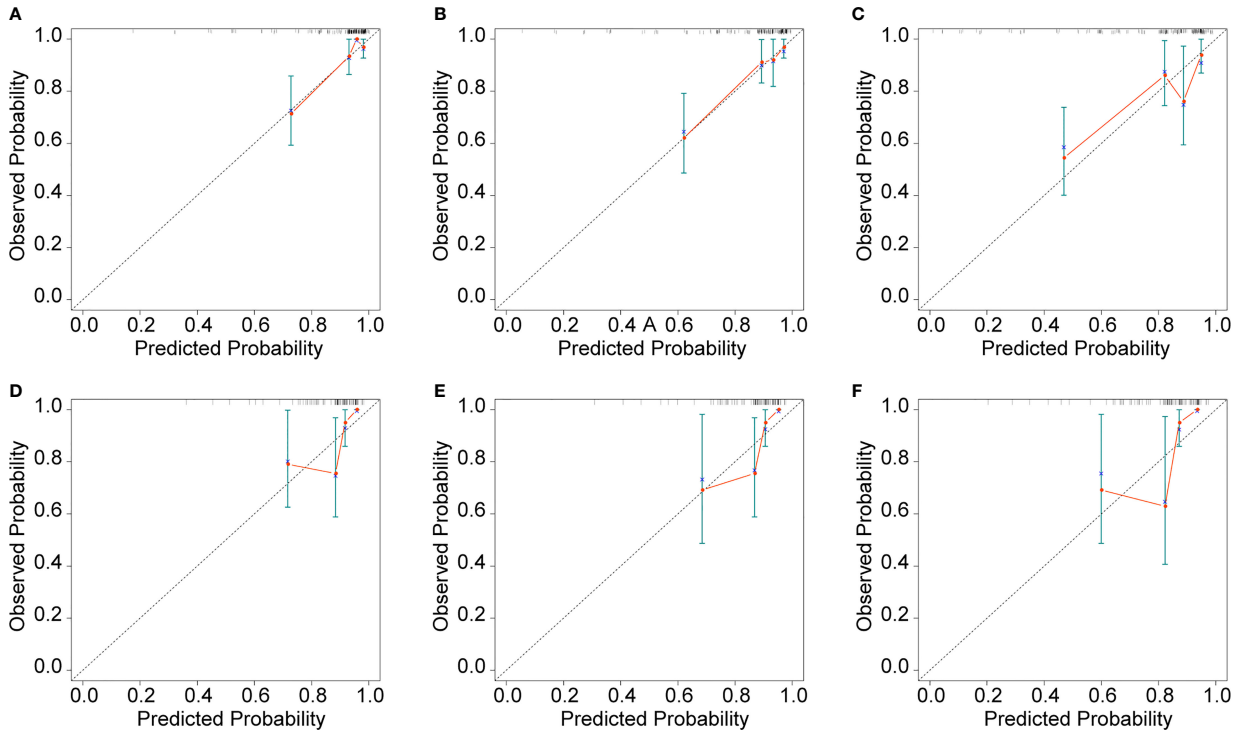

FIGURE 6 | Calibration curves of the training dataset **(A–C)** and the validation dataset **(D–F)** in 24, 36, and 60 months.

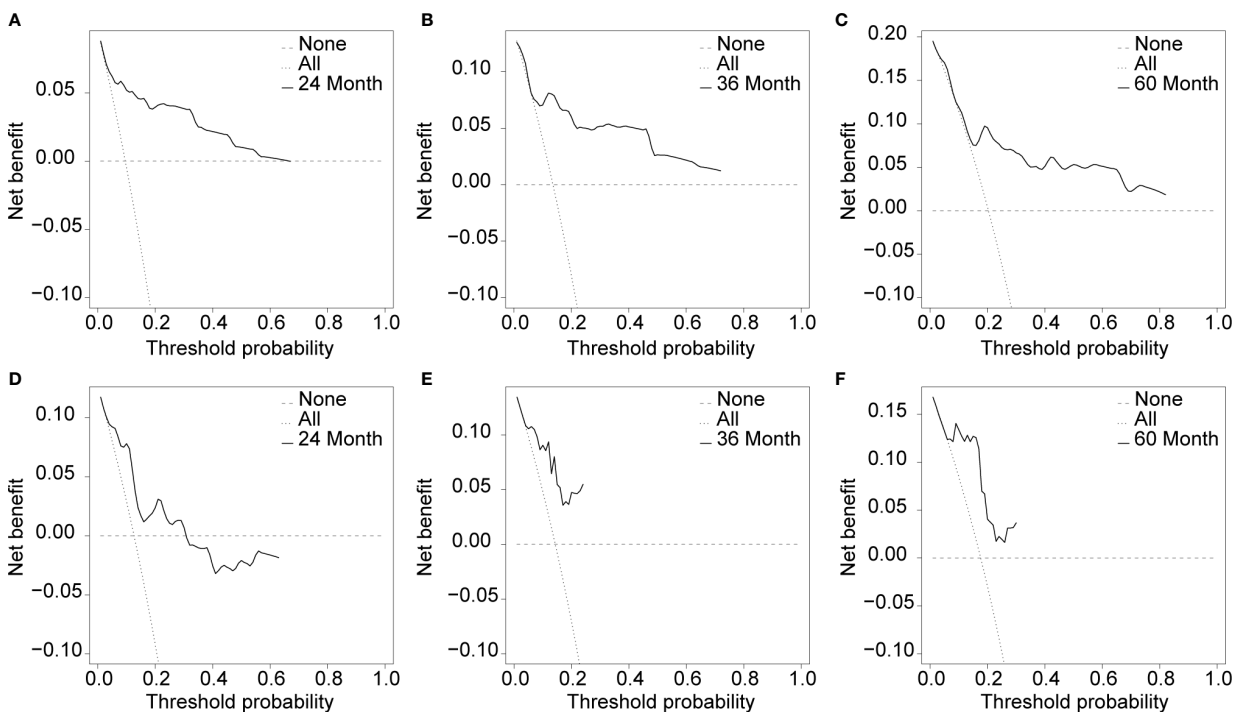

FIGURE 7 | Usefulness evaluation of the training dataset **(A–C)** and the validation dataset **(D–F)** in 24, 36, and 60 months.

consider establishing an updated model with a large sample size and detailed data that is subject to external validation.

In conclusion, both unadjusted and adjusted analyses showed that SBI is strongly associated with the risk of bone metastasis. The established SBI-based nomogram can be used to assess the risk of bone metastasis in individual LA-NPC patients.

DATA AVAILABILITY STATEMENT

The raw data supporting the conclusions of this article will be made available by the authors, without undue reservation.

ETHICS STATEMENT

The studies involving human participants were reviewed and approved by The Institutional Review Boards of Taizhou Central Hospital (Taizhou University Hospital). Written informed consent for participation was not required for this study in accordance with the national legislation and the institutional requirements.

AUTHOR CONTRIBUTIONS

BW and YT conceived the presented idea. YG and Q-GG collected the data. YG and HY analyzed the data, BW drafted the manuscript. YT improved the standard of English. All authors reviewed the manuscript and approved the submitted version.

FUNDING

This study was funded by the Medical and Health Science and Technology Program of Zhejiang Province (2020RC040).

ACKNOWLEDGMENTS

We thank the Team of Clinical Scientists for their helpful review and comments regarding the manuscript.

SUPPLEMENTARY MATERIAL

The Supplementary Material for this article can be found online at: https://www.frontiersin.org/articles/10.3389/fonc.2022.812358/full#supplementary-material

Supplementary Table 1 | Baseline characteristics of 290 locally advanced nasopharyngeal carcinoma patients grouped by hospital.

Supplementary Table 2 | Collinearity analysis of skull base invasion and covariables.

REFERENCES

1. Chen Y, Chan A, Le Q, Blanchard P, Sun Y, Ma J. Nasopharyngeal Carcinoma. *Lancet (London England)* (2019) 394(10192):64–80. doi: 10.1016/s0140-6736(19)30956-0
2. Ji MF, Sheng W, Cheng WM, Ng MH, Wu BH, Yu X, et al. Incidence and Mortality of Nasopharyngeal Carcinoma: Interim Analysis of a Cluster Randomized Controlled Screening Trial (PRO-NPC-001) in Southern China. *Ann Oncol: Off J Eur Soc Med Oncol* (2019) 30(10):1630–7. doi: 10.1093/annonc/mdz231
3. Zhang Y, Chen L, Hu GQ, Zhang N, Zhu XD, Yang KY, et al. Gemcitabine and Cisplatin Induction Chemotherapy in Nasopharyngeal Carcinoma. *New Engl J Med* (2019) 381(12):1124–35. doi: 10.1056/NEJMoa1905287
4. Liao S, Xie Y, Feng Y, Zhou Y, Pan Y, Fan J, et al. Superiority of Intensity-Modulated Radiation Therapy in Nasopharyngeal Carcinoma With Skull-Base Invasion. *J Cancer Res Clin Oncol* (2020) 146(2):429–39. doi: 10.1007/s00432-019-03067-y
5. Caglar M, Ceylan E, Ozyar E. Frequency of Skeletal Metastases in Nasopharyngeal Carcinoma After Initiation of Therapy: Should Bone Scans be Used for Follow-Up? *Nucl Med Commun* (2003) 24(12):1231–6. doi: 10.1097/00006231-200312000-00005
6. Liu FY, Chang JT, Wang HM, Liao CT, Kang CJ, Ng SH, et al. [18F] Fluorodeoxyglucose Positron Emission Tomography is More Sensitive Than Skeletal Scintigraphy for Detecting Bone Metastasis in Endemic Nasopharyngeal Carcinoma at Initial Staging. *J Clin Oncol: Off J Am Soc Clin Oncol* (2006) 24(4):599–604. doi: 10.1200/jco.2005.03.8760
7. Al Tamimi AS, Zaheer S, Ng DC, Osmany S. (18)F-Fluorodeoxyglucose-Positron Emission Tomography/Computed Tomography Imaging of Metastatic Nasopharyngeal Cancer With Emphasis on the Distribution of Bone Metastases. *World J Nucl Med* (2017) 16(3):192–6. doi: 10.4103/1450-1147.207273
8. Lu T, Guo Q, Cui X, Chen Z, Lin S, Xu L, et al. Prognostic Evaluation of Nasopharyngeal Carcinoma With Bone-Only Metastasis After Therapy. *Yonsei Med J* (2016) 57(4):840–5. doi: 10.3349/ymj.2016.57.4.840
9. Yang H, Liu C, Luo S, Ma R, Zhou Y, Yin Y, et al. Prognostic Analysis of 152 Patients With Distant Metastasis After Intensity-Modulated Radiotherapy for Nasopharyngeal Carcinoma. *Ann Palliat Med* (2021) 10(6):6824–32. doi: 10.21037/apm-21-1279
10. Yang X, Ren H, Yu W, Li H, Yang X, Fu J. Bone Metastases Pattern in Newly Diagnosed Metastatic Nasopharyngeal Carcinoma: A Real-World Analysis in the SEER Database. *BioMed Res Int* (2020) 2020:2098325. doi: 10.1155/2020/2098325
11. Li A-C, Xiao W-W, Shen G-Z, Wang L, Xu A-A, Cao Y-Q, et al. Distant Metastasis Risk and Patterns of Nasopharyngeal Carcinoma in the Era of IMRT: Long-Term Results and Benefits of Chemotherapy. *Oncotarget* (2015) 6(27):24511–21. doi: 10.18632/oncotarget.4312
12. Li YZ, Cai PQ, Xie CM, Huang ZL, Zhang GY, Wu YP, et al. Nasopharyngeal Cancer: Impact of Skull Base Invasion on Patients Prognosis and its Potential Implications on TNM Staging. *Eur J Radiol* (2013) 82(3):e107–11. doi: 10.1016/j.ejrad.2012.10.016
13. Zou GR, Li YH, Zeng WH, He Y, Gong Z, Cao XL. Correlation Between Skull Base Invasion and Bone Metastases in Locally Advanced Nasopharyngeal Carcinoma Patients. *Cancer Res Prev Treat* (2016) 43(10):4. doi: 10.3971/j.issn.1000-8578.2016.10.006
14. Yi W, Liu ZG, Li X, Tang J, Jiang CB, Hu JY, et al. CT-Diagnosed Severe Skull Base Bone Destruction Predicts Distant Bone Metastasis in Early N-Stage Nasopharyngeal Carcinoma. *OncoTarg Ther* (2016) 9:7011–7. doi: 10.2147/ott.S99717
15. Qu W, Li S, Zhang M, Qiao Q. Pattern and Prognosis of Distant Metastases in Nasopharyngeal Carcinoma: A Large-Population Retrospective Analysis. *Cancer Med* (2020) 9(17):6147–58. doi: 10.1002/cam4.3301
16. Iasonos A, Schrag D, Raj GV, Panageas KS. How to Build and Interpret a Nomogram for Cancer Prognosis. *J Clin Oncol: Off J Am Soc Clin Oncol* (2008) 26(8):1364–70. doi: 10.1200/jco.2007.12.9791
17. Peng H, Chen L, Mao Y, Tian L, Liu LJO. Nomogram-Aided Individual Induction Chemotherapy Regimen Selection in Advanced Nasopharyngeal Carcinoma. *Oral Oncol* (2021) 122:105555. doi: 10.1016/j.oraloncology.2021.105555

18. Zhang LL, Xu F, Song D, Huang MY, Huang YS, Deng QL, et al. Development of a Nomogram Model for Treatment of Nonmetastatic Nasopharyngeal Carcinoma. *JAMA Netw Open* (2020) 3(12):e2029882. doi: 10.1001/jamanetworkopen.2020.29882
19. Yang K, Zhang Q, Zhang M, Xie W, Li M, Zeng L, et al. A Nomogram for the Determination of the Necessity of Concurrent Chemotherapy in Patients With Stage II-IVa Nasopharyngeal Carcinoma. *Front Oncol* (2021) 11:640077. doi: 10.3389/fonc.2021.640077
20. Cheng YK, Liu LZ, Jiang N, Yue D, Tang LL, Zhang F, et al. MRI-Detected Skull-Base Invasion: Prognostic Value and Therapeutic Implication in Intensity-Modulated Radiotherapy Treatment for Nasopharyngeal Carcinoma. *Strahlentherapie Und Onkol: Organ Der Deutschen Rontgengesellschaft* (2014) 190(10):905–11. doi: 10.1007/s00066-014-0656-7
21. Hu W, Wang W, Yang P, Zhou C, Yang W, Wu B, et al. Phase I Study of Icotinib, an EGFR Tyrosine Kinase Inhibitor Combined With IMRT in Nasopharyngeal Carcinoma. *Int J Clin Exp Med* (2015) 8(9):15675–83.
22. Wang W, Yang H, Hu W, Shan G, Ding W, Yu C, et al. Clinical Study of the Necessity of Replanning Before the 25th Fraction During the Course of Intensity-Modulated Radiotherapy for Patients With Nasopharyngeal Carcinoma. *Int J Radiat Oncol Biol Phys* (2010) 77(2):617–21. doi: 10.1016/j.ijrobp.2009.08.036
23. Alba A, Agoritsas T, Walsh M, Hanna S, Iorio A, Devereaux P, et al. Discrimination and Calibration of Clinical Prediction Models: Users' Guides to the Medical Literature. *JAMA* (2017) 318(14):1377–84. doi: 10.1001/jama.2017.12126
24. Van Calster B, Wynants L, Verbeek J, Verbakel J, Christodoulou E, Vickers A, et al. Reporting and Interpreting Decision Curve Analysis: A Guide for Investigators. *Europ Urol* (2018) 74(6):796–804. doi: 10.1016/j.eururo.2018.08.038
25. Paget S. The Distribution of Secondary Growths in Cancer of the Breast. 1889. *Cancer Metastasis Rev* (1989) 8(2):98–101.
26. Zhao CL, Qian GQ, Chen XY, Chen C. Retrograde Analysis of Clinical Characteristics of Bone Metastasis in 1,031 Cases of Preliminarily Diagnosed Nasopharyngeal Carcinoma. *Asian Pacific J Cancer Prevention: APJCP* (2014) 15(8):3785–8. doi: 10.7314/apjcp.2014.15.8.3785
27. Guo Q, Lu T, Chen Y, Su Y, Zheng Y, Chen Z, et al. Genetic Variations in the PI3K-PTEN-AKT-mTOR Pathway are Associated With Distant Metastasis in Nasopharyngeal Carcinoma Patients Treated With Intensity-Modulated Radiation Therapy. *Sci Rep* (2016) 6:37576. doi: 10.1038/srep37576
28. Feng Y, Cao C, Hu Q, Chen X. Grading of MRI-Detected Skull-Base Invasion in Nasopharyngeal Carcinoma With Skull-Base Invasion After Intensity-Modulated Radiotherapy. *Radiat Oncol (London England)* (2019) 14(1):10. doi: 10.1186/s13014-019-1214-3
29. Chen YP, Tang LL, Zhang WN, Mao YP, Chen L, Sun Y, et al. Prognostic Value and Grading of MRI-Based T Category in Patients With Nasopharyngeal Carcinoma Without Lymph Node Metastasis Undergoing Intensity-Modulated Radiation Therapy. *Medicine* (2015) 94(43):e1624. doi: 10.1097/MD.0000000000001624
30. Wong KCW, Hui EP, Lo KW, Lam WKJ, Johnson D, Li L, et al. Nasopharyngeal Carcinoma: An Evolving Paradigm. *Nat Rev Clin Oncol* (2021) 18(11):1–17. doi: 10.1038/s41571-021-00524-x
31. Blanchard P, Lee A, Marguet S, Leclercq J, Ng WT, Ma J, et al. Chemotherapy and Radiotherapy in Nasopharyngeal Carcinoma: An Update of the MAC-NPC Meta-Analysis. *Lancet Oncol* (2015) 16(6):645–55. doi: 10.1016/s1470-2045(15)70126-9
32. Chen YP, Tang LL, Yang Q, Poh SS, Hui EP, Chan ATC, et al. Induction Chemotherapy Plus Concurrent Chemoradiotherapy in Endemic Nasopharyngeal Carcinoma: Individual Patient Data Pooled Analysis of Four Randomized Trials. *Clin Cancer Res* (2018) 24(8):1824–33. doi: 10.1158/1078-0432.CCR-17-2656
33. Wu M, Li X, Zhang T, Liu Z, Zhao Y. Identification of a Nine-Gene Signature and Establishment of a Prognostic Nomogram Predicting Overall Survival of Pancreatic Cancer. *Front Oncol* (2019) 9:996. doi: 10.3389/fonc.2019.00996
34. Xie C, Li H, Yan Y, Liang S, Li Y, Liu L, et al. A Nomogram for Predicting Distant Metastasis Using Nodal-Related Features Among Patients With Nasopharyngeal Carcinoma. *Front Oncol* (2020) 10:616. doi: 10.3389/fonc.2020.00616
35. Chen S, Qiu A, Tao Z, Zhang H. Clinical Impact of Cardiovascular Disease on Patients With Bronchiectasis. *BMC Pulm Med* (2020) 20(1):101. doi: 10.1186/s12890-020-1137-7
36. Chen C, Wu JB, Jiang H, Gao J, Chen JX, Pan CC, et al. A Prognostic Score for Nasopharyngeal Carcinoma With Bone Metastasis: Development and Validation From Multicenter. *J Cancer* (2018) 9(5):797–806. doi: 10.7150/jca.22663
37. Yao JJ, Jin YN, Liu ZG, Liu QD, Pei XF, Zhou HL, et al. Do All Patients With Advanced N-Stage Nasopharyngeal Carcinoma Benefit From the Addition of Induction Chemotherapy to Concurrent Chemoradiotherapy? *Ther Adv Med Oncol* (2019) 11:1758835919833863. doi: 10.1177/1758835919833863

Conflict of Interest: The authors declare that the research was conducted in the absence of any commercial or financial relationships that could be construed as a potential conflict of interest.

frontiers | Frontiers in Oncology

CLINICAL TRIAL
published: 27 April 2022
doi: 10.3389/fonc.2022.842281

A Single-Arm Phase 2 Trial on Induction Chemotherapy Followed by Concurrent Chemoradiation in Nasopharyngeal Carcinoma Using a Reduced Cumulative Dose of Cisplatin

Zhiyuan Xu[1,2†], Li Yang[2†], Wai-Tong Ng[2,3], Aya El Helali[2,3], Victor Ho-Fun Lee[2,3], Lingyu Ma[2], Qin Liu[2], Jishi Li[2], Lin Shen[2], Jijie Huang[2], Jiandong Zha[2], Cheng Zhou[1], Anne W. M. Lee[2,3] and Longhua Chen[1]*

[1] Department of Radiation Oncology, Nanfang Hospital, Southern Medical University, Guangzhou, China, [2] Clinical Oncology Centre, The University of Hong Kong - Shenzhen Hospital, Shenzhen, China, [3] Department of Clinical Oncology, The University of Hong Kong, Hong Kong, Hong Kong SAR, China

OPEN ACCESS

Edited by:
Steffi Ulrike Pigorsch,
Technical University of Munich,
Germany

Reviewed by:
Zhen Tao,
Tianjin Medical University Cancer Institute and Hospital, China
Govind Babu Kanakasetty,
HCG Cancer Hospital, India
Zhong Lin,
The Fifth Affiliated Hospital of Sun Yat-sen University, China

***Correspondence:**
Longhua Chen
18307555170@163.com

[†]These authors have contributed equally to this work

Specialty section:
This article was submitted to Head and Neck Cancer, a section of the journal Frontiers in Oncology

Received: 23 December 2021
Accepted: 25 March 2022
Published: 27 April 2022

Citation:
Xu Z, Yang L, Ng W-T, Helali AE, Lee VH-F, Ma L, Liu Q, Li J, Shen L, Huang J, Zha J, Zhou C, Lee AWM and Chen L (2022) A Single-Arm Phase 2 Trial on Induction Chemotherapy Followed by Concurrent Chemoradiation in Nasopharyngeal Carcinoma Using a Reduced Cumulative Dose of Cisplatin. Front. Oncol. 12:842281. doi: 10.3389/fonc.2022.842281

Background: We conducted this study to evaluate if a reduced cumulative dose of induction and concurrent cisplatin conferred similar favorable outcomes when compared to trial NPC-0501.

Methods: Newly diagnosed nasopharyngeal carcinoma (NPC) with stage III-IVA were prospectively recruited from January 2015 to September 2019. Induction chemotherapy (IC) consisted of cisplatin 80mg/m^2 on day 1 and capecitabine 1000mg/m^2 twice daily from day 1 to 14 every 3 weeks for 3 cycles followed by concurrent chemoradiotherapy (CCRT) with 2 cycles of cisplatin 100mg/m^2 given every 3 weeks. Tumor response was evaluated according to RECIST v1.1. Acute and late adverse events (AEs) were graded with CTCAE v4.0 and Late Radiation Morbidity Scoring of the RTOG, respectively.

Results: 135 patients were recruited. At 16 weeks after CCRT, all 130 patients who completed the entire course of radiotherapy (RT) had a complete response upon final assessment. With a median follow-up of 36.2 months, 22 treatment failures and 8 deaths were observed. The 3-year progression-free survival, overall survival, locoregional recurrence-free survival, and distant recurrence-free survival were 83.7%, 94.1%, 94.1%, and 85.9%, respectively. Our survival data outcomes were similar to those reported in the cisplatin and capecitabine (PX) induction arm of the 0501 trial. 103 patients (76.3%) reported acute grade 3-4 AEs. Two patients (1.5%) had late grade 3-4 complications, numerically fewer than those reported in the NPC-0501 trial.

Conclusions: Induction PX and concurrent cisplatin with a reduced cumulative cisplatin dose yield survival outcomes comparable to those reported in the NPC-0501 trial with

excellent tolerability. Therefore, a reduced cumulative dose of cisplatin is a promising treatment scheme for nasopharyngeal carcinoma.

Keywords: nasopharyngeal carcinoma, induction chemotherapy, cisplatin, capecitabine, progression-free survival

INTRODUCTION

Nasopharyngeal carcinoma (NPC) is an endemic malignancy with a specific geographical distribution. It will affect an estimated 133,354 patients worldwide in 2020, with the highest incidences occurring in South China, Southeast Asia, and North Africa (1, 2). More than 70% of NPC patients have locoregionally advanced disease at the time of presentation (3). Intensity-modulated radiation therapy (IMRT) with concurrent platinum-based chemotherapy constitutes the backbone of treatment for locoregionally advanced nasopharyngeal carcinoma (LA NPC). Although the locoregional control rate in NPC has been substantially improved, distant metastasis remains the predominant pattern of treatment failure (4).

The addition of chemotherapy as induction or adjuvant regimen to concurrent chemoradiotherapy (CCRT) has been extensively investigated. Since the first report of significant survival benefits by the Intergroup 0099 study (5), the addition of adjuvant cisplatin and 5-fluorouracil (PF) to CCRT has become a standard of care recommendation for patients with LA NPC (6). However, a significant concern regarding the concurrent-adjuvant approach is poor compliance (approximately 60%) to three cycles of adjuvant chemotherapy (7). Compared with adjuvant chemotherapy (AC), induction chemotherapy (IC) offers improved tolerability, early eradication of micrometastases, wider margin, and better radiation coverage during subsequent CCRT. A phase 3 randomized controlled trial in Hong Kong (NPC-0501) evaluated the therapeutic gain of changing the chemotherapy sequence from concurrent-adjuvant to induction-concurrent and replacing 5-fluorouracil with capecitabine for patients with LA NPC (7, 8). This trial revealed that changing the chemotherapy sequence from a concurrent-adjuvant to an induction-concurrent sequence could improve efficacy without adversely impacting toxicities. Furthermore, replacing 5- fluorouracil with capecitabine significantly lowered the risk of progression and death. Induction cisplatin plus capecitabine (PX) incurred fewer toxicities such as neutropenia and electrolyte disturbance than induction PF (7, 8). In addition, capecitabine has shown a promising survival benefit in maintenance therapy for metastatic nasopharyngeal carcinoma (9). However, the switch from 5-fluorouracil to oral capecitabine warrants further validation given its convenience, favorable toxicity profile, and favorable trends in efficacy.

Patients allocated to the induction-PX arm in the NPC-0501 trial received induction cisplatin 100 mg/m^2 on day 1 plus capecitabine 1000 mg/m ^{2} twice daily on days 1 to 14 every 21 days for 3 cycles and concurrent cisplatin 100mg/m^2 on day 1 every 21 days for 3 cycles. The proportion of patients that received 3 concurrent cycles was 33% in the induction-PX arm. Most induction platinum-based doublet chemotherapy regimens implemented a cisplatin dose of 75-80mg/m^2 for 2 to 3 cycles (10–12). Furthermore, some evidence suggested that a cumulative cisplatin dose of 200 mg/m^2 during CCRT may be adequate to achieve a survival benefit (13, 14). However, whether or not a reduced cumulative cisplatin dose in both induction PX and the CCRT phases provide comparable treatment outcomes to that reported in the NPC-0501 trial remains unclear. Therefore, we conducted this prospective, single-arm, phase 2 trial to investigate the efficacy and safety of reduced cumulative cisplatin in PX induction chemotherapy and CCRT in LA NPC.

METHODS

Study Design and Patients

This study was a prospective, single-arm, phase 2 trial conducted in a single institute in China. Eligibility was defined as newly diagnosed, previously untreated, histologically confirmed non-keratinizing NPC, stage III-IVB disease as per the 7th edition of the American Joint Committee on Cancer–Union for International Cancer Control (AJCC-UICC TNM-7) for patients diagnosed before 2018 or stage III-IVA disease as per AJCC-UICC TNM-8 for patients diagnosed on or after 2018 (except T3N0). Re-staging was performed using AJCC-UICC TNM-8 for patients enrolled prior to 2018 by two independent oncologists before the final analyses of this study. Any discrepancy in staging was resolved by consensus. Other inclusion criteria were age 18 to 75 years, an Eastern Cooperative Oncology Group (ECOG) performance status (PS) ≤ 2, adequate hematologic, hepatic, and renal function. Key exclusion criteria were the following: treatment for palliative intent; a history of prior malignancy; a history of previous chemotherapy, radiotherapy, or surgery (except diagnostic procedures) to the primary tumor or nodes; pregnancy or lactation; or any severe comorbidity. The local institutional ethics committee approved the trial protocol (reference number 201627). The trial was conducted according to the Declaration of Helsinki and Good Clinical Practice guidelines. All patients provided written informed consent before enrollment. Patients could withdraw consent at any time after enrollment. This trial is registered on clinicaltrials.gov as NCT03427359, (https://clinicaltrials.gov/ct2/show/NCT03427359?term=NCT03427359&draw=2&rank=1).

Pre-treatment assessment included the following: complete history and physical examination; complete blood count, renal and liver function tests; Epstein-Barr virus- deoxyribonucleic acid (EBV-DNA) test; dental, audiometric, and nutritional assessment; fiberoptic nasopharyngoscopy; magnetic resonance imaging (MRI) or contrast-enhanced computed tomography (CT) of the head and neck region (if MRI was contraindicated)

for primary tumor staging; contrast-enhanced CT of the chest and abdomen, together with skeletal scintigraphy for distant metastasis staging. 18F-fluorodeoxyglucose-positron-emission tomography with integrated computed tomography (PET-CT) scan was recommended though not mandatory.

Treatment and Assessment

Patients received induction PX with cisplatin at a dose of 80 mg/m^2 as an intravenous infusion on day 1 plus oral capecitabine at a dose of 1000 mg/m^2 twice daily from day 1 to 14 every 21 days for 3 cycles. In the CCRT phase, cisplatin was delivered concurrently with radiotherapy (RT) and administered intravenously at a dose of 100 mg/m^2 on days 1 and 22 for 2 cycles. Details of the chemotherapy dose modifications are available in the **Supplementary Appendix**.

Treatment with intensity-modulated radiotherapy (IMRT) or volumetric modulated arc therapy (VMAT) was mandatory for all patients. Doses of 70 Gy, 63 Gy, and 56 Gy were delivered to planning target volumes (PTV) at three levels (high, intermediate, and low risk, respectively) in 35 fractions over 7 weeks. An optional RT boost was allowed for patients with residual disease after CCRT. The details regarding RT are provided in the **Supplementary Appendix**. It was recommended that patients commence CCRT within 3 to 4 weeks after the first day of the last cycle of IC.

After completing IC and 16 weeks following RT, tumor responses were assessed with complete physical examination, fiberoptic nasopharyngoscopy, and MRI of the head and neck region, according to the Response Evaluation Criteria in Solid Tumors version 1.1 (RECIST v1.1) (15). Further investigations with contrast-enhanced CT scan of the thorax and abdomen (or PET-CT) were arranged when indicated. Complete physical examination at the end of RT and fiberoptic nasopharyngoscopy with random nasopharyngeal biopsies 8 weeks after the completion of RT were recommended to assess if RT boost was needed. Persistent primary or lymph node disease 16 weeks after the completion of RT was considered a locoregional failure. Acute toxicities during IC and CCRT were evaluated according to the Common Terminology Criteria for Adverse Events version 4.0 (CTCEA v4.0). Late RT-related toxicities were graded according to the Late Radiation Morbidity Scoring Criteria of the Radiation Therapy Oncology Group (16).

In the first 3 years of follow-up, all the patients had regular assessments every 3 months and every 6 months thereafter until death. Whenever possible, locoregional or distant recurrences were confirmed by fine-needle aspiration or biopsy. All endpoints were assessed or confirmed by the primary treating physician.

End Points

The primary endpoint was progression-free survival (PFS), defined as the time from the start of IC to the first failure at any site (either distant metastasis or locoregional recurrence) or death from any cause, whichever occurred first. Secondary endpoints included overall survival (OS) (the time from the start of IC to death from any cause), locoregional recurrence-free survival (LRFS) (the time from the start of IC to first locoregional failure), distant metastasis-free survival (DMFS) (the time from the start of IC to distant failure), tumor response, compliance to treatment, and severe (grade ≥ 3) acute and late toxicities.

Statistical Analysis

This non-inferiority trial aimed to evaluate whether the PFS of induction PX-CCRT with reduced cumulative cisplatin dose in LA NPC was not inferior to PFS reported in the NPC-0501 trial. The reported 3-year PFS in the induction PX-CCRT group (Arm 3A) in the NPC-0501 trial was 81% (7). Given the threshold of non-inferior effect δL= -10%, we estimated that 101 NPC cases could achieve 80.1% power by one-side log-rank test at the significance level of 0.05 (17, 18). Assuming 5% early dropout or loss to follow-up, the target accrual was a minimum of 107 patients.

Efficacy analyses were done in both intention-to-treat and per-protocol populations (see the **Supplementary Appendix**). Only patients who received at least 1 cycle of induction PX were included in the safety analyses. Patient demographics, clinicopathologic, and treatment-related factors were reported by descriptive statistics. For each chemotherapy drug of PX, the dose intensity (DI) was calculated as the ratio of the total dose per square meter of the patient, divided by the total treatment duration (mg/m^2/week). The relative DI was calculated as the ratio of the DI delivered to the DI planned by the protocol. Kaplan–Meier curves were used to describe time-to-event data, and the subgroups were compared with the log-rank tests. All statistical analyses were performed by R software version 3.6.1 and SPSS software version 26.0 (IBM). A two-sided P-value less than 0.05 was considered clinically significant.

RESULTS

Patients Characteristics

From January 2015 to September 2019, 135 eligible patients were accrued (**Figure 1**). The median age was 45 years (range 19-70), and 95 (70.4%) patients were male. The detailed characteristics of the patients are shown in **Table 1**.

Treatment Tolerance and Compliance

All 135 patients started protocol-defined induction IC (**Figure 1**). A total of 128 patients (94.8%) completed 3 cycles of induction PX. 7 patients (5.2%) failed to complete 3 cycles of induction PX. 2 (1.5%) patients received only one cycle, and 5 (3.7%) patients received two cycles. The reasons for discontinuing PX were shown in **Figure 1**. During IC, 7 patients (5.2%) required dose reductions of cisplatin and/or capecitabine because of neutropenia (n= 1 patient), severe vomiting (n= 2 patients), renal impairment (n= 1 patient), electrolyte disturbance (n= 1 patient), legs edema (n= 1 patient), and common cold (n=1 patient). 1 patient forgot to take the medication. Overall, the median relative DI was 96.2% (interquartile range [IQR], 91.2% to 99.0%) for cisplatin and 93.1% (IQR, 88.7% to 97.2%) for capecitabine (**Table 2**).

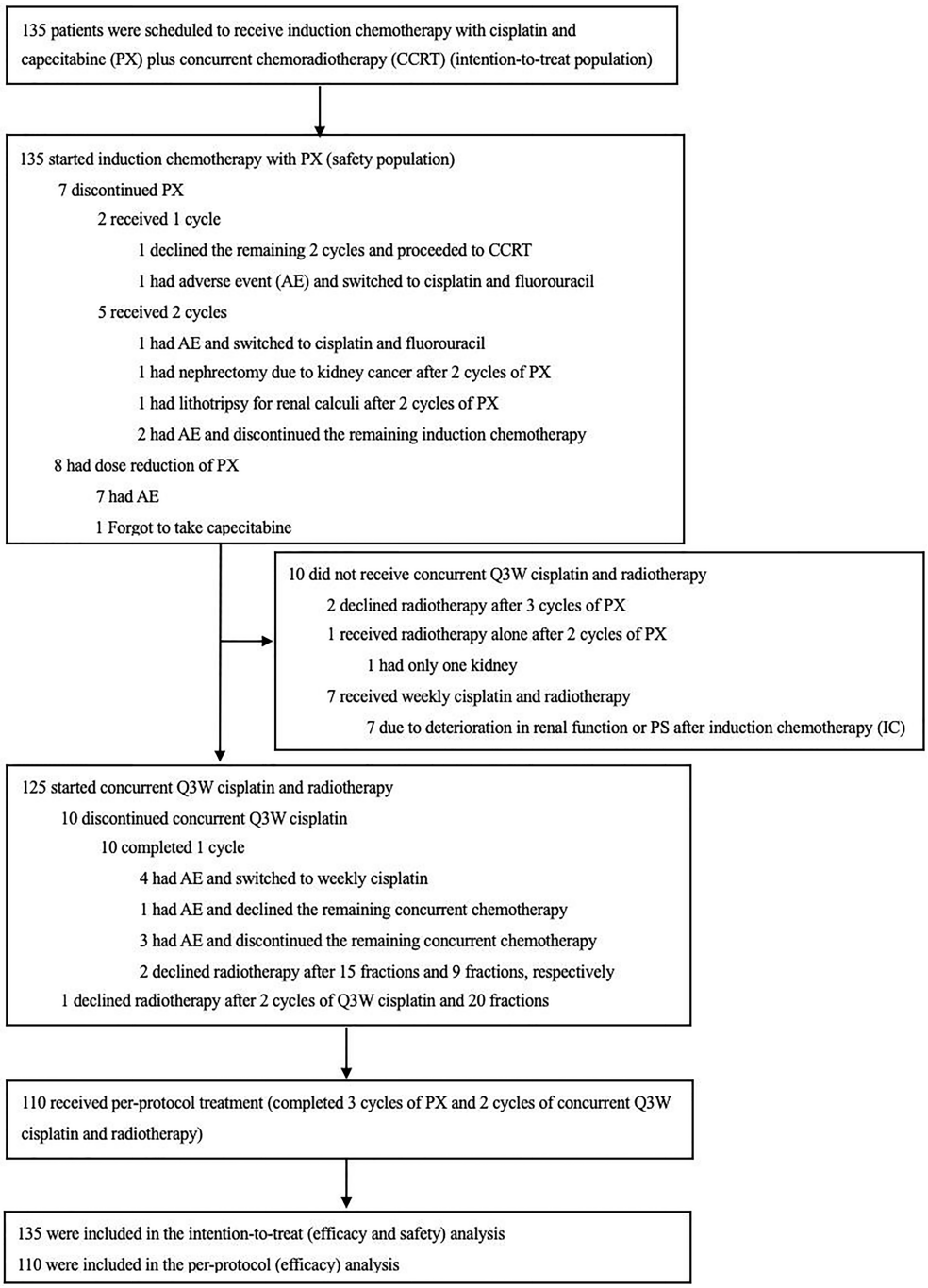

FIGURE 1 | Enrollment and Follow-up.

Regarding concurrent cisplatin, 125 patients (92.6%) started protocol-defined Q3W cisplatin, 7 patients (5.2%) started weekly cisplatin (at 40mg/m^2) due to deterioration in renal function or performance status (PS) after IC. Additionally, three patients (2.2%) received no chemotherapy, one patient received RT alone due to a single kidney, and two patients declined RT. A total of 115 of the 135 patients (85.2%) completed 2 cycles of concurrent Q3W cisplatin, and ten patients (7.4%) received only one cycle of concurrent Q3W cisplatin (**Figure 1**). Only one patient (0.7%) switched to concurrent carboplatin due to deterioration in renal function. Overall, 97 of 135 patients (71.9%) received at least 200mg/m^2 of concurrent cisplatin (including Q3W and weekly cisplatin). 93 patients (68.9%) received the full protocol-defined cumulative cisplatin dose of 440mg/m2 (**Table 2**). However in

TABLE 1 | Patient clinicopathological characteristics at baseline.

Characteristics	Number of Patients (%)
Total patients	135
Median age (range) – year old	45 (19–70)
Gender	
Male	95 (70.4)
Female	40 (29.6)
Technology	
IMRT	60(44.4)
VMAT	75(55.6)
ECOG performance status	
0	9 (6.7)
1	125 (92.6)
2	1 (0.7)
Tumor category (T)[£]	
T1	11 (8.1)
T2	30 (22.2)
T3	65 (48.1)
T4	29 (21.5)
Lymph node category (N)[£]	
N0	3 (2.2)
N1	16 (11.9)
N2	83 (61.5)
N3	33 (24.4)
Disease stage[£]	
III	78 (57.8)
IVA	57 (42.2)

IMRT, Intensity-modulated radiotherapy; VMAT, Volumetric Modulated Arc Therapy; ECOG, Eastern Cooperative Oncology Group.

[£]Tumor and node categories and disease stage were assessed according to the 8th edition of the American Joint Committee on Cancer–Union for International Cancer Control stage classification system.

practice, when we calculate chemotherapy doses based on body surface area, we would round to the nearest whole number. The actual median cumulative dose of cisplatin in the overall patient population was 430mg/m^2 (IQR, 410 to 440).

Regarding RT, 133 patients (98.5%) started RT, and the remaining 2 patients (1.5%) declined RT after completing 3 cycles of induction PX. A total of 130 patients (96.3%) completed protocol-defined IMRT/VMAT, and another 3 patients (2.2%) declined treatment after 18Gy, 30Gy, and 40 Gy of RT, respectively. On completion of RT, one patient (0.7%) had residual disease of cervical metastatic lymph nodes and received an electron boost to the residual disease. At eight weeks after RT, the pathology-proven residual disease of primary tumor of nasopharynx was detected in one patient (0.7%), and a VMAT boost was delivered. The median time from the start of the last cycle of IC to the commencement of RT was 21 days (IQR, 21 to 24). The median time from the start of the first cycle of IC to the completion of RT was 116 days (IQR, 113 to 121).

Efficacy

Among the 135 patients recruited to the study, 127 patients (94.1%) achieved a response after IC before the commencement of RT. 15 patients (11.1%) had a complete response (CR), 112 patients (83.0%) had a partial response (PR), and 8 patients (5.9%) had stable disease (SD). No patients had disease progression after IC. At 16 weeks after radiotherapy, all 130 patients (96.3%) who completed the entire course of RT achieved CR. The response of 5 patients (3.8%) who did not complete RT was unavailable (**Table S1 in the Supplementary Appendix**).

At the last follow-up on April 4, 2021, the median follow-up duration was 36.2 months (IQR, 26.1 to 51.8). Twenty-two patients (16.3% of the trial population) experienced disease recurrence, and 8 patients died. Details regarding the patterns of relapse and cause of death are provided in **Table S2 in the Supplementary Appendix**.

For the intention-to-treat population, the 3-year PFS, OS, LRFS, and DMFS were 83.7% (95% confidence interval [CI], 76.4% to 89.5%), 94.1% (95% CI, 88.7% to 97.4%), 94.1% (95% CI, 88.7% to 97.4%), and 85.9% (95% CI, 78.9% to 91.3%), respectively (**Table 3** and **Figures 2A-D**).

For per-protocol population, the 3-year PFS, OS, LRFS, and DMFS were 85.5% (95% CI, 77.5% to 91.5%), 94.5% (95% CI, 88.5% to 98.0%), 94.5% (95% CI, 88.5% to 98.0%), and 87.3% (95% CI, 79.6% to 92.9%), respectively (**Figures S1A-D in the Supplementary Appendix**).

Adverse Events

During IC, 29 patients (21.5%) experienced acute grade 3 or 4 (G3-4) adverse events (AEs). Neutropenia was the most common G3-4 AEs (14.8%), followed by electrolyte disturbance (8.9%) and anemia (7.4%). G3-4 capecitabine-related hand-foot syndrome was uncommon (0.7%). During CCRT, 74.1% of patients reported G3-4 AEs. Leukopenia was the most common G3-4 AEs (43.7%), followed by mucositis (28.9%) and anemia (25.9%) (**Table 4**). As for any late toxicity, only 2 out of 135 patients (1.5%) had ≥ G3-4 late RT toxicities (**Table 4**). There was no treatment-related death.

TABLE 2 | Compliance/tolerance of chemotherapy.

	Induction	Concurrent
No. of cycles of chemotherapy (%)		
3 cycles	128 (94.8)	0 (0)
2 cycles	5 (3.7)	115 (85.2)
1 cycle	2 (1.5)	10 (7.4)
None	0 (0)	3 (2.2)
Cumulative dose (mg/m^2)		
Cisplatin (Median, IQR)	240 (230-240)	200 (175-200)
Capecitabine (Median, IQR)	5800 (5500-6000)	–

IQR, interquartile range.

TABLE 3 | Survival to Treatment.

Variable	Survival
Progression-free survival	
Progression or death — no. (%)	22 (16.3)
Percentage of patients alive and without progression at 3 yr (95% CI)	83.7% (76.4% - 89.5%)
Overall survival	
Death — no. (%)	8 (5.9)
Percentage of patients alive at 3 yr (95% CI)	94.1% (88.7% - 97.4%)
Locoregional recurrence–free survival	
Locoregional recurrence — no. (%)	8 (5.9)
Percentage of patients without locoregional recurrence at 3 yr (95% CI)	94.1% (88.7% - 97.4%)
Distant metastasis–free survival	
Distant metastasis — no. (%)	19 (14.1)
Percentage of patients without distant metastasis at 3 yr (95% CI)	85.9% (78.9% - 91.3%)

CI, confidence interval.

Univariate and Multivariate Cox Regression on PFS

With the short follow-up, only univariate and multivariate analyses of PFS rather than OS were performed. As shown in **Figure 3**.

Significant factors of PFS indentified by univariate analyses included tumor stage (IVA/III) and cumulative concurrent cisplatin dose, either as continuous or categorical (reduced-dose/standard-dose) variable (hazard ratio [HR] 3.157, 95% CI 1.287-7.745, P = 0.012; HR 0.989, 95% CI 0.982-0.996, P = 0.003; and HR 2.384, 95% CI 1.006-5.649, P = 0.048; respectively). On multivariate analyses, cumulative concurrent cisplatin dose as categorical variable (HR 2.242, 95% CI 0.943- 5.333, P = 0.068) remained significant when adjusted for tumor stage (HR 3.036, 95% CI 1.236- 7.461, P = 0.015).

DISCUSSION

The results showed that induction PX-CCRT with a reduced cumulative cisplatin dose in both the induction (80mg/m^2 x 3 cycles) and concurrent (100mg/m^2 x 2 cycles) phases was non-inferior to the corresponding induction PX group (Arm 3A) with induction (100mg/m^2 x 3 cycles) and concurrent (100mg/m^2 x 3 cycles) cisplatin dose in NPC-0501 trial in terms of PFS (3 yr 83.7% vs. 81%) and OS (3yr 94.1% vs. 91%) in LA NPC, keeping in mind the caveats of cross-study comparisons.

Capecitabine has shown efficacy in IC (8), first-line (19), second-line (20), and maintenance therapy (21) of locoregionally advanced or metastic NPC. IC can minimize the volume of radiation delivered by reducing the tumor size, thus decreasing the radiation dose administered to normal tissue, resulting in improved quality of life (22–24). Theoretically, IC could improve the tolerance to treatment. As expected, the compliance to three cycles of induction PX in our study was numerically higher than in the NPC-0501 trial (94.8% vs. 85%). However, during CCRT, the rate of patients completing 2 cycles of concurrent Q3W cisplatin was numerically lower than in the NPC-0501 trial (85.2% vs. 91%) (7). The most common reason for failing to complete the 2 cycles of Q3W cisplatin was 1) the switch to weekly cisplatin due to deterioration of PS (8.1%), 2) treatment toxicities (3.0%), or 3) withdrawal of consent (3.7%). The proportion of patients receiving at least 200mg/m^2 of concurrent cisplatin (including Q3W and weekly cisplatin) was 71.9%. Similar to our study, previous studies showed that the cumulative cisplatin dose during CCRT substantially affected locoregional control and OS. Patients who received ≥ 200mg/m^2 of concurrent cisplatin achieved better OS than those who received a lower dose (13, 14, 25, 26). Although patients received somewhat lower doses of induction and concurrent cisplatin, the survival outcomes of our study were non-inferior to that of NPC-0501. We speculate that this may occur due to the chemotherapy/radiation sensitive nature of NPC (27).

The study published by Mai and colleagues concluded that IMRT plus 2 cycles of concurrent 100 mg/m^2 cisplatin without induction chemotherapy could be an alternative option for patients with low-risk locoregionally advanced NPC with Epstein-Barr virus (EBV) DNA levels < 4000 copies/ml (28). But for LA NPC, several recently published randomized phase III trials conducted in a similar ethnic patient cohort demonstrated that IC followed by concurrent systemic therapy/RT had better survival benefit than concurrent systemic therapy/RT alone (10–12, 29, 30). Concerning different IC regimens in LA NPC, a network meta-analysis of 9 clinical trials showed that docetaxel + cisplatin (DC), gemcitabine + cisplatin (GP), and PX had favorable OS benefits. GP and PX were the most promising IC regimens to date in the era of IMRT (10). In comparison with induction GP-CCRT, as reported by Zhang and colleagues (11), our trial showed similar results in terms of 3-year survival outcomes and toxicities. The 3-year PFS, OS, LRFS, and DMFS in our study were 83.7%, 94.1%, 94.1%, and 85.9%, respectively; and the corresponding results were 85.3%, 94.6%, 91.8% and 91.1%, respectively. Our locoregional control was better (3-year LRFS: 94.1% vs. 91.8%), and the distant control rate was numerically lower (3-year DMFS: 85.9% vs. 91.1%) than the results in induction GP-CCRT by Zhang et al. (11). This is likely due to fewer patients with T3-4 and more patients with N2-3 in our trial. Compared with the induction GP-CCRT trial by Zhang et al., patients in this study received a lower cumulative dose of cisplatin (430mg/m^2 vs. 440mg/m^2), and more patients had N2-3 disease (85.9% vs. 52.9%). Nevertheless, the OS of the two studies

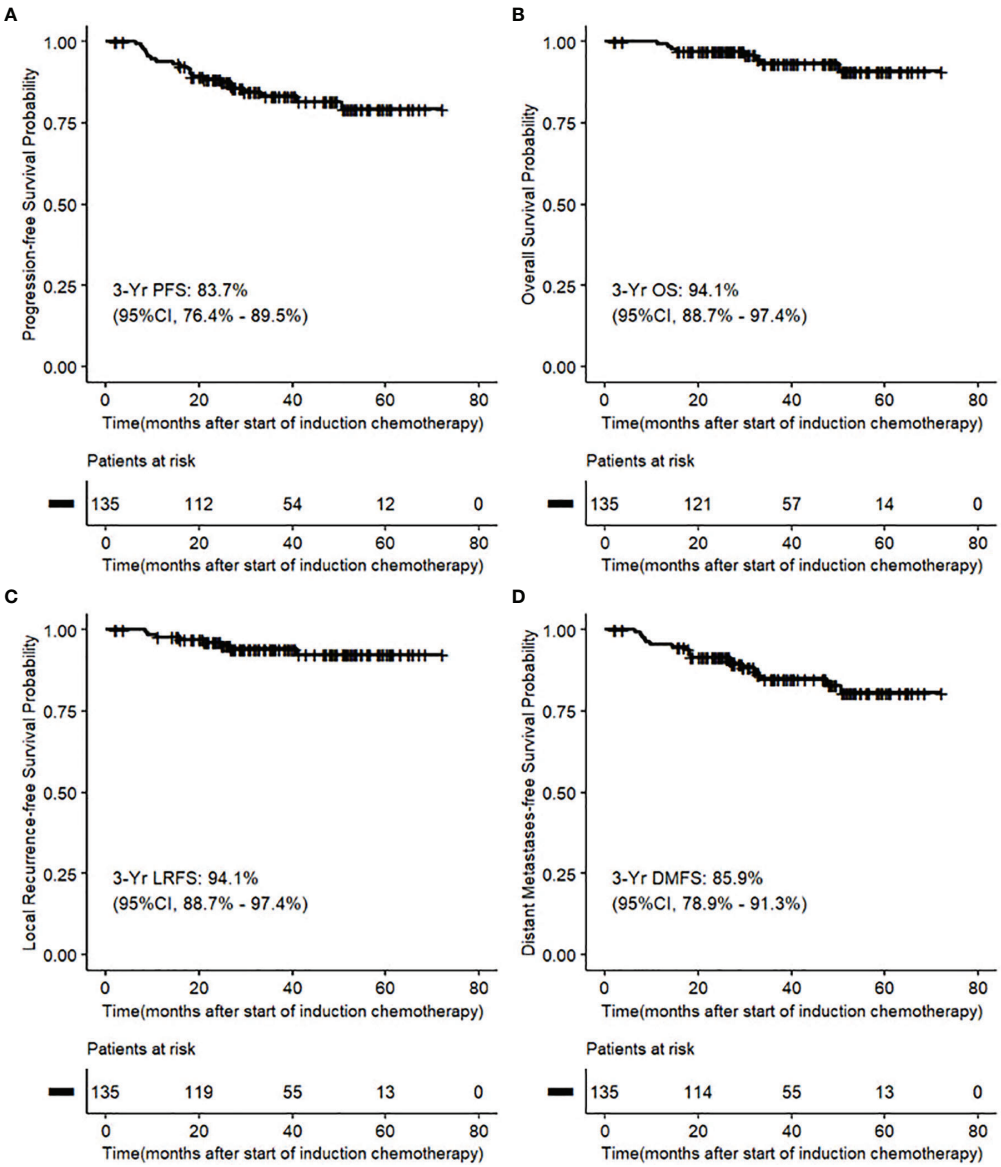

FIGURE 2 | **(A-D)** Kaplan–Meier Analysis of survival outcomes in intention-to-treat population.

were similar (3-year OS 94.1% vs. 94.6%). Concerning toxicities, the incidence of grade 3-4 acute toxicities in the present study was similar to the induction GP-CCRT regimen by Zhang et al. (76.3% vs. 75.7%). The percentage of patients who received protocol-defined cumulative cisplatin dose was 68.9% and 26.4% in the present study and GP-CCRT regimen by Zhang et al., respectively. In general, the reduced cumulative cisplatin treatment schedule in our study produced comparable treatment outcomes compared to other trials and was well tolerated with convenient administration of oral capecitabine. These factors taken together make induction PX-CCRT with reduced cumulative cisplatin dose an appealing treatment option for patients with LA NPC, given the emerging enthusiasm of de-escalation strategy for this disease (31).

Given the paucity of comparative data, the choice of either a gemcitabine-based or capecitabine-based IC regimen could be made based on the expected adverse events matched against the patient's performance status and comorbidities. The intensity of chemotherapy may be tailored based on various stage subgroups in LA NPC; some studies suggest that patients with stage IV or N2/N3 may benefit from a higher cumulative dose of cisplatin (32, 33).

We have identified some limitations to this study. Firstly, this is a single-arm trial. Prospective randomized controlled clinical trials are needed to confirm the clinical benefit of this reduced cisplatin dose treatment modality. Secondly, we did not include non-anatomical prognostic biomarkers to select eligible participants, especially plasma Epstein-Barr virus (EBV) DNA. Since no prognostic biomarkers have been included in the international staging system

TABLE 4 | AEs, according to treatment phase and Grade[#].

AEs	induction PX Grade 3-4, NO. (%)	concurrent P +RT Grade 3-4, NO. (%)	Whole course Grade 3-4, NO. (%)
Any acute AE	29 (21.5)	100 (74.1)	103 (76.3)
Leukopenia	7 (5.2)	59 (43.7)	61 (45.2)
Neutropenia	20 (14.8)	34 (25.2)	45 (33.3)
Neutropenic fever	3 (2.2)	8 (5.9)	11 (8.1)
Infection	1 (0.7)	13 (9.6)	13 (9.6)
Anemia	10 (7.4)	35 (25.9)	37 (27.4)
Thrombocytopenia	3 (2.2)	12 (8.9)	14 (10.4)
Renal function impairment	2 (1.5)	2 (1.5)	4 (3.0)
Electrolyte disturbance	12 (8.9)	14 (10.4)	22 (16.3)
Nausea/vomiting	3 (2.2)	4 (3.0)	6 (4.4)
Diarrhea	2 (1.5)	0 (0.0)	2 (1.5)
Weight loss	0 (0.0)	9 (6.7)	9 (6.7)
Neuropathy	1 (0.7)	3 (2.2)	3 (2.2)
Hand-foot syndrome	1 (0.7)	NA	1 (0.7)
Dermatitis	NA	17 (12.6)	17 (12.6)
Stomatitis (mucositis)	NA	39 (28.9)	39 (28.9)
Any late AE	NA	NA	2 (1.5)
Deafness or otitis	NA	NA	1 (0.7)
Neck tissue damage	NA	NA	1 (0.7)

PX, cisplatin plus capecitabine; CCRT, concurrent chemoradiotherapy; NA, not available.
[#]This analysis was conducted in the safety population, which included patients who began receiving the trial treatment.

for NPC and the treatment recommendation is mainly based on TNM staging. No prognostic biomarkers were included in this study. Thirdly, our trial and the induction-PX regimen in the NPC-0501 trial were not designed random control groups; they were independent and heterogeneous; due to objective reasons, there was no detailed comparison of the patient populations and the results between this study and NPC-0501. Lastly, the median follow-up for the analysis in this study was 3 years, and longer follow-up will be needed to assess long-term survival benefits and late toxic effects fully. Nonetheless, the findings of our study provide valuable data for guiding clinical practice and supporting a reduced cumulative cisplatin dose for future de-escalation clinical trials.

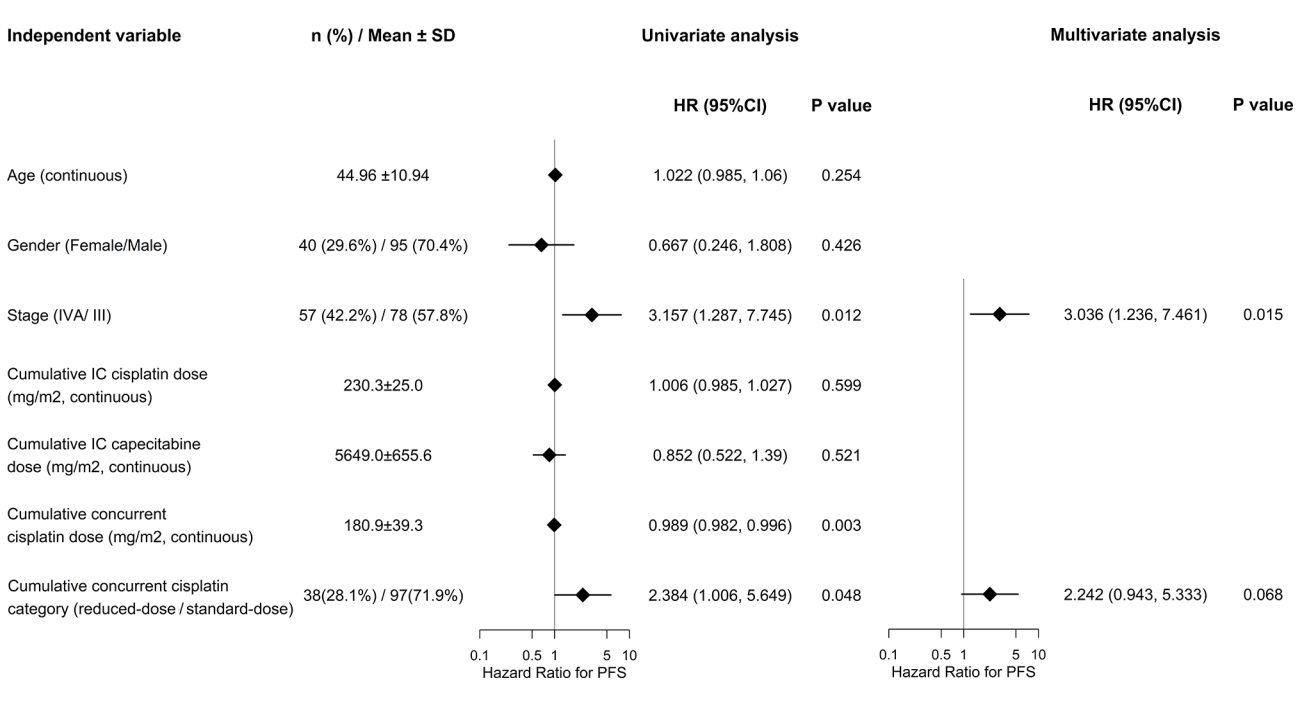

FIGURE 3 | Univariate and multivariate Cox regression on PFS.

In conclusion, the present study demonstrated that the reduced cumulative cisplatin dose in both induction and concurrent phases could achieve comparable outcomes to the NPC-0501 trial and favorable toxicity profile in LA NPC. However, long-term follow-up and randomized controlled clinical trials are needed to confirm the clinical benefit.

DATA AVAILABILITY STATEMENT

The original contributions presented in the study are included in the article/**Supplementary Material**. Further inquiries can be directed to the corresponding author.

ETHICS STATEMENT

The studies involving human participants were reviewed and approved by The institutional ethics committee of the University of Hong Kong - Shenzhen Hospital. The patients/participants provided their written informed consent to participate in this study. Written informed consent was obtained from the individual(s) for the publication of any potentially identifiable images or data included in this article.

AUTHOR CONTRIBUTIONS

This was an investigator-initiated trial. The first author wrote the first draft of the manuscript, which all the authors reviewed. No pharmaceutical companies were involved in the trial design, data collection or analysis, or manuscript preparation or review. The last author vouches for the completeness and accuracy of the data and the adherence of the trial to the protocol. All authors contributed to the article and approved the submitted version.

FUNDING

This project is supported in part by the Health Commission of Guangdong Province, China (NO. B2020100), Shenzhen Science and Technology Program (JCYJ20210324114600002), High Level-Hospital Program, Health Commission of Guangdong Province, China (NO. HKUSZH201902031, HKUSZH201901017, and HKUSZH201901038) and Shenzhen Key Medical Discipline Construction Fund (No. SZXK014).

ACKNOWLEDGMENTS

I want to express my gratitude to all patients and their families and those who have helped me during the writing of this paper, not only co-authors but also doctors, therapists, physicists, and nurses from our department.

SUPPLEMENTARY MATERIAL

The Supplementary Material for this article can be found online at: https://www.frontiersin.org/articles/10.3389/fonc.2022.842281/full#supplementary-material

REFERENCES

1. Sung H, Ferlay J, Siegel RL, Laversanne M, Soerjomataram I, Jemal A, et al. Global Cancer Statistics 2020: GLOBOCAN Estimates of Incidence and Mortality Worldwide for 36 Cancers in 185 Countries. *CA: Cancer J Clin* (2021) 71(3):209–49. doi: 10.3322/caac.21660
2. International Agency for Research on Cancer (IARC). *Global Cancer Observatory* (2020). World Health Organization. Available at: https://gco.iarc.fr/ (Accessed September 20, 2020).
3. Mao YP, Xie FY, Liu LZ, Sun Y, Li L, Tang LL, et al. Re-Evaluation of 6th Edition of AJCC Staging System for Nasopharyngeal Carcinoma and Proposed Improvement Based on Magnetic Resonance Imaging. *Int J Radiat Oncol Biol Phys* (2009) 73(5):1326–34. doi: 10.1016/j.ijrobp.2008.07.062
4. Lee AW, Ma BB, Ng WT, Chan AT. Management of Nasopharyngeal Carcinoma: Current Practice and Future Perspective. *J Clin Oncol* (2015) 33(29):3356–64. doi: 10.1200/jco.2015.60.9347
5. Al-Sarraf M, LeBlanc M, Giri PG, Fu KK, Cooper J, Vuong T, et al. Chemoradiotherapy Versus Radiotherapy in Patients With Advanced Nasopharyngeal Cancer: Phase III Randomized Intergroup Study 0099. *J Clin Oncol* (1998) 16(4):1310–7. doi: 10.1200/jco.1998.16.4.1310
6. NCCN. *The NCCN Head and Neck Cancers Clinical Practice Guidelines in Oncology (Version 3.2021)*. Pennsylvania: NCCN (2021). Available at: http://www.nccn.org/professionals/physician_gls/f_guidelines.asp.
7. Lee AW, Ngan RK, Tung SY, Cheng A, Kwong DL, Lu TX, et al. Preliminary Results of Trial NPC-0501 Evaluating the Therapeutic Gain by Changing From Concurrent-Adjuvant to Induction-Concurrent Chemoradiotherapy, Changing From Fluorouracil to Capecitabine, and Changing From Conventional to Accelerated Radiotherapy Fractionation in Patients With Locoregionally Advanced Nasopharyngeal Carcinoma. *Cancer* (2015) 121 (8):1328–38. doi: 10.1002/cncr.29208
8. Lee AWM, Ngan RKC, Ng WT, Tung SY, Cheng AAC, Kwong DLW, et al. NPC-0501 Trial on the Value of Changing Chemoradiotherapy Sequence, Replacing 5-Fluorouracil With Capecitabine, and Altering Fractionation for Patients With Advanced Nasopharyngeal Carcinoma. *Cancer* (2020) 126 (16):3674–88. doi: 10.1002/cncr.32972
9. Ng WT, Chua MLK, Lee AWM. Maintenance Capecitabine in Recurrent or Metastatic Nasopharyngeal Carcinoma-Magic Bullet or Pandora's Box? *JAMA Oncol* (2022). doi: 10.1001/jamaoncol.2021.7365
10. Choi HC, Chan SK, Lam KO, Chan SY, Chau SC, Kwong DL, et al. The Most Efficacious Induction Chemotherapy Regimen for Locoregionally Advanced Nasopharyngeal Carcinoma: A Network Meta-Analysis. *Front Oncol* (2021) 11:626145. doi: 10.3389/fonc.2021.626145
11. Zhang Y, Chen L, Hu GQ, Zhang N, Zhu XD, Yang KY, et al. Gemcitabine and Cisplatin Induction Chemotherapy in Nasopharyngeal Carcinoma. *N Engl J Med* (2019) 381(12):1124–35. doi: 10.1056/NEJMoa1905287
12. Yang Q, Cao SM, Guo L, Hua YJ, Huang PY, Zhang XL, et al. Induction Chemotherapy Followed by Concurrent Chemoradiotherapy Versus Concurrent Chemoradiotherapy Alone in Locoregionally Advanced Nasopharyngeal Carcinoma: Long-Term Results of a Phase III Multicentre Randomised Controlled Trial. *Eur J Cancer* (2019) 119:87–96. doi: 10.1016/j.ejca.2019.07.007
13. Peng H, Chen L, Zhang Y, Li WF, Mao YP, Zhang F, et al. Prognostic Value of the Cumulative Cisplatin Dose During Concurrent Chemoradiotherapy in Locoregionally Advanced Nasopharyngeal Carcinoma: A Secondary Analysis of a Prospective Phase III Clinical Trial. *Oncol* (2016) 21(11):1369–76. doi: 10.1634/theoncologist.2016-0105

14. Wen DW, Li ZX, Chen FP, Lin L, Peng BY, Kou J, et al. Individualized Cumulative Cisplatin Dose for Locoregionally-Advanced Nasopharyngeal Carcinoma Patients Receiving Induction Chemotherapy and Concurrent Chemoradiotherapy. *Oral Oncol* (2020) 107:104675. doi: 10.1016/j.oraloncology.2020.104675
15. Eisenhauer EA, Therasse P, Bogaerts J, Schwartz LH, Sargent D, Ford R, et al. New Response Evaluation Criteria in Solid Tumours: Revised RECIST Guideline (Version 1.1). *Eur J Cancer (Oxford Engl 1990)* (2009) 45(2):228–47. doi: 10.1016/j.ejca.2008.10.026
16. Cox JD, Stetz J, Pajak TF. Toxicity Criteria of the Radiation Therapy Oncology Group (RTOG) and the European Organization for Research and Treatment of Cancer (EORTC). *Int J Radiat Oncol Biol Phys* (1995) 31(5):1341–6. doi: 10.1016/0360-3016(95)00060-c
17. Schmidt R, Kwiecien R, Faldum A, Berthold F, Hero B, Ligges S. Sample Size Calculation for the One-Sample Log-Rank Test. *Stat Med* (2015) 34(6):1031–40. doi: 10.1002/sim.6394
18. Wu J. Sample Size Calculation for the One-Sample Log-Rank Test. *Pharm Stat* (2015) 14(1):26–33. doi: 10.1002/pst.1654
19. Chua DT, Yiu HH, Seetalarom K, Ng AW, Kurnianda J, Shotelersuk K, et al. Phase II Trial of Capecitabine Plus Cisplatin as First-Line Therapy in Patients With Metastatic Nasopharyngeal Cancer. *Head Neck* (2012) 34(9):1225–30. doi: 10.1002/hed.21884
20. Chua D, Wei WI, Sham JS, Au GK. Capecitabine Monotherapy for Recurrent and Metastatic Nasopharyngeal Cancer. *Jpn J Clin Oncol* (2008) 38(4):244–9. doi: 10.1093/jjco/hyn022
21. Sun XS, Liu SL, Liang YJ, Chen QY, Li XY, Tang LQ, et al. The Role of Capecitabine as Maintenance Therapy in *De Novo* Metastatic Nasopharyngeal Carcinoma: A Propensity Score Matching Study. *Cancer Commun (Lond)* (2020) 40(1):32–42. doi: 10.1002/cac2.12004
22. Yang H, Chen X, Lin S, Rong J, Yang M, Wen Q, et al. Treatment Outcomes After Reduction of the Target Volume of Intensity-Modulated Radiotherapy Following Induction Chemotherapy in Patients With Locoregionally Advanced Nasopharyngeal Carcinoma: A Prospective, Multi-Center, Randomized Clinical Trial. *Radiother Oncol* (2018) 126(1):37–42. doi: 10.1016/j.radonc.2017.07.020
23. Lee AW, Ng WT, Pan JJ, Chiang C-L, Poh SS, Choi HC, et al. International Guideline on Dose Prioritization and Acceptance Criteria in Radiation Therapy Planning for Nasopharyngeal Carcinoma. *Int J Radiat Oncol Biol Physics* (2019) 105(3):567–80. doi: 10.1016/j.ijrobp.2019.06.2540
24. Lee AW, Ng WT, Pan JJ, Poh SS, Ahn YC, AlHussain H, et al. International Guideline for the Delineation of the Clinical Target Volumes (CTV) for Nasopharyngeal Carcinoma. *Radiother Oncol* (2018) 126(1):25–36. doi: 10.1016/j.radonc.2017.10.032
25. Lee AW, Tung SY, Ngan RK, Chappell R, Chua DT, Lu TX, et al. Factors Contributing to the Efficacy of Concurrent-Adjuvant Chemotherapy for Locoregionally Advanced Nasopharyngeal Carcinoma: Combined Analyses of NPC-9901 and NPC-9902 Trials. *Eur J Cancer (Oxford Engl 1990)* (2011) 47 (5):656–66. doi: 10.1016/j.ejca.2010.10.026
26. Loong HH, Ma BB, Leung SF, Mo F, Hui EP, Kam MK, et al. Prognostic Significance of the Total Dose of Cisplatin Administered During Concurrent Chemoradiotherapy in Patients With Locoregionally Advanced Nasopharyngeal Carcinoma. *Radiother Oncol* (2012) 104(3):300–4. doi: 10.1016/j.radonc.2011.12.022
27. Lee AW, Lau WH, Tung SY, Chua DT, Chappell R, Xu L, et al. Preliminary Results of a Randomized Study on Therapeutic Gain by Concurrent Chemotherapy for Regionally-Advanced Nasopharyngeal Carcinoma: NPC-9901 Trial by the Hong Kong Nasopharyngeal Cancer Study Group. *J Clin Oncol* (2005) 23(28):6966–75. doi: 10.1200/jco.2004.00.7542
28. Mai H-Q, Li XY, Mo H-Y, Ling G, Luo D-H, Sun R, et al. De-Intensified Chemoradiotherapy for Locoregionally Advanced Nasopharyngeal Carcinoma Based on Plasma EBV DNA: A Phase 2 Randomized Noninferiority Trial. *J Clin Oncol* (2021) 39(15_suppl):110. doi: 10.1200/JCO.2021.39.15_suppl.110
29. Sun Y, Li W-F, Chen N-Y, Zhang N, Hu G-Q, Xie F-Y, et al. Induction Chemotherapy Plus Concurrent Chemoradiotherapy Versus Concurrent Chemoradiotherapy Alone in Locoregionally Advanced Nasopharyngeal Carcinoma: A Phase 3, Multicentre, Randomised Controlled Trial. *Lancet Oncol* (2016) 17(11):1509–20. doi: 10.1016/s1470-2045(16)30410-7
30. Chan S, Chan S, Tong C, Lam K, Kwong D, Leung T, et al. Comparison of Efficacy and Safety of Three Induction Chemotherapy Regimens With Gemcitabine Plus Cisplatin (GP), Cisplatin Plus Fluorouracil (PF) and Cisplatin Plus Capecitabine (PX) for Locoregionally Advanced Previously Untreated Nasopharyngeal Carcinoma: A Pooled Analysis of Two Prospective Studies. *Oral Oncol* (2021) 114:105158. doi: 10.1016/j.oraloncology.2020.105158
31. Lee A, Chow JCH, Lee NY. Treatment Deescalation Strategies for Nasopharyngeal Cancer: A Review. *JAMA Oncol* (2021) 7(3):445–53. doi: 10.1001/jamaoncol.2020.6154
32. Ou X, Xu T, He X, Ying H, Hu C. Who Benefited Most From Higher Cumulative Dose of Cisplatin Among Patients With Locally Advanced Nasopharyngeal Carcinoma Treated by Intensity-Modulated Radiation Therapy? A Retrospective Study of 527 Cases. *J Cancer* (2017) 8(14):2836–45. doi: 10.7150/jca.19725
33. Oliva M, Huang S, Taylor R, Su J, Xu W, Hansen A, et al. Impact of Cumulative Cisplatin Dose and Adjuvant Chemotherapy in Locally-Advanced Nasopharyngeal Carcinoma Treated With Definitive Chemoradiotherapy. *Oral Oncol* (2020) 105:104666. doi: 10.1016/j.oraloncology.2020.104666

Conflict of Interest: The authors declare that the research was conducted in the absence of any commercial or financial relationships that could be construed as a potential conflict of interest.

frontiers | Frontiers in Oncology

ORIGINAL RESEARCH
published: 26 May 2022
doi: 10.3389/fonc.2022.829761

A New Online Dynamic Nomogram: Construction and Validation of an Assistant Decision-Making Model for Laryngeal Squamous Cell Carcinoma

Yuchen Liu[1,2†], Yanxun Han[1,2†], Bangjie Chen[2,3†], Jian Zhang[4], Siyue Yin[2,3], Dapeng Li[1,2], Yu Wu[1,2], Yuan Jiang[1,2], Xinyi Wang[2], Jianpeng Wang[2], Ziyue Fu[2], Hailong Shen[1,2], Zhao Ding[1,2], Kun Yao[4], Ye Tao[1], Jing Wu[1] and Yehai Liu[1*]*

[1] Department of Otolaryngology, Head and Neck Surgery, The First Affiliated Hospital of Anhui Medical University, Hefei, China, [2] Anhui Medical University, Hefei, China, [3] Department of Oncology, The First Affiliated Hospital of Anhui Medical University, Hefei, China, [4] Department of Otolaryngology, Head and Neck Surgery, The Fuyang Hospital Affiliated to Anhui Medical University, Fuyang, China

OPEN ACCESS

Edited by:
Markus Wirth,
Klinikum rechts der Isar, Germany

Reviewed by:
Manish Devendra Mair,
University Hospitals of Leicester NHS Trust, United Kingdom
Maria Helena Ornellas,
Universidade Estadual do Rio de Janeiro, Brazil

***Correspondence:**
Jing Wu
wujing@ahmu.edu.cn
Yehai Liu
liuyehai@ahmu.edu.cn

[†]These authors have contributed equally to this work and share first authorship

Specialty section:
This article was submitted to Head and Neck Cancer, a section of the journal Frontiers in Oncology

Received: 06 December 2021
Accepted: 25 April 2022
Published: 26 May 2022

Citation:
Liu Y, Han Y, Chen B, Zhang J, Yin S, Li D, Wu Y, Jiang Y, Wang X, Wang J, Fu Z, Shen H, Ding Z, Yao K, Tao Y, Wu J and Liu Y (2022) A New Online Dynamic Nomogram: Construction and Validation of an Assistant Decision-Making Model for Laryngeal Squamous Cell Carcinoma. Front. Oncol. 12:829761. doi: 10.3389/fonc.2022.829761

Background: Laryngeal squamous cell carcinoma (LSCC) is the most common type of head and neck squamous cell carcinoma. However, there are currently no reliable biomarkers for the diagnosis and prognosis of LSCC. Thus, this study aimed to identify the independent risk factors and develop and validate a new dynamic web-based nomogram that can predict auxiliary laryngeal carcinogenesis.

Methods: Data on the medical history of 221 patients who were recently diagnosed with LSCC and 359 who were recently diagnosed with benign laryngeal lesions (BLLs) at the First Affiliated Hospital of Anhui Medical University were retrospectively reviewed. Using the bootstrap method, 580 patients were divided in a 7:3 ratio into a training cohort (LSCC, 158 patients; BLL, 250 patients) and an internal validation cohort (LSCC, 63 patients; BLL, 109 patients). In addition, a retrospective analysis of 31 patients with LSCC and 54 patients with BLL from Fuyang Hospital affiliated with Anhui Medical University was performed as an external validation cohort. In the training cohort, the relevant indices were initially screened using univariate analysis. Then, least absolute shrinkage and selection operator logistic analysis was used to evaluate the significant potential independent risk factors ($P<0.05$); a dynamic online diagnostic nomogram, whose discrimination was evaluated using the area under the ROC curve (AUC), was constructed, while the consistency was evaluated using calibration plots. Its clinical application was evaluated by performing a decision curve analysis (DCA) and validated by internal validation of the training set and external validation of the validation set.

Results: Five independent risk factors, sex (odds ratio [OR]: 6.779, $P<0.001$), age (OR: 9.257, $P<0.001$), smoking (OR: 2.321, $P=0.005$), red blood cell width distribution (OR: 2.698, $P=0.001$), albumin (OR: 0.487, $P=0.012$), were screened from the results of the multivariate logistic analysis of the training cohort and included in the LSCC diagnostic nomogram. The nomogram predicted LSCC with AUC values of 0.894 in the training

cohort, 0.907 in the internal testing cohort, and 0.966 in the external validation cohort. The calibration curve also proved that the nomogram predicted outcomes were close to the ideal curve, the predicted outcomes were consistent with the real outcomes, and the DCA curve showed that all patients could benefit. This finding was also confirmed in the validation cohort.

Conclusion: An online nomogram for LSCC was constructed with good predictive performance, which can be used as a practical approach for the personalized early screening and auxiliary diagnosis of the potential risk factors and assist physicians in making a personalized diagnosis and treatment for patients.

Keywords: laryngeal squamous cell carcinoma, dynamic nomogram, diagnosis, risk factors, LASSO regression

INTRODUCTION

Laryngeal squamous cell carcinoma (LSCC) is one of the most common type of head and neck squamous cell carcinoma. In 2020, 12,370 newly discovered Laryngeal cancer cases and 3,750 deaths due to Laryngeal cancer were reported in the United States (1). LSCC originates from the epithelial cells, and the structural and cytological alterations in laryngeal squamous epithelial cells lead to the occurrence of LSCC. Various factors affect the incidence of LSCC; however, the underlying mechanisms remain unclear (2). Treatments of LSCC include surgery, radiotherapy, and chemotherapy. Although the therapeutic modalities have gradually developed over the past two decades, due to the low percentage of early diagnosis, the clinical prognosis has not significantly improved (1). Several patients with LSCC have unremarkable early symptoms, and most of them are only admitted in the hospital if they experience hoarseness and pain during swallowing, progressive aggravation of dysphagia, and radiating ear pain (3). In China, although the popularity of laryngoscopy has increased the rate of early diagnosis of LSCC, laryngoscopy is an invasive procedure, and the incidence of LSCC is relatively low; therefore, laryngoscopy is not used as a routine screening examination for diseases of the pharynx and larynx in the population. However, most of the people living in remote areas in China have poor awareness of the different medical treatments, and the level of medical treatment in these areas is still underdeveloped. Results of previous studies on laryngoscopy performed in this patient group lacked clarity, and white-light endoscopy had a limited ability to detect lesions, which precluded the establishment of an accurate diagnosis (4). The relatively high cost of laryngoscopy led to the underdiagnosis and prevented the early treatment of malignant diseases in the laryngopharynx. In this era of personalized cancer therapy, nomograms are statistical tools that can consider various factors simultaneously to help patients visualize their probability of developing a disease. In addition, nomograms have been several advantages in the treatment of cancer, including personalized assessment, user friendliness, and ease of understanding. However, to our knowledge, no study has developed a dynamic prediction model for LSCC. Therefore, this study aimed to develop an online dynamic nomogram to assist physicians in providing a personalized early diagnosis and treatment of patients with LSCC.

Abbreviations: AUC, area under the ROC curve; BLL, benign laryngeal lesions; CI, confidence interval; DCA, decision curve analysis; LASSO, least absolute shrinkage and selection operator; LSCC, Laryngeal squamous cell carcinoma; OR, odds ratio; RDW, red blood cell width distribution; ROC, receiver operating characteristic.

MATERIALS AND METHODS

Patient Data

This study was approved by the Ethics Committee of the First Affiliated Hospital of the Anhui Medical University. All participants provided informed consent. The clinical data of patients with laryngeal diseases admitted in the First Affiliated Hospital of Anhui Medical University, a high-volume surgical center, from April 2017 to October 2020 were obtained. The diagnosis was made based on the results of the postoperative specimen examination performed by two experienced pathologists. Patients (1) with benign laryngeal lesion or stage I to IV LSCC as confirmed by postoperative pathology (2), with complete clinicopathological data, and (3) who signed an informed consent to collect the medical data were included in the study. By contrast, patients (1) who had undergone surgery, chemotherapy, and radiotherapy prior to admission and (2) whose disease was complicated by other malignant tumors, hematologic diseases, active inflammatory diseases (e.g., autoimmune disease and infection), liver and kidney diseases, or long-term use of oral anticoagulant drugs and corticosteroids were excluded. All patients underwent routine physical examination, fibrolaryngoscopy, electrocardiography, and laboratory examination for a comprehensive evaluation. In addition, the clinical data of patients with laryngeal diseases admitted in another high-volume surgical center, Fuyang Hospital, affiliated with Anhui Medical University, were collected.

Data Collection

The following clinicopathological data were obtained: age, sex, smoking history, and alcohol consumption history. Considering the small volume and less vascular and nerve invasion in most

laryngeal diseases, it is difficult to accurately measure them using preoperative computed tomography (CT) and endoscopy; therefore, these relevant imaging findings were not included in this study. Fasting venous blood was collected from patients with laryngeal diseases in the morning within 24 h after admission and was used for routine blood routine and blood biochemical analyses.

Statistical Analysis

All computations were performed using the R software (version 4.1.2) and various packages. The dataset collected from the First Affiliated Hospital of Anhui Medical University was randomly divided into training and validation cohorts at a ratio of 7:3, and the variables were compared. Non-normal data were presented as median (interquartile ranges). In the univariate analysis, the chi-square test was used to analyze the categorical variables, while the Student's t-test or rank-sum test was used to examine the continuous variables. In the training cohort, the least absolute shrinkage and selection operator (LASSO) logistic regression analysis was used for multivariate analysis to screen the independent risk factors and build a prediction nomogram for the diagnosis of LSCC (5). The performance of the nomogram was assessed using the receiver operating characteristic (ROC) curve and calibration curve, with the area under the ROC curve (AUC) ranging from 0.5 (no discriminant) to 1 (complete discriminant) (6). A decision curve analysis (DCA) was also performed to determine the net benefit threshold of prediction (7). Spearman's correlation analysis was performed to analyze the correlations among variables. To facilitate their incorporation into the clinical practice, an interactive web-based dynamic nomogram application was built using Shiny, version 0.13.2.26. Results with a p-value of <0.05 were considered significant.

RESULTS

Patient Cohorts and Clinicopathologic Features

The detailed flow diagram is presented in **Figure 1**. A total of 221 patients with LSCC and 359 patients with benign laryngeal lesions (BLLs), who diagnoses were pathologically confirmed after surgical treatment at the Department of Otolaryngology, Head and neck Surgery of the First Affiliated Hospital of Anhui Medical University from April 2017 to October 2020, and 31 patients with LSCC and 54 patients with BLL who were admitted in Fuyang Hospital affiliated with Anhui Medical University were enrolled in the study. All patients met the inclusion and exclusion criteria. Finally, among the patients included in the study at the First Affiliated Hospital of Anhui Medical University, 70% were selected as the training cohort, while 30% were selected as the internal validation cohort using a computer random method. Patients from Fuyang Hospital affiliated with Anhui Medical University were included in the external validation cohort. The clinicopathological characteristics of the patients are summarized in **Table 1**.

The Wilcoxon test and chi-square test were used to compare the indices between the LSCC and BLL groups. In the training cohort, nine significant indicators (P<0.05, **Table 2**) were selected, including sex (P<0.001), age (P<0.001), smoking history (P<0.001), drinking history (P<0.001), red blood cell width distribution (RDW, P<0.001), albumin (ALB, P<0.001), neutrophil/lymphocyte ratio (NLR, P<0.001), lymphocyte/monocyte ratio (LMR, P<0.001), and platelet/lymphocyte ratio (PLR, P=0.048).

Factor Selection for the Predictive Model, Calibration, and Validation of the Nomogram

The above nine variables were included in the original model, which were then reduced to seven potential predictors using LASSO regression analysis performed in the training cohort. The coefficients are shown in **Supplementary Table S1**, and a coefficient profile is plotted in **Figure 2A**. A cross-validated error plot of the LASSO regression model is shown in **Figure 2B**. As shown in **Figure 2B**, the most regularized and parsimonious model, with a cross-validated error within one standard error of the minimum, included seven variables.

As shown in **Figure 3**, the ROC analysis of the abovementioned variables yielded AUC values greater than 0.5 for sex (AUC=0.690), age (AUC=0.786), smoking (AUC=0.677), RDW (AUC=0.684), ALB (AUC=0.692), LMR (AUC=0.652), and PLR (AUC=0.558). The cutoff values, sensitivity, and specificity of these parameters are shown in **Table 3**.

To clarify whether the abovementioned seven variables were independent risk factors for LSCC, further multivariate logistic analysis excluding other confounding factors was carried out and showed that age (odds ratio [OR]=9.257, 95% confidence interval [CI]=5.251–16.757, P<0.001; **Figure 4A**), sex (OR=6.779, 95% CI=2.795–18.579, P<0.001; **Figure 4A**), smoking history (OR=2.321, 95% CI=1.294–4.228, P=0.005; **Figure 4A**), RDW (OR=2.698, 95% CI=1.498–4.900, P=0.001; **Figure 4A**), and ALB (OR=0.487, 95% CI=0.277–0.854, P=0.012; **Figure 4A**) were significantly associated with LSCC. Similar results were obtained in the internal and external validation cohorts (**Figures 4B, C**). Results of the correlation analysis showed that the five factors were all linearly correlated with each other, while ALB was negatively correlated with other indices (**Figure 5**).

The final logistic model included five independent predictors (age, sex, smoking history, RDW, and ALB) and was developed as a simple-to-use nomogram, which is illustrated in **Figure 6A** and available online (https://hanchenchen.shinyapps.io/LSCCNomapp/) and presented in **Figure 6B**. The specific coefficients of each factor are shown in **Supplementary Figure S1**.

As shown in **Figures 7A–C**, the AUCs of the model in the training cohort, internal validation cohort, and external validation cohort were 0.894, 0.907, and 0.966, respectively, showing good predictive ability. In addition, we also calculated the model AUC of early T stage (T1+T2) patients in three cohorts specifically, which were 0.899, 0.911 and 0.960, respectively, suggesting that nomogram may play an important role in the early screening of LSCC. The internal validation and calibration of the nomogram were performed using 1,000

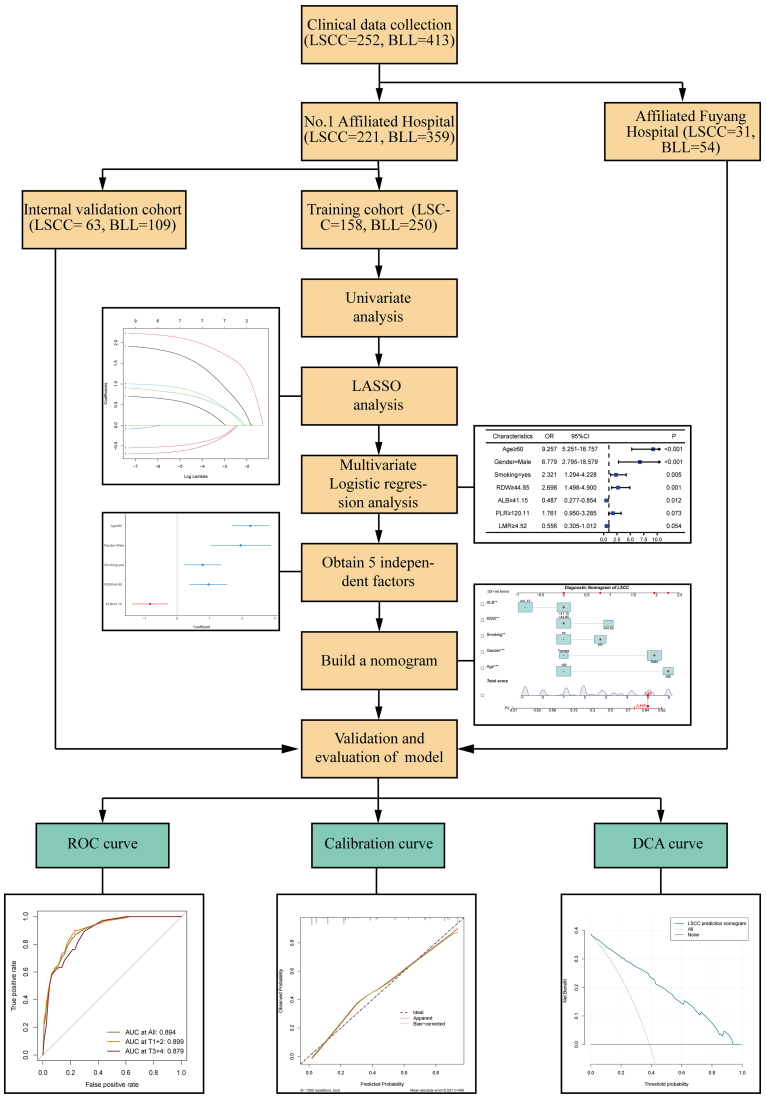

FIGURE 1 | Flow chart of the study process. ** p<0.01, *** p<0.001.

bootstrap analyses. The calibration plots of the nomogram in the three cohorts are plotted in **Figures 7D–F**, which demonstrate a good correlation between the observed and predicted development of LSCC. The above results showed that the original nomogram was still valid for use in the inner and outer validation sets, and the calibration curve of this model was relatively close to the ideal curve, which indicates that the predicted results were consistent with the actual findings.

Decision Curve Analysis

The DCA curves for the nomogram are presented in **Figures 8A–C**. A high-risk threshold probability is the probability of serious deviation in the prediction of the model when clinicians have serious defects using a nomogram for diagnosis and decision-making. In this study, the DCA curve demonstrated that the nomogram had good net benefits for clinical use.

DISCUSSION

More than 80,000 people die of laryngeal cancer every year worldwide, and LSCC accounts for approximately 90% of all laryngeal malignancies. Although the therapeutic modalities for LSCC, such as radiotherapy, chemotherapy, and surgical techniques, have made tremendous progress, the survival rate of patients with LSCC remains stagnant over the past 30 years due to the low rate of early diagnosis (8). In 2020, the European Society of Oncology suggested that the diagnosis of LSCC should

TABLE 1 | Patient demographics and clinicopathological characteristics.

Characteristics		The First Affiliated Hospital				Affiliated Fuyang Hospital	
		Training Cohort		Internal Test Cohort		External Test Cohort	
		BLL n (%)	LSCC n (%)	BLL n (%)	LSCC n (%)	BLL n (%)	LSCC n (%)
All		250	158	109	63	54	31
Age (years)	<60	216 (86.4)	46 (29.1)	100 (91.7)	26 (41.3)	51 (94.4)	12 (38.7)
	≥60	34 (13.6)	112 (70.9)	9 (8.3)	37 (58.7)	3 (5.6)	19 (61.3)
Gender	Male	144 (57.6)	151 (95.6)	61 (56.0)	59 (93.7)	23(42.6)	2 (6.5)
	Female	106 (42.4)	7 (4.4)	48 (44.0)	4 (6.3)	31 (57.4)	29(93.5)
Smoking history	No	182 (72.8)	59(37.3)	77 (70.6)	20 (31.7)	42 (77.8)	5 (16.1)
	Yes	68 (27.2)	99 (62.7)	32 (29.4)	43 (68.3)	12 (22.2)	26 (83.9)
Drinking history	No	201 (80.4)	87 (55.1)	91 (83.5)	34 (54.0)	46 (85.2)	12 (38.7)
	Yes	49 (19.6)	71 (44.9)	18 (16.5)	29 (46.0)	8 (14.8)	19 (61.3)
Tumor site	Supra-glottic	50 (20.0)	40 (25.3)	19 (17.4)	20 (31.7)	4 (7.4)	5 (16.1)
	Glottic	200 (80.0)	109 (69.0)	90 (82.6)	41(65.1)	50 (92.6)	26 (83.9)
	Sub-glottic	0 (0)	9 (5.7)	0 (0)	2 (3.2)	0 (0)	0 (0)
Tumor size	≤ 2	243 (97.2)	84 (53.2)	100 (91.7)	31(49.2)	54 (100.0)	28 (90.3)
	>2	7 (2.8)	74 (46.8)	9 (8.3)	32 (50.8)	0(0)	3 (9.7)
T stage	T1+T2	–	120 (75.9)	–	51 (81.0)	–	22 (71.0)
	T3+T4	–	38 (24.1)	–	12 (19.0)	–	9 (29.0)
Lymph node metastasis	N0	–	109 (69.0)	–	51 (81.0)	–	29 (93.4)
	N1	–	18(11.4)	–	4 (6.3)	–	1 (3.2)
	N2	–	29 (18.4)	–	8 (12.7)	–	1 (3.2)
	N3	–	2 (1.3)	–	0 (0)	–	0 (0)
Distant metastasis	No	–	155 (98.1)	–	63 (100.0)	–	31(100.0)
	Yes	–	3 (1.9)	–	0 (0)	–	0 (0)
TNM stage	I+II	–	95 (60.1)	–	43 (68.3)	–	22 (71.0)
	III+IV	–	63 (39.9)	–	20 (31.7)	–	9 (29.0)
Differentiation grade	Well	–	50 (31.6)	–	19 (30.2)	–	26 (83.9)
	Poor	–	33 (20.9)	–	13 (20.6)	–	2 (6.5)
	Moderate	–	75 (47.5)	–	31 (49.2)	–	3 (9.7)

BLL, benign laryngeal lesion; LSCC, laryngeal squamous cell carcinoma.

TABLE 2 | Comparison of variables between LSCC group and BLL group.

Variables	The First Affiliated Hospital						Affiliated Fuyang Hospital		
	Training Cohort			Internal Test Cohort			External Test Cohort		
	BLL	LSCC	P	BLL	LSCC	P	BLL	LSCC	P
N	250	158		109	63		54	31	
Gender n (%)			<0.001			<0.001			<0.001
Female	106 (42.4%)	7 (4.4%)		48(44.0%)	4 (6.3%)		32 (59.3%)	2 (6.5%)	
Male	144 (57.6%)	151 (95.6%)		61(56.0%)	59 (93.7%)		22 (40.7%)	29 (93.5%)	
Age n (%)			<0.001			<0.001			<0.001
< 60	216 (86.4%)	46 (29.1%)		100(91.7%)	26 (41.3%)		51(94.4%)	11 (35.5%)	
≥60	34 (13.6%)	112 (70.9%)		9(8.3%)	37 (58.7%)		3 (5.6%)	20 (64.5%)	
Smoking n (%)			<0.001			<0.001			<0.001
No	182 (72.8%)	59 (37.3%)		77(70.6%)	20 (31.7%)		42 (77.8%)	5 (16.1%)	
Yes	68 (27.2%)	99 (62.7%)		32(29.4%)	43 (68.3%)		12 (22.2%)	26 (83.9%)	
Drinking n (%)			<0.001			<0.001			<0.001
No	201 (80.4%)	87 (55.1%)		91(83.5%)	34 (5.0%)		46 (85.2%)	12 (38.7%)	
Yes	49 (19.6%)	71 (44.9%)		18 (16.5%)	29 (46.0%)		8 (14.8%)	19 (61.3%)	
RDW fL (median (IQR))	42.30 (3.80)	44.90 (4.18)	<0.001	42.00 (4.10)	44.30 (4.80)	<0.001	41.80 (3.38)	44.70 (3.95)	0.001
PDW fL (median (IQR))	13.05 (3.78)	13.10 (3.45)	0.551	13.7 (4.00)	13.1 (2.85)	0.131	16.30 (0.50)	16.30 (0.45)	0.616
MPV fL (median (IQR))	10.90 (1.75)	11.10 (1.50)	0.301	11.1 (1.80)	10.9 (1.50)	0.256	11.00 (1.88)	10.10 (2.35)	0.074
PA mg/L (median (IQR))	251.50 (70.00)	239.00 (84.75)	0.062	244.0 (98.00)	264.0 (77.50)	0.094	243.50 (106.25)	224.00 (62.50)	0.169
ALB g/L (median (IQR))	42.10 (4.08)	39.90 (4.73)	<0.001	41.80 (4.30)	41.70 (5.15)	0.346	42.35 (2.65)	41.00 (3.55)	0.001
NLR (median (IQR))	1.87 (0.99)	2.20 (1.14)	<0.001	1.92 (1.05)	2.19 (1.13)	0.029	1.84 (0.62)	2.22 (1.45)	0.043
LMR (median (IQR))	5.22 (2.01)	4.25 (2.23)	<0.001	5.25 (2.40)	4.13 (2.25)	0.001	4.66 (1.53)	3.82 (2.31)	0.258
PLR (median (IQR))	105.48 (46.86)	117.59 (62.06)	0.048	124.56 (56.72)	124.55 (69.57)	0.008	110.97 (40.81)	118.07 (70.22)	0.018

RDW, red blood cell width distribution; PDW, platelet distribution width; MPV, mean platelet volume; PA, prealbumin; ALB, albumin; NLR, neutrophil/lymphocyte ratio; LMR, lymphocyte/monocyte ratio; PLR, platelet/lymphocyte ratio; LSCC, laryngeal squamous cell carcinoma; BLL, benign laryngeal lesions. Red font text means statistically significant.

not only be based on the patient's medical history, complete physical examination results, electronic fiber laryngoscopy findings, enhanced CT or magnetic resonance imaging findings, and pathological diagnosis but should also include the evaluation of biochemical and hematological indicators (9). However, for some patients with laryngeal cancer, especially those with early-stage laryngeal cancer (TNM stage I + II), most have limited and small lesions, and preoperative CT and endoscopy cannot accurately determine their size, morphology, local invasion, and the safe margin of the lesions. Many lesions develop in the deep areas of the mucosa and show endophytic expansive growth. The mucosal surface is smooth and regular. The patient's irritated choking reflex was very strong on preoperative biopsy, which reduced its success rate and accuracy. Therefore, for patients with difficulty in differentiating laryngeal cancer from benign lesions of the larynx (vocal fold polyps, vocal Reinke's edema, laryngeal knot nuclei, papilloma of the larynx, keratosis of the larynx, amyloidosis of the larynx, etc.), the establishment of a nomogram for preoperative prospective quantitative prediction can help overcome these problems and allow the surgeon to formulate an individualized surgical approach for patients preoperatively. In this study, age, sex, smoking history, preoperative nutritional status (ALB), and preoperative RDW were significant predictors, and these independent factors influenced the occurrence and development of laryngeal diseases; moreover, the calibration plot of the nomogram closely matched the ideal standard line, indicating that the nomogram had sufficient statistical power to predict the incidence of diseases. Due to the inconvenience of traditional nomograms for clinical use, online versions of the nomograms were built based on traditional nomogram models. Online versions can be easily accessed by computers, smartphones, or other mobile devices and more effectively provide accurate and individualized diagnosis prediction for patients with LSCC. Therefore, in the diagnosis and treatment of malignant and benign diseases of the larynx, this model provides a practical and convenient navigation tool for preoperative propensity diagnosis, individualized treatment implementation, surgical modality selection, and clinical trial design.

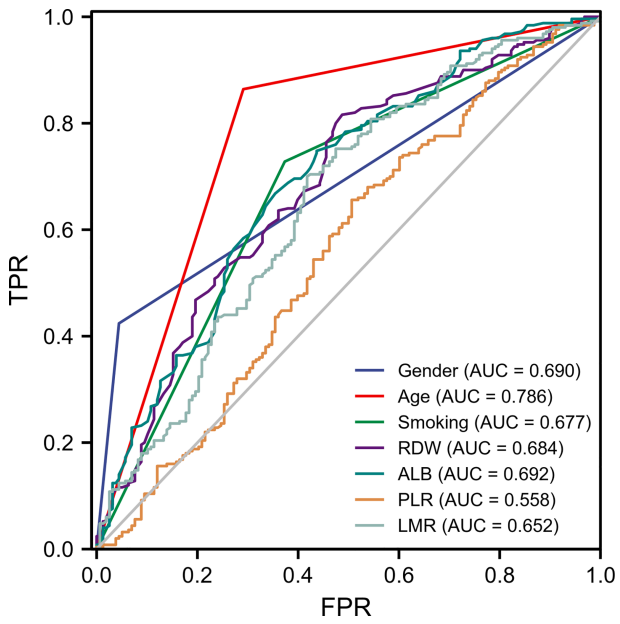

FIGURE 3 | ROC curve analysis of seven candidate diagnostic indicators.

In our study, age ≥60 years was an independent risk predictor for the development of LSCC, which was consistent with the result of most previous studies (10). Relevant studies have shown that the age-standardized incidence rate of laryngeal cancer by the world standard population (ASIRW) is 2.0/100,000. However, the ASIRW was 3.6/100,000 for men and 0.48/100,000 for women. This notion was also confirmed by our study that malignant laryngeal lesions were more common in men than in women; therefore, sex was also included in the nomogram (11). Although female patients with malignant laryngeal lesions are generally older, most are in the postmenopausal state, while a small proportion are in the premenopausal state. Age is associated with menopausal status, indicating that it might complicate the relationship between menopausal status and the development of laryngeal cancer (12). However, due to the small sample of female

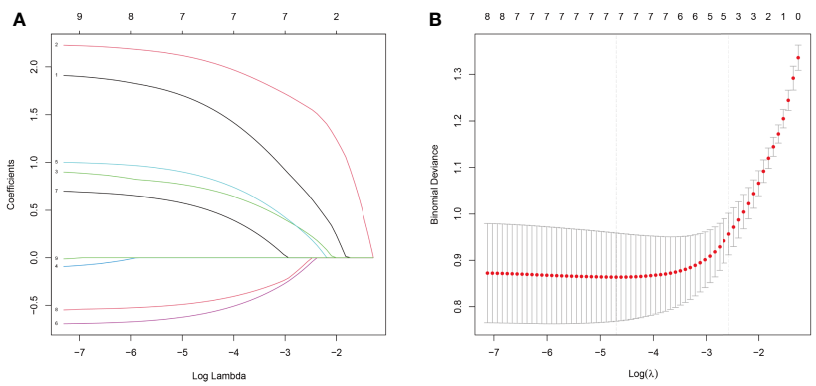

FIGURE 2 | Results of the LASSO regression analysis. **(A)** Plot of the LASSO coefficient profiles. **(B)** Tuning parameter (λ) selection cross-validation error curve.

TABLE 3 | The Results of receiver operating characteristic (ROC) curve.

Variables	AUC	Cut-off value	Youden index	Sensitivity	Specificity	95%CI	P-Value
Gender	0.690	–	0.380	0.424	0.956	0.655-0.725	<0.001
Age	0.786	–	0.573	0.864	0.709	0.745-0.828	<0.001
Smoking	0.677	–	0.355	0.728	0.627	0.630-0.724	<0.001
RDW	0.684	44.85	0.329	0.816	0.513	0.631-0.738	<0.001
ALB	0.692	41.15	0.314	0.668	0.646	0.639-0.745	<0.001
LMR	0.652	4.52	0.282	0.700	0.582	0.597-0.708	<0.001
PLR	0.558	120.11	0.150	0.656	0.494	0.499-0.617	0.048

RD, red blood cell width distribution; ALB, albumin; LMR, lymphocyte/monocyte ratio; PLR, platelet/lymphocyte ratio.

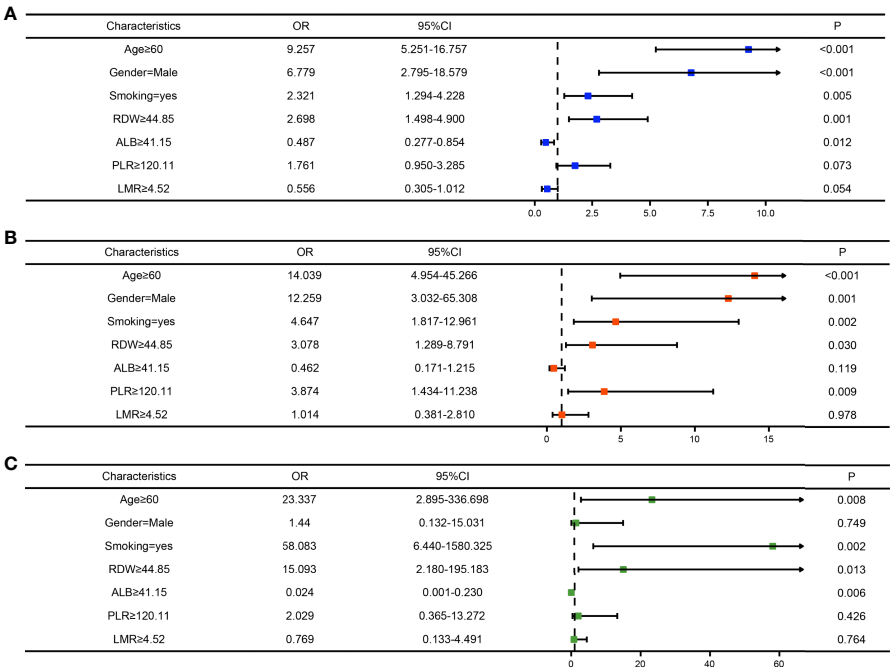

FIGURE 4 | Forest maps of the logistic regression analysis of the training cohort **(A)**, internal test cohort **(B)**, and, external test cohort **(C)**.

patients with laryngeal cancer, information on reproduction, hormone levels, use of oral contraceptives, and menopausal hormone replacement therapy status in female patients was not taken into account. Moreover, a correlation analysis was not performed in this study; hence, further exploration of the action of estrogen and its receptor could provide new insights into the diagnosis and treatment of female patients with laryngeal cancer.

Laryngeal cancer belongs to the group of tobacco-dependent malignancies including passive smoking. This cancer rarely occurs among nonsmokers (13). The increased risk of laryngeal cancer among individuals who started smoking at an earlier age is mainly due to the longer duration of smoking and higher cumulative tobacco exposure (14). Smoking cessation reduces the probability of developing laryngeal cancer, especially among former smokers who have quit smoking for 15 or more years (15). Tobacco increases the relative risk of developing laryngeal cancer in women than in men (12). This study showed that a history of smoking was a significant risk factor for the development of laryngeal cancer, and the possible mechanisms were determined. Many chemicals in tobacco have toxic effects, including polycyclic aromatic hydrocarbons (phenyltoluene), N-nitrosamines, heavy metals (nickel, cadmium, chromium, and arsenic), alkaloids (nicotine and its main metabolites, and infectious agents), and aromatic amines. Tobacco induced LSCC pathogenesis including inflammatory and immune changes, genetic alterations, oxidative damage, endothelial dysfunction, and cellular senescence (16). A significant difference was observed in the rate of drinking (45.2%, 71/221) and non-drinking (67.9%, 150/221) among the patients with LSCC admitted to the First Affiliated Hospital of Anhui Medical University. However, history of drinking was not an independent predictor of laryngeal cancer in our study, although most studies suggest that long-term heavy drinking is an independent risk factor for the development of laryngeal cancer (17), which is inconsistent with the findings of our study. Due to the insufficient sample size and regional dietary cultural differences, there may be deviations in the results of this study, which can be

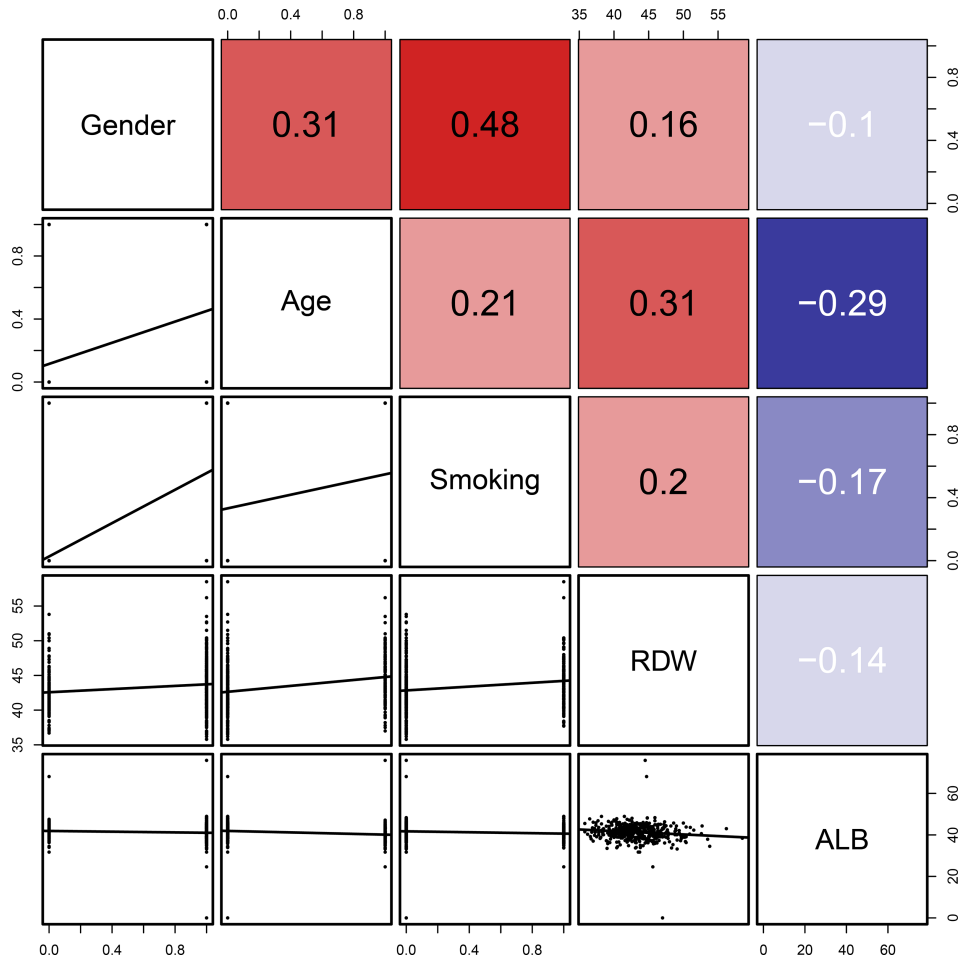

FIGURE 5 | Linear correlation analysis of the five indicators (age, sex, smoking history, RDW, and ALB). The number in the right of the plot was the correlation coefficient.

further evaluated by extending the coverage of the center and expanding the sample size in the future.

Chronic inflammation and lack of nutrition are closely related to the occurrence and development of various malignant tumors. Chronic inflammation induces tumor angiogenesis and DNA damage, and promotes tumor proliferation and metastasis by preventing apoptosis (18). However, the diagnosis of LSCC based on the changes in inflammatory biomarkers in the peripheral blood has not yet been reported. In patients with LSCC, the ALB levels were significantly reduced, while the RDW levels were significantly increased, both of which were independent risk factors for LSCC; this finding suggests that ALB and RDW are potential biomarkers for the diagnosis of LSCC.

Previous clinical applications of RDW were limited to the diagnosis of iron-deficient anemia. Recent studies have revealed elevated RDW levels in patients with cardiovascular diseases, venous thromboembolism, rheumatoid arthritis, diabetes, and cancer. RDW was positively associated with the levels of plasma inflammatory biomarkers (C-reactive protein (19, 20), erythrocyte sedimentation rate (21), and interleukins), which are considered inflammatory tumor biomarkers. Elevated RDW levels were probably related to the release of inflammatory factors (e.g., IL-6 and IFN-γ) that could inhibit EPO production, resulting in an increased proportion of immature erythroblasts in the peripheral blood (22, 23). In addition, elevated RDW levels are biomarkers of inflammation and oxidative stress-induced damage, which affects the occurrence and development of various types of cancer by maintaining proliferation signals, escaping growth inhibitors, resisting cell death, inducing angiogenesis, and activating invasion and metastasis (24, 25). The lack of nourishment, including various mineral and vitamin deficiencies (e.g., iron, folic acid, and vitamin B12) in patients with cancer, increases the RDW levels (26). Recent studies have found that RDW levels in patients with colon cancer are significantly higher than those in patients with colon polyps (27–29). Moreover, patients who developed esophageal cancer, breast cancer, lung cancer, gastric cancer, colon cancer, prostate cancer, lymphoma, and other malignant

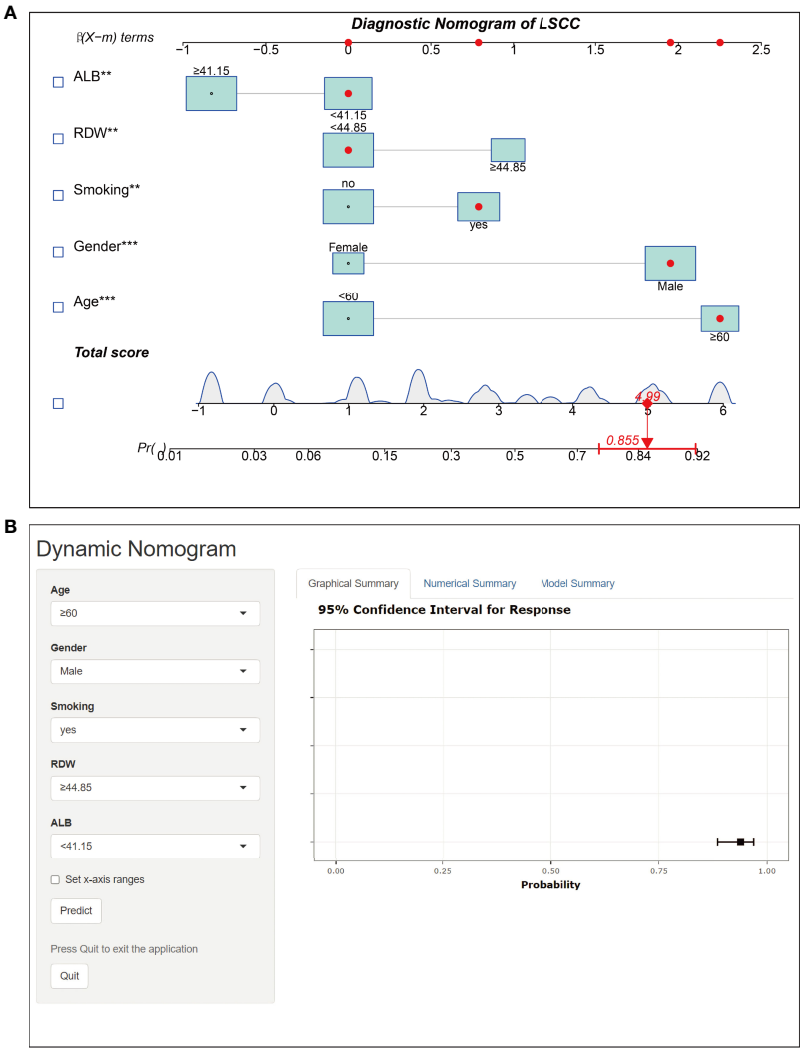

FIGURE 6 | Nomogram prediction model for LSCC diagnosis. **(A)** Established nomogram in the training cohort by incorporating the following five parameters: age, sex, smoking history, RDW, and, ALB.** p<0.01, *** p<0.001. **(B)** Online dynamic nomogram accessible at https://hanchenchen.shinyapps.io/LSCCNomapp/.

tumors with high RDW levels have a poor prognosis (28, 30, 31). Hence, RDW levels indicate chronic inflammation and malnutrition in patients with cancer. However, there is a lack of relevant research evaluating the role of RDW levels in the diagnosis, staging, and metastasis of LSCC. In this study, ROC curve analysis showed that the AUC of RDW in the diagnosis of LSCC was 0.684, suggesting a diagnostic significance for LSCC.

As a water-soluble liver protein, ALB acts as a transporter of several hormones, minerals, and fatty acids, and helps maintain the capillary colloidal osmotic pressure. ALB acts as an antioxidant in the plasma and interstitial space, providing amino acids for matrix deposition and cell proliferation (32). ALB is the primary protective factor against stable DNA replication and cell growth. High concentrations of ALB significantly inhibits the growth of various tumor cells. The inflammatory response and nutrition in patients with cancer can lead to a reduction in ALB production (33, 34). For instance, cancer promotes the expression of TNF-α (a pro-inflammatory factor), which can downregulate the transcription of the albumin gene and inhibit albumin synthesis in hepatocytes. However, TNF-α also increases the permeability of microvessels and exudation of albumin through the capillaries (35, 36), reducing the ALB levels. Previous clinical studies have shown that cancer patients usually present with a severe nutritional status at the time of diagnosis. Innutrition is known to play a vital role in the occurrence and development of cancer cachexia as well as the recurrence and progression of various cancer types (37). Hence, low levels of ALB in patients with different malignant tumors have been associated with poor prognosis (34, 38), which was consistent with our results. In this study, the ALB levels in the LSCC group were significantly lower than those in the BLL control group. Additionally, the cut-off value of ALB in the

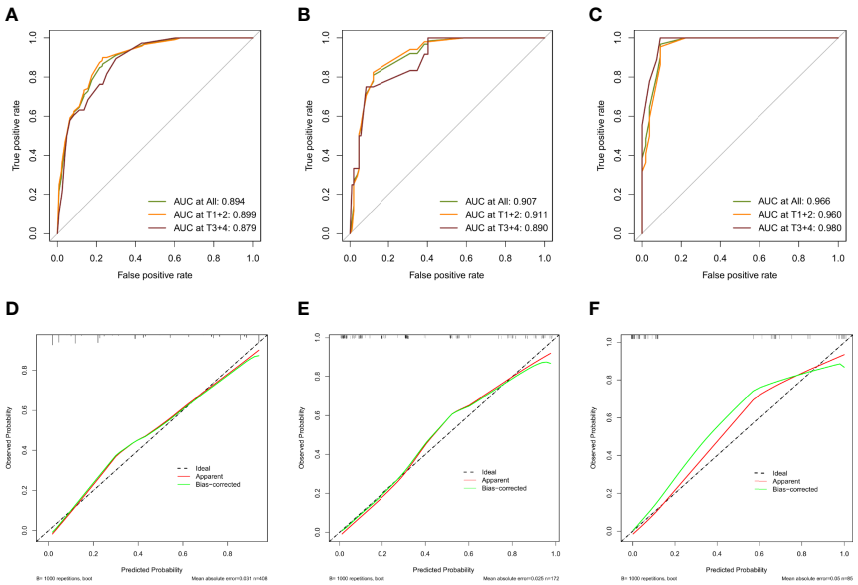

FIGURE 7 | Evaluation of validity and reliability of the model. ROC curves of the nomogram prediction model in the training cohort **(A)**, internal test cohort **(B)**, and, external test cohort **(C)**; calibration curves of the nomogram prediction model for the training cohort **(D)**, internal test cohort **(E)**, and, external test cohort **(F)**.

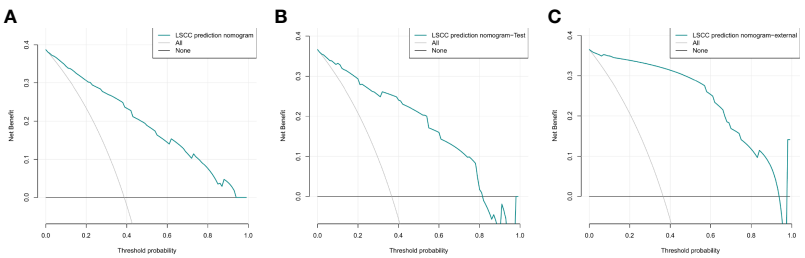

FIGURE 8 | Decision curve analysis of the nomogram of the training cohort **(A)**, internal test cohort **(B)**, and, external test cohort **(C)**.

diagnosis of LSCC was 41.15, with a sensitivity of 66.8%, a specificity of 64.6%, and a 95% CI of 0.639–0.745, thus indicating that it was an excellent diagnostic indicator.

Taken together, we conclude that ALB and RDW are potential biomarkers for the auxiliary diagnosis of LSCC. Independent analysis showed that both inflammation-related indicators were independent predictors of risk factors for LSCC. Therefore, by combining these two inflammatory biomarkers with other clinical factors (age, sex, and smoking history), an online predictive nomogram model was constructed, which is valuable in the auxiliary diagnosis and may be useful for early treatment of LSCC.

However, our study some limitations. First, this was a retrospective study with some inevitable bias. Therefore, a multicenter randomized controlled clinical study with a larger sample size could be performed in the future to verify the clinical benefits. Moreover, whether the incidence of laryngeal cancer in women is correlated with menopausal status and estrogen levels should be explored further. Second, the prediction model and dynamic nomogram were based on known risk factors, but some factors influencing the incidence of LSCC have not been studied and justified. Hence, relevant indicators can be continuously refined in the future with the development of molecular biology, which can further improve the diagnostic accuracy of the dynamic online nomogram. Third, the establishment of the model is based on the perioperative data; therefore, preoperative prediction is impossible. Finally, this algorithm only considered patients undergoing surgery; therefore, there may be selection bias compared with other nomograms.

CONCLUSION

This study was the first to develop and validate online nomograms based on the independent risk factors to dynamically predict diagnosis in individuals with LSCC. These novel models

demonstrated superior performance and discriminative power, which can provide vital information for otolaryngologists when designing customized clinical treatments.

DATA AVAILABILITY STATEMENT

The original contributions presented in the study are included in the article/supplementary material. Further inquiries can be directed to the corresponding authors.

ETHICS STATEMENT

The studies involving human participants were reviewed and approved by the medical ethics committees of The First Affiliated Hospital of Anhui Medical University (Reference number: Quick -PJ 2021-15-32). The patients/participants provided their written informed consent to participate in this study.

AUTHOR CONTRIBUTIONS

All the authors worked together to complete the paper. YeL, as the Corresponding Authors guided the design of the entire experiment and the writing of the paper. Yu L, YH, and BC are responsible for the collection of specimens, the writing of papers, design of the experiment, and other scattered work, they contributed equally to this work as first authors. YT, JW, DL, ZD, ZF, SY, JPW, KY, JZ, HS, YW, XW, and YJ were engaged in the collection of the clinical data. All authors contributed to the article and approved the submitted version.

FUNDING

This project was supported by National Natural Science Fund (82171127).

SUPPLEMENTARY MATERIAL

The Supplementary Material for this article can be found online at: https://www.frontiersin.org/articles/10.3389/fonc.2022.829761/full#supplementary-material

Supplementary Figure 1 | The coefficients of multivariate logistic regression analysis.

Supplementary Table 1 | The coefficients of Lasso regression analysis.

REFERENCES

1. Siegel RL, Miller KD, Jemal A. Cancer Statistics, 2020. *CA Cancer J Clin* (2020) 70(1):7–30. doi: 10.3322/caac.21590
2. Marcos CA, Alonso-Guervos M, Prado NR, Gimeno TS, Iglesias FD, Hermsen M, et al. Genetic Model of Transformation and Neoplastic Progression in Laryngeal Epithelium. *Head Neck* (2011) 33(2):216–24. doi: 10.1002/hed.21432
3. Gamez ME, Blakaj A, Zoller W, Bonomi M, Blakaj DM. Emerging Concepts and Novel Strategies in Radiation Therapy for Laryngeal Cancer Management. *Cancers (Basel)* (2020) 12(6):21. doi: 10.3390/cancers12061651.Citedin:Pubmed
4. Ni XG, Zhang QQ, Wang GQ. Narrow Band Imaging Versus Autofluorescence Imaging for Head and Neck Squamous Cell Carcinoma Detection: A Prospective Study. *J Laryngol Otol* (2016) 130(11):1001–6. doi: 10.1017/S0022215116009002
5. Friedman J, Hastie T, Tibshirani R. Regularization Paths for Generalized Linear Models *via* Coordinate Descent. *J Stat Software* (2010) 33(1):1–22. doi: 10.18637/jss.v033.i01
6. Zhou ZR, Wang WW, Li Y, Jin KR, Wang XY, Wang ZW, et al. In-Depth Mining of Clinical Data: The Construction of Clinical Prediction Model With R. *Ann Transl Med* (2019) 7(23):796. doi: 10.21037/atm.2019.08.63
7. Zhang Z, Rousson V, Lee WC, Ferdynus C, Chen M, Qian X, et al. Written on Behalf of AMEB-DCTCG. *Decision Curve Analysis* (2018) 6(15):308. doi: 10.21037/atm.2018.07.02
8. Lucas Grzelczyk W, Szemraj J, Kwiatkowska S, Jozefowicz-Korczynska M. Serum Expression of Selected miRNAs in Patients With Laryngeal Squamous Cell Carcinoma (LSCC). *Diagn Pathol* (2019) 14(1):49. doi: 10.1186/s13000-019-0823-3
9. Machiels JP, Rene Leemans C, Golusinski W, Grau C, Licitra L, Gregoire V, et al. Reprint of "Squamous Cell Carcinoma of the Oral Cavity, Larynx, Oropharynx and Hypopharynx: EHNS-ESMO-ESTRO Clinical Practice Guidelines for Diagnosis, Treatment and Follow-Up". *Oral Oncol* (2021) 113:105042. doi: 10.1016/j.oraloncology.2020.105042
10. Zhang SS, Xia QM, Zheng RS, Chen WQ. Laryngeal Cancer Incidence and Mortality in China, 2010. *J Cancer Res Ther* (2015) 11(Suppl 2):C143–8. doi: 10.4103/0973-1482.168175
11. Bray F, Ferlay J, Soerjomataram I, Siegel RL, Torre LA, Jemal A. Global Cancer Statistics 2018: GLOBOCAN Estimates of Incidence and Mortality Worldwide for 36 Cancers in 185 Countries. *CA Cancer J Clin* (2018) 68(6):394–424. doi: 10.3322/caac.21492
12. Gallus S, Bosetti C, Franceschi S, Levi F, Negri E, La Vecchia C. Laryngeal Cancer in Women: Tobacco, Alcohol, Nutritional, and Hormonal Factors. *Cancer Epidemiol Biomarkers Prev* (2003) 12(6):514–7.
13. Majszyk D, Bruzgielewicz A, Osuch-Wojcikiewicz E, Rzepakowska A, Niemczyk K. Gender-Related Incidence, Risk Factors Exposure and Survival Rates of Laryngeal Cancers - The 10-Years Analysis of Trends From One Institution. *Otolaryngol Pol* (2019) 73(3):6–10. doi: 10.5604/01.3001.0013.1003
14. Chang CP, Chang SC, Chuang SC, Berthiller J, Ferro G, Matsuo K, et al. Age at Start of Using Tobacco on the Risk of Head and Neck Cancer: Pooled Analysis in the International Head and Neck Cancer Epidemiology Consortium (INHANCE). *Cancer Epidemiol* (2019) 63:101615. doi: 10.1016/j.canep.2019.101615
15. Zuo JJ, Tao ZZ, Chen C, Hu ZW, Xu YX, Zheng AY, et al. Characteristics of Cigarette Smoking Without Alcohol Consumption and Laryngeal Cancer: Overall and Time-Risk Relation. A Meta-Analysis of Observational Studies. *Eur Arch Otorhinolaryngol* (2017) 274(3):1617–31. doi: 10.1007/s00405-016-4390-x
16. Qiu F, Liang CL, Liu H, Zeng YQ, Hou S, Huang S, et al. Impacts of Cigarette Smoking on Immune Responsiveness: Up and Down or Upside Down? *Oncotarget* (2017) ;8(1):268–84. doi: 10.18632/oncotarget.13613
17. Di Credico G, Polesel J, Dal Maso L, Pauli F, Torelli N, Luce D, et al. Alcohol Drinking and Head and Neck Cancer Risk: The Joint Effect of Intensity and Duration. *Br J Cancer* (2020) 123(9):1456–63. doi: 10.1038/s41416-020-01031-z
18. Trinchieri G. Cancer and Inflammation: An Old Intuition With Rapidly Evolving New Concepts. *Annu Rev Immunol* (2012) 30:677–706. doi: 10.1146/annurev-immunol-020711-075008
19. Wan GX, Chen P, Cai XJ, Li LJ, Yu XJ, Pan DF, et al. Elevated Red Cell Distribution Width Contributes to a Poor Prognosis in Patients With Esophageal Carcinoma. *Clin Chim Acta* (2016) 452:199–203. doi: 10.1016/j.cca.2015.11.025

20. Wang PF, Song SY, Guo H, Wang TJ, Liu N, Yan CX. Prognostic Role of Pretreatment Red Blood Cell Distribution Width in Patients With Cancer: A Meta-Analysis of 49 Studies. *J Cancer* (2019) 10(18):4305–17. doi: 10.7150/jca.31598
21. Meng S, Ma Z, Lu C, Liu H, Tu H, Zhang W, et al. Prognostic Value of Elevated Red Blood Cell Distribution Width in Chinese Patients With Multiple Myeloma. *Ann Clin Lab Sci* (2017) 47(3):282–90.
22. Means RTJr., Krantz SB. Inhibition of Human Erythroid Colony-Forming Units by Tumor Necrosis Factor Requires Beta Interferon. *J Clin Invest* (1993) 91(2):416–9. doi: 10.1172/JCI116216
23. Pavese I, Satta F, Todi F, Di Palma M, Piergrossi P, Migliore A, et al. High Serum Levels of TNF-Alpha and IL-6 Predict the Clinical Outcome of Treatment With Human Recombinant Erythropoietin in Anaemic Cancer Patients. *Ann Oncol* (2010) 21(7):1523–8. doi: 10.1093/annonc/mdp568
24. Hsueh CY, Lau HC, Li S, Tao L, Zhang M, Gong H, et al. Pretreatment Level of Red Cell Distribution Width as a Prognostic Indicator for Survival in a Large Cohort Study of Male Laryngeal Squamous Carcinoma. *Front Oncol* (2019) 9:271. doi: 10.3389/fonc.2019.00271
25. Zhao Z, Liu T, Li J, Yang W, Liu E, Li G. Elevated Red Cell Distribution Width Level Is Associated With Oxidative Stress and Inflammation in a Canine Model of Rapid Atrial Pacing. *Int J Cardiol* (2014) 174(1):174–6. doi: 10.1016/j.ijcard.2014.03.189
26. Douglas SW, Adamson JW. The Anemia of Chronic Disorders: Studies of Marrow Regulation and Iron Metabolism. *Blood* (1975) 45(1):55–65. doi: 10.1182/blood.V45.1.55.55
27. Ay S, Eryilmaz MA, Aksoy N, Okus A, Unlu Y, Sevinc B. Is Early Detection of Colon Cancer Possible With Red Blood Cell Distribution Width? *Asian Pac J Cancer Prev* (2015) 16(2):753–6. doi: 10.7314/apjcp.2015.16.2.753
28. Kara M, Uysal S, Altinisik U, Cevizci S, Guclu O, Derekoy FS. The Pre-Treatment Neutrophil-to-Lymphocyte Ratio, Platelet-to-Lymphocyte Ratio, and Red Cell Distribution Width Predict Prognosis in Patients With Laryngeal Carcinoma. *Eur Arch Otorhinolaryngol* (2017) 274(1):535–42. doi: 10.1007/s00405-016-4250-8
29. Yang D, Quan W, Wu J, Ji X, Dai Y, Xiao W, et al. The Value of Red Blood Cell Distribution Width in Diagnosis of Patients With Colorectal Cancer. *Clin Chim Acta* (2018) 479:98–102. doi: 10.1016/j.cca.2018.01.022
30. Lippi G, Targher G, Montagnana M, Salvagno GL, Zoppini G, Guidi GC. Relation Between Red Blood Cell Distribution Width and Inflammatory Biomarkers in a Large Cohort of Unselected Outpatients. *Arch Pathol Lab Med* (2009) 133(4):628–32. doi: 10.1043/1543-2165-133.4.62810.5858/133.4.628
31. Riedl J, Posch F, Konigsbrugge O, Lotsch F, Reitter EM, Eigenbauer E, et al. Red Cell Distribution Width and Other Red Blood Cell Parameters in Patients With Cancer: Association With Risk of Venous Thromboembolism and Mortality. *PloS One* (2014) 9(10):e111440. doi: 10.1371/journal.pone.0111440
32. Bourdon E, Blache D. The Importance of Proteins in Defense Against Oxidation. *Antioxid Redox Signal* (2001) 3(2):293–311. doi: 10.1089/152308601300185241
33. Seaton K. Albumin Concentration Controls Cancer. *J Natl Med Assoc* (2001) 93(12):490–3.
34. Xuan Q, Yang Y, Ji H, Tang S, Zhao J, Shao J, et al. Combination of the Preoperative Albumin to Globulin Ratio and Neutrophil to Lymphocyte Ratio as a Novel Prognostic Factor in Patients With Triple Negative Breast Cancer. *Cancer Manag Res* (2019) 11:5125–31. doi: 10.2147/CMAR.S195324
35. Gabay C, Kushner I. Acute-Phase Proteins and Other Systemic Responses to Inflammation. *N Engl J Med* (1999) 340(6):448–54. doi: 10.1056/NEJM199902113400607
36. Zhou T, Yu ST, Chen WZ, Xie R, Yu JC. Pretreatment Albumin Globulin Ratio has a Superior Prognostic Value in Laryngeal Squamous Cell Carcinoma Patients: A Comparison Study. *J Cancer* (2019) 10(3):594–601. doi: 10.7150/jca.28817
37. Chung JW, Park DJ, Chun SY, Choi SH, Lee JN, Kim BS, et al. The Prognostic Role of Preoperative Serum Albumin/Globulin Ratio in Patients With Non-Metastatic Renal Cell Carcinoma Undergoing Partial or Radical Nephrectomy. *Sci Rep* (2020) 10(1):11999. doi: 10.1038/s41598-020-68975-3
38. Gupta D, Lis CG. Pretreatment Serum Albumin as a Predictor of Cancer Survival: A Systematic Review of the Epidemiological Literature. *Nutr J* (2010) 9:69. doi: 10.1186/1475-2891-9-69

Conflict of Interest: The authors declare that the research was conducted in the absence of any commercial or financial relationships that could be construed as a potential conflict of interest.

frontiers | Frontiers in Oncology

ORIGINAL RESEARCH
published: 27 May 2022
doi: 10.3389/fonc.2022.793318

Gastrointestinal Endoscopy Performed by Gastroenterologists: Opportunistic Screening Strategy for Newly Diagnosed Head and Neck Cancers

Chih-Wei Yang[1], *Yueng-Hsiang Chu*[2], *Hsin-Chien Chen*[2], *Wei-Chen Huang*[1], *Peng-Jen Chen*[1] *and Wei-Kuo Chang*[1]*

[1] Division of Gastroenterology, Department of Internal Medicine, Tri-Service General Hospital, National Defense Medical Center, Taipei, Taiwan, [2] Department of Otolaryngology-Head and Neck Surgery, Tri-Service General Hospital, National Defense Medical Center, Taipei, Taiwan

Aim: Approximately 66% of head and neck cancers are diagnosed at an advanced stage. This prospective study aimed to detect newly diagnosed head and neck cancers using regular upper gastrointestinal (UGI) endoscopy with oral-pharynx-larynx examination.

Methods: A total of 2,849 patients underwent UGI endoscopy with an additional oral-pharynx-larynx examination. Patients aged < 20 years, those who were pregnant, had a history of head and neck cancers, were undergoing emergency endoscopy, and had a poor laryngopharyngeal view were excluded. The symptoms, incidence, location, pathology, and stage of malignant neoplasms were investigated.

Results: A total of 2,720 patients were enrolled. Endoscopically observable 23 abnormal findings (0.85%) included 18 (0.66%) benign lesions and 5 (0.18%) newly diagnosed malignant neoplasms. Notably, 4 (80%) of 5 patients with malignant neoplasms were diagnosed at an early stage (Stage 0, I, and II).

Conclusions: UGI endoscopy with oral-pharynx-larynx examination can achieve opportunistic head neck cancer screening and is recommended for every patient in endoscopy units.

Keywords: upper gastrointestinal endoscopy, endoscopy, screening, cancer, head and neck cancer

OPEN ACCESS

Edited by:
Markus Wirth,
Klinikum rechts der Isar, Germany

Reviewed by:
Abdelbaset Mohamed Elasbali,
Al Jouf University, Saudi Arabia
Seng-Kee Chuah,
Kaohsiung Chang Gung Memorial Hospital, Taiwan

***Correspondence:**
Wei-Kuo Chang
weikuohome@hotmail.com

Specialty section:
This article was submitted to Head and Neck Cancer, a section of the journal Frontiers in Oncology

Received: *11 October 2021*
Accepted: *02 May 2022*
Published: *27 May 2022*

Citation:
Yang C-W, Chu Y-H, Chen H-C, Huang W-C, Chen P-J and Chang W-K (2022) Gastrointestinal Endoscopy Performed by Gastroenterologists: Opportunistic Screening Strategy for Newly Diagnosed Head and Neck Cancers. Front. Oncol. 12:793318. doi: 10.3389/fonc.2022.793318

INTRODUCTION

Head and neck cancer is the sixth most common cancer worldwide (1). An estimated 53,000 new cases of head and neck cancer were reported in the United States in 2019 (2). Approximately 66% of head and cancer patients are diagnosed at an advanced stage and have a poor performance status (3). Gastrointestinal (GI) community studies reported that newly diagnosed head and neck cancer, ranging from 67% to 100% at an early curable stage, were incidentally detected with regular upper gastrointestinal (UGI) endoscopy (4–6).

Approximately 6 million upper endoscopies were performed in the United States in 2013 (7). The newly diagnosed cancer detection rate, ranging from 0.08% to 0.18%, was reported during regular UGI

endoscopy (4–6). Assuming a newly diagnosed head and neck cancer detection rate of 0.1% for all endoscopies, regular upper endoscopy may provide an excellent opportunity to detect as many as 6,000 new potentially curable head and neck cancers each year.

Most national cancer screening programs are well organized and selective and target the population who is at the highest risk (8). The Taiwan Health Promotion Administration (HPA) provides national oral cancer screening for head and neck cancers (9). The HPA has commissioned the Taiwan Dental Association and the Taiwan Head and Neck Society to provide training on oral mucosa tests to dentists and ear, nose, and throat (ENT) doctors. The HPA has also authorized local governments to conduct oral mucus educational training for non-dental and non-ENT doctors once a year. A total of 412 non-dental and non-ENT doctors underwent this training in 2016. The HPA has collaborated with local health centers to hold practical training events at medical institutions conducting oral cancer testing and helped the trained doctors to perform opportunity cancer screening during daily practice (9, 10). The HPA regularly organizes a cancer screening education training program for non-dental and non-ENT physicians. This workshop was tailored toward GI physicians who provide care for patients at the endoscopy units and was designed to help them acquire the necessary knowledge and skill to promote head and neck cancer screening in the endoscopy units.

The oral cavity, pharynx, and larynx are located at the entrance to the esophagus and must be passed through during UGI endoscopy. GI endoscopists have performed opportunistic endoscopic screening at no additional cost; this was found effective on a large number of patients and offered both physicians and patients an opportunity for early detection of cancers (8, 11). However, the oral cavity, pharynx, and larynx are generally considered to be a field of otolaryngology. Gastroenterologists may be unfamiliar with the oral-pharynx-larynx examination. It is often impractical to ask patients to move their tongue upward and laterally to obtain a clear view of the oral cavity during the endoscopic examination. Endoscopic movements may cause the scope to touch the pharyngeal walls, trigger the coughing and gag reflex, and result in a poor laryngopharyngeal view. Several methods have been developed to overcome the challenges of UGI endoscopy with an additional oral-pharynx-larynx examination (6, 12–20).

UGI endoscopy with an additional oral-pharynx-larynx examination requires minimal additional time and is well tolerated by patients (6, 12, 14, 18, 19, 21). This prospective multidisciplinary study aimed to detect newly diagnosed head and neck cancers, by using regular UGI endoscopy with oral-pharynx-larynx examination.

MATERIALS AND METHODS

Study Design

Patients undergoing regular UGI endoscopy at Tri-Service General Hospital, Taiwan, from December 2015 to December 2019 were included in the study. Patients aged < 20 years and those who were pregnant, undergoing emergency endoscopy, and had a poor laryngopharyngeal view were excluded. Before commencing the study, endoscopists were trained to perform UGI endoscopy with oral-pharynx-larynx examination, recognize the most common pathological findings, and summarize the possible pathologies. Demographic characteristics included sex, age, and presenting symptoms. Habits of cigarette smoking, alcohol drinking, and betel nut chewing were recorded. The present study was approved by the Institutional Review Board of the Tri-Service General Hospital, Taiwan (TSGHIRB 2-108-05-136). All methods were performed in accordance with the relevant guidelines and regulations. Patients were fully informed of the purpose of the study and they provided signed informed consent.

Endoscopy Instruments

The UGI endoscopic examinations were performed using narrow-band imaging (EVIS LUCERA ELITE CVL-290; Olympus Optical Co Ltd, Tokyo, Japan) fitted with an endoscope (GIF-H260, GIF-H260Z, GIF-Q260, GIF-Q260Z, GIF-H290, GIF-HQ290, and GIF-H290Z; Olympus). Endoscopy with oral-pharynx-larynx examination was performed using a digital video recorder (HVO-550MD; Sony, Tokyo, Japan) (12, 15, 22).

UGI Endoscopy With Oral-Pharynx-Larynx Examination

Patients were asked to fast for at least 4 hours (6, 12, 18, 23–25). Premedication varied according to the preference of the individual endoscopist, but consisted mostly of topical anesthesia, sometimes in combination with intravenous midazolam. Patients were placed in the left lateral decubitus position. The distal end of the endoscope was held approximately 30 cm away from the tip. The tip of the endoscope was inserted through a mouth-piece. With advancement of the endoscope along the midline of the palate, the uvula could be visualized over the base of the tongue. After the patient takes a deep breath, the epiglottis moves upward and forward, expanding and opening-up the larynx and vocal cord, which then provides a clear laryngopharyngeal view. The endoscope was rotated slightly, passed through the uvula, and gently advanced with anterior flexion to visualize the pyriform sinus, laryngeal vestibule, vocal cords, and upper part of the trachea. The vocal cords were observed at rest and during phonation of the word "e". The pyriform sinus was inspected with minimal lateral deflection. Patients were monitored for their heart rate, electrocardiography findings, and oxygen saturation.

Pathological and Diagnosis Confirmation

Endoscopically observable abnormal findings such as cysts, polyps, ulcers, leukoplakia, and telangiectasia in the oral-pharynx-larynx area were carefully investigated. Patients with endoscopically observable abnormal lesions were directly referred to an ENT specialist or oral surgeon for later review, where they underwent the standard method for examination and/or pathological confirmation. Premalignant or malignant neoplasms were histologically confirmed according to the World Health Organization criteria (26). The 8th edition of the American Joint Committee on Cancer (AJCC) was used for tumor staging (27). The treatment planning was conducted

through tumor board review, which is composed of expert opinions from gastroenterologists, ENT specialists, radio-oncologists, and surgical, dental, and medical oncologists.

Statistical Analysis

The data were analyzed using Excel 2010. Data are presented as means ± standard deviation for continuous variables with normal distribution and percentages (%) for categorical variables.

RESULTS

Patient Characteristics

The characteristics of the 23 patients with endoscopically observable abnormal findings are shown in **Table 1**. The patients included 18 men and 5 women, aged 65.5 ± 12.4 years. Some patients had a habit of cigarette smoking (n = 17), alcohol consumption (n = 16), and betel nut chewing (n = 9). The presenting symptoms included globus sensation (n = 9), epigastric pain (n = 10), dysphagia (n = 9), GI bleeding (n = 2), acid regurgitation (n = 4), and body weight loss (n = 4).

TABLE 1 | Characteristics of 23 patients with abnormal endoscopic findings.

Variable	Patients (n = 23)
Male/Female	18/5
Age (years), mean (SD)	65.5 ± 12.4
Smoking cigarettes, no. (%)	17 (74%)
Alcohol drinking, no. (%)	16 (70%)
Betel nut chewing, no. (%)	9 (39%)
Symptom, no. (%)	
Globus sensation	9 (39%)
Epigastric pain	10 (45%)
Dysphagia	9 (39%)
GI bleeding	2 (8%)
Acid regurgitation	4 (17%)
Body weight loss	4 (17%)

GI, gastrointestinal; no, number; SD, standard deviation.

UGI Endoscopy With Oral-Pharynx-Larynx Examination

During the study period, UGI endoscopies were performed in 3,275 patients (**Figure 1**); 2,849 patients (87%) successfully completed UGI endoscopy with oral-pharynx-larynx examination. The added endoscopy time ranged from 17 to 60 seconds with a mean of 30 seconds.

Endoscopically Observable Abnormal Findings

Twenty-three (0.85%) endoscopically observable abnormal findings (**Figure 2**) were found, including 18 (0.66%) benign lesions (vocal cord cyst, n = 4; vocal cord polyp, n = 7; vocal cord leucoplakia, n = 1; oral ulcer, n = 3; and telangiectasia, n = 3) and 5 (0.18%) pathologically confirmed malignant neoplasms (squamous cell carcinoma, n = 5).

Newly Diagnosed Malignant Neoplasms

Five newly diagnosed malignant neoplasms (0.18%) were found in 2,720 patients without a history of head and neck cancer (**Table 2**). All five patients had a habit of smoking cigarettes, alcohol drinking, or betel nut chewing (**Table 3**). The five newly diagnosed malignant neoplasms were located in the pharynx

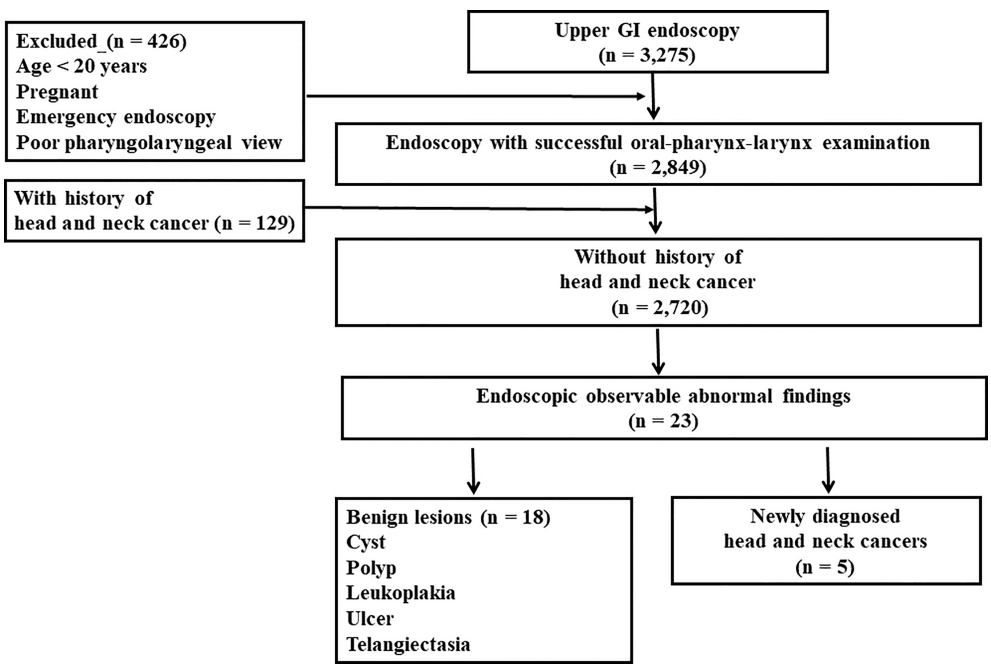

FIGURE 1 | Flowchart of data processing. GI, gastrointestinal.

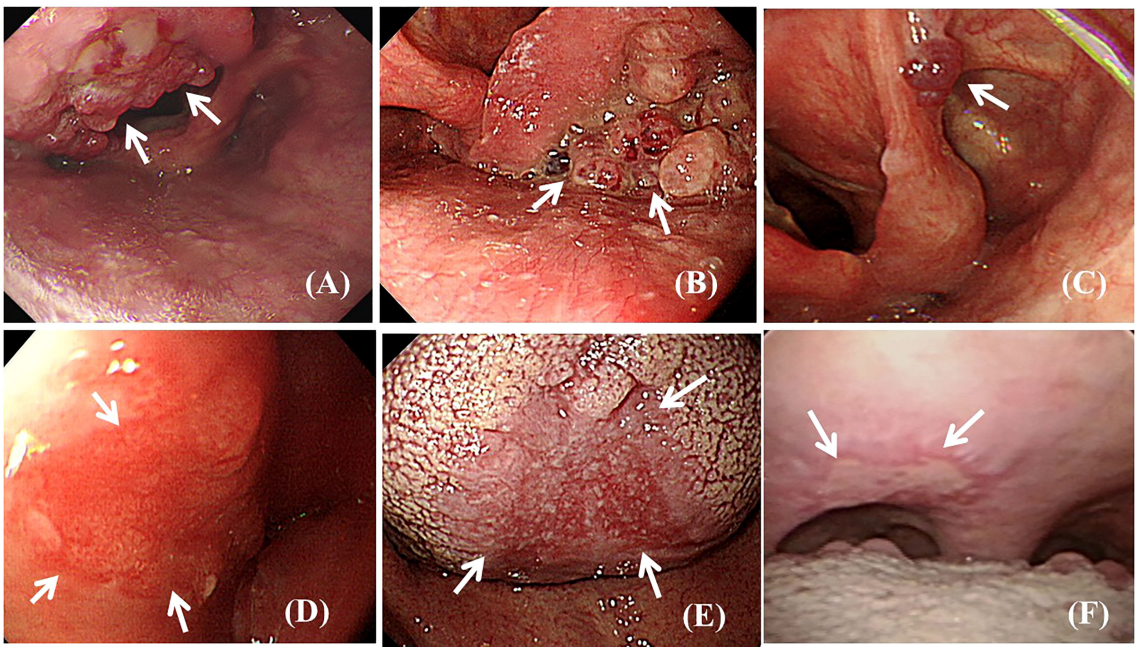

FIGURE 2 | Endoscopic view of observable abnormal findings (arrows). **(A)** Polypoid squamous cell carcinoma lesion at the epiglottis. **(B)** Polypoid squamous cell carcinoma lesion at the left side piriform sinus. **(C)** Polypoid low-grade dysplasia lesion at the aryepiglottic fold. **(D)** Superficial flat squamous cell carcinoma lesion at the lateral wall of the hypopharynx. **(E)** Superficial flat squamous cell carcinoma lesion at the middle area of the dorsal tongue. **(F)** Superficial ulcerative low-grade dysplasia lesion at the soft palate.

(n = 3), larynx (n = 1), and oral cavity (n = 1). Notably, 80% of malignant neoplasms (n = 4) were found at an early stage (AJCC stage 0, I, and II). Three patients (cases # 1, # 2, and # 3) were suitable for minimally invasive treatment, such as local surgery or endoscopic mucosal resection.

DISCUSSION

Summary of New Highlights in This Manuscript

This is a large prospective study that reported observable abnormal findings in the oral cavity, pharynx, and larynx, using regular UGI endoscopy. Five newly diagnosed malignant neoplasms (0.18%) were observed in 2,720 patients without a history of head and neck cancer. Four (80%) of the newly diagnosed malignant neoplasms were at an early stage without obstructive symptoms, which made curative treatment possible. Upper GI endoscopy with oral-pharynx-larynx screening examination can provide several advantages regarding the necessary information for further therapeutic interventions. Our number of UGI endoscopies (n = 2,800) is similar to that seen in previous gastrointestinal (GI) community studies (n = 1120, n = 1623) that used UGI endoscopy with an additional oral-pharynx-larynx examination to perform opportunistic endoscopic head and neck cancer screening. Our results are similar to those of previous studies (**Table 2**), where the cancer

TABLE 2 | Newly diagnosed head and neck cancers detected with regular UGI Endoscopy.

Study	Endoscopy with Oral-pharynx-larynx Examination			Newly diagnosed head and neck cancer			
	Total	Success		New cancer		Early stage*	
	(n)	(n)	(%)	(n)	(%)	(n)	(%)
Watanabe et al, 1996 (4)	N.R.	1,623	N.R.	3	0.18	2	67
Lehman et al, 1982 (5)	N.R.	1,120	N.R.	1	0.09	1	100
Mullhaupt et al, 2004 (6)	1,311	1,209	93	1	0.08	1	100
Current study	3,275	2,852	87	5	0.15	4	80

UGI, upper gastrointestinal; N.R, not recorded; American Joint Committee on Cancer clinical stage 0, I, or II.*

TABLE 3 | Characteristics of five newly diagnosed head and neck cancers.

Case	Age	Sex	Symptom	Risk factor	Tumor location	Pathology	TNM system	AJCC stage	Treatment
1	56	M	Dysphagia	A, C	Pharynx	SCC	$T_{is}N_0M_0$	0	Local surgery
2	62	M	Globus	A, C	Pharynx	SCC	$T_{1a}N_0M_0$	I	EMR-C
3	64	M	Regurgitation	A, B, C	Oral cavity	SCC	$T_1N_0M_0$	I	Local surgery
4	72	M	Dysphagia	A, C	Larynx	SCC	$T_2N_0M_0$	II	CCRT
5	68	M	Dysphagia	A, B, C	Pharynx	SCC	$T_3N_{2b}M_0$	IVA	CCRT, surgery

M, male; A, alcohol drinking; B, betel nut chewing; C, cigarette smoking; SCC, squamous cell carcinoma; EMR-C, endoscopic mucosal resection with a cap; CCRT, concurrent chemoradiotherapy; AJCC, American Joint Committee on Cancer; TNM, tumor, nodes, and metastases.

detection rate ranged from 0.08% to 0.18%, with the proportion of early-stage cancers ranging from 67% to 100% (4–6).

Majority of Newly Diagnosed Head and Neck Cancer Without Obstructive Symptoms

The Taiwan HPA provides national oral cancer screening for high-risk populations (9). Moreover, the HPA organizes an oral cancer screening training program for non-dental and non-ENT physicians. The HPA expects the trained GI physicians to monitor precancerous lesions and perform opportunistic oral cancer screening during daily practice (9, 10). The oral cavity, pharynx, and larynx are located at the entrance to the esophagus and must be passed through during UGI endoscopy. GI endoscopists should be aware of diseases of the oral-pharynx-larynx when performing UGI endoscopy. GI endoscopists have performed opportunistic endoscopic screening at no additional cost; this was found effective on a large number of patients and offered both physicians and patients an excellent opportunity for very early detection of cancers.

Symptom-directed, selective endoscopy is an efficient and cost-effective means to detect head and neck cancer (28). Head and neck cancer symptoms may include a lump in the neck, soreness in the mouth or throat that makes swallowing difficult, and a change or hoarseness in the voice. It is recommended that UGI endoscopy be conducted with an extra view of the blind spot of potential malignant neoplasms: the area underneath the tongue or in the space between the gum and cheeks. Unfortunately, majority of patients with laryngeal abnormalities (88%) did not report laryngeal symptoms, such as chronic hoarseness, throat clearing, or coughing, and would probably never have sought medical assistance. Thorough investigation of this area (oral-pharynx-larynx cavity) is considered mandatory to ensure provision of high quality endoscopic services. However, most GI endoscopists are unfamiliar with the oral-pharynx-larynx examination. Several gastrointestinal (GI) community studies using UGI endoscopy with an additional oral-pharynx-larynx examination have overcome the challenges of UGI endoscopy with an additional oral-pharynx-larynx examination. Newly diagnosed head and neck cancer, ranging from 67% to 100% at an early curable stage, were incidentally detected with regular UGI endoscopy (6, 12, 14, 15, 17, 19).

This study demonstrated that the majority of newly diagnosed malignant neoplasms were at an early stage without obstructive symptoms, which may be removed with minimally invasive treatment.

UGI Endoscope for Oral-Larynx-Pharyngeal Screening

The commonly used UGI endoscope (GIF-H290, Olympus) is preferred to the ENT laryngoscope (ENF-VH, Olympus) for endoscopic oral-pharynx-larynx examination. GI endoscopes have a larger outer diameter (8.9 mm vs. 3.9 mm) than ENT endoscopes and are available with a suction channel without impairing optics, providing powerful magnification images (85 times optical magnification vs. no optical magnification). The longer working channel length (103 cm vs. 30 cm) ensures that tumor screening is not only focused on the oral cavity, pharynx, and larynx, but also is extended into the esophagus. Flexible UGI endoscopes can easily perform a delicate endoscope manipulation and show an abnormal lesion hidden in the piriform sinus, postcricoid area, or posterior pharyngeal wall.

Conventional GI endoscopists tend to pass the endoscope quickly through the throat, with the intention of minimizing patient discomfort and without trying to perform an oral-pharynx-larynx examination. There is no standard technique for UGI endoscopy with oral cavity, pharynx, or larynx examination. Several methods were developed in this study to overcome the challenges of oral-pharynx-larynx examination.

GI Endoscopists Unfamiliar With the Oral-Pharynx-Larynx Examination

Successful UGI endoscopy for oral-pharynx-larynx examination requires adequate knowledge and procedural skills. However, current GI specialist training programs do not provide structured training in the ENT field. GI specialists are unfamiliar with UGI endoscopy when used for oral-pharynx-larynx examination. Therefore, there is a need to develop multidisciplinary teamwork and training programs for the implementation of UGI endoscopy with oral-pharynx-larynx examination.

GI specialists can never replace ENT specialists in the management of oral, pharyngeal, and laryngeal disorders. Oral cavity, pharynx, or larynx biopsies are not performed by GI endoscopists. A biopsy may cause pain because of a lack of local anesthesia and risk of bleeding (5, 14). After initial detection of an abnormal finding, patients should be directly referred to ENT specialists or oral surgeons for further diagnosis and treatment. Video recordings can be used to review the endoscopic examination later on a monitor, which can reduce the possibility

of missed observations (15, 22, 29, 30). Video recordings can also be used for communication, teaching, research, and education. Connection of a video recording system is recommended for endoscopy with oral-pharynx-larynx examination (6, 12, 15, 19).

Simplifying the Endoscopic Oral Examination

It was not practical to ask patients to move their tongue upward and laterally to obtain a clear view of the oral cavity during the endoscopic examination. It was especially difficult for patients who were critically ill, having neurological conditions, or under conscious sedation. To simplify the endoscopic oral examination, we did not routinely screen lesions hidden underneath the tongue or in the space between the gum and cheeks. Therefore, endoscopic oral examination can only have a view of the lips, palate, uvula, and dorsal surface of the tongue.

Having a Clear Laryngopharyngeal View

When the scope passes the uvula, the epiglottis may guard and cover the opening of the larynx and vocal cords and present an anatomically closed field; therefore, the scope cannot provide a clear view of the laryngopharyngeal area. When the patient takes a deep breath, the epiglottis moves upward and forward; the larynx and vocal cord then expand and open up and provide a wide and clear laryngopharyngeal view.

*T*he accumulation and pooling of secretions might fill in the lowermost area of the right side of the pyriform sinus, flow into the laryngeal vestibule or vocal cords, and increase the risk of aspiration pneumonia. To minimize the risk of aspiration and ensure a clear endoscopic view, secretions in the pharyngolaryngeal region were suctioned before inserting the endoscope into the esophagus.

Minimizing the Coughing and Gag Reflex

Topical pharyngeal sprays with anesthetic agents can be directed to the posterior pharyngeal wall to suppress coughing and gag reflex (22). A prospective study of 2,000 UGI endoscopic examinations without sedation and topical pharyngeal anesthesia (10% lidocaine spray) reported a safe, quick, and well-tolerated procedure (31). Topical pharyngeal anesthesia is not beneficial for conscious sedated patients (32).

Notably, a compassionate, relaxed, physician with a soothing bedside manner may be more effective than a topical pharyngeal spray (33). GI endoscopists may hold the distal end of the endoscope approximately 30 cm away from the tip (18). Therefore, when the scope passes from the uvula and pharynx into the upper esophagus, it is not necessary to change the hand-holding position, and it is much easier to make a delicate endoscope manipulation. Careful and slow endoscopic movements can avoid touching the pharyngeal walls. Creating an air or water infusion may irritate the throat or airway and trigger the coughing and gag reflex (6, 15, 22).

Limitations

The oral cavity, pharynx, and larynx are generally considered to be a field of otolaryngology. Limited training in the field of otolaryngology and the use of conventional vs. high-resolution endoscopic equipment could be considered as limitations. UGI endoscopy may have a blind spot when potential malignant neoplasms are located underneath the tongue or in the space between the gum and cheeks. This single-center study was conducted in Taiwan; therefore, the findings may not be generalizable to other populations. Further larger-scale study is necessary to develop an optimal screening program for head and neck cancers across different populations.

CONCLUSIONS

The UGI endoscope passes into the esophagus and with careful maneuvering and observation, GI endoscopists were able to extend observation into the oral cavity, pharynx, and larynx. UGI endoscopy with an additional oral-pharynx-larynx examination required minimal additional time, at no additional cost, and was well tolerated by patients. Most of the endoscopically observable malignant neoplasms were detected early enough for curative therapy. UGI endoscopy with oral-pharynx-larynx examination can achieve opportunistic head neck cancer screening and is recommended for every patient in endoscopy units.

DATA AVAILABILITY STATEMENT

The original contributions presented in the study are included in the article/supplementary material. Further inquiries can be directed to the corresponding author.

ETHICS STATEMENT

The studies involving human participants were reviewed and approved by the Institutional Review Board of the Tri-Service General Hospital, Taiwan (TSGHIRB 2-108-05-136). The patients/participants provided their written informed consent to participate in this study.

AUTHOR CONTRIBUTIONS

C-WY contributed to conception, design, and analysis, and interpretation of data. Y-HC, and H-CC contributed to conception, design, analysis and interpretation of data. W-CH and P-JC contributed to the analysis plan and wrote the manuscript. W-KC contributed to the study design and supervised the study. All authors reviewed the manuscript.

All authors contributed to the article and approved the submitted version.

FUNDING

We are grateful for the financial support provided by the Ministry of National Defense-Medical Affairs Bureau, Tri-Service General Hospital (TSGH-C108-070), Taiwan for this study.

ACKNOWLEDGMENTS

We thank Enago for English language editing service.

REFERENCES

1. Parkin DM, Bray F, Ferlay J, Pisani P. Global Cancer Statistics, 2002. *CA Cancer J Clin* (2005) 55(2):74–108. doi: 10.3322/canjclin.55.2.74
2. Siegel RL, Miller KD, Jemal A. Cancer Statistics, 2019. *CA Cancer J Clin* (2019) 69(1):7–34. doi: 10.3322/caac.21551
3. Cognetti DM, Weber RS, Lai SY. Head and Neck Cancer: An Evolving Treatment Paradigm. *Cancer* (2008) 113(7 Suppl):1911–32. doi: 10.1002/cncr.23654
4. Watanabe S, Matsuda K, Arima K, Uchida Y, Nishioka M, Haruo T, et al. Detection of Subclinical Disorders of the Hypopharynx and Larynx by Gastrointestinal Endoscopy. *Endoscopy* (1996) 28(3):295–8. doi: 10.1055/s-2007-1005456
5. Lehman G, Compton M, Meadows J, Elmore M. Screening Examination of the Larynx and Pharynx During Upper Gastrointestinal Panendoscopy. *Gastrointest Endosc* (1982) 28(3):176–8. doi: 10.1016/s0016-5107(82)73046-9
6. Mullhaupt B, Jenny D, Albert S, Schmid S, Fried M. Controlled Prospective Evaluation of the Diagnostic Yield of a Laryngopharyngeal Screening Examination During Upper Gastrointestinal Endoscopy. *Gut* (2004) 53 (9):1232–4. doi: 10.1136/gut.2003.030130
7. Peery AF, Crockett SD, Murphy CC, Lund JL, Dellon ES, Williams JL, et al. Burden and Cost of Gastrointestinal, Liver, and Pancreatic Diseases in the United States: Update 2018. *Gastroenterology* (2019) 156(1):254–72.e11. doi: 10.1053/j.gastro.2018.08.063
8. Brocklehurst PR, Speight PM. Screening for Mouth Cancer: The Pros and Cons of a National Programme. *Br Dent J* (2018) 225(9):815–9. doi: 10.1038/sj.bdj.2018.918
9. Huang CC, Lin CN, Chung CH, Hwang JS, Tsai ST, Wang JD. Cost-Effectiveness Analysis of the Oral Cancer Screening Program in Taiwan. *Oral Oncol* (2019) 89:59–65. doi: 10.1016/j.oraloncology.2018.12.011
10. Ho PS, Wang WC, Huang YT, Yang YH. Finding an Oral Potentially Malignant Disorder in Screening Program Is Related to Early Diagnosis of Oral Cavity Cancer - Experience From Real World Evidence. *Oral Oncol* (2019) 89:107–14. doi: 10.1016/j.oraloncology.2018.12.007
11. Mohan P, Richardson A, Potter JD, Coope P, Paterson M. Opportunistic Screening of Oral Potentially Malignant Disorders: A Public Health Need for India. *JCO Glob Oncol* (2020) 6:688–96. doi: 10.1200/JGO.19.00350
12. Cammarota G, Galli J, Agostino S, De Corso E, Rigante M, Cianci R, et al. Accuracy of Laryngeal Examination During Upper Gastrointestinal Endoscopy for Premalignancy Screening: Prospective Study in Patients With and Without Reflux Symptoms. *Endoscopy* (2006) 38(4):376–81. doi: 10.1055/s-2006-925127
13. Chang WK, Huang HH, Lin HH, Tsai CL. Evaluation of Oropharyngeal Dysphagia in Patients Who Underwent Percutaneous Endoscopic Gastrostomy: Stratification Risk of Pneumonia. *JPEN J Parenter Enteral Nutr* (2019) 44(2):239–45. doi: 10.1002/jpen.1592
14. Fatima H. Oropharyngeal Findings at Upper Endoscopy. *Clin Gastroenterol Hepatol* (2019) 17(12):2423–8. doi: 10.1016/j.cgh.2019.05.038
15. Katsinelos P, Kountouras J, Chatzimavroudis G, Zavos C, Beltsis A, Paroutoglou G, et al. Should Inspection of the Laryngopharyngeal Area be Part of Routine Upper Gastrointestinal Endoscopy? A Prospective Study. *Dig Liver Dis* (2009) 41(4):283–8. doi: 10.1016/j.dld.2008.06.015
16. Kang SH, Hyun JJ. Preparation and Patient Evaluation for Safe Gastrointestinal Endoscopy. *Clin Endosc* (2013) 46(3):212–8. doi: 10.5946/ce.2013.46.3.212
17. Park KS. Observable Laryngopharyngeal Lesions During the Upper Gastrointestinal Endoscopy. *Clin Endosc* (2013) 46(3):224–9. doi: 10.5946/ce.2013.46.3.224
18. Park KS. Introduction to Starting Upper Gastrointestinal Endoscopy: Proper Insertion, Complete Observation, and Appropriate Photographing. *Clin Endosc* (2015) 48(4):279–84. doi: 10.5946/ce.2015.48.4.279
19. Raju GS. Value of Screening the Laryngopharyngeal Area During Routine Upper Gastrointestinal Endoscopy. *Nat Clin Pract Gastroenterol Hepatol* (2005) 2(1):22–3. doi: 10.1038/ncpgasthep0064
20. Zullo A, Manta R, De Francesco V, Fiorini G, Hassan C, Vaira D. Diagnostic Yield of Upper Endoscopy According to Appropriateness: A Systematic Review. *Dig Liver Dis* (2019) 51(3):335–9. doi: 10.1016/j.dld.2018.11.029
21. Cammarota G, Agostino S, Rigante M, Cesaro P, Parrilla C, La Mura R, et al. Preliminary Laryngeal Examination During Magnifying Upper Gastrointestinal Video Endoscopy in Two Patients With Reflux Symptoms. *Endoscopy* (2006) 38(3):287. doi: 10.1055/s-2006-925216
22. Kamarunas EE, McCullough GH, Guidry TJ, Mennemeier M, Schluterman K. Effects of Topical Nasal Anesthetic on Fiberoptic Endoscopic Examination of Swallowing With Sensory Testing (FEESST). *Dysphagia* (2014) 29(1):33–43. doi: 10.1007/s00455-013-9473-x
23. Lee SH, Park YK, Cho SM, Kang JK, Lee DJ. Technical Skills and Training of Upper Gastrointestinal Endoscopy for New Beginners. *World J Gastroenterol* (2015) 21(3):759–85. doi: 10.3748/wjg.v21.i3.759
24. Chang WK, Huang HH, Lin HH, Tsai CL. Percutaneous Endoscopic Gastrostomy Versus Nasogastric Tube Feeding: Oropharyngeal Dysphagia Increases Risk for Pneumonia Requiring Hospital Admission. *Nutrients* (2019) 11(12):2969. doi: 10.3390/nu11122969
25. Wu CC, Huang HH, Lin HH, Chang WK. Oropharyngeal Dysphagia Increased the Risk of Pneumonia in Patients Undergoing Nasogastric Tube Feeding. *Asia Pac J Clin Nutr* (2020) 29(2):266–73. doi: 10.6133/apjcn.202007_29(2).0009
26. Gale N, Poljak M, Zidar N. Update From the 4th Edition of the World Health Organization Classification of Head and Neck Tumours: What Is New in the 2017 WHO Blue Book for Tumours of the Hypopharynx, Larynx, Trachea and Parapharyngeal Space. *Head Neck Pathol* (2017) 11(1):23–32. doi: 10.1007/s12105-017-0788-z
27. Lydiatt WM, Patel SG, O'Sullivan B, Brandwein MS, Ridge JA, Migliacci JC, et al. Head and Neck Cancers-Major Changes in the American Joint Committee on Cancer Eighth Edition Cancer Staging Manual. *CA Cancer J Clin* (2017) 67 (2):122–37. doi: 10.3322/caac.21389
28. Benninger MS, Shariff A, Blazoff K. Symptom-Directed Selective Endoscopy: Long-Term Efficacy. *Arch Otolaryngol Head Neck Surg* (2001) 127(7):770–3.
29. Sulica L, Carey B, Branski RC. A Novel Technique for Clinical Assessment of Laryngeal Nerve Conduction: Normal and Abnormal Results. *Laryngoscope* (2013) 123(9):2202–8. doi: 10.1002/lary.23950
30. Kaneoka A, Krisciunas GP, Walsh K, Raade AS, Langmore SE. A Comparison of 2 Methods of Endoscopic Laryngeal Sensory Testing: A Preliminary Study. *Ann Otol Rhinol Laryngol* (2015) 124(3):187–93. doi: 10.1177/0003489414550241
31. al-Atrakchi HA. Upper Gastrointestinal Endoscopy Without Sedation: A Prospective Study of 2000 Examinations. *Gastrointest Endosc* (1989) 35(2):79–81. doi: 10.1016/s0016-5107(89)72712-7
32. Davis DE, Jones MP, Kubik CM. Topical Pharyngeal Anesthesia Does Not Improve Upper Gastrointestinal Endoscopy in Conscious Sedated Patients. *Am J Gastroenterol* (1999) 94(7):1853–6. doi: 10.1111/j.1572-0241.1999.01217.x

33. Isenberg G. Topical Anesthesia: To Use or Not to Use–That Is the Question. *Gastrointest Endosc* (2001) 53(1):130–3. doi: 10.1067/mge.2001.112093

Conflict of Interest: The authors declare that the research was conducted in the absence of any commercial or financial relationships that could be construed as a potential conflict of interest.

Publisher's Note: All claims expressed in this article are solely those of the authors and do not necessarily represent those of their affiliated organizations, or those of the publisher, the editors and the reviewers. Any product that may be evaluated in this article, or claim that may be made by its manufacturer, is not guaranteed or endorsed by the publisher.

frontiers | Frontiers in Oncology

ORIGINAL RESEARCH
published: 30 May 2022
doi: 10.3389/fonc.2022.793351

Lymph Node Metastasis Spread Patterns and the Effectiveness of Prophylactic Neck Irradiation in Sinonasal Squamous Cell Carcinoma (SNSCC)

*Qian Liu, Yuan Qu, Kai Wang, Runye Wu, Ye Zhang, Xiaodong Huang, Jianghu Zhang, Xuesong Chen, Jingbo Wang, Jianping Xiao, Junlin Yi, Guozhen Xu and Jingwei Luo**

Department of Radiation Oncology, National Cancer Center/National Clinical Research Center for Cancer/Cancer Hospital, Chinese Academy of Medical Sciences and Peking Union Medical College, Beijing, China

OPEN ACCESS

Edited by:
Scott M. Langevin, University of Cincinnati, United States

Reviewed by:
Kee Howe Wong, Royal Marsden NHS Foundation Trust, United Kingdom
Manish Devendra Mair, University Hospitals of Leicester NHS Trust, United Kingdom

***Correspondence:**
Jingwei Luo
jingwei-luo@outlook.com

Specialty section:
This article was submitted to Head and Neck Cancer, a section of the journal Frontiers in Oncology

Received: *12 October 2021*
Accepted: *25 April 2022*
Published: *30 May 2022*

Citation:
Liu Q, Qu Y, Wang K, Wu R, Zhang Y, Huang X, Zhang J, Chen X, Wang J, Xiao J, Yi J, Xu G and Luo J (2022) Lymph Node Metastasis Spread Patterns and the Effectiveness of Prophylactic Neck Irradiation in Sinonasal Squamous Cell Carcinoma (SNSCC). Front. Oncol. 12:793351. doi: 10.3389/fonc.2022.793351

Objectives: To analyze the incidence and spread of lymph node metastasis (LNM) and the effectiveness of prophylactic neck irradiation in patients with SNSCC.

Methods: A total of 255 patients with SNSCC were retrospectively reviewed. The LNM spread pattern was revealed. The clinical parameters related to LNM, and the prognostic value of elective neck irradiation (ENI) were assessed. A 1:1 matching with propensity scores was performed between ENI group and observation (OBS) group.

Results: The initial LNM rate was 20.8%, and the regional recurrence (RR) rate was 7.5%. Lymphatic spreading in SNSCC followed the common trajectories: a. level Ib ➔ level II ➔ level Va/level III/IV lymph nodes (LNs); b. retropharyngeal lymph nodes (RPLNs) ➔ level II LNs. The most frequently involved site was level II LNs (16.1%), followed by level Ib LNs (10.2%), RPLNs (4.7%), level III LNs (3.2%), level Va LNs (1.6%), level IVa LNs (1.4%) and level VIII LNs (0.8%). The median follow-up time was 105 months. The 5-year overall survival (OS) was 55.7% for N0 patients and 38.5% for patients with initial N+ or N- relapse ($p = 0.009$). After PSM, the 5-year regional recurrence-free survival was 71.6% and 94.7% ($p = 0.046$) in OBS and ENI group, respectively. The multivariate analysis showed that ENI ($p = 0.013$) and absence of nasopharynx involvement ($p = 0.026$) were associated with a significantly lower RR rate.

Conclusions: Patients with LNM had poorer survival than those who never experienced LNM. Lymphatic spread in SNSCC followed predictable patterns. ENI effectively reduced the RR rate in patients at high risk.

Keywords: lymph node spread pattern, lymph node metastasis, sinonasal malignancies, elective neck irradiation, node-negative neck

INTRODUCTION

Sinonasal malignancies (SNMs) account for 3%~5% of all head and neck cancers (1, 2) and constitute a broad spectrum of histopathologic subtypes, of which squamous cell carcinoma represents 50%~80% (3). However, due to the insidiousness of symptoms in the early stage and primary tumors being located adjacent to critical structures, the management of SNM is challenging, resulting in a 5-year overall survival (OS) rate of approximately 50% (4).

Recently, several studies reported that regional metastasis was a prognostic factor for survival (5–7). The best management remains unclear for patients with node-negative (N0) necks. During the 1980s, many oncology teams opposed prophylactic neck treatment due to the rarity of regional metastases (8, 9). However, from the 1990s to the 2000s, the MD Anderson group (10) and Paulino et al. (11) advocated for elective ipsilateral neck irradiation in all patients with maxillary sinus squamous cell carcinoma because they found that up to 33% of N0 patients would eventually present regional failure during the follow-up after a 'watch and wait' strategy. Since then, the debate has continued regarding whether elective neck irradiation (ENI) should be performed for N0 sinonasal cancers. The National Comprehensive Cancer Network (NCCN) guidelines recommend ENI in patients with T3-4 disease based on the rationale that ENI of the N0 neck is warranted if the probability of occult cervical metastasis is greater than 20% (12).

Nevertheless, several questions remain unsolved. First, the incidence of lymph node metastasis (LNM) at SNSCC presentation varies widely from 3% to 20.6%, with differences based on race, histopathology, T stage, involved structure and treatment of the primary tumor (13). Second, the prediction of the likely location of regional metastasis is essential but challenging due to the complex lymphatic network of the nasal cavity, paranasal sinuses and neighboring structures. Also, the sentinel lymph node (SLN) approach is hard to implement in SNM (14). Third, the population at high risk for LNM needs to be identified. Except for advanced tumors (T3-4), some investigators found that T2 tumors had a higher rate than more advanced tumors (6). In addition, previous studies reported the invasion of various structures as a risk factor associated with developing regional metastasis, such as invasion of the oral cavity, nasopharynx, hard palate, and sinonasal cavity osseous confines into adjacent structures like the dura, infratemporal fossa and palate (15, 16). Moreover, most studies have included a higher proportion of patients who received no neck treatment; as such, the safety and effectiveness of ENI has not been able to be directly evaluated.

In light of these controversial issues, we conducted a retrospective study in SNSCC to evaluate the influence of LNM on oncology outcomes and LNM incidence and spread patterns. We also analyzed the effectiveness of prophylactic neck irradiation in preventing neck failure and the risk factors associated with nodal involvement at presentation and after treatment.

METHODS AND MATERIALS

Patients

Between Jan 1999 and Dec 2016, consecutive patients with a histopathological diagnosis of squamous cell carcinoma arising from the nasal cavity and paranasal sinus at a single academic tertiary referral center were included. Patients were excluded if they had a new malignant tumor diagnosed in the previous five years, if distant metastases were present at diagnosis, or if clinicopathologic and follow-up information were incomplete. The patient selection and treatment flow chart are depicted in **Figure 1**.

All patients were restaged according to the 8th edition of the AJCC staging system. Clinical LNM was determined by the results of pretreatment imaging examinations (CT/MRI): a minimal axial diameter (MID) of cervical LNs ≥ 10 mm, and a MID of retropharyngeal lymph nodes (RPLNs) ≥ 5 mm; nodal grouping, as defined as three or more contiguous LNs, any one of which had an MID ≥ 8 mm; and the presence of signs of necrosis or extracapsular invasion in any sized LN. The pathologic confirmation of LNM was obtained when it was difficult to certain nodal metastases based on imaging.

Initial Treatment of Primary Tumors

All patients underwent pretreatment evaluation. After clinical assessment and review, the final treatment modality was decided by the multidisciplinary team.

A preoperative radiotherapy (RT) strategy was preferred if the primary tumor had invaded vital organs, like orbital structures or the brain parenchyma. We routinely assessed the tumor response of patients who received preoperative RT at 50 Gy by CT, MRI and/or endoscopy examination. Nonresponders (<80% reduction of primary lesion) underwent resection of the primary tumor and modified neck dissection 4~6 weeks after receipt of preoperative 50 Gy at 2.0 Gy per fraction. Responders (≥80% reduction of primary lesion) received a boost to PTV up to a total dose of 70 Gy.

Postoperative RT was recommended for patients with selected risk factors, including advanced T stage, perineural/lymphatic/vascular invasion, nonnegative surgical margin, and multiple positive nodes with or without extranodal extension. The prescribed dose was 30 fractions of 60 Gy over six weeks. A higher dose (70 Gy) was recommended for patients with extranodal extension or positive margins.

In patients except for the responders who received preoperative RT, RT was considered a definitive treatment for patients who were unfit for or refused surgery. Typically, the prescribed dose based on primary gross tumor volume (GTVp) was 70 Gy within 6.5~7 weeks.

Initial Treatment of Neck Lymph Nodes

If the patients had clinically positive lymph nodes at presentation, neck dissection, RT, or a combined treatment regimen was considered. The nodal clinical target volume (CTVnd) encompassed all regions with nodal involvement and extended to the adjacent levels. In addition, bilateral treatment was implemented if a tumor approached or crossed the midline

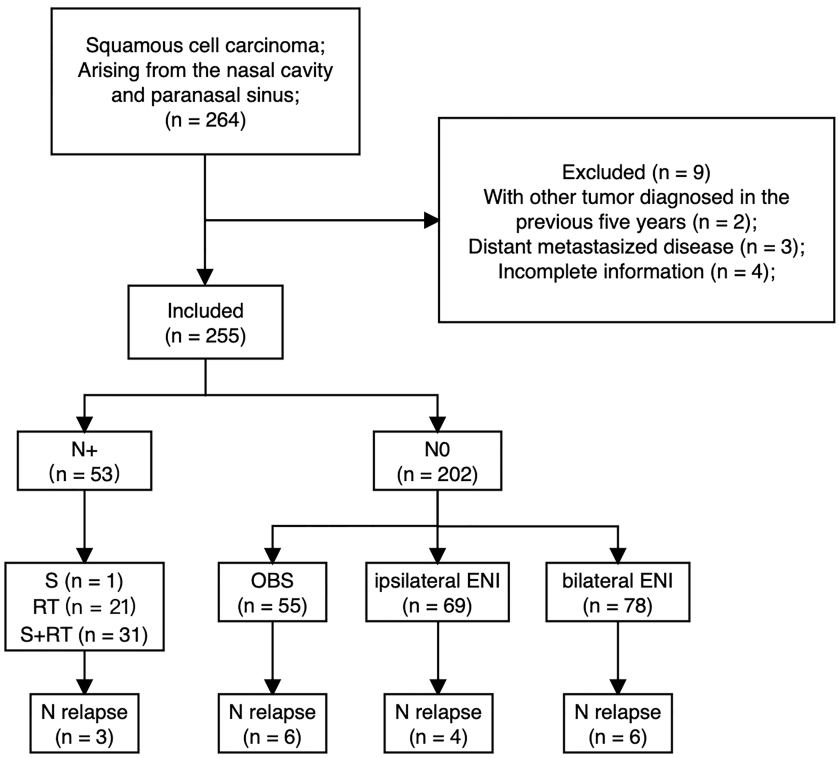

FIGURE 1 | Patient selection and treatment flow chart.

or involved some anatomic regions with crossing lymph node drainage, such as the soft palate, oral cavity, and nasopharynx.

No patients with clinical stage N0 disease received elective nodal dissection, and prophylactic neck irradiation was generally administered to patients with T3-4 SNSCC or any patients with T2 disease with rich lymphatic network structure extension. The preferred prophylactic dose of ENI was 50~60 Gy in 30~33 fractions over 6~7 weeks to high-risk regions.

Systemic Therapy

Systemic therapy was decided by the multidisciplinary team according to clinicopathologic factors, comorbidity, and patient preference. Induction and adjuvant chemotherapy included the TPF and TP regimens. In concurrent chemoradiotherapy cases, patients received cisplatin weekly or triweekly or docetaxel weekly. Alternatively, patients received nimotuzumab as targeted therapy.

Definition of Endpoints

OS was defined as the duration from the date of initial diagnosis to death due to any cause or the last follow-up. Local recurrence-free survival (LRFS), regional recurrence-free survival (RRFS) and distant metastasis-free survival (DMFS) were defined as the duration from the date of initial diagnosis to the first failure. Instances of locoregional or distant recurrence were documented by biopsy unless there was clear radiographic evidence of disease. Local treatment failure was defined as recurrence at the site of the initial primary tumor, regional treatment failure was defined as the development of recurrence in head and neck lymph nodes, and distant treatment failure was defined as recurrence in an organ outside of the head or neck.

Statistical Methods

Normally distributed continuous data are presented as the means with ranges and were compared using the independent samples t-test. Nonnormally distributed continuous data are presented as medians with interquartile ranges (IQRs) and were compared using the Mann-Whitney U test. Categorical data are presented as frequencies with percentages and were compared using the chi-square test with correction for continuity when necessary. Logistic regression was performed to estimate predictors of initial LNM. The OS curve was generated using the Kaplan-Meier method with a log-rank comparison, if needed. The instances of local, regional, and distant treatment failure are depicted in cumulative incidence plots and were compared using the Fine & Gray test. Deaths not related to the event of interest were considered as competing risk events. Multivariate Cox regression analysis was carried out to identify prognostic factors associated with lymph node recurrence for the N0 cases. Logistic regression was performed to estimate predictors of ENI or OBS. Propensity scores were calculated given the covariates of variables estimated from the logistic regression mentioned above using another logistic regression model with a caliper of 0.2; 1:1 matching was performed with the nearest-neighbor algorithm. After matching, normally distributed

continuous data were compared using the paired-samples t-test (17). The Wilcoxon signed-rank test was used for nonnormally distributed continuous data; categorical data were compared with McNemar's test. All analyses were 2-sided and used a significance level of $p<0.05$. Statistical analyses were performed with SPSS version 26 (IBM Corp) and R version 3.2 (http://www.R-project.org).

RESULTS

Patient Characteristics

A total of 255 patients with SNSCC were identified. The detailed characteristics of the patients are shown in **Table 1**.

Regarding the initial treatment of primary tumors, among 81 patients managed with preoperative RT, the median dose of GTVp was 60 Gy (range: 48~80 Gy). Among 95 patients who received postoperative RT, the median dose of tumor bed volume (GTVtb) was 67 Gy (range: 56~82 Gy).

Regarding the initial neck treatment, for 53 patients with node-positive neck disease, 3 patients underwent neck dissection alone, 23 patients received neck irradiation alone with a median dose of 69.96 Gy (range: 55~80 Gy), and 27 patients received neck dissection combined with irradiation with a median dose was 66 Gy (range: 50~70 Gy). Among 202 patients without clinically metastatic LNs, 147 patients were treated with ENI at a median dose of 60 Gy (range: 50~60 Gy), while 55 patients underwent observation (OBS). Of those who received ENI, 78

TABLE 1 | Patients' characteristics.

Variables	Nasal Cavityn = 76 (29.8%)	Maxillary Sinusn = 149 (58.4%)	Ethmoid Sinusn = 30 (11.8%)	Totaln = 255 (100%)
Median age (range)	53 (11~85)	56 (16~83)	49 (14~75)	54 (11~85)
Age				
≤50	36 (47.40%)	48 (32.20%)	16 (53.30%)	100 (39.20%)
>50	40 (52.60%)	101 (67.80%)	14 (46.70%)	155 (60.80%)
Sex				
Female	19 (25.0%)	39 (26.20%)	7 (23.30%)	65 (25.50%)
Male	57 (75.0%)	110 (73.8%)	23 (76.7%)	190 (74.5%)
Year of diagnosis				
1999-2007	31 (40.80%)	51 (34.20%)	16 (53.30%)	98 (38.40%)
2008-2016	45 (59.20%)	98 (65.80%)	14 (46.70%)	157 (61.60%)
AJCC Stage				
I	5 (6.6%)	0 (0.0%)	0 (0.0%)	5 (2.0%)
II	6 (7.9%)	5 (3.4%)	0 (0.0%)	11 (4.3%)
III	19 (25.0%)	31 (20.8%)	2 (6.7%)	52 (20.4%)
IVA	25 (32.9%)	68 (45.6%)	10 (33.3%)	103 (40.4%)
IVB	21 (27.6%)	45 (30.2%)	18 (60.0%)	82 (33.0%)
T stage				
T1	5(6.6%)	0 (0.0%)	0 (0.0%)	5 (2.0%)
T2	9 (11.8%)	6 (4.00%)	0 (0.0%)	15 (5.9%)
T3	20 (26.30%)	34 (22.8%)	2 (6.7%)	56 (22.0%)
T4a	21(27.6%)	67 (45.0%)	10 (33.3%)	98 (38.40%)
T4b	21(27.6%)	42 (28.2%)	18 (60.0%)	81 (31.80%)
N stage				
N0	56 (73.7%)	120 (80.5%)	26 (86.7%)	202 (79.2%)
N1	7 (9.20%)	14 (9.4%)	1(3.30%)	22 (8.6%)
N2	12 (15.8%)	13 (8.7%)	3 (10.0%)	28 (11.0%)
N3	1 (1.3%)	2 (1.3%)	0 (0.0%)	3 (1.2%)
Primary tumor treatment modality				
S+RT	35 (46.10%)	51 (34.20%)	9 (30.00%)	95 (37.30%)
RT+S	16 (21.10%)	56 (37.60%)	9 (30.00%)	81 (31.80%)
RT	19 (25.00%)	36 (24.20%)	11 (36.70%)	66 (25.90%)
S	6 (7.90%)	6 (4.00%)	1 (3.30%)	13 (5.10%)
N+ neck treatment modality				
S	0 (0.0%)	3 (10.3%)	0 (0.0%)	3 (5.7%)
RT	11 (55.0%)	11 (37.9%)	1 (25.0%)	23 (43.4%)
S+RT	9 (45.0%)	15 (51.7%)	3 (75.0%)	27 (50.9%)
N0 neck treatment modality				
ENI	29 (51.8%)	99 (82.5%)	19 (73.1%)	147 (72.8%)
OBS	27 (48.2%)	21 (17.5%)	7 (26.9%)	55 (27.2%)
Systemic therapy				
Chemotherapy	23 (30.30%)	48 (32.20%)	12 (40.00%)	83 (32.50%)
Target therapy	7 (9.20%)	13 (8.70%)	1 (3.30%)	21 (8.20%)
RT technology				
Non-IMRT	32 (45.7%)	54 (37.8%)	13 (44.8%)	99 (40.9%)
IMRT	38 (54.3%)	89 (62.2%)	16 (55.2%)	143 (59.1%)

S, Surgery; RT, Radiotherapy; S+RT, Surgery followed by postoperative radiotherapy; RT+S, preoperative radiotherapy followed by surgery.

(53.1%) received bilateral irradiation, and 69 (46.9%) received ipsilateral irradiation.

Regarding systemic therapy, 83 (32.5%) patients received chemotherapy, and 21 (8.2%) received nimotuzumab targeted therapy. The most common induction or adjuvant chemotherapeutic strategy was the TP regimen (75%, 12/16), while the most common concurrent chemotherapeutic agent was cisplatin (88.9%, 64/72).

Survival Outcomes

The median follow-up time was 105 months (IQR 65-147 months) in the whole cohort. The 5-year OS and 10-year OS for all patients were 51.3% and 41.3%, respectively. The 5-year OS of the primary tumor site, as ranked from high to low, was as follows: nasal cavity (60.8%), maxillary sinus (51.7%) and ethmoid sinus (27.2%). The treatment failure patterns are summarized in **Figure 2**. At five years, LRFS, RRFS and DMFS were 56.9%, 91.3% and 80.2%, respectively, among all patients.

There was a significant association between LNM and OS. The 5-year OS was 55.7% for patients with N0 disease and 38.5% for those with initial N+ or N-relapse (HR = 1.604, 95%CI: 1.121-2.295, p = 0.009, **Figure 3**).

Patients With N0 Disease: ENI vs. OBS

Of all patients, 202 patients with N0 neck at diagnosis, while 53 patients with initial LNM. To evaluate the value of prophylactic neck irradiation in the N0 neck, we compared the outcomes of the ENI (55 patients) and OBS (147 patients) groups. **Table 2** outlines the characteristics of the 202 N0 patients.

For the unmatched group, at a median follow-up time of 111 months (IQR 68-149 months), the 5-year OS was 52.9% and 54% (HR = 1.073; 95%CI: 0.697-1.653; p = 0.748), the 5-year LRFS was 60.1% and 44.6% (HR = 0.661, 95%CI: 0.417-1.05, p = 0.077), the 5-year RRFS was 92.2% and 87.7% (HR = 0.6, 95%CI: 0.218-1.63, p = 0.31, **Figure 4A**), and the 5-year DMFS was 77.9% and 86.5% (HR = 1.9, 95%CI: 0.791-4.58, p = 0.15) in the ENI and OBS group, respectively.

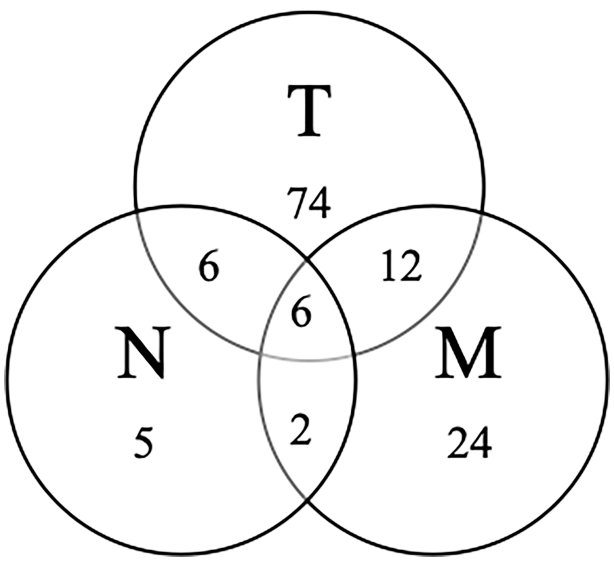

FIGURE 2 | Failure patterns for the 129 patients with SNSCC.

The 1:1 matching for OBS versus ENI resulted in 36 matched pairs, and tests indicated negligible differences across all demographics and clinicopathological variables in the matched cohort.

After PSM, the median follow-up time was 135 months (IQR 42–176 months) for OBS group and 148 months (IQR 65–176 months) for ENI group. Sixteen patients in the OBS group and 15 in the ENI group died. The median OS were 31 and 39 months in the OBS and ENI group, respectively. Additionally, 5-year OS rates was 46.9% in the OBS group and 46.7% (HR = 0.830, 95% CI: 0.449-1.534, p = 0.553), 5-year LRFS was 46.9% and 49.0% (HR = 0.844, 95%CI: 0.449-1.583, p = 0.597), 5-year RRFS was 71.6% and 94.7% (HR = 0.118, 95%CI: 0.014-0.962, p = 0.046, **Figure 4B**), and 5-year DMFS was 76.4% and 75.6% (HR = 1.088, 95%CI: 0.345-3.432, p = 0.886) in the OBS and ENI group, respectively.

In a multivariate Cox regression model (**Table 5**), compared with OBS, ENI resulted in a significantly lower rate of regional failure (HR = 0.169, 95%CI: 0.041-0.690; p = 0.013).

Incidence and Spread Pattern of Clinically Metastatic LNs

LNM Rate and Spread Pattern of LNM at Diagnosis

Of all 255 patients, 53 (20.8%) patients had LNM at diagnosis. Patients with nasal cavity SCC had the highest incidence of LNM (20/76, 26.3%), followed by patients with maxillary sinus SCC (29/149, 19.5%) and those with ethmoid sinus SCC (4/30, 13.3%). The incidence and distribution of LNM based on the primary tumor site are shown in **Table 3**.

Of these 53 patients, 73.6% had ipsilateral LNM, and 26.4% had bilateral LNM, while isolated contralateral LNM was not observed. The most frequently involved sites were level II LNs (41/255, 16.1%), followed by level Ib LNs (26/255, 10.2%) and RPLNs (12/255, 4.7%). Middle and lower jugular LN involvement was rare (level III LNs: 3.2%, level Iva LNs: 1.4%). In addition, metastatic LNs at level Va were observed in 4 (1.6%) patients, and only 2 (0.8%) patients had metastatic level VIII (preauricular) LNs. We further analyzed the spread of ipsilateral clinically metastatic lymph nodes (**Figure 5**) and found that no patient presented with skip metastasis.

LNM Rate and Spread Pattern of LNM During Follow-Up

Of all 255 patients, 19 (7.5%) patients (with involvement of the nasal cavity, 7/76, 9.2%; with involvement of the maxillary sinus, 9/148, 6%; with involvement of the ethmoid sinus, 3/30, 10%) experienced regional recurrence (RR), and 84% (16/19) developed RR during the first two years of follow-up. Detailed information on the 19 patients with nodal relapse is shown in **Table 4**. Isolated RR was present in 5 (2%) patients, and 4 of them successfully underwent salvage surgery.

Of the patients with delayed appearance of metastatic LNs, 11 patients had the metastases develop in the ipsilateral neck, 7 had

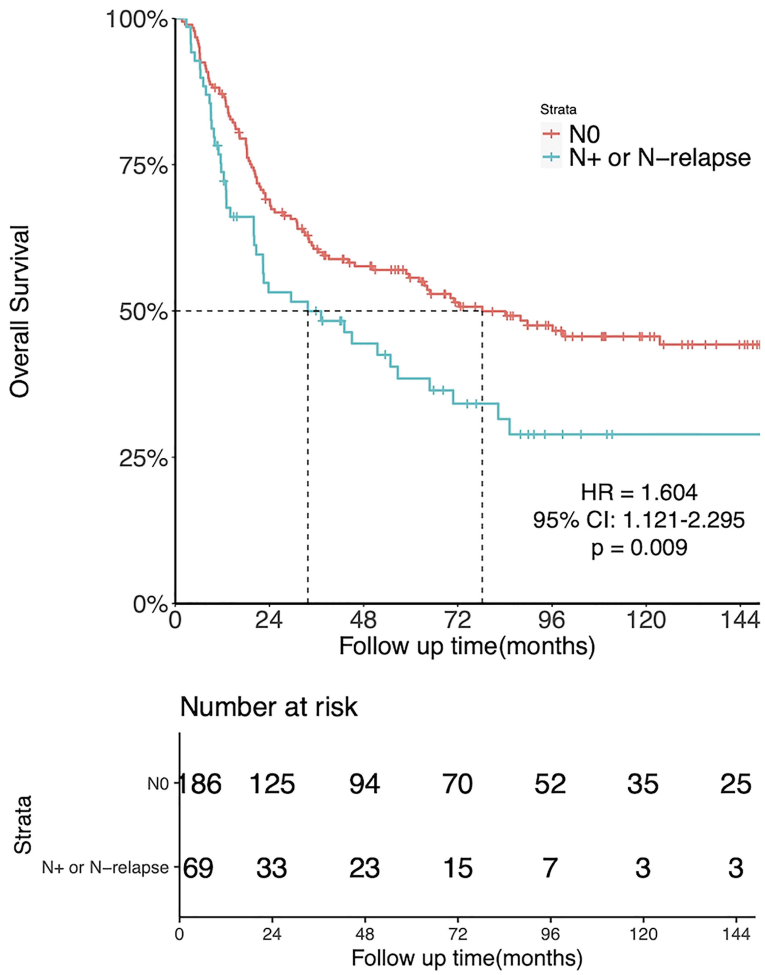

FIGURE 3 | Kaplan-Meier estimates of OS in N0 patients and patients with N+ or N-relapse patients.

the metastases develop in the bilateral neck, and 1 patient developed nodal failure in the contralateral neck alone. Level II LNs were the most involved lymphatic site, with 18 patients showing level II LN involvement, followed by level Ib LNs (7 patients), level III LNs (3 patients), level IV LNs (3 patients), level VIII LNs (2 patients), level Va LNs (1 patient), and RPLNs (1 patient).

Risk Factors for LNM

Multivariate logistic analysis (**Table 5**) revealed that nasopharyngeal invasion was associated with a higher rate of initial LNM (OR = 3.43, 95%CI: 1.435-8.196, p = 0.006).

For delayed lymph node recurrence during follow-up, in addition to ENI, predictors also included nasopharyngeal involvement (HR = 11.736, 95%CI: 1.352-101.857, p = 0.026); however, although it reached the significance level, the wide confidence intervals may influence the statistical power. Pterygopalatine fossa involvement was associated with a lower rate of RR (HR = 0.033, 95%CI: 0.004-0.533, p = 0.014).

DISCUSSION

In the present study, we confirmed that regional LNM was a negative prognostic factor for survival in SNSCC (5y-OS, N0: 55.7%; N+ of N-relapse: 38.5%). In our cohort, prophylactic neck irradiation was associated with a lower rate of RR after PSM. We also found that the rate of initial LNM was 20.8%, and the highest rate presented in nasal cavity tumors was 26.3%, while the delayed nodal recurrence rate was 7.5%. In addition, lymphatic spreading followed orderly patterns. Last, nasopharynx and pterygopalatine fossa involvement were independent factors for predicting RR.

Despite recent advances in therapeutic technology, the treatment of SNSCC remains a challenge. The inferior prognosis caused by regional lymph node issues is worth noting. In this series, the 5-year OS was 55.7% in patients with an initial N0 neck vs. 38.5% in those with LNM at diagnosis or after treatment, which are similar to the findings in previous studies, in which the 5-year OS and DSS were reduced by 10~40% for patients with N+ compared with N0 disease (5–7).

TABLE 2 | Characteristics of N0 patients undergoing observation (OBS) or elective neck irradiation (ENI) before and after PSM.

	Before PSM		p	After PSM		p
	OBS	ENI		OBS	ENI	
n	55	147		36	36	
Median age (mean (SD))	57.04 (11.64)	53.90 (14.46)	0.151	55.72 (11.70)	50.03 (16.13)	0.091
Sex			0.379			0.792
Male	43 (78.2%)	104 (70.7%)		27 (75.0%)	25 (69.4%)	
Female	12 (21.8%)	43 (29.3%)		9 (25.0%)	11 (30.6%)	
Primary tumor site			<0.001			0.076
Nasal cavity	27 (49.1%)	29 (19.7%)		13 (31.6%)	5 (13.9%)	
Maxillary sinus	21 (38.2%)	99 (67.3%)		16 (44.4%)	24 (66.7%)	
Ethmoid sinus	7 (12.7%)	19 (12.9%)		7 (19.4%)	7 (19.4%)	
T stage			<0.001			0.703
T1	5 (9.1%)	0 (0.0%)		1 (2.8%)	0 (0.0%)	
T2	8 (14.5%)	3 (2.0%)		1 (2.8%)	2 (5.6%)	
T3	14 (25.5%)	33 (22.4%)		8 (22.2%)	9 (25.0%)	
T4	28 (50.9%)	111 (75.5%)		26 (72.2%)	25 (69.4%)	
Treatment modality			<0.001			0.699
S+RT	21 (38.2%)	63 (42.9%)		15 (41.7%)	13 (36.1%)	
RT+S	15 (27.3%)	46 (31.3%)		13 (36.1%)	13 (38.9%)	
RT	7 (12.7%)	38 (25.9%)		7 (19.4%)	9 (25.0%)	
S	12 (21.8%)	0 (0.0%)		1 (2.8%)	0 (0.0%)	
Year of diagnosis			0.001			0.149
1999-2007	34 (61.8%)	50 (34.0%)		25 (69.4%)	18 (50.0%)	
2008-2016	21 (38.2%)	97 (66.0%)		11 (30.6%)	18 (50.0%)	

S, Surgery; RT, Radiotherapy.

ENI resulted in a lower regional failure rate than OBS, as revealed by the PSM analysis and multivariate Cox regression analysis. The fact that a majority of (72.8%) patients underwent ENI may explain why the rate of RR was slightly lower in our findings than in others. Abu-Ghanem et al. (13) summarized publications since the 1900s and found that nodal recurrence was detected in 0~4.3% of the patients in the ENI group and in 9.1% ~33% of patients in the OBS group. The researchers indicated that ENI could significantly reduce the nodal recurrence rate for patients with maxillary sinus SCC. In nasal cavity SCC, Ahn et al. (18) reported a nodal recurrence rate of 18.8% for N0 patients with no ENI.

Similarly, another meta-analysis found an 18.1% RR rate for nasal cavity tumors with or without ENI. The study also suggested that ENI is an effective method for reducing RR (19). The same conclusion was also drawn by Galloni et al. (20). Moreover, Jiang et al. and Paulino et al. reported high RR rates of 33% and 28.9%, respectively, for N0 patients, and a lack of ENI was associated with significantly worse survival (10, 11). As a result, MD Anderson Cancer Center changed its guidance to include irradiation of the neck in T2-4 maxillary SCC.

The researchers indicated that most patients with failure in the neck have simultaneous or preceding local failure, and the rate of isolated RR was low at 0%-16.7% (21). We hypothesized that the local lesion is potentially the source of metastatic dissemination to lymph nodes. Besides, due to the rarity and high salvageability of isolated RR, some investigators oppose routine ENI (15, 22). Regarding the especially high LNM rates found by Paulino et al. (11), in that study, the isolated neck failure rate was only 10.5%. This low rate of isolated nodal failure was also found by Mirghani et al (23), ranging from 2.8% to 13% (23). Moreover, in these isolated RR cases, salvage treatment results in good oncologic outcomes. Cantù et al. (6) reported that 97% (28/30) of patients were successfully salvaged. Similarly, both Dirix (24) and Porceddu (25) reported a high salvageability of over 50%. Notably, in a multi-institutional study (15), among 5 patients with isolated LNM, 3 patients were successfully salvaged, and 2 failed because of RPLN metastasis. Thus, the prophylactic irradiation of RPLNs deserves consideration because salvage surgery is difficult. In our results, the rate of isolated RR was only 2%, but the effectiveness of ENI indicated that the rate of isolated RR might be unequal to that of occult LNM at diagnosis.

The incidence of lymph node metastasis (LNM) at presentation or during follow-up varies widely from 3% to 33%. The initial incidence of LNM was 20.8% in the current study. According to the primary site, the rate of initial LNM was 26.3% in the nasal cavity, 19.5% in the maxillary sinus and 13.3% in the ethmoid sinus. Ahn et al. revealed rates of 7.9% and 15.2% for nasal cavity and maxillary sinus nodal involvement, respectively, in 2888 patients (18). A meta-analysis of nasal cavity SCC identified a rate of initial LNM of 0~27% (below the 10% rate in most of the enrolled articles) (19), and another study showed a rate of 3~20.6% (10% ~20% in most of the enrolled articles) in maxillary sinus SCC (13). Similar results depending on site were also found in evaluations of the SEER (26) and NCDB (27) databases. Cantù et al. (6) reported that 305 ethmoid sinus tumors had 1.6% rate of nodal metastasis at presentation. Contrary to their findings, we found that nasal cavity tumors had the highest rate of initial LNM, and the rate of LNM in ethmoid sinus tumors was higher than that in others' results. One reason for this finding is that there were fewer early-stage tumors in

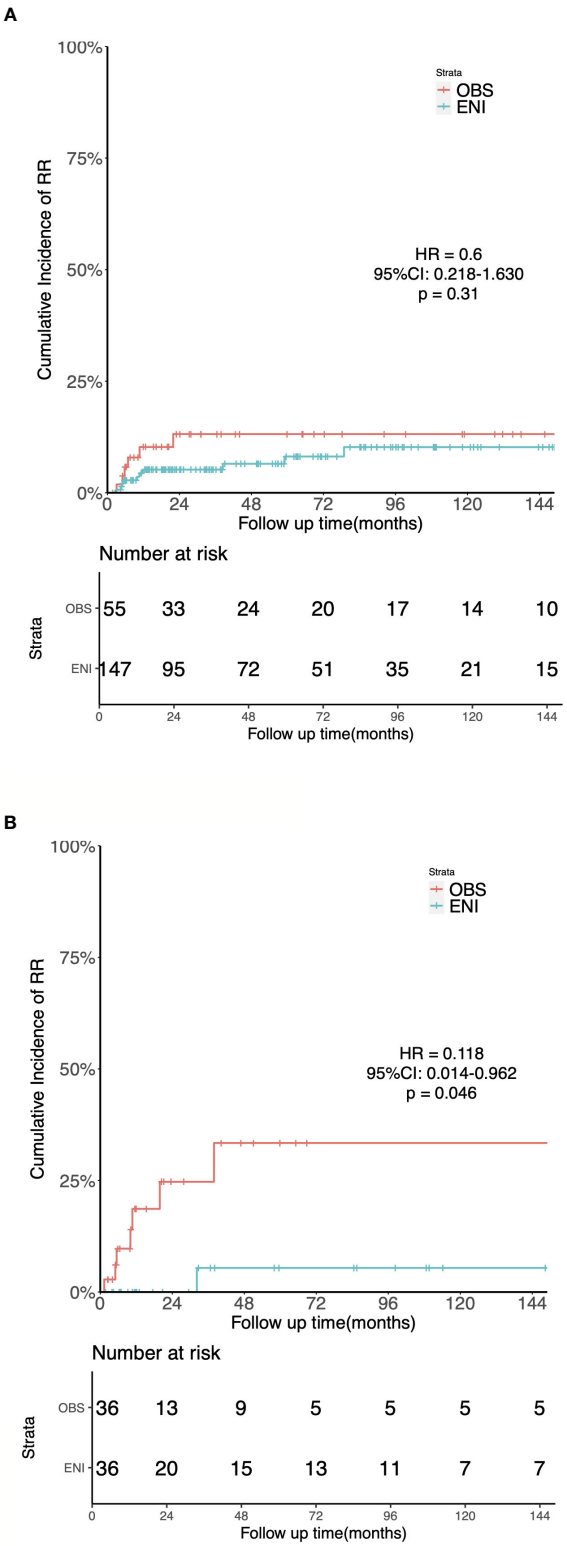

FIGURE 4 | Kaplan-Meier estimates of the cumulative incidence of regional recurrence in the ENI and OBS groups. **(A)** Regional Recurrence in the entire cohort. **(B)** Regional Recurrence in the matched cohort.

TABLE 3 | Incidence and distribution of clinically metastatic lymph node at diagnosis.

	Total (n = 255)			Nasal Cavity (n = 76)			Maxillary Sinus (n = 148)			Ethmoid Sinus (n = 30)		
	ipsi-lateral	bi-lateral	contra-lateral	ipsi-lateral	bi-lateral	contra-lateral	ipsi-lateral	bi-lateral	contra-lateral	ipsi-lateral	bi-lateral	contra-lateral
Ib	22 (8.6%)	3 (1.2%)	1 (0.4%)	9 (11.8%)	1 (1.3%)	0 (0.0%)	11 (7.4%)	2 (1.4%)	1 (0.7%)	2 (6.7%)	0 (0.0%)	0 (0.0%)
II	31 (12.2%)	9 (3.5%)	1 (0.4%)	8 (10.5%)	5 (6.6%)	0 (0.0%)	20 (13.5%)	4 (2.7%)	0 (0.0%)	3 (10.0%)	0 (0.0%)	1 (3.3%)
III	6 (2.4%)	2 (0.8%)	0 (0.0%)	2 (2.6%)	1 (1.3%)	0 (0.0%)	3 (2.0%)	1 (0.7%)	0 (0.0%)	1 (3.3%)	0 (0.0%)	0 (0.0%)
IVa	2 (0.8%)	1 (0.4%)	1 (0.4%)	1 (1.3%)	0 (0.0%)	0 (0.0%)	2 (1.4%)	1 (0.7%)	0 (0.0%)	0 (0.0%)	0 (0.0%)	1 (3.3%)
Va	2 (0.8%)	2 (0.8%)	0 (0.0%)	1 (1.3%)	0 (0.0%)	0 (0.0%)	2 (1.4%)	1 (0.7%)	0 (0.0%)	0 (0.0%)	0 (0.0%)	0 (0.0%)
RPN	7 (2.7%)	5 (2.0%)	0 (0.0%)	3 (3.9%)	2 (2.6%)	0 (0.0%)	3 (2.0%)	3 (2.0%)	0 (0.0%)	1 (3.3%)	0 (0.0%)	0 (0.0%)
VIII	2* (0.8%)	0 (0.0%)	0 (0.0%)	0 (0.0%)	0 (0.0%)	0 (0.0%)	1 (0.7%)	0 (0.0%)	0 (0.0%)	1 (3.3%)	0 (0.0%)	0 (0.0%)

**Both patients had pre-auricular lymph node metastasis.*

TABLE 4 | Details of 19 patients with regional recurrence.

Pt. no	Primary tumor site	Stage	Tx	NeckTx	ENI target volume	Failure event	Neck failure location	Neck salvage Tx	Neck salvage results	Status following salvage therapy
1	Maxillary sinus	T2N1	S +RT	S#		N	contra: II	S	CR	Died of renal failure
2	Nasal cavity	T2N2c	RT	RT	ipsi: Ib, II, III, IV, V; contra: Ib, II, III, IV, V.	N	ipsi: II, III, IV, V; contra: II, III, IV, V, RPLN.	S	CR	Died from accident
3	Nasal cavity	T4aN3b	RT	RT	ipsi: Ib, II, III, IV, V; contra: Ib, II, III, IV, V.	N	ipsi: Ib.	S	CR	Alive
4	Maxillary sinus	T3N0	S +RT	ENI	ipsi: Ib, II, III; contra: II.	T+N	ipsi: Ib, II, III; contra: Ib, II, III.	S	CR	Alive
5	Nasal cavity	T4aN0	S +RT	ENI	ipsi: RPLN; contra: RPLN.	T→N→M	ipsi: Ib, II; contra: II.	S	CR	Died of cancer
6	Ethmoid sinus	T4bN0	RT	ENI	ipsi: II, III, IV; contra: II, III, IV.	T+N+M	ipsi: Ib; contra: Ib.	Chemotherapy		Died of cancer
7	Maxillary sinus	T4aN0	S +RT	ENI	ipsi: II; contra: II.	T+N+M	ipsi: II.	Chemotherapy	SD	Died of cancer
8	Maxillary sinus	T4bN0	S +RT	ENI	ipsi: II;	T+N+M	ipsi: Ib, VIII.	_		Died of cancer
9	Maxillary sinus	T4aN0	RT +S	ENI	ipsi: Ib, II, III;	N	ipsi: II.	S	CR	
10	Maxillary sinus	T4aN0	RT +S	ENI	ipsi: Ib, II, III, RPLN; contra: Ib, II, III, RPLN.	N	ipsi: IVa.	_		Died of intercurrent diseases
11	Ethmoid sinus	T4bN0	RT	ENI	ipsi: II, III; contra: II, III.	N→2thN→M	ipsi: II.	S	CR	Died of cancer
12	Ethmoid sinus	T4bN0	S +RT	ENI	ipsi: Ib, II, III, IV; contra: Ib, II, III, IV.	N→T→M	ipsi: II.	S+RT	CR	Died of cancer
13	Nasal cavity	T4bN0	RT	ENI	ipsi: Ib, II.	N+M	ipsi: II; contra: II.	_		Died of cancer
14	Maxillary sinus	T4bN0	S +RT	OBS		T+N	ipsi: Ib.	_		Died of cancer
15	Maxillary sinus	T3N0	S +RT	OBS		T+N	ipsi: II.	S	CR	Died of cancer

(Continued)

TABLE 4 | Continued

Pt. no	Primary tumor site	Stage	Tx	NeckTx	ENI target volume	Failure event	Neck failure location	Neck salvage Tx	Neck salvage results	Status following salvage therapy
16	Maxillary sinus	T4bN0	RT +S	OBS		T+N→T	contra: II.	S	CR	Died of cancer
17	Nasal cavity	T4bN0	S +RT	OBS		T→N	ipsi: IVb; contra: Ib.	RT	PD	Died of intercurrent diseases
18	Nasal cavity	T4aN0	S +RT	OBS		T→N	ipsi: II, VIII.	_		Died of cancer
19	Nasal cavity	T4aN0	S +RT	OBS		T→N+M	ipsi: II, III; contra: II, III.	Chemotherapy	PD	Died of cancer

Pt, Patients; Tx, Treatment; S, Surgery; RT, Radiotherapy; ENI, Elective Neck Irradiation; OBS, observation; T, Local failure; N, Nodal failure; M, Distant metastasis; ipsi, ipsilateral; contra, contralateral; CR, complete response; PD, progressive disease.

[#]No.1 patient underwent the ipsilateral neck dissection.

TABLE 5 | Multivariate logistic analysis of risk factors for initial lymph node metastasis.

Variables	Initial LNMs (all patients)	%	OR	95%CI		p	Delayed LNMs (N0 patients)	%	HR	95%CI		p
Age												
≤50	21/100	21.00%	1				8/79	10.10%	1			
>50	32/155	20.60%	0.734	0.356	1.511	0.401	8/123	6.50%	0.284	0.068	1.185	0.084
Sex												
Male	43/190	22.60%	1				12/147	8.20%	1			
Female	10/65	15.40%	0.617	0.255	1.493	0.284	4/55	7.30%	0.562	0.151	2.098	0.392
Primary site						0.196						0.922
Nasal cavity	20/76	26.30%	1				5/56	8.90%	1			
Maxillary sinus	29/149	19.50%	0.505	0.216	1.178	0.114	8/120	6.70%	1.349	0.171	10.632	0.776
Ethmoid sinus	4/30	13.30%	0.418	0.216	1.178	0.244	3/26	11.50%	1.213	0.235	6.261	0.818
T stage						0.670						0.985
T1	0/5	0.00%	0	0	–	0.999	0/5	0.00%	0	0	–	0.992
T2	4/15	26.70%	2.623	0.574	11.98	0.213	0/11	0.00%	0	0	–	0.988
T3	9/56	16.10%	1.304	0.436	3.904	0.635	2/47	4.30%	0.669	0.089	5.036	0.696
T4	40/179	22.30%	1				14/139	10.10%	1			
Orbit invasion												
Yes	35/170	20.60%	0.705	0.275	1.807	0.466	14/135	10.40%	4.185	0.69	25.365	0.119
No	18/85	21.20%	1				2/67	3.00%	1			
Pterygopalatine fossa invasion												
Yes	29/97	29.90%	1.569	0.608	4.047	0.352	2/68	2.90%	0.044	0.004	0.533	0.014
No	24/158	15.20%	1				14/134	10.40%	1			
Infratemporal fossa invasion												
Yes	22/93	23.70%	0.805	0.297	2.18	0.669	5/71	7.00%	1.526	0.199	11.705	0.684
No	31/162	19.10%	1				11/131	8.40%	1			
Dura invasion												
Yes	11/32	34.40%	2.831	0.934	8.576	0.066	3/21	14.30%	2.407	0.455	12.722	0.301
No	42/223	18.80%	1				13/181	7.20%	1			
Nasopharynx invasion												
Yes	22/48	45.80%	3.43	1.435	8.196	0.006	3/26	11.5%	11.736	1.352	101.857	0.026
No	31/207	15.00%	1				13/176	7.40%	1			
Hard palate invasion												
Yes	24/75	32.00%	0.748	0.231	2.415	0.627	4/51	7.80%	0.884	0.082	9.517	0.919
No	29/180	16.10%	1				12/151	7.90%	1	0.566	12.701	0.214
Soft palate invasion												
Yes	6/12	50.00%	1.879	0.435	8.108	0.398	0/6	0.00%	1			
No	47/243	19.30%	1				16/196	8.20%	0	0	.	0.994
Oral cavity invasion												
Yes	28/89	31.50%	2.248	0.435	8.108	0.161	5/61	8.10%	2.097	0.178	24.627	0.556
No	25/165	15.20%	1				11/140	7.90%	1	0.151	2.098	0.392
Facial soft tissue invasion												0.922
Yes	23/74	31.10%	2.106	0.932	4.758	0.073	6/51	11.80%	2.682	0.566	12.701	0.214
No	30/181	16.60%	1				10/151	6.60%	1	0.171	10.632	0.776
Treatment modality												
S+RT							10/84	11.90%	1			

(Continued)

TABLE 5 | Continued

Variables	Initial LNMs (all patients)	%	OR	95%CI	p	Delayed LNMs (N0 patients)	%	HR	95%CI		p
RT+S						3/61	4.90%	0.239	0.048	1.184	0.079
RT						3/45	6.70%	0.517	0.105	2.545	0.417
S						0/12	0%	0	0	–	0.986
Chemotherapy											
Yes						4/50	7.40%	0.964	0.310	2.996	0.949
No						12/136	8.10%	1			
Neck Treatment											
ENI						10/147	6.80%	0.169	0.041	0.690	0.013
OBS						6/55	10.90%	1			

our study than other studies, and the tumor staging was the most important factor for dissemination including lymph nodes and distant organs. Due to the medical diversion system, as a tertiary hospital, the proportion of advanced-stage patients treated in our hospital has increased in recent years (**eTable 2**). This might explain why there were more advanced-stage patients in our hospital than in others. In the present study, 6.6% of patients had T1 disease; while in Dutta's study, Becker's study and Cantù's study, 44.9%, 38.5%, and 24% of patients had T1 disease (6, 26, 28). While the rate of LNM at diagnosis was higher in our study, the incidence of RR (7.5%) was lower than that in most of the existing studies. We consider that the low RR rate of cervical lymph nodes is due to the fact that 72.8% of patients have received ENI.

If ENI is to be delivered, there is no consensus about the optimal neck irradiation volume or dose for ENI. The nasal cavity and paranasal sinuses are thought to be areas with two main pathways of lymphatic drainage: the anterior route runs around the facial artery vessels, draining into the submandibular nodes (level I); and the posterior route runs to the upper jugular nodes (level 2) through retropharyngeal or parapharyngeal nodes (29). Recently, Fernández et al. performed lymphoscintigraphy during sentinel lymph node biopsy for patients with sinonasal tumors and found that levels I and II most commonly contained the sentinel node (14).

The distribution of LNM in this study was consistent with previous research. The most common levels involved were levels II and Ib of the ipsilateral neck. Level IV or V nodal involvement was observed in a minority of patients with level II and III nodal metastasis, which may be related to the intrinsic aggressiveness of the individual disease or the advanced stage of the primary tumor (18). Notably, the incidence of recurrence in RPLNs was the lowest of all the regions after treatment, though the incidence of RPLN recurrence ranked third at presentation. It is possible that the retropharyngeal space received radiation doses as a CTV or outside the CTV enough to lead the occult metastasis to cause death. Guan et al (30) found that 18.6% (11/59) of patients had RPLN involvement at diagnosis, but only 1 patient developed RPLN recurrence during follow-up. Dosimetric analysis showed

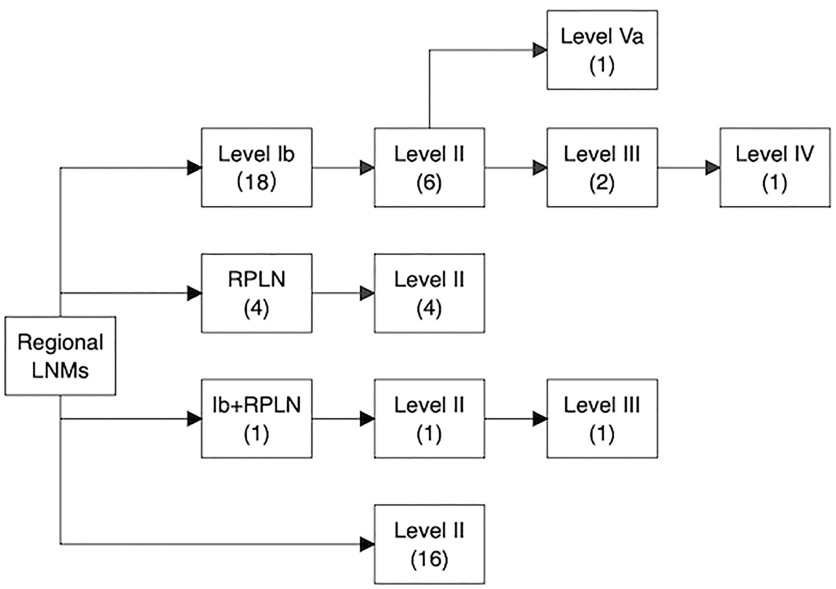

FIGURE 5 | Pathways of ipsilateral lymph node spread in SNSCC. The number in the bracket represents the number of patients who had nodal involvement in specific lymph node levels.

that the median CTV dose delivered to the retropharyngeal space was 43.3 Gy. Therefore, the researchers suggested that only ipsilateral levels Ib and II be prophylactically irradiated. However, Gangl et al (31) reported that the rate of initial RPLN involvement was 45.5% (10/23) in SNSCC, and it was a prognostic factor for OS and locoregional control. Regretfully, the incidence of RPLN recurrence after treatment was not provided. Thus, whether RPLNs are routinely included in prophylactic irradiation fields and the optimal dose need to be assessed in future studies.

In our study, the multivariate analysis showed that nasopharyngeal invasion was a risk factor for initial or delayed LNM. Similarly, Homma et al (15) reported that involvement of the nasopharynx was correlated with LNM, and involvement of the hard palate was also identified. These two areas are known to be rich in lymphatic networks that can lead to LNM development. Regarding the pterygopalatine fossa, the sample size may be a reason for the decreased RR rate.

We acknowledge that our analysis had limitations inherent to retrospective studies, such as the small number of RRs may have limited the statistical power to identify some other associations, although our study included larger sample sizes of Asian populations with significant long-term follow-up outcomes. In addition, some patients received preoperative RT in this article, which is inconsistent with the practice of surgery combined with postoperative RT adopted by most international institutions, but it does not violate the multimodal therapy recommended in advanced disease by the NCCN guidelines. As the largest cancer treatment type in Asia, the preoperative RT strategy has been successfully utilized in head and neck squamous cell carcinoma for decades (32, 33). The results of clinical practice have shown that planned preoperative RT can improve the orbital retention rate without affecting the survival outcomes (34, 35). Moreover, in this study, the proportion of patients receiving preoperative and postoperative RT was similar in the OBS group and ENI group.

In conclusion, patients who developed lymph node metastasis at diagnosis or during follow-up had poorer survival. The rate of LNM was consistent with previous studies, and lymphatic spreading in SNSCC followed predictable patterns. Prophylactic neck irradiation could effectively reduce the rate of RR in patients with SNSCC.

DATA AVAILABILITY STATEMENT

The raw data of this article will be made available by the corresponding author upon appropriate request.

ETHICS STATEMENT

This observational study was carried out following the declaration of Helsinki and approved with exemption from informed consent by the Independent Ethics Committee of Cancer Hospital, Chinese Academy of Medical Sciences.

AUTHOR CONTRIBUTIONS

QL contributed conception and design of the study; QL organized the database; QL performed the statistical analysis; QL wrote the first draft of the manuscript; QL wrote sections of the manuscript. All authors contributed to the article and approved the submitted version.

SUPPLEMENTARY MATERIAL

The Supplementary Material for this article can be found online at: https://www.frontiersin.org/articles/10.3389/fonc.2022.793351/full#supplementary-material

Supplementary Figure 1 | Kaplan-Meier estimates of the cumulative incidence of regional recurrence **(A)** and overall survival **(B)** in different RT technologies. Among 147 patients who received ENI, 94 patients were treated with IMRT, and 53 patients were treated with 3D-CRT. We depicted the KM survival curve of cumulative incidence of regional recurrence and compared IMRT and 3D-CRT using the log-rank test. There was no significant difference between IMRT and 3D-CRT on RR.

Supplementary Figure 2 | Kaplan-Meier estimates of the cumulative incidence of regional recurrence **(A)** and overall survival **(B)** in different diagnosis time periods. **(A)** Regional Recurrence in different diagnosis time periods. **(B)** Overall Survival in different diagnosis time periods.

Supplementary Table 1 | Univariate and multivariate analysis of risk factors associated with overall survival in 202 patients with N0 neck. S, Surgery; RT, Radiotherapy.

Supplementary Table 2 | The proportion of tumor stage and neck treatment in different diagnosis time.

REFERENCES

1. Siegel RL, Miller KD, Jemal A. Cancer Statistics, 2020. *CA Cancer J Clin* (2020) 70(1):7–30. doi: 10.3322/caac.21590
2. Curado MP, Edwards B, Shin HR, Storm H, Ferlay J, Heanue M, et al. Cancer Incidence in Five Continents. Volume IX. *IARC Sci Publ* (2008) 160):1–837.
3. El-Naggar AK, Chan JKC, Grandis JR, Takata T, Slootweg PJ. *WHO Classification of Head and Neck Tumours*. Lyon: International Agency for Research on Cancer (2017).
4. Turner JH, Reh DD. Incidence and Survival in Patients With Sinonasal Cancer: A Historical Analysis of Population-Based Data. *Head Neck* (2012) 34 (6):877–85. doi: 10.1002/hed.21830
5. Le QT, Fu KK, Kaplan MJ, Terris DJ, Fee WE, Goffinet DR. Lymph Node Metastasis in Maxillary Sinus Carcinoma. *Int J Radiat Oncol Biol Phys* (2000) 46(3):541–9. doi: 10.1016/S0360-3016(99)00453-8
6. Cantù G, Bimbi G, Miceli R, Mariani L, Colombo S, Riccio S, et al. Lymph Node Metastases in Malignant Tumors of the Paranasal Sinuses: Prognostic Value and Treatment. *Arch Otolaryngol Head Neck Surg* (2008) 134(2):170–7. doi: 10.1001/archoto.2007.30
7. Dubal PM, Bhojwani A, Patel TD, Zuckerman O, Baredes S, Liu JK, et al. Squamous Cell Carcinoma of the Maxillary Sinus: A Population-Based Analysis. *Laryngoscope* (2016) 126(2):399–404. doi: 10.1002/lary.25601
8. Lavertu P, Roberts JK, Kraus DH, Levine HL, Wood BG, Medendorp SV, et al. Squamous Cell Carcinoma of the Paranasal Sinuses: The Cleveland Clinic Experience 1977-1986. *Laryngoscope* (1989) 99(11):1130–6. doi: 10.1288/00005537-198911000-00005
9. Giri SP, Reddy EK, Gemer LS, Krishnan L, Smalley SR, Evans RG. Management of Advanced Squamous Cell Carcinomas of the Maxillary Sinus. *Cancer* (1992) 69(3):657–61. doi: 10.1002/1097-0142(19920201)69:3<657::AID-CNCR2820690310>3.0.CO;2-7

10. Jiang GL, Ang KK, Peters LJ, Wendt CD, Oswald MJ, Goepfert H. Maxillary Sinus Carcinomas: Natural History and Results of Postoperative Radiotherapy. *Radiother Oncol* (1991) 21(3):193–200. doi: 10.1016/0167-8140(91)90037-H
11. Paulino AC, Fisher SG, Marks JE. Is Prophylactic Neck Irradiation Indicated in Patients With Squamous Cell Carcinoma of the Maxillary Sinus? *Int J Radiat Oncol Biol Phys* (1997) 39(2):283–9. doi: 10.1016/S0360-3016(97)00293-9
12. Weiss MH, Harrison LB, Isaacs RS. Use of Decision Analysis in Planning a Management Strategy for the Stage N0 Neck. *Arch Otolaryngol Head Neck Surg* (1994) 120(7):699–702. doi: 10.1001/archotol.1994.01880310005001
13. Abu-Ghanem S, Horowitz G, Abergel A, Yehuda M, Gutfeld O, Carmel NN, et al. Elective Neck Irradiation Versus Observation in Squamous Cell Carcinoma of the Maxillary Sinus With N0 Neck: A Meta-Analysis and Review of the Literature. *Head Neck* (2015) 37(12):1823–8. doi: 10.1002/hed.23791
14. Fernandez JM, Santaolalla F, Del Rey AS, Martinez-Ibarguen A, Gonzalez A, Iriarte MR. Preliminary Study of the Lymphatic Drainage System of the Nose and Paranasal Sinuses and its Role in Detection of Sentinel Metastatic Nodes. *Acta Otolaryngol* (2005) 125(5):566–70. doi: 10.1080/00016480510036457
15. Homma A, Hayashi R, Matsuura K, Kato K, Kawabata K, Monden N, et al. Lymph Node Metastasis in T4 Maxillary Sinus Squamous Cell Carcinoma: Incidence and Treatment Outcome. *Ann Surg Oncol* (2014) 21(5):1706–10. doi: 10.1245/s10434-014-3544-6
16. Peck BW, Van Abel KM, Moore EJ, Price DL. Rates and Locations of Regional Metastases in Sinonasal Malignancies: The Mayo Clinic Experience. *J Neurol Surg B Skull Base* (2018) 79(3):282–8. doi: 10.1055/s-0037-1607288
17. Austin PC. Comparing Paired vs non-Paired Statistical Methods of Analyses When Making Inferences About Absolute Risk Reductions in Propensity-Score Matched Samples. *Stat Med* (2011) 30(11):1292–301. doi: 10.1002/sim.4200
18. Ahn PH, Mitra N, Alonso-Basanta M, Palmer JN, Adappa ND, O'Malley BW Jr, et al. Risk of Lymph Node Metastasis and Recommendations for Elective Nodal Treatment in Squamous Cell Carcinoma of the Nasal Cavity and Maxillary Sinus: A SEER Analysis. *Acta Oncol* (2016) 55(9-10):1107–14. doi: 10.1080/0284186X.2016.1216656
19. Scurry WC Jr, Goldenberg D, Chee MY, Lengerich EJ, Liu Y, Fedok FG. Regional Recurrence of Squamous Cell Carcinoma of the Nasal Cavity: A Systematic Review and Meta-Analysis. *Arch Otolaryngol Head Neck Surg* (2007) 133(8):796–800. doi: 10.1001/archotol.133.8.796
20. Galloni C, Locatello LG, Bruno C, Cannavicci A, Maggiore G, Gallo O. The Role of Elective Neck Treatment in the Management of Sinonasal Carcinomas: A Systematic Review of the Literature and a Meta-Analysis. *Cancers (Basel)* (2021) 13(8):1842. doi: 10.3390/cancers13081842
21. Dooley L, Shah J. Management of the Neck in Maxillary Sinus Carcinomas. *Curr Opin Otolaryngol Head Neck Surg* (2015) 23(2):107–14. doi: 10.1097/MOO.0000000000000138
22. Dulguerov P, Jacobsen MS, Allal AS, Lehmann W, Calcaterra T. Nasal and Paranasal Sinus Carcinoma: Are We Making Progress? A Series of 220 Patients and a Systematic Review. *Cancer* (2001) 92(12):3012–29. doi: 10.1002/1097-0142(20011215)92:12<3012::AID-CNCR10131>3.0.CO;2-E
23. Mirghani H, Mortuaire G, Armas GL, Hartl D, Aupérin A, El Bedoui S, et al. Sinonasal Cancer: Analysis of Oncological Failures in 156 Consecutive Cases. *Head Neck* (2014) 36(5):667–74. doi: 10.1002/hed.23356
24. Dirix P, Nuyts S, Geussens Y, Jorissen M, Vander Poorten V, Fossion E, et al. Malignancies of the Nasal Cavity and Paranasal Sinuses: Long-Term Outcome With Conventional or Three-Dimensional Conformal Radiotherapy. *Int J Radiat Oncol Biol Phys* (2007) 69(4):1042–50. doi: 10.1016/j.ijrobp.2007.04.044
25. Porceddu S, Martin J, Shanker G, Martin J, Shanker G, Weih L, et al. Paranasal Sinus Tumors: Peter MacCallum Cancer Institute Experience. *Head Neck* (2004) 26(4):322–30. doi: 10.1002/hed.10388
26. Dutta R, Dubal PM, Svider PF, Liu JK, Baredes S, Eloy JA. Sinonasal Malignancies: A Population-Based Analysis of Site-Specific Incidence and Survival. *Laryngoscope* (2015) 125(11):2491–7. doi: 10.1002/lary.25465
27. Ranasinghe VJ, Stubbs VC, Reny DC, Fathy R, Brant JA, Newman JG. Predictors of Nodal Metastasis in Sinonasal Squamous Cell Carcinoma: A National Cancer Database Analysis. *World J Otorhinolaryngol Head Neck Surg* (2020) 6(2):137–41. doi: 10.1016/j.wjorl.2020.01.006
28. Becker C, Kayser G, Pfeiffer J. Squamous Cell Cancer of the Nasal Cavity: New Insights and Implications for Diagnosis and Treatment. *Head Neck* (2016) 38 Suppl 1:E2112–7. doi: 10.1002/hed.24391
29. Rouviere H. Chapter 2. Lymphatic System of the Head and Neck. In: *Anatomy of the Human Lymphatic System* Ann Arbor: JW Edwards (1938).
30. Guan X, Wang X, Liu Y, Hu C, Zhu G. Lymph Node Metastasis in Sinonasal Squamous Cell Carcinoma Treated With IMRT/3D-CRT. *Oral Oncol* (2013) 49(1):60–5. doi: 10.1016/j.oraloncology.2012.07.009
31. Gangl K, Nemec S, Altorjai G, Pammer J, Grasl MC, Erovic BM. Prognostic Survival Value of Retropharyngeal Lymph Node Involvement in Sinonasal Tumors: A Retrospective, Descriptive, and Exploratory Study. *Head Neck* (2017) 39(7):1421–7. doi: 10.1002/hed.24782
32. Yi J, Huang X, Xu Z, Liu S, Wang X, He X, et al. Phase III Randomized Trial of Preoperative Concurrent Chemoradiotherapy Versus Preoperative Radiotherapy for Patients With Locally Advanced Head and Neck Squamous Cell Carcinoma. *Oncotarget* (2017) 8(27):44842–50. doi: 10.18632/oncotarget.15107
33. Zhang ZM, Tang PZ, Gang XZ, Fa QY, Zh XG. Significance of Different Preoperative Radiotherapy Doses in Combined Therapy for Hypopharyngeal Squamous Cell Carcinoma. *Chin J Radiat Oncol* (2004) 13(1):1–3. doi: 10.3760/j.issn:1004-4221.2004.01.001
34. Wang Z, Qu Y, Wang K, Wu R, Zhang Y, Huang X, et al. The Value of Preoperative Radiotherapy in the Treatment of Locally Advanced Nasal Cavity and Paranasal Sinus Squamous Cell Carcinoma: A Single Institutional Experience. *Oral Oncol* (2020) 101:104512. doi: 10.1016/j.oraloncology.2019.104512
35. Zhang ZM, Tang PZ, Xu ZG, Li ZJ. Squamous Cell Carcinoma of Naso-Ethmoid Sinus: Analysis of 146 Cases. *Zhonghua Er Bi Yan Hou Tou Jing Wai Ke Za Zhi* (2010) 45(7):555–9. doi: 10.3760/cma.j.issn.1673-0860.2010.07.007

Conflict of Interest: The authors declare that the research was conducted in the absence of any commercial or financial relationships that could be construed as a potential conflict of interest.

frontiers | Frontiers in Oncology

SYSTEMATIC REVIEW
published: 01 June 2022
doi: 10.3389/fonc.2022.820808

Risk of CVD Following Radiotherapy for Head and Neck Cancer: An Updated Systematic Review and Meta-Analysis

Ping-Yi Lin[1,2†], Ping-Chia Cheng[2,3†], Wan-Lun Hsu[4], Wu-Chia Lo[2,3], Chen-Hsi Hsieh[2,5,6,7], Pei-Wei Shueng[2,5,6] and Li-Jen Liao[2,3,8]*

[1] Oral Maxillofacial Surgery, Far Eastern Memorial Hospital, Taipei, Taiwan, [2] Head and Neck Cancer Surveillance and Research Group, Far Eastern Memorial Hospital, New Taipei, Taiwan, [3] Otolaryngology, Far Eastern Memorial Hospital, Taipei, Taiwan, [4] Genomics Research Center, Academia Sinica, Taipei, Taiwan, [5] Division of Radiation Oncology, Department of Radiology, Far Eastern Memorial Hospital, New Taipei City, Taiwan, [6] Faculty of Medicine, School of Medicine, National Yang-Ming University, Taipei, Taiwan, [7] Institute of Traditional Medicine, School of Medicine, National Yang-Ming University, Taipei, Taiwan, [8] Department of Electrical Engineering, Yuan Ze University, Taoyuan, Taiwan

OPEN ACCESS

Edited by:
Markus Wirth, Klinikum rechts der Isar, Germany

Reviewed by:
Francesco Ricchetti, Sacro Cuore Don Calabria Hospital (IRCCS), Italy
Christoph Straube, Technical University of Munich, Germany

***Correspondence:**
Li-Jen Liao
liaolj@ntu.edu.tw

†These authors have contributed equally to this work

Specialty section:
This article was submitted to Head and Neck Cancer, a section of the journal Frontiers in Oncology

Received: *23 November 2021*
Accepted: *02 May 2022*
Published: *01 June 2022*

Citation:
Lin P-Y, Cheng P-C, Hsu W-L, Lo W-C, Hsieh C-H, Shueng P-W and Liao L-J (2022) Risk of CVD Following Radiotherapy for Head and Neck Cancer: An Updated Systematic Review and Meta-Analysis. Front. Oncol. 12:820808. doi: 10.3389/fonc.2022.820808

Background: The relative risk for cerebrovascular disease (CVD) is increased in patients with head and neck cancer (HNC) treated with radiotherapy (RT). However, the current relative risk for CVD following RT has not been well clarified. The purpose of this study was to analyze the effect of RT and update the risk of CVD following RT in HNC patients through a systematic review and meta-analysis.

Material and Methods: We conducted an online database search and systematic review of observational studies that reported on CVD and extracranial carotid stenosis in patients with HNC who had undergone RT. Articles published in Medline and PubMed from 1980 to 2021 were identified and collected.

Results: Of the forty-seven articles identified from PubMed and forty-four articles identified from 3 systematic reviews, twenty-two studies were included. We found that neck RT was a significant risk factor for CVD (HR 3.97, 95% CI: 2.89-5.45). Patients with HNC treated by RT had an increased OR (7.36, 95% CI: 4.13-13.11) for CVD, and approximately 26% (95% CI: 22%-31%) of HNC patients treated with RT were at risk for CVD with more than 50% reduction in carotid diameter.

Conclusion: The risk of CVD is increased in patients with HNC treated by RT, and recent improvements in RT techniques may have contributed to the decreased risk of CVD. These results suggest that regular follow-up and appropriate screening for CVD should be required for patients with HNC.

Keywords: cerebrovascular disease, head and neck cancer, radiotherapy, radiotherapy - adverse effects, systematic review and meta-analysis

BACKGROUND

In the United States, cancer-related mortality has declined with improved treatment, and consequently, the number of cancer survivors increased to 17 million in 2019 (1). Due to the increasing number of head and neck cancer survivors, cancer-therapy-related cardiovascular complications impact both morbidity and mortality (2). Among these complications, radiation-induced cerebrovascular disease (CVD) is one of the most important issues.

Radiotherapy (RT) or concurrent with chemoradiation therapy (CCRT) is an essential therapeutic modality for patients with head and neck cancer (HNC). However, CVD in patients with HNC is under-identified and undertreated (3). The increased risk in ischemic CVD following RT has been reported in several cohort studies (4–8). Although previous systematic reviews have been reported, the quantitative method has not been updated, and there are limitations in the study design. Because of the risk of RT-related CVD, we organized a task force to conduct a comprehensive review on the risk of RT-related CVD in HNC survivors.

In the current study, a quantitative meta-analysis of the risk of CVD in post-RT/ CCRT HNC patients was designed and studied. Moreover, the assessment/screening for CVD in post-RT/CCRT HNC patients and the prevention/treatment of CVD in post-RT/CCRT HNC patients were investigated to provide potential clinical applications.

MATERIAL AND METHODS

We conducted a search on Medline and PubMed with the MeSH terms "Cerebrovascular disease AND head and neck cancer AND Radiotherapy (((head and neck cancer) AND radiotherapy [MeSH Terms]) AND Cerebrovascular disease [MeSH Terms] in the PubMed database)" in October 2021 following the PRISMA (Preferred Reporting Items for Systematic reviews and Meta-Analyses) guidelines (**Figure 1**) to identify relevant studies in the published literature. The search was performed for articles published from 1980 to 2021. Additional records from other review articles were also extracted (9–11).

Literature Inclusion Criteria

1) Studies that were original research; 2) studies that evaluated patients with histopathologically proven head and neck cancer who underwent radiotherapy; 3) studies that provided data about cerebrovascular events, such as carotid stenosis, carotid intima-media thickness or ischemia stroke; 4) studies published between 1980 and 2021; an 5) studies published in English.

Literature Exclusion Criteria

1) Studies that did not meet our inclusion criteria, 2) studies for which the data had already been published or were duplicate data and 3) studies with incomplete raw data.

Extracted Information, Excel Spreadsheet, and Information Retrieval

1) The general information extracted included the title, first author, and publication date. 2) The relative risk (RR) or hazard ratio (HR) and 95% CI were extracted for cohort studies; the number of patients with RT-related treatment and the number of patients in the control group were extracted for case–control studies; and the number of cases of CVD among the total number of RT patients was extracted for prevalence studies.

Statistical Synthesis and Analysis

The hazard ratio (HR) with 95% confidence interval (CI) was calculated to evaluate the risk of CVD in the general population and in those receiving different treatment modalities by using a random-effects model meta-analysis. The odds ratio (OR) with the corresponding 95% CI was used to compare the clinical characteristics of the post-RT vs. non-RT groups. The cumulative incidence of carotid stenosis and the 95% confidence interval (CI) were computed to estimate the prevalence of CVD (more than 50% of carotid artery diameter stenosis). The I-squared statistic was used to assess heterogeneity. An I-squared greater than 50% indicated significant heterogeneity. A random-effects model was used to pool the effect size of significant heterogeneity. A forest plot was used to graphically display the effect size in each study and the pooled estimates. A p value < 0.05 was considered significant. We performed the meta-analysis with two R software packages: "meta" (12) was used for pooling the hazard ratio and OR, while the package "metaphor" (13) was used for meta-regression to elucidate the possible etiology of heterogeneity.

RESULTS

Search Results

The search process is shown in **Figure 1**. The initial literature search yielded 91 potentially relevant records after duplicates were removed, 47 from a PubMed search (N=47) and 44 from 3 other systematic reviews (9–11). After screening the titles and abstracts, 73 articles were retrieved for full-text evaluation. Twenty-two studies met the predetermined eligibility criteria and were included in the meta-analysis, as shown in the PRISMA flow diagram.

Twenty-two studies were included (4–7, 14–31). Within the 22 studies, there were six cohort studies, of which two studies reported RR (6, 14), and another four studies reported HR (4, 5, 15, 16). Moreover, there were 13 studies with case–control study designs (7, 17–28), and another three studies (29–31) reported the number of patients with carotid stenosis after neck radiation. A total of 35,160 patients had a history of head and neck cancer treated with radiation therapy. Most patients were diagnosed with laryngeal carcinoma (32%), followed by undesignated head and neck squamous cell carcinoma (18%), oral cancer (17%), nasopharyngeal cancer (14%), oropharyngeal cancer (12%), hypopharyngeal cancer (3%), salivary gland cancer (3%), and

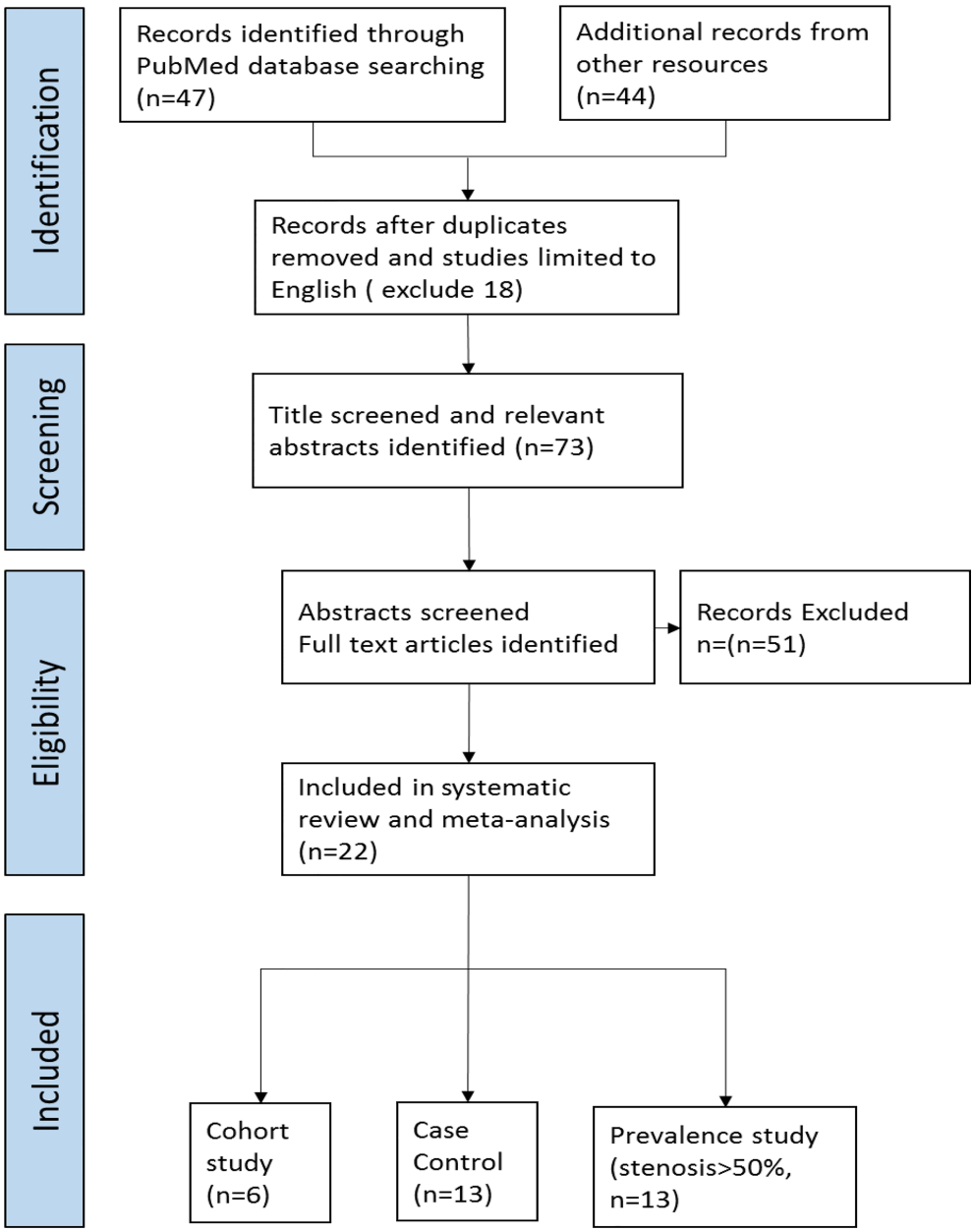

FIGURE 1 | PRISMA flow diagram of searching process.

nasal cavity or sinus cancer (1%). The imaging modalities used for the detection of carotid stenosis were Doppler ultrasound (most of the included studies) and magnetic resonance angiography (one study) (28). In the cohort study reporting the RR of CVD following radiation, Dorresteijn et al. (2002) (6) reported that radiation to the neck significantly increased the RR (5.6, 95% CI: 3.1-9.4) of stroke compared to the general population. Haynes et al. (2002) (14) also reported that radiation to the neck with/without surgery increased the relative risk of stroke (RR 2.09, 95% CI: 1.28-3.22) compared to that of the general population (**Table 1).**

Comparing the HR of CVD in the general population (Pop) with that of patients receiving different treatment modalities, RT alone for head and neck patients indeed increased the risk of CVD [HR 3.97(2.89-5.45)] compared with that in the general population in the random-effects model (**Figure 2**). Additionally, concurrent chemoradiation therapy also increased the HR [3.26 (2.43-4.38)] for CVD. Interestingly, compared to RT with surgery, RT alone significantly increased the risk of CVD (HR: 1.42, 1.14-1.77) (**Figure 2**).

Thirteen case–control studies reported carotid stenosis in patients with HNC (**Table 1**). The RT-related CCA

TABLE 1 | Summary of the 22 included studies.

	Author	Treat1	Treat2/ Control	RR or HR	lower.HR	upper.HR	Country	Cancer	Remark	Study type	Methods for CVD	Treat1 incidence (%)	Treat2 incidence (%)	RT dose (Gy)
1	Haynes (2002) (14)	RT +-SUG	Population	RR 2.09	1.28	3.22	USA	HNC	Stroke	Retro	No. of stroke	4.8	Nli	64
2	Dorresteijn (2002) (6)	RT	Population	RR 5.6	3.1	9.4	Netherland	HNC	Stroke	Retro	No. of stroke	3.8	Nil	50-66
3	Smith (2008) (4)	RT	Surgery	HR 1.50	1.18	1.90	USA	HNC	CVD	Retro	No. of stroke, carotid revascularization, or stroke death	4	3	Nil
		RT	Surgery + RT	HR 1.42	1.14	1.77	USA	HNC		Retro		4	3	Nil
4	Arthurs (2016) (5)	RT	Surgery	HR 1.70	1.41	2.05	Canada	HNC	Stroke	Retro	No. of stroke	Nil	Nil	Nil
5	Chen (2019) (15)	RT	Population	HR3.97	2.89	5.44	Taiwan	NPC	Stroke	Retro	No. of stroke	Nil	1.3	Nil
		CCRT	Population	HR 3.26	2.43	4.38	Taiwan	NPC		Retro		Nil	1.3	Nil
6	Swisher (2019) (16)	RT	Surgery	HR 1.75	1.04	2.96	USA	Glottic cancer	Fatal CVA	Retro	No. of death from CVA	2.8	1.5	Nil

	Author	Case/ RT	Noncase/ RT	Case/ Control	Noncase/Control	Country	Cancer	Grade of carotid stenosis	Study type	Methods for CVD	RT dose (Gy)
7	Moritz (1990) (17)	16	37	2	36	USA	HNC	50%	Retro	Doppler US	>50
8	Cheng (2000) (18)	35	61	8	88	HK	NPC	70%	Retro	Doppler US	64-72
9	Carmody (1999) (19)	5	18	2	44	USA	HNC	70%	Retro	Doppler US	Nil
10	Lam_H&N (2001) (20)	24	56	0	58	HK	NPC	50%	Retro	Doppler US	56.6
11	Lam_Cancer (2001) (21)	21	50	0	51	HK	NPC	50%	Retro	Doppler US	Nil
12	Chang (2009) (22)	38	154	0	98	TW	HNC	50%	Retro	Doppler US	>60
13	Greco (2012) (23)	9	30	3	51	Italy	HNC	50%	Pros	Doppler US	Nil
14	Dubec (1998) (24)	17	28	13	335	Canada	HNC	50%	Retro	Doppler US	59.5
15	Cheng (2004) (25)	43	87	22	73	HK	HNC	50%	Retro	Doppler US	60
16	Martin (2005) (26)	6	34	1	39	Canada	HNC	60%	Retro	Doppler US	>35
17	Brown (2005) (7)	8	36	3	41	USA	HNC	50%	Pros	Doppler US	>45
18	Tai (2013) (27)	8	39	1	46	Malaysia	NPC	50%	Retro	Doppler US	66
19	Zhou (2015) (28)	33	111	2	98	China	NPC	50%	Pros	MR angiography	66
20	Griewing (1995) (29)	4	12	NA	NA	Germany	HNC	50%	Retro	Doppler US	56.2
21	Steele (2004) (30)	16	24	NA	NA	USA	HNC	50%	Pros	Doppler US	64.2
22	Carpenter (2018) (31)	58	308	NA	NA	USA	HNC	50%	Retro	Doppler US	48

HNC (head and neck cancer), NPC (nasopharyngeal carcinoma), HK (Hong Kong), TW (Taiwan), USA (United States of America), Retro (retrospective study), Pros (prospective study), No. of stroke (Numbers of stroke), Pop (population), RT (radiotherapy), Surg (surgery).

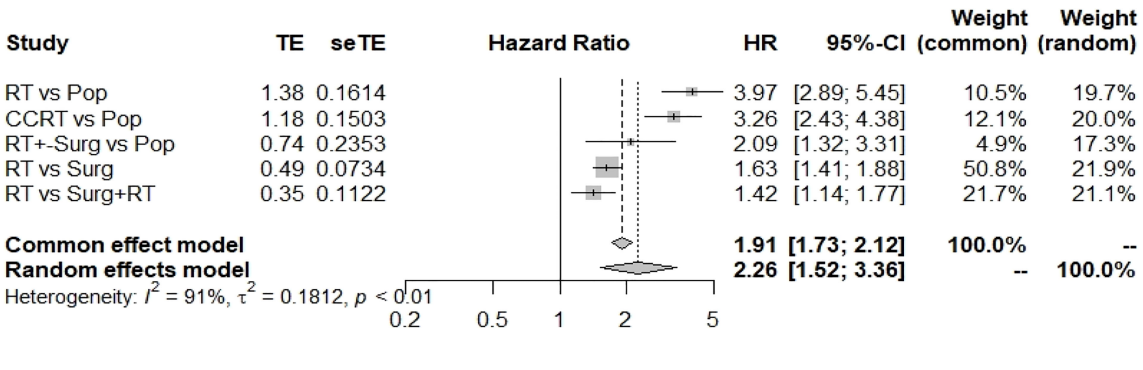

FIGURE 2 | Summary of the hazard ratios for CVD for different treatment methods. Pop, population; RT, radiotherapy; Surg, surgery.

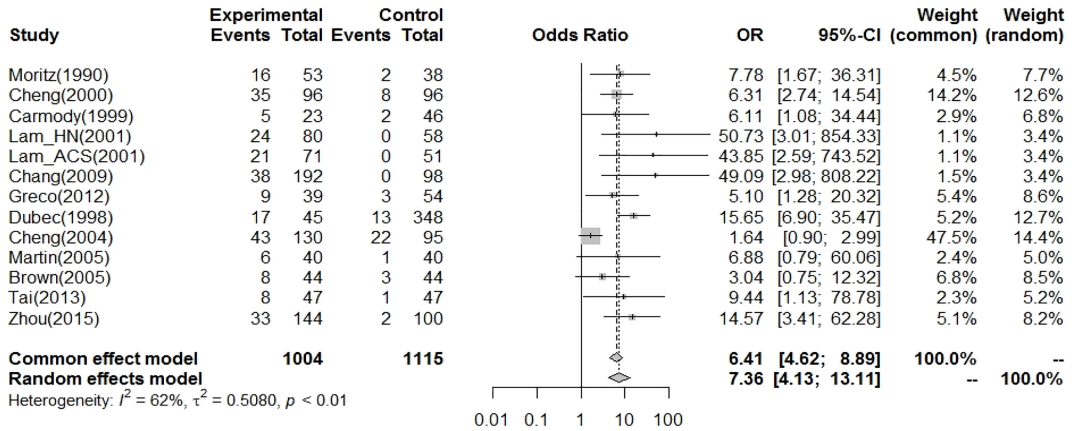

FIGURE 3 | In case–control studies, the pooled OR for radiation-related CA vasculopathy (carotid artery stenosis>50%~%70 as risk) was 7.36 (95% CI: 4.13-13.11).

vasculopathy results are shown in **Figure 3**. The pooled OR (odds ratio) for an increased risk of CVD was 7.36 (4.13-13.11) using a cutoff point of 50% carotid artery stenosis in the random-effects model. However, there was significant heterogeneity among studies.

The current study demonstrated that the prevalence of CVD with more than 50% carotid stenosis in post-RT HNC patients was 26% (95% CI: 22%-31%, **Table 2** and **Figure 4**). In meta-regression analysis to clarify the possible factors contributing to the heterogeneity among studies, we found that the publication year was a significant factor that contributed to the heterogeneity (p-value < 0.001, **Table 2**). In studies published before 2004, the prevalence of CVD with more than 50% carotid stenosis in post-RT HNC patients was 33% (95% CI: 29%-38%).

DISCUSSION

We collected multiple studies and combined different study designs to clarify the effects of radiation effect to the neck. We concluded that radiation is a significant risk factor for CVD (HR 3.97, 95% CI: 2.89-5.45). Post-RT head and neck cancer patients had an increased OR (7.36, 95% CI: 4.13-13.11) for the risk of CVD, and approximately 26% of patients were at risk for CVD, defined as having more than 50% carotid diameter reduction. Our findings provide scientific evidence and are helpful for the development of protocols for the diagnosis and prevention of CVD.

Another meta-analysis of eight studies reported the pooled relative risk (9) and RR (7.54, 95% CI: 3.65-15.59) for high-grade carotid stenosis. Because the total number of patients at risk was not followed prospectively, the effect size should be calculated as the OR (32). Our OR for carotid stenosis more than 50% results is similar (7.36, 95% CI: 4.13-13.11).

The cost-effectiveness of carotid artery stenosis screening depends on the prevalence. One study revealed that the prevalence of carotid stenosis in the general population was 0% to 7.5% for moderate stenosis (carotid stenosis >50%) and 0% to 3.1% for severe stenosis (carotid stenosis >70%) (33). CVD screening is recommended if the prevalence of carotid artery stenosis is more than 20% (34). Previous meta-analysis reported that the prevalence of carotid stenosis in post-RT HNC patients was 25% (95% CI: 19%-32%) for moderate stenosis, 12% (95% CI: 7%-17%) for severe stenosis, and 4% (95% CI: 2%-8%) (11) for carotid occlusion. In our study, we estimated that the pooled prevalence for carotid stenosis (>50% luminal stenosis) was 26% (95% CI: 22%-31%). This result indicates that screening in post-RT HNC patients is necessary.

CVD is an underestimated condition for head and neck cancer patients (3). Okoye et al. reported that approximately 23% (27/115) of head and neck cancer patients have cardiovascular disease at diagnosis. Among these patients, 15% (17/115) had coronary artery disease and 9% (10/115) had carotid artery disease (35). A high prevalence of cardiovascular disease risk factors at HNC diagnosis requires personalized

TABLE 2 | Results of meta-regression analysis with the R package metafor, showing that the year of publication and subsites of cancer were significant contributing factors to the heterogeneity.

Characteristics	% of CA stenosis>50%	z-val	p-val
Publication year		5.0234	<.0001
Before 2004	33% (29-38%)		
After 2004	19% (16-22%)		
Overall	26% (22-31%)		

CA, carotid artery.

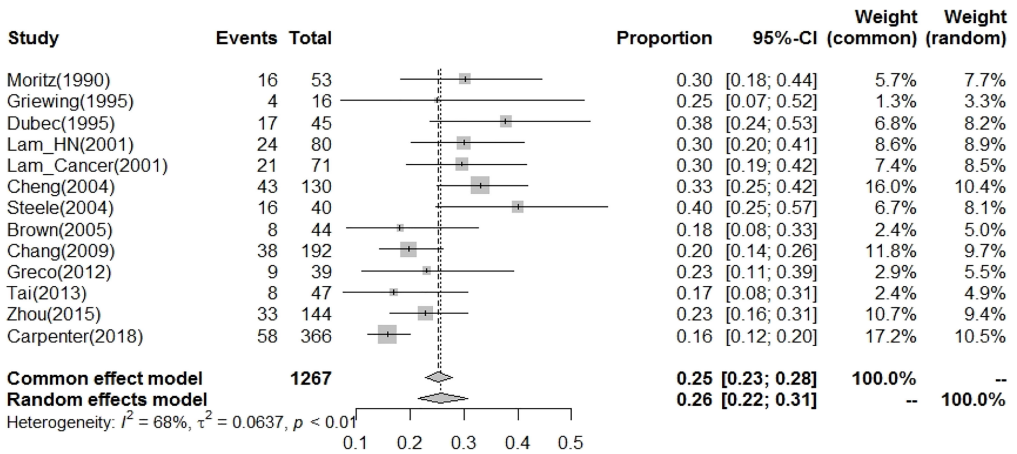

FIGURE 4 | The prevalence of CVD risk (CA stenosis>50% as increasing risk for CVD) for patients after radiotherapy to the neck was 26% (95% CI: 22%-31%).

lifestyle changes and risk factor modifications to achieve LDL, blood pressure and blood sugar targets as early as possible (36).

Radiation-related carotid vasculopathy is a dynamic and progressive process that can result in the depletion of parenchymal and vascular endothelial cells, with both macro- and microvascular effects (37). Oxidative stress caused by reactive oxygen species promotes endothelial dysfunction and inflammatory changes in the radiation field (38). Accordingly, RT induces the release of thromboxane (39) and increases the level of von Willebrand factor, which causes platelet adhesion to endothelial cells and predisposes patients to arterial thrombosis (40). Simonetto et al. reported an increase in carotid intima media thickness (CIMT) one year after radiation for hypopharyngeal cancers (41). Therefore, it is necessary to screen the carotid artery one year after neck radiation. The late effects of radiation to the carotid artery will progress (42); therefore, regular extracranial color-coded duplex sonography examination is reasonable.

Neck irritation will induce inflammation in the arteries; however, the mechanism through which this occurs is still poorly understood. To date, there are no guidelines for medication in the prevention of radiation-associated CVD. In radiotherapy-induced carotid artery vasculopathy, CIMT was reported to be related to LDL cholesterol levels (43). According to a retrospective study, statin use was associated with a significant reduction in the incidence of stroke of 32% among cancer patients after radiation to the thorax, head and neck (44). There is growing evidence of anti-inflammatory medication to prevent radiation-associated CVDs, such as statins, colchicine and aspirin (45). More evidence is necessary for anti-inflammatory medication to prevent radiation-associated CVD.

The treatment of head and neck cancer requires a multidisciplinary team, including head and neck surgeons, radiation oncologists, hemato-oncologists and cardio-oncologists. Novel models for comprehensive head and neck cancer survival are necessary to provide a multidisciplinary approach to the prevention, screening and treatment of radiation-related CVD.

Due to technical innovations, the prevalence of radiation-related carotid vasculopathy may be decreased. In our studies, we found that publication year was an important factor in the heterogeneity among studies. One study reported that IMRT can reduce the risk for CVD compared to 2D RT (46). However, Addison et al. reported that patients with HPV-related head and neck cancer who underwent radiation had an increased risk for CVD (HR 4.4, 95% CI: 1.5-13.2) compared to HPV-negative patients (47). In addition, advances in head and neck cancer treatment have led to increased survival. Radiation-related CVD will still be an important issue in the future due to the emergence of HPV-related HNC.

There are limitations in the current study. First, there was significant heterogeneity among the collected studies, which may be due to various radiation dosages, radiation protocols, radiation techniques, and follow-up times. However, there were no sufficient information about the radiation dosages, protocols, and techniques from the included studies. The follow-up duration of the included studies was varying. The radiation dosages were either recorded as main tumor, neck or carotid region. The radiation protocols and techniques were mostly not mentioned. Thus, we cannot achieve further analysis. Second, the enrolled studies were nonrandomized and were observation studies. Only four of the included reports were prospective cohort studies, and others were retrospective studies. Third, there are still no solid guidelines for screening and treatment, and further studies are necessary to develop cost-effective methods in the management of radiation-related CVD. Fourth, the timeframe of the included articles is very large, the CVD risk may be change by radiation technique, HPV status and patients' survival condition.

CONCLUSION

The included studies demonstrated that the prevalence of CVD with more than 50% carotid stenosis in post-RT HNC patients was 26%. Based on our analysis, RT for HNC patients can increase the risk of CVD. To combat this complication, close

follow-up studies and appropriate screenings for CVD are recommended for HNC patients who receive RT

DATA AVAILABILITY STATEMENT

The raw data supporting the conclusions of this article will be made available by the authors, without undue reservation.

AUTHOR CONTRIBUTIONS

1. Conceived and designed the study: P-CC, W-LH, and L-JL; 2. Collected the data: P-YL, P-CC, W-LH, W-CL, C-HH, P-WS, and L-JL; 3. Performed the analysis P-CC, W-LH, and L-JL; 4. Wrote the paper: P-YL, P-CC, W-LH, W-CL, C-HH, P-WS, and L-JL. All authors contributed to the article and approved the submitted version.

FUNDING

This work was supported by grants from the Far Eastern Memorial Hospital (FEMH -2021-C-011, PI20190002) and National Science Council of the Republic of China (MOST-109-2314-B-418-004).

ACKNOWLEDGMENTS

We also thank our colleagues in the Head and Neck Cancer Surveillance & Research Group, Far Eastern Memorial Hospital.

SUPPLEMENTARY MATERIAL

The Supplementary Material for this article can be found online at: https://www.frontiersin.org/articles/10.3389/fonc.2022.820808/full#supplementary-material

Supplementary Figure 1 | The prevalence of CVD risk (CA stenosis>50% as increasing risk for CVD) for patients after radiotherapy to the neck was 33% (95% CI: 29%-38%) among studies published before 2004.

Supplementary Figure 2 | The prevalence of CVD risk (CA stenosis>50% as increasing risk for CVD) for patients after radiotherapy to the neck was 19% (95% CI: 16%-22%) among studies published after 2004.

REFERENCES

1. Siegel RL, Miller KD, Jemal A. Cancer Statistics, 2019. *CA Cancer J Clin* (2019) 69(1):7–34. doi: 10.3322/caac.21551
2. Wang L, Wang F, Chen L, Geng Y, Yu S, Chen Z. Long-Term Cardiovascular Disease Mortality Among 160 834 5-Year Survivors of Adolescent and Young Adult Cancer: An American Population-Based Cohort Study. *Eur Heart J* (2021) 42(1):101–9. doi: 10.1093/eurheartj/ehaa779
3. Yeh YC, Fang KM, Hsu W-L, Liao L-J. It is Time to Take Action to Prevent Cardiovascular Disease in Postirradiation Head and Neck Cancer Patients. *Eur Arch Oto-Rhino-Laryngol* (2019) 276(8):2361–2. doi: 10.1007/s00405-019-05492-8
4. Smith GL, Smith BD, Buchholz TA, Giordano SH, Garden AS, Woodward WA, et al. Cerebrovascular Disease Risk in Older Head and Neck Cancer Patients After Radiotherapy. *J Clin Oncol* (2008) 26(31):5119–25. doi: 10.1200/JCO.2008.16.6546
5. Arthurs E, Hanna TP, Zaza K, Peng Y, Hall SF. Stroke After Radiation Therapy for Head and Neck Cancer: What Is the Risk? *Int J Radiat Oncol Biol Phys* (2016) 96(3):589–96. doi: 10.1016/j.ijrobp.2016.07.007
6. Dorresteijn LD, Kappelle AC, Boogerd W, Klokman WJ, Balm AJ, Keus RB, et al. Increased Risk of Ischemic Stroke After Radiotherapy on the Neck in Patients Younger Than 60 Years. *J Clin Oncol* (2002) 20(1):282–8. doi: 10.1200/JCO.2002.20.1.282
7. Brown PD, Foote RL, McLaughlin MP, Halyard MY, Ballman KV, Collie AC, et al. A Historical Prospective Cohort Study of Carotid Artery Stenosis After Radiotherapy for Head and Neck Malignancies. *Int J Radiat Oncol Biol Phys* (2005) 63(5):1361–7. doi: 10.1016/j.ijrobp.2005.05.046
8. Lee JY, Kim YA, Kim HS, Back JH, Jung YH, Lee DH, et al. Radiotherapy can Increase the Risk of Ischemic Cerebrovascular Disease in Head and Neck Cancer Patients: A Korean Population-Based Cohort Study. *Radiother Oncol* (2020) 142:85–91. doi: 10.1016/j.radonc.2019.09.025
9. Bashar K, Healy D, Clarke-Moloney M, Burke P, Kavanagh E, Walsh SR. Effects of Neck Radiation Therapy on Extra-Cranial Carotid Arteries Atherosclerosis Disease Prevalence: Systematic Review and a Meta-Analysis. *PloS One* (2014) 9(10):e110389. doi: 10.1371/journal.pone.0110389
10. Plummer C, Henderson RD, O'Sullivan JD, Read SJ. Ischemic Stroke and Transient Ischemic Attack After Head and Neck Radiotherapy: A Review. *Stroke* (2011) 42(9):2410–8. doi: 10.1161/STROKEAHA.111.615203
11. Texakalidis P, Giannopoulos S, Tsouknidas I, Song S, Rivet DJ, Reiter ER. Prevalence of Carotid Stenosis Following Radiotherapy for Head and Neck Cancer: A Systematic Review and Meta-Analysis. *Head Neck* (2020) 42 (5):1077–88. doi: 10.1002/hed.26102
12. Balduzzi S, Rücker G, Schwarzer G. How to Perform a Meta-Analysis With R: A Practical Tutorial. *Evidence-Based Ment Health* (2019) 22(4):153–60. doi: 10.1136/ebmental-2019-300117
13. Viechtbauer W. Conducting Meta-Analyses in R With the Metafor Package. *J Stat Softw* 36(3):1–48. doi: jss.v036.i03/jss.v036.i03
14. Haynes JC, Machtay M, Weber RS, Weinstein GS, Chalian AA, Rosenthal DI. Relative Risk of Stroke in Head and Neck Carcinoma Patients Treated With External Cervical Irradiation. *Laryngoscope* (2002) 112(10):1883–7. doi: 10.1097/00005537-200210000-00034
15. Chen MC, Kuan FC, Huang SF, Lu CH, Chen PT, Huang CE, et al. Accelerated Risk of Premature Ischemic Stroke in 5-Year Survivors of Nasopharyngeal Carcinoma. *Oncologist* (2019) 24(9):e891–7. doi: 10.1634/theoncologist.2018-0747
16. Swisher-McClure S, Mitra N, Lin A, Ahn P, Wan F, O'Malley B. Risk of Fatal Cerebrovascular Accidents After External Beam Radiation Therapy for Early-Stage Glottic Laryngeal Cancer. *Head Neck* (2014) 36(5):611–6. doi: 10.1002/hed.23342
17. Moritz MW, Higgins RF, Jacobs JR. Duplex Imaging and Incidence of Carotid Radiation Injury After High-Dose Radiotherapy for Tumors of the Head and Neck. *Arch Surg* (1990) 125(9):1181–3. doi: 10.1001/archsurg.1990.01410210107017
18. Cheng SW, Ting AC, Lam LK, Wei WI. Carotid Stenosis After Radiotherapy for Nasopharyngeal Carcinoma. *Arch Otolaryngol Head Neck Surg* (2000) 126 (4):517–21. doi: 10.1001/archotol.126.4.517
19. Carmody BJ, Arora S, Avena R, Curry KM, Simpkins J, Cosby K, et al. Accelerated Carotid Artery Disease After High-Dose Head and Neck Radiotherapy: Is There a Role for Routine Carotid Duplex Surveillance? *J Vasc Surg* (1999) 30(6):1045–51. doi: 10.1016/S0741-5214(99)70042-X
20. Lam WW, Yuen HY, Wong KS, Leung SF, Liu KH, Metreweli C. Clinically Underdetected Asymptomatic and Symptomatic Carotid Stenosis as a Late Complication of Radiotherapy in Chinese Nasopharyngeal Carcinoma Patients. *Head Neck* (2001) 23(9):780–4. doi: 10.1002/hed.1111
21. Lam WW, Leung SF, So NM, Wong KS, Liu KH, Ku PK, et al. Incidence of Carotid Stenosis in Nasopharyngeal Carcinoma Patients After Radiotherapy. *Cancer* (2001) 92(9):2357–63. doi: 10.1002/1097-0142(20011101)92:9<2357::AID-CNCR1583>3.0.CO;2-K
22. Chang YJ, Chang TC, Lee TH, Ryu SJ. Predictors of Carotid Artery Stenosis After Radiotherapy for Head and Neck Cancers. *J Vasc Surg* (2009) 50(2):280–5. doi: 10.1016/j.jvs.2009.01.033

23. Greco A, Gallo A, De Virgilio A, Marinelli C, Macri GF, Fusconi M, et al. Carotid Stenosis After Adjuvant Cervical Radiotherapy in Patients With Head and Neck Cancers: A Prospective Controlled Study. *Clin Otolaryngol* (2012) 37(5):376–81. doi: 10.1111/coa.12007
24. Dubec JJ, Munk PL, Tsang V, Lee MJ, Janzen DL, Buckley J, et al. Carotid Artery Stenosis in Patients Who Have Undergone Radiation Therapy for Head and Neck Malignancy. *Br J Radiol* (1998) 71(848):872–5. doi: 10.1259/bjr.71.848.9828801
25. Cheng SW, Ting AC, Ho P, Wu LL. Accelerated Progression of Carotid Stenosis in Patients With Previous External Neck Irradiation. *J Vasc Surg* (2004) 39(2):409–15. doi: 10.1016/j.jvs.2003.08.031
26. Martin JD, Buckley AR, Graeb D, Walman B, Salvian A, Hay JH. Carotid Artery Stenosis in Asymptomatic Patients Who Have Received Unilateral Head-and-Neck Irradiation. *Int J Radiat Oncol Biol Phys* (2005) 63(4):1197–205. doi: 10.1016/j.ijrobp.2005.04.017
27. Tai SM-L, Niyaz M, Ng C-G, Govindasamy GK, Tan C-T. Extracranial Carotid Stenosis After Radiotherapy in Nasopharyngeal Carcinoma, a Malaysian Study. *Neurol Asia* (2013) 18(2): 143–51.
28. Zhou L, Xing P, Chen Y, Xu X, Shen J, Lu X. Carotid and Vertebral Artery Stenosis Evaluated by Contrast-Enhanced MR Angiography in Nasopharyngeal Carcinoma Patients After Radiotherapy: A Prospective Cohort Study. *Br J Radiol* (2015) 88(1050):20150175. doi: 10.1259/bjr.20150175
29. Griewing B, Guo Y, Doherty C, Feyerabend M, Wessel K, Kessler C. Radiation-Induced Injury to the Carotid Artery: A Longitudinal Study. *Eur J Neurol* (1995) 2(4):379–83. doi: 10.1111/j.1468-1331.1995.tb00143.x
30. Steele SR, Martin MJ, Mullenix PS, Crawford JV, Cuadrado DS, Andersen CA. Focused High-Risk Population Screening for Carotid Arterial Stenosis After Radiation Therapy for Head and Neck Cancer. *Am J Surg* (2004) 187(5):594–8. doi: 10.1016/j.amjsurg.2004.01.014
31. Carpenter DJ, Mowery YM, Broadwater G, Rodrigues A, Wisdom AJ, Dorth JA, et al. The Risk of Carotid Stenosis in Head and Neck Cancer Patients After Radiation Therapy. *Oral Oncol* (2018) 80:9–15. doi: 10.1016/j.oraloncology.2018.02.021
32. Ranganathan P, Aggarwal R, Pramesh CS. Common Pitfalls in Statistical Analysis: Odds Versus Risk. *Perspect Clin Res* (2015) 6(4):222–4. doi: 10.4103/2229-3485.167092
33. de Weerd M, Greving JP, Hedblad B, Lorenz MW, Mathiesen EB, O'Leary DH, et al. Prevalence of Asymptomatic Carotid Artery Stenosis in the General Population: An Individual Participant Data Meta-Analysis. *Stroke* (2010) 41(6):1294–7. doi: 10.1161/STROKEAHA.110.581058
34. Yin D, Carpenter JP. Cost-Effectiveness of Screening for Asymptomatic Carotid Stenosis. *J Vasc Surg* (1998) 27(2):245–55. doi: 10.1016/S0741-5214(98)70355-6
35. Okoye CC, Bucher J, Tatsuoka C, Parikh SA, Oliveira GH, Gibson MK, et al. Cardiovascular Risk and Prevention in Patients With Head and Neck Cancer Treated With Radiotherapy. *Head Neck* (2017) 39(3):527–32. doi: 10.1002/hed.24646
36. Yang EH, Marmagkiolis K, Balanescu DV, Hakeem A, Donisan T, Finch W, et al. Radiation-Induced Vascular Disease-A State-Of-the-Art Review. *Front Cardiovasc Med* (2021) 8:652761. doi: 10.3389/fcvm.2021.652761
37. Kim JH, Jenrow KA, Brown SL. Mechanisms of Radiation-Induced Normal Tissue Toxicity and Implications for Future Clinical Trials. *Radiat Oncol J* (2014) 32(3):103–15. doi: 10.3857/roj.2014.32.3.103
38. Ping Z, Peng Y, Lang H, Xinyong C, Zhiyi Z, Xiaocheng W, et al. Oxidative Stress in Radiation-Induced Cardiotoxicity. *Oxid Med Cell Longev* (2020) 2020:3579143. doi: 10.1155/2020/3579143
39. Virmani R, Farb A, Carter AJ, Jones RM. Pathology of Radiation-Induced Coronary Artery Disease in Human and Pig. *Cardiovasc Radiat Med* (1999) 1(1):98–101. doi: 10.1016/S1522-1865(98)00010-9
40. Verheij M, Dewit LG, Boomgaard MN, Brinkman HJ, van Mourik JA. Ionizing Radiation Enhances Platelet Adhesion to the Extracellular Matrix of Human Endothelial Cells by an Increase in the Release of Von Willebrand Factor. *Radiat Res* (1994) 137(2):202–7. doi: 10.2307/3578813
41. Simonetto C, Mayinger M, Ahmed T, Borm K, Kundrát P, Pigorsch S, et al. Longitudinal Atherosclerotic Changes After Radio(chemo)therapy of Hypopharyngeal Carcinoma. *Radiat Oncol* (2020) 15:102. doi: 10.1186/s13014-020-01541-3
42. Huang TL, Hsu HC, Chen HC, Lin HC, Chien CY, Fang FM, et al. Long-Term Effects on Carotid Intima-Media Thickness After Radiotherapy in Patients With Nasopharyngeal Carcinoma. *Radiat Oncol* (2013) 8:261. doi: 10.1186/1748-717X-8-261
43. Pereira EB, Gemignani T, Sposito AC, Matos-Souza JR, Nadruz WJr. Low-Density Lipoprotein Cholesterol and Radiotherapy-Induced Carotid Atherosclerosis in Subjects With Head and Neck Cancer. *Radiat Oncol* (2014) 9:134. doi: 10.1186/1748-717X-9-134
44. Boulet J, Peña J, Hulten EA, Neilan TG, Dragomir A, Freeman C, et al. Statin Use and Risk of Vascular Events Among Cancer Patients After Radiotherapy to the Thorax, Head, and Neck. *J Am Heart Assoc* (2019) 8(13):e005996. doi: 10.1161/JAHA.117.005996
45. Camara Planek MI, Silver AJ, Volgman AS, Okwuosa TM. Exploratory Review of the Role of Statins, Colchicine, and Aspirin for the Prevention of Radiation-Associated Cardiovascular Disease and Mortality. *J Am Heart Assoc* (2020) 9(2):e014668. doi: 10.1161/JAHA.119.014668
46. Liao W, Zhou H, Fan S, Zheng Y, Zhang B, Zhao Z, et al. Comparison of Significant Carotid Stenosis for Nasopharyngeal Carcinoma Between Intensity-Modulated Radiotherapy and Conventional Two-Dimensional Radiotherapy. *Sci Rep* (2018) 8(1):13899. doi: 10.1038/s41598-018-32398-y
47. Addison D, Seidelmann SB, Janjua SA, Emami H, Staziaki PV, Hallett TR, et al. Human Papillomavirus Status and the Risk of Cerebrovascular Events Following Radiation Therapy for Head and Neck Cancer. *J Am Heart Assoc* (2017) 6(9):e006453. doi: 10.1161/JAHA.117.006453

Conflict of Interest: The authors declare that the research was conducted in the absence of any commercial or financial relationships that could be construed as a potential conflict of interest.

frontiers | Frontiers in Oncology

ORIGINAL RESEARCH
published: 07 June 2022
doi: 10.3389/fonc.2022.830496

Apparent Diffusion Coefficient Map–Based Radiomics Features for Differential Diagnosis of Pleomorphic Adenomas and Warthin Tumors From Malignant Tumors

Baohong Wen[1†], Zanxia Zhang[1†], Jing Zhu[1], Liang Liu[1], Yinhua Li[1], Haoyu Huang[2], Yong Zhang[1] and Jingliang Cheng[1]*

[1] Department of MRI, the First Affiliated Hospital of Zhengzhou University, Zhengzhou, China, [2] Advanced Technical Support, Philips Healthcare, Shanghai, China

OPEN ACCESS

Edited by:
Max Heiland,
Charité Universitätsmedizin Berlin, Germany

Reviewed by:
Caterina Giannitto,
Humanitas Research Hospital, Italy
Xiaohu Li,
First Affiliated Hospital of Anhui Medical University, China

***Correspondence:**
Jingliang Cheng
fcchengjl@zzu.edu.cn

[†]These authors have contributed equally to this work

Specialty section:
This article was submitted to Head and Neck Cancer, a section of the journal Frontiers in Oncology

Received: 07 December 2021
Accepted: 25 April 2022
Published: 07 June 2022

Citation:
Wen B, Zhang Z, Zhu J, Liu L, Li Y, Huang H, Zhang Y and Cheng J (2022) Apparent Diffusion Coefficient Map–Based Radiomics Features for Differential Diagnosis of Pleomorphic Adenomas and Warthin Tumors From Malignant Tumors. Front. Oncol. 12:830496. doi: 10.3389/fonc.2022.830496

Purpose: The magnetic resonance imaging (MRI) findings may overlap due to the complex content of parotid gland tumors and the differentiation level of malignant tumor (MT); consequently, patients may undergo diagnostic lobectomy. This study assessed whether radiomics features could noninvasively stratify parotid gland tumors accurately based on apparent diffusion coefficient (ADC) maps.

Methods: This study examined diffusion-weighted imaging (DWI) obtained with echo planar imaging sequences. Eighty-eight benign tumors (BTs) [54 pleomorphic adenomas (PAs) and 34 Warthin tumors (WTs)] and 42 MTs of the parotid gland were enrolled. Each case was randomly divided into training and testing cohorts at a ratio of 7:3 and then was compared with each other, respectively. ADC maps were digitally transferred to ITK SNAP (www.itksnap.org). The region of interest (ROI) was manually drawn around the whole tumor margin on each slice of ADC maps. After feature extraction, the Synthetic Minority Oversampling TEchnique (SMOTE) was used to remove the unbalance of the training dataset. Then, we applied the normalization process to the feature matrix. To reduce the similarity of each feature pair, we calculated the Pearson correlation coefficient (PCC) value of each feature pair and eliminated one of them if the PCC value was larger than 0.95. Then, recursive feature elimination (RFE) was used to process feature selection. After that, we used linear discriminant analysis (LDA) as the classifier. Receiver operating characteristic (ROC) curve analysis was used to evaluate the diagnostic performance of the ADC.

Results: The LDA model based on 13, 8, 3, and 1 features can get the highest area under the ROC curve (AUC) in differentiating BT from MT, PA from WT, PA from MT, and WT from MT on the validation dataset, respectively. Accordingly, the AUC and the accuracy of

the model on the testing set achieve 0.7637 and 73.17%, 0.925 and 92.31%, 0.8077 and 75.86%, and 0.5923 and 65.22%, respectively.

Conclusion: The ADC-based radiomics features may be used to assist clinicians for differential diagnosis of PA and WT from MTs.

Keywords: radiomics, diffusion-weighted image, apparent diffusion coefficient, parotid gland tumor, magnetic resonance imaging

INTRODUCTION

Salivary gland tumors constitute about 3%–6% of head and neck tumors (1), about 70% of them are located in the parotid gland (2). About 80%–85% of parotid gland tumors are benign tumors (BTs), most of them are pleomorphic adenoma (PA) (about 65% of parotid gland tumors), and Warthin tumor (WT) is the second most common BT (about 15%–20% of parotid tumors) (3). Malignant salivary gland tumors constitute about 15%–30% of parotid gland tumors. Mucoepidermoid carcinoma is the most common parotid gland malignant tumor (MT) (4, 5). About 1.8%–6.2% of PA transforms into MT or carcinoma ex PA, and the recurrence of PA is reported in 0%–3% of patients (6). In contrast, WT rarely undergoes malignant evolution and recurs (7). For the treatment of BT, superficial parotidectomy is preferred, whereas total parotidectomy combined with radiotherapy is preferred for the treatment of MT (2). Specifically, the treatment of PA requires excision by either partial or total parotidectomy, which results in a risk of facial nerve injury (8, 9), the results of the study by Mercante et al. show that total parotidectomy should be the treatment of choice in case of benign parotid gland tumors and in particular for PA (10), whereas the treatment of WT could potentially avoid excision as it can be monitored. Therefore, accurate preoperative diagnosis is essential for treatment.

Fine needle aspiration cytology (FNAC) is a reliable examination that can provide preoperative information about the treatment plan and postoperative procedures (11). As this technology is cheap, fast, safe, and relatively non-invasive, it is commonly used as a mature solution. However, it still suffered from considerable variability in the accuracy, high non-diagnostic rates, and poor sensitivity or specificity (12). When done blindly by clinicians with different levels of experience, poor technique or inaccurate or inadequate sampling can result in a high rate of non-representative or insufficient aspiration (13).

Imaging technology is used to determine the stage of the tumor based on the TNM classification and the suitability of the surgery, which is the main treatment for most parotid gland tumors. Currently, there are a variety of imaging techniques that can be used to study the parotid gland tumors, such as ultrasound, computed tomography (CT), and magnetic resonance imaging (MRI). Ultrasound is an inexpensive and effective tool for delineating cystic or solid tumors, tumor borders, and cervical lymph nodes; however, it has poor visualization of deep lobe and relies on the expertise of the operator (14). CT is not a preferred method for parotid gland tumor evaluation for parotid tumor assessment due to ionizing radiation. MRI plays a crucial role in preoperatively differentiating parotid gland tumors noninvasively (15). The morphological features of parotid gland tumors from conventional MRI can help to distinguish BT and MT (16). Diffusion-weighted imaging (DWI) determines the motion of water molecules qualitatively and translates it into a coefficient called the apparent diffusion coefficient (ADC) (17), which is used to evaluate quantitative water molecule movement through ADC value. DWI is becoming a popular diagnostic and research tool for differential diagnosis of parotid gland tumors. The ADC value of BT is higher than that of MT, and BT is successfully distinguished from MT (16–21). However, previous studies (22–24) reported that ADC value cannot be satisfactorily distinguished between BT and MT, and they did not combine the various ordered imaging features of the whole-tumor region of interest (ROI) with machine learning methods. Even in squamous cell carcinoma of the oral cavity and oropharynx, Bonello et al. did not observe any statistically significant correlation between ADC values and clinical–histological characteristics of SCCA of the oral cavity and oropharynx (25).

Radiomics is one of the most innovative fields of tumor imaging, which involves the use of computer-aided techniques to detect and quantify mathematical patterns in digital images. With the development of artificial intelligence and algorithms, the computer-aided quantitative image evaluation is increasingly applied to improving the accuracy of preoperative diagnosis of parotid gland tumors (26–29), whereas the ADC map–based radiomics in differentiating parotid gland tumors has been addressed in only a few studies and needs further validation (28, 29). The purpose of this study is to evaluate the performance of ADC map–based radiomics analysis with the whole-tumor ROI for differentiating parotid gland (BT vs. MT, PA vs. WT, PA vs. MT, and WT vs. MT).

MATERIALS AND METHODS

Patients

This study was approved by the Ethics Committee of the First Affiliated Hospital of Zhengzhou University (2019-KY-0015-002). The Institutional Review Board waived the requirement of informed consent. All patients' informed consents were waived for the retrospective nature of this study.

This study retrospectively evaluated the MRI examinations of 130 patients with parotid gland tumors from August 2019 to

December 2020. Histopathology diagnosis was obtained in all cases by biopsy or surgical resection. The exclusion criteria were patients (a) with a maximum tumor diameter less than 5 mm, (b) with recurrent tumor, and (c) with poor imaging that was unsuitable for the ROI delineation. A total of 130 patients who underwent a pre-treatment MRI study included 83 men and 47 women, with an average age of 48.22 ± 17.71 years (range 1–85 years). Eighty-eight cases were BT, including 54 (41.54%) PA and 34 (26.15%) WT. The other 42 lesions were MT. The details of patient and tumor characteristics are shown in **Table 1**.

MRI Acquisition Protocols

The MRI data of patients were obtained from the picture archiving and communication system (PACS) of the First Affiliated Hospital of Zhengzhou University. Preoperative plain and contrast-enhanced MRI of the parotid gland was performed for each patient with parotid gland lesion in this study. MRI was performed on three 3.0 T MRI scanners with head/neck coil: a Skyra scanner (Siemens Healthineers, Germany), a Discovery 750 scanner (GE Healthcare, USA), and an Ingenia CX scanner (Philips Healthcare, Holland). The conventional scanning sequences including T1-weighted imaging (T1WI) in axial planes; T2-weighted imaging (T2WI) in axial, sagittal, and coronal planes, axial DWI, and post-contrast (Gadolinium, 0.1 mmol/kg) T1WI in axial, sagittal, and coronal planes were performed. The ADC maps were generated inline after the data acquisition and exported from the PACS workstation to a personal computer in DICOM format (30). A detailed overview of the MRI parameters is listed in **Table 2**. For the MRI data of our 130 patients, cases from Skyra scanner, Discovery 750 scanner, and Ingenia scanner were 92, 26, and 12, respectively.

TABLE 1 | Distribution of parotid gland tumors.

Characteristic	Number
Patient	130
Age (years) mean ± standard deviation	48.22 ± 17.71
Sex (male/female)	83/47 (63.85%/36.15%)
Tumor type, n (%)	130 (100%)
Benign tumor	88 (67.69%)
Pleomorphic adenoma	54 (41.54%)
Warthin tumor	34 (26.15%)
Malignant tumor	42 (32.31%)
Mucoepidermoid carcinoma	10 (7.69%)
Salivary duct carcinoma	4 (3.08%)
Adenoid cystic carcinoma	4 (3.08%)
Squamous cell carcinoma	4 (3.08%)
Acinar cell carcinoma	4 (3.08%)
Lymphoma	4 (3.08%)
Secretory carcinoma	2 (1.54%)
Mixed carcinoma	2 (1.54%)
Carcinoma in pleomorphic adenoma	2 (1.54%)
Myoepithelial carcinoma	1 (0.77%)
Epithelial-myoepithelial carcinoma	1 (0.77%)
Basal cell carcinoma	1 (0.77%)
Adenocarcinoma	1 (0.77%)
Rhabdomyosarcoma	1 (0.77%)
Sebaceous carcinoma	1 (0.77%)

ROI Segmentation

The ADC maps were used for our radiomics study. Axial ADC maps were digitally transferred to ITK SNAP (www.itksnap.org). The ROI was manually drawn around the whole tumor margin on each slice of ADC maps (**Figure 1**). All lesions were separately segmented and evaluated by two independent radiologists with 9 and 6 years of experience, respectively, in MRI. The radiologists know nothing about the histological results.

Feature Extraction

We used the open-source PyRadiomics toolbox to quantify radiomics features from the ADC maps (https://pyradiomics.readthedocs.io/). Three image types (original, wavelet, and gradient) were enabled and then, from each (original and/or derived) image type, extracted the following feature classes: first-order statistics (19 features), gray level co-occurrence matrix (GLCM, 24 features), gray level run length matrix (GLRLM, 16 features), gray level size zone matrix (GLSZM, 16 features), neighboring gray tone difference matrix (NGTDM, 5 features), and gray level dependence matrix (GLDM, 14 features). Meanwhile, 14 shape-based (three-dimensional) features were also extracted from the original image. In total, 944 features were extracted.

To evaluate the relationship between tumor segmentation and extracted imaging features, the intra-class correlation coefficient (ICC) was used to evaluate interobserver reproducibility for the extracted imaging features from the ROI drawn by the two radiologists. The ICC ranged from 0 to 1.00 and was interpreted as follows: $r < 0.20$, poor; $r = 0.20–0.40$, fair; $r = 0.41–0.60$, moderate; $r = 0.61–0.75$, good; and $r > 0.75$, excellent. Finally, 260 features were excellent, and the rest 684 features were good.

Statistical Analysis

In this study, 88 BT (54 PA and 34 WT) and 42 MT of the parotid gland were enrolled. Each case was randomly divided into training and testing cohorts at a ratio of 7:3 and then was compared with each other, respectively, after the following pipeline.

The Synthetic Minority Oversampling TEchnique (SMOTE) was used to remove the unbalance of the training dataset. Then, we applied the normalization process on the feature matrix. For each feature vector, we calculated the mean value and the standard deviation. Each feature vector was subtracted by the mean value and was divided by the standard deviation. After the normalization process, each vector has zero center and unit standard deviation. To reduce the similarity of each feature pair, we calculated the Pearson correlation coefficient (PCC) value of each feature pair and eliminated one of them if the PCC value was larger than 0.95 so that each feature was independent to each other. Then, we used recursive feature elimination (RFE) algorithm to process feature selection, which is based on a classifier that recursively considers smaller set of features in the training dataset by ranking features by importance until the specified number of features remains.

We used linear discriminant analysis (LDA) as the classifier. LDA was a linear classifier by fitting class conditional densities to the data and using Bayes' rule. To determine the hyper-

TABLE 2 | MRI main sequence parameters.

Parameters	T2WI	T2WI	T2WI	T1WI	DWI	CE-T1WI	CE-T1WI	CE-T1WI
Skyra								
Imaging technique	TSE	TSE	TSE	TSE	Readout-segmented EPI	TSE	TSE	TSE
Orientation	Coronal	Sagittal	Axial	Axial	Axial	Axial	Sagittal	Coronal
TR(ms)	4,500	4,000	4,300	250	3,900	884	884	565
TE(ms)	82	82	82	2.5	55	6.9	6.9	6.9
Field of view (mm^2)	230 × 230	230 × 230	230 × 230	230 × 230	220 × 220	240 × 240	240 × 240	240 × 240
Slice thickness (mm)	4	4	4	4	4	4	4	4
No. of slices	27	25	27	27	24	20	20	20
b-values (s/mm^2)	NA	NA	NA	NA	0/1,000	NA	NA	NA
Acquisition time	1 min 13 s	1 min 13 s	1 min 13 s	1 min	1 min 47 s	1 min 37 s	1 min 58 s	59 s
Discovery 750								
Imaging technique	FSE	FSE	FSE	FSE	EPI	FSE	FSE	FSE
Orientation	Coronal Ideal	Sagittal	Axial Ideal	Axial	Axial	Axial	Sagittal Ideal	Coronal
TR (ms)	3,410	3,000	2,824	478	3,044.5	550	604	567
TE (ms)	68	85	68	Min Full	60.5	Min Full	Min Full	Min Full
Field of view (mm^2)	240 × 240	240 × 240	240 × 240	240 × 240	240 × 240	240 × 240	240 × 240	240 × 240
Slice thickness (mm)	4.5	4	4	4	4	4	4	4.5
No. of slices	18	22	20	20	20	20	20	20
b-values (s/mm^2)	NA	NA	NA	NA	0/800	NA	NA	NA
Acquisition time	1 min 56 s	2 min 2 s	1 min 42 s	38 s	1 min 42 s	1 min 53 s	1 min 56 s	1 min 36 s
Ingenia CX								
Imaging technique	TSE	TSE	TSE	TSE	EPI	TSE	TSE	TSE
Orientation	Coronal	Sagittal	Axial	Axial	Axial	Axial	Sagittal	Coronal
TR (ms)	3,400	2,388	3,500	574	3,914	548	486	611
TE (ms)	100	66	85	6.5	60	7.1	7.5	7.5
Field of view (mm^2)	180 × 180	220 × 220	180 × 180	180 × 180	200 × 224	200 × 200	180 × 180	200 × 200
Slice thickness (mm)	4	4	4	4	4	4	4	4
No. of slices	24	24	24	24	24	20	19	24
b-values (s/mm^2)	NA	NA	NA	NA	0/800	NA	NA	NA
Acquisition time	1 min 32 s	1 min 33 s	1 min 56 s	1 min 30 s	1 min 38 s	1 min 55 s	2 min 12 s	1 min 43 s

T2WI, T2-weighted imaging; T1WI, T1-weighted imaging; DWI, diffusion-weighted imaging; TSE, turbo spin-echo; EPI, echo-planar imaging; TR, repetition time; TE, echo time; NA, not applicable; FSE, fast spin-echo; CE, contrast enhance.

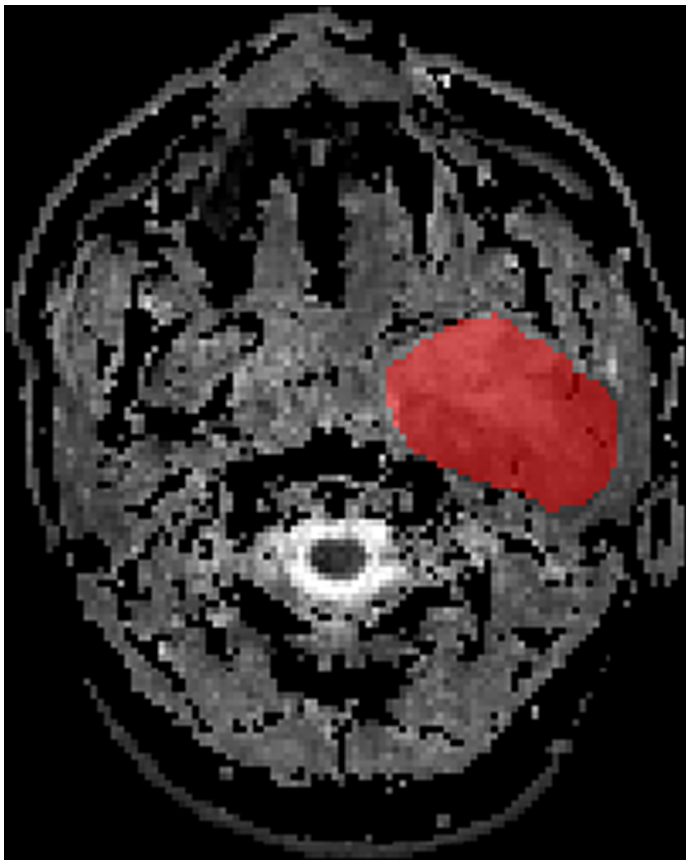

FIGURE 1 | ROI delineation of PA on ADC in ITK SNAP.

parameter (e.g., the number of features) of a model, we applied cross-validation with five-fold on the training dataset. The hyper-parameters were set according to the model performance on the validation dataset.

Receiver operating characteristic (ROC) curve analysis was used to evaluate the diagnostic performance of the ADC map–based radiomics features for differential diagnosis of parotid gland tumors (BT and MT, PA and WT, PA and MT, and WT and MT). The area under the ROC curve (AUC) was calculated for quantification. The accuracy, sensitivity, specificity, positive predictive value (PPV), and negative predictive value (NPV) were also calculated at a cutoff value that maximized the value of the Youden index. We also estimated the 95% confidence interval by bootstrap with 1,000 samples. All the above processes were implemented with FeAture Explorer Pro (FAEPro, version 0.4.0) on Python (3.7.6).

RESULTS

BT (PA + WT) vs. MT

The LDA model based on eight features can get the best diagnostic performance on the testing set in differentiating BT (PA + WT) from MT. The AUC and the accuracy could achieve 0.7637 and 73.17%, yielding sensitivity and specificity 84.62% and 67.86%, respectively. The diagnostic performance of significant ADC radiomics parameters and the selected features in differentiating PA from MT were shown in **Tables 3**, **4**. The ROC curve was shown in **Figure 2A**.

PA vs. WT

The LDA model based on 13 features can get the best diagnostic performance on the testing set in differentiating PA from WT. The AUC and the accuracy could achieve 0.925 and 92.31%, yielding sensitivity and specificity 80.00% and 100.00%,

TABLE 3 | ROC analysis of ADC radiomics parameters.

Statistics	Value
Accuracy	0.7317
AUC	0.7637
AUC 95% CIs	[0.6179–0.9106]
NPV	0.9048
PPV	0.5500
Sensitivity	0.8462
Specificity	0.6786
Youden Index	0.3673

TABLE 4 | The coefficients of features in the model.

Features	Coef in Model
Original shape sphericity	−1.436
Wavelet-LHL first-order mean	1.223
Wavelet-LHH gldm large dependence low–gray level emphasis	−1.313
Wavelet-HHL first-order mean	−0.423
Wavelet-HHL glszm small-area low–gray level emphasis	1.909
Wavelet-LLL glszm small-area low–gray level emphasis	0.230
Gradient glcm cluster tendency	0.885
Original glszm small-area low–gray level emphasis	−1.854

respectively. The diagnostic performance of significant ADC radiomics parameters and the selected features in differentiating PA from WT were shown in **Tables 5**, **6**. The ROC curve was shown in **Figure 2B**.

PA vs. MT

The LDA model based on three features can get the best diagnostic performance on the testing set in differentiating PA from MT. The AUC, the accuracy, sensitivity, and specificity could achieve 0.8077, 75.86%, 100.00%, and 56.25%, respectively. The diagnostic performance of significant ADC radiomics parameters and the selected features in differentiating PA from

TABLE 5 | ROC analysis of ADC radiomics parameters.

Statistics	Value
Accuracy	0.9231
AUC	0.9250
AUC 95% CIs	[0.7778–1.0000]
NPV	0.8889
PPV	1.0000
Sensitivity	0.8000
Specificity	1.0000
Youden Index	0.9554

TABLE 6 | The coefficients of features in the model.

Features	Coef in Model
Wavelet-LHL glrlm gray level non-uniformity normalized	−2.398
Wavelet-LHL glszm small-area low–gray level emphasis	1.179
Wavelet-HLL first-order median	1.300
Wavelet-HLH glszm gray level non-uniformity normalized	0.095
Wavelet-HLH glszm gray level variance	−3.308
Wavelet-HHH glcm Imc1	−1.490
Gradient ngtdm complexity	0.115
Original first-order 10 percentile	−4.296
Original first-order median	2.820
Original first-order skewness	1.726
Original gldm large dependence high gray level emphasis	0.929
Original glcm autocorrelation	−5.527
Original glcm joint average	4.310

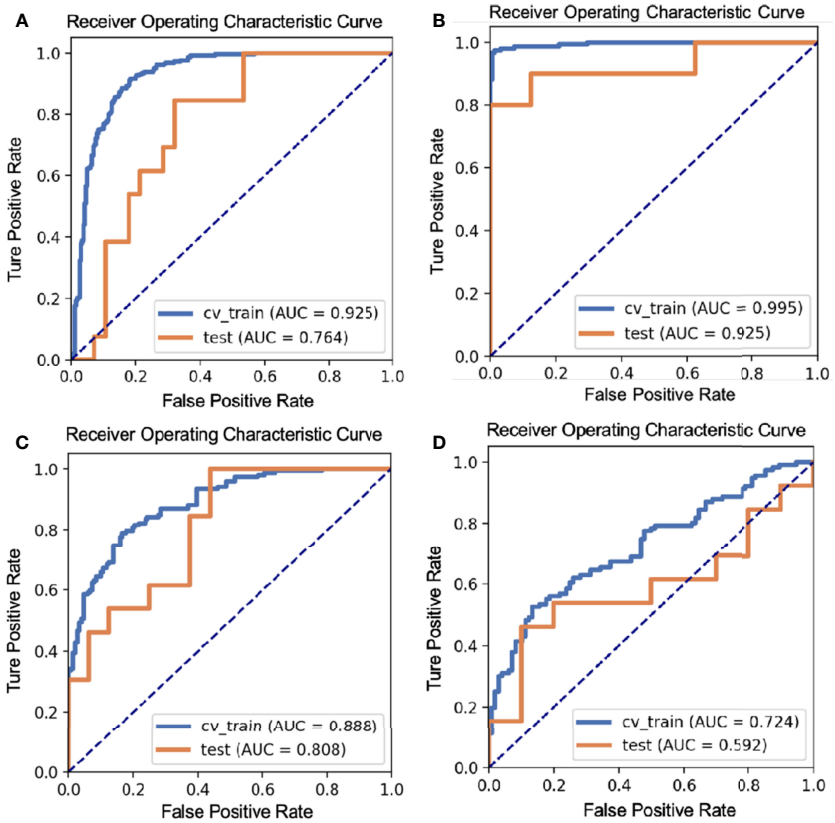

FIGURE 2 | The ROC curves of different parotid gland tumors: **(A)** BT vs. MT; **(B)** PA vs. WT; **(C)** PA vs. MT; **(D)** WT vs. MT.

MT were shown in **Tables 7**, **8**. The ROC curve was shown in **Figure 2C**.

WT vs. MT

The LDA model based on one feature can get the highest AUC on the testing set in differentiating WT from MT. The AUC, accuracy, sensitivity, and specificity could achieve 0.5923, 65.22%, 46.15%, and 90.00%, respectively. The diagnostic performance of significant ADC radiomics parameters and the selected features in differentiating WT from MT was shown in **Tables 9**, **10**. The ROC curve was shown in **Figure 2D**.

DISCUSSION

Using ADC-based radiomics analysis to detect parotid gland tumors has increasingly shown its value on different histopathological entities (30–33). ADC-based texture analysis, as a non-invasive and quantitative additional supporting tool, can extract features of entire tumors and go beyond individual-based visual assessment (34). Previously, many studies (26, 34–42) have explored the computer-assisted discrimination of benign and malignant parotid gland tumors, but only a few studies have evaluated the role of ADC-based radiomics features in the differentiation of parotid lesions (29, 31, 34). In our study, the ADC-based radiomics features were from three different manufacturers, which still shows a good performance in differentiating PA and WT from MTs. This implies the advantage of the generalization of our ADC-based features that can cross different manufacturers.

It was observed that intra/inter-tumoral heterogeneity and overlap of ADC values between BT and MT could be overcome by making a whole-tumor analysis (30, 31, 43). Previously, Ma et al. reported that no significant difference between BT and MT was found in ADC histogram parameters extracted from the ROI of whole-tumor ADC map (30). We used LDA as the classifier and found a significant difference in ADC map–based radiomics features between parotid gland BT and MT. The AUC of this model is 0.7637 in sensitivity of 84.62% and specificity of 67.86%, which may be explained by that WT was not the dominant tumor among BT. The specificity of our result is slightly lower, this could arise from that both parotid gland BT and MT have been well-differentiated and exhibiting cytological overlap.

In the comparison of PA and WT, we found extracted radiomics features get excellent diagnostic performance; the AUC is 0.925 in sensitivity of 80.00% and specificity of 100.00%; these results agree with findings of previous reports (28, 30, 31), and it may be due to the tumor components. PA exhibits a variety of histopathologic characteristics, and the presence of epithelial, mesenchymal-like tissues and rich mucus is the main diagnostic feature, which leads to facilitated water diffusibility and the highest ADC values (18, 44, 45). However, WT has lymphoid stroma with low ADC values (17, 46).

We found that the AUC was 0.8077 in sensitivity of 100.00% and specificity of 56.25% in distinguishing PA from MT, and the diagnostic performance of ADC map–based radiomics features was high, which agreed with findings of previous reports (28, 30, 31). Heterogeneous ADC maps were seen in MT (47). Investigators reported that myxoid lymphosarcomas, adenoid cystic carcinomas, and mucoepidermoid carcinomas had higher ADC values compared with other malignant neoplasms, whereas lymphomas had lower ADC values (17), but ADC values of MT were lower than these of PA.

Comparing WT with MT, our study showed that the AUC was 0.592 in sensitivity of 46.15% and specificity of 90.00%, and the diagnostic performance of ADC map–based radiomics features was not high, which is due to WT having high cellularity. The histologic structure of WT that can resemble MT includes both an oncocytic epithelial component and lymphoid stroma (17, 46, 48).

TABLE 7 | ROC analysis of ADC radiomics parameters.

Statistics	Value
Accuracy	0.7586
AUC	0.8077
AUC 95% CIs	[0.6381–0.9474]
NPV	1.0000
PPV	0.6500
Sensitivity	1.0000
Specificity	0.5625
Youden Index	0.4557

TABLE 8 | The coefficients of features in the model.

Features	Coef in Model
Wavelet-LLH first-order 90 percentile	0.684
Wavelet-LHH gldm large dependence low–gray level emphasis	–0.497
Original first-order 10 percentile	–1.468

TABLE 9 | ROC analysis of ADC radiomics parameters.

Statistics	Value
Accuracy	0.6522
AUC	0.5923
AUC 95% CIs	[0.3413–0.8250]
NPV	0.5625
PPV	0.8571
Sensitivity	0.4615
Specificity	0.9000
Youden Index	0.6549

TABLE 10 | The coefficients of features in the model.

Features	Coef in Model
Wavelet-LHH glcm Imc1	0.763

This study has some limitations. First, the data were performed on three 3.0 T MRI scanners, and different parameters might affect the diagnostic performances of the ADC map–based radiomics features; MRI acquisition parameters certainly need to be considered in the further clinical application of this technology. Second, we only constructed radiologic features based on ADC maps, and combining T2WI and contrast-enhanced T1WI is needed to accumulate more evidence for future clinical applications. Third, it is a retrospective study with relatively fewer cases, especially some pathological categories in MT. They included only PA and WT as BTs and that the dataset was unbalanced (BT was more represented than MT). We will continue to collect cases and expand the sample size. Last but not least, we did not validate our model with an external dataset. Multicenter studies with a larger number of patients are needed to further research.

CONCLUSION

In this study, we proposed to use ADC-based radiomics features for differential diagnosis of PA and WT from MT, which shows very good predictive performance. This implies that the radiomics analysis can be used as an additional tool for supporting radiologists' decisions. Further validation in a larger prospective study is required for this method.

DATA AVAILABILITY STATEMENT

The original contributions presented in the study are included in the article/supplementary material. Further inquiries can be directed to the corresponding author.

ETHICS STATEMENT

This study was conducted with approval from the Review Committee of the First Affiliated Hospital of Zhengzhou University (No: 2019-KY-0015-002). All patients' informed consents were waived for the retrospective nature of this study. Written informed consent from the participants' legal guardian/next of kin was not required to participate in this study in accordance with the national legislation and the institutional requirements.

AUTHOR CONTRIBUTIONS

BW and HH designed this study. BW, ZZ, and YL acquired data. BW and ZZ drafted the manuscript. HH, JZ, and LL performed the data and statistical analysis. JC and YZ contributed substantially to its revision. All authors contributed to the article and approved the submitted version.

FUNDING

This work was supported by the Fund of Henan Medical Science and Technology Research Plan (LHGJ20190157).

ACKNOWLEDGMENTS

We are particularly grateful to all the people who have given us help on our article. This work was supported by the First Affiliated Hospital of Zhengzhou University. We thank Liangjie Lin, PhD (Philips Healthcare), for the benefit discussion on the design of this study.

REFERENCES

1. Gao M, Hao Y, Huang MX, Ma DQ, Chen Y, Luo HY, et al. Salivary Gland Tumours in a Northern Chinese Population: A 50-Year Retrospective Study of 7190 Cases. *Int J Oral Maxillofac Surg* (2017) 46:343–9. doi: 10.1016/j.ijom.2016.09.021
2. Gökçe E. Multiparametric Magnetic Resonance Imaging for the Diagnosis and Differential Diagnosis of Parotid Gland Tumors. *J Magn Reson Imaging* (2020) 52:11–32. doi: 10.1002/jmri.27061
3. Freling N, Crippa F, Maroldi R. Staging and Follow-Up of High-Grade Malignant Salivary Gland Tumours: The Role of Traditional Versus Functional Imaging Approaches – A Review. *Oral Oncol* (2016) 60:157–66. doi: 10.1016/j.oraloncology.2016.04.016
4. Coudert H, Mirafzal S, Dissard A, Boyer L, Montoriol PF. Multiparametric Magnetic Resonance Imaging of Parotid Tumors: A Systematic Review. *Diagn Interv Imaging* (2021) 102:121–30. doi: 10.1016/j.diii.2020.08.002
5. To VSH, Chan JYW, Tsang RKY, Wei WI. Review of Salivary Gland Neoplasms. *ISRN Otolaryngol* (2012) 2012:1–6. doi: 10.5402/2012/872982
6. Valstar MH, de Ridder M, van den Broek EC, Stuiver MM, van Dijk BAC, van Velthuysen MLF, et al. Salivary Gland Pleomorphic Adenoma in the Netherlands: A Nationwide Observational Study of Primary Tumor Incidence, Malignant Transformation, Recurrence, and Risk Factors for Recurrence. *Oral Oncol* (2017) 66:93–9. doi: 10.1016/j.oraloncology.2017.01.004
7. Chulam TC, Noronha Francisco AL, Goncalves Filho J, Pinto Alves CA, Kowalski LP. Warthin's Tumour of the Parotid Gland: Our Experience. *Acta Otorhinolaryngol Ital* (2013) 33:393–7.
8. Wang CW, Chu YH, Chiu DY, Shin N, Hsu HH, Lee JC, et al. JOURNAL CLUB: The Warthin Tumor Score: A Simple and Reliable Method to Distinguish Warthin Tumors From Pleomorphic Adenomas and Carcinomas. *AJR Am J Roentgenol* (2018) 210:1330–7. doi: 10.2214/AJR.17.18492
9. Espinoza S, Felter A, Malinvaud D, Badoual C, Chatellier G, Siauve N, et al. Warthin's Tumor of Parotid Gland: Surgery or Follow-Up? Diagnostic Value of a Decisional Algorithm With Functional MRI. *Diagn Interv Imaging* (2016) 97:37–43. doi: 10.1016/j.diii.2014.11.024
10. Mercante G, Makeieff M, Guerrier B. Ruolo Della Chirurgia Nelle Recidive Dei Tumori Benigni Della Parotide [Recurrent Benign Tumors of Parotid Gland: The Role of the Surgery]. *Acta Otorhinolaryngol Ital* (2002) 22:80–5. doi: 10.11604/pamj.2019.33.65.18259
11. Bouatay R, Ben Nasr R, Moussa A, El Korbi A, Harrathi K, Koubaa J. The importance of fine needle aspiration biopsy in the diagnosis of parotid tumors. *Pan Afr Med J* (2019) 33:1–9. doi: 10.11604/pamj.2019.33.65.18259
12. Pierre SK, Moody AB, Howlett DC. The Diagnostic Value of Fine Needle Aspiration in Parotid Lumps. *Ann R Coll Surg Engl* (2014) 96:253. doi: 10.1308/003588414X13814021676639
13. Howlett DC, Skelton E, Moody AB. Establishing an Accurate Diagnosis of a Parotid Lump: Evaluation of the Current Biopsy Methods - Fine Needle Aspiration Cytology, Ultrasound-Guided Core Biopsy, and Intraoperative Frozen Section. *Br J Oral Maxillofac Surg* (2015) 53:580–3. doi: 10.1016/j.bjoms.2015.03.015
14. Xu Y, Shu Z, Song G, Liu Y, Pang P, Wen X, et al. The Role of Preoperative Computed Tomography Radiomics in Distinguishing Benign and Malignant

Tumors of the Parotid Gland. *Front Oncol* (2021) 11:634452. doi: 10.3389/fonc.2021.634452
15. Jia CH, Wang SY, Li Q, Qiu JM, Kuai XP. Conventional, Diffusion, and Dynamic Contrast-Enhanced MRI Findings for Differentiating Metaplastic Warthin's Tumor of the Parotid Gland. *Sci Prog* (2021) 104:1–18. doi: 10.1177/00368504211018583
16. Yuan Y, Tang W, Tao X. Parotid Gland Lesions: Separate and Combined Diagnostic Value of Conventional MRI, Diffusion-Weighted Imaging and Dynamic Contrast-Enhanced MRI. *Br J Radiol* (2016) 89:20150912. doi: 10.1259/bjr.20150912
17. Munhoz L, Ramos EA dos A, Im DC, Hisatomi M, Yanagi Y, Asaumi J, et al. Application of Diffusion-Weighted Magnetic Resonance Imaging in the Diagnosis of Salivary Gland Diseases: A Systematic Review. *Oral Surg Oral Med Oral Pathol Oral Radiol* (2019) 128:280–310. doi: 10.1016/j.oooo.2019.02.020
18. Celebi I, Mahmutoglu AS, Ucgul A, Ulusay SM, Basak T, Basak M. Quantitative Diffusion-Weighted Magnetic Resonance Imaging in the Evaluation of Parotid Gland Masses: A Study With Histopathological Correlation. *Clin Imaging* (2013) 37:232–8. doi: 10.1016/j.clinimag.2012.04.025
19. Milad P, Elbegiermy M, Shokry T, mahmoud H, Kamal I, Taha MS, et al. The Added Value of Pretreatment DW MRI in Characterization of Salivary Glands Pathologies. *Am J Otolaryngol - Head Neck Med Surg* (2017) 38:13–20. doi: 10.1016/j.amjoto.2016.09.002
20. Elmokadem AH, Abdel Khalek AM, Abdel Wahab RM, Tharwat N, Gaballa GM, Elata MA, et al. Diagnostic Accuracy of Multiparametric Magnetic Resonance Imaging for Differentiation Between Parotid Neoplasms. *Can Assoc Radiol J* (2019) 70:264–72. doi: 10.1016/j.carj.2018.10.010
21. Zhang W, Zuo Z, Luo N, Liu L, Jin G, Liu J, et al. Non-Enhanced MRI in Combination With Color Doppler Flow Imaging for Improving Diagnostic Accuracy of Parotid Gland Lesions. *Eur Arch Oto-Rhino-Laryngol* (2018) 275:987–95. doi: 10.1007/s00405-018-4895-6
22. Matsushima N, Maeda M, Takamura M, Takeda K. Apparent Diffusion Coefficients Of Benign And Malignant Salivary Gland Tumors. Comparison to histopathological Findings. *J Neuroradiol* (2007) 34:183–9. doi: 10.1016/j.neurad.2007.04.002
23. Habermann CR, Arndt C, Graessner J, Diestel L, Petersen KU, Reitmeier F, et al. Diffusion-Weighted Echo-Planar MR Imaging of Primary Parotid Gland Tumors: Is a Prediction of Different Histologic Subtypes Possible? *Am J Neuroradiol* (2009) 30:591–6. doi: 10.3174/ajnr.A1412
24. Yerli H, Aydin E, Haberal N, Harman A, Kaskati T, Alibek S. Diagnosing Common Parotid Tumours With Magnetic Resonance Imaging Including Diffusion-Weighted Imaging vs Fine-Needle Aspiration Cytology: A Comparative Study. *Dentomaxillofac Radiol* (2010) 39:349–55. doi: 10.1259/dmfr/15047967
25. Bonello L, Preda L, Conte G, Giannitto C, Raimondi S, Ansarin M, et al. Squamous Cell Carcinoma of the Oral Cavity and Oropharynx: What Does the Apparent Diffusion Coefficient Tell Us About its Histology? *Acta Radiol* (2016) 57:1344–51. doi: 10.1177/0284185115587734
26. Liu Y, Zheng J, Zhao J, Yu L, Lu X, Zhu Z, et al. Magnetic Resonance Image Biomarkers Improve Differentiation of Benign and Malignant Parotid Tumors Through Diagnostic Model Analysis. *Oral Radiol* (2021) 37:658–68. doi: 10.1007/s11282-020-00504-4
27. Liu Y, Zheng J, Lu X, Wang Y, Meng F, Zhao J, et al. Radiomics-Based Comparison of MRI and CT for Differentiating Pleomorphic Adenomas and Warthin Tumors of the Parotid Gland: A Retrospective Study. *Oral Surg Oral Med Oral Pathol Oral Radiol* (2021) 131:591–9. doi: 10.1016/j.oooo.2021.01.014
28. Abdel Razek AAK, Gadelhak BN, El Zahabey IA, Elrazzak GAEA, Mowafey B. Diffusion-Weighted Imaging With Histogram Analysis of the Apparent Diffusion Coefficient Maps in the Diagnosis of Parotid Tumours. *Int J Oral Maxillofac Surg* (2021) 51:166–74. doi: 10.1016/j.ijom.2021.03.019
29. Piludu F, Marzi S, Ravanelli M, Pellini R, Covello R, Terrenato I, et al. Mri-Based Radiomics to Differentiate Between Benign and Malignant Parotid Tumors With External Validation. *Front Oncol* (2021) 11:656918. doi: 10.3389/fonc.2021.656918
30. Ma G, Zhu LN, Su GY, Hu H, Qian W, Bu SS, et al. Histogram Analysis of Apparent Diffusion Coefficient Maps for Differentiating Malignant From Benign Parotid Gland Tumors. *Eur Arch Oto-Rhino-Laryngol* (2018) 275:2151–7. doi: 10.1007/s00405-018-5052-y
31. Zhang Z, Song C, Zhang Y, Wen B, Zhu J, Cheng J. Apparent Diffusion Coefficient (ADC) Histogram Analysis: Differentiation of Benign From Malignant Parotid Gland Tumors Using Readout-Segmented Diffusion-Weighted Imaging. *Dentomaxillofac Radiol* (2019) 48:1–8. doi: 10.1259/dmfr.20190100
32. Wada T, Yokota H, Horikoshi T, Starkey J, Hattori S, Hashiba J, et al. Diagnostic Performance and Inter-Operator Variability of Apparent Diffusion Coefficient Analysis for Differentiating Pleomorphic Adenoma and Carcinoma Ex Pleomorphic Adenoma: Comparing One-Point Measurement and Whole-Tumor Measurement Including Radiomics. *Jpn J Radiol* (2020) 38:207–14. doi: 10.1007/s11604-019-00908-1
33. Yabuuchi H, Matsuo Y, Kamitani T, Setoguchi T, Okafuji T, Soeda H, et al. Parotid Gland Tumors: Can Addition of Diffusion-weighted Mr Imaging to Dynamic Contrast- Enhanced MR Imaging Improve Diagnostic Accuracy in Purpose. *Methods: Results: Conclusion* (2008) 249:909–16. doi: 10.1148/radiol.2493072045
34. Nardi C, Tomei M, Pietragalla M, Calistri L, Landini N, Bonomo P, et al. Texture Analysis in the Characterization of Parotid Salivary Gland Lesions: A Study on MR Diffusion Weighted Imaging. *Eur J Radiol* (2021) 136:109529. doi: 10.1016/j.ejrad.2021.109529
35. Sarioglu O, Sarioglu FC, Akdogan AI, Kucuk U, Arslan IB, Cukurova I, et al. MRI-Based Texture Analysis to Differentiate the Most Common Parotid Tumours. *Clin Radiol* (2020) 75:877.e15–e23. doi: 10.1016/j.crad.2020.06.018
36. Fruehwald-Pallamar J, Czerny C, Holzer-Fruehwald L, Nemec SF, Mueller-Mang C, Weber M, et al. Texture-Based and Diffusion-Weighted Discrimination of Parotid Gland Lesions on MR Images at 3.0 Tesla. *NMR BioMed* (2013) 26:1372–9. doi: 10.1002/nbm.2962
37. Chang YJ, Huang TY, Liu YJ, Chung HW, Juan CJ. Classification of Parotid Gland Tumors by Using Multimodal MRI and Deep Learning. *NMR BioMed* (2021) 34:1–9. doi: 10.1002/nbm.4408
38. Gabelloni M, Faggioni L, Attanasio S, Vani V, Goddi A, Colantonio S, et al. Can Magnetic Resonance Radiomics Analysis Discriminate Parotid Gland Tumors? A Pilot Study. *Diagnostics* (2020) 10:1–14. doi: 10.3390/diagnostics10110900
39. Zheng Ym, Li J, Liu S, Cui J, Zhan Jf, Pang J, et al. Mri-Based Radiomics Nomogram for Differentiation of Benign and Malignant Lesions of the Parotid Gland. *Eur Radiol* (2021) 31:4042–52. doi: 10.1007/s00330-020-07483-4
40. Xia X, Feng B, Wang J, Hua Q, Yang Y, Sheng L. Deep Learning for Differentiating Benign From Malignant Parotid Lesions on MR Images. *Front Oncol* (2021) 11:1–10. doi: 10.3389/fonc.2021.632104
41. Zheng YM, Chen J, Xu Q, Zhao WH, Wang XF, Yuan MG, et al. Development and Validation of an MRI-based Radiomics Nomogram for Distinguishing Warthin's Tumour From Pleomorphic Adenomas of the Parotid Gland. *Dentomaxillofac Radiol* (2021) 50:20210023. doi: 10.1259/dmfr.20210023
42. Vernuccio F, Arnone F, Cannella R, Verro B, Comelli A, Agnello F, et al. Diagnostic Performance of Qualitative and Radiomics Approach to Parotid Gland Tumors: Which is the Added Benefit of Texture Analysis ? *Br J Radiol* (2021) 94:20210340. doi: 10.1259/bjr.20210340
43. Matsuo H, Nishio M, Kanda T, Kojita Y, Kono AK, Hori M, et al. Diagnostic Accuracy of Deep-Learning With Anomaly Detection for a Small Amount of Imbalanced Data: Discriminating Malignant Parotid Tumors in MRI. *Sci Rep* (2020) 10:1–9. doi: 10.1038/s41598-020-76389-4
44. Ishibashi M, Fujii S, Kawamoto K, Nishihara K, Matsusue E, Kodani K, et al. Capsule of Parotid Gland Tumor: Evaluation by 3.0 T Magnetic Resonance Imaging Using Surface Coils. *Acta Radiol* (2010) 51:1103–10. doi: 10.3109/02841851.2010.519716
45. Ito FA, Jorge J, Vargas PA, Lopes MA. Histopathological Findings of Pleomorphic Adenomas of the Salivary Glands. (2009) 14:E57–61.
46. Zhang W, Zuo Z, Huang X, Jin G, Su D. Value of Diffusion-Weighted Imaging Combined With Susceptibility-Weighted Imaging in Differentiating Benign From Malignant Parotid Gland Lesions. *Med Sci Monit* (2018) 24:4610–6. doi: 10.12659/MSM.911185
47. Eida S, Sumi M, Sakihama N, Takahashi H, Nakamura T. Apparent Diffusion Coefficient Mappinq of Salivary Gland Tumors: Prediction of the Benignancy and Malignancy. *Am J Neuroradiol* (2007) 28:116–21.
48. Sagiv D, Witt RL, Glikson E, Mansour J, Shalmon B, Yakirevitch A, et al. Warthin Tumor Within the Superficial Lobe of the Parotid Gland: A

Suggested Criterion for Diagnosis. *Eur Arch Oto-Rhino-Laryngol* (2017) 274:1993–6. doi: 10.1007/s00405-016-4436-0

Conflict of Interest: Author HH was employed by Philips Healthcare.

The remaining authors declare that the research was conducted in the absence of any commercial or financial relationships that could be construed as a potential conflict of interest.

Publisher's Note: All claims expressed in this article are solely those of the authors and do not necessarily represent those of their affiliated organizations, or those of the publisher, the editors and the reviewers. Any product that may be evaluated in this article, or claim that may be made by its manufacturer, is not guaranteed or endorsed by the publisher.

frontiers | Frontiers in Oncology

ORIGINAL RESEARCH
published: 24 June 2022
doi: 10.3389/fonc.2022.792462

Postoperative Complications of Free Flap Reconstruction in Moderate-Advanced Head and Neck Squamous Cell Carcinoma: A Prospective Cohort Study Based on Real-World Data

Delong Li[1†], Chong Wang[1†], Wei Wei[2], Bo Li[1], Huan Liu[1], Aoming Cheng[1], Qifang Niu[1], Zhengxue Han[1] and Zhien Feng[1]*

[1] Department of Oral and Maxillofacial-Head and Neck Oncology, Beijing Stomatological Hospital, Capital Medical University, Beijing, China, [2] Clinical Epidemiology and EBM Unit, National Clinical Research Center for Digestive Diseases, Beijing Friendship Hospital, Capital Medical University, Beijing, China

Background: Postoperative complications (POCs) of moderate-advanced head and neck squamous cell carcinoma (HNSCC) after free flap reconstruction have received little attention. We investigated the risk factors that lead to POCs and their impact on management and prognosis.

Patients and Methods: A single-center, prospective cohort study was conducted at Beijing Stomatological Hospital on primary HNSCC patients treated between 2015 and 2020.

Results: In total, 399 consecutive HNSCC patients who underwent radical resection of the primary tumor and free flap reconstruction were enrolled in this study, 155(38.8%) experienced POCs. The occurrence of POCs directly led to worse short-term outcomes and poorer long-term overall survival (P=0.0056). Weight loss before the operation (P=0.097), Tumor site (P=0.002), stage T4b (P=0.016), an ACE-27 index of 2-3 (P=0.040), operation time≥8h (P=0.001) and Clindamycin as antibiotic prophylaxis (P=0.001) were significantly associated with POCs.

Conclusions: The occurrence of POCs significantly leads to worse short-term outcomes and increases the patients' burden.

Keywords: postoperative complications, head and neck cancer, free flap reconstruction, risk factors, prediction model

OPEN ACCESS

Edited by:
Markus Wirth,
Klinikum rechts der Isar, Germany

Reviewed by:
Richa Vaish,
Tata Memorial Hospital, India
Andreas Fichter,
Technical University of Munich, Germany
Samer Alkhudari,
Cleveland Clinic, United States

****Correspondence:***
Zhien Feng
jyfzhen@126.com

[†]These authors have contributed equally to this work and share first authorship

Specialty section:
This article was submitted to Head and Neck Cancer, a section of the journal Frontiers in Oncology

Received: *10 October 2021*
Accepted: *30 May 2022*
Published: *24 June 2022*

Citation:
Li D, Wang C, Wei W, Li B, Liu H, Cheng A, Niu Q, Han Z and Feng Z (2022) Postoperative Complications of Free Flap Reconstruction in Moderate-Advanced Head and Neck Squamous Cell Carcinoma: A Prospective Cohort Study Based on Real-World Data. Front. Oncol. 12:792462. doi: 10.3389/fonc.2022.792462

INTRODUCTION

The long-term survival of patients with moderate-advanced head and neck squamous cell carcinoma (HNSCC) has not improved significantly in the past 40 years (1). During this period, surgery has remained the most common and effective treatment for primary HNSCC (2). Radical resection for moderate-advanced HNSCC involves large-scale tumor resection and neck dissection (ND), and some procedures involve free flap reconstructions and tracheostomy (3, 4). Even if the defect is repaired and reconstructed intraoperatively, a decline or loss of important functions and aesthetics is common after a major operation (2, 5).

Postoperative complications (POCs) as the most important reason for surgical failure, not only increase the patient's health and economic burden, delay adjuvant treatment, and reduce short-term or long-term quality of life but also increase the risk of sequelae and a poor prognosis. Therefore, the prevention and management of surgical complications is becoming an issue that deserves more attention (6–8). It is important for HNSCC patients who undergo free flap reconstruction to obtain primary recovery without any POC, which may have a significant correlation with short-term outcomes and long-term survival (9, 10).

Many valuable works had been done about POCs of free-flap reconstruction for head and neck cancers, and reported rates of POCs ranged from 15% to 62% in published studies (10–15). Most of the literatures are retrospective study based on medical records or public database, while the occurrence and severity of complications were usually not defined or described so clearly (10–13). Despite many indexes, including the Frailty index (16), Kaplan-Feinstein score comorbidity index (17), Washington University Head and Neck Comorbidity Index (WUHNCI) (12), and Adult Comorbidity Evaluation-27 (ACE-27) (18), have been used to evaluate the preoperative status of populations with head and neck cancers and demonstrated to be related to increased risks of complications and decreased survival rates with increasing index scores, standardized methods for risk prediction developed specifically for POCs of HNSCC surgery with free flap reconstruction were still in need.

This prospective study was designed to investigate predictors of POCs occurring after HNSCC surgery with free flap reconstruction and their influence on survival in a real-world setting. Specifically, we sought to better characterize short-term and long-term outcomes after HNSCC surgery with free flap reconstruction and evaluate whether specific patient characteristics would be predictive of treatment effects, with the goal of providing useful guidance for clinical decision making.

PATIENTS AND METHODS

Datasets

The data used in this study originated from POROMS, a Prospective, Observational, Real-world Oral Malignant Tumors Study (ClinicalTrials.gov identifier: NCT02395367). Chinese patients with newly diagnosed and pathologically confirmed stage II-IV HNSCC (UICC/AJCC classification 8th edition) were treated in the Department of Oral and Maxillofacial-Head and Neck Oncology, Beijing Stomatological Hospital, Capital Medical University, between March 2015 and May 2020. This prospective study was carried out in accordance with ethical principles according to the World Medical Association Declaration of Helsinki (2002 version) and was approved by the Institutional Review Board of Beijing Stomatological Hospital.

Inclusion and Exclusion Criteria

To be included in this study, patients were required to fulfill the following criteria: (a) newly diagnosed HNSCC confirmed by pathology and no previous radiological or major surgical treatment; (b) a tumor located in the tongue, lower/upper gingiva, buccal mucosa, floor of the mouth, oropharynx or hard palate; (c) no evidence of distant metastasis; and (d) HNSCC with tumor stage II-IV according to UICC/AJCC classification 8th edition.

The exclusion criteria were as follows: (a) patients who had unresectable disease at the time of surgery; (b) patients who refused major surgical treatment due to personal will; and (c) patients who underwent operation without free flap reconstruction.

Goals and the Definition of Complications

The main goal of this study was to explore in-hospital complications and postoperative 42 days complications. POCs were defined as (a) postoperative respiratory or cardiac failure requiring critical care admission, (b) flap crisis, hematoma or any other complications requiring bedside treatment or reoperation, and (c) Surgical site infection (SSI) or pneumonia defined by the individual investigator or confirmed by bacterial cultivation. The length of hospital stay after the operation and total cost of hospital care were measured according to baseline records.

The Clavien-Dindo classification (CDC) is a widely accepted grading system based on an ordinal scale and demonstrated reliability for precisely classifying the severity of POCs (19). POCs were graded by the CDC system to classify severity: a minor complication was defined as grade I or II, while a severe complication was defined as grade III, IV or V (20) including death, life-threatening complications requiring Intensive Care/ Intensive Care Unit (IC/ICU) management or complications requiring surgical, endoscopic or radiological intervention. The highest grade of POCs were recoded as the CDC grade of patients.

Outcomes

The short-term outcomes included POCs, length of hospital stay after the operation and total cost of hospital care. The long-term outcomes were overall survival (OS) and disease-free survival (DFS). OS was calculated as the length of time from the first operation to all-cause death or the last follow-up. DFS was defined as the length of time from the first operation until first recurrence, metastasis, or death. One-year and 2-year postoperative all-cause mortality were compiled with complete follow-up data.

COVARIATES

Demographic factors (age, sex, Body Mass Index (BMI) and weight loss), tumor anatomy and pathological features (tumor site, T stage, pathological nodal [pN] stage, clinical features, and

growth patterns) and operation-related variables (operation time, blood loss, intraoperative fluid, tracheostomy[yes/no], type of flaps used, ND (unilateral/bilateral), type of antibiotic prophylaxis and red blood cell (RBC) transfusion during the operation[yes/no]) were recorded. Based on World Health Organization (WHO) cutoff points of BMI status, BMI were categorized into obese (≥30.0 kg/m^2), overweight (25.0–29.9 kg/m^2), normal weight (18.5–24.9 kg/m^2), and underweight (<18.5 kg/m^2) (14). Weight loss was defined as "weight loss >10% of the body weight within the past 6 months (21). Preoperative comorbidities (ACE-27 comorbidity index, hypertension, and diabetes) and habitual factors (smoking and alcohol histories) were collected and recorded through a person-to-person survey before surgery.

Statistical Analyses

Baseline data are summarized as descriptive statistics. Categorical variables are presented as frequencies and percentages, and continuous variables are presented as the means ± standard deviations or medians (P25, P75). Univariate and multivariate logistic regression analyses were applied to explore risk factors for POCs and to build a forest plot. The odds ratios (ORs) with their 95% confidence intervals (CIs) and two-tailed P values are reported. A prediction model that included all candidate predictors selected from the multivariate logistic regression analysis was built, and the results are presented as a nomogram. The concordance index (C-index) was used to determine discrimination ability of the nomogram. The area under the receiver operating characteristic curve (AUC) and ROC curve analysis were used to measure the difference between the predicted and observed outcomes. A calibration curve was adopted to compare the observed and predicted outcomes for the nomogram. Decision curve analysis (DCA) was used to test the predictive value of the model.

The survival curves were plotted by the Kaplan–Meier method to depict the associations of each group and the main outcome indexes, OS and DFS. Log-rank tests were used to compare survival outcomes between different groups. The Cox proportional hazards regression model was used to assess the impacts of prognostic factors on DFS and OS. All tests were two-sided, and P values <0.05 were considered statistically significant.

The data were analyzed with SPSS (version 17) and R software (version 4.0.4; https://www.R-project.org). The packages used included rms, pROC, rmda, forestplot, survival and survminer.

RESULTS

Patient Characteristics

A total of 399 patients met the inclusion criteria: 250(62.7%) men and 149(37.3%) women. The mean patient age was 58.0 ± 10.7years. Of 399 patients, 155(38.8%) had complications in the perioperative period (from the day of the operation to 42 days after the operation). The results of the univariate logistic regression analysis showed that patients who experienced weight loss before the operation (P=0.021, OR 1.753, 95% [CI] 1.089-2.822) and those with a smoking history (P=0.009, OR 1.715, 95% [CI] 1.142-2.576), alcohol history (P=0.047, OR 1.509, 95% [CI] 1.006-2.264), ACE-27 index of 2-3(P=0.008, OR 2.446, 95% [CI] 1.268-4.721) and diabetes (P=0.047, OR 1.313, 95% [CI] 1.003-1.718) had a significantly higher risk of postoperative complications (**Table 1**).

The most common primary tumor site was the tongue (153, 38.3%), followed by the inferior gingiva (76, 19.0%). According to postoperative pathological reports, the T stage was distributed as follows: T2 (n=103, 25.8%), T3 (n=99, 24.8%), T4a (n=171, 42.9%), and T4b (n=26, 6.5%); the lymph node status was distributed as follows: pN0 in 218(54.4%) patients, pN2 in 89 (22.3%), pN1 in 68 (17.0%), and pN3 in 25(6.3%). Tumor location in the non-upper gingiva and non-hard palate (Abbreviated as non-upper gingiva/hard palate) (P=0.001, OR 4.857, 95% [CI] 1.856-12.709) and T4b stage (P=0.006, OR 3.217, 95% [CI] 1.396-7.413) were significantly associated with POCs (**Table 1**).

The mean operation time and blood loss were 7.29 ± 1.44h and 611.02 ± 187.47ml in the POC (-) group and 8.00 ± 1.44h and 665.58 ± 230.27ml in the POC (+) group, with significant differences. Most patients received anterolateral thigh flaps (155, 38.8%), followed by radial forearm flaps (126, 31.6%), fibula flaps (106, 26.6%) and latissimus dorsi flaps (12, 3.0%). Cephalosporin was used to treat antibiotic prophylaxis in 376 patients, while clindamycin was used in the other 23 patients due to an allergy to cephalosporin. A total of 340 (85.2%) patients underwent unilateral ND, 50 (12.3%) underwent bilateral ND, and 9 (2.3%) did not undergo ND. In total, 271 (67.9%) patients underwent tracheostomy, and 18 (6.6%) of them had infectious pneumonia, significantly higher than those without tracheostomy (2/128, 1.6%) (P=0.028). Ninety-three (23.3%) patients received an RBC transfusion during the operation. An operation time≥8.0h (P=0.001, OR 2.584, 95% [CI] 1.706-3.915), blood loss>500 ml (P=0.034, OR 1.573, 95% [CI] 1.035-2.390), Clindamycin as antibiotic prophylaxis (vs. cephalosporin) (P=0.003, OR 3.897, 95% [CI] 1.565-9.707), bilateral ND (vs. unilateral or no ND) (P=0.043, OR 1.848, 95% [CI] 1.018-3.353) and tracheostomy (P=0.033, OR 1.622, 95% [CI] 1.040-2.530) were associated with an increased risk of POCs in univariate analysis (**Table 2**).

Distributions of POCs and CDC Grades of Patients

The most common type of POC was SSI (95, 61.3%), followed by flap crisis or failure (37, 23.9%), pneumonia (20, 12.9%), hematoma (10, 6.4%), congestive heart failure (9, 5.8%), Acute Respiratory Distress Syndrome (ARDS) (6, 3.9%), Fistula (5, 3.2%), Cardio-discomfort (5, 3.2%), Pulmonary embolism (4, 2.6%), Airway-condition needs tracheotomy (4, 2.6%) and some other types.

Of all 155 patients with POCs, 88 (56.8%) patients were graded I or II in CDC, while 67 (43.2%) patients were graded III-V (**Supplemental Table 1**).

Short-Term Outcomes

The median length of hospital stay after the operation in POC (+) patients was 14.00 (10.00, 21.00) days, which was significantly

TABLE 1 | The univariate analysis between demographic and clinicopathological factors and POCs.

	Totaln = 399		POC (-) n = 244 (61.2%)	POC (+) n = 155 (38.8%)	P	OR (95% CI)
	No.	%	No. (%)	No. (%)		
Age					0.346	
>60	192	48.1	122 (50.0)	70 (45.2)		Ref.
≤60	207	51.9	122 (50.0)	85 (54.8)		1.214 (0.811-1.818)
Gender					0.300	
Male	250	62.7	148 (60.7)	102 (65.8)		Ref.
Female	149	37.3	96 (39.3)	53 (34.2)		0.801 (0.527-1.219)
BMI					0.807	
Underweight	9	2.2	6 (2.5)	3 (1.9)		Ref.
Normal	217	54.4	129 (52.9)	88 (56.8)		1.364 (0.332-5.600)
Overweight	152	38.1	97 (39.7)	55 (35.5)		1.134 (0.273-4.714)
Obese	21	5.3	12 (4.9)	9 (5.8)		1.500 (0.293-7.681)
Weight loss					0.021	
Absent	310	77.7	199 (81.6)	111 (71.6)		Ref.
Present	89	22.3	45 (18.4)	44 (28.4)		1.753 (1.089-2.822)
Smoking history					0.009	
Nonsmoker	200	50.4	135 (55.3)	65 (41.9)		Ref.
Smoker	199	49.6	109 (44.7)	90 (58.1)		1.715 (1.142-2.576)
Alcohol history					0.047	
Nondrinker	223	55.9	146 (59.8)	77 (49.7)		Ref.
Drinker	176	44.1	98 (40.2)	78 (50.3)		1.509 (1.006-2.264)
ACE-27					0.008	
0-1	358	89.6	227 (93.0)	131 (84.5)		Ref.
2-3	41	10.4	17 (7.0)	24 (15.5)		2.446 (1.268-4.721)
Hypertension					0.071	
Absent	251	62.9	162 (66.4)	89 (57.4)		Ref.
Present	148	37.1	82 (33.6)	66 (42.6)		1.465 (0.968-2.218)
Diabetes					0.047	
Absent	335	84.0	212 (86.9)	123 (79.4)		Ref.
Present	64	16.0	32 (13.1)	32 (20.6)		1.313 (1.003-1.718)
Tumor Sites					0.001	
Upper Gingiva	30	7.5	27 (11.1)	3 (1.9)		Ref.
Hard palate	9	2.3	7 (2.9)	2 (1.3)		
Tongue	153	38.3	97 (39.7)	56 (36.1)		4.857 (1.856-12.709)
Inferior gingiva	76	19.0	43 (17.6)	33 (21.3)		
Buccal Mucosa	73	18.3	39 (16.0)	34 (22.0)		
Floor of the mouth	43	10.8	21 (8.6)	22 (14.2)		
Oropharynx	15	3.8	10 (4.1)	5 (3.2)		
Growth Patterns					0.573	
Exophytic	99	24.8	64 (26.2)	35 (22.6)		Ref.
Ulcerative	153	38.3	89 (36.5)	64 (41.3)		1.315 (0.780-2.217)
Invasive	147	36.9	91 (37.3)	56 (36.1)		1.125 (0.663-1.911)
Clinical Stage					0.117	
II	87	21.8	61 (25.0)	26 (16.8)		Ref.
III	72	18.0	45 (18.4)	27 (17.4)		1.408 (0.726-2.729)
IV	240	60.2	138 (56.6)	102 (65.8)		1.734 (1.025-2.933)
T stage					0.006	
T2	103	25.8	65 (26.6)	38 (24.5)		Ref.
T3	99	24.8	65 (26.6)	34 (21.9)		
T4a	171	42.9	105 (43.0)	66 (42.6)		
T4b	26	6.5	9 (3.8)	17 (11.0)		3.217 (1.396-7.413)
pN stage					0.441	
N0	218	54.6	141 (57.8)	77 (49.7)		Ref.
pN1	68	17.1	38 (15.6)	30 (19.3)		1.446 (0.831-2.514)
pN2	89	22.3	52 (21.3)	37 (23.9)		1.303 (0.786-2.159)
pN3	24	6.0	13 (5.3)	11 (7.1)		1.549 (0.663-3.624)

POC, Postoperative complication.
BMI, body mass index.
ACE-27, Adult Comorbidity Evaluation-27 comorbidity index.

TABLE 2 | The univariate analysis between operation-related factors and POCs.

	Total n = 399		POC (-) n = 244 (61.2%)	POC (+) n = 155 (38.8%)	P	OR (95% CI)
	No.	%	No. (%)	No. (%)		
Operation time					0.001	
<8.0h	236	59.1	166 (68.0)	70 (45.2)		Ref.
≥8.0h	163	40.9	78 (32.0)	85 (54.8)		2.584 (1.706-3.915)
Blood loss					0.034	
0-500ml	160	40.1	108 (44.3)	52 (33.5)		Ref.
>500ml	239	59.9	136 (55.7)	103 (66.5)		1.573 (1.035-2.390)
Neck dissection					0.043	
None	9	2.3	7 (2.9)	2 (1.3)		Ref.
Unilateral	340	85.2	213 (87.3)	127 (81.9)		
Bilateral	50	12.5	24 (9.8)	26 (16.8)		1.848 (1.018-3.353)
Tracheostomy					0.033	
Absent	128	32.1	88 (36.1)	40 (25.8)		Ref.
Present	271	67.9	156 (63.9)	115 (74.2)		1.622 (1.040-2.530)
Flap Reconstruction					0.288	
Fibula flap	106	26.6	57 (23.4)	49 (31.6)		Ref.
Radial forearm flap	126	31.6	83 (34.0)	43 (27.8)		0.603 (0.355-1.024)
Anterolateral thigh flap	155	38.8	97 (39.7)	58 (37.4)		0.696 (0.421-1.149)
Latissimus dorsi flap	12	3.0	7 (2.9)	5 (3.2)		0.831 (0.248-2.785)
Antibiotic Prophylaxis					0.003	
Cephalosporin	376	94.2	237 (97.1)	139 (89.7)		Ref.
Clindamycin	23	5.8	7 (2.9)	16 (10.3)		3.897 (1.565-9.707)
Intraoperative Fluid					0.247	
<6000	318	79.7	199 (81.6)	119 (76.8)		Ref.
≥6000	81	20.3	45 (18.4)	36 (23.2)		1.338 (0.817-2.192)
RBC transfusion during operation					0.057	
No	306	76.7	195 (79.9)	111 (71.6)		Ref.
Yes	93	23.3	49 (20.1)	44 (28.4)		1.057 (0.987-2.522)

POC, Postoperative complication.
RBC, Red blood cell.

longer than that in POC (-) patients 9.00 (8.00, 11.75) days. The median healthcare cost in the POC (+) group was $6484.10 (5486.80,8162.90), whereas that in the POC (-) group was $5947.11 (4862.65,7081.87). A total of 137 (34.3%) patients received a transfusion while in the hospital. In total, 41.3% of patients in the POC (+) group received a transfusion, and 29.9% in the POC (-) group received a transfusion (**Table 3**).

Multivariate Logistic Regression Analysis of POCs

Multivariate logistic regression analysis on POCs showed that the independent risk factors were as follows: weight loss (P=0.097, OR 1.551, 95% [CI] 0.923-2.608), ACE-27 index:2-3 (vs. 0-1, P=0.040, OR 2.091, 95% [CI] 1.035-4.266), T4b stage (vs. T2-T4a, P=0.016, OR 3.184, 95% [CI] 1.244-8.151), tumor in the

TABLE 3 | The association between post-operation complication and major short outcomes.

	Total n = 399	POC (-) n = 244 (61.2%)	POC (+) n = 155 (38.8%)	P
Cost	$6185.12 (5033.32,7527.23)	$5947.11 (4862.65,7081.87)	$6484.10 (5486.80,8162.90)	0.001
Length of hospital stay after operation (days)	10.00 (8.05,14.00)	9.00 (8.00,11.75)	14.00 (10.00,21.00)	0.001
RBC Transfusion				0.020
Absent	262 (65.7)	171 (70.1)	91 (58.7)	
Present	137 (34.3)	73 (29.9)	64 (41.3)	
1-year overall survival		93.6%	86.0%	0.015
Survive	327 (90.6)	204	123	
Death	34 (9.4)	14	20	
N/A	38	27	11	
2-year overall survival		84.5%	72.9%	0.024
Survive	217 (79.5)	131	86	
Death	56 (20.5)	24	32	
N/A	126	90	36	

POC, Postoperative complication.
RBC, Red blood cell.

non-upper gingiva/hard palate (P=0.002, OR 4.783, 95% [CI] 1.745-13.113), operation time≥8h (P=0.001, OR 2.333, 95% [CI] 1.501-3.628), and Clindamycin as antibiotic prophylaxis (vs. cephalosporin, P=0.001, OR 5.432, 95% [CI] 2.013-14.663). The forest plot was built with the six variables (**Figure 1**).

Development of a Novel Nomogram Prediction Model of POCs

A nomogram that incorporated the six significant risk factors for predicting POCs was constructed (**Figure 2A**). The total score was calculated using the scores of the ACE-27 index, weight loss, tumor site, T stage, operation time and type of antibiotic prophylaxis.

The predictive nomogram achieved a C-index of 0.703, suggesting that the model has moderate discrimination ability. The calibration curve of the nomogram to predict POC risk after HNSCC surgery with free flap reconstruction demonstrated good consistency in this cohort (**Figure 2B**). The accuracies of the risk models were also compared using ROC curve analysis (AUC=0.703, **Figure 2C**).

DCA was used to determine whether the prediction model-based decisions were more clinically useful than default decisions for patients after surgery. The graph in **Figure 2D** shows the expected net benefit per patient to predict the risk of a POC when the nomogram score threshold was between 0.2-0.8 (red curve).

Survival Analyses

Among the 399 patients in this study, 394(98.7%) had follow-up data. The 1-year survival rates were 86.0% in the POC (+) group and 93.6% in the POC (-) group, and the 2-year survival rates were 72.9% and 84.5%, both with a significant difference.

Kaplan–Meier analysis revealed significant associations between POCs and OS (P<0.01, **Figure 3A**), and patients in the POC (-) group had a higher OS rate than those in the POC (+) group. No significant associations between POCs and DFS were observed (P=0.190, **Figure 3B**). We also found no significant difference in OS (P=0.841) or DFS (P=0.270) between patients with severe POCs and patients with minor POCs.

Among all the potential prognostic factors, T stage, N stage, hypertension, weight loss before the operation, operation time≥8.0h, RBC transfusion and POCs were all risk factors for OS (P<0.05) (**Table 4**). However, the association between POCs and OS was not significant after adjusting for other prognostic factors (P=0.128). Weight loss, N stage and RBC transfusion remained significant risk factors for OS (P<0.05). No operation-related factors were associated with a poor prognosis in the multivariate analysis of OS.

DISCUSSION

The early postoperative period is a vulnerable time for HNSCC patients who have undergone a major operation with free flaps, as the risk of complications is increased. Reducing complications has become a major target for improving the quality of patient care and healthcare cost savings. A comprehensive analysis of the rates and types of complications is essential to develop appropriate interventions to reduce them.

Immediate flap reconstruction is generally associated with fewer POCs, a shorter hospital stay, reduced treatment costs and more favorable aesthetic and functional outcomes than cancer resection without flap reconstruction (22). However, reconstructive surgery using a microvascular free flap is also considered to be a great challenge, as it may lead to a longer operation time and more blood loss, both of which have been demonstrated to be associated with a high incidence of POCs (23, 24). Therefore, the significance of free flap reconstruction in the prognosis and occurrence of complications in HNSCC patients is complicated (25).

In the current study, we first developed a novel tool to predict the risk of POCs after HNSCC surgery with free flap reconstruction based on a prospective cohort with real-world data. Six parameters that may objectively reflect the risk of POCs were evaluated: preoperative factors (ACE-27 index and weight loss), tumor characteristics (T stage and tumor site) and

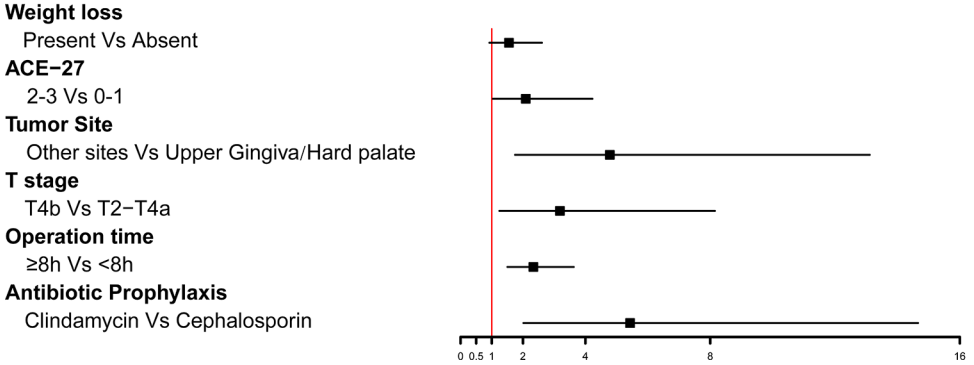

FIGURE 1 | Multivariable logistic regression analysis was applied to build forest plots.

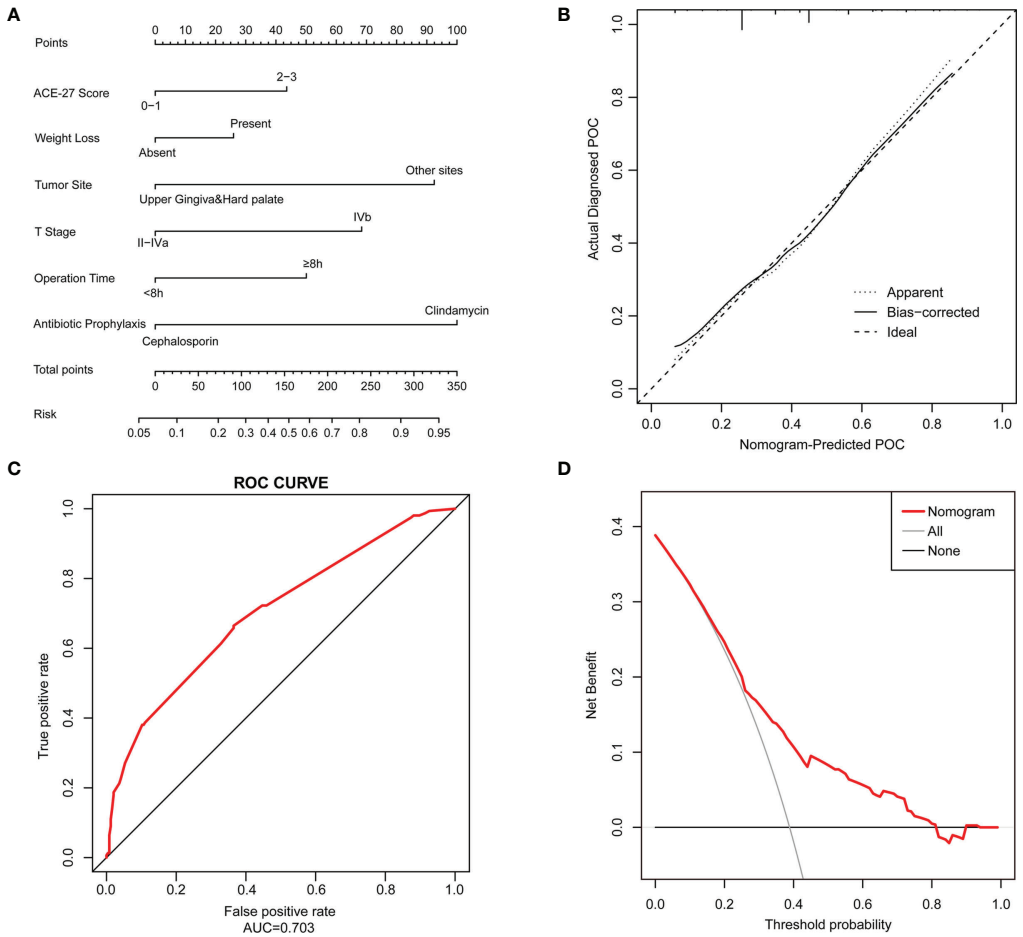

FIGURE 2 | A Nomogram model is constructed to predict the POCs. **(A)** The POC risk nomogram was developed by incorporating the following factors: ACE-27 index, weight loss, tumor site, T stage of the tumor, operation time and type of antibiotic prophylaxis; **(B)** Calibration plots of the nomogram which the y-axis is the actual rate of POCs and the x-axis is the predicted rate of POCs. The diagonal dotted line represents a perfect prediction by an ideal model. The solid line represents the bias-corrected performance of the nomogram, where a closer fit to the diagonal dotted line represents a better prediction; **(C)** The accuracy of the model for identifying patients with POCs was determined using AUC curve; **(D)** DCA showed the clinical usefulness of the nomogram. The y-axis measures the net benefit. The red solid line is the nomogram used to predict POC risk. The gray solid line assumes that all patients will develop a POC. The thin black solid line assumes that no patients will develop a POC.

perioperative factors (operation time and antibiotic prophylaxis). According to the validation, the predictive ability of our nomogram is reliable, and it can be widely used to predict POCs. However, considering that the limited number of patients may have influenced the veracity of our model, the nomogram was not externally validated.

Infective complications, including SSI and pneumonia, were the main types of POCs in HNSCC patients who underwent free flap reconstruction in this study. The probability of severe respiratory and circulatory complications is not high, which may have been due to strict preoperative preparation. While hair removal, antibiotic prophylaxis, the avoidance of hypothermia and perioperative glycemic control have been widely adopted to reduce infection-related complications (26), apart from a long surgery time and increased blood loss, ND and primary tumor site, which increase the risk of wound exposure to a microbacterial environment, can be high-level risk factors for SSI (27).

An increased risk of wound infections with flap reconstruction has been demonstrated (28, 29). Most clinicians agree that antibiotic prophylaxis is the most effective means to prevent infective complications (28, 30). According to American Society of Health-System Pharmacists (ASHP) guidelines (29, 31), cefazolin or cefuroxime with metronidazole, or ampicillin-sulbactam are recommended for oncological clean-contaminated head and neck surgery. The guidelines also suggest the use of clindamycin in patients with a beta-lactam allergy (29, 31). However, clindamycin may cause a 2-3 times higher risk of infective complications than beta-lactam in clean-contaminated head and neck cases (30, 32) and it was reported that no significant difference was observed between clindamycin and no antibiotic (33). Our study also demonstrated that

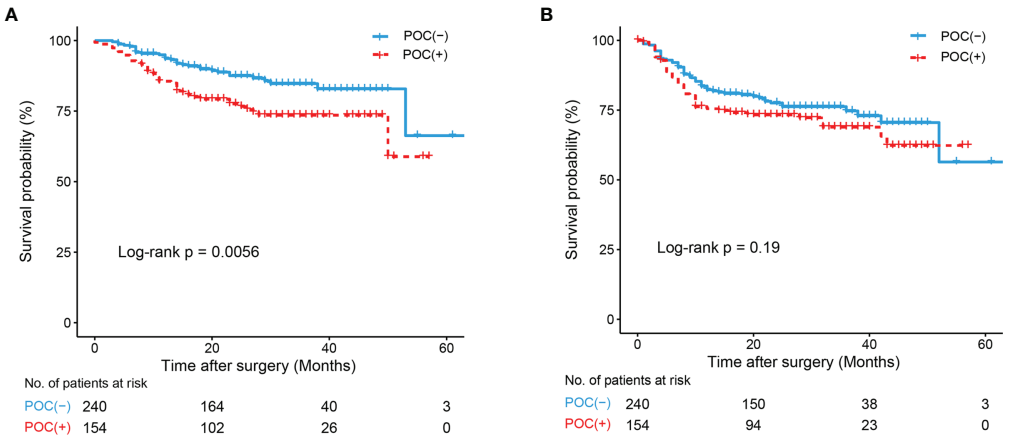

FIGURE 3 | K-M curve drawn by occurrence of POCs and Overall survival (OS) and Disease-Free Survival (DFS) of all patients. **(A)** K-M curve of POCs and OS; **(B)** K-M curve of POCs and DFS.

prophylactic clindamycin led to a substantially higher risk of POCs than cephalosporin, suggesting that clindamycin is not sufficient and a broader antibiotic is needed.

An ever-expanding complex oncological surgery with free flap reconstruction often means a higher risk of massive intraoperative or postoperative hemorrhage, which may require a blood transfusion and lead to subsequent complications. Hemoglobin (Hb) was a critical indicator and the value below 7 g/dl was considered as a threshold for blood transfusion in head and neck surgical oncology according to guidelines (34), which was also accepted and used in our department. Moreover, the literature has demonstrated that blood transfusion may be considered as an important indicator for adverse short-term outcomes in patients undergoing oncological surgery (34, 35) and it was reported an almost 30% higher five-year overall survival rate of non-transfused OSCC patients than patients with transfusion (36). In this study, we found that 34.3% of patients required an RBC transfusion during the hospital stay, with a higher rate in the POC (+) group than in the POC (-) group. The univariate analysis also showed that patients who received a transfusion during surgery had a higher risk of POCs. Transfusion was also demonstrated to be a risk factor for long-term OS in the univariate and multivariate Cox regression analyses. Transfusion should be considered an important short-term outcome and a remarkable risk factor for long-term survival.

As maximum cytoreduction has been considered the ideal treatment for advanced HNSCC for decades, aggressive removal of the tumor to the greatest extent possible to improve survival is chosen by most oral and maxillofacial surgeons (37). Tumor characteristics are the main limitation of surgery for cancer patients (38). In our study, we found that not only long-term survival but also POC occurrence was highly associated with advanced T stage and N stage. A stage T4b tumor invades many important surrounding anatomical structures, such as the pterygoid plates, skull base or internal carotid artery, making complete excision of the tumor and hemostasis difficult and leading to a higher risk of POCs such as hematoma. A wide range of tumor resection may also result in surgical dead space and postoperative infections (26). Tumors in an advanced pN stage have extensive lymphatic metastasis or extranodal extension. Both of these are strongly associated with a poor prognosis.

A poor preoperative nutritional status in surgically treated patients may be an important factor affecting surgical tolerance and increasing the risk of complications (39, 40). Preoperative weight loss and BMI often reflect the nutritional status of patients. Preoperative weight loss may be more common in oral cancer (located at the beginning of the digestive tract) than in cancers at other locations because eating function is affected. In this study, preoperative weight loss occurred in 22.3% of patients, and it was identified as an important risk factor for POC occurrence and long-term survival. Preventing a decline in the nutritional status prior to surgery could be a means to reduce these negative consequences. In another study, our team found that the incidence of complications after OSCC surgery was highest (33.3%) in the low BMI group, but no significant relationship between BMI and POCs was demonstrated in this study (14). This may be due to the stricter screening procedure before free flap reconstruction for patients enrolled in this study.

A comorbidity assessment may be a crucial predictive factor for complications (41). The ACE-27 comorbidity index is a widely accepted comorbidity evaluation system for oncology patients. The ACE-27 index consists of 12 categories and 27 subcategories, each of which quantifies a specific disease within the circulatory, respiratory, digestive or nervous system and its severity (42). The index has been proven to be a validated, relevant scoring system for patients undergoing surgery for HNSCC (43, 44). Our study showed that an ACE-27 score>1 was significantly related to complications, which means that 2 or more comorbidities or a severe comorbidity can be a high-risk factor for poor short-term outcomes but not for long-term outcomes. Thus, the ACE-27 index can be useful when

TABLE 4 | Univariate & Multivariate Cox regression of risk factors for OS in all patients with HNSCC with free flap reconstruction.

	Univariate Cox regressionHR (95% CI)	P	Multivariate Cox regressionHR (95% CI)	P
Age		0.450		
>60	Ref.			
≤60	0.828 (0.507-1.352)			
Gender		0.732		
Male	Ref.			
Female	0.915 (0.549-1.524)			
BMI		0.333		
Underweight	Ref.			
Normal weight	1.184 (0.276-5.085)			
Overweight	0.890 (0.200-3.954)			
Obese	0.238 (0.021-2.610)			
Weight loss		0.001		0.001
Absent	Ref.		Ref.	
Present	3.899 (2.383-6.379)		3.255 (1.873-5.656)	
Smoking history		0.900		
Nonsmoker	Ref.			
Smoker	0.969 (0.594-1.582)			
Alcohol history		0.840		
Nondrinker	Ref.			
Drinker	0.950 (0.580-1.558)			
ACE-27		0.133		0.989
0-1	Ref.		Ref.	
2-3	1.648 (0.859-3.161)		0.995 (0.470-2.107)	
Hypertension		0.029		0.081
Absent	Ref.		Ref.	
Present	1.731 (1.059-2.828)		1.673 (0.938-2.984)	
Diabetes		0.149		0.669
Absent	Ref.		Ref.	
Present	1. 546 (0.855-2.797)		1.075 (0.771-1.499)	
Tumor Site		0.395		
Tongue	Ref.			
Inferior gingiva	1.274 (0.651-2.496)			
Buccal Mucosa	1.280 (0.647-2.532)			
Floor of the mouth	0.494 (0.147-1.663)			
Oropharynx	2.536 (0.951-6.760)			
Upper gingiva	1.300 (0.487-3.466)			
Hard palate	0.685 (0.092-5.110)			
Growth Patterns		0.731		
Exophytic	Ref.			
Ulcerative	1.216 (0.621-2.381)			
Invasive	1.309 (0.671-2.555)			
Clinical Stage		0.001		0.219
II	Ref.		Ref.	
III	0.695 (0.166-2.908)		0.232 (0.043-1.237)	
IV	4.600 (1.842-11.488)		0.555 (0.129-2.387)	
T stage		0.001		0.264
T2	Ref.		Ref.	
T3	1.811 (0.702-4.672)		1.968 (0.642-6.029)	
T4a	3.413 (1.515-7.690)		1.973 (0.630-6.182)	
T4b	6.434 (2.473-16.744)		3.629 (0.966-13.634)	
pN stage		0.001		0.001
N0	Ref.		Ref.	
N1	1.946 (0.891-4.253)		2.939 (1.162-7.433)	
N2	4.641 (2.506-8.596)		4.977 (2.230-11.105)	
N3	11.315 (5.258-24.350)		12.975 (4.907-34.311)	
Operation time		0.001		0.702
<8h	Ref.		Ref.	
≥8h	2.274 (1.373-3.766)		0.957 (0.762-1.201)	
Blood loss		0.098		0.448
0-500ml	Ref.		Ref.	
>500ml	1.573 (0.920-2.691)		0.764 (0.381-1.530)	
Neck resection		0.096		0.837
Unilateral	Ref.		Ref.	

(Continued)

TABLE 4 | Continued

	Univariate Cox regressionHR (95% CI)	P	Multivariate Cox regressionHR (95% CI)	P
Bilateral	1.711 (0.910-3.219)		0.914 (0.385-2.166)	
Tracheostomy		0.628		
Absent	Ref.			
Present	0.882 (0.529-1.468)			
Flap Reconstruction		0.158		
Fibula flap	Ref.			
Radial forearm flap	0.900 (0.464-1.747)			
Anterolateral thigh flap	1.185 (0.639-2.200)			
Latissimus dorsi flap	3.099 (1.028-9.340)			
Intraoperative Fluid		0.230		
<6000	Ref.			
≥6000	1.415 (0.803-2.493)			
RBC Transfusion		0.002		0.038
Absent	Ref.		Ref.	
Present	2.198 (1.345-3.592)		1.846 (1.033-3.298)	
POC		0.016		0.128
Negative	Ref.		Ref.	
Positive	1.944 (1.188-3.181)		1.519 (0.869-2.656)	

POC, Postoperative complication.
RBC, Red blood cell.
Ref., Reference group.
ACE-27, Adult Comorbidity Evaluation-27 comorbidity index.

deciding which treatment option is more suitable for advanced-stage HNSCC patients.

It is well known that a prolonged operative time is often accompanied by a prolonged anesthesia time and more blood loss and may lead to many adverse events (45), such as SSI, wound disruption, reoperation or transfusion. A prolonged operative time was demonstrated to be associated with an increased risk of POCs in our studies. A long operation time increases wound exposure and decreases the effects of sterilization and antibacterial measures. It is generally believed that the operation time is closely related to the surgeon's experience, the type of reconstruction, and a good preoperative design. Tracheostomy is a useful method to prevent asphyxia caused by airway obstruction after surgery. Direct exposure of the respiratory tract caused by tracheostomy may result in contamination, leading to adverse events such as pulmonary infection, which was demonstrated in our study. Tracheostomy tends to be used during tongue, floor of mouth or mandible resection, indicating a high risk of POCs.

Several limitations to this study need to be considered. Complications after complex surgery can never be completely eliminated and may have consequences that extend well beyond the postoperative period (38). Although based on a prospective real-world study, our study is still a single-center observational study with a limited sample size. However, the lost to follow-up rate of the research is very low, and the quality of prospective data can be well guaranteed. The avoidance of POCs remains a worthwhile goal, and further work is still needed to understand their occurrence. A multicenter prospective study with a large sample size may provide useful guidance for clinical decision making.

CONCLUSION

The occurrence of POCs significantly increases the burden on patients and leads to poor long-term OS. More attention should be paid on operation time and blood loss. Measures should be taken to prevent weight loss before operation to reduce the risk of POCs. An antibiotic with a broader spectrum is better than clindamycin to prevent POCs.

DATA AVAILABILITY STATEMENT

The original contributions presented in the study are included in the article/**Supplementary Material**. Further inquiries can be directed to the corresponding author.

ETHICS STATEMENT

The studies involving human participants were reviewed and approved by Institutional Review Board of Beijing Stomatological Hospital. The patients/participants provided their written informed consent to participate in this study.

AUTHOR CONTRIBUTIONS

DL: Project administration, validation, writing-original draft, interpretation of data. CW: Data analysis, writing-original draft,

interpretation of data. BL: Validation, writing-original draft, interpretation of data. WW: Design of the work, interpretation of data, revising it critically for the intellectual content. HL, AC, QN: Resources, writing-original draft, interpretation of data. ZH: Supervision, writing-review & editing, resources. ZF: Funding acquisition, project administration, supervision, writing-original draft, interpretation of data. All authors contributed to the article and approved the final version.

FUNDING

This article is supported by the Capital's Funds for Health Improvement and Research (CFH2020-2-2143 and 2018-4-2082); the National Natural Science Foundation of China (82072984); the Project of Beijing Municipal Education Commission (KM202110025008); the Beijing Science and Technology Commission (Z161100000516201); the Discipline Construction Fund of Beijing Stomatological Hospital (18-09-21); and innovation Research Team Project of Beijing Stomatological Hospital, Capital Medical University, NO. CXTD202204.

SUPPLEMENTARY MATERIAL

The Supplementary Material for this article can be found online at: https://www.frontiersin.org/articles/10.3389/fonc.2022.792462/full#supplementary-material

REFERENCES

1. Chow LQM. Head and Neck Cancer. *N Engl J Med* (2020) 382:60–72. doi: 10.1056/NEJMra1715715
2. Cramer JD, Burtness B, Le QT, Ferris RL. The Changing Therapeutic Landscape of Head and Neck Cancer. *Nat Rev Clin Oncol* (2019) 16:669–83. doi: 10.1038/s41571-019-0227-z
3. Pfister DG, Spencer S, Adelstein D, Adkins D, Anzai Y, Brizel DM, et al. Head and Neck Cancers, Version 2.2020, NCCN Clinical Practice Guidelines in Oncology. *J Natl Compr Canc Netw* (2020) 18:873–98. doi: 10.6004/jnccn.2020.0031
4. Tolstonog G, Simon C. Trends in Surgical Research in Head and Neck Cancer. *Curr Treat Options Oncol* (2017) 18:38. doi: 10.1007/s11864-017-0475-z
5. Dort JC, Farwell DG, Findlay M, Huber GF, Kerr P, Shea-Budgell MA, et al. Optimal Perioperative Care in Major Head and Neck Cancer Surgery With Free Flap Reconstruction: A Consensus Review and Recommendations From the Enhanced Recovery After Surgery Society. *JAMA Otolaryngol Head Neck Surg* (2017) 143:292–303. doi: 10.1001/jamaoto.2016.2981
6. Choi N, Park SI, Kim H, Sohn I, Jeong HS. The Impact of Unplanned Reoperations in Head and Neck Cancer Surgery on Survival. *Oral Oncol* (2018) 83:38–45. doi: 10.1016/j.oraloncology.2018.06.004
7. Slump J, Hofer SOP, Ferguson PC, Wunder JS, Griffin AM, Hoekstra HJ, et al. Flap Reconstruction Does Not Increase Complication Rates Following Surgical Resection of Extremity Soft Tissue Sarcoma. *Eur J Surg Oncol* (2018) 44:251–9. doi: 10.1016/j.ejso.2017.11.015
8. Locatello LG, Mastronicola R, Cortese S, Beulque E, Salleron J, Gallo O, et al. Estimating the Risks and Benefits Before Salvage Surgery for Recurrent Head and Neck Squamous Cell Carcinoma. *Eur J Surg Oncol* (2021) 47:1718–26. doi: 10.1016/j.ejso.2021.01.022
9. Cash H, Abouyared M, Houlton JJ. Optimizing Value in Head and Neck Cancer Free Flap Surgery. *Curr Opin Otolaryngol Head Neck Surg* (2019) 27:413–19. doi: 10.1097/MOO.0000000000000570
10. Dooley BJ, Karassawa ZD, Mcgill MR, Awad MI, Shah JP, Wong RJ, et al. Intraoperative and Postanesthesia Care Unit Fluid Administration as Risk Factors for Postoperative Complications in Patients With Head and Neck Cancer Undergoing Free Tissue Transfer. *Head Neck* (2020) 42:14–24. doi: 10.1002/hed.25970
11. Lin PC, Kuo PJ, Kuo SCH, Chien PC, Hsieh CH. Risk Factors Associated With Postoperative Complications of Free Anterolateral Thigh Flap Placement in Patients With Head and Neck Cancer: Analysis of Propensity Score-Matched Cohorts. *Microsurgery* (2020) 40:538–44. doi: 10.1002/micr.30587
12. Awad MI, Palmer FL, Kou L, Yu C, Montero PH, Shuman AG, et al. Individualized Risk Estimation for Postoperative Complications After Surgery for Oral Cavity Cancer. *JAMA Otolaryngol Head Neck Surg* (2015) 141:960–68. doi: 10.1001/jamaoto.2015.2200
13. Awad MI, Shuman AG, Montero PH, Palmer FL, Shah JP, Patel SG. Patel: Accuracy of Administrative and Clinical Registry Data in Reporting Postoperative Complications After Surgery for Oral Cavity Squamous Cell Carcinoma. *Head Neck* (2015) 37:851–61. doi: 10.1002/hed.23682
14. Wang C, Pan Y, Xu Q, Li B, Kim K, Mao M, et al. Relationship Between Body Mass Index and Outcomes for Patients With Oral Squamous Cell Carcinoma. *Oral Dis* (2018) 25:87–96. doi: 10.1111/odi.12963
15. Kiong KL, Lin FY, Yao C, Guo T, Ferrarotto R, Weber RS, et al. Impact of Neoadjuvant Chemotherapy on Perioperative Morbidity After Major Surgery for Head and Neck Cancer. *Cancer-Am Cancer Soc* (2020) 126:4304–14. doi: 10.1002/cncr.33103
16. Kojima G, Iliffe S, Walters K. Frailty Index as a Predictor of Mortality: A Systematic Review and Meta-Analysis. *Age Ageing* (2018) 47:193–200. doi: 10.1093/ageing/afx162
17. D'Andréa G, Scheller B, Gal J, Chamorey E, Château Y, Dassonville O, et al. How to Select Candidates for Microvascular Head and Neck Reconstruction in the Elderly? Predictive Factors of Postoperative Outcomes. *Surg Oncol* (2020) 34:168–73. doi: 10.1016/j.suronc.2020.04.016
18. Grammatica A, Piazza C, Pellini R, Montalto N, Lancini D, Vural A, et al. Free Flaps for Advanced Oral Cancer in the "Older Old" and "Oldest Old": A Retrospective Multi-Institutional Study. *Front Oncol* (2019) 9:604. doi: 10.3389/fonc.2019.00604
19. Dindo D, Demartines N, Clavien PA. Classification of Surgical Complications: A New Proposal With Evaluation in a Cohort of 6336 Patients and Results of a Survey. *Ann Surg* (2004) 240:205–13. doi: 10.1097/01.sla.0000133083.54934.ae
20. Clavien PA, Barkun J, de Oliveira ML, Vauthey JN, Dindo D, Schulick RD, et al. The Clavien-Dindo Classification of Surgical Complications: Five-Year Experience. *Ann Surg* (2009) 250:187–96. doi: 10.1097/SLA.0b013e3181b13ca2
21. Zhang X, Tang M, Zhang Q, Zhang K, Guo Z, Xu H, et al. The GLIM Criteria as an Effective Tool for Nutrition Assessment and Survival Prediction in Older Adult Cancer Patients. *Clin Nutr (Edinburgh Scotland)* (2021) 40:1224–32. doi: 10.1016/j.clnu.2020.08.004
22. Chinn SB, Myers JN. Oral Cavity Carcinoma: Current Management, Controversies, and Future Directions. *J Clin Oncol* (2015) 33:3269–76. doi: 10.1200/JCO.2015.61.2929
23. Poisson M, Longis J, Schlund M, Pere M, Michel G, Delagranda A, et al. Postoperative Morbidity of Free Flaps in Head and Neck Cancer Reconstruction: A Report Regarding 215 Cases. *Clin Oral Investig* (2019) 23:2165–71. doi: 10.1007/s00784-018-2653-1
24. Cannady SB, Hatten KM, Bur AM, Brant J, Fischer JP, Newman JG, et al. Use of Free Tissue Transfer in Head and Neck Cancer Surgery and Risk of Overall and Serious Complication(s): An American College of Surgeons-National Surgical Quality Improvement Project Analysis of Free Tissue Transfer to the Head and Neck. *Head Neck* (2017) 39:702–7. doi: 10.1002/hed.24669
25. Joo YH, Cho KJ, Park JO, Kim SY, Kim MS. Surgical Morbidity and Mortality in Patients After Microvascular Reconstruction for Head and Neck Cancer. *Clin Otolaryngol* (2018) 43:502–8. doi: 10.1111/coa.13006
26. Leaper D, Ousey K. Evidence Update on Prevention of Surgical Site Infection. *Curr Opin Infect Dis* (2015) 28:158–63. doi: 10.1097/QCO.0000000000000144

27. Lin S, Chang T, Yang K, Lin Y, Lin Y. Factors Contributing to Surgical Site Infection in Patients With Oral Cancer Undergoing Microvascular Free Flap Reconstruction. *Eur Arch Otorhinolaryngol* (2018) 275:2101–08. doi: 10.1007/s00405-018-5035-z
28. Haidar YM, Tripathi PB, Tjoa T, Walia S, Zhang L, Chen Y, et al. Antibiotic Prophylaxis in Clean-Contaminated Head and Neck Cases With Microvascular Free Flap Reconstruction: A Systematic Review and Meta-Analysis. *Head Neck* (2018) 40:417–27. doi: 10.1002/hed.24988
29. Bratzler DW, Dellinger EP, Olsen KM, Perl TM, Auwaerter PG, Bolon MK, et al. Clinical Practice Guidelines for Antimicrobial Prophylaxis in Surgery. *Surg Infect* (2013) 14:73–156. doi: 10.1089/sur.2013.9999
30. Mitchell RM, Mendez E, Schmitt NC, Bhrany AD, Futran ND. Antibiotic Prophylaxis in Patients Undergoing Head and Neck Free Flap Reconstruction. *JAMA Otolaryngol Head Neck Surg* (2015) 141:1096–103. doi: 10.1001/jamaoto.2015.0513
31. Cohen LE, Finnerty BM, Golas AR, Ketner JJ, Weinstein A, Boyko T, et al. Perioperative Antibiotics in the Setting of Oropharyngeal Reconstruction: Less Is More. *Ann Plast Surg* (2016) 76:663–7. doi: 10.1097/SAP.0000000000000291
32. ASHP Therapeutic Guidelines on Antimicrobial Prophylaxis in Surgery. American Society of Health-System Pharmacists. *Am J Health Syst Pharm* (1999) 56:1839–88. doi: 10.1093/ajhp/56.18.1839
33. Iocca O, Copelli C, Ramieri G, Zocchi J, Savo M, Di Maio P. Antibiotic Prophylaxis in Head and Neck Cancer Surgery: Systematic Review and Bayesian Network Meta-Analysis. *Head Neck* (2022) 44:254–61. doi: 10.1002/hed.26908
34. Fischer D, Neb H, Choorapoikayil S, Zacharowski K, Meybohm P. Red Blood Cell Transfusion and its Alternatives in Oncologic Surgery—A Critical Evaluation. *Crit Rev Oncol Hematol* (2019) 134:1–9. doi: 10.1016/j.critrevonc.2018.11.011
35. McSorley ST, Tham A, Dolan RD, Steele CW, Ramsingh J, Roxburgh C, et al. Perioperative Blood Transfusion is Associated With Postoperative Systemic Inflammatory Response and Poorer Outcomes Following Surgery for Colorectal Cancer. *Ann Surg Oncol* (2020) 27:833–43. doi: 10.1245/s10434-019-07984-7
36. Spanier G, Böttcher J, Gerken M, Fischer R, Roth G, Lehn P, et al. Prognostic Value of Perioperative Red Blood Cell Transfusion and Anemia on Survival and Recurrence in Oral Squamous Cell Carcinoma. *Oral Oncol* (2020) 107:104773. doi: 10.1016/j.oraloncology.2020.104773
37. Marur S, Forastiere AA. Head and Neck Squamous Cell Carcinoma: Update on Epidemiology, Diagnosis, and Treatment. *Mayo Clin Proc* (2016) 91(3):386–96. doi: 10.1016/j.mayocp.2015.12.017
38. Nathan H, Yin H, Wong SL. Postoperative Complications and Long-Term Survival After Complex Cancer Resection. *Ann Surg Oncol* (2017) 24:638–44. doi: 10.1245/s10434-016-5569-5
39. Weimann A, Braga M, Harsanyi L, Laviano A, Ljungqvist O, Soeters P, et al. ESPEN Guidelines on Enteral Nutrition: Surgery Including Organ Transplantation. *Clin Nutr* (2006) 25:224–44. doi: 10.1016/j.clnu.2006.01.015
40. Schandl A, Kauppila JH, Anandavadivelan P, Johar A, Lagergren P. Predicting the Risk of Weight Loss After Esophageal Cancer Surgery. *Ann Surg Oncol* (2019) 26:2385–91. doi: 10.1245/s10434-019-07352-5
41. Strombom P, Widmar M, Keskin M, Gennarelli RL, Lynn P, Smith JJ, et al. Assessment of the Value of Comorbidity Indices for Risk Adjustment in Colorectal Surgery Patients. *Ann Surg Oncol* (2019) 26:2797–804. doi: 10.1245/s10434-019-07502-9
42. Paleri V, Wight RG, Silver CE, Haigentz M Jr, Takes RP, Bradley PJ, et al. Comorbidity in Head and Neck Cancer: A Critical Appraisal and Recommendations for Practice. *Oral Oncol* (2010) 46:712–9. doi: 10.1016/j.oraloncology.2010.07.008
43. Schimansky S, Lang S, Beynon R, Penfold C, Davies A, Waylen A, et al. Association Between Comorbidity and Survival in Head and Neck Cancer: Results From Head and Neck 5000. *Head Neck* (2019) 41:1053–62. doi: 10.1002/hed.25543
44. Omura G, Ando M, Saito Y, Kobayashi K, Yamasoba T, Asakage T. Comorbidity as Predictor Poor Prognosis for Patients With Advanced Head and Neck Cancer Treated With Major Surgery. *Head Neck* (2016) 38:364–9. doi: 10.1002/hed.23897
45. Guan X, Lu Z, Wang S, Liu E, Zhao Z, Chen H, et al. Comparative Short- and Long-Term Outcomes of Three Techniques of Natural Orifice Specimen Extraction Surgery for Rectal Cancer. *Eur J Surg Oncol* (2020) 46:e55–61. doi: 10.1016/j.ejso.2020.06.023

Conflict of Interest: The authors declare that the research was conducted in the absence of any commercial or financial relationships that could be construed as a potential conflict of interest.

Publisher's Note: All claims expressed in this article are solely those of the authors and do not necessarily represent those of their affiliated organizations, or those of the publisher, the editors and the reviewers. Any product that may be evaluated in this article, or claim that may be made by its manufacturer, is not guaranteed or endorsed by the publisher.

frontiers | Frontiers in Oncology

ORIGINAL RESEARCH
published: 07 July 2022
doi: 10.3389/fonc.2022.809760

Construction of a lncRNA–mRNA Co-Expression Network for Nasopharyngeal Carcinoma

Chunmei Fan[1,2,3†], Fang Xiong[1,2,3†], Yanyan Tang[1], Panchun Li[4], Kunjie Zhu[1], Yongzhen Mo[5], Yumin Wang[3], Shanshan Zhang[3], Zhaojiang Gong[4], Qianjin Liao[1], Guiyuan Li[1,5], Zhaoyang Zeng[1,5], Can Guo[1,5], Wei Xiong[1,5] and He Huang[2*]*

[1] NHC Key Laboratory of Carcinogenesis and Hunan Key Laboratory of Cancer Metabolism, Hunan Cancer Hospital and the Affiliated Cancer Hospital of Xiangya School of Medicine, Central South University, Changsha, China, [2] Department of Histology and Embryology, Xiangya School of Medicine, Central South University, Changsha, China, [3] Department of Stomatology, Xiangya Hospital, Central South University, Changsha, China, [4] Department of Oral and Maxillofacial Surgery, The Second Xiangya Hospital, Central South University, Changsha, China, [5] Key Laboratory of Carcinogenesis and Cancer Invasion of the Chinese Ministry of Education, Cancer Research Institute, Central South University, Changsha, China

OPEN ACCESS

Edited by:
Li-Ang Lee,
Linkou Chang Gung Memorial Hospital, Taiwan

Reviewed by:
Wei Cao,
Shanghai Jiao Tong University, China
Yongmei Li,
Tianjin Medical University, China

***Correspondence:**
Wei Xiong
xiongwei@csu.edu.cn
He Huang
huanghe@csu.edu.cn

[†]These authors have contributed equally to this work

Specialty section:
This article was submitted to Head and Neck Cancer, a section of the journal Frontiers in Oncology

Received: *05 November 2021*
Accepted: *06 June 2022*
Published: *07 July 2022*

Citation:
Fan C, Xiong F, Tang Y, Li P, Zhu K, Mo Y, Wang Y, Zhang S, Gong Z, Liao Q, Li G, Zeng Z, Guo C, Xiong W and Huang H (2022) Construction of a lncRNA–mRNA Co-Expression Network for Nasopharyngeal Carcinoma. Front. Oncol. 12:809760. doi: 10.3389/fonc.2022.809760

Long non-coding RNAs (lncRNAs) widely regulate gene expression and play important roles in the pathogenesis of human diseases, including malignant tumors. However, the functions of most lncRNAs remain to be elucidated. In order to study and screen novel lncRNAs with important functions in the carcinogenesis of nasopharyngeal carcinoma (NPC), we constructed a lncRNA expression profile of 10 NPC tissues and 6 controls through a gene microarray. We identified 1,276 lncRNAs, of which most are unknown, with different expression levels in the healthy and NPC tissues. In order to shed light on the functions of these unknown lncRNAs, we first constructed a co-expression network of lncRNAs and mRNAs using bioinformatics and systematic biological approach. Moreover, mRNAs were clustered and enriched by their biological functions, and those lncRNAs have similar expression trends with mRNAs were defined as functional molecules with potential biological significance. The module may help identify key lncRNAs in the carcinogenesis of NPC and provide clues for in-depth study of their functions and associated signaling pathways. We suggest the newly identified lncRNAs may have clinic value as biomarkers and therapeutic targets for NPC diagnosis and treatment.

Keywords: nasopharyngeal carcinoma, long non-coding RNA, weighted gene co-expression network analysis, genomic instability, p53, MYC

INTRODUCTION

Nasopharyngeal carcinoma (NPC) is a kind of malignant tumor that originates from the nasopharyngeal epithelial cells (1). It is a common head and neck malignancy in southeast Asia and south China (2). However, NPC differs markedly from other head and neck malignancies in terms of epidemiology, etiology, pathological characteristics, and treatment strategies. NPC exhibits

Abbreviations: ceRNA, competitive endogenous RNA; GEO, Gene Expression Omnibus; GSEA, gene set enrichment analysis; IPA, Ingenuity Pathway Analysis; KEGG, Kyoto Encyclopedia of Genes and Genomes; lncRNA, long non-coding RNA; miRNA, microRNA; MSigDB, molecular signatures database; NPC, nasopharyngeal carcinoma; NPE, nasopharyngeal epithelium; SAM, Significant Analysis of Microarray; WGCNA, weighted gene co-expression network analysis.

distinctive ethnic and regional distribution characteristics. In most parts of the world, the incidence of NPC is very low (1 in 100,000 people) but high in southeast Asia, north Africa, and other regions; in particular, the Guangdong province of south China has an incidence of NPC up to 30 in 100,000 people (3). NPC carcinogenesis is caused by pathogenic environmental factors and genetic factors (4). Environmental factors including exposure to carcinogenic chemicals (such as nitrosamines in food) and Epstein-Barr virus infection (5–12). Genetic factors, or genetic susceptibility, also plays an important role in the pathogenesis of NPC (13–15). Most cases of NPC are low-grade differentiated squamous cell carcinomas, which are relatively sensitive to radiation (16–19). Radiotherapy achieves good curative effects for patients with an early-stage of NPC, whose five-year survival rate exceeds 90%. However, due to the primary site of NPC is not readily visible, early symptoms of NPC are not evident, which makes it easy to be overlooked or misdiagnosed clinically. In addition, most NPC patients have a high degree of malignancy and a strong tendency to metastasis (20–24). Therefore, most patients with NPC occur metastases at the time of diagnosis and the effects of radiotherapy lose their in-time efficacy. Recurrence and metastasis are the main causes of treatment failure in NPC.

Many genes have been reported to be dysregulated and multiple signal transduction pathways function abnormally during NPC carcinogenesis (25–28). However, the mechanism of NPC development has not been fully elucidated. An increasing number of studies showed that, in addition to protein-coding genes, non-coding RNAs also play important roles in the development of malignant tumors. Most non-coding RNAs are longer than 200 nt and have been classified as long non-coding RNAs (lncRNAs) (29–31). At present, more than 90,000 lncRNA genes, encoding more than 140,000 transcripts, have been identified in the human genome (32), far more than the number of protein-coding genes. LncRNAs regulate gene expression at multiple levels, such as the epigenetic, transcriptional, and post-transcriptional levels, with important effects on biological functions (33–37). So far more than 100 lncRNAs have been found associated with NPC (38–42), however, these lncRNAs were just the tip of the iceberg. The roles and mechanisms of most lncRNAs in the development of NPC remain obscure. Therefore, a whole transcriptomic expression profile of lncRNA will enable effective screening and identification of important lncRNAs associated with NPC. Furthermore, it will enable us to explore the key driving factors during transformation of inflammation to carcinoma.

The identification of functinal lncRNAs remains difficult as many lncRNAs are undiscovered. However, regulation of protein-coding genes and non-coding RNAs is governed by certain rules (43). Genes with similar expression patterns may have common characteristics, such as may be regulated by common factors or participated in the same signaling pathway. Therefore, after we obtained lncRNA and mRNA expression profiles for NPC and the control tissues, we constructed the lncRNA–mRNA co-expression network based on their expression patterns. We defined functional modules by clustering and enriching mRNAs based on their biological functions and by determining lncRNAs with similar expression trends.

Another important cluster of RNA, the microRNAs (miRNAs), regulates gene expression in the transcriptome (44–46). miRNAs bind to other RNA molecules to induce the degradation of target RNA, thereby altering gene expression. LncRNAs and mRNAs that share the same miRNA binding site reciprocally regulate each other by competing for miRNAs (45). Although we did not use a gene chip with miRNA probes in this study, we performed miRNA target gene enrichment analysis through gene set enrichment analysis (GSEA) (47), to find RNAs share the same miRNA recognition site to build a competitive endogenous RNA (ceRNA) (48) co-expression network. We hypothesize that these functional modules may reveal lncRNAs with potential biological significance, which may provide clues for screening candidate lncRNAs and may aid the exploration of possible mechanisms of NPC.

MATERIALS AND METHODS

Clinical Samples

We selected 6 non-cancerous nasopharyngeal epithelium (NPE) tissues and 10 NPC tissues for construction of lncRNA and mRNA expression profiles. And then we collected another 10 NPE and 26 NPC tissue samples for validation of lncRNA expression. All NPC tissues were from newly diagnosed patients who did not undergo treatment. The tissue specimens were stored in liquid nitrogen. This study was authorized by the Ethics Committee of the Central South University. All patients provided written informed consent.

RNA Extraction, cDNA Synthesis, and Labeling

We minced the tissues (50 mg–100 mg) in liquid nitrogen and extracted total RNA using the TRIzol® reagent according to the manufacturer's instructions. We quantified RNA using a NanoDrop™ ND-2000 (Thermo Scientific) and assessed its integrity with an Agilent 2100 Bioanalyzer (Agilent Technologies). We reverse-transcribed double-stranded cDNA from RNA and synthesized a complementary RNA labeled with cyanine-3-CTP using the kit provided by Agilent.

Chip Selection, Hybridization, and Image Acquisition

We profiled lncRNA and mRNA expression with the Agilent 4×180K lncRNA Array, which contains all known lncRNAs and mRNAs from multiple databases, such as NCBI RefSeq, UCSC, and Ensembl. The labeled complementary RNA was hybridized to the chip, then scanned with an Agilent Scanner G2505C (Agilent Technologies) after elution. Raw expression data were extracted from the images using the Agilent Feature Extraction software (version 10.7.1.1, Agilent Technologies). We standardized the data using GeneSpring software (version 13.1,

Agilent Technologies) to obtain lncRNA and mRNA expression values from each sample for subsequent data analysis. The raw data for all the 16 tissues used in this project have been uploaded to the Gene Expression Omnibus (GEO) database (Accession number: GSE61218).

Differential Expression Analysis

We filtered data to reduce the "background noise" for subsequent analysis. We retained lncRNAs or mRNAs that were detectable in at least one of the two sample groups (NPC or NPE). The filtered data were analyzed with the Significant Analysis of Microarray (SAM) software (49); standard parameters (fold change ≥ 1.5 and the false discovery rate q value ≤ 0.05) were used to identify significantly and differentially expressed transcripts. The differentially expressed lncRNAs and mRNAs were displayed in heatmap created using the Genesis software to visualize their expression patterns in the two groups of the samples.

Cell Culture

NPC cell CNE2 was cultured in RPMI-1640 (Life Technologies, Grand Island, NY, USA) with 10% fetal bovine serum (FBS; Life Technologies) and 1% penicillin/streptomycin (Life Technologies), at 37 °C in a humid incubator with 5% CO2.

Cell Transfection, RNA Extraction and qPCR

Cells were seeded in a 6-well plate and cultured overnight, the next day, cells were transfected with 50 nM siRNA and 5 μL Hiperfect (Qiagen). After 48 hours, total RNA was extracted with TRIzol (Invitrogen, CA, USA), 1 μg RNAs were reverse transcribed into cDNA using HiScript II Q RT SuperMix (Vazyme, Nanjing, China), and qPCR was performed using 2×SYBR Green qPCR Master Mix (Bimake, Changsha, China). Sequences of primers and siRNAs were shown in **Supplementary Table 1**.

Wound Healing Assay

Cells were seeded in a 6-well plate and transfected with siRNAs or nc when cell density reached 50%. When the cells reached 100% confluency, the plate was scratched using a 10 μL pipette tip, making each gap as uniform as possible. The cells were cultured with 2% FBS and hydroxyurea (inhibit cell growth, 40 μg/mL). The gap was imaged at different time points using an inverted microscope (IX51, Olympus, Japan).

Transwell Assay

Chambers (8-mm pores, Corning, NY, USA) were placed in a 24-well plate. Matrigel (BD Biosciences, NJ, USA) was diluted 1:9 with RPMI-1640 and 20 μL diluted Matrigel was added to the chambers following by incubating at 37 °C for 2h. Transfected cells were digested, and diluted to a density of 20,000 cells per 200 μL and then added to upper chamber and 800 μL 20% FBS was added to the bottom of 24-well plate. After incubation for 24-48 hours, the cells were fixed with 4% formaldehyde, stained with 0.1% crystal violet, and cells inside the chamber were wiped off, cells outside chamber were imaged using an inverted microscope (IX51, Olympus, Japan).

CCK8

Cells were seeded in a 6-well plate and transfected with siRNAs or nc when cell density reached 50%. After 24 hours, the cells were digested and diluted to 800 per 200 μL, then cells were seeded in 96-well plates. Each group was set with 5 parallel wells. Then CCK8 (Hanbio, shanghai, China) was added and incubated for 2 hours, absorbance was measured at 450nm.

Weighted Gene Co-Expression Network Analysis

LncRNAs and mRNAs share similar expression trends in the NPC and controls were calculated using the weighted gene co-expression network analysis (WGCNA) algorithm (50). We used those expression trends to construct the lncRNA–mRNA co-expression networks, which were visualized using the Cytoscape software.

GSEA

GSEA is a computational method that determines whether *a priori* defined set of genes shows statistically significant, concordant differences between the two biological states, e.g. normal vs disease (47). We used GSEA to analyze the gene sets in which the differentially expressed molecules were enriched. Using a combination of the GSEA results and the lncRNA–mRNA co-expression network, we defined the lncRNA–mRNA modules that may share the characteristics of the enriched gene sets.

Ingenuity® Pathway Analysis

The Ingenuity® Pathway Analysis (IPA®; http://www.ingenuity.com) is an integrated bioinformatic analysis software based on the Ingenuity Knowledge Base and the cloud computing provided by Qiagen (51). We imported data of our lncRNA and mRNA expression profile to obtain several potential core transcriptional regulatory factors. We then integrated those findings with the lncRNA co-expression network to construct a core transcription factor-driven lncRNA–mRNA co-expression module.

RESULTS

Differentially Expressed lncRNAs and mRNAs in NPC

We successfully profiled lncRNA and mRNA expression in 10 NPC tissues and 6 controls by a gene array. By filtering and analyzing data, we found 3,734 differentially expressed molecules, of which 1,276 were lncRNAs (405 up-regulated and 871 down-regulated in NPC) and 2,458 mRNAs (1,677 up-regulated and 781 down-regulated in NPC), as shown in **Supplementary Table 2**. A heatmap displaying the differentially expressed RNAs has been shown in **Figure 1**.

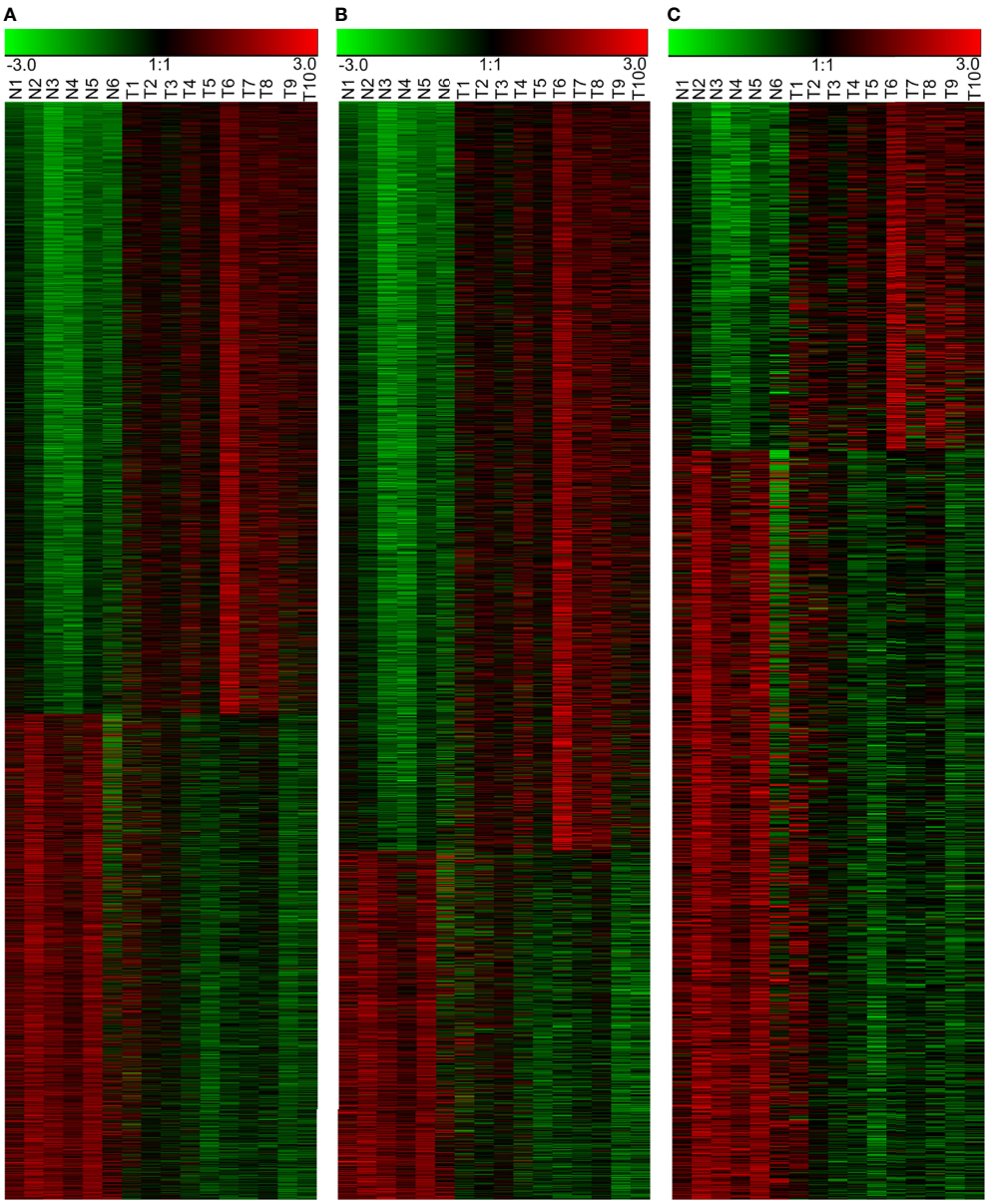

FIGURE 1 | Differentially expressed RNAs in the NPC and the control NPE samples. **(A)** Heatmap of all differentially expressed RNAs, including lncRNAs and mRNAs. **(B)** Differentially expressed mRNAs. **(C)** Differentially expressed lncRNAs. N: normal nasopharyngeal epithelium; T: nasopharyngeal carcinoma.

Differentially Expressed lncRNAs Were Validated in NPC Tissues

In order to verify the reliability of our gene array, we collected another 26 NPC tissues and 10 normal controls for qPCR detection. We randomly selected 6 lncRNAs from down-regulated or up-regulated modules, respectively. The results showed that LINC01420, PVT1, LINC01503, LOC730101, LINC00673, TUG1 was upregulated in NPC tissues, while ZNF667-AS1, WDR86-AS1, CCNT2-AS1, LOC730227, TRAF3IP2-AS1, HAR1A was downregulated in NPC tissues, which were consistent with gene array data (**Figure 2**).

Biological Function of Differentially Expressed lncRNAs

To further prove that our differentially expressed lncRNAs have biological function. We selected WDR86-AS1 from down-regulated module and LINC00673 from up-regulated module for phenotype verification, which have not been reported in NPC. Firstly, the effect of knockdown using siRNAs was detected by qPCR (**Figure 3A**). CCK8 assays, transwell assays and wound healing assays demonstrated that siWDR86-AS1 promoted proliferation, invasion and migration ability of NPC cells, while siLINC00673 showed opposite effect (**Figures 3B-D**).

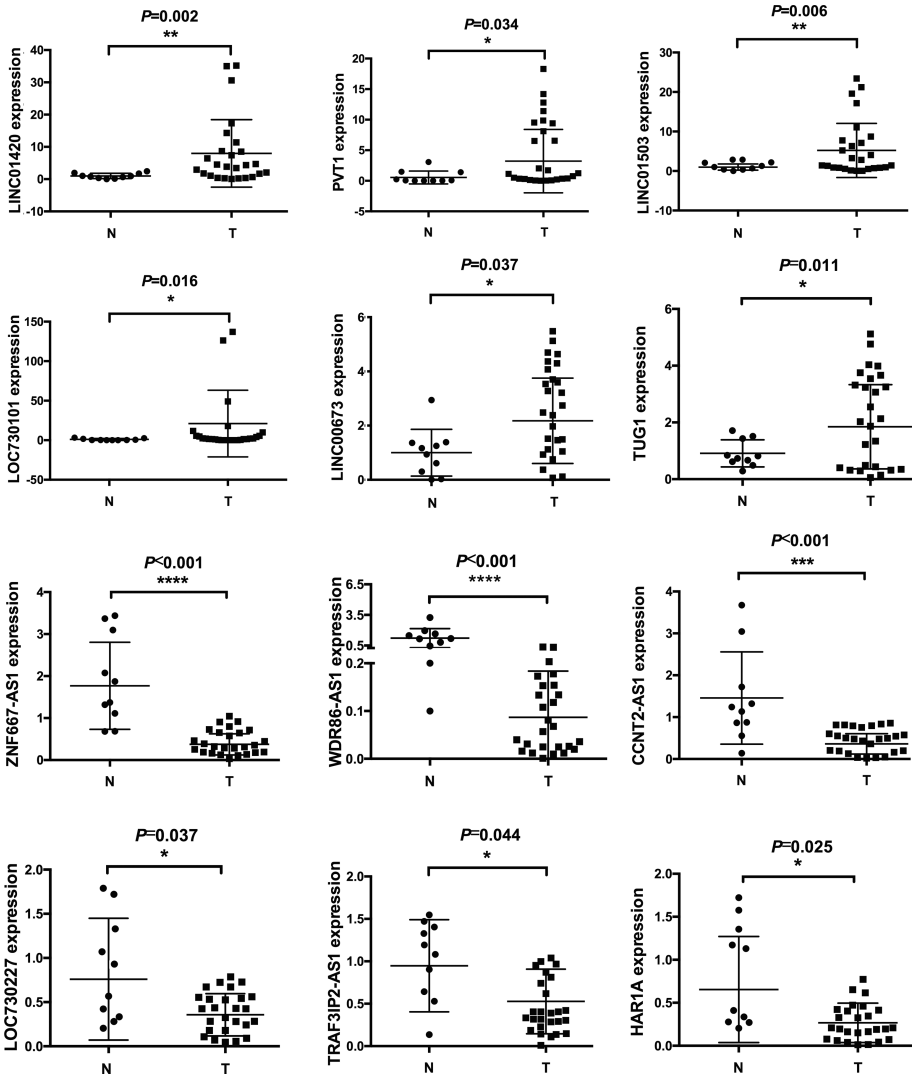

FIGURE 2 | Differentially expressed lncRNAs were validated by qPCR. 10 normal and 26 cancerous tissues were used to detect expression levels of lncRNAs. Six upregulated and six downregulated lncRNAs were validated. * means p<05, ** means p<0.01, *** means p<0.001, **** means p<0.0001.

Chromosome Co-Localization of Differentially Expressed lncRNAs and mRNAs

Genomic instability, especially loss or amplification of chromosome fragments, is a special characteristic of NPC (1). The loss or amplification of certain chromosomal segments can alter gene expression in certain chromosomal region. Therefore, we investigated if the differentially expressed lncRNAs and mRNAs in NPC were enriched by a chromosomal localization. We analyzed differentially expressed genes with GSEA using gene set of chromosomal position (c1: positional gene sets). We found that there were significant enrichments in five chromosome segments. Of those, 12q24, 22p11, and 3q21 were significantly up-regulated together, suggesting that these chromosome segments may be amplified in NPC. However, the other two enriched segments, 3p21 and 11p15, were significantly down-regulated, suggesting that these chromosome segments may be absent in the NPC. The most significantly enriched chromosome is 12q24, and the expression patterns of mRNA and lncRNA in this chromosome segment have been shown in **Figure 4**, as an example of the chromosomal co-localization of the differentially expressed lncRNAs and mRNAs.

Construction of a lncRNA and mRNA Co-Expression Network Using WGCNA

At present, the functions of most lncRNAs in NPC remain unknown. However, we constructed the lncRNA–mRNA co-expression network to establish relationship between functionally annotated mRNAs and novel lncRNAs with unknown biological functions. We used the WGCNA algorithm to calculate the topological overlap between 3,734 differentially expressed RNAs and classify them according to their expression patterns, then we constructed a hierarchical

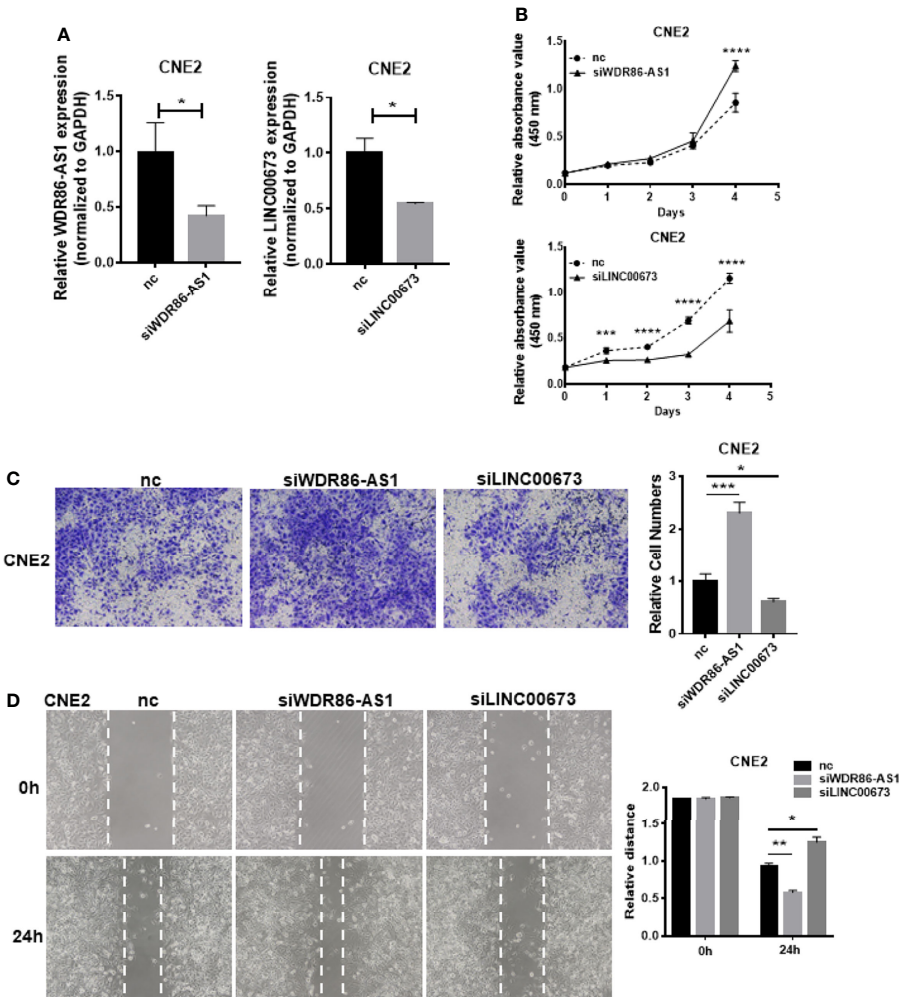

FIGURE 3 | Biological function of differentially expressed lncRNAs. **(A)** The efficiency of knock down was detected by qPCR. **(B)** CCK8 was used to measure the proliferation ability of lncRNAs. **(C)** Transwell assays were performed to detect the invasion potential of lncRNAs after knock down. **(D)** Wound healing assays were employed to assess the migration rate. * means p<0.05, ** means p<0.01, *** means p<0.001, **** means p<0.0001.

clustering tree (**Figure 5A**, upper left). The branches of the clustering tree contained genes with similar expression patterns and represented a different gene module. We next constructed a correlation coefficient matrix of the differentially expressed RNAs (1,276 lncRNAs and 2,458 mRNAs, which formed a 3,734×3,734 matrix). The matrix has been represented as a heatmap (**Figure 5A**). Finally, we constructed the lncRNA–mRNA co-expression network for molecules with topological overlap greater than 0.09 (**Figure 5B**). This network included a total of 2,196 nodes (915 lncRNAs and 1,281 mRNAs) and 35,290 connections (relationships). The remaining 361 lncRNAs and 1,177 mRNAs did not exceed the threshold (0.09) for a co-expression relationship.

ceRNA Modules Enriched by Common miRNA Binding Sites

Using the WGCNA algorithm, we determined the full lncRNA–mRNA co-expression network for NPC (**Figure 3B**). However, the biological significance of the lncRNA–mRNA modules was unclear. Using GSEA, we identified lncRNAs and mRNAs that shared miRNA recognition sites. We found that targets for miR-142-3p, miR506, and miR-17 family (including miR-17-5p, miR-20a, miR-106a, miR-106b, miR-20b, and miR-519d) were the most significantly enriched in the setting of NPC. **Figure 6** shows the lncRNA/miR-142-3p/mRNA ceRNA module as an example.

Construction of lncRNA–mRNA Co-Expression Modules Based on Signaling Pathway

In addition to finding lncRNA–mRNA co-expression modules based on the chromosomal co-localization and the ceRNAs, we enriched modules based on signaling pathways. Using GSEA, we analyzed gene sets that contained all the pathways from the Kyoto Encyclopedia of Genes and Genomes (KEGG) to enrich for the signaling pathways associated with the differentially expressed RNAs. We found that the p53 signaling pathway

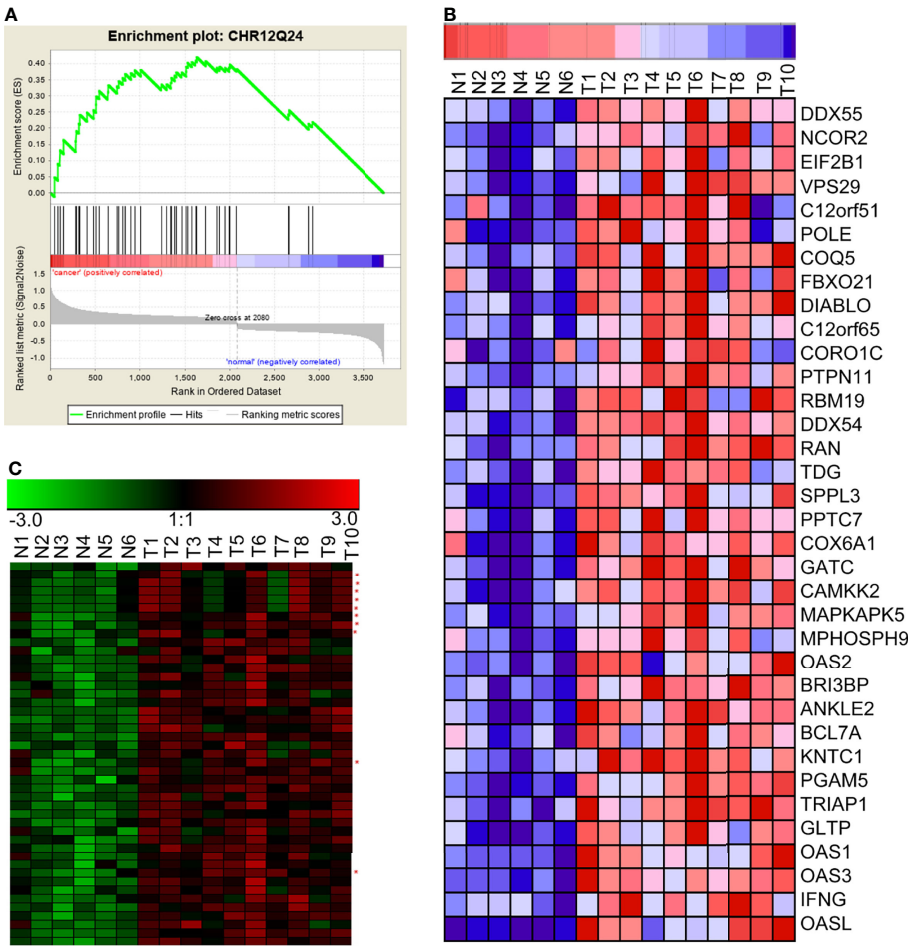

FIGURE 4 | GSEA revealed the concurrent up-regulation of a branch of lncRNAs and mRNAs located on the chromosome 12q24 region. **(A)** GSEA showed that genes in the chromosome 12q24 region were significantly enriched in NPC. **(B)** mRNAs in the chromosome 12q24 region were significantly up-regulated in NPC. **(C)** lncRNAs and mRNAs in the chromosome 12q24 region were concurrently up-regulated (red asterisks beside the right of the heatmap indicate lncRNAs; the rest of the rows represent mRNAs). N, the nasopharyngeal epithelium; T, nasopharyngeal carcinoma.

(KEGG_P53_SIGNALING_PATHWAY), the cell cycle regulatory pathway (KEGG_CELL_CYCLE), and the tumor-associated pathway (KEGG_PATHWAYS_IN_CANCER) were significantly enriched in NPC. We then used WGCNA to construct the lncRNA–mRNA co-expression modules based on the signaling pathways. In **Figure 7**, the p53 pathway has been used as an example of the lncRNA–mRNA co-expression module for an enriched pathway.

Classification of lncRNA–mRNA Co-Expression Modules by Key Transcriptional Regulatory Factors

Transcriptional regulatory factors drive the transcription of many genes, especially in the process of carcinogenesis. Therefore, assessment on co-regulation of lncRNA–mRNA co-expression network is important for the determination of regulatory mechanism of NPC. We used IPA to perform an integrated analysis of all differentially expressed lncRNAs and mRNAs, and found that β-estradiol, MYC, p53, E2F4, and ERBB2 were important upstream regulatory factors in the NPC transcriptome. We integrated the analyses from IPA and WGCNA, and constructed the lncRNA–mRNA co-expression modules that were driven by these core transcriptional regulatory factors. **Figure 8** shows the MYC-driven lncRNA–mRNA co-expression module as an example.

DISCUSSION

The study of lncRNAs is a hotspot of biomedical research due to the abundance of lncRNAs, their extensive participation in the regulation of other genes, and their roles in the development of a variety of human diseases (52–54). Research about lncRNAs is at the frontier of science as only a small portion of lncRNAs has been studied. The biological functions and molecular mechanisms of most lncRNAs remain unknown. The

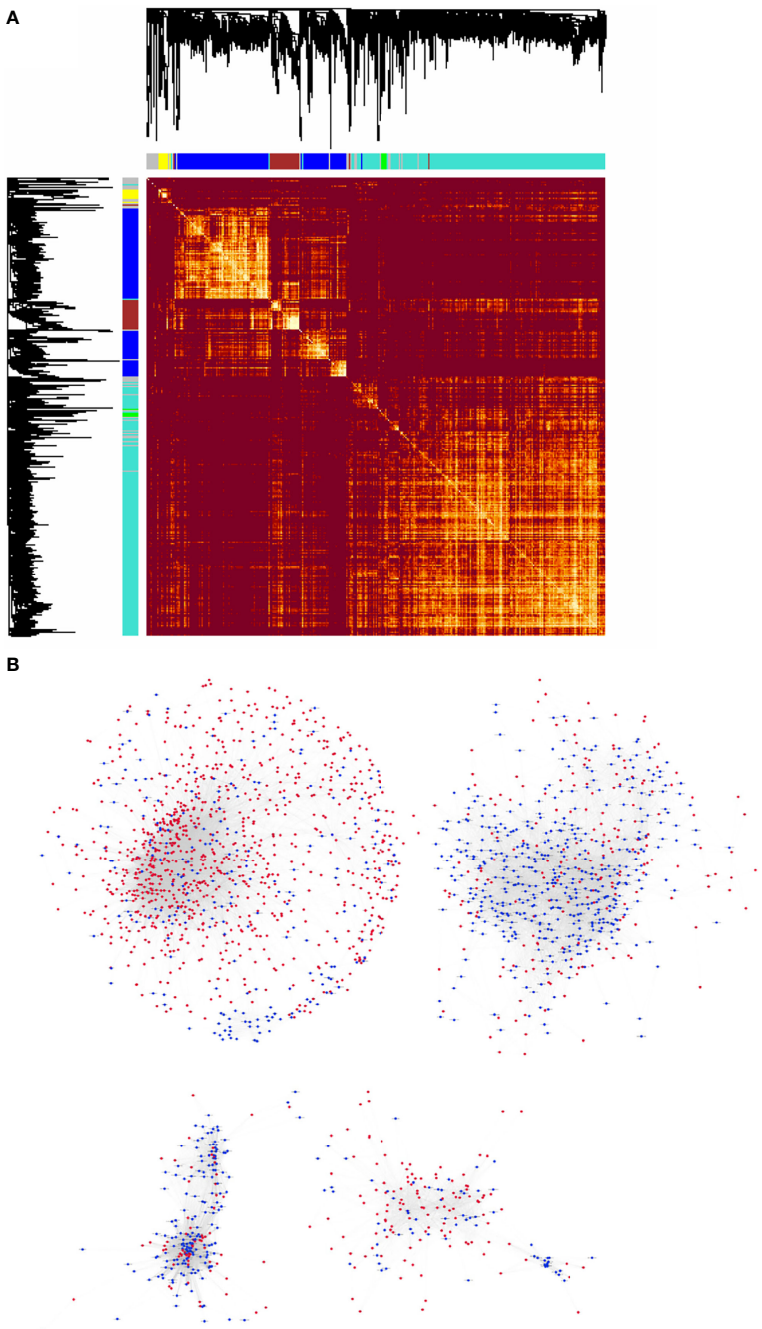

FIGURE 5 | The lncRNA–mRNA co-expression network for NPC was constructed using WGCNA. **(A)** Heatmap of the topological overlap matrix of all the differentially expressed lncRNAs and mRNAs in NPC. The elements above and the left of the heatmap are hierarchical clustering trees. The different branches of the clustering tree represent different gene modules and have been displayed as different colored boxes. **(B)** Highly correlated, co-expressed lncRNAs and mRNAs with topological overlap greater than 0.09 were selected. They formed the basis of the lncRNA–mRNA co-expression network of NPC, which was illustrated using the Cytoscape software. There were 2,196 nodes (915 lncRNAs and 1,281 mRNAs) and 35,290 connections (or relationships) in the co-expression network.

construction of lncRNA expression profiles and screening for differentially expressed lncRNAs are critical for the identification of disease-relevant lncRNAs and their pathogenic mechanisms. Given the generally low incidence of NPC globally, the small size of the nasopharyngeal cavity, and the limited availability of biopsy tissues, there have been few reports on lncRNA expression profiles in NPC (55–57). In this study, we constructed lncRNA and mRNA expression profiles using 10 NPC tissues and 6 normal controls, which were uploaded to the public database. These profiles will provide a basis for further

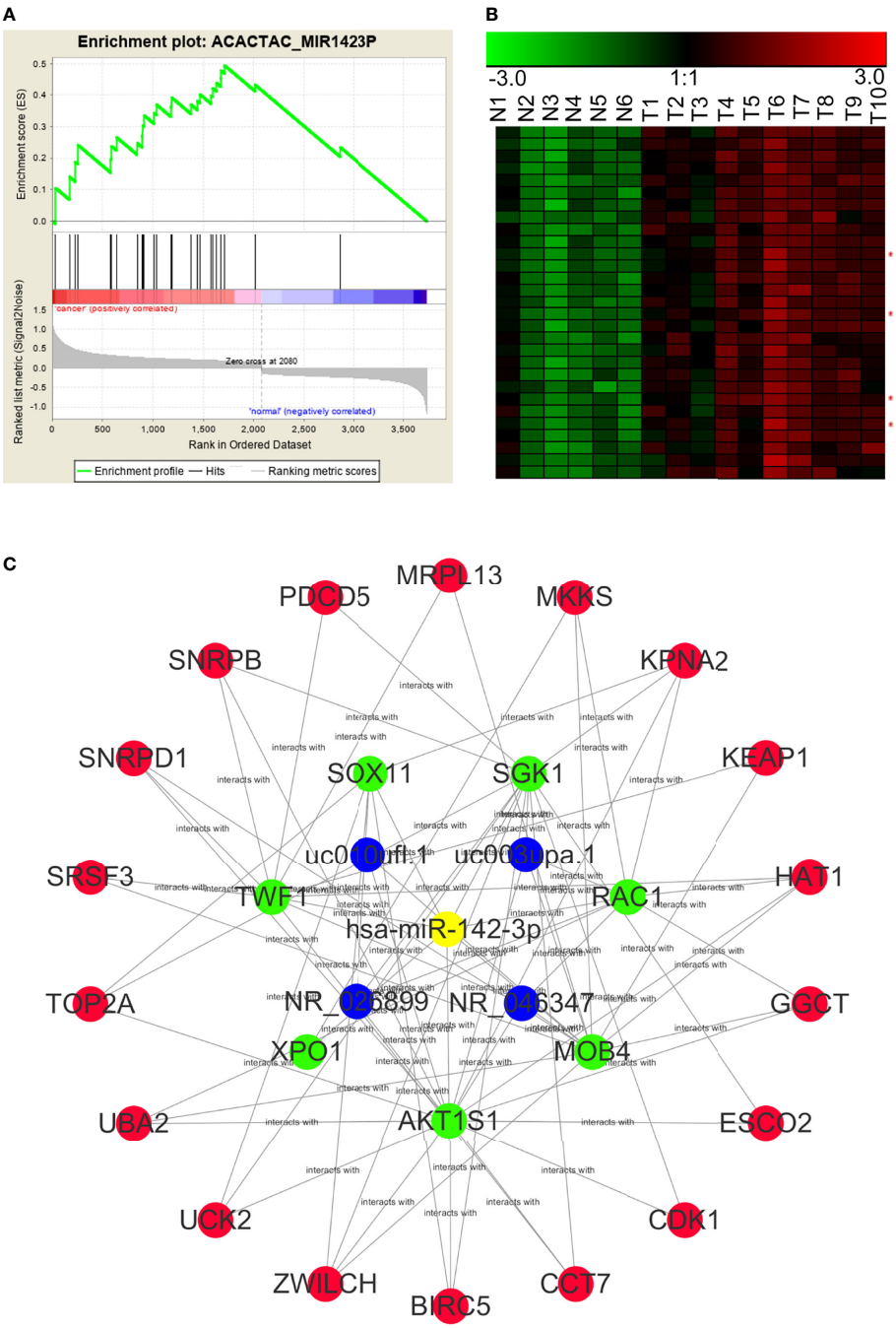

FIGURE 6 | A potential NPC lncRNA–mRNA ceRNA module based on the competition for miR-142-3p. **(A)** GSEA predicted that miR-142-3p target genes were significantly enriched among the RNAs that were differentially expressed in NPC. **(B)** Expression profiles of lncRNAs and mRNAs that may be targeted by miR142-3p in NPC (red asterisks indicate lncRNAs). N, the nasopharyngeal epithelium; T, nasopharyngeal carcinoma. **(C)** An NPC lncRNA–mRNA regulatory module based on the competition for miR142-3p, constructed through GSEA and WGCNA.

screening and multi-center verification of lncRNAs that play an important role in the carcinogenesis of NPC.

We identified 1,275 lncRNAs and 2,485 mRNAs that were significantly and differently expressed in the NPC samples compared to controls. Among these differentially expressed lncRNAs, some have been previously reported associated with NPC; for example, AFAP1-AS1 (41), LOC284454 (42), PVT1 (16) and LINC01420 (40) have been reported upregulated in NPC tissues and promoted migration and invasion ability of NPC cells, these findings verified the reliability of our gene array

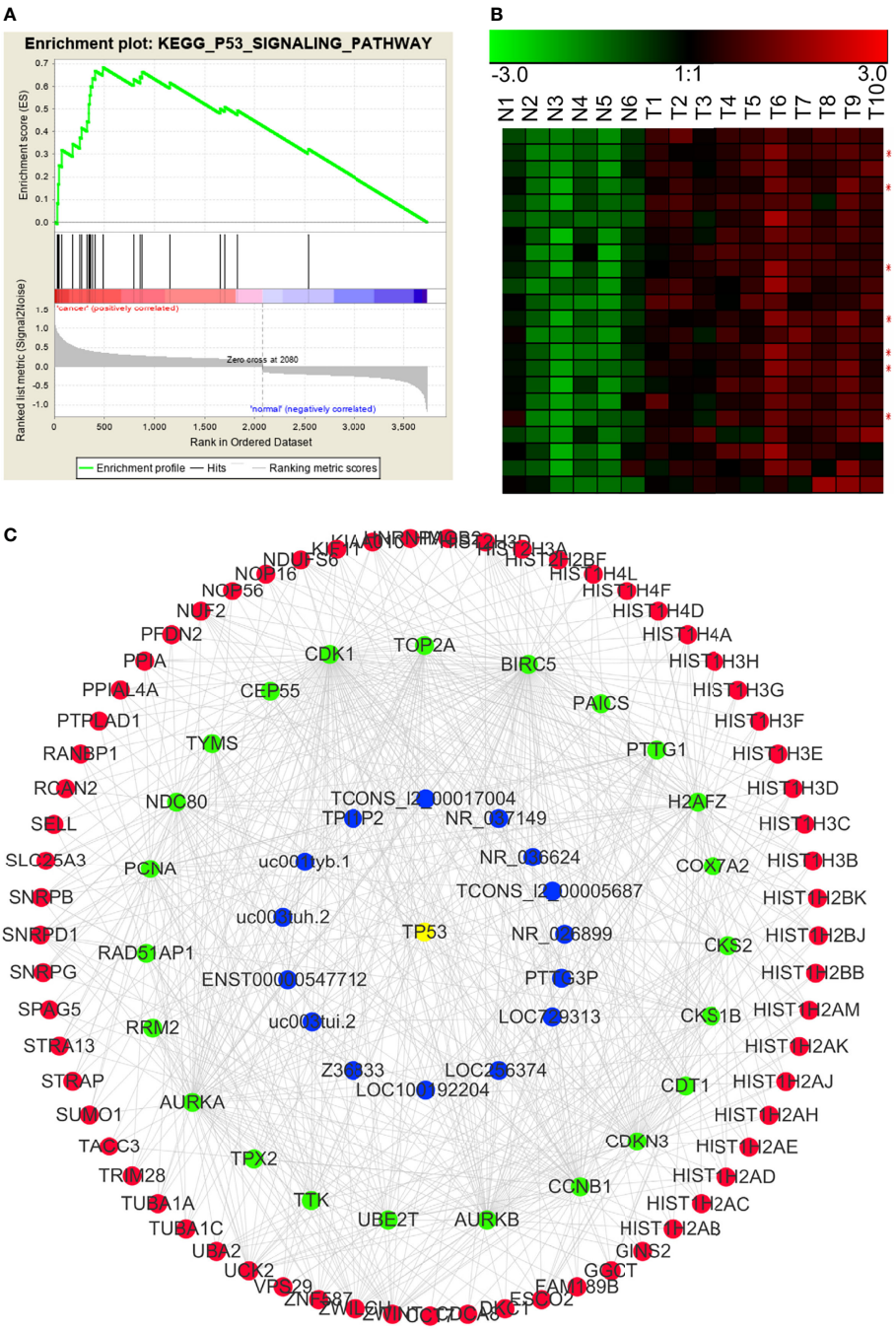

FIGURE 7 | p53 pathway-related lncRNA-mRNA co-expression modules in NPC. **(A)** GSEA revealed that involvement in the p53 signal pathway was significantly enriched in the differentially expressed RNAs in NPC. **(B)** Many genes in the p53 pathway were significantly up-regulated in NPC (red asterisks indicate lncRNAs). N: the control nasopharyngeal epithelium, T, nasopharyngeal carcinoma. **(C)** We used GSEA and WGCNA to construct the lncRNA–mRNA co-expression module related to the p53 signaling pathway.

data. However, most of the other lncRNAs have not been reported in the literature. Screening for important lncRNA molecules for subsequent research will not only expand our knowledge about pathogenesis of NPC, but also provide new annotations for functions of these lncRNAs.

Among these differentially expressed lncRNAs, some may be driving factors of nasopharyngeal epithelial carcinogenesis (58). In contrast, other differentially expressed lncRNAs may be simply associated with the carcinogenesis, which may be caused by a disordered transcriptional regulation during carcinogenesis (59).

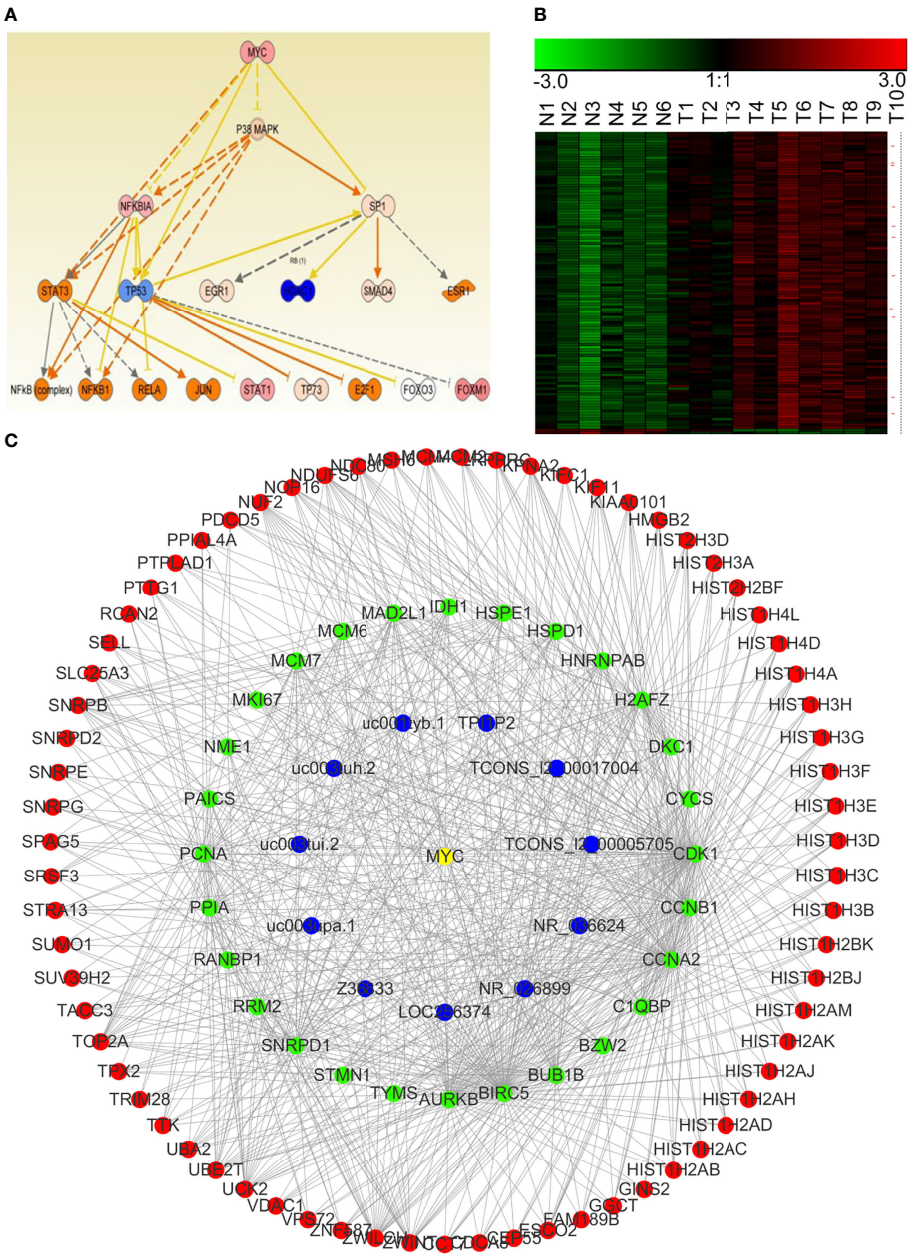

FIGURE 8 | The MYC-driven lncRNA–mRNA co-expression network module in NPC. **(A)** The regulatory model for MYC and the other transcription factors involved in NPC (obtained using IPA). **(B)** Expression of the potential mRNAs and lncRNAs downstream of MYC in NPC (red asterisk indicates lncRNAs). N, the control nasopharyngeal epithelium; T, nasopharyngeal carcinoma. **(C)** We generated a MYC-driven lncRNA–mRNA co-expression network module for NPC by integrating the IPA and the WGCNA results.

The ability to find true driving factors (lncRNAs) is the key to further success. Fortunately, we used gene chip technology to simultaneously obtain the mRNA expression profile while constructing the lncRNA expression profile of NPC, and most of the protein-coding genes were found to have functional annotations. This allowed us to cluster lncRNAs and mRNAs with similar expression patterns, which provided clues for the unknown functions of these lncRNAs.

WGCNA is a systematic biological algorithm to describe patterns of gene association between different samples (60). Compared with the traditional one-size-fits-all, hard-threshold algorithm, WGCNA sets a soft threshold and calculates the correlation coefficient weighting value, so that the connections between genes in the network obey scale-free networks. We found the sensible biological flexibility of the algorithm. We used the WGCNA algorithm to analyze the 1,275 differentially

expressed lncRNAs and 2,485 differentially expressed mRNAs in NPC, and found the co-expression correlations between 915 lncRNAs and 1,281 mRNAs. We constructed the first lncRNA–mRNA co-expression network of NPC, which contained 35,290 correlations. The network provides important information for studying the functions of new lncRNAs that drive NPC carcinogenesis.

Genomic instability is one of the biological characteristics of malignant tumors. The frequency of point mutations in the NPC genome is the lowest while variation in the copy number occurs widely in the NPC genome (61–63). There are two copies of genes on the autosomes, both of which may be transcribed in normal cells. If a chromosome segment is lost or amplified during carcinogenesis, the change in the chromosome may result in down-regulation or up-regulation of genes on the chromosome. In this article, we used GSEA to cluster the chromosomal positions of the differentially expressed RNAs in NPC and found that genes in the chromosome regions 12q24, 22p11, and 3q21 were significantly up-regulated, suggesting that these chromosome segments may be amplified. There may be oncogenes, including oncogenic lncRNAs, in these segments. Genes in the chromosome segments 3p21 and 11p15 were significantly down-regulated. The down-regulation of the tumor suppressor genes, including lncRNAs, in these two chromosome segments may be an initiating factor for NPC. This hypothesis is consistent with previous studies of genomic instability in NPC (64–68).

One of the most important ways for lncRNAs to exert their biological functions is to act as sponges by competitively adsorbing miRNAs, thus indirectly regulating the expression of other mRNAs (69–71). The ceRNA hypothesis was first proposed by Professor Pandolfi in 2011. He posited that RNA molecules (mRNAs or lncRNAs) share miRNA response elements, or miRNA-binding sites, may compete with miRNA, thereby regulating each other's expression and forming a large, complex ceRNA regulatory network in cells (48). The probes used in our gene chip were 60 mers that were not suitable for detecting miRNAs (~20 nt long). However, there are gene sets of miRNA target genes in the molecular signatures database (MSigDB) in GSEA. GSEA classifies genes by sharing an miRNA-binding site (47). Using GSEA, we successfully enriched a series of target genes that share binding sites for individual miRNAs. We combined those results with our WGCNA results to construct competitive endogenous lncRNA–mRNA co-expression modules. These modules provide important functional clues for future study of lncRNAs driving NPC. For example, miR-142-3p is an important tumor suppressor miRNA (72–74). Using GSEA and WGCNA, we suggest that a group of mRNAs and lncRNAs with similar expression trends in NPC may share a miR-142-3p-binding site. These newly identified lncRNAs may play an important role in the development of NPC by competing for miR-142-3p, thereby regulating some important mRNAs, such as *BIRC5*, *CDK1*, and *TOP2A*. Based on this finding, we propose further in-depth research using the co-expression networks to yield new discoveries about the mechanisms governing NPC.

We also performed a pathway enrichment analysis on differentially expressed genes in NPC using the KEGG. As expected, the p53 signaling pathway, cell cycle pathway, and pathways in cancer were most significantly enriched. The KEGG pathways in cancer refer to a large signaling pathway formed by the integration of multiple signaling pathways related to tumor development, including p53 and cell cycle pathways. Abnormal cell cycle regulation is a fundamental aspect of malignant tumors (75), and the *TP53* gene is one of the most important tumor suppressor genes. The p53 protein encoded by this gene is widely involved in the initiation and development of malignant tumors. The enrichment of these signal pathways in our analysis indicates that our results of gene chip are reliable. It also suggests that lncRNAs enriched in these signaling pathway modules, as indicated by GSEA and WGCNA, may be regulated by p53 or may participate in the regulation of the p53 signaling pathway (76). Similarly, we found potential core transcriptional regulatory factors that may drive the dysregulation of NPC transcriptome through IPA. Among these factors, MYC (77), p53, and E2F4 are important nuclear transcription factors that regulate expression levels of genes involved in cell cycle, apoptosis, metabolism, and other cell functions (78–81). For example, a series of important proteins, such as MAPK (82), NF-κB (83), and STAT3 (84), may be regulated by c-Myc (85); there are series of lncRNAs and mRNAs that are regulated by these proteins, which constitute complex lncRNA–mRNA co-expression network modules. The lncRNAs in these modules may also be important in NPC carcinogenesis.

Noteworthy, the core regulatory factors β-estradiol and ERBB2 were enriched according to the IPA. β-estradiol is an estrogen that activates the estrogen receptor and regulates the expression of downstream genes (86–89). The protein encoded by ERBB2 is the well-known oncoprotein HER-2 (90). β-estradiol and HER-2 have been known to be the main driving factors of breast cancer. The expression of estrogen receptor and HER-2 remain as the main criteria for the clinicopathological classification of breast cancer (86–90). However, their roles in NPC have not been well-studied. Recent reports suggest that the estrogen receptor may be a tumor suppressor gene, or a protective factor, in tumors such as gastric cancer (91). Given the lower estrogen levels in men, a role for the estrogen receptor as a tumor suppressor may be a contributing factor to the higher incidence of NPC in men than women (92). Therefore, β-estradiol- and HER-2-driven downstream lncRNA–mRNA regulatory modules, especially the lncRNAs, constitute an exciting new area of research into the pathogenesis of NPC.

In conclusion, the role of lncRNAs in the pathogenesis of NPC remains to be elucidated, and a large number of functional lncRNAs have not been thoroughly studied. For the first time, we constructed a co-expression network of lncRNAs and mRNAs in the transcriptome of NPC using bioinformatics and systematic biological methods. Through functional clustering and the enrichment of differentially expressed mRNAs in NPC, we identified functional modules with potential biological significance for carcinogenesis of NPC. These modules will aid in the discovery of key lncRNAs in NPC and will provide clues for the mechanistic study of novel lncRNAs.

DATA AVAILABILITY STATEMENT

The datasets presented in this study can be found in online repositories. The names of the repository/repositories and accession number(s) can be found in the article/**Supplementary Material**.

ETHICS STATEMENT

The tissue specimens were stored in liquid nitrogen. This study was authorized by the Ethics Committee of the Central South University. All patients provided written informed consent.

AUTHOR CONTRIBUTIONS

CF contributed to drafting and editing the manuscript. WX and HH designed, revised, and finalized the manuscript. FX, YT, and PL participated in the drafting. KZ, YM, and YW participated in the revision. SZ, ZG, QL, GL and ZZ, CG contributed to the literature search. All authors contributed toward data analysis, drafting, and revising and agreed to submit. All authors contributed to the article and approved the submitted version.

FUNDING

This work has been supported by the National Natural Science Foundation of China (81872278, 81803025 and 81972776), the Natural Science Foundation of Hunan Province (2018JJ3815, 2018SK21210, 2018SK21211), and open sharing fund for the large-scale instruments and equipments of Central South University(CSUZC202235).

SUPPLEMENTARY MATERIAL

The Supplementary Material for this article can be found online at: https://www.frontiersin.org/articles/10.3389/fonc.2022.809760/full#supplementary-material

Supplementary Table 2 | Upregulated and downregulated mRNA or lncRNAs.

Supplementary Table 3 | Clinical information of NPC patients.

REFERENCES

1. Zeng Z, Huang H, Zhang W, Xiang B, Zhou M, Zhou Y, et al. Nasopharyngeal Carcinoma: Advances in Genomics and Molecular Genetics. *Sci China Life Sci* (2011) 54(10):966–75. doi: 10.1007/s11427-011-4223-5
2. Wu C, Li M, Meng H, Liu Y, Niu W, Zhou Y, et al. Analysis of Status and Countermeasures of Cancer Incidence and Mortality in China. *Sci China Life Sci* (2019) 62(5):640–7. doi: 10.1007/s11427-018-9461-5
3. Chen YP, Chan ATC, Le QT, Blanchard P, Sun Y, Ma J. Nasopharyngeal Carcinoma. *Lancet* (2019) 394(10192):64–80. doi: 10.1016/S0140-6736(19)30956-0
4. Xiong F, Deng S, Huang HB, Li XY, Zhang WL, Liao QJ, et al. Effects and Mechanisms of Innate Immune Molecules on Inhibiting Nasopharyngeal Carcinoma. *Chin Med J (Engl)* (2019) 132(6):749–52. doi: 10.1097/CM9.0000000000000132
5. Yan Q, Zeng Z, Gong Z, Zhang W, Li X, He B, et al. EBV-miR-BART10-3p Facilitates Epithelial-Mesenchymal Transition and Promotes Metastasis of Nasopharyngeal Carcinoma by Targeting BTRC. *Oncotarget* (2015) 6(39):41766–82. doi: 10.18632/oncotarget.6155
6. Xiao K, Yu Z, Li X, Li X, Tang K, Tu C, et al. Genome-Wide Analysis of Epstein-Barr Virus (EBV) Integration and Strain in C666-1 and Raji Cells. *J Cancer* (2016) 7(2):214–24. doi: 10.7150/jca.13150
7. Zeng Z, Fan S, Zhang X, Li S, Zhou M, Xiong W, et al. Epstein-Barr Virus-Encoded Small RNA 1 (EBER-1) Could Predict Good Prognosis in Nasopharyngeal Carcinoma. *Clin Transl Oncol* (2016) 18(2):206–11. doi: 10.1007/s12094-015-1354-3
8. Tu C, Zeng Z, Qi P, Li X, Yu Z, Guo C, et al. Genome-Wide Analysis of 18 Epstein-Barr Viruses Isolated From Primary Nasopharyngeal Carcinoma Biopsy Specimens. *J Virol* (2017) 91(17):e00301-17. doi: 10.1128/JVI.00301-17
9. Fan C, Tang Y, Wang J, Xiong F, Guo C, Wang Y, et al. The Emerging Role of Epstein-Barr Virus Encoded microRNAs in Nasopharyngeal Carcinoma. *J Cancer* (2018) 9(16):2852–64. doi: 10.7150/jca.25460
10. Duan S, Guo W, Xu Z, He Y, Liang C, Mo Y, et al. Natural Killer Group 2d Receptor and Its Ligands in Cancer Immune Escape. *Mol Cancer* (2019) 18(1):29. doi: 10.1186/s12943-019-0956-8
11. Wu Y, Wei F, Tang L, Liao Q, Wang H, Shi L, et al. Herpesvirus Acts With the Cytoskeleton and Promotes Cancer Progression. *J Cancer* (2019) 10(10):2185–93. doi: 10.7150/jca.30222
12. Ren D, Hua Y, Yu B, Ye X, He Z, Li C, et al. Predictive Biomarkers and Mechanisms Underlying Resistance to PD1/PD-L1 Blockade Cancer Immunotherapy. *Mol Cancer* (2020) 19(1):19. doi: 10.1186/s12943-020-1144-6
13. Xiong W, Zeng ZY, Xia JH, Xia K, Shen SR, Li XL, et al. A Susceptibility Locus at Chromosome 3p21 Linked to Familial Nasopharyngeal Carcinoma. *Cancer Res* (2004) 64(6):1972–4. doi: 10.1158/0008-5472.can-03-3253
14. Zeng Z, Zhou Y, Zhang W, Li X, Xiong W, Liu H, et al. Family-Based Association Analysis Validates Chromosome 3p21 as a Putative Nasopharyngeal Carcinoma Susceptibility Locus. *Genet Med* (2006) 8(3):156–60. doi: 10.1097/01.gim.0000196821.87655.d0
15. Xiao L, Wei F, Liang F, Li Q, Deng H, Tan S, et al. TSC22D2 Identified as a Candidate Susceptibility Gene of Multi-Cancer Pedigree Using Genome-Wide Linkage Analysis and Whole-Exome Sequencing. *Carcinogenesis* (2019) 40(7):819–27. doi: 10.1093/carcin/bgz095
16. He Y, Jing Y, Wei F, Tang Y, Yang L, Luo J, et al. Long non-Coding RNA PVT1 Predicts Poor Prognosis and Induces Radioresistance by Regulating DNA Repair and Cell Apoptosis in Nasopharyngeal Carcinoma. *Cell Death Dis* (2018) 9(2):235. doi: 10.1038/s41419-018-0265-y
17. Tang L, Wei F, Wu Y, He Y, Shi L, Xiong F, et al. Role of Metabolism in Cancer Cell Radioresistance and Radiosensitization Methods. *J Exp Clin Cancer Res* (2018) 37(1):87. doi: 10.1186/s13046-018-0758-7
18. Wei F, Tang L, He Y, Wu Y, Shi L, Xiong F, et al. BPIFB1 (LPLUNC1) Inhibits Radioresistance in Nasopharyngeal Carcinoma by Inhibiting VTN Expression. *Cell Death Dis* (2018) 9(4):432. doi: 10.1038/s41419-018-0409-0
19. Ge J, Wang J, Wang H, Jiang X, Liao Q, Gong Q, et al. The BRAF V600E Mutation Is a Predictor of the Effect of Radioiodine Therapy in Papillary Thyroid Cancer. *J Cancer* (2020) 11(4):932–9. doi: 10.7150/jca.33105
20. Zhang W, Huang C, Gong Z, Zhao Y, Tang K, Li X, et al. Expression of LINC00312, a Long Intergenic Non-Coding RNA, Is Negatively Correlated With Tumor Size But Positively Correlated With Lymph Node Metastasis in Nasopharyngeal Carcinoma. *J Mol Histol* (2013) 44(5):545–54. doi: 10.1007/s10735-013-9503-x
21. He B, Li W, Wu Y, Wei F, Gong Z, Bo H, et al. Epstein-Barr Virus-Encoded miR-BART6-3p Inhibits Cancer Cell Metastasis and Invasion by Targeting Long non-Coding RNA Loc553103. *Cell Death Dis* (2016) 7(9):e2353. doi: 10.1038/cddis.2016.253
22. Deng X, Xiong F, Li X, Xiang B, Li Z, Wu X, et al. Application of Atomic Force Microscopy in Cancer Research. *J Nanobiotechnol* (2018) 16(1):102. doi: 10.1186/s12951-018-0428-0

23. Tang Y, He Y, Zhang P, Wang J, Fan C, Yang L, et al. LncRNAs Regulate the Cytoskeleton and Related Rho/ROCK Signaling in Cancer Metastasis. *Mol Cancer* (2018) 17(1):77. doi: 10.1186/s12943-018-0825-x
24. Wei F, Wu Y, Tang L, He Y, Shi L, Xiong F, et al. BPIFB1 (LPLUNC1) Inhibits Migration and Invasion of Nasopharyngeal Carcinoma by Interacting With VTN and VIM. *Br J Cancer* (2018) 118(2):233–47. doi: 10.1038/bjc.2017.385
25. Zeng Z, Zhou Y, Xiong W, Luo X, Zhang W, Li X, et al. Analysis of Gene Expression Identifies Candidate Molecular Markers in Nasopharyngeal Carcinoma Using Microdissection and cDNA Microarray. *J Cancer Res Clin Oncol* (2007) 133(2):71–81. doi: 10.1007/s00432-006-0136-2
26. Zeng ZY, Zhou YH, Zhang WL, Xiong W, Fan SQ, Li XL, et al. Gene Expression Profiling of Nasopharyngeal Carcinoma Reveals the Abnormally Regulated Wnt Signaling Pathway. *Hum Pathol* (2007) 38(1):120–33. doi: 10.1016/j.humpath.2006.06.023
27. Zeng Z, Huang H, Huang L, Sun M, Yan Q, Song Y, et al. Regulation Network and Expression Profiles of Epstein-Barr Virus-Encoded microRNAs and Their Potential Target Host Genes in Nasopharyngeal Carcinomas. *Sci China Life Sci* (2014) 57(3):315–26. doi: 10.1007/s11427-013-4577-y
28. Wang YA, Li XL, Mo YZ, Fan CM, Tang L, Xiong F, et al. Effects of Tumor Metabolic Microenvironment on Regulatory T Cells. *Mol Cancer* (2018) 17 (1):168. doi: 10.1186/s12943-018-0913-y
29. Gong Z, Zhang S, Zhang W, Huang H, Li Q, Deng H, et al. Long Non-Coding RNAs in Cancer. *Sci China Life Sci* (2012) 55(12):1120–4. doi: 10.1007/s11427-012-4413-9
30. Yu J, Liu Y, Gong Z, Zhang S, Guo C, Li X, et al. Overexpression Long Non-Coding RNA LINC00673 is Associated With Poor Prognosis and Promotes Invasion and Metastasis in Tongue Squamous Cell Carcinoma. *Oncotarget* (2017) 8(10):16621–32. doi: 10.18632/oncotarget.14200
31. Yu J, Liu Y, Guo C, Zhang S, Gong Z, Tang Y, et al. Upregulated Long Non-Coding RNA LINC00152 Expression Is Associated With Progression and Poor Prognosis of Tongue Squamous Cell Carcinoma. *J Cancer* (2017) 8 (4):523–30. doi: 10.7150/jca.17510
32. Zhao Y, Li H, Fang S, Kang Y, Wu W, Hao Y, et al. NONCODE 2016: An Informative and Valuable Data Source of Long Non-Coding RNAs. *Nucleic Acids Res* (2016) 44(D1):D203–208. doi: 10.1093/nar/gkv1252
33. Fan C, Tang Y, Wang J, Xiong F, Guo C, Wang Y, et al. Role of Long Non-Coding RNAs in Glucose Metabolism in Cancer. *Mol Cancer* (2017) 16 (1):130. doi: 10.1186/s12943-017-0699-3
34. Tang Y, Wang J, Lian Y, Fan C, Zhang P, Wu Y, et al. Linking Long non-Coding RNAs and SWI/SNF Complexes to Chromatin Remodeling in Cancer. *Mol Cancer* (2017) 16(1):42. doi: 10.1186/s12943-017-0612-0
35. Wang Y, Mo Y, Yang X, Zhou R, Wu Z, He Y, et al. Long non-Coding RNA AFAP1-AS1 Is a Novel Biomarker in Various Cancers: A Systematic Review and Meta-Analysis Based on the Literature and GEO Datasets. *Oncotarget* (2017) 8(60):102346–60. doi: 10.18632/oncotarget.21830
36. Yang L, Tang Y, Xiong F, He Y, Wei F, Zhang S, et al. LncRNAs Regulate Cancer Metastasis *via* Binding to Functional Proteins. *Oncotarget* (2018) 9 (1):1426–43. doi: 10.18632/oncotarget.22840
37. Wu P, Mo Y, Peng M, Tang T, Zhong Y, Deng X, et al. Emerging Role of Tumor-Related Functional Peptides Encoded by lncRNA and circRNA. *Mol Cancer* (2020) 19(1):22. doi: 10.1186/s12943-020-1147-3
38. Bo H, Gong Z, Zhang W, Li X, Zeng Y, Liao Q, et al. Upregulated Long Non-Coding RNA AFAP1-AS1 Expression Is Associated With Progression and Poor Prognosis of Nasopharyngeal Carcinoma. *Oncotarget* (2015) 6 (24):20404–18. doi: 10.18632/oncotarget.4057
39. Tang Y, He Y, Shi L, Yang L, Wang J, Lian Y, et al. Co-Expression of AFAP1-AS1 and PD-1 Predicts Poor Prognosis in Nasopharyngeal Carcinoma. *Oncotarget* (2017) 8(24):39001–11. doi: 10.18632/oncotarget.16545
40. Yang L, Tang Y, He Y, Wang Y, Lian Y, Xiong F, et al. High Expression of LINC01420 Indicates an Unfavorable Prognosis and Modulates Cell Migration and Invasion in Nasopharyngeal Carcinoma. *J Cancer* (2017) 8 (1):97–103. doi: 10.7150/jca.16819
41. Lian Y, Xiong F, Yang L, Bo H, Gong Z, Wang Y, et al. Long Noncoding RNA AFAP1-AS1 Acts as a Competing Endogenous RNA of miR-423-5p to Facilitate Nasopharyngeal Carcinoma Metastasis Through Regulating the Rho/Rac Pathway. *J Exp Clin Cancer Res* (2018) 37(1):253. doi: 10.1186/s13046-018-0918-9
42. Fan C, Tang Y, Wang J, Wang Y, Xiong F, Zhang S, et al. Long Non-Coding RNA LOC284454 Promotes Migration and Invasion of Nasopharyngeal Carcinoma *via* Modulating the Rho/Rac Signaling Pathway. *Carcinogenesis* (2019) 40(2):380–91. doi: 10.1093/carcin/bgy143
43. Zhou Y, Zeng Z, Zhang W, Xiong W, Li X, Zhang B, et al. Identification of Candidate Molecular Markers of Nasopharyngeal Carcinoma by Microarray Analysis of Subtracted cDNA Libraries Constructed by Suppression Subtractive Hybridization. *Eur J Cancer Prev* (2008) 17(6):561–71. doi: 10.1097/CEJ.0b013e328305a0e8
44. Song Y, Li X, Zeng Z, Li Q, Gong Z, Liao Q, et al. Epstein-Barr Virus Encoded miR-BART11 Promotes Inflammation-Induced Carcinogenesis by Targeting Foxp1. *Oncotarget* (2016) 7(24):36783–99. doi: 10.18632/oncotarget.9170
45. He R, Liu P, Xie X, Zhou Y, Liao Q, Xiong W, et al. Circgfra1 and GFRA1 Act as ceRNAs in Triple Negative Breast Cancer by Regulating miR-34a. *J Exp Clin Cancer Res* (2017) 36(1):145. doi: 10.1186/s13046-017-0614-1
46. Zhong Y, Du Y, Yang X, Mo Y, Fan C, Xiong F, et al. Circular RNAs Function as ceRNAs to Regulate and Control Human Cancer Progression. *Mol Cancer* (2018) 17(1):79. doi: 10.1186/s12943-018-0827-8
47. Subramanian A, Tamayo P, Mootha VK, Mukherjee S, Ebert BL, Gillette MA, et al. Gene Set Enrichment Analysis: A Knowledge-Based Approach for Interpreting Genome-Wide Expression Profiles. *Proc Natl Acad Sci U S A* (2005) 102(43):15545–50. doi: 10.1073/pnas.0506580102
48. Karreth FA, Tay Y, Perna D, Ala U, Tan SM, Rust AG, et al. *In Vivo* Identification of Tumor- Suppressive PTEN ceRNAs in an Oncogenic BRAF-Induced Mouse Model of Melanoma. *Cell* (2011) 147(2):382–95. doi: 10.1016/j.cell.2011.09.032
49. Zhang W, Zeng Z, Fan S, Wang J, Yang J, Zhou Y, et al. Evaluation of the Prognostic Value of TGF-Beta Superfamily Type I Receptor and TGF-Beta Type II Receptor Expression in Nasopharyngeal Carcinoma Using High-Throughput Tissue Microarrays. *J Mol Histol* (2012) 43(3):297–306. doi: 10.1007/s10735-012-9392-4
50. Zhang B, Horvath S. A General Framework for Weighted Gene Co-Expression Network Analysis. *Stat Appl Genet Mol Biol* (2005) 4:Article17. doi: 10.2202/1544-6115.1128
51. Jimenez-Marin A, Collado-Romero M, Ramirez-Boo M, Arce C, Garrido JJ. Biological Pathway Analysis by ArrayUnlock and Ingenuity Pathway Analysis. *BMC Proc* (2009) 3 Suppl 4:S6. doi: 10.1186/1753-6561-3-S4-S6
52. Bo H, Fan L, Li J, Liu Z, Zhang S, Shi L, et al. High Expression of lncRNA AFAP1-AS1 Promotes the Progression of Colon Cancer and Predicts Poor Prognosis. *J Cancer* (2018) 9(24):4677–83. doi: 10.7150/jca.26461
53. Bo H, Fan L, Gong Z, Liu Z, Shi L, Guo C, et al. Upregulation and Hypomethylation of lncRNA AFAP1AS1 Predicts a Poor Prognosis and Promotes the Migration and Invasion of Cervical Cancer. *Oncol Rep* (2019) 41(4):2431–9. doi: 10.3892/or.2019.7027
54. Wei F, Jing YZ, He Y, Tang YY, Yang LT, Wu YF, et al. Cloning and Characterization of the Putative AFAP1-AS1 Promoter Region. *J Cancer* (2019) 10(5):1145–53. doi: 10.7150/jca.29049
55. Yang QQ, Deng YF. Genome-Wide Analysis of Long Non-Coding RNA in Primary Nasopharyngeal Carcinoma by Microarray. *Histopathology* (2015) 66 (7):1022–30. doi: 10.1111/his.12616
56. Li G, Liu Y, Liu C, Su Z, Ren S, Wang Y, et al. Genome-Wide Analyses of Long Noncoding RNA Expression Profiles Correlated With Radioresistance in Nasopharyngeal Carcinoma *via* Next-Generation Deep Sequencing. *BMC Cancer* (2016) 16:719. doi: 10.1186/s12885-016-2755-6
57. Zhang B, Wang D, Wu J, Tang J, Chen W, Chen X, et al. Expression Profiling and Functional Prediction of Long Noncoding RNAs in Nasopharyngeal Nonkeratinizing Carcinoma. *Discov Med* (2016) 21(116):239–50.
58. Gong Z, Yang Q, Zeng Z, Zhang W, Li X, Zu X, et al. An Integrative Transcriptomic Analysis Reveals P53 Regulated miRNA, mRNA, and lncRNA Networks in Nasopharyngeal Carcinoma. *Tumour Biol* (2016) 37(3):3683–95. doi: 10.1007/s13277-015-4156-x
59. Xu K, Xiong W, Zhou M, Wang H, Yang J, Li X, et al. Integrating ChIP-Sequencing and Digital Gene Expression Profiling to Identify BRD7 Downstream Genes and Construct Their Regulating Network. *Mol Cell Biochem* (2016) 411(1-2):57–71. doi: 10.1007/s11010-015-2568-y
60. Presson AP, Sobel EM, Papp JC, Suarez CJ, Whistler T, Rajeevan MS, et al. Integrated Weighted Gene Co-Expression Network Analysis With an Application to Chronic Fatigue Syndrome. *BMC Syst Biol* (2008) 2:95. doi: 10.1186/1752-0509-2-95

61. Tu C, Zeng Z, Qi P, Li X, Guo C, Xiong F, et al. Identification of Genomic Alterations in Nasopharyngeal Carcinoma and Nasopharyngeal Carcinoma-Derived Epstein-Barr Virus by Whole-Genome Sequencing. *Carcinogenesis* (2018) 39(12):1517–28. doi: 10.1093/carcin/bgy108
62. Jiang X, Wang J, Deng X, Xiong F, Ge J, Xiang B, et al. Role of the Tumor Microenvironment in PD-L1/PD-1-Mediated Tumor Immune Escape. *Mol Cancer* (2019) 18(1):10. doi: 10.1186/s12943-018-0928-4
63. Peng M, Mo Y, Wang Y, Wu P, Zhang Y, Xiong F, et al. Neoantigen Vaccine: An Emerging Tumor Immunotherapy. *Mol Cancer* (2019) 18(1):128. doi: 10.1186/s12943-019-1055-6
64. Fang Y, Guan X, Guo Y, Sham J, Deng M, Liang Q, et al. Analysis of Genetic Alterations in Primary Nasopharyngeal Carcinoma by Comparative Genomic Hybridization. *Genes Chromosomes Cancer* (2001) 30(3):254–60. doi: 10.1002/1098-2264(2000)9999:9999<::aid-gcc1086>3.0.co;2-d
65. Or YY, Hui AB, Tam KY, Huang DP, Lo KW. Characterization of Chromosome 3q and 12q Amplicons in Nasopharyngeal Carcinoma Cell Lines. *Int J Oncol* (2005) 26(1):49–56. doi: 10.3892/ijo.26.1.49
66. Li X, Wang E, Zhao YD, Ren JQ, Jin P, Yao KT, et al. Chromosomal Imbalances in Nasopharyngeal Carcinoma: A Meta-Analysis of Comparative Genomic Hybridization Results. *J Transl Med* (2006) 4:4. doi: 10.1186/1479-5876-4-4
67. Lee CH, Fang CY, Sheu JJ, Chang Y, Takada K, Chen JY. Amplicons on Chromosome 3 Contain Oncogenes Induced by Recurrent Exposure to 12-O-Tetradecanoylphorbol-13-Acetate and Sodium N-Butyrate and Epstein-Barr Virus Reactivation in a Nasopharyngeal Carcinoma Cell Line. *Cancer Genet Cytogenet* (2008) 185(1):1–10. doi: 10.1016/j.cancergencyto.2008.03.014
68. Natasya Naili MN, Hasnita CH, Shamim AK, Hasnan J, Fauziah MI, Narazah MY, et al. Chromosomal Alterations in Malaysian Patients With Nasopharyngeal Carcinoma Analyzed by Comparative Genomic Hybridization. *Cancer Genet Cytogenet* (2010) 203(2):309–12. doi: 10.1016/j.cancergencyto.2010.07.136
69. Zhou R, Wu Y, Wang W, Su W, Liu Y, Wang Y, et al. Circular RNAs (circRNAs) in Cancer. *Cancer Lett* (2018) 425:134–42. doi: 10.1016/j.canlet.2018.03.035
70. Fan CM, Wang JP, Tang YY, Zhao J, He SY, Xiong F, et al. Circman1a2 Could Serve as a Novel Serum Biomarker for Malignant Tumors. *Cancer Sci* (2019) 110(7):2180–8. doi: 10.1111/cas.14034
71. Wang W, Zhou R, Wu Y, Liu Y, Su W, Xiong W, et al. PVT1 Promotes Cancer Progression *via* MicroRNAs. *Front Oncol* (2019) 9:609. doi: 10.3389/fonc.2019.00609
72. Lei Z, Xu G, Wang L, Yang H, Liu X, Zhao J, et al. MiR-142-3p Represses TGF-Beta-Induced Growth Inhibition Through Repression of TGFbetaR1 in non-Small Cell Lung Cancer. *FASEB J* (2014) 28(6):2696–704. doi: 10.1096/fj.13-247288
73. Godfrey JD, Morton JP, Wilczynska A, Sansom OJ, Bushell MD. MiR-142-3p is Downregulated in Aggressive P53 Mutant Mouse Models of Pancreatic Ductal Adenocarcinoma by Hypermethylation of its Locus. *Cell Death Dis* (2018) 9(6):644. doi: 10.1038/s41419-018-0628-4
74. Lu Y, Gao J, Zhang S, Gu J, Lu H, Xia Y, et al. miR-142-3p Regulates Autophagy by Targeting ATG16L1 in Thymic-Derived Regulatory T Cell (Ttreg). *Cell Death Dis* (2018) 9(3):290. doi: 10.1038/s41419-018-0298-2
75. Zhang W, Zeng Z, Zhou Y, Xiong W, Fan S, Xiao L, et al. Identification of Aberrant Cell Cycle Regulation in Epstein-Barr Virus-Associated Nasopharyngeal Carcinoma by cDNA Microarray and Gene Set Enrichment Analysis. *Acta Biochim Biophys Sin (Shanghai)* (2009) 41(5):414–28. doi: 10.1093/abbs/gmp025
76. Gong Z, Zhang S, Zeng Z, Wu H, Yang Q, Xiong F, et al. LOC401317, a P53-Regulated Long Non-Coding RNA, Inhibits Cell Proliferation and Induces Apoptosis in the Nasopharyngeal Carcinoma Cell Line Hne2. *PLos One* (2014) 9(11):e110674. doi: 10.1371/journal.pone.0110674
77. Jin K, Wang S, Zhang Y, Xia M, Mo Y, Li X, et al. Long non-Coding RNA PVT1 Interacts With MYC and its Downstream Molecules to Synergistically Promote Tumorigenesis. *Cell Mol Life Sci* (2019) 76(21):4275–89. doi: 10.1007/s00018-019-03222-1
78. Fan C, Tu C, Qi P, Guo C, Xiang B, Zhou M, et al. GPC6 Promotes Cell Proliferation, Migration, and Invasion in Nasopharyngeal Carcinoma. *J Cancer* (2019) 10(17):3926–32. doi: 10.7150/jca.31345
79. Mo Y, Wang Y, Xiong F, Ge X, Li Z, Li X, et al. Proteomic Analysis of the Molecular Mechanism of Lovastatin Inhibiting the Growth of Nasopharyngeal Carcinoma Cells. *J Cancer* (2019) 10(10):2342–9. doi: 10.7150/jca.30454
80. Mo Y, Wang Y, Zhang L, Yang L, Zhou M, Li X, et al. The Role of Wnt Signaling Pathway in Tumor Metabolic Reprogramming. *J Cancer* (2019) 10(16):3789–97. doi: 10.7150/jca.31166
81. Xia M, Zhang Y, Jin K, Lu Z, Zeng Z, Xiong W. Communication Between Mitochondria and Other Organelles: A Brand-New Perspective on Mitochondria in Cancer. *Cell Biosci* (2019) 9:27. doi: 10.1186/s13578-019-0289-8
82. Yang Y, Liao Q, Wei F, Li X, Zhang W, Fan S, et al. LPLUNC1 Inhibits Nasopharyngeal Carcinoma Cell Growth *via* Down-Regulation of the MAP Kinase and Cyclin D1/E2F Pathways. *PLos One* (2013) 8(5):e62869. doi: 10.1371/journal.pone.0062869
83. Yi M, Cai J, Li J, Chen S, Zeng Z, Peng Q, et al. Rediscovery of NF-kappaB Signaling in Nasopharyngeal Carcinoma: How Genetic Defects of NF-kappaB Pathway Interplay With EBV in Driving Oncogenesis? *J Cell Physiol* (2018) 233(8):5537–49. doi: 10.1002/jcp.26410
84. Liao Q, Zeng Z, Guo X, Li X, Wei F, Zhang W, et al. LPLUNC1 Suppresses IL-6-Induced Nasopharyngeal Carcinoma Cell Proliferation *via* Inhibiting the Stat3 Activation. *Oncogene* (2014) 33(16):2098–109. doi: 10.1038/onc.2013.161
85. Zhang Y, Xia M, Jin K, Wang S, Wei H, Fan C, et al. Function of the C-Met Receptor Tyrosine Kinase in Carcinogenesis and Associated Therapeutic Opportunities. *Mol Cancer* (2018) 17(1):45. doi: 10.1186/s12943-018-0796-y
86. Achinger-Kawecka J, Valdes-Mora F, Luu PL, Giles KA, Caldon CE, Qu W, et al. Epigenetic Reprogramming at Estrogen-Receptor Binding Sites Alters 3d Chromatin Landscape in Endocrine-Resistant Breast Cancer. *Nat Commun* (2020) 11(1):320. doi: 10.1038/s41467-019-14098-x
87. Wu J, Yan J, Fang P, Zhou HB, Liang K, Huang J. Three-Dimensional Oxabicycloheptene Sulfonate Targets the Homologous Recombination and Repair Programmes Through Estrogen Receptor Alpha Antagonism. *Cancer Lett* (2020) 469:78–88. doi: 10.1016/j.canlet.2019.10.019
88. Xiao Y, Liu G, Sun Y, Gao Y, Ouyang X, Chang C, et al. Targeting the Estrogen Receptor Alpha (ERalpha)-Mediated circ-SMG1.72/miR-141-3p/Gelsolin Signaling to Better Suppress the HCC Cell Invasion. *Oncogene* (2020) 39(12):2493–508. doi: 10.1038/s41388-019-1150-6
89. Xu G, Chhangawala S, Cocco E, Razavi P, Cai Y, Otto JE, et al. ARID1A Determines Luminal Identity and Therapeutic Response in Estrogen-Receptor-Positive Breast Cancer. *Nat Genet* (2020) 52(2):198–207. doi: 10.1038/s41588-019-0554-0
90. Prat A, Pascual T, De Angelis C, Gutierrez C, Llombart-Cussac A, Wang T, et al. HER2-Enriched Subtype and ERBB2 Expression in HER2-Positive Breast Cancer Treated With Dual HER2 Blockade. *J Natl Cancer Inst* (2020) 112(1):46–54. doi: 10.1093/jnci/djz042
91. Kang MH, Choi H, Oshima M, Cheong JH, Kim S, Lee JH, et al. Estrogen-Related Receptor Gamma Functions as a Tumor Suppressor in Gastric Cancer. *Nat Commun* (2018) 9(1):1920–32. doi: 10.1038/s41467-018-04244-2
92. Wei F, Wu Y, Tang L, Xiong F, Guo C, Li X, et al. Trend Analysis of Cancer Incidence and Mortality in China. *Sci China Life Sci* (2017) 60(11):1271–5. doi: 10.1007/s11427-017-9172-6

Conflict of Interest: The authors declare that the research was conducted in the absence of any commercial or financial relationships that could be construed as a potential conflict of interest.

frontiers | Frontiers in Oncology

SYSTEMATIC REVIEW
published: 12 July 2022
doi: 10.3389/fonc.2022.843675

A Systematic Review and Meta-Analysis of Studies Comparing Concurrent Chemoradiotherapy With Radiotherapy Alone in the Treatment of Stage II Nasopharyngeal Carcinoma

Yao-Can Xu[1], *Kai-Hua Chen*[1], *Zhong-Guo Liang*[1] *and Xiao-Dong Zhu*[1,2*]

[1] *Department of Radiation Oncology, Affiliated Tumor Hospital of Guangxi Medical University, Nanning, China,* [2] *Department of Oncology, Affiliated Wu-Ming Hospital of Guangxi Medical University, Nanning, China*

OPEN ACCESS

Edited by:
Shan Shan Guo,
Sun Yat-sen University Cancer Center (SYSUCC), China

Reviewed by:
Maria Grazia Ghi,
Veneto Institute of Oncology (IRCCS), Italy
Feng Mei,
Sichuan Cancer Hospital, China

***Correspondence:**
Xiao-Dong Zhu
zhuxdonggxmu@126.com

Specialty section:
This article was submitted to Head and Neck Cancer, a section of the journal Frontiers in Oncology

Received: *26 December 2021*
Accepted: *31 May 2022*
Published: *12 July 2022*

Citation:
Xu Y-C, Chen K-H, Liang Z-G and Zhu X-D (2022) A Systematic Review and Meta-Analysis of Studies Comparing Concurrent Chemoradiotherapy With Radiotherapy Alone in the Treatment of Stage II Nasopharyngeal Carcinoma. Front. Oncol. 12:843675. doi: 10.3389/fonc.2022.843675

Purpose: The role of concurrent chemoradiotherapy (CCRT) in stage II nasopharyngeal carcinoma (NPC) is still controversial. Our objective is to evaluate the value of concurrent chemotherapy in stage II NPC receiving radiotherapy (RT).

Methods: We searched the PubMed, Embase, and Scopus databases for studies comparing CCRT versus RT alone in stage II NPC with survival outcomes and toxicities, including locoregional recurrence-free survival (LRFS), metastasis-free survival (DMFS), progression-free survival (PFS), overall survival (OS), and grade 3–4 acute toxicities. The hazard ratios (HRs) of survival outcomes and risk ratios (RRs) of toxicities were extracted for meta-analysis. Subgroup analysis for stage N1 patients was performed to further explore whether these populations can earn benefits from concurrent chemotherapy.

Results: Nine eligible studies with a total of 4,092 patients were included. CCRT was associated with a better OS (HR = 0.61, 95% CI 0.44–0.82), LRFS (HR = 0.62, 95% CI 0.50–0.78), and PFS (HR = 0.65, 95% CI 0.54–0.79), but with similar DMFS (HR = 0.81, 95% CI = 0.46–1.45) compared with two-dimensional RT (2DRT) alone. However, CCRT showed no survival benefit in terms of OS (HR = 0.84, 95% CI 0.62–1.15), LRFS (HR = 0.85, 95% CI 0.54–1.34), DMFS (HR = 0.96, 95% CI 0.60–1.54), and PFS (HR = 0.96, 95% CI 0.66–1.37) compared with intensity-modulated RT (IMRT) alone. Subgroup analyses indicated that CCRT had similar OS (HR = 1.04, 95% CI 0.37–2.96), LRFS (HR = 0.70, 95% CI 0.34–1.45), DMFS (HR = 1.03, 95% CI 0.53–2.00), and PFS (HR = 1.04, 95% CI 0.58–1.88) in the stage N1 populations. Meanwhile, compared to RT alone, CCRT significantly increased the incidence of grade 3–4 leukopenia (RR = 4.00, 95% CI 2.29–6.97), mucositis (RR = 1.43, 95% CI 1.16–1.77), and gastrointestinal reactions (RR = 8.76, 95% CI 2.63–29.12). No significant differences of grade 3–4 toxicity in thrombocytopenia (RR = 3.45, 95% CI 0.85–13.94) was found between the two groups.

Conclusion: For unselected patients with stage II NPC, CCRT was superior to 2DRT alone with better LRFS, PFS, and OS, while adding concurrent chemotherapy to IMRT did not significantly improve survival but exacerbated acute toxicities.

Systematic Review Registration: https://www.crd.york.ac.uk/PROSPERO/, identifier CRD42022318253.

Keywords: stage II, nasopharyngeal carcinoma, chemotherapy, radiotherapy, meta-analysis

BACKGROUND

Nasopharyngeal carcinoma (NPC) is one of the major cancers within Southeastern Asia (1), with an annual incidence rate of 10 to 30 per 100,000 among these prevalence regions (2). Over 20% of patients present with stage II NPC at initial diagnosis (3). Radiotherapy (RT) is the main radical treatment for NPC and has brought outstanding disease control (4). Studies have shown that chemotherapy played a significant role in stage III–IVA patients (5, 6), while stage I patients cannot earn benefits from concurrent chemotherapy (7). However, the role of concurrent chemotherapy in stage II NPC remains controversial.

There are two small-sample prospective studies (8, 9) comparing concurrent chemoradiation (CCRT) with RT alone in stage II NPC patients. Among these two studies, the study (9) using two-dimensional radiotherapy (2DRT) technology reached positive results with better 10-year metastasis-free survival (DMFS), progression-free survival (PFS), overall survival (OS), and cancer-specific survival (CSS), in the CCRT group, while the other study (8) using IMRT technology obtained negative results with no survival benefit but higher hematological toxicity. However, multiple retrospective studies that compared CCRT with 2DRT alone or IMRT alone showed opposite results. Xu et al. (10) found that, compared with 2DRT, CCRT had no role in improving OS, DMFS, and PFS in stage II NPC patients, but it increased the incidence of acute adverse events. Ahmed et al. (11) reported that CCRT was superior to IMRT alone with significant benefits in OS. A systematic review (12) on treatment patterns for stage II NPC indicated that IMRT alone may be sufficient, but more aggressive treatment interventions may be needed for the T2N1M0 subgroup which has poorer survival outcomes than those in the T1N1M0 or T2N0M0 subgroup. In addition, there are three meta-analyses (13–15) evaluating the role of chemotherapy adding to RT alone for stage II NPC. Regrettably, patients with stage I/III or receiving CCRT combined with induction chemotherapy (IC) or adjuvant chemotherapy (AC) were included. The actual value of concurrent chemotherapy adding to RT is still uncertain. Therefore, we performed this meta-analysis to evaluate the benefit of concurrent chemotherapy on stage II NPC patients receiving RT.

We present the following article in accordance with the PRISMA reporting checklist (16) (**eTable 1 in the Supplement**).

METHODS

Search Strategy

A systematic electronic search of PubMed, Embase, and Scopus databases was performed for literature published from January 1, 1990, to December 20, 2021. The detailed search strategy is presented in **eTable 2 in the Supplement**. Furthermore, we also searched relevant studies registered on ClinicalTrials.gov. A manual search of reference lists from all available reviews was conducted to identify the ultimate selection. Two investigators (Y-CX and Z-GL) independently carried out the literature retrieval.

Selection Criteria

Studies that met the following preset specific criteria were included: (a) original English articles published in peer-reviewed journals; (b) studies that compared CCRT versus radiotherapy alone in stage II NPC patients; and (c) studies must contain time-to-event data such as locoregional recurrence-free survival (LRFS), PFS, DMFS, or OS, which could be obtained directly from the article or extracted indirectly through the method introduced by Tierney et al. (17). The LRFS was the time from the date of diagnosis to the date of first local and/or regional failure. The DMFS was considered as the interval from the date of the diagnosis to the date of distant metastasis. The PFS was defined as the interval from the date of the diagnosis to disease progression. The OS was defined as the duration from the date of diagnosis to the date of death for any reason. The exclusion criteria were as follows: (a) conference abstracts, case reports, and reviews and (b) studies involving patients who received IC and AC.

Data Extraction and Literature Quality Assessment

Two investigators (Y-CX and Z-GL) evaluated the relevant articles according to the eligible criteria independently then extracted OS, DMFS, LRRFS, PFS, and grade 3–4 acute toxicity (leukopenia, thrombocytopenia, mucositis, gastrointestinal reactions) data from the included article, evaluated the quality of the included literature, and cross-checked the extracted data. Disagreements were resolved through discussion among the two investigators or consulting a third researcher (K-HC) to reach an agreement.

The quality of randomized controlled trial (RCT) was evaluated using the revised Cochrane risk-of-bias tool for randomized trials (RoB2) (18). The tool evaluates the risk of bias in individual RCT based on six domains: the randomization process, deviations from intended interventions, missing outcome data, measurement of the outcome, and selection of the reported result. Overall bias will be considered as low risk of bias, some concerns, or high risk of bias. Any domain-level

judgement reaching a high risk of bias will result in overall high risk of bias. Some concerns for any individual domain will eventually contribute to the overall evaluation of the paper being identified as some concerns or high risk of bias. The quality of retrospective studies was assessed by the modified Newcastle–Ottawa scale assessment criteria, which comprises eight items: representativeness of the exposed cohort, selection of the non-exposed cohort, ascertainment of exposure, a demonstration that outcome of interest was not present at the start of the study, comparability of cohorts on the basis of the design or analysis, assessment of outcome, if follow-up was longer enough for outcomes to occur, and adequacy of follow-up of cohorts.

Statistical Analysis

This meta-analysis was performed with Review Manager 5.3 software. To assess survival outcomes (OS, DMFS, LRRFS, PFS) and grade 3–4 acute toxicities (leukopenia, thrombocytopenia, mucositis, gastrointestinal reactions) between CCRT and RT alone, the HRs and relative ratios (RRs) with 95% CIs were pooled, respectively. Heterogeneity between included studies was assessed with the χ^2 heterogeneity test. I^2 values of 25%, 50%, and 75% were considered as low, moderate, and high heterogeneity, respectively. The fixed-effect model was employed for meta-analysis if the heterogeneity test revealed no important heterogeneity between studies ($P > 0.10$, $I^2 < 50\%$); otherwise, the random-effect model was applied. When the HR or RR was less than 1, it indicated a better survival outcome or safety in the CCRT group. If the 95% CI did not contain the value 1, it suggested that there was a significant difference in the statistics. Sensitivity analysis was applied to assess the stability of the survival results.

According to the Cochrane Handbook for Systematic Reviews of Interventions, we did not assess publication bias because only nine studies were included in the meta-analysis, and it was not possible to assess publication bias employing a funnel plot.

RESULTS

Characteristics and Quality of Included Studies

Totally 1,009 items, including 435 from PubMed, 287 from Embase, and 287 from Scopus, were obtained after the initial search. After duplication removal, 602 studies were retrieved. Only 22 studies remained after the titles and abstracts were assessed. Among the remaining 22 studies, six studies (19–24) involving patients with adjuvant or neoadjuvant chemotherapy were excluded, another six studies (25–30) involving patients with stage I or III were eliminated, and one study (31) with insufficient data was also eliminated (**Figure 1**). Nine studies were finally included, two of which were RCTs (8, 9), and the rest were retrospective studies (10, 11, 32–36). A total of 4,092 patients were enrolled, 2,462 received CCRT, and 1,632 received RT alone. There are four studies (9, 10, 32, 34) with a total of 2,490 patients that investigated 2DRT combined with concurrent chemotherapy, and 7 studies (8, 11, 32–36) with 1,602 patients that explored IMRT plus concurrent chemotherapy (**Table 1**). According to RoB2 assessment criteria, the overall risk of bias was low for the two included RCTs (**Figure 2**). According to the Newcastle–Ottawa Scale assessment criteria, four retrospective studies received eight stars, and the other three got nine stars (**Table 2**).

Survival Outcomes

Six studies directly provided HR values and 95%CI of time-to-event data, and the other three studies (8, 10, 33) did not provide HR values but provided survival curves. The method recommended by Tierney was used to extract HR and 95% CI from survival curves. OS data were available in all included studies.

Based on different radiotherapy techniques, the included studies were separated into two categories and meta-analyses were performed respectively. It revealed that, for stage II NPC patients undergoing 2DRT, concurrent chemotherapy could significantly prolong OS (HR = 0.61, 95% CI 0.44–0.82) (heterogeneity $P = 0.08$, $I^2 = 55\%$), LRFS (HR = 0.62, 95% CI 0.50–0.78) (heterogeneity $P = 0.82$, $I^2 = 0.00\%$), and PFS (HR = 0.65, 95% CI 0.54–0.79) (heterogeneity $P = 0.67$, $I^2 = 0.00\%$), except DMFS (HR = 0.81, 95% CI = 0.46–1.45) (heterogeneity $P = 0.04$, $I^2 = 65\%$) (**Figure 3**). Nevertheless, with IMRT, no remarkable difference between the CCRT group and the IMRT-alone group was observed in terms of OS (HR = 0.84, 95% CI 0.62–1.15) (heterogeneity $P = 0.11$, $I^2 = 43\%$), LRFS (HR=0.85, 95% CI 0.54–1.34) (heterogeneity $P = 0.86$, $I^2 = 0.00\%$), DMFS (HR = 0.96, 95% CI 0.60–1.54) (heterogeneity $P = 0.87$, $I^2 = 0.00\%$), and PFS (HR = 0.96, 95% CI 0.66–1.37) (heterogeneity $P = 0.97$, $I^2 = 0.00\%$) (**Figure 4**). Moreover, to explore the potential beneficiaries of concurrent chemotherapy for stage II NPC in the IMRT era, we conducted a subgroup analysis of stage T1-2N1 patients treated with IMRT. Unfortunately, it was found that additional concurrent chemotherapy did not improve OS (HR = 1.04, 95% CI 0.37–2.96) (heterogeneity $P = 0.44$, $I^2 = 0.00\%$), LRFS (HR = 0.70, 95% CI 0.34–1.45) (heterogeneity $P = 0.85$, $I^2 = 0.00\%$), DMFS (HR = 1.03, 95% CI 0.53–2.00) (heterogeneity $P = 0.60$, $I^2 = 0.00\%$), and PFS (HR = 1.04, 95% CI 0.58–1.88) (heterogeneity $P = 0.81$, $I^2 = 0.00\%$) in this population (**Figure 5**).

A Sensitivity Analysis

The stability of the results was evaluated by removing some studies according to different standards (**Table 3**). First of all, the sensitivity analysis was conducted in IMRT studies by separately eliminating two studies (8, 35) with a sample size of less than 100 patients, four studies (11, 32, 33, 35) with a median follow-up time of fewer than 60 months, and three studies (11, 33, 34) that included concurrent chemotherapy regimens other than cisplatin, respectively. It suggested that OS, LRFS, DMFS, and PFS were similar between the CCRT group and IMRT alone group, which was consistent with that before sensitivity analysis. Then, the sensitivity analysis was carried out in 2DRT studies by

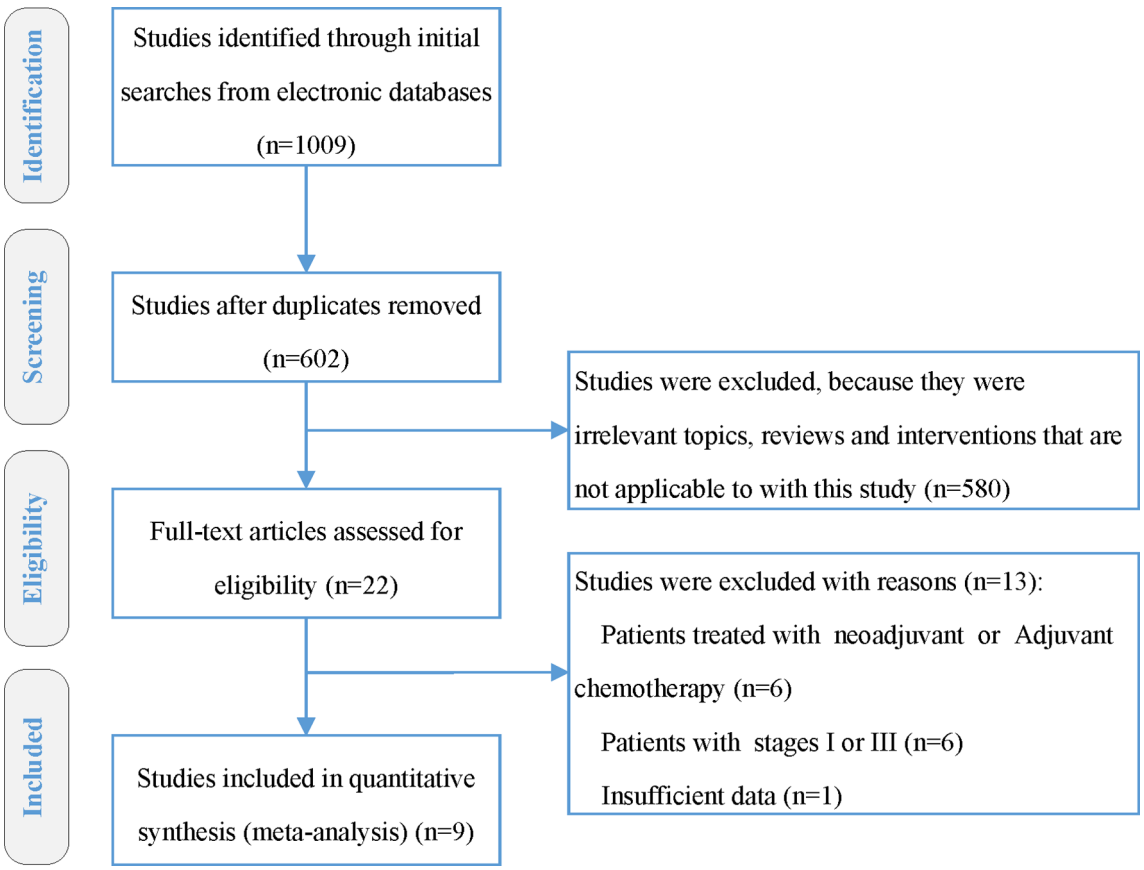

FIGURE 1 | PRISMA flow diagram.

TABLE 1 | Eligible study characteristics.

Study	Study design	No. of patients (CCRT/RT)	Inclusion period	Stage	Median follow-up (months)	Radiotherapy	Concurrent chemotherapy
Li 2021 (34)	R	2DRT: 348 (159/189) IMRT: 253 (96/157)	2003–2016	AJCC-2010 II	2DRT:103.0 IMRT: 99.0	2DRT: T66–70 Gy, N+60–62 Gy, N-50 Gy IMRT: T66–70 Gy, N+66–70 Gy	Cisplatin or nedaplatin 35 mg/m^2, qw or 80–100 mg/m2, q3w
Chen 2011 (37)/ Li 2019 (9)	RCT	230 (116/114)	2003–2007	Chinese-1992 II	125.0	2DRT: T68–70 Gy, N+60–62 Gy, N-50 Gy	Cisplatin 30 mg/m^2, qw
Xu 2015 (35)	R	86 (43/43)	2009–2011	AJCC-2002 II	37.4	IMRT: T66 Gy, N+60 Gy, N-54 Gy	Cisplatin 40 mg/m^2, qw
Jin 2021 (36)	R	354 (177/177)	2008–2016	AJCC-2017 II	69.9	IMRT: T66–72 Gy, N+64–70Gy, N-54–56 Gy	Cisplatin 40 mg/m^2, qw, or 80 mg/m^2, q3w
Ahmed 2019 (11)	R	172 (116/56)	2004–2013	AJCC-2010 II	50.4	IMRT: T66–70 Gy	NR
Liu 2020 (32)	R	2DRT: 1520 (304/1216) IMRT: 404 (202/202)	1990–2012	AJCC-2010 II	2DRT: 93 IMRT: 44.0	2DRT: T66–72 Gy, IMRT: T66–72 Gy	Cisplatin 30–40 mg/m^2 qw, or 80–100 mg/m^2 q3w
Xu 2011 (10)	R	392 (181/211)	2000–2003	AJCC-2002 II	66.0	2DRT: T70 Gy, N+66–70 Gy	Cisplatin 100 mg/m^2, q3w
Su 2016 (33)	R	24 9(143/106)	2005–2010	AJCC-2010 II	59.4	IMRT: T66–70 Gy, N+60–64 Gy, N-42–62 Gy	platinum single-agent (qw or q3w), paclitaxel, TP or PF
Huang 2020 (8)	RCT	84 (41/43)	2010–2012	AJCC-2010 II	75.0	IMRT: T69.96 Gy, N+60.06 Gy, N-50.96 Gy	Cisplatin 40 mg/m^2, qw

CCRT, concurrent chemoradiation; 2D-RT, two-dimensional radiotherapy; IMRT, intensity-modulated radiotherapy; AJCC, American Joint Committee on Cancer; R, retrospective; RCT, randomized controlled trial; NR, not reported.

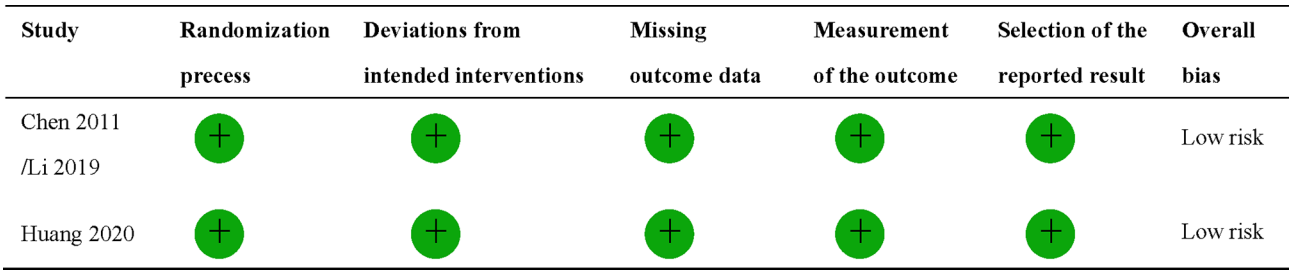

FIGURE 2 | Assessment of quality of randomized controlled trials.

excluding one study that included concurrent chemotherapy with nedaplatin. There was no statistically significant change in survival outcomes. We did not perform sensitivity analyses for sample size and follow-up time because all 2DRT studies had a sample size of more than 100 and were followed up for more than 60 months. In summary, the survival results of the meta-analysis were robust and reliable.

Acute Toxicity

The incidence of grade 3–4 acute toxicity was reported in five studies with a total of 741 patients. The results of the meta-analysis suggested that the incidence of grade 3–4 leukopenia (RR = 4.00, 95% CI 2.29~6.97) (heterogeneity $P = 0.14$, $I^2 = 41\%$), mucositis (RR = 1.43, 95% CI 1.16–1.77) (heterogeneity $P = 0.20$, $I^2 = 38\%$), and gastrointestinal reaction (RR = 8.76, 95% CI 2.63~29.12) (heterogeneity $P = 0.66$, $I^2 = 0\%$) in the CCRT group were significantly higher than those in the IMRT-alone group. The incidence of grade 3–4 thrombocytopenia (RR = 3.45, 95% CI 0.85–13.94) (heterogeneity $P = 0.97$, $I^2 = 0\%$) was similar in the two groups (**Figure 6**).

DISCUSSION

Radiotherapy is the main treatment for NPC. Stage III–IVA NPC patients receiving CCRT can further earn survival benefits from induction chemotherapy (5), but so far, whether chemotherapy can bring survival benefits to stage II patients is still controversial. The ASCO and CSCO Guideline recommends that it is not necessary for stage II NPC to routinely receive

TABLE 2 | Assessment of quality of non-randomized studies.

Study	Selection				Comparability	Outcome			Score
	Representativeness of the exposed cohort	Selection of the non-exposed cohort	Ascertainment of exposure	Demonstration that outcome of interest was not present at start of study	Comparability of cohorts on the basis of the design or analysis	Assessment of outcome	Was follow-up longer enough for outcomes to occur	Adequacy of follow-up of cohorts	
Li 2021 (34)	*	*	*	*	*	*	*	*	8
Xu 2015 (35)	*	*	*	*	*	*	*	*	8
Jin 2021 (36)	*	*	*	*	**	*	*	*	9
Ahmed 2019 (11)	*	*	*	*	**	*	*	*	9
Liu 2020 (32)	*	*	*	*	**	*	*	*	9
Xu 2011 (10)	*	*	*	*	*	*	*	*	8
Su 2016 (33)	*	*	*	*	*	*	*	*	8

"" represents the score of each item in the evaluation criteria (full score of "Selection" is 4 points, full score of "Comparability" is 2 points, full score of "Outcome" is 3 points. The higher the score is, the higher the quality of the paper is), "*" represents 1 point, "**" represents 2 points.*

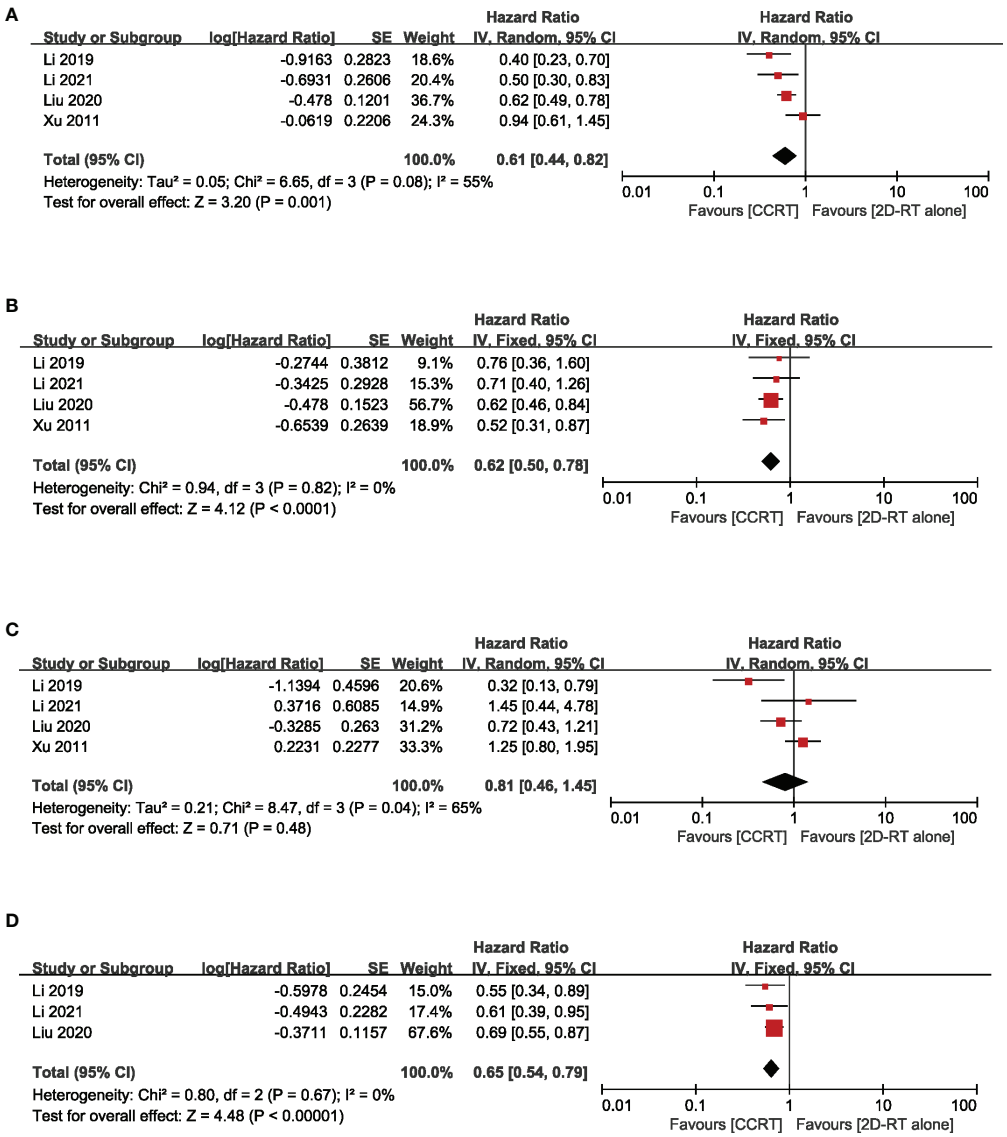

FIGURE 3 | Forest plot of the meta-analysis regarding OS **(A)**, LRFS **(B)**, DMFS **(C)**, and PFS **(D)** with CCRT vs. 2DRT alone. OS, overall survival; LRFS, locoregional recurrence-free survival; DMFS, distant metastasis-free survival; PFS, progression-free survival; CCRT, concurrent chemoradiation; 2D-RT, two-dimensional radiotherapy.

chemotherapy unless there are high-risk factors, such as high pretreatment EBV-DNA level, bulky tumor volumes, or extranodal extension (38). We assessed the therapeutic effect and toxicity of CCRT compared with 2DRT alone or IMRT alone for stage II NPC patients by conducting a meta-analysis.

Our study suggested that, compared with 2DRT alone, CCRT was associated with improved OS, LRFS, and PFS in stage II NPC patients. In the 2DRT era, a retrospective study conducted by Cheng and colleagues (23) revealed that stage II NPC patients receiving CCRT had similar PFS and LRFS compared with stage I patients receiving 2DRT alone. Another large retrospective study (39) included 1,790 patients and exhibited that the N1 subgroup of stage II NPC patients is more prone to distant metastasis, leading to a poorer prognosis. Furthermore, a combined subgroup analysis from two RCTs showed the survival benefit obtained from two or three cycles of cisplatin-based induction chemotherapy in stage II NPC (40). Hence, for stage II IPC patients treated with 2DRT, concurrent chemotherapy is highly crucial, particularly for the T1-2N1 population.

IMRT has become a daily choice for NPC. Several studies (8, 11, 32–36) have investigated whether concurrent chemotherapy can further improve the efficacy of stage II NPC patients receiving IMRT. However, the results of these studies are not completely consistent. Our meta-analysis revealed that concurrent chemotherapy had no therapeutic effect but increased toxicity in patients with stage II NPC receiving IMRT. Multiple possible

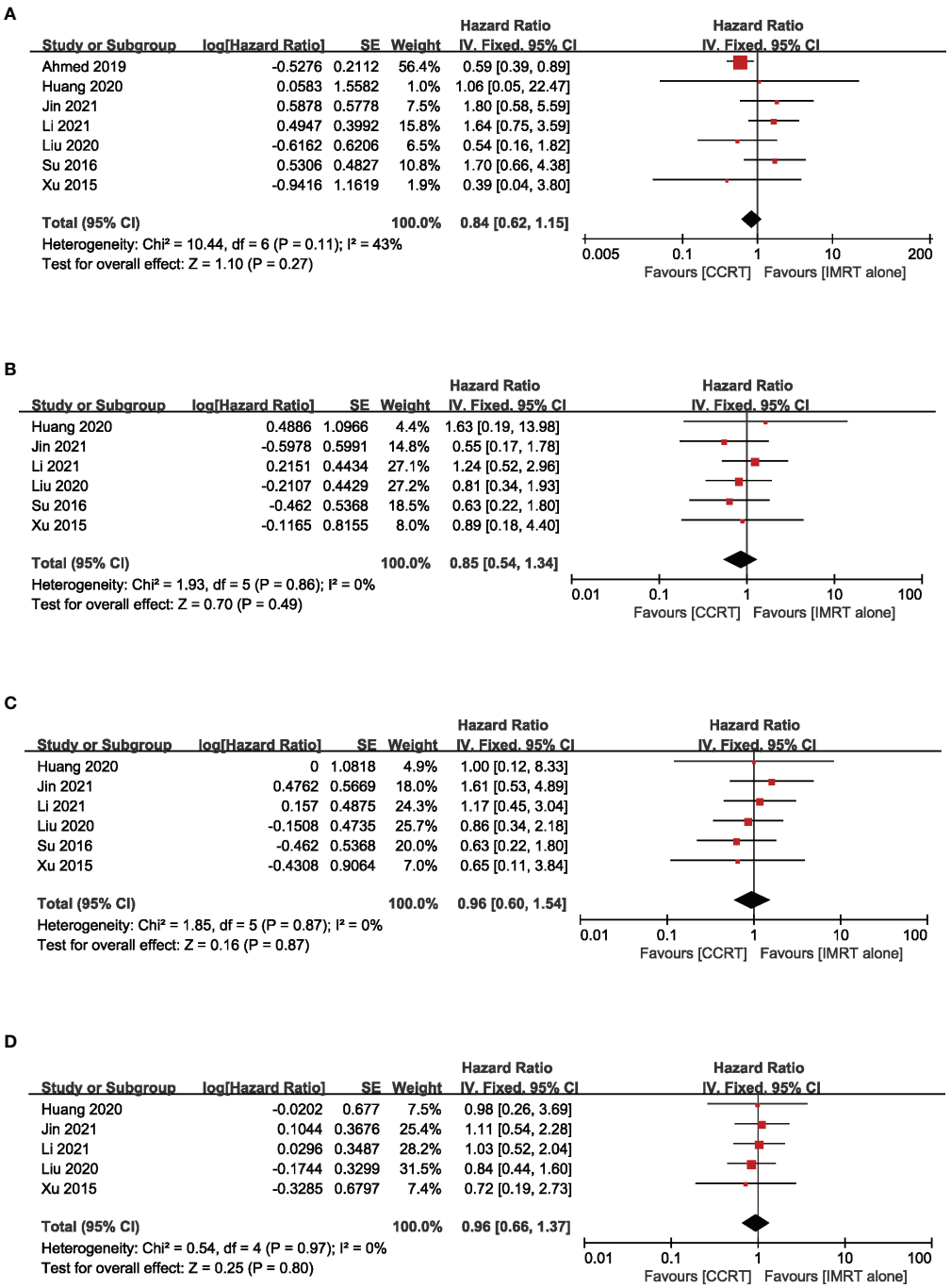

FIGURE 4 | Forest plot of the meta-analysis regarding OS **(A)**, LRFS **(B)**, DMFS **(C)**, and PFS **(D)** with CCRT vs. IMRT alone. IMRT, intensity-modulated radiotherapy.

explanations could account for the negative result in survival outcomes. First of all, as a high-precision radiotherapy therapy, IMRT can not only accurately irradiate the irregular tumor target with a higher dose but also protect the adjacent critical structures to the greatest extent. Several studies (41, 42) have consistently found that IMRT can significantly reduce radiation-induced toxicity and improve local control and long-term survival outcomes versus 2DRT, particularly for T1-2 patients (26, 41, 43). A prospective randomized study (41) comparing 2DRT with IMRT suggested that, with 2DRT, the 5-year OS and local control rates of stage II NPC were 67.1% and 84.7%, respectively, while with IMRT, they can be increased to 79.6% and 90.5%, respectively. Lai and colleagues (44) performed a retrospective study and found that IMRT significantly prolonged 5-year LRFS

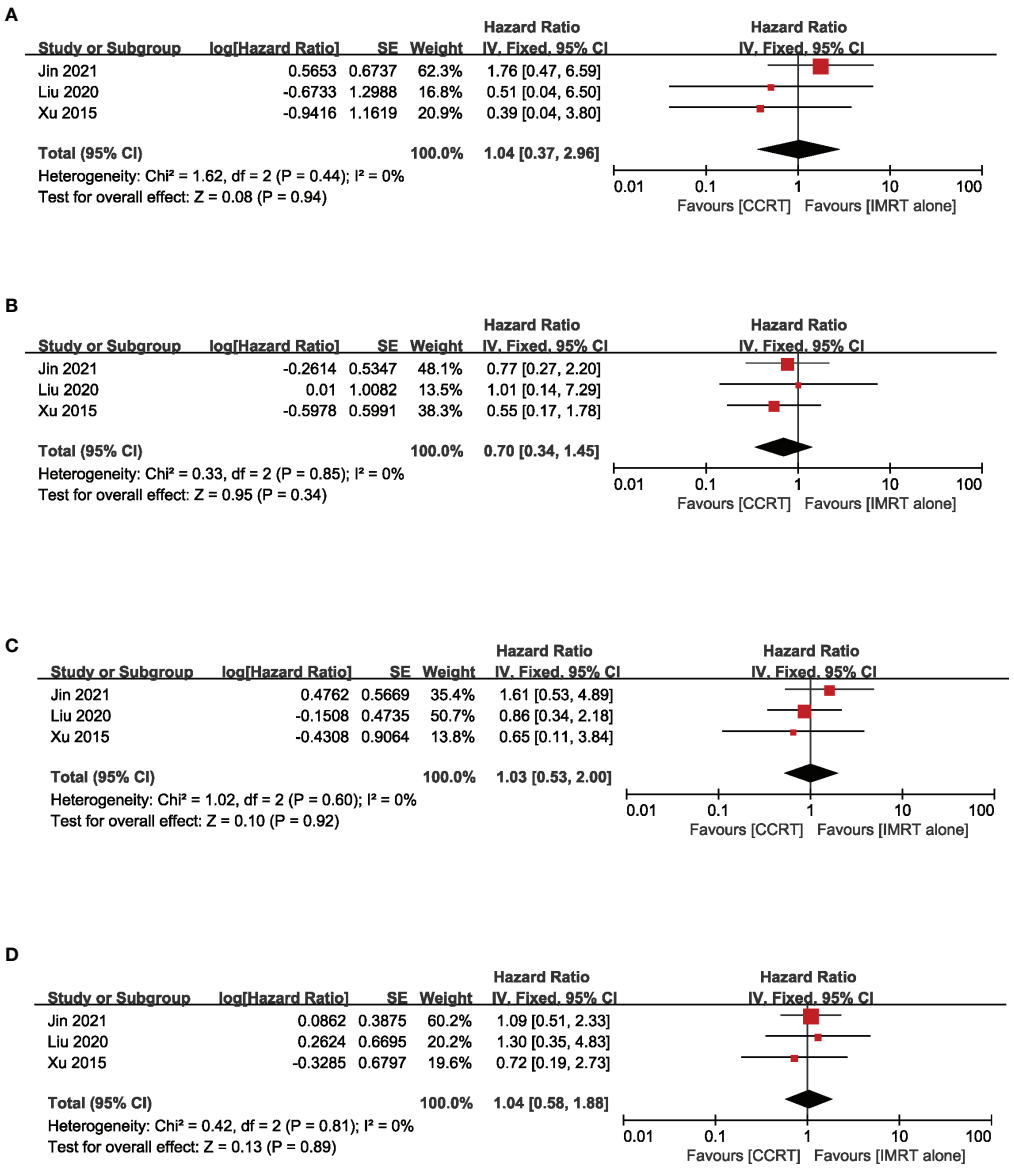

FIGURE 5 | Forest plot of the meta-analysis regarding OS **(A)**, LRFS **(B)**, DMFS **(C)**, and PFS **(D)** with CCRT vs. IMRT alone in the N1 subgroup.

for patients with stage II NPC (92.7% vs. 86.8%) compared with 2DRT. The 5-year LRFS of stage T1 patients even reached 100% in the IMRT group versus 94.4% in the 2DRT group. Interestingly, a study (26) directly comparing IMRT alone with 2DRT plus concurrent chemotherapy indicated that the two groups were similar in terms of 4-year OS, LRFS, and DMFS (97.4% vs. 97.4%; 93.8% vs. 95.7%; 96.5% vs. 97.3%, respectively). Thanks to the progress of radiation therapy technology, the 5-year OS and local control rates of stage II NPC have improved substantially in the IMRT era. Concurrent chemotherapy might not bring survival benefits to this population. Secondly, an update result from the only phase 3 RCT (9) for stage II NPC revealed that CCRT significantly improved the 10-year OS (83.6% vs. 65.8%) and PFS (76.7% vs. 64.0%) compared to RT alone. However, the enrolled patients were evaluated by the Chinese 1992 staging system, and 31 (13%) of them were reclassified as stage III/N2 based on the AJCC TNM Staging System (7th ed., 2017). The survival benefit from stage N2 patients may lead to an overestimation of the role of concurrent chemotherapy in this study. Thirdly, stage II NPC is composed of three subsets (T2N0, T1N1, and T2N1), with obvious heterogeneity. Each subgroup has a different prognosis, and N1 patients are more likely to develop distant metastases (39). Hence, we conducted an N1 subgroup analysis for stage II patients. Unfortunately, it was found that additional concurrent chemotherapy did not improve survival outcomes.

TABLE 3 | Sensitivity analysis for the comparison of CCRT and RT alone.

Outcome	Patients		Effect	*P*-value	Heterogeneity			*P*-value
	CCRT	RT alone	HR (95% CI)		χ^2	*df*	I^2 (%)	
IMRT								
Sample size >100 patients								
OS	734	698	1.05 (0.58–19.98)	0.87	9.98	4	60%	**0.04**
LRFS	618	642	0.82 (0.51–1.33)	0.42	1.56	3	0%	0.67
DMFS	618	642	0.99 (0.60–1.64)	0.97	1.65	3	0%	0.65
PFS	475	536	0.98 (0.66–1.45)	0.91	0.35	2	0%	0.84
Median follow-up time > 60 months								
OS	314	377	1.66 (0.88–3.11)	0.12	0.10	2	0%	0.95
LRFS	314	377	0.98 (0.50–1.91)	0.96	1.43	2	0%	0.49
DMFS	314	377	1.30 (0.65–2.58)	0.45	0.25	2	0%	0.88
PFS	314	377	1.06 (0.66–1.68)	0.82	0.25	2	0%	0.98
Concurrent chemotherapy with cisplatin								
OS	463	465	0.93 (0.44–1.97)	0.84	2.64	3	0%	0.45
LRFS	463	465	0.78 (0.42–1.44)	0.43	0.83	3	0%	0.84
DMFS	463	465	1.03 (0.55–1.91)	0.93	1.02	3	0%	0.80
PFS	463	465	0.93 (0.60–1.42)	0.73	0.47	3	0%	0.92
2DRT								
Concurrent chemotherapy with cisplatin								
OS	601	1743	0.63 (0.43–0.94)	**0.02**	5.88	2	66%	**0.05**
LRFS	601	1743	0.61 (0.48–0.78)	**<0.0001**	0.71	2	0%	0.70
DMFS	601	1743	0.73 (0.37–1.42)	0.35	7.78	2	74%	**0.02**
PFS	601	1736	0.66 (0.54–0.81)	**<0.0001**	0.70	1	0%	0.40

CCRT, concurrent chemoradiation; 2D-RT, two-dimensional radiotherapy; IMRT, intensity-modulated radiotherapy; HR, hazard ratio; CI, confidence interval; df, degrees of freedom; OS, overall survival; LRFS, locoregional recurrence-free survival; DMFS, distant metastasis-free survival; PFS, progression-free survival.

P values less than 0.05 are shown in bold (bold numbers), indicating that the therapeutic effect or heterogeneity of the included literature is statistically significant.

Studies have found that baseline characteristics, such as plasma EBV-DNA level (45), lymph node size (46), and extranodal extension (47, 48), were independent unfavorable factors of NPC. Growing evidence indicated that the plasma EBV-DNA level was highly associated with tumor burden and elevated pretreatment plasma EBV-DNA was related to worse clinical outcomes (49, 50). EBV DNA-positive stage II patients had similar overall survival to stage III patients (51). This is the first study to demonstrate that pretreatment plasma EBV-DNA can be used to distinguish high-risk subgroups in early-stage patients. Results from real-world research (52) indicated that high pretreatment plasma EBV-DNA levels (≥4,000 copies/ml) was an adverse independent factor in LA-NPC. Patients with high EBV-DNA levels had a comparable survival outcome to T4 or N2–3 patients, with a 5-year PFS of 69%. Another large cohort study (53) of 1,357 patients with LA-NPC revealed that, for patients with high EBV-DNA levels (>4,000 copies/ml), IMRT with concurrent chemotherapy improved OS, DFS, and DMFS compared with IMRT alone. However, there was no observed benefit with the addition of concurrent chemotherapy in patients with low EBV-DNA levels. Pretreatment EBV-DNA has been widely accepted as a useful prognostic biomarker and plays an important role in tailoring treatment strategies in the clinic (54). Therefore, stage II NPC patients with high pretreatment EBV-DNA levels might be ideal candidates for concurrent chemotherapy. However, two issues need to be addressed before EBV-DNA was widely used in clinical practice for risk stratification. Firstly, the harmonization and standardization of the quantitative plasma EBV-DNA measurement between laboratories have not been established, resulting in poor inter-laboratory concordance. Secondly, although the EBV-DNA cutoff values have been set at 2,000 or 4,000 copies/ml in most studies, there is still no consensus on the optimal thresholds for risk discretization. A retrospective study showed that the tumor volume was a significant independent predictor of increasing risk of recurrence (33). Another study (55) from Hong Kong reported no role of using concurrent chemotherapy in stage II NPC, except for lymph nodes >2 cm. However, these two studies are small-sample retrospective studies, and the value of tumor volume and lymph node size needs to be further studied. Studies demonstrated that extranodal extension played an important role in predicting distant metastasis in stage II NPC patients with N1 category (56–58). Patients with high-grade extranodal extension (including coalescent nodes and metastatic node infiltrating into adjacent structures) had a significantly higher risk of distant metastasis and death than those without (including metastatic nodes infiltrating into surrounding fat and without extranodal extension) and were suggested to be classified as cN3. However, patients with metastatic nodes infiltrating into surrounding fat (low-grade extranodal extension) had a similar outcome to those without extranodal extension. Hence, stage II nasopharyngeal carcinoma patients with high-grade extranodal invasion are likely candidates for concurrent chemotherapy. Although the risk stratification factors mentioned above might have the potential to identify candidates for concurrent chemotherapy, we were unable to conduct further subgroup analyses for these factors because they were not reported in the included literature. The tumor volume, size of metastatic lymph nodes, extranodal extension, and EBV-DNA levels were not disaggregated in the

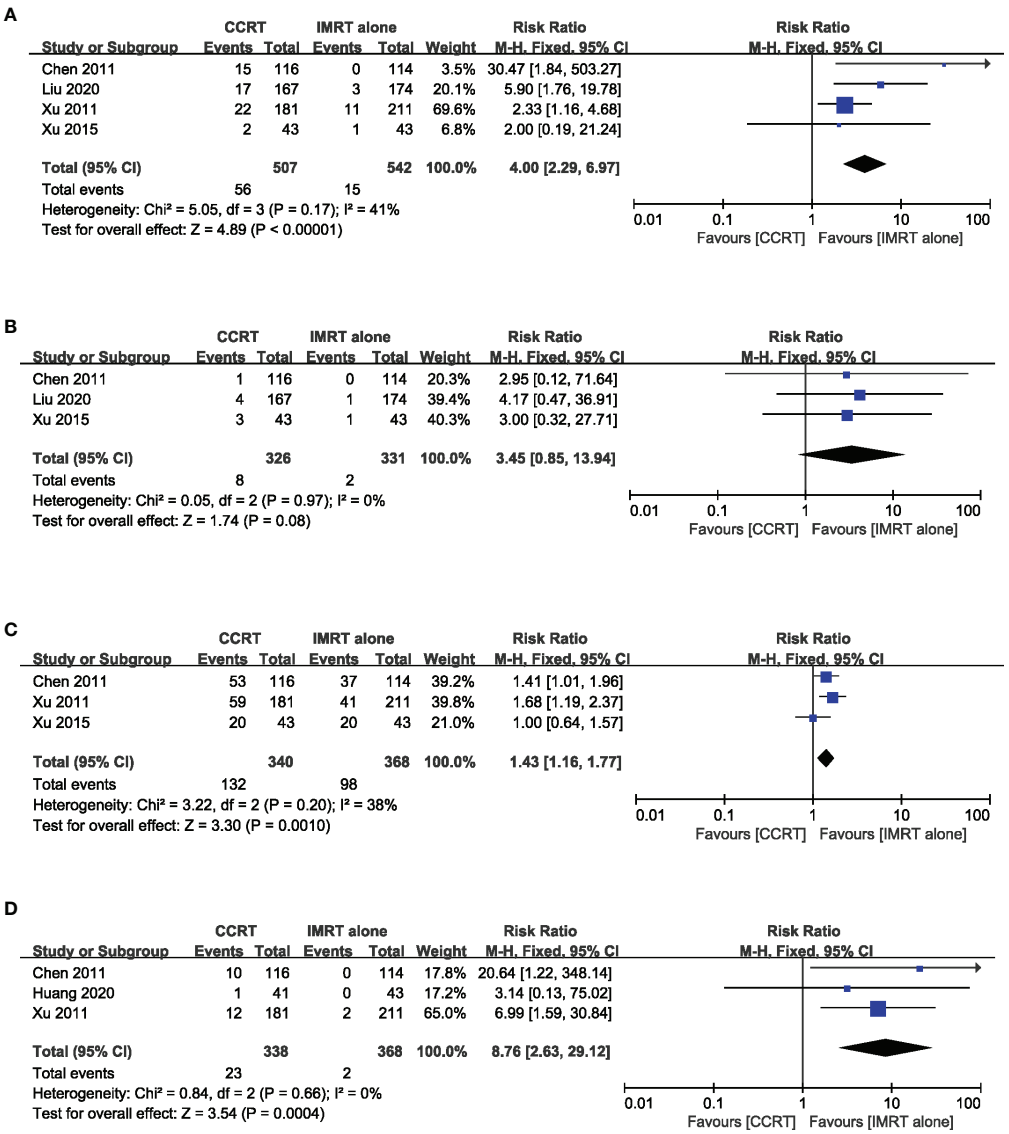

FIGURE 6 | Forest plot of the meta-analysis regarding grade 3–4 leukopenia **(A)**, thrombocytopenia **(B)**, mucositis **(C)**, and gastrointestinal reactions **(D)** with CCRT vs. IMRT alone.

N1 subgroup analysis, which may have a significant impact on the results. Therefore, the negative results of the N1 subgroup analysis in this study should be interpreted with caution. Future studies should focus on these high-risk groups who are most likely to benefit from chemotherapy.

Stage II NPC has a good prognosis, with 5-year OS 97.8%, so it is particularly significant to relieve toxicity and improve quality of life (59). Studies in terms of anti-EGFR antibodies, such as cetuximab, nimotuzumab, and Endostar, combined with RT in patients with LA-NPC have been launched. Xu and colleagues carried out a comparative study between concurrent cisplatin-chemoradiotherapy (CRT) and cetuximab-radiotherapy (ERT) (60). ERT was not superior to CRT, while it was more prone to result in acute adverse events. Similar results were obtained in another retrospective study (61); cetuximab/nimotuzumab combined concurrently with IMRT suggested equivalence to the standard CCRT in terms of DFS, LRRFS, DMFS, and OS. Skin reaction and mucositis are more common in the cetuximab/nimotuzumab group. A phase II study enrolling 23 stage III–IV NPC patients found that, compared to CCRT, radiotherapy combined with Endostar had similar efficacy, but lighter acute adverse reactions, which improved quality of life (62). In conclusion, Endostar has the potential to serve as a concurrent treatment option for the high-risk subgroup of stage II patients and deserves further study. Anti-PD1 checkpoint inhibitors, such as nivolumab (63), pembrolizumab (64), camrelizumab (65, 66),

toripalimab (67), and tislelizumab (68), had a clinically meaningful antitumor activity with a manageable safety profile. Two phase 3 trials demonstrated that, as first-line treatment for recurrent/metastatic NPC, camrelizumab or toripalimab in combination with gemcitabine and cisplatin prolonged PFS as compared to gemcitabine and cisplatin (median PFS 9.7 vs. 6.9 months, 11.7 vs. 8.0 months, respectively) (65, 67). Several phase II–III trials (NCT05305131, NCT03700476, NCT03267498, NCT04782765, NCT04227509, NCT03427827, NCT04557020, NCT04453826, NCT05211232) are in progress to clarify the efficacy and safety of PD-1 in combination with CCRT for high-risk LA-NPC (except for T3N0–1 and T4N0). Of particular concern is a phase II trial (NCT05229315) evaluating the safety and efficacy of toripalimab combined with IMRT in the treatment of stage II NPC. Nevertheless, risk stratification factors, such as EBV-DNA, lymph node size, and extranodal extension, were not evaluated as a part of eligibility criteria in most studies, with the exceptions of NCT04453826 (enrolled patients were required to have EBV-DNA >0 copies/ml after 3 cycles of induction chemotherapy) and NCT05229315 (enrolled patients were required to have EBV-DNA <4,000 copies/ml).

In terms of acute toxicities, this meta-analysis found that grade 3–4 leukopenia, mucositis, and gastrointestinal reactions were more frequent in patients receiving CCRT versus IMRT alone. A previous study (69) suggested that CCRT is related to higher incidences of treatment-related mortality (1.7% vs. 0.8%) as compared with radiotherapy alone. Leukopenia is the most common cause of death. Because of higher acute toxicity and treatment-related death, the application of concurrent chemotherapy in stage II NPC should be considered prudently. Currently, four RCTs (NCT02116231, NCT02633202, NCT02610010, NCT03068936) that evaluate the role of concurrent chemotherapy for stage II patients are ongoing in China, and the eventual results are expected to be released in the near future.

The present meta-analysis has multiple limitations. First of all, both RCTs and retrospective studies were enrolled, which may influence the level of evidence to some extent. Second, because staging systems vary in some included studies, it may contribute to heterogeneity in this meta-analysis. Third, several studies with relatively small sample sizes or median follow-up of less than 5 years were included. Finally, survival data of three studies (8, 10, 33) were obtained from survival curves by Tierney's methods, which may lead to potential bias.

CONCLUSION

In summary, for patients with stage II NPC, current evidence suggested that CCRT was superior to 2DRT alone with significantly better LRFS, PFS, and OS. However, IMRT alone was comparable to CCRT with similar efficacy but lower acute toxicities. Consequently, routine use of concurrent chemotherapy in unselected patients should not be encouraged in the IMRT era. There is an urgent need to identify subgroups of stage II patients who might derive clinical benefits from concurrent chemotherapy.

DATA AVAILABILITY STATEMENT

The original contributions presented in the study are included in the article/**Supplementary Material**. Further inquiries can be directed to the corresponding author.

AUTHOR CONTRIBUTIONS

Study design: X-DZ, K-HC; data acquisition: Y-CX, Z-GL; quality control of data: Y-CX, Z-GL, and K-HC; data analysis and interpretation: Y-CX, Z-GL; statistical analysis: Y-CX, Z-GL; manuscript preparation: Y-CX, Z-GL, and K-HC; manuscript review: X-DZ. All authors read and X-DZ approved the final manuscript. All authors contributed to the article and approved the submitted version.

SUPPLEMENTARY MATERIAL

The Supplementary Material for this article can be found online at: https://www.frontiersin.org/articles/10.3389/fonc.2022.843675/full#supplementary-material

REFERENCES

1. Bray F, Ferlay J, Soerjomataram I, Siegel RL, Torre LA, Jemal A. Global Cancer Statistics 2018: GLOBOCAN Estimates of Incidence and Mortality Worldwide for 36 Cancers in 185 Countries. *CA Cancer J Clin* (2018) 68 (6):394–424. doi: 10.3322/caac.21492
2. Wee JT, Ha TC, Loong SL, Qian CN. Is Nasopharyngeal Cancer Really a "Cantonese Cancer"? *Chin J Cancer* (2010) 29(5):517–26. doi: 10.5732/cjc.009.10329
3. Yang XL, Wang Y, Liang SB, He SS, Chen DM, Chen HY, et al. Comparison of the Seventh and Eighth Editions of the UICC/AJCC Staging System for Nasopharyngeal Carcinoma: Analysis of 1317 Patients Treated With Intensity-Modulated Radiotherapy at Two Centers. *BMC Cancer* (2018) 18 (1):606. doi: 10.1186/s12885-018-4419-1
4. Lin YH, Huang TL, Chien CY, Chen HC, Hsu HC, Huang EY, et al. Pretreatment Prognostic Factors of Survival and Late Toxicities for Patients With Nasopharyngeal Carcinoma Treated by Simultaneous Integrated Boost Intensity-Modulated Radiotherapy. *Radiat Oncol* (2018) 13(1):45. doi: 10.1186/s13014-018-0990-5
5. Zhang Y, Chen L, Hu GQ, Zhang N, Zhu XD, Yang KY, et al. Gemcitabine and Cisplatin Induction Chemotherapy in Nasopharyngeal Carcinoma. *N Engl J Med* (2019) 381(12):1124–35. doi: 10.1056/NEJMoa1905287
6. Bongiovanni A, Vagheggini A, Fausti V, Mercatali L, Calpona S, Di Menna G, et al. Induction Chemotherapy Plus Concomitant Chemoradiotherapy in Nasopharyngeal Carcinoma: An Updated Network Meta-Analysis. *Crit Rev Oncol Hematol* (2021) 160:103244. doi: 10.1016/j.critrevonc.2021.103244
7. Verma V, Ryckman JM, Simone CB2nd, Lin C. Patterns of Care and Outcomes With the Addition of Chemotherapy to Radiation Therapy for

Stage I Nasopharyngeal Cancer. *Acta Oncol* (2018) 57(2):257–61. doi: 10.1080/0284186x.2017.1351039
8. Huang X, Chen X, Zhao C, Wang J, Wang K, Wang L, et al. Adding Concurrent Chemotherapy to Intensity-Modulated Radiotherapy Does Not Improve Treatment Outcomes for Stage II Nasopharyngeal Carcinoma: A Phase 2 Multicenter Clinical Trial. *Front Oncol* (2020) 10:1314. doi: 10.3389/fonc.2020.01314
9. Li XY, Chen QY, Sun XS, Liu SL, Yan JJ, Guo SS, et al. Ten-Year Outcomes of Survival and Toxicity for a Phase III Randomised Trial of Concurrent Chemoradiotherapy Versus Radiotherapy Alone in Stage II Nasopharyngeal Carcinoma. *Eur J Cancer* (2019) 110:24–31. doi: 10.1016/j.ejca.2018.10.020
10. Xu T, Hu C, Wang X, Shen C. Role of Chemoradiotherapy in Intermediate Prognosis Nasopharyngeal Carcinoma. *Oral Oncol* (2011) 47(5):408–13. doi: 10.1016/j.oraloncology.2011.03.008
11. Ahmed Z, Kujtan L, Kennedy K, Wood V, Schomas D, Subramanian J. The Role of Chemotherapy in the Treatment of Stage II Nasopharyngeal Carcinoma: Retrospective Analysis of the National Cancer Database. *Cancer Med* (2019) 8(4):1500–7. doi: 10.1002/cam4.2033
12. Wu P, Zhao Y, Xiang L, Yang L. Management of Chemotherapy for Stage II Nasopharyngeal Carcinoma in the Intensity-Modulated Radiotherapy Era: A Review. *Cancer Manag Res* (2020) 12:957–63. doi: 10.2147/cmar.S239729
13. Xu C, Zhang LH, Chen YP, Liu X, Zhou GQ, Lin AH, et al. Chemoradiotherapy Versus Radiotherapy Alone in Stage II Nasopharyngeal Carcinoma: A Systemic Review and Meta-Analysis of 2138 Patients. *J Cancer* (2017) 8(2):287–97. doi: 10.7150/jca.17317
14. Wang S, Li S, Shen L. Combined Chemoradiation vs Radiation Therapy Alone in Stage-II Nasopharyngeal Carcinoma: A Meta-Analysis of the Published Literature. *Curr Probl Cancer* (2018) 42(3):302–18. doi: 10.1016/j.currproblcancer.2018.03.004
15. Liu F, Jin T, Liu L, Xiang Z, Yan R, Yang H. The Role of Concurrent Chemotherapy for Stage II Nasopharyngeal Carcinoma in the Intensity-Modulated Radiotherapy Era: A Systematic Review and Meta-Analysis. *PloS One* (2018) 13(3):e0194733. doi: 10.1371/journal.pone.0194733
16. Page MJ, McKenzie JE, Bossuyt PM, Boutron I, Hoffmann TC, Mulrow CD, et al. The PRISMA 2020 Statement: An Updated Guideline for Reporting Systematic Reviews. *BMJ* (2021) 372:n71. doi: 10.1136/bmj.n71
17. Tierney JF, Stewart LA, Ghersi D, Burdett S, Sydes MR. Practical Methods for Incorporating Summary Time-to-Event Data Into Meta-Analysis. *Trials* (2007) 8:16. doi: 10.1186/1745-6215-8-16
18. Sterne JAC, Savović J, Page MJ, Elbers RG, Blencowe NS, Boutron I, et al. RoB 2: A Revised Tool for Assessing Risk of Bias in Randomised Trials. *BMJ* (2019) 366:l4898. doi: 10.1136/bmj.l4898
19. Guo Q, Lu T, Lin S, Zong J, Chen Z, Cui X, et al. Long-Term Survival of Nasopharyngeal Carcinoma Patients With Stage II in Intensity-Modulated Radiation Therapy Era. *Jpn J Clin Oncol* (2016) 46(3):241–7. doi: 10.1093/jjco/hyv192
20. Wang L, Miao J, Huang H, Chen B, Xiao X, Zhu M, et al. Long-Term Survivals, Toxicities and the Role of Chemotherapy in Early-Stage Nasopharyngeal Carcinoma Patients Treated With Intensity-Modulated Radiation Therapy: A Retrospective Study With 15-Year Follow-Up. *Cancer Res Treat* (2021) 54(1):118–29. doi: 10.4143/crt.2021.101
21. Kang MK, Oh D, Cho KH, Moon SH, Wu HG, Heo DS, et al. Role of Chemotherapy in Stage II Nasopharyngeal Carcinoma Treated With Curative Radiotherapy. *Cancer Res Treat* (2015) 47(4):871–8. doi: 10.4143/crt.2014.141
22. Pan XB, Huang ST, Chen KH, Zhu XD. Chemotherapy Use and Survival in Stage II Nasopharyngeal Carcinoma. *Oncotarget* (2017) 8(60):102573–80. doi: 10.18632/oncotarget.21751
23. Cheng SH, Tsai SY, Yen KL, Jian JJ, Chu NM, Chan KY, et al. Concomitant Radiotherapy and Chemotherapy for Early-Stage Nasopharyngeal Carcinoma. *J Clin Oncol* (2000) 18(10):2040–5. doi: 10.1200/jco.2000.18.10.2040
24. Ding X-C, Fan P-P, Xie P, Fan B-J, Yang J, Jiang L-Y, et al. Ten-Year Outcomes Of Intensity-Modulated Radiotherapy (IMRT) Combine With Chemotherapy Versus IMRT Alone For Stage II Nasopharyngeal Carcinoma In The Real-World Study (RWD). *Cancer Manag Res* (2019) 11:8893–903. doi: 10.2147/CMAR.S218842
25. Zhang F, Zhang Y, Li WF, Liu X, Guo R, Sun Y, et al. Efficacy of Concurrent Chemotherapy for Intermediate Risk NPC in the Intensity-Modulated Radiotherapy Era: A Propensity-Matched Analysis. *Sci Rep* (2015) 5:17378. doi: 10.1038/srep17378
26. Zhang LN, Gao YH, Lan XW, Tang J, Su Z, Ma J, et al. Propensity Score Matching Analysis of Cisplatin-Based Concurrent Chemotherapy in Low Risk Nasopharyngeal Carcinoma in the Intensity-Modulated Radiotherapy Era. *Oncotarget* (2015) 6(41):44019–29. doi: 10.18632/oncotarget.5806
27. Aftab O, Liao S, Zhang R, Tang N, Luo M, Zhang B, et al. Efficacy and Safety of Intensity-Modulated Radiotherapy Alone Versus Intensity-Modulated Radiotherapy Plus Chemotherapy for Treatment of Intermediate-Risk Nasopharyngeal Carcinoma. *Radiat Oncol* (2020) 15(1):66. doi: 10.1186/s13014-020-01508-4
28. Luo S, Zhao L, Wang J, Xu M, Li J, Zhou B, et al. Clinical Outcomes for Early-Stage Nasopharyngeal Carcinoma With Predominantly WHO II Histology Treated by Intensity-Modulated Radiation Therapy With or Without Chemotherapy in Nonendemic Region of China. *Head Neck* (2014) 36(6):841–7. doi: 10.1002/hed.23386
29. Katano A, Takahashi W, Yamashita H, Yamamoto K, Ando M, Yoshida M, et al. Radiotherapy Alone and With Concurrent Chemotherapy for Nasopharyngeal Carcinoma: A Retrospective Study. *Medicine (Baltimore)* (2018) 97(18):e0502. doi: 10.1097/md.0000000000010502
30. Sun X, Su S, Chen C, Han F, Zhao C, Xiao W, et al. Long-Term Outcomes of Intensity-Modulated Radiotherapy for 868 Patients With Nasopharyngeal Carcinoma: An Analysis of Survival and Treatment Toxicities. *Radiother Oncol* (2014) 110(3):398–403. doi: 10.1016/j.radonc.2013.10.020
31. Pan X-B, Li L, Qu S, Chen L, Liang S-X, Zhu X-D. The Efficacy of Chemotherapy in Survival of Stage II Nasopharyngeal Carcinoma. *Oral Oncol* (2020) 101. doi: 10.1016/j.oraloncology.2019.104520
32. Liu DH, Zhou XY, Pan YG, Chen S, Ye ZH, Chen GD. Survival of Stage II Nasopharyngeal Carcinoma Patients With or Without Concurrent Chemotherapy: A Propensity Score Matching Study. *Cancer Med* (2020) 9(4):1287–97. doi: 10.1002/cam4.2785
33. Su Z, Mao YP, Tang J, Lan XW, OuYang PY, Xie FY. Long-Term Outcomes of Concurrent Chemoradiotherapy Versus Radiotherapy Alone in Stage II Nasopharyngeal Carcinoma Treated With IMRT: A Retrospective Study. *Tumour Biol* (2016) 37(4):4429–38. doi: 10.1007/s13277-015-4266-5
34. Li PJ, Lai YL, He F, Chen YY, Gu ZS, Luo W, et al. Explore the Usefulness of Concurrent Chemotherapy in Stage II Nasopharyngeal Carcinoma: A Retrospective Study. *Front Pharmacol* (2021) 12:688528. doi: 10.3389/fphar.2021.688528
35. Xu T, Shen C, Zhu G, Hu C. Omission of Chemotherapy in Early Stage Nasopharyngeal Carcinoma Treated With IMRT: A Paired Cohort Study. *Medicine (Baltimore)* (2015) 94(39):e1457. doi: 10.1097/md.0000000000001457
36. Jin YN, Tang QN, Yao JJ, Xu XW, He WZ, Wang L, et al. The Effect of Adding Concurrent Chemotherapy to Radiotherapy for Stage II Nasopharyngeal Carcinoma With Undetectable Pretreatment Epstein-Barr Virus DNA: Retrospective Analysis With a Large Institutional-Based Cohort. *Transl Oncol* (2021) 14(2):100990. doi: 10.1016/j.tranon.2020.100990
37. Chen QY, Wen YF, Guo L, Liu H, Huang PY, Mo HY, et al. Concurrent Chemoradiotherapy vs Radiotherapy Alone in Stage II Nasopharyngeal Carcinoma: Phase III Randomized Trial. *J Natl Cancer Inst* (2011) 103(23)::1761–70. doi: 10.1093/jnci/djr432
38. Chen YP, Ismaila N, Chua MLK, Colevas AD, Haddad R, Huang SH, et al. Chemotherapy in Combination With Radiotherapy for Definitive-Intent Treatment of Stage II-IVA Nasopharyngeal Carcinoma: CSCO and ASCO Guideline. *J Clin Oncol* (2021) 39(7):840–59. doi: 10.1200/jco.20.03237
39. Tang LL, Chen YP, Mao YP, Wang ZX, Guo R, Chen L, et al. Validation of the 8th Edition of the UICC/AJCC Staging System for Nasopharyngeal Carcinoma From Endemic Areas in the Intensity-Modulated Radiotherapy Era. *J Natl Compr Canc Netw* (2017) 15(7):913–9. doi: 10.6004/jnccn.2017.0121
40. Chua DT, Ma J, Sham JS, Mai HQ, Choy DT, Hong MH, et al. Improvement of Survival After Addition of Induction Chemotherapy to Radiotherapy in Patients With Early-Stage Nasopharyngeal Carcinoma: Subgroup Analysis of Two Phase III Trials. *Int J Radiat Oncol Biol Phys* (2006) 65(5):1300–6. doi: 10.1016/j.ijrobp.2006.02.016

41. Peng G, Wang T, Yang KY, Zhang S, Zhang T, Li Q, et al. A Prospective, Randomized Study Comparing Outcomes and Toxicities of Intensity-Modulated Radiotherapy vs. Conventional Two-Dimensional Radiotherapy for the Treatment of Nasopharyngeal Carcinoma. *Radiother Oncol* (2012) 104 (3):286–93. doi: 10.1016/j.radonc.2012.08.013
42. Du T, Xiao J, Qiu Z, Wu K. The Effectiveness of Intensity-Modulated Radiation Therapy Versus 2D-RT for the Treatment of Nasopharyngeal Carcinoma: A Systematic Review and Meta-Analysis. *PloS One* (2019) 14 (7):e0219611. doi: 10.1371/journal.pone.0219611
43. Lin S, Pan J, Han L, Guo Q, Hu C, Zong J, et al. Update Report of Nasopharyngeal Carcinoma Treated With Reduced-Volume Intensity-Modulated Radiation Therapy and Hypothesis of the Optimal Margin. *Radiother Oncol* (2014) 110(3):385–9. doi: 10.1016/j.radonc.2014.01.011
44. Lai SZ, Li WF, Chen L, Luo W, Chen YY, Liu LZ, et al. How Does Intensity-Modulated Radiotherapy Versus Conventional Two-Dimensional Radiotherapy Influence the Treatment Results in Nasopharyngeal Carcinoma Patients? *Int J Radiat Oncol Biol Phys* (2011) 80(3):661–8. doi: 10.1016/j.ijrobp.2010.03.024
45. Lee VH, Kwong DL, Leung TW, Choi CW, O'Sullivan B, Lam KO, et al. The Addition of Pretreatment Plasma Epstein-Barr Virus DNA Into the Eighth Edition of Nasopharyngeal Cancer TNM Stage Classification. *Int J Cancer* (2019) 144(7):1713–22. doi: 10.1002/ijc.31856
46. Toya R, Murakami R, Saito T, Murakami D, Matsuyama T, Baba Y, et al. Radiation Therapy for Nasopharyngeal Carcinoma: The Predictive Value of Interim Survival Assessment. *J Radiat Res* (2016) 57(5):541–7. doi: 10.1093/jrr/rrw038
47. Tsai TY, Chou YC, Lu YA, Kang CJ, Huang SF, Liao CT, et al. The Prognostic Value of Radiologic Extranodal Extension in Nasopharyngeal Carcinoma: Systematic Review and Meta-Analysis. *Oral Oncol* (2021) 122:105518. doi: 10.1016/j.oraloncology.2021.105518
48. Mao Y, Wang S, Lydiatt W, Shah JP, Colevas AD, Lee AWM, et al. Unambiguous Advanced Radiologic Extranodal Extension Determined by MRI Predicts Worse Outcomes in Nasopharyngeal Carcinoma: Potential Improvement for Future Editions of N Category Systems. *Radiother Oncol* (2021) 157:114–21. doi: 10.1016/j.radonc.2021.01.015
49. Zhang W, Chen Y, Chen L, Guo R, Zhou G, Tang L, et al. The Clinical Utility of Plasma Epstein-Barr Virus DNA Assays in Nasopharyngeal Carcinoma: The Dawn of a New Era?: A Systematic Review and Meta-Analysis of 7836 Cases. *Medicine (Baltimore)* (2015) 94(20):e845. doi: 10.1097/md.0000000000000845
50. Kim KY, Le QT, Yom SS, Ng RHW, Chan KCA, Bratman SV, et al. Clinical Utility of Epstein-Barr Virus DNA Testing in the Treatment of Nasopharyngeal Carcinoma Patients. *Int J Radiat Oncol Biol Phys* (2017) 98 (5):996–1001. doi: 10.1016/j.ijrobp.2017.03.018
51. Chan AT, Lo YM, Zee B, Chan LY, Ma BB, Leung SF, et al. Plasma Epstein-Barr Virus DNA and Residual Disease After Radiotherapy for Undifferentiated Nasopharyngeal Carcinoma. *J Natl Cancer Inst* (2002) 94 (21):1614–9. doi: 10.1093/jnci/94.21.1614
52. Tang SQ, Chen L, Li WF, Chan ATC, Huang SH, Chua MLK, et al. Identifying Optimal Clinical Trial Candidates for Locoregionally Advanced Nasopharyngeal Carcinoma: Analysis of 9468 Real-World Cases and Validation by Two Phase 3 Multicentre, Randomised Controlled Trial. *Radiother Oncol* (2021) 167:179–86. doi: 10.1016/j.radonc.2021.12.029
53. Liang H, Lv X, Wang L, Wu YS, Sun R, Ye YF, et al. The Plasma Epstein-Barr Virus DNA Level Guides Precision Treatment for Nasopharyngeal Carcinoma in the Intensity-Modulated Radiotherapy Era: A Large Population-Based Cohort Study From an Endemic Area. *Ther Adv Med Oncol* (2018) 10:1758835918782331. doi: 10.1177/1758835918782331
54. Lee AWM, Lee VHF, Ng WT, Strojan P, Saba NF, Rinaldo A, et al. A Systematic Review and Recommendations on the Use of Plasma EBV DNA for Nasopharyngeal Carcinoma. *Eur J Cancer* (2021) 153:109–22. doi: 10.1016/j.ejca.2021.05.022
55. Ng AWY, Tung SY, Cheung AKW, Chan PC. No Role of Using Chemoradiation in T2N0 and T1N1 With Small Lymph Node Size Stage II Nasopharyngeal Carcinoma. *Int J Radiat Oncol Biol Phys* (2015) 93(3):E306–7. doi: 10.1016/j.ijrobp.2015.07.1329
56. Hu Y, Lu T, Huang SH, Lin S, Chen Y, Fang Y, et al. High-Grade Radiologic Extra-Nodal Extension Predicts Distant Metastasis in Stage II Nasopharyngeal Carcinoma. *Head Neck* (2019) 41(9):3317–27. doi: 10.1002/hed.25842
57. Lu T, Hu Y, Xiao Y, Guo Q, Huang SH, O'Sullivan B, et al. Prognostic Value of Radiologic Extranodal Extension and its Potential Role in Future N Classification for Nasopharyngeal Carcinoma. *Oral Oncol* (2019) 99:104438. doi: 10.1016/j.oraloncology.2019.09.030
58. Chin O, Yu E, O'Sullivan B, Su J, Tellier A, Siu L, et al. Prognostic Importance of Radiologic Extranodal Extension in Nasopharyngeal Carcinoma Treated in a Canadian Cohort. *Radiother Oncol* (2021) 165:94–102. doi: 10.1016/j.radonc.2021.10.018
59. Li WZ, Wu HJ, Lv SH, Hu XF, Liang H, Liu GY, et al. Assessment of Survival Model Performance Following Inclusion of Epstein-Barr Virus DNA Status in Conventional TNM Staging Groups in Epstein-Barr Virus-Related Nasopharyngeal Carcinoma. *JAMA Netw Open* (2021) 4(9):e2124721. doi: 10.1001/jamanetworkopen.2021.24721
60. Xu T, Liu Y, Dou S, Li F, Guan X, Zhu G. Weekly Cetuximab Concurrent With IMRT Aggravated Radiation-Induced Oral Mucositis in Locally Advanced Nasopharyngeal Carcinoma: Results of a Randomized Phase II Study. *Oral Oncol* (2015) 51(9):875–9. doi: 10.1016/j.oraloncology.2015.06.008
61. You R, Sun R, Hua YJ, Li CF, Li JB, Zou X, et al. Cetuximab or Nimotuzumab Plus Intensity-Modulated Radiotherapy Versus Cisplatin Plus Intensity-Modulated Radiotherapy for Stage II-IVb Nasopharyngeal Carcinoma. *Int J Cancer* (2017) 141(6):1265–76. doi: 10.1002/ijc.30819
62. Kang M, Wang F, Liao X, Zhou P, Wang R. Intensity-Modulated Radiotherapy Combined With Endostar has Similar Efficacy But Weaker Acute Adverse Reactions Than IMRT Combined With Chemotherapy in the Treatment of Locally Advanced Nasopharyngeal Carcinoma. *Medicine (Baltimore)* (2018) 97(25):e11118. doi: 10.1097/md.0000000000011118
63. Ma BBY, Lim WT, Goh BC, Hui EP, Lo KW, Pettinger A, et al. Antitumor Activity of Nivolumab in Recurrent and Metastatic Nasopharyngeal Carcinoma: An International, Multicenter Study of the Mayo Clinic Phase 2 Consortium (NCI-9742). *J Clin Oncol* (2018) 36(14):1412–8. doi: 10.1200/jco.2017.77.0388
64. Hsu C, Lee SH, Ejadi S, Even C, Cohen RB, Le Tourneau C, et al. Safety and Antitumor Activity of Pembrolizumab in Patients With Programmed Death-Ligand 1-Positive Nasopharyngeal Carcinoma: Results of the KEYNOTE-028 Study. *J Clin Oncol* (2017) 35(36):4050–6. doi: 10.1200/jco.2017.73.3675
65. Yang Y, Qu S, Li J, Hu C, Xu M, Li W, et al. Camrelizumab Versus Placebo in Combination With Gemcitabine and Cisplatin as First-Line Treatment for Recurrent or Metastatic Nasopharyngeal Carcinoma (CAPTAIN-1st): A Multicentre, Randomised, Double-Blind, Phase 3 Trial. *Lancet Oncol* (2021) 22(8):1162–74. doi: 10.1016/s1470-2045(21)00302-8
66. Yang Y, Zhou T, Chen X, Li J, Pan J, He X, et al. Efficacy, Safety, and Biomarker Analysis of Camrelizumab in Previously Treated Recurrent or Metastatic Nasopharyngeal Carcinoma (CAPTAIN Study). *J Immunother Cancer* (2021) 9(12):e003790. doi: 10.1136/jitc-2021-003790
67. Mai HQ, Chen QY, Chen D, Hu C, Yang K, Wen J, et al. Toripalimab or Placebo Plus Chemotherapy as First-Line Treatment in Advanced Nasopharyngeal Carcinoma: A Multicenter Randomized Phase 3 Trial. *Nat Med* (2021) 27(9):1536–43. doi: 10.1038/s41591-021-01444-0
68. Shen L, Guo J, Zhang Q, Pan H, Yuan Y, Bai Y, et al. Tislelizumab in Chinese Patients With Advanced Solid Tumors: An Open-Label, non-Comparative, Phase 1/2 Study. *J Immunother Cancer* (2020) 8(1):e000437. doi: 10.1136/jitc-2019-000437
69. Zhang AM, Fan Y, Wang XX, Xie QC, Sun JG, Chen ZT, et al. Increased Treatment-Related Mortality With Additional Cisplatin-Based Chemotherapy in Patients With Nasopharyngeal Carcinoma Treated With Standard Radiotherapy. *Radiother Oncol* (2012) 104(3):279–85. doi: 10.1016/j.radonc.2012.08.022

Conflict of Interest: The authors declare that the research was conducted in the absence of any commercial or financial relationships that could be construed as a potential conflict of interest.

frontiers | Frontiers in Oncology

TYPE Original Research
PUBLISHED 22 July 2022
DOI 10.3389/fonc.2022.831583

OPEN ACCESS

EDITED BY
Yoshihiko Yano,
Kobe University, Japan

REVIEWED BY
Nguyen Minh Duc,
Pham Ngoc Thach University of Medicine, Vietnam
Raluca Dumache,
Victor Babes University of Medicine and Pharmacy, Romania
Huixu Xie,
Sichuan University, China

*CORRESPONDENCE
Xinwei Han
dreamweaver08@126.com
Jianzhuang Ren
rrjjzzjrk@126.com

†These authors have contributed equally to this work and share first authorship

SPECIALTY SECTION
This article was submitted to Head and Neck Cancer, a section of the journal Frontiers in Oncology

RECEIVED 08 December 2021
ACCEPTED 28 June 2022
PUBLISHED 22 July 2022

CITATION
Bi Y, Du T, Pan W, Tang F, Wang Y, Jiao D, Han X and Ren J (2022) Transcatheter Arterial Chemoembolization Is Safe and Effective for Patients With Late-Stage or Recurrent Oral Carcinoma. *Front. Oncol.* 12:831583. doi: 10.3389/fonc.2022.831583

Transcatheter arterial chemoembolization is safe and effective for patients with late-stage or recurrent oral carcinoma

Yonghua Bi[1†], Tianfeng Du[2†], Wenting Pan[2†], Fan Tang[1], Yang Wang[1], Dechao Jiao[1], Xinwei Han[1*] and Jianzhuang Ren[1*]

[1]Department of Interventional Radiology, The First Affiliated Hospital of Zhengzhou University, Zhengzhou, China, [2]Department of Stomatology, The First Affiliated Hospital of Zhengzhou University, Zhengzhou, China

Objective: We reported the long-term outcomes of transcatheter chemoembolization (TACE) for patients with late-stage or recurrent oral carcinoma.

Methods: This retrospective study enrolled 18 patients with late-stage or recurrent oral carcinoma between December 2015 and April 2021. The tumor-feeding artery was catheterized, and cisplatin/oxaliplatin and 5-FU/raltitrexed were infused with embolization using polyvinyl alcohol or gelatin sponge. Computed tomography was performed at about 1, 3, and 6 months after the procedure, and every 6 months after that. During the procedure and follow-up, procedure outcomes, complications, treatment efficacy, and overall survival were analyzed.

Results: A total of 31 sessions of TACE were performed, with a technical success rate of 100%. Of 12 patients combined with oral hemorrhage, two patients showed rebleeding 35 and 37 days later, with a clinical efficiency of hemostasis of 88.9%. Mild complications were observed in 11 patients (61.1%). Severe complications or procedure-related deaths were not observed during or after the procedure. The objective response rate and disease control rate were 20.0% and 86.7%, 38.5% and 61.5%, and 25.0% and 50.0% at 1, 3, and 6 months later, respectively. Seventeen patients (94.4%) were followed up, with a median duration of 37.8 months (IQR 22.3–56.8). Nine patients died of tumor progression, one died of massive rebleeding, and one died of severe lung infection. The median overall survival was 23.8 months.

Conclusion: TACE is a safe and effective procedure with minimal invasiveness for treating late-stage or recurrent oral carcinoma. TACE can be recommended as a palliative treatment, particularly for patients with oral hemorrhage.

KEYWORDS

TACE, oral carcinoma, oral hemorrhage, complications, oxaliplatin, raltitrexed

Introduction

As one of the most common carcinomas in the head and neck, about half of the patients with oral carcinoma are diagnosed or treated at their late stage, resulting in a poor prognosis. Oral carcinoma can be effectively managed by traditional surgery. However, surgical resection may affect facial appearance and damage oral function, and tumor recurrence may be inevitable for some patients. For late-stage inoperable patients, conventional chemoradiotherapy can be used as a palliative treatment and targeted therapy has been carried out as a novel management (1). Unfortunately, those patients often suffer side effects and adverse events after receiving palliative treatment.

Transcatheter chemoembolization (TACE) has been widely performed for the palliative treatment of late-stage carcinomas (2, 3), including advanced head and neck cancers (4–6). Besides, preoperative TACE has also been used to decrease tumor size to improve surgical success rate or reduce the recurrence rate of postoperative tumors (7, 8). To date, few studies that have reported the clinical outcomes of TACE for treating late-stage or recurrent oral carcinoma (6, 9). In this study, we reported the long-term outcomes of TACE for treating patients with late-stage or recurrent oral carcinoma.

Materials and methods

Patients

This retrospective study included 18 patients with oral carcinoma between December 2015 and April 2021. Including criteria were 1) histopathologically diagnosed as oral carcinoma, both primary and recurrent carcinoma (**Figures 1A–C**); 2) being of stages IIIA–IV (**Figures 2A, B, 3A, B**); 3) estimated survival >3 months; 4) without severe dysfunction in the heart, liver, and kidney; and 5) white blood cells >3 × 10^9/L. There were 11 male and seven female patients, including tongue cancer (n = 5), gingival cancer (n = 2), carcinoma of the mouth floor (n = 6), palate carcinoma (n = 2), and cancer of the mandible/maxilla (n = 3). The ages of the patients ranged from 26 to 84 years, with a median age of 58.5 years. There were 10 recurrent cases after surgical resection, and the remaining eight cases had an initial onset. Only five patients had no metastases. The remaining patients showed lymphatic (n = 8), liver (n = 3), bone (n = 3), and lung metastases (n = 2), respectively. Twelve patients showed massive oral bleeding on admission (**Table 1**). Ethical approval was waived by the Institutional Review Board of the University due to its retrospective nature. Written informed consent was obtained from all patients before the TACE procedure.

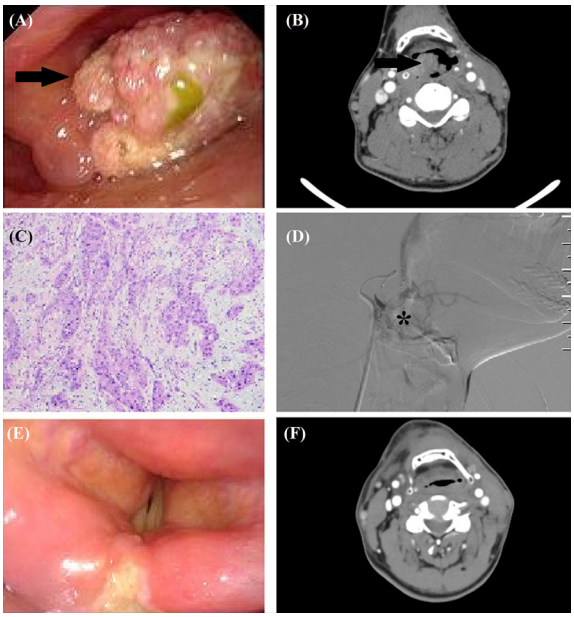

FIGURE 1
TACE for a 56-year male with recurrent squamous cells carcinoma after tongue cancer resection. **(A, B)** A recurrent tumor (arrow) was shown by laryngoscopy and computed tomography. **(C)** The tumor was histopathologically diagnosed as squamous cells carcinoma. **(D)** Tumor staining (*) was shown by angiography. **(E, F)** Laryngoscopy and computed tomography confirmed that the tumor disappeared 7 months after TACE.

TACE Procedure

All procedures were performed under local anesthesia and fluoroscopical guidance. The femoral artery was punctured using Sedinger's method. Angiography was performed with a 5F catheter to show the tumor staining and tumor-feeding arteries. Anticarcinogens including cisplatin (60 mg/m^2) or oxaliplatin (60 mg/m^2), 5-FU(600 mg/m^2) or raltitrexed (4 mg) were infused into the arteries and 350–560 μm of gelatin sponge or polyvinyl alcohol were used to block all tumor-feeding arteries (**Figures 1D, 2C, D, 3C, D**).

Follow Up

Patients underwent computed tomography examinations about 1, 3, and 6 months after the first TACE procedure (**Figures 1E, F, 2E, F, 3F**) and efficacy was evaluated according to the guidelines by Response Evaluation Criteria in Solid Tumors (RECIST) (10). Completely relieved was considered if all target lesions disappeared and partially relieved was considered if the tumor diameter decreased by

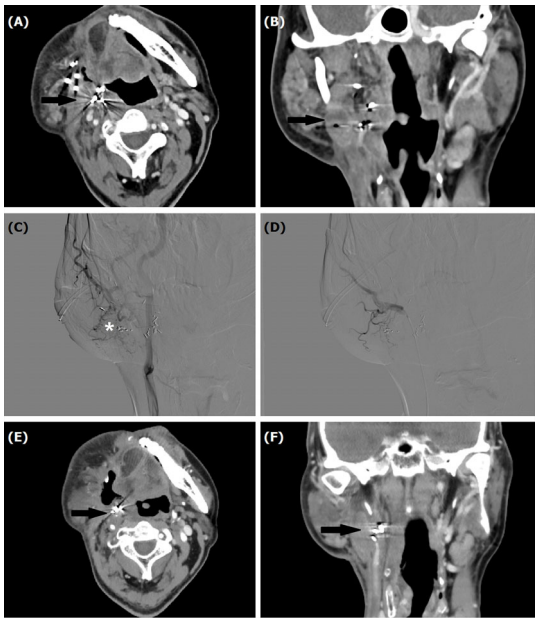

FIGURE 2
A 53-year male treated by TACE for recurrent mucoepidermoid carcinomas in tongue. **(A, B)** Computed tomography showed a recurrent tumor with Iodine-125 seeds (arrow). **(C, D)** Tumor staining (*) was shown by angiography, which disappeared after TACE. **(E, F)** A decreased tumor (arrow) was shown by computed tomography examination about 1 month later.

30% or more. Progressive development was defined as an increase in tumor diameter of 20% or greater. The objective response rate was defined as the sum of completely relieved and partially relieved. The disease control rate was defined as the sum of completely relieved, partially relieved, and stable development. All patients were followed up until death or loss to follow-up. Adverse reactions were evaluated using the National Cancer Institute Common Terminology Criteria for Adverse Events Version 3.0.

Results

TACE

Selective angiography showed that the tumor-feeding arteries appeared thickened and disordered, with irregular staining of the oral carcinoma, which vanished after embolization. During transcatheter perfusion, median dosages of cisplatin and oxaliplatin (n = 9) were of 90.0 mg and 100 mg, respectively; 5-FU or raltitrexed was 750 mg and 4 mg, respectively. Gelatin sponge (350–560 μm), polyvinyl alcohol (350–560 μm), and microspheres (300–500 μm) were used for embolization in eight, seven, and three patients, respectively. The microcoil (2 ∗ 20 mm) was used for one patient with massive oral hemorrhage. The median procedure time was 92.5 min (Table 2).

Efficacy

A total of 31 sessions of TACE were performed on 18 patients, with a technical success rate of 100%. For 12 patients combined with oral hemorrhage, hemorrhage was effectively controlled in all patients after TACE, and two patients showed rebleeding 35 and 37 days later, with a clinical efficiency of hemostasis of 88.9%. Two patients received Iodine-125 implantation before or after TACE (Figure 3E). Six months after the first sessions of TACE, completely relieved, partially relieved, and stable development were observed in one, two, and three patients, respectively. The objective response rate and disease control rate were 20.0% and 86.7%, 38.5% and 61.5%, and 25.0% and 50.0% at 1, 3, and 6 months later, respectively (Table 3).

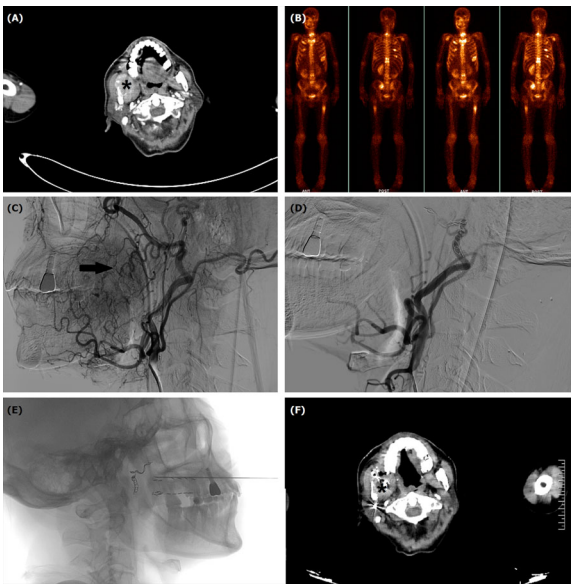

FIGURE 3
TACE for a 63-year male with oral hemorrhage due to recurrent squamous cells carcinoma in mandible and maxilla. **(A)** Computed tomography showed a tumor (*) in right mandible and maxilla. **(B)** Numerous bone metastases were visible in systemic bone imaging. **(C)** Tumor staining (arrow) and varies blood vessels were shown by angiography. **(D)** The tumor staining and tumor-feeding arteries disappeared after TACE. **(E)** Iodine-125 seeds implantation was performed about 1 month after TACE. **(F)** The tumor (*) decreased 4 months after TACE.

TABLE 1 Baseline clinicopathological characteristics of the study patients.

Variables	TACE
Number of patients	18
Mean age, years	58.5 (46.0, 68.8)
Gender, male	11 (61.1%)
Disease course, months	11.0 (4.5, 24.0)
Pathological types of tumors	
Squamous cells carcinoma	13 (72.2%)
Mucoepidermoid carcinomas	1 (5.6%)
Adenocarcinoma	1 (5.6%)
Others	3 (16.7%)
The sites of tumors	
Tongue	5 (27.8%)
Gingival	2 (11.1%)
Floor of mouth	6 (33.3%)
Palate	2 (11.1%)
Mandible/maxilla	3 (16.7%)
Recurrence after surgery	10 (55.6%)
Radiochemotherapy	14 (77.8%)
Oral hemorrhage	12 (66.7%)

Complication

All TACE procedures were safe, with no skin necrosis, cerebral infarction caused by ectopic embolization, or procedure-related death. Mild complications were observed in 11 patients (61.1%). Of these, mild-to-moderate local pain (44.4%) was the most common complication, which was easily relieved by treatment with analgesics. Nausea or vomiting and fever were observed in three and two cases, respectively.

TABLE 2 Clinical data on TACE procedure and tumor diameter change.

Variables	TACE
Technique success	18 (100%)
Rebleeding	2 (11.1%)
Hospital stay, days	12.0 (10.0, 14.5)
Procedure time, min	92.5 (65.0, 120.0)
Medical cost, $\times 10^4$ ¥	3.4 (2.9, 4.7)
Complications	11 (61.1%)
Local pain	8 (44.4%)
Nausea or vomiting	3 (16.7%)
Fever	2 (11.1%)
Oral mucosal ulcers	1 (5.6%)
Tumor diameter, mm	
Before TACE	46.0 (30.5, 66.0)
1 month later	36.5 (22.8, 70.8)
3 months later	44.0 (23.0, 57.0)
6 months later	36.5 (15.0, 67.8)

¥, Renminbi (RMB) "yuan".

Follow Up

Seventeen patients (94.4%) were followed up, with a median duration of 37.8 months (IQR 22.3, 56.8). Nine patients died of tumor progression, one died of massive rebleeding, and one died of severe lung infection. The median overall survival was 23.8 months.

Discussion

Half of the patients with oral carcinoma are diagnosed and managed as already being at a late stage, making the treatment challenging and difficult (11). Early-stage oral carcinomas can be effectively managed by surgery. However, tumor recurrence may be inevitable for some patients, and surgery has quite limited efficacy for patients with late-stage or recurrent oral carcinoma (12). Besides, traditional resection may damage oral function, and affect facial appearance, seriously affect the quality of life of patients. Conventional chemoradiotherapy is the main treatment strategy for patients with late-stage or recurrent oral carcinoma. However, medications in high doses may lead to severe adverse reactions and the clinical efficacy may be limited in cases of resistance. Due to the extensive involvement with or without metastatic lymph nodes, complete resection may be impossible for late-stage patients, with a high rate of recurrence after surgery (13).

Currently, TACE has been emerging as a palliative treatment for many kinds of late-stage carcinomas. By using local infusion of chemotherapeutic drugs at high dosage and embolization of tumor-feeding arteries for nutritional deprivation, TACE can cause tumor to shrink, necrosis, or even disappear (14–16). Besides, preoperative TACE may be beneficial to distinguish tumor boundaries from normal surrounding tissue and improve the resection rate by decreasing tumor volume and intraoperative bleeding (10), when compared with traditional treatments (17, 18).

Transcatheter infusion of high-dose anticarcinogens has been used for late-stage carcinoma of the head and neck, with or without concurrent radiation therapy (19–22). Regine et al. (18) reported that transcatheter cisplatin infusion is feasible for late-stage cancer of the head and neck if combined with hyperfractionated radiation therapy. Currently, there are few studies reporting the clinical outcomes of TACE for treating late-stage or recurrent oral carcinoma (6, 9). Kovaces et al. (9) reported that TACE using degradable starch microspheres and cisplatin showed a high overall response for late-stage cancer of the head and neck. Tomura et al. (6) performed TACE using

TABLE 3 Treatment responses of the study patients.

Response	1 month	3 months	6 months
Completely relieved	0 (0.0%)	0 (0.0%)	1 (8.3%)
Partially relieved	3 (20.0%)	5 (38.5%)	2 (16.7%)
Stable development	10 (66.7%)	3 (23.1%)	3 (25.0%)
Progressive development	2 (13.3%)	5 (38.5%)	6 (50.0%)
Objective response rate	3 (20.0%)	5 (38.5%)	3 (25.0%)
Disease control rate	13 (86.7%)	8 (61.5%)	6 (50.0%)

carboplatin microcapsules for 14 patients with malignant tumors in the head and neck and achieved obvious tumor reduction.

In this study, the objective response rate and disease control rate were 20% and 86.7%, 38.5% and 61.5%, and 25% and 50% at 1, 3, and 6 months later, respectively. The median overall survival was 23.8 months. Besides, oral hemorrhage was effectively controlled in all patients after TACE. Theoretically, TACE allowed better efficacy by direct delivery of anticarcinogens into the tumor and lower adverse events by protecting the kidney, liver, and bone marrow from systemic effects (23). Mild complications were observed in this study, and local pain was the most common complication. This was similar to the study by Tomura et al. (6), in which only mild-to-moderate local pain was observed after TACE using carboplatin microcapsules.

There were some limitations to this study. This is a retrospective study with a long time study period of 2015–2021 and was only performed in a single center. The sample size of enrolled patients is small, and we could not avoid some bias for the evaluation of clinical outcomes.

Conclusion

TACE is a safe and effective procedure with minimal invasiveness for the treatment of late-stage or recurrent oral carcinoma. TACE can be recommended as a palliative treatment, especially for patients with oral hemorrhage.

Data availability statement

The original contributions presented in the study are included in the article/supplementary material. Further inquiries can be directed to the corresponding author.

Ethics statement

The studies involving human participants were reviewed and approved by the Institutional Review Board of Zhengzhou University. The patients/participants provided their written informed consent to participate in this study.

Author contributions

XH and JR conceptualized the study. YB, TD, and WP developed the methodology. XH, and JR validated the study. YB, TD, WP, FT, YW, and DJ performed the formal analysis. YB wrote and prepared the original draft. YB, TD, and WP wrote, reviewed, and edited the article. XH and JR conducted the visualization. XH and JR supervised the study. All authors listed have made a substantial, direct, and intellectual contribution to the work and approved it for publication.

Conflict of interest

The authors declare that the research was conducted in the absence of any commercial or financial relationships that could be construed as a potential conflict of interest.

Publisher's note

All claims expressed in this article are solely those of the authors and do not necessarily represent those of their affiliated organizations, or those of the publisher, the editors and the reviewers. Any product that may be evaluated in this article, or claim that may be made by its manufacturer, is not guaranteed or endorsed by the publisher.

References

1. Dutta PR, Maity A. Cellular responses to EGFR inhibitors and their relevance to cancer therapy. *Cancer Lett* (2007) 254:165–77. doi: 10.1016/j.canlet.2007.02.006

2. Bi Y, Yi M, Yu Z, Han X, Ren J. Clinical outcomes of transarterial chemotherapy and embolization for vaginal cancer. *J Obstet Gynaecol Res* (2020) 46:924–30. doi: 10.1111/jog.14234

3. Bi Y, Shi X, Ren J, Yi M, Han X, M Song. Transarterial chemoembolization with doxorubicin-loaded beads for inoperable or recurrent colorectal cancer. *Abdom Radiol (NY)* (2021) 46:2833–38. doi: 10.1007/s00261-020-02877-w

4. Kovacs AF, Turowski B. Chemoembolization of oral and oropharyngeal cancer using a high-dose cisplatin crystal suspension and degradable starch microspheres. *Oral Oncol* (2002) 38:87–95. doi: 10.1177/02841851960371P111

5. Bi Y, Shi X, Zhang W, Lu L, Han X, Ren J. Feasibility of drug-eluting embolics chemoembolization for the management of recurrent/advanced head and neck cancer. *J Vasc Interv Radiol* (2022) 12:S1051–0443(22)00901-0. doi: 10.1016/j.jvir.2022.05.002

6. Tomura N, Kobayashi M, Hirano J, Watarai J, Okamoto Y, Togawa K, et al. Chemoembolization of head and neck cancer with carboplatine microcapsules. *Acta Radiol* (1996) 37:52–6. doi: 10.1177/02841851960371P111

7. Szabo G. New steps in the intra-arterial chemotherapy of head and neck tumors. *Oncology* (1985) 42:217–23. doi: 10.1159/000226034

8. Korogi Y, Hirai T, Nishimura R, Hamatake S, Sakamoto Y, Murakami R, et al. Superselective intraarterial infusion of cisplatin for squamous cell carcinoma of the mouth: preliminary clinical experience. *AJR Am J Roentgenol* (1995) 165:1269–72. doi: 10.2214/ajr.165.5.7572516

9. Kovacs AF, Turowski B. Chemoembolization of oral and oropharyngeal cancer using a high-dose cisplatin crystal suspension and degradable starch microspheres. *Oral Oncol* (2002) 38:87–95. doi: 10.1016/s1368-8375(01)00088-4

10. Eisenhauer EA, Therasse P, Bogaerts J, Schwartz LH, Sargent D, Ford R, et al. New response evaluation criteria in solid tumours: revised RECIST guideline (version 1.1). *Eur J Cancer* (2009) 45:228–47. doi: 10.1016/j.ejca.2008.10.026

11. Vernham GA, Crowther JA. Head and neck carcinoma–stage at presentation. *Clin Otolaryngol Allied Sci* (1994) 19:120–4. doi: 10.1111/j.1365-2273.1994.tb01194.x

12. Kurtin SE. Systemic therapies for squamous cell carcinoma of the head and neck. *Semin Oncol Nurs* (2009) 25:183–92. doi: 10.1016/j.soncn.2009.05.001

13. Li WZ, Ma ZB, Zhao T. Transcatheter arterial chemoembolization of oral squamous-cell carcinoma: a clinicopathological observation. *Di Yi Jun Yi Da Xue Xue Bao* (2004) 24:614–8.

14. Bi Y, Shi X, Ren J, Yi M, Han X, M Song. Clinical outcomes of doxorubicin-eluting CalliSpheres(R) beads-transarterial chemoembolization for unresectable or recurrent esophageal carcinoma. *BMC Gastroenterol* (2021) 21:231. doi: 10.1186/s12876-021-01816-3

15. Bi Y, Shi X, Yi M, Han X, Ren J. Pirarubicin-loaded CalliSpheres(R) drug-eluting beads for the treatment of patients with stage III-IV lung cancer. *Acta Radiol* (2022) 63:311–8. doi: 10.1177/0284185121994298

16. Bi Y, Wang Y, Zhang J, Shi X, Wang Y, Xu M, et al. Clinical outcomes of uterine arterial chemoembolization with drug-eluting beads or advanced-stage or recurrent cervical cancer. *Abdom Radiol (NY)* (2021) 46:5715–22. doi: 10.1007/s00261-021-03267-6

17. Kovacs AF, Turowski B, Ghahremani MT, Loitz M. Intraarterial chemotherapy as neoadjuvant treatment of oral cancer. *J Craniomaxillofac Surg* (1999) 27:302–7. doi: 10.1054/jcms.1999.0900

18. Milazzo J, Mohit-Tabatabai MA, Hill GJ, Raina S, Swaminathan A, Cheung NK, et al. Preoperative intra-arterial infusion chemotherapy for advanced squamous cell carcinoma of the mouth and oropharynx. *Cancer* (1985) 56:1014–7. doi: 10.1002/1097-0142

19. Wilson WR, Siegel RS, Harisiadis LA, Davis DO, Nguyen HH, WO Bank. High-dose intra-arterial cisplatin therapy followed by radiation therapy for advanced squamous cell carcinoma of the head and neck. *Arch Otolaryngol Head Neck Surg* (2001) 127:809–12.

20. Fuwa N, Ito Y, Matsumoto A, Kamata M, Kodaira T, Furutani K, et al. A combination therapy of continuous superselective intraarterial carboplatin infusion and radiation therapy for locally advanced head and neck carcinoma. *Phase I study Cancer* (2000) 89:2099–105. doi: 10.1002/1097-0142

21. Regine WF, Valentino J, John W, Storey G, Sloan D, Kenady D, et al. High-dose intra-arterial cisplatin and concurrent hyperfractionated radiation therapy in patients with locally advanced primary squamous cell carcinoma of the head and neck: report of a phase II study. *Head Neck* (2000) 22:543–9. doi: 10.1002/1097-0347

22. Andreasson L, Biorklund A, Mercke C, Scheike O, Andersson T, Brismar J, et al. Intra-arterial mitomycin c and intravenous bleomycin as induction chemotherapy in advanced head and neck cancer–a phase II study. *Radiother Oncol* (1986) 7:37–45. doi: 10.1016/s0167-8140(86)80123-2

23. Kerber CW, Wong WH, Howell SB, Hanchett K, Robbins KT. An organ-preserving selective arterial chemotherapy strategy for head and neck cancer. *AJNR Am J Neuroradiol* (1998) 19:935–41.

frontiers | Frontiers in Oncology

ORIGINAL RESEARCH
published: 02 August 2022
doi: 10.3389/fonc.2022.835965

Retinoblastoma in Adults: Clinical Features, Gene Mutations and Treatment Outcomes: *A Study of Six Cases*

*Nan Zhou, Lihong Yang, Xiaolin Xu, Yueming Liu and Wenbin Wei**

Beijing Tongren Eye Center, Beijing Key Laboratory of Intraocular Tumor Diagnosis and Treatment, Medical Artificial Intelligence Research and Verification Laboratory of the Ministry of Industry and Information Technology, Beijing Tongren Hospital, Capital Medical University, Beijing, China

Purpose: To report six Asian adult patients with retinoblastoma (RB).

Design: Retrospective and observational small case series.

Participants: Six patients with a white dome-shaped tumor of the retina were evaluated from May 10, 1995, to September 10, 2021.

Main Outcome Measures: Initial tumor and associated fundus features, pathology, gene mutation, treatment, tumor course on follow-up, and salvage globe outcome.

Results: The six affected Asian patients consisted of three men and three women. The mean age at the time of diagnosis was 36.5 years (median: 31 years, range: 20-55 years). All patients were unilateral. In all cases, the tumors were white, dome-shaped, with full-thickness retinal involvement, and mushroom-like protrusions into the vitreous cavity. The mean tumor thickness measured by ultrasonography was 4.5 mm (median: 3.2 mm, range: 3.2-6.8 mm). Associated characteristic symptoms included dilated retinal feeding artery and draining vein (100%), surrounding subretinal infiltration (83%), exudative retinal detachment (83%), and vitreous seeds (67%). Local tumor resection was performed in three patients, I-125 plaque brachytherapy combined with transpupillary thermotherapy (TTT) and intravitreous injection of melphalan (combination treatment) in one patient, I-125 plaque brachytherapy in two patients, and enucleation in one (20%) patient. RB1 gene testing was carried out on four patients and pathological diagnosis on five patients. Genetic analysis revealed that the RB1 mutation was a mosaic c.709dupG (p.Glu237GlyfsTer4) duplication in one patient, a mosaic c.763C>T(p.Arg255Ter) mutation in another patient, while the remaining two patients were RB1 negative. At the end of the follow-up, none of the patients had developed tumor-related metastasis or died. The findings were consistent in all patients who had an adequate follow-up. This study focused on this rare lesion to distinguish it from other intraocular white lesions in adults, including choroidal osteoma, vitreoretinal lymphoma, and retinal capillary hemangioma, all of which are different clinical entities.

OPEN ACCESS

Edited by:
Jun Itami,
Shinmatsudo Central General Hospital, Japan

Reviewed by:
Andrea Di Cataldo,
University of Catania, Italy
Ahmet Kaan Gündüz,
Ankara University, Turkey

***Correspondence:**
Wenbin Wei
weiwenbintr@163.com

Specialty section:
This article was submitted to Head and Neck Cancer, a section of the journal Frontiers in Oncology

Received: *15 December 2021*
Accepted: *02 May 2022*
Published: *02 August 2022*

Citation:
Zhou N, Yang L, Xu X, Liu Y and Wei W (2022) Retinoblastoma in Adults: Clinical Features, Gene Mutations and Treatment Outcomes: A Study of Six Cases. Front. Oncol. 12:835965. doi: 10.3389/fonc.2022.835965

Conclusion: In adults, RB is typically a white, full-thickness retinal mass that is unilateral, often combining with retinal feeding vessels, subretinal infiltration, and vitreous seeds. Genetic studies on adult-onset RB are essential and still require elucidation. Despite RB being a malignant tumor, patient survival was minimally affected.

Keywords: retinoblastoma, onset in adult, clinical features, genetic analysis, treatment outcomes

INTRODUCTION

Retinoblastoma (RB), a tumor originating from the sensory retina, is the most common primary malignant intraocular tumor in children, with an incidence of one case per 15,000-20,000 live births (1). Approximately 90% of children with RB are diagnosed between birth and five years old, and the tumor has been associated with the RB1 mutation (2).

The occurrence of RB in adults is uncommon, and there is limited published literature on the onset of RB in adults. In 1919, Maghy initially first reported a 20-year-old Caucasian female with bilateral RB (3). Since then, studies on this demographically rare variety of RB have been progressively increasing (4–6). There are less than 30 cases of RB in patients above the age of 20 at the time of diagnosis, with the oldest patient being a 74-year-old man (5). However, because most of them were isolated cases, there was a lack of clinical features and genetic studies on adult-onset RB patients.

The presentation of adult-onset RB can be quite different compared to its pediatric counterpart. Due to its atypical clinical symptoms and delayed diagnosis, elderly RB patients have typically been managed with enucleation. It is important to note the clinical characteristic differences between childhood and adult-onset RB, especially distinguish it from other intraocular white lesions in adults. In this study, we describe the clinical features, treatment outcomes, and review the literature on adult-onset RB based on our experience with six patients.

CASE REPORTS

A summary of the clinical features, gene mutations, ultrasonographic features, and treatment outcomes of all six cases are provided in **Table 1**.

Patient 1

A 20-year-old female was referred to our clinic after experiencing floaters in her right eye for two weeks. The patient had no significant medical history. Upon examination, her visual acuity was 20/50 in the right eye and 20/20 in the left eye. The intraocular pressure (IOP) in the right and left eyes was 12 mmHg and 15 mmHg, respectively. A slit-lamp examination revealed that the anterior segment of both eyes was normal. A dilated fundus examination of the right eye detected a white mass with feeding vessels located in the inferonasal peripheral fundus, which was surrounded by a few vitreous cellularities (**Figure 1A**). The condition of the left eye was normal. Fundus fluorescein angiography (FA) of the neoplasm showed multiple areas of mottled hyperfluorescence in the early stages, followed by obvious staining in the late stages. In contrast, the indocyanine green angiography (ICGA) showed hypofluorescence at all stages (**Figure 1B**). The patient underwent color Doppler imaging (CDI), which revealed a pedunculated mass with moderately inconsistent reflectivity and no choroidal excavation, as well as arterial blood signals in the tumor and no obvious calcification (**Figure 1C**). The size of the elevated lesion was $5.2 \times 3.9 \times 5.9$ mm^3. Optical coherence tomography (OCT) revealed that the tumor had a sloped dome-shaped elevation with a hyperreflective anterior surface and vitreous seeds, as well as normal fovea horizontally and vertically (**Figure 1D**). MRI showed the right globe with the tumor located far from the optic nerve, demonstrating a slight hyperintensity (arrow) than vitreous in axial T1-weighted MRI, hypointensity (arrow) in the axial T2-weighted MRI, and moderate enhancement of the tumor in the axial contrast-enhanced T1-weighted, fat-saturated MRI (**Figure 1E**). According to genetic analysis, the RB1 gene variant identified in the patient was a mosaic c.709dupG (p.Glu237GlyfsTer4) duplication, which was estimated to be present in approximately 10% of the patient's blood leukocytes. Targeted PCR-NGS was used to validate the presence of this mosaic variant. The results pointed to RB, which confirmed to the diagnosis. No tumor metastasis was found with 18F-FDG PET/CT. The RB gene test results of the patient's first-degree relatives were negative.

Combination treatment was then performed. The patient underwent I-125 plaque brachytherapy and three times of transpupillary thermotherapy (TTT) treatments, with a four-week interval between the first and second treatments and an eight-week interval between the second and third treatments. At the last follow-up, which was 30 months following initial presentation and 15 months since last treatment, the RB completely regressed into a partially calcified scar, with complete resolution of intravitreal seeds and no evidence of tumor recurrence (**Figure 1F**). The patient's visual acuity improved to 20/33 in the right eye and there were no adverse effects during the entire treatment.

Three years after the combination therapy, the recurrence of vitreous seeds was examined with an ophthalmoscope, and the patient was administered intravitreal injection of melphalan (30 ug). After one day of IV-Melphalan, the patient's BCVA dropped to LP, her IOP was 7 mmHg, and fundus examination revealed that the vitreous seeds had disappeared. However, exudative retinal detachment, choroidal detachment, and preretinal hemorrhage had occurred (**Figure 1G**), which were due to toxicity of intravitreal melphalan-hemorrhagic retinopathy.

TABLE 1 | Active retinoblastoma in adults: a study of 6 Cases.

Patient	Age/ Gender, Years	Laterality/ Tumor Location	Tumor-size (mm)	Gene Mutation	IRCB/ IRSS	Primary Treatment	Globe Salvage	Outcome	Final BCVA	Follow-up Duration, Months
1	20/F	Unilateral/ Intraocular	5.2×3.9×5.9	mosaic c.709dupG (p.Glu237GlyfsTer4) duplication	ICRB-C	Combination Therapy-TTT (3 times), IV-Melphalan	Yes	Alive	NLP	36
2	24/M	Unilateral/ Intraocular	5.0×4.3×6.8	mosaic c.763C>T (p.Arg255Ter) mutation in 1	ICRB-D	I-125 plaque brachytherapy; ultimately enucleation	No	Alive	–	46
3	45/F	Unilateral/ Intraocular	6.2×4.5×3.9	–	ICRB-C	Local resection	Yes	Alive	20/ 100	180
4	55/M	Unilateral/ Intraocular	5.8×3.9×3.8	–	ICRB-C	Local resection	Yes	Alive	20/ 200	120
5	38/F	Unilateral/ Intraocular	6.1×5.5×6.0	–	ICRB-C	Local resection	Yes	Alive	20/ 200	72
6	24/F	Unilateral/ Intraocular	13.7×4.8×4.7	RB 1 mutation negative	ICRB-D	I-125 plaque brachytherapy-	Yes	Alive	20/40	3

F, Female; M, Male; TTT, transpupillary thermotherapy; BCVA, best corrected visual acuity; IV-Melphalan, intravitreous injection of melphalan; ICRB, International Classification of Retinoblastoma; IRSS, International Retinoblastoma Staging System.

The patient was given oral prednisone (70 mg/per day) and topical triamcinolone acetonide periocular injection twice, but her condition did not improve. The patient ultimately developed phthisis bulbi (**Figure 1H**) but refused to be enucleated.

Patient 2

A 24-year-old male reported reduced visual acuity in the right eye. Upon examination, his visual acuity was 20/400 in the right eye and 20/20 in the left eye. The condition of the left eye was unremarkable and the anterior segment was normal. Ophthalmoscopic examination of the right eye revealed a circumscribed, nodular, white lesion of the retina located in the peripheral quadrant, coupled with tortuous feeding vessels and diffused subretinal yellow-white deposits (**Figure 2A**). The lesion was 3.2 mm thick and its largest basal diameter was 5.6 mm, as measured by CDI (**Figure 2B**). Swept source-optical coherence tomography angiography (SS-OCT, VG200D, SVision Imaging, Ltd., China, central wavelength: 1050nm; transverse resolution: 15μm [optical]; longitudinal resolution: 5μm [optical]); B-scan revealed that the multifocal subretinal lesions displayed medium- to hyper-reflectivity and exudative retinal detachment involving the macular (**Figure 2C**). Notably, similar punctate lesions with medium to high reflectivity, such as subretinal deposits observed on the lamina cribrosa, as well as around and within the optic nerve, were observed (**Figure 2C**).

Genetic analysis revealed that the RB1 gene variant identified in the patient was a mosaic c.763C>T(p.Arg255Ter) mutation in 1. We performed I-125 plaque brachytherapy, which resulted in significant tumor regression. However, the patient's condition could not be monitored due to the COVID-19 epidemic. When he returned around 10 months later, we discovered a recurrence of the tumor, which had grown bigger, multifocal, and more diffused than before, as well as fine vitreous seeds overlying the lesion. Enucleation was performed and pathological findings revealed no infiltration in the optic nerve head and the sclera (**Figure 2D**). Furthermore, the subretinal tumor cell clusters shown by pathology corresponded to the multifocal subretinal lesions shown by SS-OCT (**Figure 2C**). At the 18-month follow-up, there was no tumor-related metastasis or death.

Patient 3

A 45-year-old female was found to have a non-pigmented lesion in her right eye during a routine examination. According to the patient, a recurrence of vitreous hemorrhage had occurred twice before the lesion was initially detected two years earlier, but she recovered spontaneously both times. Her visual acuity was 20/20 in each eye. The condition of the left eye was unremarkable. In the fundus of the right eye, there was a white, dome-shaped lesion of the retina with fine vitreous hemorrhage. The vitreous seeds were unclear. The mass was 4.5 mm thick and its largest basal diameter was 6.2 mm. The mass was found in the inferotemporal fundus, and the peripheral portion of the lesion was flat, while the central portion appeared nodular and fibrotic with subtle tortuous retinal vessels, as well as associated radial macular traction (**Figure 3A**). There was a minimally dilated feeding retinal arteriole and draining venules, with associated macular edema, retinal exudation, and subretinal fluid. PET/CT scan was performed to exclude the possibility of metastases. Considering the age of the patient, a benign diagnosis was favorable, and local resection was performed using a 20-gauge vitrectomy for excision of intraocular tumors. The neoplasm was analyzed by pathology and immunohistochemistry. The findings revealed the foci of Flexner-Wintersteiner rosettes, confirming the diagnosis of RB in adults (**Figures 3B, C**). At the 15-year follow-up, the patient's final visual acuity was 20/100, and there was no evidence of tumor recurrence (**Figure 3D**). Furthermore, there was no tumor-related metastasis or death. The patient declined to undergo genetic testing.

Patient 4

A 55-year-old male experienced mild visual loss over a period of six months in his right eye. Upon examination, his visual acuity

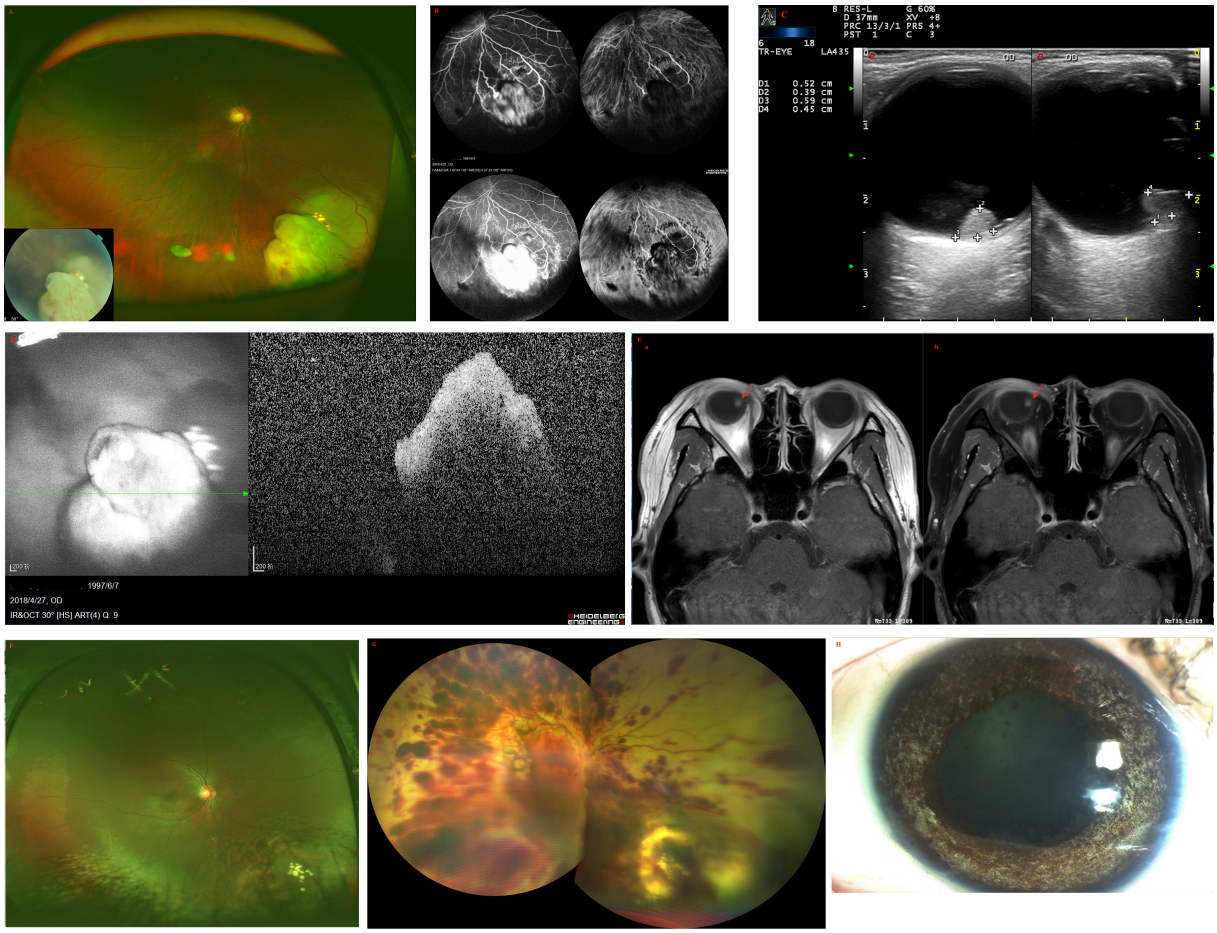

FIGURE 1 | **(A)** Fundus examination of the right eye of patient 1 revealed a large white dome-shaped retinal tumor in the inferonasal quadrant with feeding vessels and a few vitreous cellularities. **(B)** On fundus fluorescein angiography (FA), multiple areas of the tumor displayed mottled hyperfluorescence in the early phase and hyperfluorescence with intense leakage in the late phase. On indocyanine green angiography (ICGA), the tumor showed hypofluorescence during all stages. **(C)** Color Doppler imaging (CDI) revealed a pedunculated mass with inconsistent reflectivity of moderate-intensity and no choroidal excavation, as well as arterial blood signals in the tumor. The size of the elevated lesion was 5.2 × 3.9 × 5.9 mm^3. **(D)** Optical coherence tomography (OCT) revealed that the tumor had a sloped dome-shaped elevation, with a hyperreflective anterior surface and vitreous seeds, and normal macular fovea. **(E)** MRI revealed that the tumor was far from the optic nerve in the right globe, demonstrating a slightly higher hyperintensity (arrow) than vitreous in **(a)** axial T1-weighted MRI, hypointensity (arrow) in **(b)** axial T2-weighted MRI, and moderate enhancement of the tumor in axial contrast-enhanced T1-weighted, fat-saturated MRI. **(F)** At the last follow-up 15 months after the last combination treatment, the retinoblastoma demonstrated complete regression into a partially calcified scar. **(G)** One day after IV-Melphalan, intravitreal melphalan-hemorrhagic retinopathy toxicity occurred. **(H)** The patient showed signs of iris atrophy and eventually developed phthisis bulbi.

was 20/60 in the right eye and 20/20 in the left eye. The condition of the left eye was unremarkable. In the right eye, there was a white, elevated lesion of the retina in the temporal fundus without vitreous seeds. The mass was 3.9 mm thick and its largest basal diameter was 5.8 mm, as measured by CDI. The peripheral portion of the lesion was flat and white, but the central portion was elevated, with fine retinal vessels on the surface (**Figure 4A**). The feeding retinal arteriole and venule were both minimally dilated. There were no associated vitreous seeds, macular edema, or subretinal fluid. Fluorescein angiography revealed that the mass was nonfluorescent with a prominent halo of retinal hyperfluorescence in the late phase. Ultrasonography revealed that the echogenic mass displayed moderate internal reflectivity, suggesting intrinsic vascular pulsations. The patient underwent 18F-FDG PET/CT imaging, which showed no positive uptake in the other parts of the body. The clinical presentation was not consistent with amelanotic choroidal melanoma or metastasis. The patient had local resection using a 23-gauge micro-invasive vitrectomy, and immunohistochemistry results revealed Homer-Wright rosettes and occasional fleurettes, with positive neuron-specific enolase (**Figures 4B, C**). It was then determined that the patient had RB. At the 10-year follow-up, the patient's final visual acuity was 20/200, and there was no tumor recurrence (**Figure 4D**). Furthermore, there was no tumor-related metastasis or death. Genetic analysis revealed a negative RB1 gene mutation.

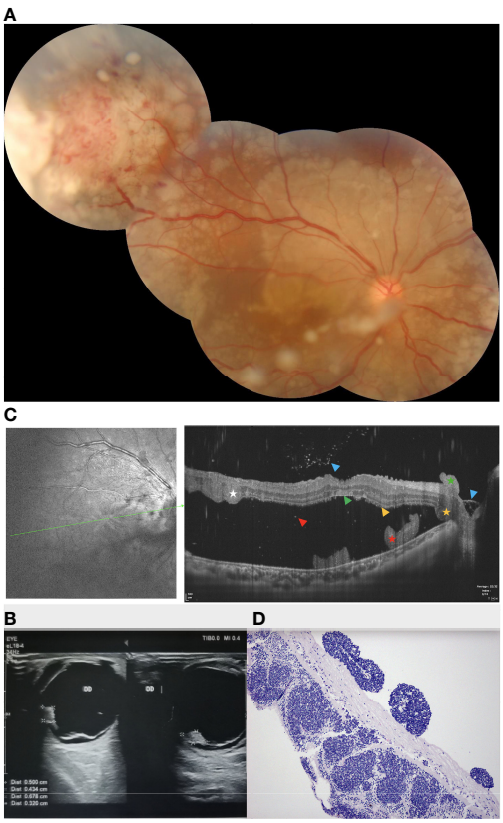

FIGURE 2 | **(A)** Fundus examination of patient 2 revealed a circumscribed, nodular, white lesion of the retina located in the peripheral quadrant, which was associated with tortious feeding vessels and subretinal yellow-white deposits. **(B)** The lesion was 4.3 mm thick and its largest basal diameter was 6.8 mm, as measured by CDI. **(C)** SS-OCT revealed multifocal, punctate, or spot subretinal lesions with medium- to hyper-reflectivity involving the lamina cribrosa and the surrounding of the optic nerve, as well as the spot lesions corresponding to subretinal tumor cells in pathological findings. (Green Triangle: superficial retinal detachment; Red Pentagram: tumor cell cluster; Yellow triangle: damaged photoreceptor cell layer and suspended tumor cells; Red triangle: discrete subretinal tumor cells; Blue triangle: tumor cells are implanted in the vitreous cavity; **(D)** Enucleation was performed and pathological findings revealed no infiltration in the optic nerve head and the sclera. Green Triangle: inner limiting membrane; Red Pentagram: tumor cell cluster; Yellow triangle: damaged photoreceptor cell layer and suspended tumor cells; Red triangle: discrete subretinal tumor cells; Blue triangle: tumor cells are implanted in the vitreous cavity; White pentagram: suspended tumor cell cluster; tumor cell clusters around the optic nerve, subretinal (yellow pentagram) and epiretinal (green pentagram).

Patient 5

A 38-year-old female reported reduced visual acuity in the right eye. Upon examination, her visual acuity was 20/200 in the right eye and 20/20 in the left eye. The condition of the left eye was unremarkable. There was mild, temporal macular traction in the right fundus, while in the left fundus, there was a white, circumscribed lesion of the retina in the superotemporal peripheral fundus, which was associated with retinal exudation and subretinal fluid. The mass was 5.5 mm thick and its largest basal diameter was 6.1 mm, as measured by CDI. The feeding retinal arteriole and venule of the tumor were both minimally dilated and convoluted. There was a mild, focal retinal hemorrhage on the nasal aspect of the lesion, with no vitreous seeds (**Figure 5A**). Fluorescein angiography revealed that the mass was nonfluorescent with a trace of overlying retinal hyperfluorescence in the late frames. Systemic examination revealed no sign of metastases. The patient had local resection using a 20-gauge vitrectomy, and immunohistochemistry results revealed rosette formation and areas of extensive necrosis, but there were no calcific foci (**Figure 5B**). It was then histology confirmed that the patient had RB. At the 6-year follow-up, the patient's final visual acuity was 20/200, and there was no tumor recurrence (**Figure 5C**). Furthermore, there was no tumor-related metastasis or death. The patient declined to undergo genetic testing.

Patient 6

A 24-year-old female reported floaters in the left eye. Upon examination, her visual acuity was 20/60 in the right eye and 20/25 in the left eye. The condition of the right eye was unremarkable. In the left fundus, there was a white, circumscribed lesion of the retina in the superotemporal peripheral fundus with tortious seeding vessels, retinal exudation, and subretinal fluid (**Figure 6A**) The feeding retinal arteriole and venule of tumor were both minimally dilated and convoluted, with significant vitreous seeds (**Figure 6B**). The

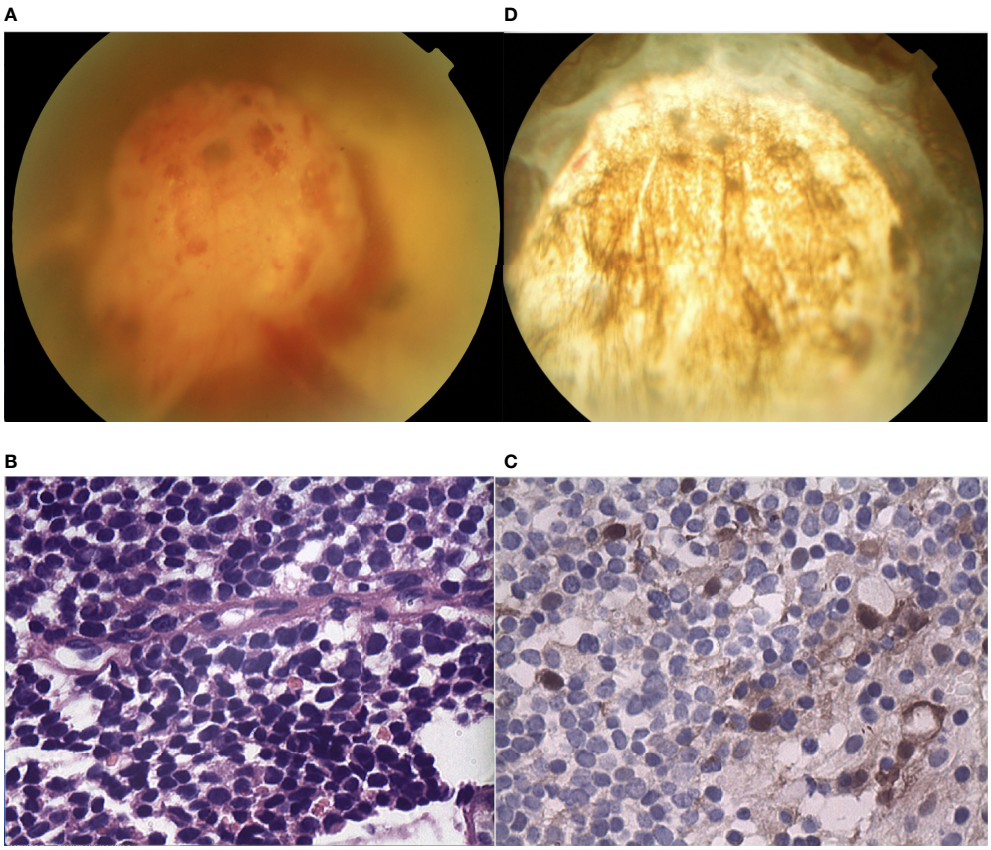

FIGURE 3 | **(A)** In the fundus of the right eye of patient 3, there was a white, dome-shaped lesion of the retina in the inferotemporal fundus, with fine vitreous hemorrhage. The central portion appeared nodular and fibrotic with subtle tortuous retinal vessels. The vitreous seeds were unclear. **(B, C)** Pathology and immunohistochemistry results revealed the foci of **(B)** Flexner-Wintersteiner rosettes that were **(C)** S100 positive. **(D)** In the last follow-up, the retina was well-attached and there was slight proliferation in the defect area of the retina.

mass was 4.8 mm thick and its largest basal diameter was 13.7 mm, as measured by CDI. SS-OCT B-scan revealed a local exudative retinal detachment surrounding the tumor, as well as subretinal deposition spots with medium to high reflectivity, not involving the macular (**Figure 6C**). Genetic analysis revealed a negative RB1 gene mutation.

Vitreous biopsy was then performed, followed by pathological analysis. The findings revealed the foci of Flexner-Wintersteiner rosettes, confirming the diagnosis of RB in the adult. We then performed I-125 plaque brachytherapy, which resulted in tumor reduction 3 months later (**Figure 6D**) and stable visual acuity. However, there were still fine white vitreous seeds overlying the lesion. Therefore, a further intravitreal injection of melphalan or topotecan was required. Systemic examination revealed no signs of metastases.

DISCUSSION

The possibilities in the diagnosis of an amelanotic mass lesion of the fundus in an adult include amelanotic melanoma, lymphoma, metastatic carcinoma, astrocytoma, tubercular choroiditis, endophthalmitis, inflammatory diseases of the retina, RB, and retinoma (4, 7–9).

The diagnosis of RB should be considered in adults with an amelanotic whitish mass lesion (pseudoretinoblastoma) (10, 11) in the fundus. However, it remains a challenge due to its rarity. Almost all RBs in adults are sporadic and unilateral. In our six cases, adult-onset RB displayed unique clinical characteristic signs on fundus appearance, including 1) unilateral diseases, 2) white mass originating from the retina with vitreous seeds, 3) tumor-associated feeding vessels, exudative retinal detachment, 4) sub-retinal discrete white-yellow deposits (tumor cells clusters), 5) uncommon calcification, and 6) rare tumor-related metastasis or death. Therefore, lesions that simulate a true retinal capillary hemangioma, as well as choroidal osteoma with retinal invasion can be mistaken for an RB lesion.

Although large white lesions with vitreous seedings can easily be identified as RB, accurate diagnosis of smaller lesions and early lesions is an issue. Ultrasonography and CT scan can reveal calcification and characteristic imaging patterns. However, in certain cases, the diagnosis may be unclear even when both

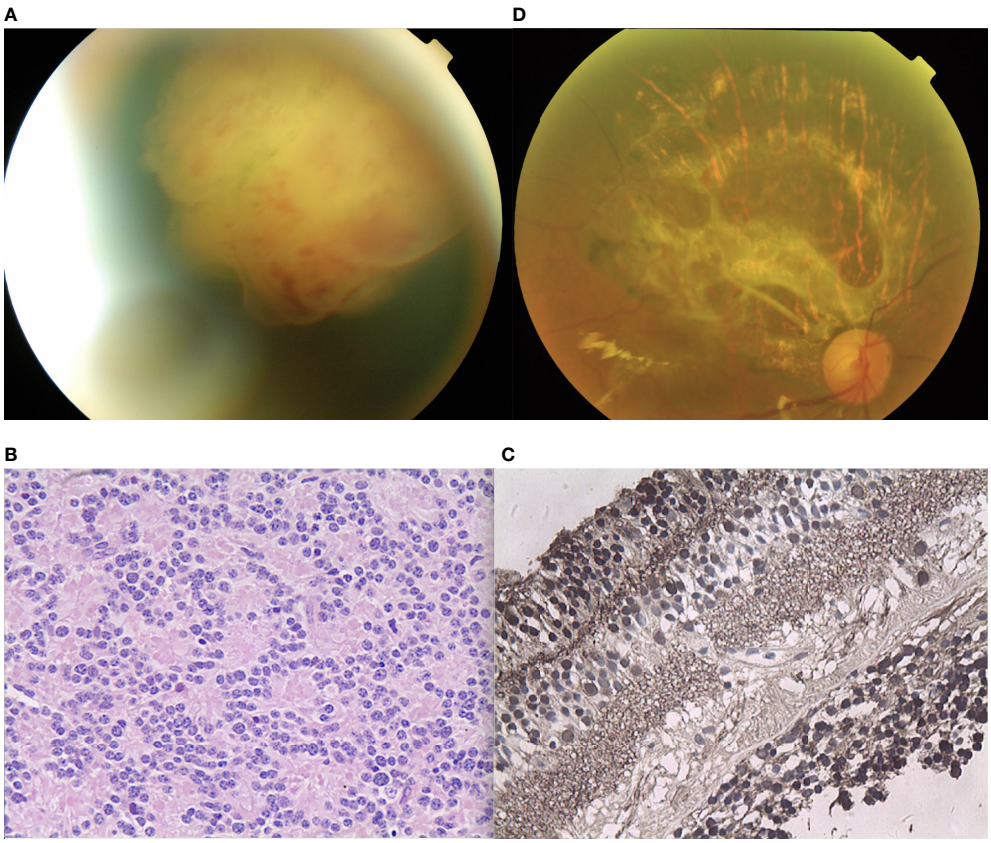

FIGURE 4 | **(A)** The peripheral portion of the lesion in patient 4 was flat and white, while the central portion was elevated. Fine retinal vessels on the surface were observed. **(B, C)** Pathology and immunohistochemistry results revealed the foci of **(B)** Flexner-Wintersteiner rosettes that were **(C)** NSE positive. **(D)** In the last follow-up, the retina was well-attached and there was slight proliferation in the defect area of the retina.

approaches are used. In all our cases, both imaging methods did not detect any calcification. Fine-needle aspiration cytology and immunohistochemistry (with neuron-specific enolase) may help confirm a diagnosis, but the former approach is controversial due to the risk of tumor cell dissemination (12). SS-OCT revealed multifocal, punctate, or spot subretinal lesions with medium- to hyper-reflectivity involving the lamina cribrosa and the surrounding of the optic nerve (**Figures 2C, D**), as well as the spot lesions corresponding to subretinal tumor cells in pathological findings (**Figures 2C, D**). These tumor cell clusters could be exfoliated, inactive tumor cells from the original mass; however, based on the theory that RB originates from ARR3-positive maturing photoreceptor precursors cells (13), these tumor cell clusters could be early RB lesions gathered by active tumor cells, which may be related to metastasis and a worse prognosis. As pathological analysis of enucleation (patient 2) showed no evidence of invasion in the optic nerve, which was not consistent with the SS-OCT findings (tumor celon the surface of the lamina cribrosa), we speculated that this may be due to the differences in the scanning direction and resolution between SS-OCT (transverse resolution: 15μm [optical]; longitudinal resolution: 5μm [optical]) and the pathological section (4 μm). Therefore, tumor invasion of the lamina cribrosa and the optic nerve should be interpreted with caution, and this patient is still being closely monitored.

Tumor histopathology or enucleation confirms the diagnosis and identifies tumor differentiation. Among our cases, patients 3 and 4 had well-differentiated RBs, while another two had undifferentiated tumors. For patient 2, enucleation pathology showed that the optic nerve head and the sclera were not infiltrated. Tumors with rosettes typically have a central lumen surrounded by a single row of cells with scanty cytoplasm and large oval nuclei with nucleoli. Nuclear pleomorphism and mitotic activity are commonly observed in these cells. Tumors displaying foci of Flexner-Wintersteiner rosettes are classified as differentiated RB.

RB, a rapidly growing tumor derived from embryonal retinal cells, is usually caused by biallelic loss of the RB1 gene, a tumor suppressor gene at chromosome 13q14, during infancy and childhood (14). RB in adults is rare (7, 9), and genetic studies on adult-onset RB patients are limited. The cause of RB in adults was speculated to be the reactivation of previously undiagnosed, spontaneously regressed, or arrested RB (also termed retinocytoma) (2). In this study, patients 1 and 2 had the RB1

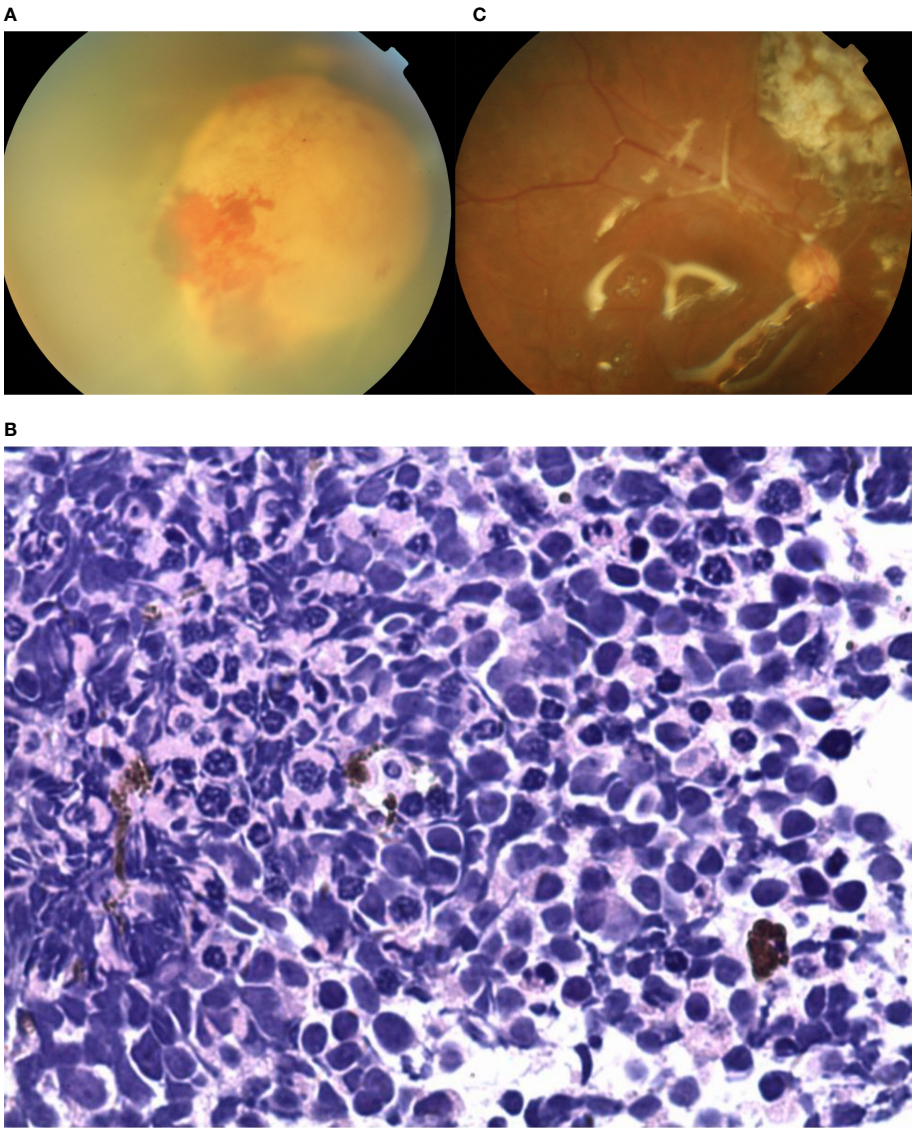

FIGURE 5 | **(A)** In patient 5, there was a white, circumscribed lesion of the retina located in the superotemporal peripheral fundus, with retinal exudation and subretinal fluid in the left fundus. The feeding retinal arteriole and venule of the tumor were minimally dilated and convoluted. There was a mild, focal retinal hemorrhage on the nasal aspect of the lesion with no vitreous seeds. **(B)** Photomicrograph revealed the foci of Flexner-Wintersteiner rosettes. **(C)** In the last follow-up, the retina was well-attached and there was slight proliferation in the defect area of the retina.

mosaic mutation. According to a recent study, the proportion of low-level deleterious copy number variant mosaicism in the blood is over 4% and low-level mosaicism is considered an under-recognized cause of disease (15). Notably, the variant of mosaic c.709dupG (p.Glu237GlyfsTer4) duplication in patient 1 had not been previously reported but was expected to cause RB due to a frameshift and premature stop codon, resulting in unstable mRNA transcript or truncated protein. Therefore, the relevant pathogenic gene was identified in adult-onset RB cases, and it is important to note the genetic differences between childhood and adult-onset RB.

Undetected RB1 mutations in fully tested tumors (RB1+/+) may include deep intronic mutations, translocations, or alterations in unknown RB1 regulatory regions. Certain unilateral RBs with undetectable RB1 mutations arise *via* an independent mechanism. Rushlow (16) and colleagues reported that there were no RB1 mutations (RB1+/+) in approximately 2.7% of unilateral, non-familial children with RB tumors. Furthermore, they identified a distinct RB1+/+MYCNA subtype that has no RB1 mutations, displays functional protein, and accounted for 1.4% of the 1068 samples. In this study, there were insufficient RB1+/+ tumor samples for gene

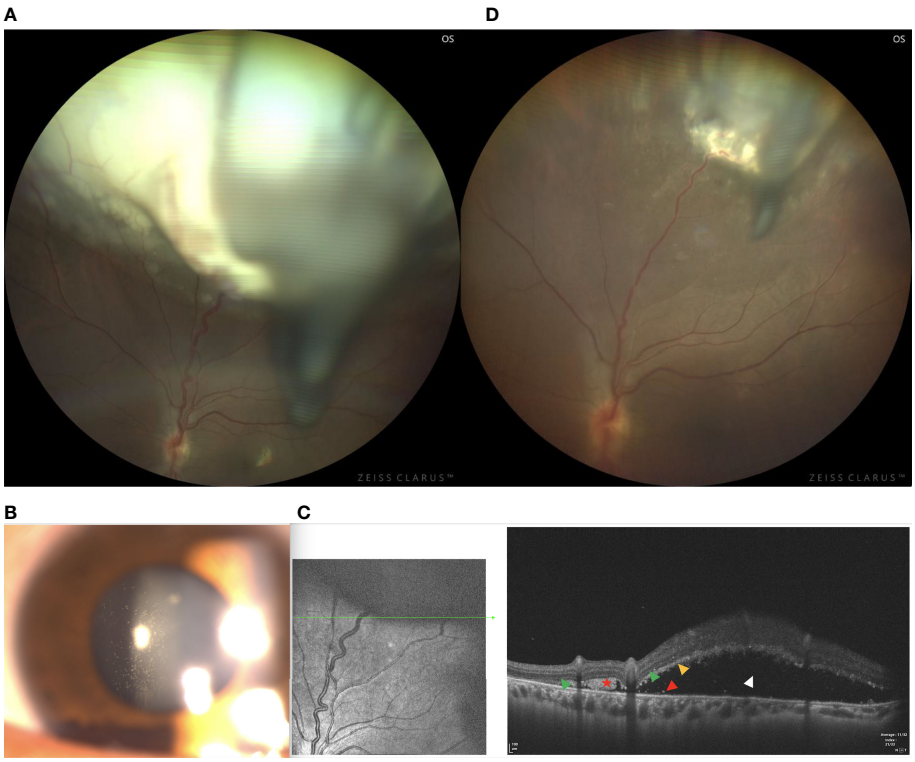

FIGURE 6 | **(A)** In patient 6, there was a white, circumscribed lesion of the retina in the superotemporal peripheral fundus, with tortious seeding vessels, retinal exudation, and subretinal fluid in the left fundus. Significant vitreous seeds were observed. **(B)** The slit lamp microscope showed significant tumor seeds floating in the vitreous cavity. **(C)** The SS-OCT B-scan revealed local exudative retinal detachment surrounding the tumor, as well as subretinal deposition spots with medium to high reflectivity without involving the macular. (Green Triangle: outer limiting membrane; Red Pentagram: tumor cell cluster; Yellow triangle: damaged photoreceptor cell layer and suspended tumor cells; Red triangle: discrete subretinal tumor cells; Blue triangle: tumor cells are implanted in the vitreous cavity; White triangle: superficial retinal detachment) **(D)** Three months after I-125 plaque brachytherapy, the tumor showed a reduction in size, resolution of subretinal fluid, normalization of the caliber and decrease in the tortuosity of feeding and draining vessels.

expression or protein analysis. There was no RB 1 mutation in two patient blood samples, while another two patients had the mosaic RB 1 mutation. These findings suggested that the prognosis of adult-onset RB is favorable and merits further investigation.

The management of adult-onset RB is determined by the stage of the disease and conditions of therapy at the time of manifestation. At present, globe preserving treatment remains a challenge for eyes with adult-onset RB. Enucleation was the primary treatment modality in most reported cases, as the lesions were detected at a fairly advanced stage and each patient had one normal eye. According to previous studies on adults with RB, the disease is usually treated with excision or enucleation at an advanced stage (Group D or E) (7, 9, 17). However, some vision in the eyes of certain unilaterally affected patients may be saved using inexpensive and non-invasive treatment. The selection criteria and treatment guidelines we followed were based on previous reports and experience with our patients. In this study, the TTT, IVM, I-125 plaque brachytherapy, surgical resection, and combination therapy were used as the primary local treatments for adult-onset RB, with none of the patients developing metastasis or died until the final follow up. In addition, because intraarterial chemotherapy is an invasive procedure and there was no indication that systemic chemotherapy was needed, we did not use chemotherapy (either intraarterial or intravenous) as the primary treatment. Similar to two of our patients, a few patients from previous studies underwent I-125 plaque brachytherapy. Although the curative effect appeared to be good for tumor regression in the early stages, there was tumor recurrence and poor results at diagnosis and follow-up in the advanced stages of the disease. Three patients underwent local tumor resection but did not experience tumor recurrence or metastasis. The optimal treatment for adult RB should still be evaluated with caution due to the rarity of the disease.

Since RB in adults is extremely rare and there are no established treatment protocols, we referred to the treatment principles of children with RB. Melphalan is the most extensively used drug to control the vitreous seeds in RB (18–22). However, Francis et al. (21, 23) discovered that melphalan injection caused a decrease in ERG response, leading them to speculate that more deeply pigmented eyes absorb increased levels of melphalan,

resulting in enhanced RPE toxicity, and, by extension, retinal and choroidal toxicity. When patient 1 was administered intravitreal injection of melphalan for Rb vitreous seeds, there was obvious drug toxicity despite its effectiveness. Therefore, the dosage or results of IVM in adult-onset RB must be interpreted with caution. Shields et al. used topotecan for vitreous seeds in RB as it was cheaper, less toxic, and effective (24–26). Melphalan is no longer used by a group from India due to its toxicity. Although some studies reported that topotecan is less effective than melphalan, Rao et al. (26) found it to be very effective. Therefore, we may use 20 ug/0.1 cc topotecan in the future for refractory or recurrent vitreous seeds in RB.

In summary, we reported a series of cases of RB in adults, describing their clinical characteristics and rare genetic make-up, as well as outcomes of local management as primary therapy. In the presence of amelanotic whitish mass lesions in the fundus of an adult, the possibility of RB as a clinical diagnosis should be taken into consideration. If the diagnosis is still unclear, RB1 gene testing may be recommended. SS-OCT can be recommended as the primary investigation method since it can detect fine lesions and shed light on the development and therapeutics of RB. Although adult patients with RB have historically poor globe salvage rates, early diagnosis of the disease and appropriate treatments improve globe salvage and long-term survival of adults with RB compared to children with RB. Based on our findings and the literature, patient survival was minimally affected, with no tumor-related metastasis or death.

DATA AVAILABILITY STATEMENT

The raw data supporting the conclusions of this article will be made available by the authors, without undue reservation.

ETHICS STATEMENT

The studies involving human participants were reviewed and approved by Institutional Review Board of Beijing Tongren Hospital. The patients/participants provided their written informed consent to participate in this study.

AUTHOR CONTRIBUTIONS

WW: Examination of the patient, interpretation of results, writing the manuscript; NZ: Interpretation of results and writing/reviewing of the manuscript; XX: Interpretation of results and reviewing of the manuscript. LY: Reviewing and examination of the manuscript. YL: Examination and treatment of the patient. All authors read and approved the final manuscript.

FUNDING

The National Natural Science Foundation of China (Nr. 81272981), the Beijing Natural Science Foundation (Nr. 7151003) provided financial support.

REFERENCES

1. Bishop JO, Madson EC. Retinoblastoma. Review of the Status. *Surv Ophthalmol* (1975) 19:342–66.
2. Pendergrass TW, Davis S. Incidence of Retinoblastoma in the United States. *Arch Ophthalmol* (1980) 98(7):1204–10. doi: 10.1001/archopht.1980.01020040056003
3. Maghy C. A Case of Bilateral Glioma of the Retina in a Girl Twenty Years of Age in Which the Second Eye was Excised After an Interval of Nearly Eighteen Years. *Br J Ophthalmol* (1919) 3:337–40. doi: 10.1136/bjo.3.8.337
4. Kaliki S, Shields CL, Gupta A, Mishra DK, Das C, Say EA, et al. Newly Diagnosed Active Retinoblastoma in Adults. *Retina* (2015) 35:2483–8. doi: 10.1097/IAE.0000000000000612
5. Sengupta S, Pan U, Khetan V. Adult-Onset Retinoblastoma. *Indian J Ophthalmol* (2016) 64(7):485–91. doi: 10.4103/0301-4738.190099
6. Gündüz AK, Mirzayev I, Temel E, Ünal E, Taçyıldız N, Dinçaslan H, et al. A 20-Year Audit of Retinoblastoma Treatment Outcomes. *Eye (Lond)* (2020) 34 (10):1916–24. doi: 10.1038/s41433-020-0898-9
7. Biswas J, Mani B, Shanmugam MP, Patwardhan D, Kumar KS, Badrinath SS. Retinoblastoma in Adults. Report of Three Cases and Review of the Literature. *Surv Ophthalmol* (2000) 44(5):409–14. doi: 10.1016/s0039-6257(99)00132-0
8. Stafford WR, Yanoff M, Parnell BL. Retinoblastoma Initially Misdiagnosed as Primary Inflammation. *Arch Ophthalmol* (1969) 82(6):771–3. doi: 10.1001/archopht.1969.00990020763008
9. Odashiro AN, Pereira PR, de Souza Filho JP, Cruess SR, Burnier MN Jr. Retinoblastoma in an Adult: Case Report and Literature Review. *Can J Ophthalmol* (2005) 40(2):188–91. doi: 10.1016/S0008-4182(05)80032-8
10. Shields CL, Schoenberg E, Kocher K, Shukla SY, Kaliki S, Shields JA. Lesions Simulating Retinoblastoma (Pseudoretinoblastoma) in 604 Cases: Results Based on Age at Presentation. *Ophthalmology* (2013) 120(2):311–6. doi: 10.1016/j.ophtha.2012.07.067
11. Mirzayev I, Gündüz AK, Biçer Ö, Tarlan B. The Final Diagnosis: Retinoblastoma or Pseudoretinoblastoma. *J Pediatr Ophthalmol Strabismus* (2021) 58(3):161–7. doi: 10.3928/01913913-20210108-01
12. Karcioglu ZA, Gordon RA, Karcioglu GL. Tumor Seeding in Ocular Fine Needle Aspiration Biopsy. *Ophthalmology* (1985) 92(12):1763–7. doi: 10.1016/s0161-6420(85)34105-2
13. Liu H, Zhang Y, Zhang YY, Li YP, Hua ZQ, Zhang CJ, et al. Human Embryonic Stem Cell-Derived Organoid Retinoblastoma Reveals a Cancerous Origin. *Proc Natl Acad Sci USA* (2020) 117(52):33628–38. doi: 10.1073/pnas.2011780117
14. Global Retinoblastoma Study Group; Fabian ID, Abdallah E, Abdullahi SU, Abdulqader RA, Boubacar SA, et al. Global Retinoblastoma Presentation and Analysis by National Income Level. *JAMA Oncol* (2020) 6(5):685–95. doi: 10.1001/jamaoncol.2019.6716
15. Campbell IM, Yuan B, Robberecht C, Pfundt R, Szafranski P, McEntagart ME, et al. Parental Somatic Mosaicism Is Under-Recognized and Influences Recurrence Risk of Genomic Disorders. *Am J Hum Genet* (2014) 95(2):173–82. doi: 10.1016/j.ajhg.2014.07.003
16. Rushlow DE, Mol BM, Kennett JY, Yee S, Pajovic S, Thériault BL, et al. Characterisation of Retinoblastomas Without RB1 Mutations: Genomic, Gene Expression, and Clinical Studies. *Lancet Oncol* (2013) 14(4):327–34. doi: 10.1016/S1470-2045(13)70045-7
17. Magan T, Khoo CT, Jabbour PM, Fuller DG, Shields CL. Intra-Arterial Chemotherapy for Adult-Onset Retinoblastoma in a 32-Year-Old Man. *J Pediatr Ophthalmol Strabismus* (2016) 53:43–6. doi: 10.3928/01913913-20160722-01
18. Francis JH, Brodie SE, Marr B, Zabor EC, Mondesire-Crump I, Abramson DH, et al. Efficacy and Toxicity of Intravitreous Chemotherapy for Retinoblastoma: Four-Year Experience. *Ophthalmology* (2017) 124(4):488–95. doi: 10.1016/j.ophtha.2016.12.015

19. Munier FL, Gaillard MC, Balmer A, Soliman S, Podilsky G, Moulin AP, et al. Intravitreal Chemotherapy for Vitreous Disease in Retinoblastoma Revisited: From Prohibition to Conditional Indications. *Br J Ophthalmol* (2012) 96 (8):1078–83. doi: 10.1136/bjophthalmol-2011-301450
20. Munier FL, Soliman S, Moulin AP, Gaillard M-C, Balmer A, Beck-Popovic M. Profiling Safety of Intravitreal Injections for Retinoblastoma Using an Anti-Reflux Procedure and Sterilisation of the Needle Track. *Br J Ophthalmol* (2012) 96(8):1084–7. doi: 10.1136/bjophthalmol-2011-301016
21. Francis JH, Abramson DH, Gaillard MC, Marr BP, Beck-Popovic M, Munier FL. The Classification of Vitreous Seeds in Retinoblastoma and Response to Intravitreal Melphalan. *Ophthalmology* (2015) 122(6):1173–9. doi: 10.1016/j.ophtha.2015.01.017
22. Shields CL, Manjandavida FP, Arepalli S, Kaliki S, Lally SE, Shields JA. Intravitreal Melphalan for Persistent or Recurrent Retinoblastoma Vitreous Seeds: Preliminary Results. *JAMA Ophthalmol* (2014) 132(3):319–25. doi: 10.1001/jamaophthalmol.2013.7666
23. Francis JH, Schaiquevich P, Buitrago E, Del Sole MJ, Zapata G, Croxatto JO, et al. Local and Systemic Toxicity of Intravitreal Melphalan for Vitreous Seeding in Retinoblastoma: A Preclinical and Clinical Study. *Ophthalmology* (2014) 121(9):1810–7. doi: 10.1016/j.ophtha.2014.03.028
24. Ghassemi F, Shields CL, Ghadimi H, Khodabandeh A, Roohipoor R. Combined Intravitreal Melphalan and Topotecan for Refractory or Recurrent Vitreous Seeding From Retinoblastoma. *JAMA Ophthalmol* (2014) 132(8):936–41. doi: 10.1001/jamaophthalmol
25. Shields CL, Douglass AM, Beggache M, Say EA, Shields JA. Intravitreous Chemotheraphy for Active Vitreous Seeding From Retinoblastoma: Outcomes After 192 Consecutive Injections. The 2015 Howard Naquin Lecture. *Retina* (2016) 36(6):1184–90. doi: 10.1097/IAE.0000000000000903
26. Rao R, Honavar SG, Sharma V, Reddy VAP. Intravitreal Topotecan in the Management of Refractory and Recurrent Vitreous Seeds in Retinoblastoma. *Br J Ophthalmol* (2018) 102(4):490–5. doi: 10.1136/bjophthalmol-2017-310641

Conflict of Interest: The authors declare that the research was conducted in the absence of any commercial or financial relationships that could be construed as a potential conflict of interest.

Frontiers in Oncology

Advances knowledge of carcinogenesis and tumor progression for better treatment and management

The third most-cited oncology journal, which highlights research in carcinogenesis and tumor progression, bridging the gap between basic research and applications to imrpove diagnosis, therapeutics and management strategies.

Discover the latest Research Topics

See more →

Frontiers

Avenue du Tribunal-Fédéral 34
1005 Lausanne, Switzerland
frontiersin.org

Contact us

+41 (0)21 510 17 00
frontiersin.org/about/contact